

A UNITED STATES
DEPARTMENT OF
COMMERCE
PUBLICATION



NAT'L INST. OF STAND & TECH



A11107 263251

NBS SPECIAL PUBLICATION 317

VOLUME I

FUNDAMENTAL
ASPECTS OF
DISLOCATION
THEORY

U.S.
DEPARTMENT
OF
COMMERCE
National
Bureau
of
Standards

UNITED STATES DEPARTMENT OF COMMERCE

Maurice H. Stans, *Secretary*

National Bureau of Standards, Lewis M. Branscomb, *Director*

FUNDAMENTAL ASPECTS OF DISLOCATION THEORY

Conference Proceedings

National Bureau of Standards, April 21-25, 1969

Edited by

John A. Simmons and R. deWit
Metallurgy Division, Institute for Materials Research,
National Bureau of Standards, Washington, D.C. 20234

R. Bullough
Theoretical Physics Division, A.E.R.E.
Harwell, Didcot, England

Volume I of 2 Volumes



U.S. National Bureau of Standards, Special Publication 317, Volume I

Nat. Bur. Stand. (U.S.), Spec. Publ. 317, Vol. I, 752 pages (Dec. 1970)

CODEN: XNBSA

Issued December 1970

For sale by the Superintendent of Documents, U.S. Government Printing Office, Washington, D.C. 20402 -
(Order by SD Catalog No. C 13.10:317) - Price \$8.25 per set of 2 volumes (sold in sets only)

JUL 4 1971

161188

22100

1967

No. 319

V. 1

1969

Copy 2.

ABSTRACT

These Proceedings contain research papers, discussions thereon, and panel discussions for the conference on "Fundamental Aspects of Dislocation Theory," held under the auspices of the Institute for Materials Research, April 21-25, 1969, at the laboratories of the National Bureau of Standards, Gaithersburg, Maryland. Approximately 75 contributed papers and two panel discussions are included. Topics covered are Discrete Dislocations in Continuum Elasticity, Lattice Theories, Dislocation-Phonon Interactions, Applications of the Geometry of Dislocations, Intrinsic Properties of Dislocations, Dislocation Field Theories, Thermally Activated Processes and Statistical Theories, Dislocation-Electron Interactions, and Future Directions for Dislocation Theory.

Key words: Conference; continuum mechanics; crystal physics; disclinations; dislocations; elasticity; electron-dislocation interactions; lattice defects; phonon-dislocation interactions; solid-state; theoretical physics; thermally activated processes; twinning.

Library of Congress Catalog Card Number: 70-602416

FOREWORD

In its role of characterizing materials and their properties, the Institute for Materials Research of the National Bureau of Standards periodically sponsors topical conferences devoted to an understanding of the fundamental quantities affecting material behavior. One such quantity is the dislocation. As line defects in crystalline solids, dislocations have a fundamental influence on mechanical, electronic, and growth properties; while they are also of prime significance as elementary sources of internal stress in any elastic material.

The organizers of this conference assembled over one hundred scientists from eighteen different nations for their meeting on Fundamental Aspects of Dislocation Theory which was held at the NBS laboratories in Gaithersburg, April 21–25, 1969. Their purpose was to provide a multidisciplinary forum seeking to intermix the viewpoints of solid state physicists and continuum mechanists on the basic properties of dislocations. The success of this venture is well attested in the following Proceedings.

J. D. HOFFMAN, *Director,*
Institute for Materials Research
National Bureau of Standards

PREFACE

These volumes comprise the proceedings of the conference on "Fundamental Aspects of Dislocation Theory" held under the auspices of the Institute for Materials Research at the Gaithersburg Laboratories of the National Bureau of Standards on April 21-25, 1969.

The purpose of the conference was to bring together workers active in all fundamental aspects of the theory of dislocations to discuss, evaluate, and contribute to the current state of understanding of these defects in crystalline materials.

Dislocations have been subject to theoretical study for some 60 years, starting with the investigations reported by Volterra. In the last 20 years there has been a steady increase in sophistication of dislocation theory from the early almost intuitive models to current theories, which range over a large portion of continuum mechanics and solid state physics. Sustained interest in dislocations has been largely due to their applications, particularly to mechanical properties of materials. Over the last 15 years the study of dislocations has received an added impetus from better correlations with experimental observations made possible by advances in such fields as electron microscopy and crystal growth. With this increase in experimental work, recent conferences have been predominantly devoted to experimental results. We, therefore, felt that this was a suitable time for a conference whose scope was limited enough to allow some in-depth treatment of various theoretical developments in the study of dislocations.

A small closed conference of about sixty people was decided upon to insure a high degree of informality and interaction. However, toward the end of our preparations the general interest had exceeded our expectations, so that a little over one hundred participants with forty percent drawn from eighteen different foreign countries finally took part; this produced a gathering of truly international character.

The conference was divided into ten sessions, each of which was organized by its chairman. Eight of these sessions were devoted to the presentation of contributed papers; however, due to the large number submitted, not all papers could be orally presented. Nonetheless, discussion time was allocated for all contributions. The remaining two sessions of the conference were panels which provided some perspective on current opinion of dislocation theory by aiming at the general questions: "How far have we come?" and "Where do we go from here?" The discussions were taped and each discusser edited his own comments. A few comments were also submitted in writing after the conference and these are labeled in the discussions as written contributions.

Constant support both for the conference and for the preparation of these Proceedings has been given from within the Institute for Materials Research and from the National Bureau of Standards as a whole. We

particularly want to thank R. B. Johnson for his invaluable counsel throughout and R. Wagner and Mrs. B. L. Oberholtzer for unstinting efforts in preparing these Proceedings—which have at times approached a printer's nightmare. Among the many groups within the NBS who have provided continuous assistance we want to mention the Special Activities Section, R. T. Cook, Chief, and the Conference Facilities Management, B. V. Como, Chief. Grateful thanks are also due Mrs. L. D. Smith, Mrs. M. C. Reid, Mrs. R. J. Morehouse, Mrs. S. F. Holdridge, and Mrs. M. L. Oland.

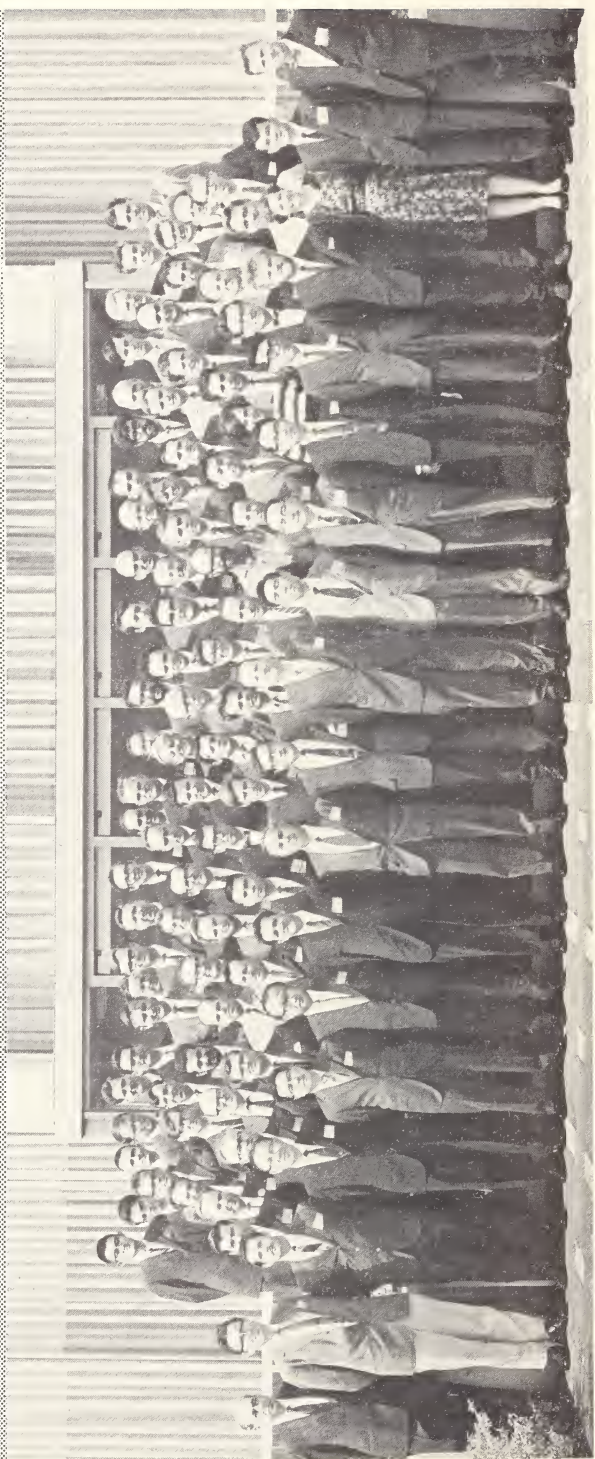
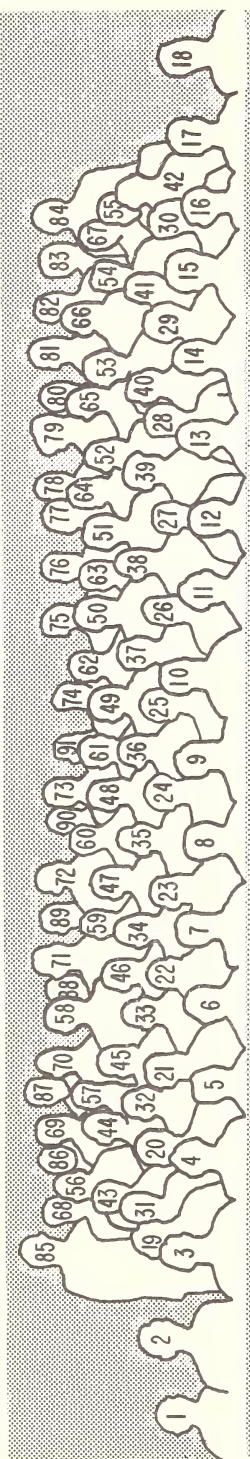
We also acknowledge the assistance of the A.E.R.E., Harwell, for their help in preparing the discussion transcriptions.

Our acknowledgements would not be complete without recognition of the basic encouragement and support which have been given us throughout this endeavor by Dr. L. M. Kushner, Dr. J. D. Hoffman, Dr. H. Sorrows, Dr. E. Passaglia, and Dr. M. R. Meyerson.

One of the important by-products of this conference was to continue the nurturing of interaction between continuum mechanists and theoretical physicists interested in understanding and describing the processes of deformation. We hope that further conferences devoted to the theory of dislocations will take place periodically and further encourage this interaction.

June 17, 1969

The Editors



FUNDAMENTAL ASPECTS OF DISLOCATION THEORY

1	N. LOUAT	24	K. MALÉN	47	R. E. GREEN	70	K. H. ANTHONY
2	R. BULLOUGH	25	W. JAUNZEMIS	48	D. J. BACON	71	R. SIEMS
3	C. S. HARTLEY	26	C. ELBAUM	49	W. P. MASON	72	W. F. HARRIS
4	R. CHANG	27	D. M. BARNETT	50	A. A. O. RUKWIED	73	W. BOILMANN
5	M. KURIYAMA	28	ANNE ENGERT	51	A. W. RUFF, JR.	74	M. KLEMÁN
6	H. SUZUKI	29	J. R. HARDY	52	J. W. FLOCKEN	75	M. S. DUESBERY
7	S. MENDELSON	30	D. O. THOMPSON	53	N. W. ASHCROFT	76	H. D. DIETZE
8	F. R. N. NABARRO	31	U. F. KOCKS	54	G. SCHOECK	77	F. BROTZEN
9	A. GRINBERG	32	P. G. KLEMENS	55	P. B. HIRSCH	78	R. O. SCATTERGOOD
10	J. A. SIMMONS	33	W. FRANK	56	J. LOTHÉ	79	G. P. HUFFMAN
11	Y. T. CHOU	34	P. GRUNER	57	J. S. KOEHLER	80	D. N. BESHERS
12	J. C. M. LI	35	J. WEERTMAN	58	T. JØSSANG	81	A. M. STONEHAM
13	T. NINOMIYA	36	G. SAADA	59	J. W. MITCHELL	82	R. THOMSON
14	T. MURA	37	B. VON TURKOVICH	60	A. K. HEAD	83	A. D. BRAILSFORD
15	M. O. TUCKER	38	S. I. BEN-ABRAHAM	61	J. H. C. THOMPSON	84	P. HAASEN
16	DORIS KUHLMANN-WILSDORF	39	M. H. YOO	62	C. TEODOSIU	85	C.-C. WANG
17	G. C. T. LIU	40	B. Z. WEISS	63	J. D. ESHELBY	86	D. SWENSON
18	R. DEWIT	41	J. J. GIJMAN	64	R. HOBART	87	N. FOX
19	L. J. TEUTONICO	42	A. A. MARADUDIN	65	H. ENGELKE	88	E. KRÖNER
20	A. C. ERINGEN	43	J. J. HREN	66	A. V. GRANATO	89	M. J. MARCINKOWSKI
21	R. J. ARSENAULT	44	W. TYSON	67	J. M. ROBERTS	90	T. R. DUNCAN
22	M. MİŞİCU	45	P. C. GEHLEN	68	F. BOISARD	91	G. P. SENDECKYJ
23	B. T. M. LOH	46	H. CONRAD	69	J. P. HIRTH		

Contributors to these Proceedings

- ANTHONY, K. H. *Max-Planck-Institut für Metallforschung, Azenbergstrasse 12, 7000 Stuttgart 1, West Germany.*
- ARSENAULT, R. J. *Chemical Engineering Department, University of Maryland, College Park, Maryland 20742.*
- ASHCROFT, N. W. *Laboratory of Atomic and Solid State Physics, Cornell University, Ithaca, New York 14850.*
- BACON, D. J. *Department of Metallurgy, University of Liverpool, Liverpool, England.*
- BARNETT, D. J. *Metallurgy Section, Scientific Research Laboratory, Ford Motor Company, 2000 Rotunda Drive, Dearborn, Michigan 48121.*
- BEN-ABRAHAM, S. I. *Departamento de Fisica, Instituto Tecnológico de Aeronáutica, C.T.A., São José dos Campos, S.P., Brazil.*
- BENNETT, L. H. *Metallurgy Division, National Bureau of Standards, Washington, D.C. 20234.*
- BERG, H. M. *Materials Science Department and Materials Research Center, The Technological Institute, Northwestern University, Evanston, Illinois 60201.*
- BESHERS, D. N. *Seeley W. Mudd Building, Henry Krumb School of Mines, Columbia University, New York, New York 10027.*
- BLOOM, J. E. *Materials Science Department and Materials Research Center, The Technological Institute, Northwestern University, Evanston, Illinois 60201.*
- BOLLMANN, W. *Battelle Institute, Advanced Studies Center, Geneva, Switzerland.*
- BRAILSFORD, A. D. *Math. and Theoretical Science, Scientific Research Laboratory, Ford Motor Company, 20000 Rotunda Drive, Dearborn, Michigan 48120.*
- BULLOUGH, R. *Theoretical Physics Division, A.E.R.E., Harwell, Didcot, Berkshire, England.*
- CHANG, R. *North American Rockwell Science Center, 1049 Camino dos Rios, Thousand Oaks, California 91360.*
- CLAUS, W. D., JR. *Textile Research Institute, Princeton, New Jersey 08540.*
- COTTERILL, R. M. J. *Structural Properties of Materials, The Technical University of Denmark, Lyngby, Denmark.*
- DATTA, B. K. *Institut für Theoretische Physik, Bergakademie Clausthal, 3392, Clausthal-Zellerfeld, West Germany.*
- DE ROSSET, W. *Department of Physics, University of Illinois, Urbana, Illinois 61801.*
- DEWIT, R. *Metallurgy Division, National Bureau of Standards, Washington, D.C. 20234.*
- DOYAMA, M. *Department of Metallurgy, Faculty of Engineering, The University of Tokyo, Bunkyo-ku, Tokyo 113, Japan.*

- DUESBURY, M. S. *Division of Pure Physics, National Research Council, Ottawa 7, Canada.*
- DUNCAN, T. R. *The University of Wisconsin, College of Engineering, Department of Minerals & Metals Engineering, Madison, Wisconsin 53706.*
- EISENBERG, M. A. *Department of Engineering Science and Mechanics, University of Florida, Gainesville, Florida 32601.*
- ELBAUM, C. *Department of Physics, Brown University, Providence, Rhode Island 02912.*
- ENGELKE, H. *Max-Planck-Institut für Metallforschung, Azenbergstrasse 12, 7000 Stuttgart 1, West Germany.*
- ENGLERT, A. *E.R.A., 95, Rue Gatti de Gammond, Bruxelles 18, Belgium.*
- ERINGEN, A. C. *Department of Aerospace & Mechanical Sciences, Princeton University, Princeton, New Jersey 08540.*
- ESHELBY, J. D. *Department of the Theory of Materials, University of Sheffield, Elmfield, Northumberland Road, Sheffield 10, England.*
- FLOCKEN, J. W. *Department of Physics, University of Nebraska, Lincoln, Nebraska 68508.*
- FOREMAN, A. J. E. *Metallurgy Division, A.E.R.E., Harwell, Didcot, Berks., England.*
- FOX, N. *Department of Applied Mathematics, University of Sheffield, Sheffield 10, England.*
- FRANK, W. *Max-Planck-Institut für Metallforschung, Azenbergstrasse 12, 7000 Stuttgart 1, West Germany.*
- FRIEDEL, J. *Service de Physique des Solides, Faculté des Sciences, Université de Paris, 91-Orsay, France.*
- GARBER, J. A. *Department of Physics, University of Illinois, Urbana, Illinois 61801.*
- GEHLEN, P. C. *Metal Science Group, Battelle Memorial Institute, Columbus, Ohio 43201.*
- GILMAN, J. J. *Materials Research Center, Allied Chemical Corporation, Morristown, New Jersey 07960.*
- GRANATO, A. V. *Department of Physics, University of Illinois, Urbana, Illinois 61801.*
- GROVES, P. P. *Department of Metallurgy, University of Liverpool, Liverpool, England.*
- GRUNER, P. *Solid State Physics Laboratory, Boeing Scientific Research Laboratories, Post Office Box 3981, Seattle, Washington 98124.*
- HAASEN, P. *Institut für Metallphysik, Universität Göttingen, Hospitalstrasse 12, 34 Göttingen, West Germany.*
- HAHN, G. T. *Metal Science Group, Battelle Memorial Institute, Columbus, Ohio 43201.*
- HARDY, J. R. *Department of Physics, University of Nebraska, Lincoln, Nebraska 68508.*
- HARRIS, W. F. *Department of Chemical Engineering, University of Minnesota, Minneapolis, Minnesota 55455.*
- HARTLEY, C. S. *Department of Engineering Science and Mechanics, University of Florida, Gainesville, Florida 32601.*
- HEAD, A. K. *CSIRO, Division of Tribophysics, University of Melbourne, Victoria 3052, Australia.*

HIKATA, A.	<i>Department of Physics, Brown University, Providence, Rhode Island 02912.</i>
HIRSCH, P. B.	<i>Department of Metallurgy, Parks Road, University of Oxford, England.</i>
HIRTH, J. P.	<i>Department of Metallurgical Engineering, The Ohio State University, Columbus, Ohio 43210.</i>
HOBART, R.	<i>Battelle Memorial Institute, Columbus, Ohio 43201.</i>
HOLDER, J.	<i>Department of Physics, University of Illinois, Urbana, Illinois 61801.</i>
HOLMES, R. R.	<i>Department of Physics, Brown University, Providence, Rhode Island 02912.</i>
HÖLZLER, A.	<i>Institut für Theoretische Physik C, Technische Hochschule Aachen, Templergraben 55, 51 Aachen, West Germany.</i>
HUFFMAN, G. P.	<i>Edgar C. Bain Laboratory for Fundamental Research, U.S. Steel Corporation Research Center, Monroeville, Pennsylvania 15146.</i>
HUMPHREYS, F. J.	<i>Department of Metallurgy, Parks Road, University of Oxford, England.</i>
ISHII, H.	<i>Materials Science Department and Materials Research Center, The Technological Institute, Northwestern University, Evanston, Illinois 60201.</i>
KLÉMAN, M.	<i>Service de Physique des Solides, Faculté des Sciences, Université de Paris, 91-Orsay, France.</i>
KLEMENS, P. G.	<i>Department of Physics, The University of Connecticut, Storrs, Connecticut 06268.</i>
KOCKS, U. F.	<i>Metallurgy Division, Argonne National Laboratory, Argonne, Illinois 60439.</i>
KOEHLER, J. S.	<i>Department of Physics, University of Illinois, Urbana, Illinois 61801.</i>
KONDO, K.	<i>The Faculty of Engineering, University of Tokyo, Bunkyo-ku, Tokyo, Japan.</i>
KRÖNER, E.	<i>Institut für Theoretische Physik, Bergakademie Clausthal, 3392, Clausthal-Zellerfeld, West Germany.</i>
KUHLMANN-WILSDORF, D.	<i>Department of Physics, University of Virginia, Charlottesville, Virginia 22903.</i>
KUNIN, I. A.	<i>Institute of Thermophysics, Academy of Sciences, Novosibirsk 90, U.S.S.R.</i>
LI, J. C. M.	<i>Materials Research Center, Allied Chemical Corporation, Morristown, New Jersey 07960.</i>
LOH, B. T. M.	<i>Metals and Ceramics Division, Oak Ridge National Laboratory, Post Office Box X, Oak Ridge, Tennessee 37830.</i>
LOTHE, J.	<i>Institute of Physics, University of Oslo, Blindern, Oslo 3, Norway.</i>
LOUAT, N.	<i>Edgar C. Bain Laboratory for Fundamental Research, U.S. Steel Corporation Research Center, Monroeville, Pennsylvania 15146.</i>
MALÉN, K.	<i>Aktiebolaget Atomenergi, Studsvik, Fack, Nyköping 1, Sweden.</i>
MARADUDIN, A. A.	<i>Department of Physics, University of California, Irvine, California 92664.</i>

- MARCINKOWSKI, M. J. *Department of Mechanical Engineering, University of Maryland, College Park, Maryland 20742.*
- MARION, R. H. *Materials Science Department and Materials Research Center, The Technological Institute, Northwestern University, Evanston, Illinois 60201.*
- MASON, W. P. *Department of Engineering and Applied Science, Columbia University, New York, New York 10027.*
- MENDELSON, S. *2660 Somerset Boulevard, Troy, Michigan 48084.*
- MITCHELL, J. W. *Department of Physics, University of Virginia, McCormick Road, Charlottesville, Virginia 22903.*
- MİŞICU, M. *Department of Mechanics of Deformable Bodies, Center of Mechanics of Solids, Academy of Sciences, Bucharest, Rumania.*
- MURA, T. *Materials Research Center, The Technological Institute, Northwestern University, Evanston, Illinois 60201.*
- NABARRO, F. R. N. *Department of Physics, University of Witwatersrand, Johannesburg, South Africa.*
- NINOMIYA, T. *Department of Physics, Faculty of Science, University of Tokyo, Bunkyo-ku, Tokyo, Japan.*
- NOURTIER, C. *Physique du Solide, Faculté des Sciences, 91 Orsay, France.*
- PEASE, D. E. *Materials Science Department and Materials Research Center, The Technological Institute, Northwestern University, Evanston, Illinois 60201.*
- RIVLIN, R. S. *Center for the Application of Mathematics, Lehigh University, Bethlehem, Pennsylvania 18015.*
- ROSENFIELD, A. R. *Metal Science Group, Battelle Memorial Institute, Columbus, Ohio 43201.*
- SAADA, G. *Departement de Physique, CUSLA, Université de Lille, BP 36/59 Lille Distribution, France.*
- SCHOECK, G. *Instituto de Fisica, Centro Atomico Bariloche, San Carlos de Bariloche, R.N., Argentina.*
- SCHRÖTER, W. *Institut für Metallphysik, Universität Göttingen, Hospitalstrasse 12, 34 Göttingen, West Germany.*
- SCHWENKER, R. O. *Department of Physics, University of Illinois, Urbana, Illinois 61801.*
- SCATTERGOOD, R. O. *Metallurgy Division, Argonne National Laboratory, Argonne, Illinois 60439.*
- SEEGER, A. *Max-Planck-Institut für Metallforschung, Azenbergstrasse 12, 7000 Stuttgart 1, West Germany.*
- SENDECKYJ, G. P. *School of Engineering, Case Western Reserve University, Cleveland, Ohio 44106.*
- SIEMS, R. *Institut für Theoretische Physik C, Technische Hochschule Aachen, Templergraben 55, 51 Aachen, West Germany.*
- SIMMONS, J. A. *Metallurgy Division, National Bureau of Standards, Washington, D.C. 20234.*
- SMITH, E. *Department of Metallurgy, University of Manchester, Manchester 13, England.*
- SPRENG, D. T. *Materials Science Department and Materials Research Center, The Technological Institute, Northwestern University, Evanston, Illinois 60201.*

- STOJANović, R. *Faculty of Sciences, Department of Mechanics, University of Belgrade, Belgrade, Yugoslavia.*
- STONEHAM, A. M. *Theoretical Physics Division, A.E.R.E., Harwell, Didcot, Berks., England.*
- SUZUKI, H. *Department of Physics, Faculty of Science, University of Tokyo, Bunkyo-ku, Tokyo, Japan.*
- TEODOSIU, C. *Mechanics of Deformable Solids, Center of Mechanics of Solids, Academy of Sciences, Bucharest, Rumania.*
- TEUTONICO, L. J. *Republic Aviation Division, Fairchild Hiller Corporation, Farmingdale, New York 11735.*
- THOMSON, R. M. *Department of Materials Science, State University of New York, Stony Brook, New York 11790.*
- TOMPA, H. *E.R.A., 95, Rue Gatti de Gammond, Bruxelles 18, Belgium.*
- TUCKER, M. O. *Department of Physics, University of Surrey, Guildford, Surrey, England.*
- VANDER SANDE, J. B. *Materials Science Department and Materials Research Center, The Technological Institute, Northwestern University, Evanston, Illinois 60201.*
- VON TURKOVICH, B. *Department of Mechanical and Industrial Engineering, University of Illinois, Urbana, Illinois 61801.*
- WAISMAN, A. M. *Institute of Thermophysics, Academy of Sciences, Novosibirsk 90, U.S.S.R.*
- WANG, C.-C. *Department of Mathematical Sciences, Rice University, Houston, Texas 77001.*
- WEERTMAN, J. *Materials Science Department and Materials Research Center, The Technological Institute, Northwestern University, Evanston, Illinois 60201.*
- WEINER, J. H. *Division of Engineering, Brown University, Providence, Rhode Island 02912.*
- WILKENS, M. *Max-Planck-Institut für Metallforschung, Azenbergstrasse 12, 7000 Stuttgart 1, West Germany.*
- YOO, M. H. *Metals and Ceramics Division, Oak Ridge National Laboratory, Post Office Box X, Oak Ridge, Tennessee 37830.*

CONTENTS—VOLUME I

	Page
Foreword.....	iii
Preface.....	v
Frontispiece.....	viii
Contributors.....	xi
I. Discrete Dislocations in Continuum Elasticity	
<i>Chairmen: J. D. ESHELBY AND R. DEWIT</i>	1
Introduction to the Session	
J. D. ESHELBY.....	3
Discrete Dislocations in Continuum Elasticity	
A. K. HEAD.....	5
The Image Force on Dislocations at Free Surfaces—	
Comments on the Concept of Line Tension	
J. LOTHE.....	11
Stability and Some Characteristics of Uniformly Moving Dislocations	
K. MALÉN.....	23
The Dislocation in a Semi-infinite Isotropic Medium	
D. J. BACON and P. P. GROVES.....	35
Theoretical Considerations on the Extension of $1/2\langle 110 \rangle \{111\}$ Dislocations in Isotropic F.C.C. Metals into Shockley Partials	
D. KUHLMANN-WILSDORF and T. R. DUNCAN.....	47
Screw Dislocations in Inhomogeneous Solids	
G. P. SENDECKYJ.....	57
Subsonic, Supersonic, and Transonic Dislocations Moving on an Interface Separating Two Media of Differing Elastic Properties	
H. M. BERG, J. E. BLOOM, H. ISHII, R. H. MARION, D. E. PEASE, D. T. SPRENG, J. B. VANDER SANDE, and J. WEERTMAN.	71
Discussion on Papers by	
A. K. HEAD, K. MALÉN, and D. KUHLMANN-WILSDORF and T. R. DUNCAN.....	83

CONTENTS—VOLUME I

	Page
Internal Stress and the Incompatibility Problem in Infinite Anisotropic Elasticity J. A. SIMMONS and R. BULLOUGH.....	89
Series Representations of the Elastic Green's Tensor for Cubic Media D. M. BARNETT.....	125
Some Problems Involving Linear Dislocation Arrays N. LOUAT.....	135
Some Recent Results on Dislocation Pileups J. C. M. LI.....	147
The Behavior of an Elastic Solid Containing Distributions of Free and Fixed Dislocations E. SMITH.....	151
The Elastic Interaction Between Grain Boundaries and Screw Dislocation Pile-ups M. O. TUCKER.....	163
Discussion on Papers by J. A. SIMMONS and R. BULLOUGH, and D. M. BARNETT.....	173
II. Lattice Theories	
<i>Chairman: R. BULLOUGH</i>	177
One-Electron Theories of Cohesion on Ion-Pair Potentials in Metals N. W. ASHCROFT.....	179
Discussion on Paper by N. W. ASHCROFT	201
Localized Vibration Modes Associated With Screw Dislocations A. A. MARADUDIN.....	205
The Method of Lattice Statics J. W. FLOCKEN and J. R. HARDY.....	219
Discussion on Papers by A. A. MARADUDIN, and J. W. FLOCKEN and J. R. HARDY.....	247
Effect of Zero-Point Motion on Peierls Stress H. SUZUKI.....	253

CONTENTS — VOLUME I

Page

Point Defects and Dislocations in Copper A. ENGLERT, H. TOMPA, and R. BULLOUGH.....	273
Atomistic Calculations of Dislocations in Solid Krypton M. DOYAMA and R. M. J. COTTERILL.....	285
A Lattice Theory Model for Peierls-Energy Calculations A. HÖLZLER and R. SIEMS.....	291
The Interaction Between a Screw Dislocation and Carbon in Body-Centered Cubic Iron According to an Atomic Model R. CHANG.....	299
The Structure of the $\langle 111 \rangle$ Screw Dislocation in Iron P. C. GEHLEN, G. T. HAHN, and A. R. ROSENFIELD.....	305
Discussion on Papers by H. SUZUKI, A. HÖLZLER and R. SIEMS, R. CHANG, and P. C. GEHLEN et al.....	309
III. Dislocation-Phonon Interactions	
Chairman: J. LOTHE.....	313
Eigenfrequencies in a Dislocated Crystal T. NINOMIYA.....	315
Discussion on Paper by T. NINOMIYA.....	359
Phonon Scattering by Dislocations and Its Influence on the Lattice Thermal Conductivity and on the Dislocation Mobility at Low Temperatures P. P. GRUNER.....	363
Phonon Scattering by Cottrell Atmospheres P. G. KLEMENS.....	391
Discussion on Papers by P. GRUNER and P. G. KLEMENS.....	395
Dragging Forces on Moving Defects by Strain-Field Phonon Scattering A. SEEGER and H. ENGELKE.....	397
Thermal Energy Trapping by Moving Dislocations J. H. WEINER.....	403

CONTENTS — VOLUME I

	Page
Discussion on Papers by	
A. SEEGER and H. ENGELKE, and J. H. WEINER.....	415
Dislocation Resonance	
J. A. GARBER and A. V. GRANATO.....	419
Disclocation Radiation	
R. O. SCHWENKER and A. V. GRANATO.....	423
The Anharmonic Properties of Vibrating Dislocations	
C. ELBAUM and A. HIKATA.....	427
A Source of Dissipation That Produces an Internal Friction Independent of the Frequency	
W. P. MASON.....	447

Discussion on Papers by

J. A. GARBER and A. V. GRANATO, R. O. SCHWENKER and A. V. GRANATO, and W. P. MASON.....	459
--	-----

IV. Applications of the Geometry of Dislocations

<i>Chairman:</i> F. R. N. NABARRO.....	463
The Meaning of Dislocations in Crystalline Interfaces	
W. BOLLMANN.....	465
Structural and Elastic Properties of Zonal Twin Dislocations in Anisotropic Crystals	
M. H. YOO and B. T. M. LOH.....	479
Non-Planar Dissociations of Dislocations	
S. MENDELSON.....	495
Propagation of Glide Through Internal Boundaries	
M. J. MARCINKOWSKI.....	531
Discussion on Papers by	
W. BOLLMANN, M. H. YOO and B. T. M. LOH, and S. MENDELSON, Including a Written Contribution by J. P. HIRTH.....	547
Kinks, Vacancies, and Screw Dislocations	
R. M. THOMSON.....	563
Discussion on Paper by	
R. M. THOMSON.....	577

CONTENTS — VOLUME I

	Page
Topological Restriction on the Distribution of Defects in Surface Crystals and Possible Biophysical Application W. F. HARRIS.....	579
Disclinations in Surfaces F. R. N. NABARRO.....	593
Application of Dislocation Theory to Liquid Crystals J. FRIEDEL and M. KLÉMAN.....	607
Nonmetric Connexions, Quasidislocations and Quasidisclinations. A Contribution to the Theory of Nonmechanical Stresses in Crystals K. H. ANTHONY.....	637
Linear Theory of Static Disclinations R. DEWIT.....	651
Discussion on Papers by F. R. N. NABARRO, K. H. ANTHONY, and R. DEWIT.....	675
 V. Panel: Intrinsic Properties of Dislocations	
<i>Chairman: J. P. HIRTH</i>	
<i>Panel Members: R. BULLOUGH, R. DEWIT, C. ELBAUM, J. D. ESHELBY, P. HAASEN and P. B. HIRSCH.....</i>	681
Introduction to the Panel Discussion J. P. HIRTH.....	683
Proceedings of the Panel J. P. HIRTH, <i>Editor</i>	687
Contributor Index.....	725

CONTENTS—VOLUME II

VI. Field Theories I

	Page
<i>Chairman: E. KRÖNER.....</i>	727
The Problem of Non-Locality in the Mechanics of Solids: Review on Present Status	
E. KRÖNER.....	729
Non-Local Theory of Elasticity for a Finite Inhomogeneous Medium—A Derivation from Lattice Theory	
E. KRÖNER and B. K. DATTA.....	737
On Problems of the Non-Local Theory of Elasticity	
I. A. KUNIN and A. M. WAISMAN.....	747
A Non-Riemannian Construction of Variational Criteria for Plastic Manifolds With Special Reference to the Theory of Yielding	
K. KONDO.....	761
Derivation of a Continuum Theory of Dislocations on the Basis of an Estimative Analysis of Crystal Lattices	
M. MIŠICU.....	785
The Elastic Generalized Cosserat Continuum With Incompatible Strains	
R. STOJANOVIĆ.....	817
Discussion on Papers by	
E. KRÖNER, and E. KRÖNER and B. K. DATTA.....	831
A Dynamic Theory of Dislocations and Its Applications to the Theory of the Elastic-Plastic Continuum	
C. TEODOSIU.....	837
Non-Linear Dynamic Problems for Anisotropic Elastic Bodies in the Continuum Theory of Dislocations	
C. TEODOSIU and A. SEEGER.....	877
On the Thermodynamics of Inhomogeneous Bodies	
C.-C. WANG.....	907
Elastic-Plastic Plane Bending of a Single Crystal	
C. S. HARTLEY and M. A. EISENBERG.....	925

CONTENTS—VOLUME II

Page

Generalized Stress and Non-Riemannian Geometry S. I. BEN-ABRAHAM.....	943
Discussion on Papers by C. TEODOSIU, and C. S. HARTLEY and M. A. EISENBERG Including Two Written Contributions by S. I. BEN-ABRAHAM..	963
VII. Field Theories II	
<i>Chairman: J. A. SIMMONS</i>	975
The Elastic Field of Moving Dislocations and Disclinations T. MURA.....	977
Discussion on Paper by T. MURA.....	997
Kinematics of Continuously Distributed Dislocations S. I. BEN-ABRAHAM.....	999
Discussion on Paper by S. I. BEN-ABRAHAM.....	1021
A Micromorphic Approach to Dislocation Theory and Its Relation to Several Existing Theories A. C. ERINGEN and W. D. CLAUS, JR.....	1023
On the Continuum Theory of Dislocations N. FOX.....	1041
Discussion on Papers by A. C. ERINGEN and W. D. CLAUS, JR., and N. FOX.....	1053
VIII. Thermally Activated Processes and Statistical Theories	
<i>Chairman: A. SEEGER.....</i>	1063
Dislocation Dynamics in the Presence of a Multiple Spectrum of Thermally Surmountable Barriers W. FRANK.....	1065
Flow and the Arrhenius Equation in the Statistical Framework U. F. KOCKS	1077
Movement of a Dislocation Through Random Arrays of Point and Parallel Line Obstacles A. J. E. FOREMAN, P. B. HIRSCH, and F. J. HUMPHREYS.....	1083
Strain Rates in Dislocation Dynamics W. DE ROSSET and A. V. GRANATO.....	1099

CONTENTS — VOLUME II

	Page
Discussion on Papers by	
W. FRANK and U. F. KOCKS.....	1107
On the Mechanism of Cross-Slip of Dislocations at Particles	
M. S. DUESBERY and P. B. HIRSCH.....	1115
Discussion on Paper by	
M. S. DUESBERY and P. B. HIRSCH.....	1135
Theories of Thermally Activated Processes and their Application to Dislocation Motions in Crystals	
H. ENGELKE.....	1137
Slightly Dissociated Dislocations	
R. H. HOBART.....	1157
Discussion on Papers by	
H. ENGELKE and R. H. HOBART.....	1163
The Broadening of Resonance Lines by Dislocations	
A. M. STONEHAM.....	1169
Discussion on Paper by	
A. M. STONEHAM.....	1175
Dislocation Pair Interaction in a Finite Body	
R. O. SCATTERGOOD and U. F. KOCKS.....	1179
The Mean Square Stresses $\langle \sigma^2 \rangle$ for a Completely Random and a Restrictedly Random Distribution of Dislocations in a Cylindrical Body	
M. WILKENS.....	1191
Theoretical Aspects of Kinematical X-Ray Diffraction Profiles from Crystals Containing Dislocation Distributions	
M. WILKENS.....	1195
Thermodynamic Properties of Solids Containing Dislocations	
J. HOLDER and A. V. GRANATO.....	1223
Discussion on Papers by	
M. WILKENS, and J. HOLDER and A. V. GRANATO.....	1227
IX. Dislocation-Electron Interactions	
<i>Chairman:</i> R. M. THOMSON.....	1229
Charged Dislocations in the Diamond Structure	
P. HAASEN and W. SCHRÖTER.....	1231

CONTENTS—VOLUME II

	Page
Discussion on Paper by	
P. HAASEN and W. SCHRÖTER.....	1255
Electronic Effects Associated With Stacking Faults in Normal Metals	
C. NOURTIER and G. SAADA.....	1259
Theory of Surface States on Stacking Faults	
R. M. THOMSON.....	1279
Discussion on Paper by	
C. NOURTIER and G. SAADA.....	1289
Interactions of Dislocations With Electrons in Metals	
C. ELBAUM and A. HIKATA.....	1291
Electronic Energy States of Dislocations; The Case of Covalent-Ionic Solids	
C. ELBAUM and R. R. HOLMES.....	1293
Interactions Between Electrons and Moving Dislocations	
G. P. HUFFMAN and N. LOUAT.....	1303
Discussion: Closing Comments by	
R. M. THOMSON.....	1323
X. Panel: Future Directions for Dislocation Theory	
Chairman: A. SEEGER	
Panel Members: N. W. ASHCROFT, A. C. ERINGEN, E. KRÖNER, J. LOTHE, A. A. MARADUDIN and J. A. SIMMONS	1325
Questions Submitted to the Panel.....	1327
Report on the Panel Discussion	
A. SEEGER.....	1329
Contributor Index.....	1337

I DISCRETE DISLOCATIONS IN CONTINUUM ELASTICITY

Chairmen:

J. D. ESHELBY

R. DEWIT

INTRODUCTION TO THE SESSION ON DISCRETE DISLOCATIONS IN CONTINUUM ELASTICITY

J. D. Eshelby

*Department of the Theory of Materials
University of Sheffield
Sheffield, England*

This section is concerned with that part of dislocation theory which treats the elastic fields of discrete dislocation lines according to linear continuum mechanics. It forms the basis for much of dislocation theory in the narrower sense, and, by giving an approximation to the positions of the atoms in a crystal lattice, serves to relate the theory to other parts of physics. Where non-linear effects are important they can usually be dealt with by perturbation theory starting from the linear solution; if this is inadequate it is usually necessary to take into account the atomic structure as well.

The papers presented show that the subject matter of this section, though the longest-established (or most old-fashioned) part of dislocation theory is far from being worked-out.

The opening paper by Head presents his views on some important topics in the present field.

Many dislocation calculations are concerned with problems relating to specific configurations of one or more dislocation lines. There is, of course, indefinite scope for the solution of such problems, but if they are not to serve simply as an excuse for a display of mathematical weight-lifting they must be chosen carefully, either to cover a wide range of special cases, or to refer to a specific situation of interest (e.g. some configuration observed in the electron microscope), or they should be concerned with some simple situation chosen so as to bring out a physical point.

A number of the papers presented in this section fall into this category and meet these requirements. Bacon and Groves treat the case of a dislocation loop near a free surface, Li finds the elastic field of a finite grain boundary, and Sendeckyj presents some general theorems and special solutions for screw dislocations interacting with inclusions or cavities. Smith gives some new results relating to the equilibrium form of dislocation pile-ups under the influence of fixed dislocations and applied stresses. The papers by Kuhlmann-Wilsdorf and Duncan, and by Lothe, use the results of elasticity calculations to elucidate the physical behavior of dislocations. Kuhlmann-Wilsdorf and Duncan are concerned with the extent to which

4 FUNDAMENTAL ASPECTS OF DISLOCATION THEORY

dislocations in f.c.c. metals split into Shockley partials. Lothe deals with the image force on a dislocation terminating at a free surface.

Several of the papers in this section use anisotropic elasticity, but three in particular are concerned specifically with the problem of anisotropy. The theory of two-dimensional problems (infinite straight dislocations) is in reasonably good shape. To solve three-dimensional problems (e.g. to find the strain field of a dislocation loop) one in effect needs to know the elastic Green's function, that is, the response of the anisotropic medium to a point force. Even if the method used does not make explicit use of this function the analysis will sooner or later come up against the same difficulties as present themselves in the calculation of the Green's function.

It is only for crystals of the hexagonal system, which are elastically invariant under rotation round the six-fold axis, that the Green's function can always be written down explicitly. For cubic crystals an analytic solution (a particularly simple one) can apparently be obtained only for the theoretically possible but seemingly non-existent solid which satisfies $C_{12} = -C_{44}$ in the usual notation. Generally one has to use some kind of series expansion. One way is to do a perturbation calculation starting from an isotropic medium. Its elastic constants may be chosen largely at will. Barnett's paper on series representations of the Green's tensor throws light on the effect of this choice. Simmons and Bullough treat the problem of how to find the stress field in a finite anisotropic solid when the incompatible strain or the incompatibility tensor is prescribed.

The last-named contribution evidently trespasses into the realm of the theory of continuous distributions of dislocations. So also, in a sense, do the papers of Tucker and Louat. If it contains a large number of dislocations a dislocation pile-up can be replaced by a linear continuous distribution of infinitesimal dislocations. This "smear technique" (Louat) has also been found useful as a mathematical tool in solving some of the crack problems of fracture mechanics. Though not the most erudite, it is, perhaps, so far, the most productive part of the theory of continuous distributions of dislocations. Tucker uses this technique to discuss screw dislocation pile-ups near grain boundaries in anisotropic crystals. Louat considers the solution of the integral equations which appear when one is concerned with a number of continuous pile-ups, not necessarily in the same plane.

Finally, included in this section are two papers on dynamic problems, which however, reduce to modified static problems when viewed by a suitable steadily-moving observer. Malén is concerned with the stability of moving dislocations in anisotropic media, and Weertman and his colleagues discuss the elastic fields of dislocations moving in the interface between two different isotropic media.

DISCRETE DISLOCATIONS IN CONTINUUM ELASTICITY

A. K. Head

*Commonwealth Scientific and Industrial Research Organization
Division of Tribophysics
University of Melbourne
Victoria, Australia*

As a framework in which to survey some of the current questions in this long-established part of dislocation theory, the problem of the experimental determination of stacking fault energy is considered. Attention is restricted to those methods which observe and measure in the electron microscope a simple dislocation-stacking fault configuration. It is assumed that the configuration is in equilibrium with the forces between the dislocation balancing the surface tension of the stacking fault. The stacking fault energy then follows if these dislocation forces are known from theory for the observed dimensions of the configuration.

Experimental techniques have improved to the point where a reproducibility of 1 to 5 percent standard deviation is claimed. This calls for theory which has at least a similar standard of accuracy. It is doubtful if the theory which is in current use has this accuracy and this is surveyed under the following headings: (a) The treatment of the core; (b) Elastic anisotropy; (c) Zig-zag instabilities; (d) The effect of the stacking fault; (e) The observation of dislocations by electron microscopy.

Key words: Dislocation observations; dislocation theory; status and problems.

I. Introduction

A historical survey of this part of dislocation theory is quite impracticable in the time available and I am sure it would not be appreciated since you already know all about it. This is where dislocation theory started, as dislocations in an elastic continuum with the quantization of Burgers vectors and slip planes in recognition of the real lattice as opposed to the idealized continuum. Books have been written on the subject, it is taught to undergraduates, it is in everyday use, and it is, I suspect, often taken to be the truth, the whole truth, and nothing but the truth. Most of it is of course true enough as far as it goes but I will use this occasion to consider if in fact it does go far enough for the needs of the present.

Fundamental Aspects of Dislocation Theory, J. A. Simmons, R. de Wit, and R. Bullough, Eds. (Nat. Bur. Stand. (U.S.), Spec. Publ. 317, I, 1970).

There is one general characteristic of dislocation problems in this field, that they are questions in continuum elasticity and as such show many of the features of continuum elasticity in general. These features include the simplicity of two dimensional problems as compared with three dimensions and, especially in the case of two dimensions, the wide variety of mathematical methods which can be used in any particular case. The choice of any particular mathematical apparatus has been largely a matter of personal taste but a new variable is appearing as more complicated problems are tackled. This choice is whether the end product shall be in a form best for human understanding or a form best for computers. These often coincide in simple cases but may diverge widely in cases of complexity. I think that this divergence will become increasingly apparent.

As a framework in which to survey some current questions, I will consider the problem of the experimental determination of stacking fault energy. There are a number of different ways in which this can be estimated but, in keeping with the spirit of this conference, I will only consider direct methods which observe and measure in the electron microscope a simple dislocation-stacking fault configuration. Examples would be the separation into partials of a straight dislocation or a three-fold dislocation node. It is then assumed that the configuration is in equilibrium with the forces between dislocations balancing the surface tension of the stacking fault. If this is so, then the stacking fault energy follows if these dislocation forces are known from theory for the observed dimensions of the configuration.

Experimental techniques have improved to the point where a reproducibility of 1 to 5 percent standard deviation is claimed. To maintain this accuracy in deduced values of stacking fault energy calls for theory with at least a similar standard of accuracy. I would suggest that current theory probably does not meet this standard in a number of respects and I will attempt to survey some areas of continuum dislocation theory where improvement appears to be needed.

II. The Dislocation Core

The core of the dislocation does not really belong to this part of the conference, being the nonlinear, noncontinuum part of the dislocation but I mention it because our ignorance is often disguised as a linear continuum question, the choice of an inner cutoff radius. There are various conventional ways of prescribing this cutoff but they are just conventions and give no guide as to what value this cutoff should have in order that the true total energy of the dislocation is reproduced. A typical choice could be that the inner cutoff is taken as a fixed multiple of the Burgers vector of the dislocation. But any such choice forces the nonlinear core energy

to vary in proportion to the linear elastic energy for changes in the screw-edge character of the dislocation, for changes in the Burgers vector, or for differing elastic constants. It seems unlikely that the real situation could be that simple, but a better description will not come from continuum theory.

III. Elastic Anisotropy

The fact that most metals are elastically anisotropic and that most dislocation theory has used isotropic elasticity is well known. This is understandable as isotropic theory is so much simpler and can often give neat little formulae when the anisotropic equivalent only gives numerical results for specific cases. But even in simple cases for simple metals it is unlikely that the isotropic approximation is good to 1 percent and an example given in the next section suggests it is much worse than that.

Three dimensional problems in anisotropic elasticity are especially difficult and are rarely considered. Recent Russian work is therefore important in showing that some three dimensional dislocation problems can be reduced, in a certain sense, to two dimensional problems. This is a technique which is awaiting fuller exploitation.

The theory of two dimensional elastic anisotropy is well known and is being used increasingly in dislocation theory. Results have been numerical except when special symmetries have allowed simplification. But there does seem to be a mistaken belief that numerical results are the only possibility in the general case as the roots of a sextic polynomial are involved. This may be because it is often loosely said that Abel has proved that the roots of a general polynomial cannot be determined explicitly if the degree of the polynomial is greater than four. But what Abel proved was that the roots cannot be determined explicitly in terms of radicals.

The appropriate question for higher degree polynomials is then, what new types of higher function will explicitly solve the polynomial? The answer is known for the general quintic to be elliptic modular functions and for the general sextic, of interest to us, to be hyper-elliptic functions. I do not suggest that this explicit solution of a sextic polynomial is simple nor that it would replace numerical methods when specific numerical results are needed. But the type of question where it may be of use could be the following. Consider the common slip dislocations of fcc metals which lie on $\langle 111 \rangle$ planes. The general direction in a $\langle 111 \rangle$ plane does not fall in one of the symmetry categories for which explicit factorization of the sextic is presently possible. But in this case the six coefficients of the sextic are functions of only three parameters, one angle specifying the dislocation direction and two ratios of elastic constants. So this sextic is far from general and perhaps the solution of this sextic by hyper-elliptic functions would reveal just how special it really is.

IV. Zig-Zag Instability

The zig-zag instability of dislocations is a feature which is specific to elastic anisotropy and cannot occur for isotropy. The occurrence of such instability is a sign that the isotropic approximation is inappropriate. Such zig-zag dislocations have previously been observed in β -brass, which is very anisotropic, with good agreement between theory and experiment. But we have recently observed in Cu-15 percent Al, which is about as anisotropic as copper, that for the common $\frac{1}{2}\langle 110 \rangle$ slip dislocations, one partial has a zig-zag form. This suggested that we examine theoretically the question of zig-zag instability of partial dislocations in fcc metals and we find that it can be expected in copper, silver and gold and their dilute alloys.

These metals are of course just the ones which have been most intensively studied in determinations of stacking fault energy yet they are sufficiently anisotropic for the partials, which are involved in these determinations, to have zig-zag instability. This raises doubts as to the accuracy of stacking fault energies which have been derived from isotropic theory. For instance many values have been derived from the measurement of the shape and size of three-fold nodes. This shape depends directly on the variation of energy of a partial as a function of its screw-edge character. But it is just this energy variation, and the fact that it is significantly different from the isotropic approximation, which produces zig-zag instability.

V. The Stacking Fault

The most obvious property of the stacking fault is that it has an energy per unit area and exerts a force per unit length on the dislocation which bounds it. It also has a second property which has not been taken into account, that across the fault the cubic packing of atoms is changed to hexagonal and in the approximation of continuum elasticity it should be represented as a thin layer of material with different elastic constants. The importance of this is rather difficult to estimate for although the layer is thin, it usually is in regions of high strain energy.

A possible illustration of the importance of this effect may be shown by the zig-zag partials in Cu-15 percent Al which have been mentioned above. The theoretical calculations of the forbidden directions of such dislocations give a forbidden range of directions which is symmetrical about the edge orientation of the partial but the experimental measurements show a small but definite asymmetry. This cannot be due to the stress field of the other partial nor to the stacking fault as a source of line force on the dislocation but could be due to the stacking fault as a region of differing elasticity which is created or destroyed as the dislocation moves.

VI. Electron Microscopy

The experiments I have been considering involve the measurement of electron micrographs of dislocations to determine their positions or spacings, and what is needed is the position of the centre of the dislocation. The theory of electron microscopy is complicated and general rules are few but one rule would be that in almost all cases the centre of the dislocation is not at the blackest point of the image. It may be to one side or the other, displaced by distances which may be tens of Angstroms and depending not only on the experimental parameters of the electron microscope but on the precise nature of the dislocation.

So if the position of the centre of the dislocation is required with precision, then it is necessary to interpret the micrographs with some care. Now for any particular situation this can be done by computing the theoretical image the dislocation should have and then the position of the dislocation centre can be located. What is required is the displacement field of the dislocation in a suitable form for a computer to simulate the passage of the electron waves through the distorted crystal. It has been said that a dislocation is revealed in the electron microscope by a complicated analogue of photoelasticity and the detailed form of its image, which is really an image of its displacement field, has no simple interpretation. But the image can be calculated if the displacements are known and for accurate measurements of the positions of dislocations, this needs to be done.

VII. Conclusion

Any estimation of the influence of these various effects on deduced values of stacking fault energy can, at the moment, be no more than a personal guess. My guess is that all these things would have to be taken into account if 1 percent accuracy is the target and a number of them would have influences of over 10 percent. I have only considered one field of application of the continuum theory of discrete dislocations but the same thing is probably true in other situations, that with increasing accuracy and sophistication of experiments, the theory of yesterday may no longer be sufficient and its assumptions and approximations need continual scrutiny in the light of today's needs.

THE IMAGE FORCE ON DISLOCATIONS AT FREE SURFACES—COMMENTS ON THE CONCEPT OF LINE TENSION

J. Lothe

*Institute of Physics
University of Oslo
Blindern, Oslo, Norway*

It is shown that a straight dislocation emerging at a planar free surface is acted upon by a force distributed according to the law $dF = \lambda^{-1}(-E \cotan \theta + \partial E / \partial \theta) d\lambda$. Here θ is angle of inclination to surface. E is dislocation energy factor, and λ is distance from surface along the dislocation. The proof involves use of a slightly generalized version of the energy flow theorem for straight dislocations (Lothe, Phil. Mag. **15**, 9 (1967)). The above formula is the exact linear elasticity law corresponding to the usual approximate line tension result. According to this law there are certain angles of incidence for which the forces vanish so that the dislocation can be straight. Similarly, when only elastic terms are considered, there are certain node orientations for which the forces on the branches vanish so that the branches can be truly straight (Indenbom and Dubnova, Sovj. Phys. (Solid State), **9**, 915 (1967)). In this paper a discussion is given of how core energy terms may modify the results. It is concluded that also for nodes in the characteristic orientation for no elastic forces on the branches, some branch curvature will be present near the node.

Key words: Dislocation-surface interactions; dislocations-image series; line tension of dislocations; dislocation nodes.

I. Introduction

The elastic energy per unit length between two cylinders of radii r_0 and r coaxial about an infinite straight dislocation is

$$W/L = E \log (r/r_0). \quad (1)$$

The prelogarithmic factor E , the energy factor, is well defined and independent of r and r_0 . Dislocation calculations are often performed in the so-called line tension approximation in which an energy per unit

Fundamental Aspects of Dislocation Theory, J. A. Simmons, R. de Wit, and R. Bullough, Eds. (Nat. Bur. Stand. (U.S.), Spec. Publ. 317, I, 1970).

length W/L as given by (1) is ascribed to the dislocations, and one is then always confronted with the problem of deciding on appropriate cutoff parameters r_0 and r . However, let us temporarily ignore this difficulty and consider the logarithmic factor as just some constant. Consider a straight dislocation making an angle θ with a free planar surface. From the virtual displacement indicated in figure 1, one concludes that the dislocation is acted upon by a force

$$F \sim (-E \cotan \theta + \partial E / \partial \theta). \quad (2)$$

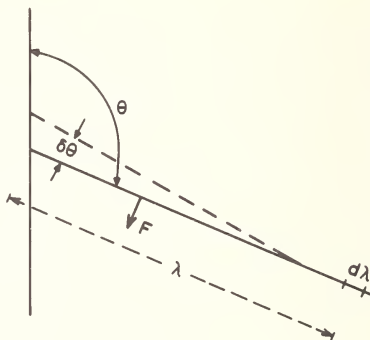


FIGURE 1. A straight dislocation emerging at a free surface. Stapled line indicates a virtual displacement.

Actually the force will be distributed according to a $1/\lambda$ law,

$$dF = \lambda^{-1} (-E \cotan \theta + \partial E / \partial \theta) d\lambda. \quad (3)$$

Here dF is the force on a dislocation element of length $d\lambda$. A sketchy proof of this theorem has previously been given by Lothe [1] for the special case of normal incidence. In this paper a complete proof will be given. The proof involves use of a somewhat generalized version of the energy flow theorem for straight dislocations (Lothe [2]). Generalization of the energy flow theorem is considered in the first part of this paper.

The above image law (3) and similar laws for the forces on the branches of dislocation bends (Lothe [3]) or dislocation nodes (Indenbom and Orlov [4]) can be used for a discussion of the validity of the concept of line tension in some of the simplest applications. However, in all of these laws only purely elastic terms are considered. This paper concludes with a discussion, in which the effect of core energy terms is also considered.

II. Generalized Energy Flow Theorem

Consider an infinite straight dislocation in the x - z plane and parallel with the z -axis. When the dislocation is moved a distance δx in the negative direction as indicated in figure 2, the displacements at a given point change by $(\partial u_i / \partial x) \delta x$. Thus, an energy $P \delta x$, where

$$P = \int \sigma_{zi} (\partial u_i / \partial x) dS_z + \int \sigma_{xi} (\partial u_i / \partial x) dS_x + \int \sigma_{yi} (\partial u_i / \partial y) dS_y \quad (4)$$

will be transmitted through a plane cutting the dislocation. The transmission factor P for that part of the plane which is between two cylinders of radii r_1 and r_2 coaxial about the dislocation, can be written in the form

$$P = p \log (r_2/r_1) \quad (5)$$

where the prelogarithmic factor p is independent of r_1 and r_2 .

It will be shown that

$$p = E \tan \alpha - \partial E / \partial \theta. \quad (6)$$

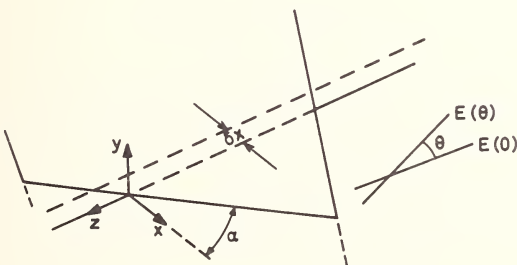


FIGURE 2. α is the angle between the x -axis and the intersection line between the x - z plane and the intersecting plane.

Here α is the angle between the x -axis and the line of intersection between the x - z plane and the intersecting plane. See figure 2. The energy flow theorem (6) has previously been proved by Lothe [2] for the special case of an intersecting plane normal to the dislocation, $\alpha=0$.

Consider first the last term in (4),

$$P_y = p_y \log (r_2/r_1) = \int_S \sigma_{yi} (\partial u_i / \partial x) dS_y. \quad (7)$$

Now,

$$dS_y \cos \psi_3 = dS_z \cos \psi_2, \quad (8)$$

where $\cos \psi_i$ are the direction cosines for the normal of the intersecting plane. In the z -projection the cross-section S is bounded by two circles. Thus

$$p_y \cos \psi_3 = r \cos \psi_2 \int_0^{2\pi} \sigma_{yi} (\partial u_i / \partial x) r d\phi \quad (9)$$

where in the integral r is constant. See figure 3. Now, since generally $\sigma_{ij} = r^{-1} \alpha_{ij}(\phi)$ and $(\partial u_i / \partial x_j) = r^{-1} \beta_{ij}(\phi)$, where $\alpha_{ij}(\phi + \pi) = -\alpha_{ij}(\phi)$ and $\beta_{ij}(\phi + \pi) = -\beta_{ij}(\phi)$, (9) can be written in the form

$$p_y \cos \psi_3 = 2y \cos \psi_2 \int_{-\infty}^{+\infty} \sigma_{yi} (\partial u_i / \partial x) dx \quad (10)$$

where the integral is along the L_y line parallel with the x -axis, figure 3.

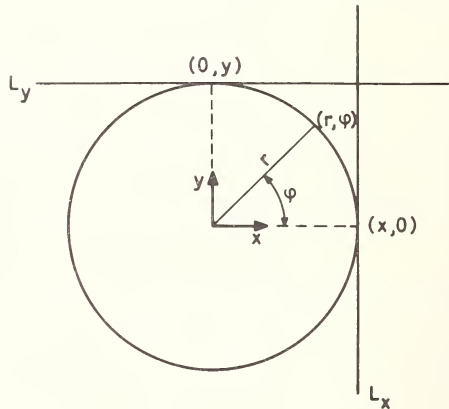


FIGURE 3. z -projection of the cross-section

It is clear that

$$-\delta x \int_{-\infty}^{+\infty} \sigma_{yi} (\partial u_i / \partial x) dx$$

is the energy per unit length of dislocation transmitted through an infinite plane parallel with the x - z plane when the dislocation moves by δx .

If the integral is different from zero, it will depend on y as y^{-1} . But this would imply that the energy per unit length in a slab parallel with the dislocation changes with a displacement of the dislocation parallel with the slab, because of nonzero divergence $\partial y^{-1}/\partial y \sim y^{-2}$, and this is a contradictory conclusion. Consequently the integral is zero, so that

$$p_y = 0. \quad (11)$$

For p_x the equation similar to (10) is

$$p_x \cos \psi_3 = 2x \cos \psi_1 \int_{-\infty}^{+\infty} \sigma_{xi} (\partial u_i / \partial x) dy, \quad (12)$$

where the integral is now along L_x .

The energy factor E need not be defined by a circular integral as implied in the definition (1). Using the same technique as in going from (9) to (10), one sees that the energy factor E can also be defined by the relation

$$d(W/L) = (E/2x) dx, \quad (13)$$

for the energy per unit length in a slab of thickness dx parallel with the y - z plane and a distance x from the dislocation.

It follows from (12) that $-p_x \cos \psi_3 \delta x / 2 \cos \psi_1 x$ is the energy per unit length transmitted through an infinite plane parallel with the y - z plane when the dislocation moves by δx . The divergence of this energy transmission must correspond to the change of energy in a slab along this plane. $-\delta x \partial(E/2x) / \partial x$. Thus

$$-(\partial/\partial x)(p_x \cos \psi_3 / 2 \cos \psi_1 x) = -(\partial/\partial x)(E/2x) \quad (14)$$

or

$$p_x = E \tan \alpha, \quad (15)$$

since geometrically $\tan \alpha = \cos \psi_1 / \cos \psi_3$.

The first term in (6) is now established. Lothe [2] has previously proved that

$$p_z = -\partial E / \partial \theta. \quad (16)$$

III. The Image Force on Dislocations at Free Surfaces

Consider a straight dislocation ending at a planar free surface S , figure 4. α is the angle between the x -axis and the intersection line between the surface and the $x-z$ plane. It will be shown that forces with a component

$$dF = \lambda^{-1}(E \tan \alpha - \partial E / \partial \theta) d\lambda \quad (17)$$

in the $x-z$ plane act on the dislocation.

Forces act on the dislocation in so far as the stresses along the dislocation are different from those characteristic of the infinite straight dislocation. It follows that if external forces $\sigma^d dS$ are applied to the surface S , where σ^d is the stress tensor characteristic of the infinite straight dislocation, no forces act on the dislocation. When such external forces are present, the displacements will also be the characteristics dislocation displacements \mathbf{u}^d . Next superpose additional external forces $\sigma^r dS$ such that

$$\sigma^r dS = -\sigma^d dS. \quad (18)$$

A free surface then results. The forces $\sigma^r dS$ will give rise to additional stresses σ^r in the medium and additional displacements \mathbf{u}^r . The forces on the dislocation are due to σ^r . Define σ^r as

$$\sigma^r = \mathbf{b}(\sigma^r \mathbf{j})/b. \quad (19)$$

Then the force dF on the element $d\lambda$ is

$$dF = \sigma^r b d\lambda. \quad (20)$$

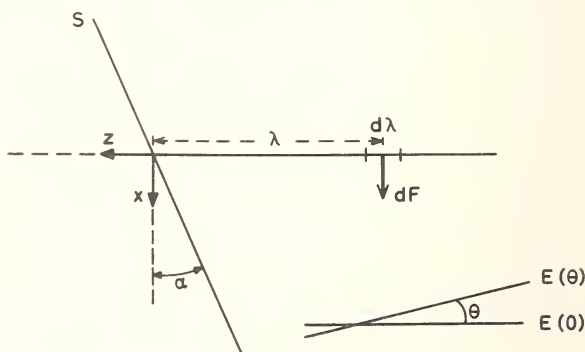


FIGURE 4. Dislocation at free surface. A force dF acts on the element $d\lambda$.

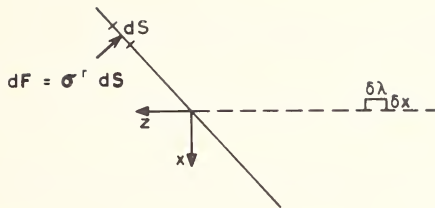


FIGURE 5. A dislocation loop $\delta x\delta\lambda$ in a half infinite medium.

Consider figure 5, a half infinite medium like in figure 4, but without dislocation and only with external forces $\sigma^r d\mathbf{S}$ applied at the surface. If a small loop $\delta x\delta\lambda$ is formed, it will give rise to displacements $\delta\mathbf{u}$ at the surface. According to the general principle that the work done against σ^r equals the work done on the external mechanism maintaining σ^r (Eshelby [5]) one can write

$$\int_S \delta\mathbf{u} (\sigma^r d\mathbf{S}) = -\sigma^r b \delta x \delta\lambda. \quad (21)$$

The problem of determining σ^r in (20) would thus be solved if the integral in (21) could be determined.

By superposition, the displacement field $\delta\mathbf{u}$ due to a small loop is the same as that due to a corresponding bulge on a dislocation.

Let $\delta\mathbf{u}^d$ be the displacements due to a pair of bulges (say pair *A* in fig. 6) on an *infinite* straight dislocation in an *infinite* medium. $\delta\mathbf{u}^d$ is

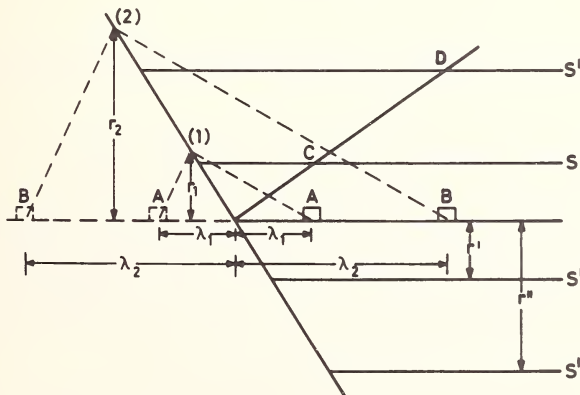


FIGURE 6. The orientation of point (1) relative to the pair of bulges *A* is equivalent to the orientation of point (2) relative to the pair of bulges *B*. Image stresses at *C* and *D* are equivalent.

different from the $\delta\mathbf{u}$ due to *one* bulge under a *free* surface, and we define the relaxation $\delta\mathbf{u}^r$ so that

$$\delta\mathbf{u} = \delta\mathbf{u}^d + \delta\mathbf{u}^r. \quad (22)$$

It is now convenient to define functions \mathbf{v} so that in the surface S

$$\delta\mathbf{u} = \mathbf{v}\delta x\delta\lambda, \quad (23a)$$

$$\delta\mathbf{u}^d = \mathbf{v}^d\delta x\delta\lambda, \quad (23b)$$

and

$$\delta\mathbf{u}^r = \mathbf{v}^r\delta x\delta\lambda. \quad (23c)$$

Equation (21) can then be written as

$$\sigma^{rb} = \int_S \mathbf{v}^d(\boldsymbol{\sigma}^d dS) - \int_S \mathbf{v}^r(\boldsymbol{\sigma}^r dS) \quad (24)$$

when (18) is used.

Since a stiff forward displacement δx of the dislocation can be considered as due to bulges along the entire dislocation, it follows that

$$\partial\mathbf{u}/\partial x - (\partial\mathbf{u}/\partial z) \tan \alpha = \int_0^\infty \mathbf{v} d\lambda, \quad (25a)$$

$$\partial\mathbf{u}^d/\partial x = \int_0^\infty \mathbf{v}^d d\lambda, \quad (25b)$$

$$\text{and } \partial\mathbf{u}^r/\partial x - (\partial\mathbf{u}^r/\partial z) \tan \alpha = \int_0^\infty \mathbf{v}^r d\lambda, \quad (25c)$$

where the left-hand side quantities are surface values.

The pair of bulges *A*, figure 6, will give rise to displacements at (1) equivalent to those at (2) due to the pair *B*. The coordinates $(r/\lambda, \phi)$ are the same for the two cases. ϕ is the angle between the axial plane considered and the $x-z$ plane. By dimensional considerations one can show that the displacements will be in the ratio r_1^{-2}/r_2^{-2} . Thus, one may write

$$\mathbf{v}^d = r^{-2} \mathbf{g}^d(r/\lambda, \phi). \quad (26a)$$

Similarly

$$\mathbf{v} = r^{-2} \mathbf{g}(r/\lambda, \phi) \quad (26b)$$

and

$$\mathbf{v}^r = r^{-2} \mathbf{g}^r(r/\lambda, \phi). \quad (26c)$$

Further, it will be convenient to introduce a function $\mathbf{f}^d(\phi)$ so that in the surface

$$\boldsymbol{\sigma}^d \mathbf{n} = -\boldsymbol{\sigma}^r \mathbf{n} = r^{-1} \mathbf{f}^d(\phi). \quad (27)$$

\mathbf{n} is surface normal.

The first term in (24) can now readily be connected with the energy flow theorem (6), which we write in the form

$$\int_0^{2\pi} (\boldsymbol{\sigma}^d \mathbf{n}) (\partial \mathbf{u}^d / \partial x) d\phi = \cos \psi_3 r^{-2} [E \tan \alpha - \partial E / \partial \theta]. \quad (28)$$

By (25b), (26a), and (27) and with introduction of the dimensionless variable $\xi = r/\lambda$, (28) becomes

$$E \tan \alpha - \partial E / \partial \theta = (\cos \psi_3)^{-1} \int_0^{2\pi} \int_0^\infty \xi^{-2} \mathbf{f}^d(\phi) \mathbf{g}^d(\xi, \phi) d\phi d\xi. \quad (29)$$

With the same substitutions, the first term in (24) becomes

$$\begin{aligned} \int_S \mathbf{v}^d (\boldsymbol{\sigma}^d dS) &= (\cos \psi_3)^{-1} \int_0^{2\pi} \int_0^\infty r^{-2} \mathbf{f}^d(\phi) \mathbf{g}^d(r/\lambda, \phi) d\phi dr \\ &= \lambda^{-1} (\cos \psi_3)^{-1} \int_0^{2\pi} \int_0^\infty \xi^{-2} \mathbf{f}^d(\phi) \mathbf{g}^d(\xi, \phi) d\phi d\xi \end{aligned} \quad (30)$$

So, by comparison between (30) and (29),

$$\int_S \mathbf{v}^d (\boldsymbol{\sigma}^d dS) = \lambda^{-1} (E \tan \alpha - \partial E / \partial \theta). \quad (31)$$

The last term in (24) can be shown to be zero. Since \mathbf{u}^r is single-valued, the conservation theorem (see Eshelby [5])

$$\int_{\Sigma} \mathbf{T} d\mathbf{S} = 0, \quad (32)$$

where

$$T_{ij} = w \delta_{ij} - \sigma_{jm} \partial u_m / \partial x_i \quad (33)$$

can be used for a region bounded by a closed surface Σ . w is energy

density. Combining x and z components of (32), one may write

$$\int_{\Sigma} (\partial \mathbf{u}^r / \partial x - \tan \alpha \partial \mathbf{u}^r / \partial z) (\boldsymbol{\sigma}^r d\mathbf{S}) = \int_{\Sigma} w^r (dS_x - \tan \alpha dS_z). \quad (34)$$

Equation (34) can be applied to the surface consisting of two cylinders coaxial with the dislocation and the section of the free surface between the cylinders, figure 6. The integrals over the two cylindrical surfaces S' and S'' will exactly cancel. Stresses $\boldsymbol{\sigma}^r$ at equivalent points C and D differ only in strength and will be in the ratio $(r')^{-1}/(r'')^{-1}$. Thus w^r at the two points will be in the ratio $(r')^{-2}/(r'')^{-2}$, and similar for the other terms in (34). Corresponding surface elements will be in the ratio $(r')^2/(r'')^2$. Corresponding surface normals are oppositely directed.

On the free surface section, $dS_x = \tan \alpha dS_z$, and the righthand side of (34) vanishes.

It follows then that the lefthand side integral of (34) over the free surface section is zero, or,

$$\int_2^{2\pi} (\boldsymbol{\sigma}^r \mathbf{n}) (\partial \mathbf{u}^r / \partial x - \tan \alpha \partial \mathbf{u}^r / \partial z) d\phi = 0. \quad (35)$$

where the integral is along the elliptic intersection between a cylinder of radius r and the free surface. Comparing (35) with the last term in (24) in the same way as (28) was compared with the first term in (24), it follows that

$$\int_S \mathbf{v}^r (\boldsymbol{\sigma}^r d\mathbf{S}) = 0. \quad (36)$$

Equations (24), (31), and (36) prove the image force theorem (17).

IV. Discussion. Comments on the Concept of Line Tension

For simplicity consider the equilibrium of a glide dislocation emerging at a free surface when only motion in the glide plane is allowed, figure 7a. By simple line tension arguments such as outlined in the introduction, the equilibrium inclination is determined by the condition

$$E \tan \alpha - \partial E / \partial \theta = 0, \quad (37)$$

and indeed, according to the image law (17), exact in the approximation of linear elasticity, no forces act on the dislocation when it is in this orientation and it can be truly straight in this orientation. However, core terms should also be considered. Roughly representing the core terms by a

constant orientation-independent core energy, one concludes that the core terms will tend to align the dislocation normal to the surface. However, the overall orientation cannot change. If it did, long range image forces, (17), will swing the dislocation back. The only possibility is an asymptotic orientation agreeing with (37) and some curvature very near the surface so that the orientation locally, at the surface, is a compromise between elastic terms and core terms, figure 7b.

The effect of the core cannot be completely taken into account as just a line tension contribution. Core terms should strictly be considered in σ_d and hence in the force distribution $\sigma^r dS$ of (18). Thus, the core terms will contribute to the image stresses and lead to deviations from (17). However, as far as long range effects are concerned, the effect of core terms can at most (depending on the model) amount to the equivalent of an external point force applied at the point of emergence, and this would give stresses decaying as λ^{-2} along the dislocation. It remains true, then, that (17) is the correct long-range term, and that core effects only can cause some curvature and alter the inclination very near the surface.

The problem of node equilibrium is somewhat more complicated. Fulfillment of simple line tension criteria for equilibrium does not assure

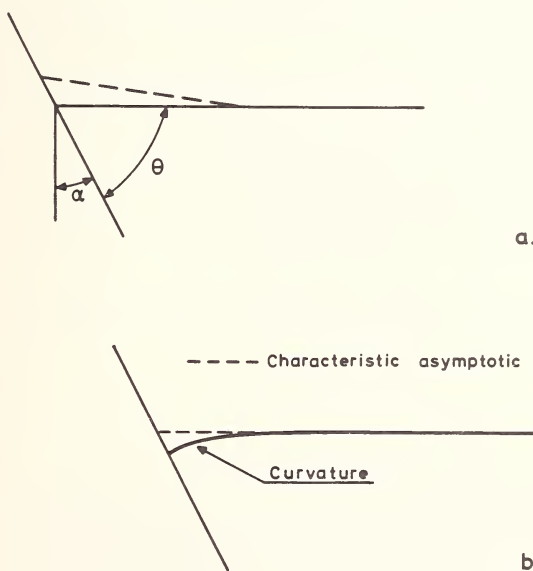


FIGURE 7. (a) Dislocation at free surface. Virtual displacement is indicated. (b) Near the surface, the dislocation will be curved. The stapled line gives the asymptotic orientation.

absence of long range elastic forces on the branches (Indenbom and Dubnova [6], Sætre [7], Indenbom and Orlov [4]). In general, forces

will be present which tend to rotate the node. Only for certain orientations of the branches are the forces absent so that the branches can be truly straight in the approximation that only elastic terms are considered. It is convenient to call such a node an equilibrium node. The line tension criterion is a necessary but not sufficient criterion for equilibrium (Indenbom and Orlov [4]).

For the characteristic equilibrium nodes, the elastic forces balance. However, if the core terms do not independently balance for the same orientation of the branches, the branches must be curved very near the node so that the core terms are given some relaxation.

Rough estimates indicate that local curvature and orientations different from the characteristic asymptotic orientations should not be appreciable (say 5° deviation) beyond $\sim 50b$ from the nodal point or from the point of emergence.

V. References

- [1] Lothe, J., *Physica Norvegica* **2**, 153 (1967).
- [2] Lothe, J., *Phil. Mag.* **15**, 9 (1967).
- [3] Lothe, J., *Phil. Mag.* **15**, 353 (1967).
- [4] Indenbom, V. L., and Orlov, S. S., *Sovj. Physics (Crystallography)* **12**, 849 (1968).
- [5] Eshelby, J. D., in *Solid State Physics* **3**; F. Seitz and D. Turnbull, Eds. (Academic Press, New York, 1956) p. 99 and p. 105.
- [6] Indenbom, V. L., and Dubnova, G. N., *Sovj. Physics (Solid State)* **9**, 915 (1967).
- [7] Sætre, T., Master's Thesis, Univ. of Oslo (1967).

STABILITY AND SOME CHARACTERISTICS OF UNIFORMLY MOVING DISLOCATIONS

K. Malén

*AB Atomenergi
Studsvik, Sweden*

The stability of uniformly moving dislocations has been studied in the case of elastic anisotropy using computer. The velocity for instability to occur for a screw dislocation in an isotropic medium is so high, $0.98 C_t$, with C_t the transverse sound velocity, that it may well be unattainable. Inclusion of anisotropy gives the possibility of more reasonable instability velocities. Some data showing this for Fe, Li and Cr are given.

The stress field around a uniformly moving dislocation has been studied. Increasing the velocity of a dislocation corresponds to some extent to a change in the anisotropy of the crystal.

In uniform motion above the lowest velocity of sound in the direction of motion one can have associated with the moving dislocation 2, 4 or 6 Cerenkov waves, above the next sound velocity 4 or 6 and above the highest sound velocity 6 waves.

The formula developed earlier for the stress field around a uniformly moving planar dislocation loop can be generalized directly to three dimensions using the theorems of Indenbom and Orlov for the fields from three-dimensional sources using data for two-dimensional sources.

The generalization can also be made using the fact that the choice of cut surface is arbitrary.

Key words: Anisotropic elasticity; Cerenkov waves; dislocation dynamics; dislocation stability.

I. Introduction

As found by Beltz et al. [1], instability can occur for a straight screw dislocation in uniform motion in an isotropic medium. Since the velocity at which this happens is very high a computer study has been made of the effects of anisotropy. In the latter case instability can occur at more reasonable velocities. In this connexion the stability criterion is examined (cf. Indenbom and Orlov [2]). An obvious extension to an expression for

Fundamental Aspects of Dislocation Theory, J. A. Simmons, R. de Wit, and R. Bullough, Eds. (Nat. Bur. Stand. (U.S.), Spec. Publ. 317, I, 1970).

the stress field around a curved nonplanar dislocation loop in uniform motion is closely related to the stability criterion, cf. [1, 2]. A study is made of complications in Čerenkov wave creation at a uniformly moving straight dislocation due to elastic anisotropy.

II. Stability Criterion

A recent analysis of the stability criterion for a static dislocation bend is given by Indenbom and Orlov [2]. This stability criterion is derived by Lothe [3], by studying the restoring force on a bent dislocation for a bend with angle $(\pi - \theta)$ (fig. 1). λ , θ , and dl are defined in figure 1.

$$dF = \lambda^{-1} \left(\frac{E(0)}{\sin \theta} - \frac{E(\theta)}{\tan \theta} + \frac{\partial E(\theta)}{\partial \theta} \right) dl = 0. \quad (1)$$

$E(\theta)$ is the energy factor defined through the elastic energy $W(\theta)$ per unit dislocation length in a cylindrical annulus with inner radius r_1 and outer radius r_2 around a straight dislocation with the direction determined by θ .

$$W(\theta) = E(\theta) \ln (r_2/r_1).$$

In the limit of a straight dislocation this gives, for stability,

$$dF = \frac{\theta}{2\lambda} (E(0) + E''(0)) dl \geq 0. \quad (2)$$

This criterion is thus the same as that for zero or positive line tension. As Indenbom and Orlov have shown [2], a plot $(E(\theta))^{-1}$ as a function of angle can be used to graphically construct dF in these eqs (1) and (2).

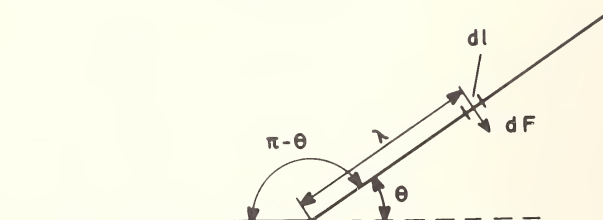


FIGURE 1. Force on a dislocation bend.

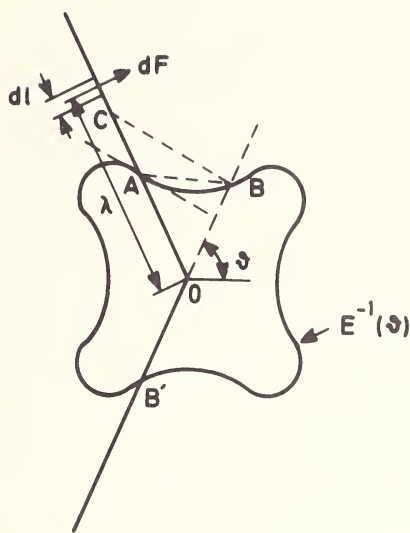


FIGURE 2. Construction of the force (dF) on a dislocation bend

$$\lambda \cdot \frac{dF}{dl} = \frac{OA - OC}{S_{AOB}},$$

where S_{AOB} is the area of AOB . The figure shows an unstable dislocation bend.

(fig. 2). Points with a common tangent correspond to a possible bent configuration (cf. Head [4]). Some consideration also shows that equation (2), with an equality sign, describes a flat portion of the curve and that a convex part of the curve defines a stable direction and a concave one an unstable (fig. 2) [4]. It is also clear that points with a common tangent giving real stability are on two convex parts of the curve and other such combinations are metastable.

III. Instability of Dislocations in Uniform Motion

As shown by Beltz et al. [1], the stability criterion for a bent and a straight dislocation in uniform motion is found from the criterion for the static case by replacing $E(\theta)$ by $L(\theta)$, where the Lagrangian factor L is defined as $L = E - T$ with E = total energy factor and T = kinetic energy factor. The criterion

$$L(\theta) + L''(\theta) \geq 0 \quad (3)$$

has been examined for anisotropic media.

Beltz et al. [1] showed that a screw dislocation with velocity v in an isotropic medium becomes unstable at $v \approx 0.98C_t$ for $0 < \nu < 0.5$, where C_t is the transverse sound velocity and ν is Poisson's ratio.

It is known (e.g., Head [4]) that, in anisotropic media, dislocations can be unstable already at zero velocity. For $v = 0.98C_t$, resistance to the motion might make the velocity unattainable, cf. Rogula [5, 6].

For an edge dislocation (i.e. $\bar{b} = \frac{b_0}{\sqrt{3}} [11\bar{1}]$ in Fe lying along [112] in the $(\bar{1}10)$ plane, and moving in the $[11\bar{1}]$ direction, the critical velocity is found to be $v \approx 0.80C_t$ with $C_t = (C_{55}/\rho)^{1/2}$ ($= 2975$ m/s) the appropriate shear sound velocity for this direction. ρ is the density. The interaction of two edge dislocations in the same slip plane changes sign at a higher velocity ($v \approx 0.92C_t$). A screw dislocation (i.e., $\bar{b} = \frac{b_0}{\sqrt{6}} [112]$) under the same conditions as above is stable at all velocities below C_t . The critical velocity above which Čerenkov waves are created is $v \approx 0.95C_t$. (See table 1.)

TABLE 1. *Velocities for instability (zero line tension) and velocities for change of sign of the interaction between like dislocations in the same slip plane (zero Lagrangian) as well as the limiting velocity. The dislocation is along [112] and moving in the $[11\bar{1}]$ direction. Materials studied are Fe, Li, and Cr.*

Material	Velocity (v/C_t) for zero line tension		Velocity (v/C_t) for zero Lagrangian		Limiting velocity (v/C_t)	A	H [10^{11} dyn cm $^{-2}$]
	Edge	Screw	Edge	Screw			
Fe $C_t = 2975$ m/s	0.80	stable	0.922	> 0.93	0.948	2.36	12.9
Li $C_t = 2860$ m/s	0.50	0.65	¹ 0.803	¹ 0.794	¹ 0.808	9.4	1.93
Cr $C_t = 4300$ m/s	stable	0.90	0.87	> 0.95	0.97	0.69	-10.0

¹ Teutonico [7] gives for zero Lagrangian $v/C_t = 0.804$ for an edge and $v/C_t = 0.794$ for a screw

He also gives the limiting velocity $v/C_t = 0.809$

$$A = 2C_{44}(C_{11} - C_{12})^{-1}; \quad H = 2C_{44} + C_{12} - C_{11}.$$

In Li, which has a very high anisotropy coefficient,

$$A = 9.4 \quad (A = 2C_{44}/(C_{11} - C_{12}) \quad A \text{ for Fe} = 2.36),$$

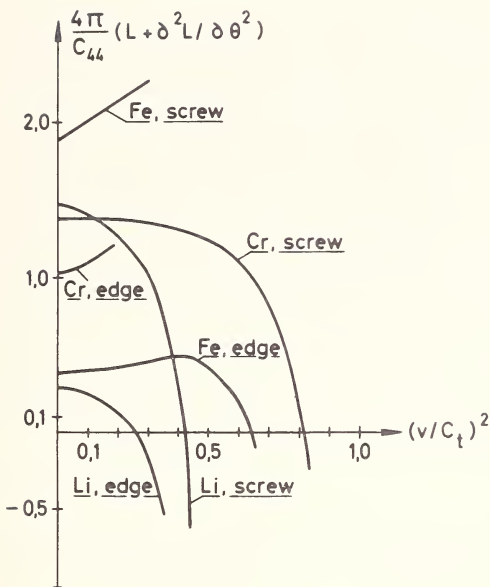


FIGURE 3. Line tension for edge and screw dislocations in Fe, Li and Cr. The dislocations are along [112] and are moving in the [111] direction.

the effect is still more pronounced. Edge dislocations (as above) become unstable at $v \approx 0.50C_t$, and screw dislocations become unstable at $v \approx 0.65C_t$ ($C_t = 2860$ m/s). The interaction of edge dislocations moving in the same slip plane changes sign at $v \approx 0.80C_t$ and for screw dislocations the interaction changes sign at $v \approx 0.79C_t$, i.e., before the edge. The critical velocity for Čerenkov wave creation is $v \approx 0.81C_t$. These three last data agree with the data found by Teutonico [7] and are thus a check of the computer program.

It is interesting that, contrary to the behaviour for isotropic media, the instability velocity is lower in these cases than the velocity for the change of sign of the interaction between like dislocations in the same slip plane.

For Cr, which has an anisotropy coefficient smaller than 1, ($A = 0.69$) one finds for the special direction chosen (direction [112] and motion in the $[1\bar{1}\bar{1}]$ direction) that the edge dislocation is stable for all velocities and that the screw dislocation becomes unstable at $v \approx 0.90C_t$ ($C_t = 4300$ m/s). Data for Fe, Li and Cr are collected in Table 1 and in figure 3.

IV. Stress Field Around a Uniformly Moving Straight Dislocation

It is a well-known fact that anisotropy can change the general character of the stress field around a dislocation, e.g., Lie and Koehler [8] or Chou [9]. This can be said to be due to higher order terms becoming more important as anisotropy increases [8].

The same effect of course arises when one increases the velocity of a dislocation (see fig. 4). The motion increases the effect of higher order terms. In particular, one notices that stresses change considerably in the region where a Čerenkov wave appears at higher velocities. This is the same behaviour as for the isotropic case where the stresses are most affected around the plane $x=0$ in motion along the x -axis with the dislocation along the z -axis. The plane $x=0$ is where a Čerenkov wave appears as the dislocation attains the transverse sound velocity. In the anisotropic case this need not be this plane, but can be any plane containing the z -axis depending on the elastic constants.

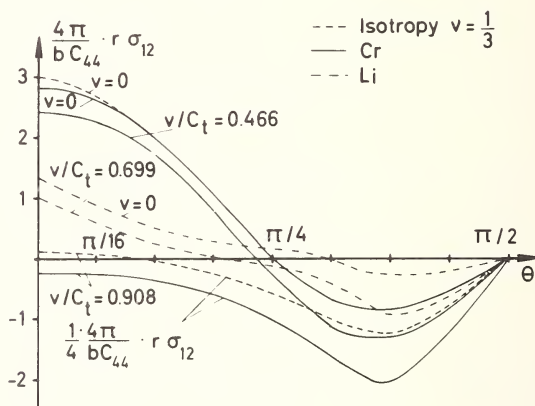


FIGURE 4. Stress field (σ_{12}) around an edge dislocation in uniform motion in Cr, Li and an isotropic medium. The dislocations are along [112] and are moving in the $[1\bar{1}\bar{1}]$ direction.

The change of character of the stress field noticed by Chou [9] on changing the degree of anisotropy is also found as the velocity increases. This is not surprising, as the effect of increasing the velocity is to make the roots of the sixth-order equation determining the properties of the medium more and more real, i.e., making the imaginary part go to zero. The same thing happens as Chou changes his parameter C toward -4 . $C+4=0$ implies real roots.

V. Possible Čerenkov Waves During Supersonic Motion

Supersonic motion in the isotropic case gives rise to new Čerenkov waves only as one increases the velocity past a sound velocity. (See, e.g., Stroh [10]). Thus, at sufficiently high velocities (above the highest sound velocity) six waves are developed. In an anisotropic medium there is possibility for a more complicated behaviour.

Mathematically the situation can be analyzed by considering the slowness surface in the y_1y_2 -plane for cylindrical waves with the dislocation direction as axis (y_3). The equation for this surface which is used in the theory of wave propagation in anisotropic elastic media, is (e.g., Stroh [10])

$$\|C_{i1k1}y_1^2 - (C_{i1k2} + C_{i2k1})y_1y_2 + C_{i2k2}y_2^2 - \rho\delta_{ik}\| = 0, \quad (4)$$

where C_{ijkl} are the elastic constants for the medium and ρ the density. The criterion for development of a Čerenkov wave at a dislocation is that there is a real root (p) to the equation

$$\|C_{i1k1} + p(C_{i1k2} + C_{i2k1}) + p^2C_{i2k2} - \rho v^2\delta_{ik}\| = 0 \quad (5)$$

(v is the dislocation velocity).

We see that setting

$$y_1 = v^{-1}$$

$$y_2 = -pv^{-1}$$

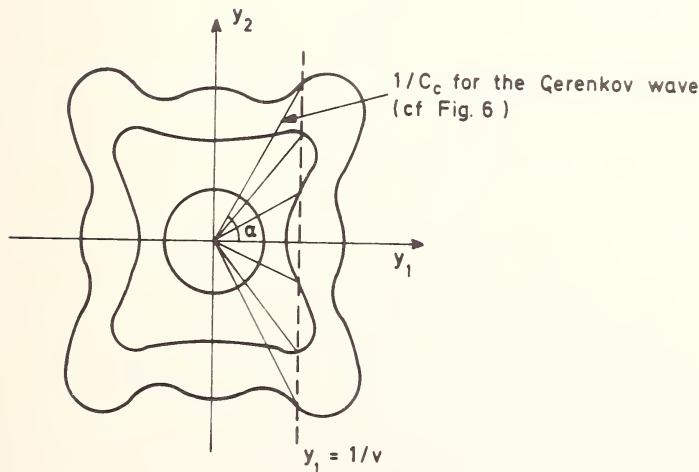


FIGURE 5. Possible slowness surface. The intersection with the line $y_1 = 1/v$ defines the Čerenkov waves accompanying a dislocation moving in the x_1 -direction at velocity v .

makes the two equations equivalent and a study of the first one (4) gives information about the solutions to the second one (5). The surface (4) (a cylinder with generators parallel to the y_3 -axis) is a sextic surface in the space y_i consisting of three closed sheets. Thus the form can be as in figure 5 (See e.g.. Duff [11]). The plane

$$y_1 = v^{-1}$$

thus cuts the curves for $v=0$ at no point, but as v is increased one starts to cut the outer surface and there one can get 2, 4 (!) or 6(!) cuts and thus real roots ($p=-y_2/y_1$) (at tangency there is a double root). Thus, at any velocity above the lowest velocity for Čerenkov wave creation one can have 2, 4, or 6 waves. When one has started to cut the next sheet the possibility is 4 or 6 and cutting the innermost sheet (i.e., at sufficiently high velocity) leaves the possibility of 6 waves only.

This use of the slowness surface to give information on Čerenkov waves is of course easily explained in physical terms—and gives the same criterion as is usual for Čerenkov waves. Anisotropy simply complicates matters somewhat.

The radius vector to the slowness surface represents a possible wave normal in the medium with the inverse length representing the phase velocity (fig. 6a). Figure 6b shows the normal construction of the wave front for a Čerenkov wave. Comparing $\cos \alpha = C_c/v$ shows that the criteria indeed are equivalent.

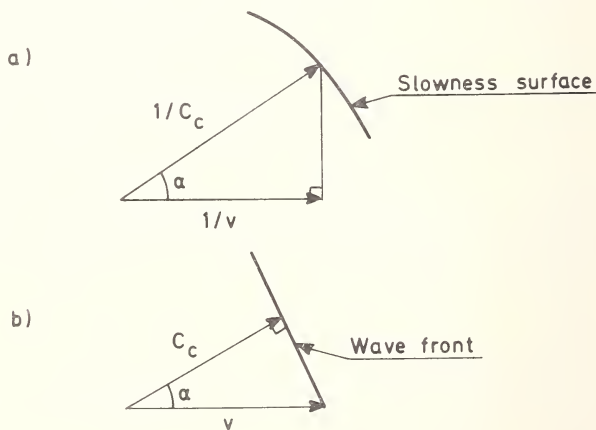


FIGURE 6. Comparison of Čerenkov wave velocity C_c constructed from
 a) slowness surface
 b) wave front
 $\cos \alpha = (1/C_c)/(1/v) = C_{c/r}$
 The two methods of construction are equivalent.

VI. Formula for the Stress Field Around a Curved Three-Dimensional Loop in Uniform Motion in Terms of Data for a Straight Dislocation

It is worth mentioning here that the formula developed by Beltz et al. [1] for the stress field around a uniformly moving curved dislocation in terms of data for a straight dislocation also applies to a three-dimensional loop (the proof in [1] applies only to a planar loop moving in its slip plane). The extension to three dimensions follows immediately from the proof of the general three-dimensional theorem given by Indenbom and Orlov [2]. The important thing for the proof is that the field drops off as r^{-1} . In the case of uniform motion this still holds if one replaces r by

$$\mathbf{r}^x = \sqrt{(x - v_x t)^2 + (y - v_y t)^2 + (z - v_z t)^2}$$

and use of appropriate data for uniformly moving dislocations (cf. [1]) gives a formula similar to the one for the static case.

The three-dimensional relationship can also be deduced directly from the expression for a planar loop. In the static case it is well-known that the cut surface defining the dislocation can be chosen at will as long as it is spanned by the dislocation loop, when one is interested in the stress and strain fields. One can thus divide a loop into infinitesimal planar loops as in figure 7 and use the theorem for planar loops. The field point must lie on all these loop planes and must thus be at P in figure 7. As the cut surface can be chosen at will this gives no restriction to the possible

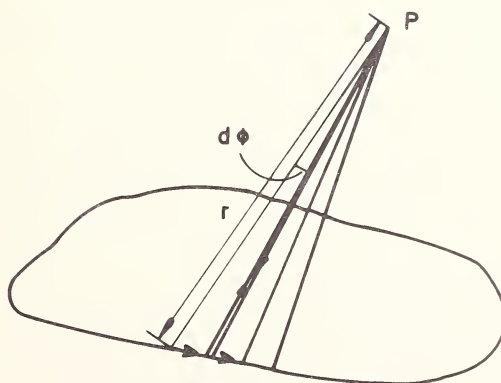


FIGURE 7. Use of infinitesimal loops to construct the stress and strain fields around a three-dimensional loop from Brown-Lothe's theorem for a planar loop [13, 3]. P is the field point. A new surface is needed for every point P .

field points. The loop sides connecting the original loop with the field point P sum up to give zero net contribution and one is left with an integral around the original dislocation loop

$$\sigma = \oint (\Sigma + \partial^2 \Sigma / \partial \phi^2) r^{-1} d\phi \quad (6)$$

where Σ is chosen as in the planar case.

In uniform motion the same argument holds as in the static case. This can for instance be seen through the possibility of transforming the surface integral describing the strain field into a line integral over the dislocation loop. (This is shown in general by Mura [12].) This line integral can then be transformed by Stokes theorem into a surface integral over an arbitrary surface spanned by the loop. In general this has to be done for every moment of the dislocation motion. In uniform motion one can, however, choose the same shape for the whole motion. It is thus possible to study the field at a point moving with the dislocation using the method described above as in the static case.

VII. Summary

The stability criterion for a uniformly moving straight dislocation is that the polar plot of $L^{-1}(\theta)$ should be convex, which is equivalent to the criterion

$$L(\theta) + \partial^2 L(\theta) / \partial \theta^2 > 0. \quad (7)$$

This corresponds to a similar relationship in the static case with $E(\theta)$ instead of $L(\theta)$.

This criterion used on a uniformly moving dislocation in an anisotropic medium shows that instability can be introduced at more reasonable velocities than in the isotropic case [1].

A relationship given by Indenbom and Orlov [2] has been used to derive an expression for the stress field around a uniformly moving nonplanar dislocation loop in terms of data for straight dislocations. A simple proof based on [1] and on the possibility of deforming the surface spanned by a loop when calculating the stress or strain field might throw more light on the relations in [2].

The change of the stress field around a straight dislocation on increasing its velocity is to some extent similar to the changes one finds on varying the degree of anisotropy observed by Chou [9].

Çerenkov wave creation is shown to exhibit a more complicated behaviour when anisotropy is introduced. The appearance of six simultaneous wave fronts at the lowest critical velocity for Çerenkov wave creation is possible.

VIII. Acknowledgement

The author thanks AB Atomenergi for permission to publish this paper.

IX. References

- [1] Beltz, R. J., Davis, T. L., Malén, K., Phys. Status Solidi **26**, 621 (1968).
- [2] Indenbom, V. L., Orlov, S. S., Soviet Phys.-Cryst. **12**, 849 (1968).
- [3] Lothe, J., Phil. Mag. **15**, 353 (1967).
- [4] Head, A. K., Phys. Status Solidi **19**, 185 (1967).
- [5] Rogula, D., Bull. Acad. Polon. Sci., Ser. Sci. Tech. **13**, 337 (1965).
- [6] Rogula, D., Bull. Acad. Polon. Sci., Ser. Sci. Tech. **14**, 159 (1966).
- [7] Teutonico, L. J., Phys. Rev. **127**, 413 (1962).
- [8] Lie, K-H. C., Koehler, J. S., Advan. Phys. **17**, 421 (1968).
- [9] Chou, Y. T., J. Appl. Phys. **34**, 429 (1963).
- [10] Stroh, A. N., J. Math. Phys. **41**, 77 (1962).
- [11] Duff, G. F. D., Phil. Trans. Roy. Soc. London **A252**, 249 (1959/60).
- [12] Mura, T., Phil. Mag. **8**, 843 (1963).
- [13] Brown, L. M., Phil. Mag. **15**, 363 (1967).

THE DISLOCATION IN A SEMI-INFINITE ISOTROPIC MEDIUM

D. J. Bacon and P. P. Groves

Department of Metallurgy and Materials Science

*The University
Liverpool, England*

The displacement associated with an infinitesimal dislocation loop (displacement dipole) of arbitrary orientation in an isotropic, semi-infinite elastic medium has been obtained, and on integration this yields the displacement associated with a finite dislocation loop. The solution for the infinitesimal loop has been obtained by finding the relationship between point forces and displacement dipoles in an infinite medium, and using the same relations with Mindlin's solution for the point force in an elastic half-space. This approach leads to a rather simpler analysis than that of Steketee, and the expressions for the displacements of all the infinitesimal loops near a free surface are presented here for the first time. The solution is being used to study the stability of a prismatic dislocation loop on a glide prism of square cross-section near a free surface. Preliminary results are presented for the forces on the loop sides and changes in loop energy on rotation for the situation in which the Burgers vector is normal to the surface.

Key words: Dislocation loops; elasticity; finite bodies.

I. Introduction

A dislocation near the free surface of a crystal experiences forces induced by the presence of the surface which, if larger than the lattice frictional force opposing dislocation motion, can remove the dislocation from the crystal or change its shape and orientation. A good estimate of these forces can be obtained by using linear elasticity theory to evaluate the stress field of the dislocation, and in the present work this method is being used to investigate the stability of a prismatic dislocation loop near the free surface of a semi-infinite isotropic medium. This was prompted by a similar study [1] of the influence of a free surface on the edge dislocation dipole, where it was shown that the effects on the stability and equilibrium orientations can be significant.

Fundamental Aspects of Dislocation Theory, J. A. Simmons, R. de Wit, and R. Bullough, Eds. (Nat. Bur. Stand. (U.S.), Spec. Publ. 317, I, 1970).

In order to carry out the present investigation, it is necessary to obtain the stress field associated with a dislocation loop of arbitrary shape, orientation and Burgers vector in an elastic half-space. The method of Hankel transforms used by Baštecká [2] to determine the stress field of a circular loop with Burgers vector normal to the surface is not appropriate for a situation without cylindrical symmetry. We have used a method which, although analogous to the general procedure of Steketee [3], avoids the tedious integrations and analysis of his approach. Our method uses the fact that the elastic field of a finite dislocation loop can be determined by using infinitesimal loops, and that these may be constructed from certain combinations of point forces. We have therefore used the solution for the point force in half-space in order to provide a basic solution for the finite dislocation loop. The analysis is described in section II, where we describe how dislocations and point forces are related and then derive expressions for the displacements of an arbitrary infinitesimal loop near a free surface. As an example of the case of a prismatic dislocation loop near a free surface, we are considering a loop on a glide prism of square cross-section. For simplicity, the loop is being taken to be planar and rectangular in shape, and we are first studying the case when the Burgers vector is normal to the surface. Preliminary results are presented in section III. The results of the paper are discussed in section IV.

II. The Arbitrary Infinitesimal Loop in Half-Space

We introduce rectangular Cartesian reference axes with unit base vectors \mathbf{x}_i so that the coordinates x_i of the point with position vector \mathbf{x} are given by $\mathbf{x} = x_i \mathbf{x}_i$. (Repeated suffices imply summation; and later the convention $i \equiv \partial/\partial x_i$ is used). The displacement $\mathbf{u}(\mathbf{x}) = u_i(\mathbf{x}) \mathbf{x}_i$ at point \mathbf{x} due to a point force $\mathbf{F}(\mathbf{x}') = F_i(\mathbf{x}') \mathbf{x}_i$ acting at $\mathbf{x}' = x'_i \mathbf{x}_i$ has the components

$$u_i(\mathbf{x}) = U_{ij}(\mathbf{x} - \mathbf{x}') F_j(\mathbf{x}'), \quad (1)$$

where the $U_{ij}(\mathbf{x} - \mathbf{x}')$ are components of the tensor Green's function, which for an infinite isotropic medium are given by [4]

$$U_{ij}(\mathbf{x}) = Q [(3 - 4\nu) \delta_{ij}/x + x_i x_j/x^3], \quad (2)$$

where $Q = 1/16\pi\mu(1 - \nu)$, μ is the shear modulus and ν is Poisson's ratio. Consider now a dislocation line of arbitrary shape, orientation and Burgers vector $\mathbf{b} = b_i \mathbf{x}_i$, the sign of which is defined by the **FS/RH** convention. Following de Wit [4], it may be shown that the displacements at \mathbf{x} due to

such a dislocation are given by

$$u_i(\mathbf{x}) = b_j \int_S c_{jkmn} U_{mi,n}(\mathbf{x} - \mathbf{x}') dS'_k - \int_A u_j(\mathbf{x}') c_{jkmn} U_{mi,n'}(\mathbf{x} - \mathbf{x}') dA'_k, \quad (3)$$

where c_{jkmn} are components of the elastic stiffness tensor, S is the surface of the cut used to formally generate the dislocation, and A is the traction-free outer surface of the body. Thus, the displacements due to an infinitesimal loop ('displacement dipole') of area dS and normal components dS_k at the origin are

$$u_i(\mathbf{x}) = b_j dS_k c_{jkmn} U_{mi,n}(\mathbf{x}) - \int_A u_j(\mathbf{x}') c_{jkmn} U_{mi,n'}(\mathbf{x} - \mathbf{x}') dA'_k. \quad (4)$$

Here, the $u_j(\mathbf{x}')$ appearing in the integral make A traction free, but evaluation of the integral can be avoided as follows. We note that the integral vanishes for a medium of indefinite extent, so that for the case of isotropy for which $U_{ij}(\mathbf{x})$ in (2) is symmetric, eq (4) reduces to

$$u_i(\mathbf{x}) = \mu b_j dS_k \left[U_{ij,k}(\mathbf{x}) + U_{ik,j}(\mathbf{x}) + \frac{2\nu}{(1-2\nu)} \delta_{jk} U_{im,m}(\mathbf{x}) \right], \quad (5)$$

where $U_{ij}(\mathbf{x})$ is given by (2). Equation (5) completely defines the relationship between dislocations and the classical "point nuclei of strain" [5]. For example, for a pure edge loop with $b_i = \delta_{i3}b$ and $dS_i = \delta_{i3}dS$, say,

$$u_i(\mathbf{x}) = 2\mu b dS \left[U_{i3,3}(\mathbf{x}) + \frac{\nu}{(1-2\nu)} U_{ik,k}(\mathbf{x}) \right], \quad (6)$$

so that the loop is equivalent to a "double force without moment" plus a "centre of compression." For a pure shear loop with $b_i = \delta_{i1}b$ and $dS_i = \delta_{i3}dS$, say,

$$u_i(\mathbf{x}) = \mu b dS [U_{i1,3}(\mathbf{x}) + U_{i3,1}(\mathbf{x})], \quad (7)$$

which is a pair of "force dipoles with moment," the moments being of equal magnitude but opposite sense about \mathbf{x}_2 . The way in which force dipoles and displacement dipoles (infinitesimal loops) are thus related enables results in a recent paper [6] to be easily understood [7].

These relationships may also be used to derive the displacements associated with infinitesimal loops in a bounded isotropic medium provided the appropriate force dipole displacements are used. Thus for the half-space, for which Mindlin [8] has given the point force solution,

the displacements due to force dipoles with or without moment can be determined by differentiation, and the displacements due to an arbitrary infinitesimal loop written down immediately. This method avoids the integrations of Skeketee's [3] approach. If the reference axes are such that the origin is on the surface with \mathbf{x}_3 orthogonal to the surface and pointing into the medium, then Mindlin's solution [8] for the i th component of displacement due to a unit force acting in the \mathbf{x}_j direction at $(0, 0, c)$ can be shown to be given by:

$$M_{ij}(\mathbf{x}, c\mathbf{x}_3) = U_{ij}(\mathbf{x} - c\mathbf{x}_3) + V_{ij}(\mathbf{x} + c\mathbf{x}_3), \quad (8)$$

where U_{ij} is given by eq (2) and,

$$\begin{aligned} V_{ij}(\mathbf{x}) &= U_{ij}(\mathbf{x}) + 2cU_{i3,j}(\mathbf{x}) + \frac{c^2}{(1-2\nu)} U_{ik,kj}(\mathbf{x}) - 2(1-2\nu)Q\left(\frac{x_j}{x}\right)_i \\ &\quad + 4(1-\nu)(1-2\nu)Q[1-2\delta_{(i)3}]\left(\frac{x_j}{x+x_3}\right)_i \quad (\text{for } j=1, 2); \\ V_{ij}(\mathbf{x}) &= (3-4\nu)U_{ij}(\mathbf{x}) - 2cU_{i3,j}(\mathbf{x}) + 2cU_{ik,k}(\mathbf{x}) - \frac{c^2}{(1-2\nu)} U_{ik,kj}(\mathbf{x}) \\ &\quad - 4(1-\nu)(1-2\nu)Q[\ln(x+x_3)]_i \quad (\text{for } j=3). \end{aligned}$$

By expanding $M_{ij}(\mathbf{x}, c\mathbf{x}_3)$ using Taylor's theorem, the displacements due to force dipoles in half-space can be derived by differentiation. (Care must be exercised since even though these displacements are of the form $M_{ij,k}(\mathbf{x}, c\mathbf{x}_3)$, they are not equal to $U_{ij,k}(\mathbf{x} - c\mathbf{x}_3) + V_{ij,k}(\mathbf{x} + c\mathbf{x}_3)$ when $k=3$). Then, using the force dipole relationships discussed above, the displacements due to an arbitrary infinitesimal loop may be obtained. The $u_i(\mathbf{x})$ due to an infinitesimal loop at $c\mathbf{x}_3$ in half-space can be denoted by:

$$u_i(\mathbf{x}) = u_i^z(\mathbf{x}) + u_i^l(\mathbf{x}) + u_i^s(\mathbf{x}), \quad (9)$$

where $u_i^z(\mathbf{x})$ are the displacements due to the loop at $c\mathbf{x}_3$ in an infinite medium, $u_i^l(\mathbf{x})$ are the displacements due to a loop of opposite sign at $-c\mathbf{x}_3$ in an infinite medium, and $u_i^s(\mathbf{x})$ are the displacements required to completely annul the tractions on the surface. The displacements u_i^z and u_i^l can be obtained directly from eq (5), and the terms u_i^s can be derived from the force dipole displacements determined from eq (8). After some analysis the displacements u_i^s for the 9 distinct infinitesimal loops in half-space are found to be given by the following 4 equations:

(a) $\mathbf{b} = b\mathbf{x}_3$, $\mathbf{dS} = dS\mathbf{x}_3$ (edge loop):—

$$u_i^S(\mathbf{x}) = Kc \left\{ A_{i3} \left(\frac{1}{R} \right)_{,i3} - \left(\frac{x_3}{R} \right)_{,i33} \right\}, \quad (10a)$$

(b) $\mathbf{b} = b\mathbf{x}_j$, $\mathbf{dS} = dS\mathbf{x}_j$; $j = 1$ or 2 (edge loop):—

$$\begin{aligned} u_i^S(\mathbf{x}) = & K \left\{ (A_{ij} - 2\nu A_{i3}) \left(\frac{1}{R} \right)_{,i} - 2(1-\nu) R_{,ijj} + 2\nu \left(\frac{x_3}{R} \right)_{,i3} - c \left(\frac{x_3}{R} \right)_{,ijj} \right. \\ & \left. + 4(1-\nu)c \left(\frac{\delta_{i3}}{R} \right)_{,jj} + 2(1-\nu)(1-2\nu)(1-2\delta_{i3}) \left(\frac{x_j}{R+x_3+c} \right)_{,ij} \right\}, \end{aligned} \quad (10b)$$

(j is not summed in this equation)

(c) $\mathbf{b} = b\mathbf{x}_j$, $\mathbf{dS} = dS\mathbf{x}_3$; or $\mathbf{b} = b\mathbf{x}_3$, $\mathbf{dS} = dS\mathbf{x}_j$; $j = 1$ or 2 (shear loop):—

$$u_i^S(\mathbf{x}) = Kc \left\{ -A_{i3} \left(\frac{1}{R} \right)_{,ij} + \left(\frac{x_3}{R} \right)_{,ij3} \right\}, \quad (10c)$$

(d) $\mathbf{b} = b\mathbf{x}_1$, $\mathbf{dS} = dS\mathbf{x}_2$; or $\mathbf{b} = b\mathbf{x}_2$, $\mathbf{dS} = dS\mathbf{x}_1$ (shear loop):—

$$\begin{aligned} u_i^S(\mathbf{x}) = & K \left\{ 2(1-\nu) \left[\left(\frac{\delta_{i1}}{R} \right)_{,2} + \left(\frac{\delta_{i2}}{R} \right)_{,1} + 2c \left(\frac{\delta_{i3}}{R} \right)_{,12} - R_{,i12} \right] \right. \\ & \left. - c \left(\frac{x_3}{R} \right)_{,i12} + 2(1-\nu)(1-2\nu)(1-2\delta_{i3}) \left(\frac{x_1}{R+x_3+c} \right)_{,i2} \right\}, \end{aligned} \quad (10d)$$

where

$$K = bdS/4\pi(1-\nu); A_{ij} = 2\nu + 4(1-\nu)\delta_{ij}; R^2 = x_1^2 + x_2^2 + (x_3 + c)^2.$$

The displacements associated with a finite dislocation in half-space may be obtained by integration of the displacements in eq (9) over the surface of the cut used to generate the dislocation. The stresses due to the dislocation can be found by applying Hooke's law before or after the surface integration. In either case, the stresses arising from the terms u_i^x and u_i^y in (9) are the same as those given by the Peach and Koehler equations [4] and are thus obtained from a line integral rather than a surface integral. It does not appear to be generally possible to transform the double integral for the stresses arising from the displacements u_i^S to a line integral by using Stoke's theorem, but because the expressions in eqs (10) have been left in differential form, the double integral for the stresses does reduce to a single integral in many cases.

III. The Prismatic Loop With b Normal to the Surface

The analysis of the preceding section has been developed in order that a study may be made of the effect of a free surface on the stability and equilibrium orientation of a prismatic dislocation loop. Because of its geometrical simplicity, we are considering first a planar loop of rectangular shape on a glide prism of square cross-section. For the preliminary results to be presented here, the situation in which the Burgers vector \mathbf{b} of the loop is normal to the surface has been considered. The prismatic loop is shown diagrammatically in figure 1, where the loop ABCD is shown rotated through an angle θ from the pure edge orientation with its centre a distance a from the surface. The glide prism size is given by h , and at present we have only obtained results for the case $h = 50b$.

The stress tending to make segments of the loop move by glide has been determined at a number of points on the loop perimeter. It has been found convenient to express the stress at a point as the sum of three parts arising from the terms u_i^∞ , u_i^t and u_i^S in the displacement of the infinitesimal loop (eq (9)). As noted in section II, the first two parts in the stress can be obtained from the Peach and Koehler integrals, and so the relevant stresses due to the straight segments AB, BC, CD, DA and their images can be evaluated directly from the analytic expressions for the stress field of a finite straight segment given by Li [9]. The third part of the stress at a point may be found by applying Hooke's law to u_i^S given by eqs (10a) and (10c), and integrating over the surface of the loop. Because of the differential form of the right-hand side of eqs (10a) and (10c), this double integral easily

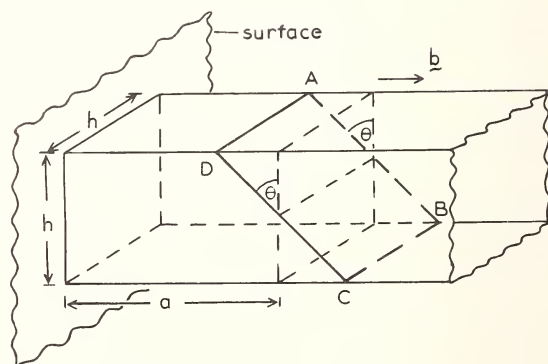


FIGURE 1. Diagrammatic representation of a rectangular loop ABCD on a glide prism of square cross section with axis normal to a free surface.

reduces to a single integral which we have evaluated numerically on a computer. The stresses arising from u_i^I and u_i^S are finite on the loop itself, and infinities in the terms arising from u_i^∞ may be avoided at all points except the corners because the segments AD and BC experience no self-stress and the self-stresses of AB and CD may easily be found from Brown's definition of self-stress [10] and Li's stress expressions [9]. Forces on any segment within a distance of $5b$ of a corner have not been considered because the stress on one side due to the adjacent side diverges as the distance from the corner decreases.

Consider first the pure edge sides AD and BC. Curves showing how the force per unit length (in units of $\mu b/4\pi(1-\nu)$) due to the infinite body part of the stress, F^∞ , the image part, F^I , and the surface traction erasing part, F^S , at the midpoint of AD varies with θ for different values of a are shown in figure (2a); the variation of the net force F^T is shown in figure (2b). (ν has been taken as $1/3$ in all calculations). The forces are taken to be positive when acting away from the surface. Similar curves for the mid-

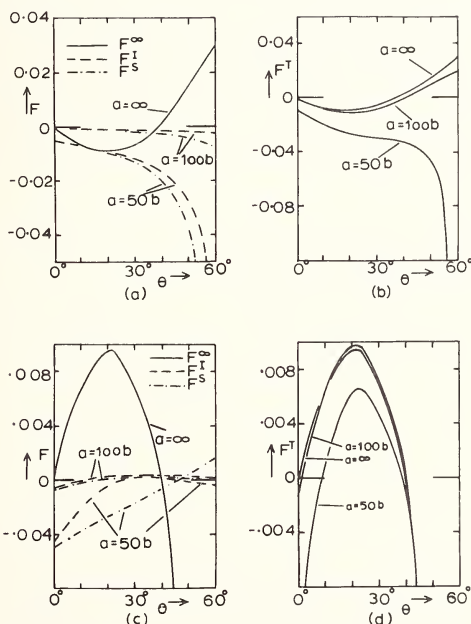


FIGURE 2. Variation of the force per unit length (units of $\mu b/4\pi(1-\nu)$) with θ at the midpoint of AD ((a) and (b)) and BC ((c) and (d)). F^∞ is the infinite body force, F^I is the force due to an image loop, F^S is the force due to the other traction erasing stresses, and F^T is the net force ($=F^\infty + F^I + F^S$).

point of BC are shown in figures (2c) and (2d). It can be seen that the forces F^\times on AD and BC tend to rotate the loop from the unstable equilibrium orientation $\theta=0$ to the orientation $\theta=38^\circ$. The side AD is attracted to the surface by the forces F^I and F^S for all values of θ , whereas the side BC is sometimes repelled. F^I and F^S are of the same order of magnitude and act in the same sense for most values of θ . The magnitudes of the forces change with position along the sides, the changes being comparatively small for F^I and F^S ($< 20\%$ when $a=50b$ and $< 2\%$ when $a=200b$) but large for F^\times ($100-300\%$ for $0 < \theta \leq 60^\circ$). The variation in F^T is less than that in F^\times for finite a . Simple line tension calculations indicate that if curvature of AD and BC due to this effect were allowed, it would be small.

The sides AB and CD are identical by symmetry and we need only consider the forces on AB. The force F^\times is zero at the midpoint of AB and the forces F^I and F^S attract AB to the surface for all θ and a , their magnitudes being larger for points closer to the surface. Again, F^S is of the same order of magnitude as F^I except when θ is large. Curves showing how F^I and F^S and the net force per unit length F^T (all in units of $\mu b/4\pi(1-\nu)$) vary with θ and a at the midpoint of AB are presented in figure (3a). The force F^\times increases in magnitude towards the corners A and B, and its effect is to produce a torque on AB tending to rotate it to $\theta=0$ for all values of θ , i.e., it opposes the effect of F^\times on AD and BC. This effect is modified by the forces F^I and F^S , as can be seen in figure (3b), where F^T on AB at points $5b$ from ends A and B is plotted against θ for $a=50b$ and $a=\infty$:

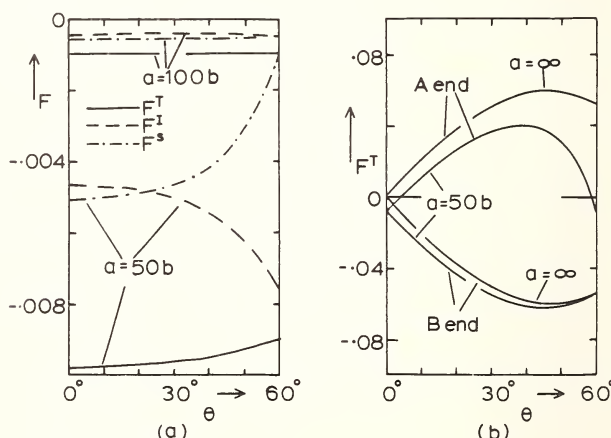


FIGURE 3. Variation of the force per unit length (units of $\mu b/4\pi(1-\nu)$) with θ at (a) the midpoint of AB, and (b) points $5b$ from ends A and B on AB.

curves for $a = 100b$ are indistinguishable from those for $a = \infty$ for the scale used for F^T . It can be seen that the surface has a considerable effect on points at the A end of AB as θ increases and they can in fact be attracted to the surface because of strong image effects.

The rectangular loop on a square glide prism of side $50b$ in an infinite medium has a minimum in its elastic energy at $\theta \approx 26^\circ$ [11]. The results of figures 2 and 3 indicate that such a loop can only achieve this orientation against the opposition of the forces on the rotating sides. We have therefore examined the relation between the forces on the loop and its energy for finite values of a by determining the change in loop energy ΔE for various rotations from the edge orientation. This has been done, not by the usual elastic energy calculation methods, but by calculating the work done by the forces discussed above in producing a given rotation θ , i.e., we have integrated F^T along each side and then integrated the result over θ . The results are shown in figure 4 where ΔE (in units of $\mu b^3/4\pi(1-\nu)$) is plotted against θ . A positive ΔE indicates that a positive amount of work has to be done on the loop to enable it to rotate to the particular value of θ . The equilibrium orientation when $a = \infty$ is at $\theta = 30^\circ$,

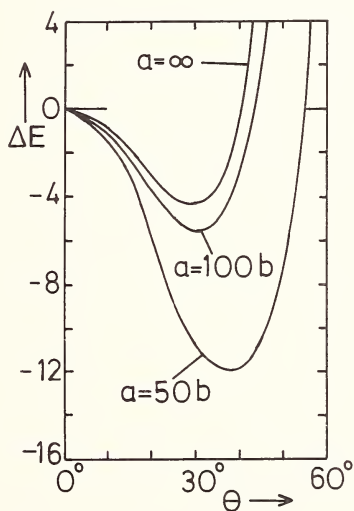


FIGURE 4. The change in the elastic energy of the loop ΔE (units of $\mu b^3/4\pi(1-\nu)$) for rotations of θ from the edge orientation.

which is close to the value found previously [11]; the difference is probably associated with our cutoff of $5b$ at the corners. The effect of the surface is to deepen the energy minimum and displace it to larger values of θ . The elastic energy will of course decrease again when AD comes close to the surface.

In principle, the results of figures 2–4 can be used together, so that for a given value of a , the minimum energy orientation of the loop can be found and then, assuming a value for the lattice friction stress opposing dislocation motion, the stability of the loop under the action of the forces examined. The results of this approach, however, are difficult to interpret because of the magnitudes of the F^\times terms near the loop corners. It may be more reasonable to ignore the force F^\times altogether, or to consider its value only at the midpoint of the sides. Because of the complex nature of this problem, we shall leave this discussion to a later paper when results for other loop sizes and Burgers vector orientations are available.

IV. Discussion and Conclusions

The only previous study of a dislocation loop near a free surface was by Baštecká [2] who considered a pure edge circular loop with Burgers vector normal to the surface. Her method of using Hankel transforms is only suitable for cases of cylindrical symmetry and cannot therefore be used to determine the forces on loops with more general shapes and orientations. We have used an approach which enables the displacements and stresses of an arbitrary infinitesimal loop to be determined directly from Mindlin's point force solution [8]. This leads to a solution for the arbitrary finite loop which can be expressed as the sum of three parts (eq (9)). Two of these can be obtained from the well-known infinite body solutions, and the third involves a double integral which in many situations reduces to at most a single integral. Our method is similar in principle to that of Steketee [3] who also makes use of the relationship between point forces and dislocations, but by making use of Mindlin's solution we have avoided the integrations of Steketee's procedure for they have, in effect, already been carried out by Mindlin. Steketee's presents the displacements for just one infinitesimal loop with $\nu=1/4$, and eqs (9) and (10) of the present paper give the displacements due to an arbitrary infinitesimal loop in half-space for the first time.

Our investigation into the stability of a prismatic dislocation loop near a free surface is in its early stages and in section III we have presented only the preliminary results. Several important features emerge however. First, the forces arising from the stresses which, with those of the image loop, make the surface traction free are not negligible for any values of a and are generally of the same order of magnitude as the forces due to the

image loop. Second, the form of the forces for glide on the loop perimeter varies strongly with loop orientation and proximity to the surface. Third, the results for the forces are in some cases difficult to interpret because the force can vary markedly along a side and because the forces on adjacent sides can tend to oppose each other. This problem is likely to arise in any analysis in which the loop is restricted to a planar form. An attempt has been made to relate the forces on the loop to the energy changes associated with loop rotation, but difficulties are still encountered in deciding how to deal with the force F^∞ . We have therefore been content to merely present the results and to leave a full discussion of loop stability near a free surface to a later paper.

V. Acknowledgement

One of us (P.P.G.) wishes to thank the States of Jersey for the award of a research studentship.

VI. References

- [1] Bacon, D. J., Phys. Stat. Sol. **29**, 543 (1968).
- [2] Baštecká, J., Czech. J. Phys. **14**, 430 (1964).
- [3] Steketee, J. A., Can. J. Phys. **36**, 192 (1958).
- [4] de Wit, R., in Solid State Physics **10**. F. Seitz and D. Turnbull, Eds. (Academic Press, New York, 1960) p. 249.
- [5] Love, A. E. H., The Mathematical Theory of Elasticity, 4th ed. (Cambridge University Press, 1952).
- [6] Koehler, J. S., J. Appl. Phys. **37**, 4351 (1966).
- [7] Groves, P. P., and Bacon, D. J., J. Appl. Phys. **40**, 4207 (1969).
- [8] Mindlin, R. D., Physics **7**, 195 (1936).
- [9] Li, J. C. M., Phil. Mag. **10**, 1097 (1964).
- [10] Brown, L. M., Phil. Mag. **10**, 441 (1964).
- [11] Bacon, D. J., and Crocker, A. G., Phil. Mag. **13**, 217 (1966).

THEORETICAL CONSIDERATIONS ON THE EXTENSION OF $\frac{1}{2}\langle 110 \rangle$, {111} DISLOCATIONS IN ISOTROPIC F.C.C. METALS INTO SHOCKLEY PARTIALS

Doris Kuhlmann-Wilsdorf

*Department of Materials Science
University of Virginia
Charlottesville, Virginia 22903*

and

T. R. Duncan

*Department of Minerals and Metals Engineering
University of Wisconsin
Madison, Wisconsin 53706*

The energy changes and equilibrium separations associated with the extension of $\frac{1}{2}\langle 110 \rangle$, {111} dislocations in fcc metals into Shockley partials have been calculated and were found considerably smaller than the previous corresponding values due to Seeger and Schöck. The new results may be shown to be credible on the basis of the following simple estimates:

The theoretical shear fracture strength of a crystal may be written as $\tau_{crit} = G/q$, with G the appropriate shear modulus, and the numerical parameter q near 30 for {111} planes in fcc metals. The resolved shear stress required to force the Shockley partials into coincidence at vanishing stacking fault energy, $(\tau_{eq})_{Max}$, must approach but cannot exceed τ_{crit} so that $(\tau_{eq})_{Max} \lesssim G/30$, i.e. much smaller than the value of $\sqrt{6}G/8\pi \approx G/9$ previously assumed. Similarly, the stacking fault energy cannot exceed the value of $\gamma_{crit} = Ga/\sqrt{6}q$ with a the lattice constant, and the dislocation core energy must be in the order of $E_c \approx 2r_0 \gamma_{crit} \approx \frac{1}{4}E_D$ where E_D is the total dislocation energy, and the core radius, r_0 , is taken to be that distance from the dislocation axis at which the resolved shear stress on the slip plane would become equal to τ_{crit} in linear elastic behavior. Lastly, D_0 , the actual equilibrium separation between the partials must be considerably smaller than D_0^* , the separation calculated from linear elastic theory, as long as $D_0^* < 2r_0$. One finds easily that $D_0^* \leq 2r_0$ for $\gamma \gtrsim \gamma_{crit}/6$ and $\gamma \gtrsim \gamma_{crit}/10$ for edge and screw dislocations, respectively, de-

pending somewhat on Poisson's ratio, so that only in silver will edge dislocations have an equilibrium separation a little larger than $2r_0$, but much less than $2r_0$ in the other common pure fcc metals. For $D_0 = 2r_0$, when the core energy is reduced by about $\frac{1}{3}$ according to the rule of the square of the Burgers vectors but the elastic energy is virtually unaffected, and remembering that work $2r_0\gamma$ with $\gamma = \gamma_{crit}/6$ must be done to spread out the stacking fault, the relative energy gain due to the extension of edge dislocations is simply estimated as $(\Delta E/E_D)_{\perp} \approx [\frac{1}{3}E_c/4E_c - \frac{1}{6}\gamma_{crit}/4\gamma_{crit}] \approx 4\%$ which may be compared to the calculated value of 4.6% in silver.

Key words: Dislocation geometry; stacking faults; Shockley partials.

I. Introduction

The geometrically and experimentally well-known extension of the common $\frac{1}{2}\langle 110 \rangle, \{111\}$ glide dislocations of fcc metals into $\frac{1}{6}\langle 112 \rangle$ partials has received comparatively little theoretical attention. This is the more surprising because this effect is believed to govern cross slip, which in turn is widely held to determine the magnitude of τ_{III} , the stress at the onset of stage III. Particularly lacking are reliable estimates for the fractional energy gain associated with dislocation splitting, as well as for the resolved shear stress required to force the Shockley partials of an extended dislocation back into coincidence. For these two quantities, the earlier estimates by Seeger, and Seeger and Schöck, based on a sinusoidal interaction potential are almost universally accepted.

These are, with respect to the fractional energy gain as shown by Seeger [1] and Seeger and Schöck [2], 11.2 percent for edge dislocations in copper assuming a stacking fault energy of $\gamma = 40$ ergs/cm² and 3.7 percent for aluminum with $\gamma = 200$ ergs/cm², and with respect to the maximum shear stress to force coincidence as given by Seeger [3],

$$(\tau_{eq})_{Max} = \sqrt{6}G/8\pi \quad (1)$$

where G is the modulus of rigidity. Note here that eq (1) does not depend on Poisson's ratio, which certainly must be involved, and thus could not possibly be reliable. Further, no expression seems ever to have been given to relate the values of $(\tau_{eq})_{Max}$ to the relative orientation of the dislocation, i.e., whether the unextended dislocation is of edge, screw, or mixed type.

II. Estimate of the Maximum Stress of Repulsion Between Shockley Partials

The reason for the lack of theoretical information in the field under discussion lies in the great mathematical difficulties encountered for small separations. The problem concerns the interaction between overlapping cores of partial dislocations. In this, the Peierls-Nabarro treatment is greatly complicated by the fact that two nonparallel Burgers vectors are involved. Moreover, the assumption of basically sinusoidal interaction potentials between the atoms on either side of the slip plane is inadequate since it greatly overestimates the critical shear, and with it τ_{crit} , the highest resolved shear stress which a defect-free crystal could support on the slip system considered. This is a most important aspect because, on the one hand, the highest shear stress which can occur on the slip plane within the dislocation core cannot much exceed τ_{crit} , while, on the other hand, τ_{crit} must be reached at or in the core. Hence, it seems a foregone conclusion that a stress not far from τ_{crit} will be needed to force two partials together, but that this same stress, $(\tau_{\text{eq}})_{\text{Max}}$, cannot possibly be larger than τ_{crit} , the stress which spontaneously generates dislocations all over the slip plane.

Most conveniently, τ_{crit} should be written as

$$\tau_{\text{crit}} = G/q \quad (2a)$$

since, to a good first approximation, the critical stress for any potential slip plane and any crystal structure is expected to be proportional to the relevant modulus of rigidity. The factor $q = G/\tau_{\text{crit}}$, then, is primarily of geometrical nature. For the case of $\{111\}$ planes in fcc metals, the value of $q = 30$ found by Mackenzie [4] has been widely adopted as the best estimate, while for a simple sinusoidal interaction potential, much as was used in the calculations leading to eq (1), one readily obtains

$$q_s = 2\pi h/p \quad (2b)$$

where h is the separation between the slip planes and p is the periodicity interval. For slip on $\{111\}$ planes from a regular position into a stacking fault position, $h = a/\sqrt{3}$ and $p = a/\sqrt{6}$ with a the lattice constant so that for this case one finds $q_s = 2\pi\sqrt{2}$ and $(\tau_{\text{crit}})_s = G/\sqrt{8}\pi$. By our preceding argument this latter value should be the upper limit of, but not far from, $(\tau_{\text{eq}})_{\text{Max}}$ for the case of sinusoidal interaction potentials. Not surprisingly, the ratio of $(\tau_{\text{eq}})_{\text{Max}}$ of eq (1) to $(\tau_{\text{crit}})_s$ is found at $\sqrt{3}/4 = 0.865$, i.e., $(\tau_{\text{eq}})_{\text{Max}}$ is found just below the value of τ_{crit} that corresponds to the model used.

However, while eq (1) is thus consistent with the model on which it was based, this model is quite unrealistic because it predicts $q_s = \sqrt{8}\pi \approx 9$ while the best accepted value is $q = 30$, as pointed out above. Correspondingly, one must suspect eq (1) to be an overestimate by a factor on the order of 3 or 4.

III. Estimate of the Energy Gain Due to Dislocation Splitting

As there is no reason to believe other than that the replusive force between the partials assumes its largest value at coincidence, no extension will occur, and thus no energy will be gained due to extension, if the equivalent stress on the partials due to the surface energy of the stacking fault is larger than $(\tau_{eq})_{Max}$; i.e., the critical stacking fault energy above which no extension takes place at all is given by

$$\gamma_{crit} = (\tau_{eq})_{Max}a/\sqrt{6} \leq Ga/\sqrt{6}q \quad (3)$$

TABLE I. *Upper limit for the values of the stacking fault energy which the metal listed could have*

Metal	$\gamma_{crit} \leq \frac{Ga}{q\sqrt{6}}$
Al	147 ergs/cm ²
Cu	229 ergs/cm ²
Ag	164 ergs/cm ²
Au	157 ergs/cm ²
Ni	372 ergs/cm ²

which, with $q = 30$, yields the values listed in table I. Thus dislocations in aluminum cannot be extended and no energy can be gained unless the stacking fault energy is significantly less than 147 ergs/cm²—much less than the 200 ergs/cm² usually assumed as the correct value.¹ In any event, the stacking fault energy of aluminum cannot be as high as 200 ergs/cm². Namely, it could not possibly require a shear stress in excess of τ_{crit} to produce a stacking fault by shear of a {111} plane through the displacement of $a/\sqrt{6}$ in ⟨112⟩ direction, i.e., from the faulted position into the stacking fault position. Hence, the stacking fault energy

¹ A recent, careful determination of the intrinsic stacking fault energy of aluminum due to P. S. Dobson, P. J. Goodhew, and R. E. Smallman, Phil. Mag. **16**, 9 (1967), has yielded the value of $\gamma = 135 \pm 20$ ergs/cm².

must be less than $\tau_{\text{crit}} a/\sqrt{6}$, so that γ_{crit} of eq (3) and the values in table I are, at the same time, the highest possible values of the stacking fault energy.

Previously, Kuhlmann-Wilsdorf [5] has interpreted the core radius of dislocations as the distance from the dislocation axis at which the resolved shear stress on the slip plane would reach the value of $\tau_{\text{crit}} = G/q$ according to linear elastic theory. For distances closer to the core than that, linear elasticity must certainly be a very poor approximation. Since the misfit on the slip plane within the core represents about the highest possible energy density on the slip plane which, as we saw, is given by γ_{crit} , we may estimate the core energy as

$$E_c \approx 2r_0\gamma_{\text{crit}} \approx qb\gamma_{\text{crit}}/\pi g \approx Gb^2/\sqrt{3}\pi g \quad (4)$$

where $b = a/\sqrt{2}$ is the Burgers vector of undissociated $\frac{1}{2} < 110 > \{111\}$ dislocations and g is an orientation factor, equal to $(1-\nu)$ for edge dislocations and equal to unity for screw dislocations. Thus, at least to a first approximation, the dislocation core energy is independent of q , i.e., is independent of the choice of slip plane and of core radius, as previously pointed out by Cottrell [6]. Further, the core energy seems to depend on the elastic constants, Burgers vector, and relative dislocation orientation in the same manner as the elastic energy of the dislocation. Consequently, the dislocation energy may be written as

$$E = \{Gb^2/4\pi g\} \{\ln(R/r_0) + C\} \quad (5)$$

with $C \approx 4/\sqrt{3} \approx 2$ according to eq (4). Thus with $R/r_0 \approx 600$, which would follow for $r_0 \approx qb/2\pi g \approx 16\text{\AA}$ and $R \approx 1$ micron, the core energy amounts to roughly one-quarter of the total dislocation energy.

The equilibrium distance of separation between Shockley partials, assuming completely elastic interaction, as given by Read [7], is

$$D_0^* = Gb^2(1 - \nu/2 - \nu \cos 2\phi)/\{12\pi(1-\nu)\gamma\} \quad (6a)$$

where ϕ is the angle between the dislocation axis and the Burgers vector of the undissociated dislocation, or

$$(D_0^*)_\perp = Gb^2(1 + \nu/2)/\{12\pi(1-\nu)\gamma\} \quad (6b)$$

for edge dislocations. Generally, D_0^* as given in eq (6) is an overestimate for the actual separation between the partials because the shear stress in the cores, and with it the repulsive forces between the partials, is less than

calculated from linear elasticity theory. The corresponding discrepancy between D_0 , the actual equilibrium distance of separation, and D_0^* of eq (6), is considerable as long as the cores of the partials overlap, say, for $D_0 \leq 2r_0$.

As may be seen from eq (6b), an edge dislocation will split to $(D_0^*)_{\perp} = 2r_0$ when the stacking fault energy equals about 1/6 of γ_{crit} , i.e., with an assumed stacking fault energy of 40 ergs/cm² in copper, the partials' cores of an extended dislocation would still overlap. As the greatest possible fractional reduction in core energy due to splitting is about 1/3, while the core energy amounts to about 1/4 of the total dislocation energy, we thus expect the energy gain to be less than about 1/12, i.e., less than about 8 percent, unless the partials are well separated, and hence conclude that the value of 11.4 percent for copper assuming $\gamma=40$ ergs/cm² quoted in the introduction, must be a substantial overestimate.

IV. Evaluation of Equilibrium Separation, Maximum Repulsive Stress, and Energy Gain, on the Basis of a Simple Model

In accordance with the considerations in the preceding sections, realistic values for $(\tau_{\text{eq}})_{\text{Max}}$, for D_0 , and for the relative energy reduction due to the extension of glide dislocations to their equilibrium configurations can be derived as follows:

The energy of the undissociated dislocation is given by

$$E_u = Gb^2 \{ \ln (R/r_0) + C \} \{ 1 - (\nu/2)(1 + \cos 2\phi) \} / \{ 4\pi(1-\nu) \} \quad (7)$$

where

$$r_o = qb \{ 1 - (\nu/2)(1 + \cos 2\phi) \} / \{ 2\pi(1-\nu) \}, \quad (8)$$

while the energy of the dissociated dislocation is the sum of the energy of the two partials when widely separated (assuming R to remain the same), plus their interaction energy, plus the energy of the stacking fault ribbon stretched out between the partials. The sum of the energy of the partials is

$$E_{p1} + E_{p2} = Gb^2 \{ 2 - \nu - (\nu \cos 2\phi)/2 \} \{ \ln (\sqrt{3}R/r_o) + C \} / \{ 12\pi(1-\nu) \}. \quad (9)$$

Here, for simplicity's sake, the core radii of the two partials are taken to be equal to $r_{op} = r_o/\sqrt{3}$, i.e., the slight difference in core radii due to the reorientation of the Burgers vectors is neglected.

The interaction energy between the partials consists of the elastic interaction energy,

$$eE_{\text{int}} = Gb^2 \{1 - \nu/2 - \nu \cos 2\phi\} \{\ln [R/(r_0/\sqrt{3} + D_o)]\}/\{12\pi(1-\nu)\} \quad (10)$$

and the interaction energy between their cores, cE_{int} . An expression for cE_{int} may be derived from the following three requirements: (i) The reduction in core energy due to splitting shall be in the same relation to the elastic constants, the Burgers vector, and the angle ϕ , as the reduction in the elastic energy. (ii) For $D_o=0$ the core energy of the undissociated dislocation shall be equal to the sum of the core energies of the two coincident partials plus their interaction energy for $D_o=0$, plus the energy of that part of the elastic stress field which lies between $r_{\text{op}}=r_0/\sqrt{3}$, the smaller core radius of the partials, and r_o , the core radius of the undissociated dislocation. (iii) The core interaction energy shall decrease monotonically with increasing separation between the partials such that at separations of $D_o \gtrsim 2r_o$ the linear elastic solution shall become an increasingly good approximation.

With the above requirements for the core interaction, assembling the different contributions listed, and after some arithmetic, one finds for the relative energy reduction at equilibrium separation

$$(\Delta E/E_u)_0 \approx B(\phi) \{\ln (1 + D_o/r_{\text{op}}) + (2C^*/\pi) \text{arc tan } (\ell D_o/r_{\text{op}}) - D_o/D_o^*\}/\{3(\ln(R/r_o) + C)\} \quad (11a)$$

with

$$B(\phi) = \{1 - \nu/2 - \nu \cos 2\phi\}/\{1 - (\nu/2)(1 + \cos 2\phi)\} \quad (11b)$$

with

$$C^* = C - 3 \ln \sqrt{3} = C - 1.65, \quad (11c)$$

with ℓ an adjustable parameter not far from unity, and with D_o^* as given by eq (6). Varying ℓ within reasonable limits has only an insignificant influence on the numerical results.

Figure 1 gives D_o/D_o^* as a function of D_o/r_{op} for different assumed values of the core energy parameter, C , which as explained in section III is believed to be near 2. Values of $(\Delta E/E_u)_0/B(\phi)$ as a function of $(\gamma/Gb)/B(\phi)$ are given in figure 2, again for different values of C .

Lastly, the maximum stress between the partials is found as

$$(\tau_{\text{eu}})_{\text{Max}} = \{\tau_{\text{crit}} B(\phi) (1 + 2C^*/\pi)\}/2 \quad (12)$$

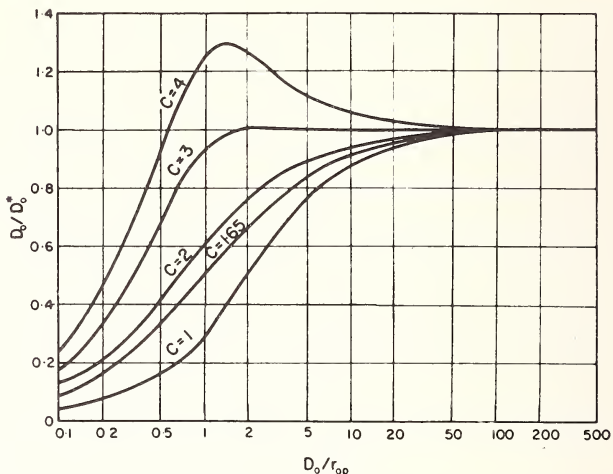


FIGURE 1. Equilibrium distances of separation between Shockley partials, D_o , compared to D_o^* , the separation distances which would be calculated assuming linear elastic behavior throughout.

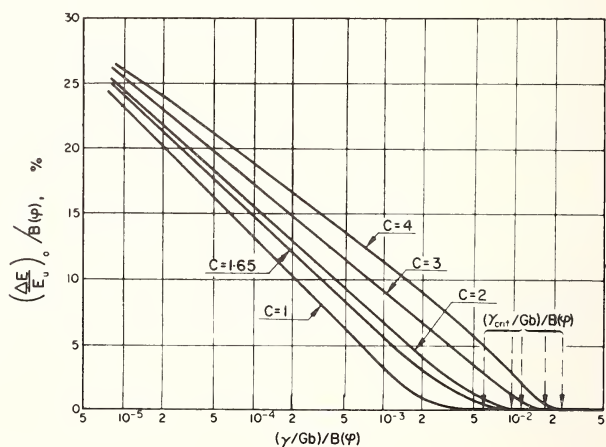


FIGURE 2. The relative energy gain due to the extension of $1/2\langle 110 \rangle, \{111\}$ dislocations into Shockley partials, $(\Delta E/E_u)_o$, as a function of the stacking fault parameter γ/Gb . The function $B(\phi)$, representing the dependence on relative dislocation orientation, is given by eq (11b).

i.e., not far from but somewhat smaller than τ_{crit} in conformity with the considerations in section II above.

Table II summarizes some of the pertinent data for the case of edge and screw dislocations with $q=30$, $C=2$, $R/r_0=600$, and $\ell=1$ for six fcc metals. A more detailed treatment of the model is given elsewhere by Kuhlmann-Wilsdorf and Duncan [8].

TABLE II. Approximate values of $(\Delta E/E_u)_0$, the fractional energy gain due to the extension of $1/2 \langle 110 \rangle$, $\{111\}$ edge and screw dislocations into partials, and of D_0 , the equilibrium distance between the Shockley partials, calculated for the values of Poisson's ratio, ν , stacking fault energy, γ , and shear modulus, G , as listed, assuming $q=30$, $C=2$, $R/r_0=600$, and $\ell=1$. These latter values are believed to be the most likely or representative.

Metal	ν	$G \times 10^{-11}$ {dyne/cm ² }	γ assumed {erg/cm ² }	$\frac{\gamma}{Gb} \times 10^3$	Edge dislocations		Screw dislocations	
					$(\Delta E/E_u)_0$ percent	$D_0 \{\text{\AA}\}$	$(\Delta E/E_u)_0$ percent	$D_0 \{\text{\AA}\}$
Al	0.34	2.68	200	26.0	0	0	0	0
Cu	0.35	4.64	85	7.2	1.1	11	~ 0.06	~ 3
Ag	0.37	2.94	20	2.6	4.6	48	~ 2.0	~ 18
Au	0.42	2.82	55	6.7	1.4	15	~ 0.02	~ 1
Ni	0.31	7.85	300	16.0	0	0	0	0
α -brass	0.37	3.8	8	0.8	9.7	150	~ 5	~ 90

V. Acknowledgement

The financial support of this research by the U.S. Atomic Energy Commission is gratefully acknowledged. Part of this research was carried out while T. R. Duncan held a postdoctoral research fellowship at the Physics Department of the University of the Witwatersrand.

VI. References

- [1] Seeger, A., Z. Naturforschung **9a**, 856 (1954).
- [2] Seeger, A., and Schöck, G., Acta Met. **1**, 519 (1953).
- [3] Seeger, A., Dislocations and Mechanical Properties of Crystals, (J. Wiley & Sons, New York, 1957) p. 243.
- [4] Mackenzie, J. K., Ph.D. Thesis, Bristol, 1949 (unpublished); see A. H. Cottrell, Dislocations and Plastic Flow in Crystals, (The Clarendon Press, Oxford, England, 1953) p. 10.
- [5] Kuhlmann-Wilsdorf, D., Phys. Rev. **120**, 773 (1960).
- [6] Cottrell, A. H., Dislocations and Plastic Flow in Crystals, (The Clarendon Press, Oxford, 1953) p. 39.
- [7] Read, W. T., Dislocations in Crystals, (McGraw-Hill Book Co., New York, 1953).
- [8] Kuhlmann-Wilsdorf, D., and Duncan, T. R., Acta Met. **16**, 1401 (1968).

SCREW DISLOCATIONS IN INHOMOGENEOUS SOLIDS

G. P. Sendeckyj

*School of Engineering
Case Western Reserve University
Cleveland, Ohio 44106*

The problem of screw dislocations interacting with free surfaces and inhomogeneities is reconsidered and a general method is presented for solving a large class of screw dislocation problems. The method is based on knowledge of certain general solutions in the theory of antiplane deformation of elastic solids. It can be shown that all the known screw dislocation solutions for solids undergoing antiplane deformation can be found by using this approach.

As an illustration of the method, three new solutions for screw dislocations near inhomogeneities are given. These are the screw dislocation near (1) an elastic elliptic cylindrical inclusion, (2) two circular cylindrical inclusions, and (3) a *curvilinear* cavity or rigid inclusion. The interaction energy between the dislocation and the inhomogeneities is also computed.

Key words: Dislocations-elasticity; dislocation surface interactions; finite elasticity; inhomogeneities.

I. Introduction

Even though the interaction of dislocations with free surfaces and inhomogeneities is of considerable importance in materials science, only a handful of solutions can be found in the literature [1-12]. This seems to be due to the apparent complexity of the elastic boundary value problems that have to be solved.

In the present work, the problem of screw dislocations interacting with free surfaces and inhomogeneities is reconsidered and a general method is presented for solving a large class of screw dislocation problems. This method is based on knowledge of certain general solutions in the theory of antiplane deformation of elastic solids. It can be shown that all the known screw dislocation solutions [1-12] for solids undergoing antiplane deformation may be found by using this approach.

In the next section the required general results are summarized. Next the problem of a screw dislocation near an elastic elliptic cylindrical inclusion is considered. The analysis simplifies considerably for the case of a *curvilinear cavity* or rigid inclusion; and the general solution is found for this case. The problem of a screw dislocation near two elastic circular cylindrical inclusions is also solved. Finally the interaction energy between the screw dislocation and the inhomogeneities is computed. Some general features of the interaction are discussed.

II. General Results in Antiplane Deformation

In the case of antiplane deformation (Milne-Thomson, [13]), one has

$$u=v=0, \quad w=w(x,y), \quad (1)$$

where u , v , w are the displacements along the coordinate axes. The nonzero stress components are related to $w(x, y)$ by

$$\sigma_{zx} = \mu(\partial w / \partial x) \quad \sigma_{yz} = \mu(\partial w / \partial y), \quad (2)$$

where μ is the shear modulus. In the absence of body forces, the general solution of the stress equilibrium equations can be written as

$$\mu w = \operatorname{Re} \{F(z)\}, \quad (3)$$

where $F(z)$ is an analytic function of the complex variable $z=x+iy$ and $\operatorname{Re} \{ \}$ is used to denote the real part of the function in the brackets. The stresses are now determined from

$$\sigma_{zx} - i\sigma_{yz} = \partial F / \partial z. \quad (4)$$

Curvilinear Coordinates. Let us consider two complex planes, the z - and ζ -plane. Letting ρ and ψ be polar coordinates in the ζ -plane, we have $\zeta = \rho e^{i\psi}$. Consider the transformation

$$z = \omega(\zeta) = \left[\zeta + \sum_{n=1}^{\infty} A_n \zeta^{-n} \right] \quad (5)$$

from the ζ -plane into the z -plane. Equation (5) maps the unit circle $|\zeta|=1$, or $\rho=1$, in the ζ -plane into a closed curvilinear contour Σ in the z -plane. *Points exterior to the circle $|\zeta|=1$ are mapped uniquely into points exterior to Σ if and only if the coefficients A_n are restricted appropriately.*

For example, in the transformation

$$z = \omega(\zeta) = c[\zeta + A_n \zeta^{-n}],$$

coefficients c and A_n must satisfy the conditions

$$c > 0, \quad 0 \leq A_n \leq 1/n;$$

otherwise the mapping function will not transform the exterior of the unit circle $|\zeta|=1$ into the exterior of the curvilinear contour Σ . Variables ρ and ψ can be thought of as forming a curvilinear coordinate system for the z -plane, with $\rho=1$ corresponding to the curvilinear contour Σ .

In terms of ρ and ψ , the displacements and stresses are

$$\mu w = \operatorname{Re} \{F(\zeta)\}, \quad (6)$$

$$\sigma_{\rho z} - i\sigma_{\psi z} = \zeta F'(\zeta)/\rho |\omega'(\zeta)| \quad (7)$$

where a prime on a function is used to denote differentiation with respect to its argument. From (7), it is seen that the stresses will, in general, be singular at the points

$$|\omega'(\zeta)| = 0, \quad (8)$$

which are the singular points of transformation (5). Furthermore, (5) maps points inside $|\zeta|=1$ all over the z -plane; that is, points inside the circle $\rho=1$ do not necessarily correspond to points inside Σ . This precludes the use of classical conformal mapping techniques in solving elastic inclusion problems.

The difficulties are readily avoided by using the following procedure: The elastic fields inside the inclusion are assumed to be given by a function of z . Equations (5), (6), and (7) are used to write the displacements and stresses on Σ in terms of ρ and ψ .¹ The boundary conditions are then satisfied at the interface by the appropriate choice of the complex potential for the matrix. This yields the desired solution. This approach is used below to get some general results for curvilinear inclusion problems.

Inclusion Problems. Consider an elastic matrix containing a single curvilinear inclusion whose boundary is given by Σ . Letting subscripts 1 and 2 on elastic quantities refer to the matrix and inclusion respectively, the boundary conditions at the interface corresponding to a perfect bond

¹ This can always be done since conformal mapping (5) is *not* applied to the inclusion region. It is only used to write the stresses and displacements, due to the assumed elastic fields inside the inclusion, in terms of ρ and ψ on Σ . This may be seen from the following argument: An unbounded region, with properties of the inclusion, is loaded so that the elastic fields inside the region, bounded by Σ , are equal to the assumed ones. The stresses and displacements on boundary Σ of the inclusion region are expressed in terms of ρ and ψ by using conformal map (5), which applies in this case.

are

$$w_1 = w_2, \quad \sigma_{\rho z_1} = \sigma_{\rho z_2} \text{ for } \rho = 1. \quad (9)$$

It is required to find the general form of the solution satisfying (9). This is easily done by following the procedure outlined above. Hence, one has

THEOREM 1: *The general form of displacement potentials $F_i(z)$ satisfying boundary conditions (9) on Σ in the z -plane is*

$$F_1(z) = f(z) - K\bar{f}[\omega(1/\zeta)], \quad F_2(z) = (1+K)f(z), \quad (10)$$

where $z = \omega(\zeta)$ and

$$K = (\mu_2 - \mu_1)/(\mu_2 + \mu_1). \quad (11)$$

PROOF: That this is the solution is readily verified by direct substitution of (10) into boundary conditions (9).

REMARKS: It should be noted that the stress field inside the inclusion is given in terms of the variable z and that the region inside Σ is *not* transformed. The conformal mapping is used only as a convenient tool in satisfying boundary conditions (9).

As a consequence of Theorem 1, it follows:

COROLLARY 1: (Smith, [1]) *The general solution of the circular inclusion problem is*

$$F_1(z) = f(z) - K\bar{f}(1/z), \quad F_2(z) = (1+K)f(z). \quad (12)$$

COROLLARY 2: *The general solution of the curvilinear cavity (rigid inclusion) problem is*

$$F(\zeta) = f(\zeta) \pm \bar{f}(1/\zeta), \quad (13)$$

where the plus (minus) sign should be taken.

COROLLARY 3: *The ellipse, and its geometric limits, is the only inclusion shape for which a uniform applied stress at infinity induces a uniform state of stress inside the inclusion.*

PROOF: Let the stress be uniform inside the inclusion, that is

$$F_2(z) = (1+K)Az,$$

where A is a complex constant. By Theorem 1,

$$F_1(z) = A\omega(\zeta) - \bar{A}K\omega(1/\zeta) = Ac \left[\zeta + \sum_{n=1}^{\infty} A_n \zeta^{-n} \right] - K\bar{A}c \left[\zeta^{-1} + \sum_{n=1}^{\infty} A_n \zeta^n \right].$$

Upon substituting this expression for $F_1(z)$ into (7), one sees that terms with $n > 1$ induce stresses that are not uniform at infinity. Hence for constant applied stress at infinity, $A_n = 0$ ($n > 1$) and, consequently, $\omega(\zeta) = c[\zeta + A_1\zeta^{-1}]$, which is the mapping function for an ellipse. *Q.E.D.*

Joined Half-Spaces. Another useful result is the general solution for two joined half-spaces which may be stated as:

THEOREM 2: Consider two joined elastic half-spaces undergoing antiplane deformation. Let the interface lie along the x -axis. Let subscripts 1 and 2 on elastic quantities refer to the upper ($y > 0$) and lower ($y < 0$) half-planes, respectively. If a source of stress with complex potential $f(z)$ is put in region 1, then the solution satisfying the conditions of a perfect weld at the interface is:

$$F_1(z) = f(z) - K\bar{f}(z), \quad F_2(z) = (1+K)f(z). \quad (14)$$

PROOF: This result is readily verified by substituting (14) into the boundary conditions.

Now let us turn to the application of these results to problems of screw dislocations in inhomogeneous solids. In the next section, a screw dislocation near a curvilinear inclusion is considered.

III. Screw Dislocation Near Curvilinear Inclusion

Screw Dislocation near an Elliptic Inclusion. Let us consider application of the general results to the problem of a screw dislocation near an elliptic inclusion. In this case, the appropriate mapping function is

$$z = \omega(\zeta) = c[\zeta + \lambda\zeta^{-1}], \quad c > 0, 0 \leq \lambda \leq 1, \quad (15)$$

where c and λ are real constants related to the semi-axes a and b of the ellipse by

$$c = (a+b)/2, \quad \lambda = (a-b)/(a+b). \quad (16)$$

Assuming that the interface between the matrix and inclusion is mechanically coherent (that is, boundary conditions (9) must be satisfied at the interface), putting the dislocation on the x -axis at a distance z_0 ($a < z_0 < \infty$) from the center of the inclusion as indicated on figure 1, and using Theorem 1 yields

$$^1F_1(z) = (\mu_1 b_z / 2\pi i) \{ \log [\omega(\zeta) - \omega(\beta)] + K \log [\omega(1/\zeta) - \omega(\beta)] \}, \quad (17)$$

$$^1F_2(z) = (\mu_1 b_z / 2\pi i) (1+K) \log (z - z_0), \quad (18)$$

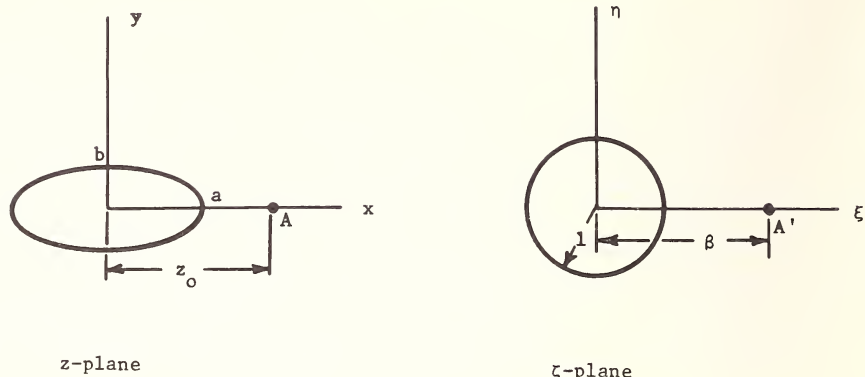


FIGURE 1. The complex z - and ζ -plane for elliptic inclusion problems. Dislocation is put at point A .

$$z = \omega(\zeta) = c[\zeta + \lambda\zeta^{-1}]$$

where $(\mu_1 b_z / 2\pi i) \log(z - z_0)$ is the potential for a dislocation acting at the point z_0 and β is the point in the ζ -plane corresponding to z_0 in the z -plane. Equation (17) can be rewritten as

$$\begin{aligned} {}^1F_1(z) &= (\mu_1 b_z / 2\pi i) \{ \log(\zeta - \beta) + K \log(\zeta - 1/\beta) + \log(\zeta - \lambda/\beta) \\ &\quad + K \log(\zeta - \beta/\lambda) - (1+K) \log \zeta + \log c + K \log c \zeta \}, \end{aligned}$$

from which it is seen that ${}^1F_1(z)$ consists of some rigid body terms and five dislocations in the ζ -plane, placed at $\zeta = 0, \beta, 1/\beta, \beta/\lambda, \lambda/\beta$. The term containing β/λ corresponds to a dislocation in the matrix at $\zeta = \beta/\lambda$ in the ζ -plane. It violates the condition of a dislocation only at β ; hence, it must be eliminated by putting a dislocation at the corresponding point in the z -plane. This introduces a dislocation at $\zeta = \beta/\lambda^2$ in the ζ -plane. Repeating this procedure, one finally gets

$$\begin{aligned} F_1(z) &= (\mu_1 b_z / 2\pi i) \sum_{n=0}^{\infty} (-K)^n \{ \log [\omega(\zeta) - \omega(\beta/\lambda^n)] \\ &\quad + K \log [\omega(1/\zeta) - \omega(\beta/\lambda^n)] \}, \end{aligned} \quad (19)$$

$$F_2(z) = (\mu_1 b_z / 2\pi i) (1+K) \sum_{n=0}^{\infty} (-K)^n \log [z - \omega(\beta/\lambda^n)], \quad (20)$$

which is the required solution. An alternate expression for $F_1(z)$ is

$$F_1(z) = (\mu_1 b_z / 2\pi i) \{ \log(\zeta - \beta) + K [\log(\zeta - 1/\beta) - \log \zeta] \\ + (1 - K^2) \sum_{n=0}^{\infty} (-K)^n [\log(\zeta - \lambda^{n+1}/\beta) - \log \zeta] \}. \quad (21)$$

By using (21) it is easily shown that this solution contains the results of Smith [1] and Dundurs [2] as special cases.

Screw Dislocation near a Circular Boundary. The solution for a screw dislocation near a circular inclusion of radius a can be obtained directly from Corollary 1. Thus for a dislocation with Burgers vector $b = (0, 0, b_z)$ placed at the point $z = z_0 (|z_0| > 0)$, one has

$$F_1(z) = (\mu_1 b_z / 2\pi i) \{ \log(z - z_0) + K [\log(z - a^2/\bar{z}_0) - \log z - \pi i] \}, \\ F_2(z) = (\mu_1 b_z / 2\pi i) (1 + K) \log(z - z_0). \quad (22)$$

For a dislocation, put at $z = z_1 (|z_1| < a)$ inside the inclusion, Corollary 1 yields

$$F_1(z) = (\mu_2 b_z / 2\pi i) [1/(1 + K)] \{ \log(z - z_1) + K [\log(z - a^2/\bar{z}_1) - \log z - \pi i] \}, \\ F_2(z) = (\mu_2 b_z / 2\pi i) \log(z - z_1). \quad (23)$$

From the first of equations (23), it is seen that the solution contains an inadmissible singularity in the matrix. Removing it by another application of Corollary 1 results in

$$F_1(z) = (\mu_2 b_z / 2\pi i) \{ (1 - K) \log(z - z_1) - K \log z - K\pi i \}, \\ F_2(z) = (\mu_2 b_z / 2\pi i) \{ \log(z - z_1) - K \log(z - a^2/\bar{z}_1) \}, \quad (24)$$

which is the desired solution. Solutions (22) and (24) are in agreement with the results of Dundurs [2] and Smith [1]. Upon letting the rigidity of the matrix or inclusion go to zero, one recovers the solutions, due to Siems [3] and Eshelby [4], for a screw dislocation inside a circular cylinder and in an unbounded solid containing a cylindrical cavity.

Screw Dislocation near a Curvilinear Cavity or Rigid Inclusion. The solution for a screw dislocation near an elastic elliptic inclusion gives some indication of the complexity of the general curvilinear inclusion problem. In fact, it seems that only limited results can be generated for the case of an elastic inclusion.

If the inclusion is rigid, the analysis simplifies considerably and the general solution can be found immediately from Corollary 2. Thus, the

solution is

$$F(\zeta) = (\mu b_z / 2\pi i) \{ \log (\zeta - \zeta_0) + \log (\zeta - 1/\bar{\zeta}_0) - \log \zeta - \pi i \}, \quad (25)$$

where ζ is related to z by $z = \omega(\zeta)$. The transformation $\omega(\zeta)$ must be restricted so that it maps the exterior of $|\zeta| = 1$ into the exterior of Σ . The dislocation is put at the point z_0 which is related to ζ_0 by $z_0 = \omega(\zeta_0)$. In the case of a rigid elliptic inclusion, (25) reduces to the results of Smith [1].

For a dislocation near a curvilinear cavity, Corollary 2 yields

$$F(\zeta) = (\mu b_z / 2\pi i) \{ \log (\zeta - \zeta_0) - \log (\zeta - 1/\bar{\zeta}_0) + \log \zeta + \pi i \}. \quad (26)$$

For an elliptic cavity, (26) reduces to the results of Smith [1].

IV. Screw Dislocation Near Two Circular Inclusions

Now consider the problem of a screw dislocation near two circular inclusions. For the sake of simplicity, assume that both inclusions are of unit radius and have the same shear modulus. Superscripts I and II will be used to distinguish the two inclusions. Let a screw dislocation with Burgers vector b_z be put at $z = z_0$ as shown in figure 2. By Corollary 1, the potentials satisfying the boundary conditions between inclusion I and the

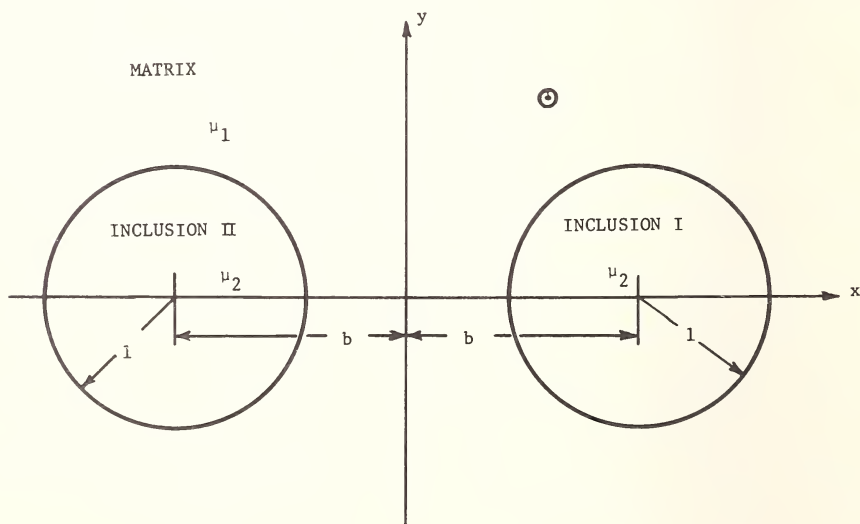


FIGURE 2. Screw dislocation \odot near two equal inclusions of unit radius.

matrix (interface I) are

$$F_1(z) = (\mu_1 b_z / 2\pi i) \{ \log(z - z_0) + K \log [1/(z - b) + b - \bar{z}_0] \},$$

$$F'_2(z) = (\mu_1 b_z / 2\pi i) (1 + K) \log(z - z_0).$$

Even though the boundary conditions at interface I are satisfied, those at the inclusion II-matrix interface (interface II) are not. They can be satisfied by applying Corollary 1 to inclusion II. This yields

$$\begin{aligned} F_1(z) &= (\mu_1 b_z / 2\pi i) \{ \log(z - z_0) + K[\log \{1/(z - b) + b - \bar{z}_0\} \\ &\quad + \log \{1/(z + b) - b - \bar{z}_0\}] + K^2 \log [1/\{1/(z + b) - 2b\} + b - z_0] \}, \end{aligned}$$

$$F'_2(z) = (\mu_1 b_z / 2\pi i) (1 + K) \log(z - z_0),$$

$$F''_2(z) = (\mu_1 b_z / 2\pi i) (1 + K) \{ \log(z - z_0) + K \log [1/(z - b) + b - \bar{z}_0] \}.$$

The continuity conditions at interface I are now violated. Applying Corollary 1 to this interface will guarantee the required continuity at interface I, while violating the conditions at interface II. Repeated application of the corollary finally yields

$$\begin{aligned} F_1(z) &= (\mu_1 b_z / 2\pi i) \left\{ \log(z - z_0) + \sum_{n=1}^{\infty} K^{2n-1} [\log(g_{2n-1} + b - \bar{z}_0) \right. \\ &\quad \left. + \log(h_{2n-1} - b - \bar{z}_0)] \right. \\ &\quad \left. + \sum_{n=1}^{\infty} K^{2n} [\log(g_{2n} - b - z_0) + \log(h_{2n} + b - z_0)] \right\}, \end{aligned} \quad (27)$$

$$\begin{aligned} F'_2(z) &= (\mu_1 b_z / 2\pi i) (1 + K) \left\{ \log(z - z_0) + \sum_{n=1}^{\infty} [K^{2n-1} \log(h_{2n-1} - b - \bar{z}_0) \right. \\ &\quad \left. + K^{2n} \log(h_{2n} + b - z_0)] \right\}, \end{aligned} \quad (28)$$

$$\begin{aligned} F''_2(z) &= (\mu_1 b_z / 2\pi i) (1 + K) \left\{ \log(z - z_0) + \sum_{n=1}^{\infty} [K^{2n-1} \log(g_{2n-1} + b - \bar{z}_0) \right. \\ &\quad \left. + K^{2n} \log(g_{2n} - b - z_0)] \right\}, \end{aligned} \quad (29)$$

where

$$\begin{aligned} h_1 &= 1/(z + b), \quad h_{2n} = 1/(h_{2n-1} - 2b), \quad h_{2n+1} = 1/(h_{2n} + 2b), \\ g_1 &= 1/(z - b), \quad g_{2n} = 1/(g_{2n-1} + 2b), \quad g_{2n+1} = 1/(g_{2n} - 2b). \end{aligned} \quad (30)$$

Contractions h_n and g_n may be rewritten in a more tractable form as

$$h_n = \frac{a_n + c_n(z+b)}{d_n + e_n(z+b)}, \quad g_n = \frac{\alpha_n + \beta_n(z-b)}{\delta_n + \gamma_n(z-b)}, \quad (31)$$

where

$$a_n = d_{n-1}, \quad c_n = e_{n-1}, \quad \alpha_n = \delta_{n-1}, \quad \beta_n = \gamma_{n-1}, \quad (32a)$$

$$d_n = a_{n-1} + 2bd_{n-1}, \quad e_n = c_{n-1} + 2be_{n-1}, \quad (n \text{ odd}), \quad (32b)$$

$$\delta_n = \alpha_{n-1} - 2b\delta_{n-1}, \quad \gamma_n = \beta_{n-1} - 2b\gamma_{n-1},$$

$$d_n = a_{n-1} - 2bd_{n-1}, \quad e_n = c_{n-1} - 2be_{n-1}, \quad (n \text{ even}), \quad (32c)$$

$$\delta_n = \alpha_{n-1} + 2b\delta_{n-1}, \quad \gamma_n = \beta_{n-1} + 2b\gamma_{n-1},$$

with

$$a_1 = c_1 = \alpha_1 = \gamma_1 = 1, \quad c_1 = d_1 = \beta_1 = \delta_1 = 0. \quad (33)$$

That (27), (28) and (29) constitute the desired solution is readily verified by using contractions (31).

V. Screw Dislocation in Solids With Plane Boundaries

Finally, consider application of theorem 2 to screw dislocations in solids with plane boundaries. Using the notation of theorem 2, the solution for a screw dislocation at z_0 in region 1 of the two joined half-planes is

$$F_1(z) = (\mu_1 b_z / 2\pi i) \{ \log(z - z_0) + K \log(z - \bar{z}_0) \}, \quad (34)$$

$$F_2(z) = (\mu_1 b_z / 2\pi i) (1 + K) \log(z - z_0).$$

This solution can be shown to be equivalent to the results of Head [9]. Solutions for solids with more complicated plane boundaries may be obtained by the procedure used in the two inclusion problem. Since the results for most problems of practical interest are available in the literature (Chou [6, 7], Head [8], Leibfried and Dietze [10]), these solutions will not be repeated here.

VI. Energy of Screw Dislocation Near Finite Inclusions

The strain energy due to the presence of the dislocation may be computed as the work required to introduce the screw dislocation into the material, that is,

$$W = \frac{1}{2} b \int_{x_0 + \epsilon}^R \sigma_{yz} \Big|_{y=y_0} dx, \quad (35)$$

where R is a distance corresponding to the material size and ϵ is the core radius of the dislocation. Since $\sigma_{yz} = -\text{Im} \{ \partial F(z)/\partial z \}$, one formally has (Siems, [3])

$$\begin{aligned} W &= -\frac{1}{2} b \int_{x_0+\epsilon}^R \text{Im} \{ \partial F(z)/\partial z \} dx \\ &= (\mu b^2/4\pi) \log(R/\epsilon) + (b/2) \text{Im} \{ F^*(z_0) \}, \end{aligned} \quad (36)$$

where $F^*(z_0)$ consists of the part of the potential remaining after the dislocation singularity has been removed. The first term in (36) is the self energy of the screw dislocation. Equation (36) is the appropriate expression for the interaction energy of a screw dislocation put in the matrix. The results have to be modified for a dislocation inside the inclusion.

Since the dislocation tends to seek the region of minimum interaction energy, some qualitative insight into the interaction of a dislocation with finite inhomogeneities may be gained by examining the energy surface or function. This is done next.

Dislocation Near a Circular Inclusion. Equation (36) is applicable in the case of a screw dislocation near a circular inclusion. Substituting (22) into (36) yields

$$\begin{aligned} W &= (\mu_1 b^2/4\pi) \{ \log(R/\epsilon) - K \log [(z_0 \bar{z}_0 - a^2)/z_0 \bar{z}_0] \} \\ &= (\mu_1 b^2/4\pi) \{ \log(R/\epsilon) + K \log [\beta^2/(\beta^2 - 1)] \}, \quad (1 < \beta < \infty), \end{aligned} \quad (37)$$

where β is the radial distance from the center of the inclusion. The strain energy tends to a maximum or minimum value at the interface as K varies from one to minus one. Since the dislocation seeks the minimum energy configuration, one immediately has that the dislocation is repelled by a hard inclusion ($K > 0$) and attracted by a soft one ($K < 0$), with no equilibrium positions near the inclusion.

Dislocation Near a Curvilinear Cavity or Rigid Inclusion. The energy for a screw dislocation near a rigid curvilinear inclusion can be found by substituting (25) into (36) and using the result that $F_1(z)$ is identically equal to $F_1(\zeta)$. Thus one has

$$W = (b^2 \mu / 4\pi) \{ \log(R/\epsilon) - \log [(\zeta_0 \bar{\zeta}_0 - 1)/\zeta_0 \bar{\zeta}_0] \}. \quad (38)$$

Similarly for a screw dislocation near a curvilinear cavity, (26) gives

$$W = (b^2 \mu / 4\pi) \{ \log(R/\epsilon) + \log [(\zeta_0 \bar{\zeta}_0 - 1)/\zeta_0 \bar{\zeta}_0] \}. \quad (39)$$

From (38) and (39), it is seen that a rigid curvilinear inclusion will always

repell a screw dislocation, while a curvilinear cavity will attract the dislocation. Furthermore, the conformal nature of the mapping used indicates that no equilibrium positions exist near the inclusion.

Screw Dislocation Near an Elastic Elliptic Inclusion. For a screw dislocation near an elliptic inclusion, (21) yields

$$W = (b^2 \mu_1 / 4\pi) \left\{ \log (R/\epsilon) + K \log [\beta^2 / (\beta^2 - 1)] + (1 - K^2) \sum_{n=0}^{\infty} (-K)^n \log [\beta^2 / (\beta^2 - \lambda^{n+1})] \right\}, \quad (40)$$

where β specifies the position of the dislocation on the x -axis through the transformation $x_0 = c[\beta + \lambda\beta^{-n}]$. It seems that a hard inclusion ($K > 0$) will repell the dislocation, while a soft one ($K < 0$) will attract it. Whether an equilibrium position exists near the inclusion can not be ascertained without summing the series; but it seems that no such equilibrium position exists, based on the structure of the energy function.

Screw Dislocation Near Two Circular Inclusions. For the screw dislocation near two circular inclusions, (27) gives

$$W = (\mu_1 b_z^2 / 4\pi) \left\{ \log (R/\epsilon) - \sum_{n=1}^{\infty} K^{2n-1} [\log (g_{2n-1}^* + b - \bar{z}_0) + \log (h_{2n-1}^* - b - \bar{z}_0)] - \sum_{n=1}^{\infty} K^{2n} [\log (g_{2n}^* - b - z_0) + \log (h_{2n}^* + b - z_0)] \right\}, \quad (41)$$

where g_i^* and h_i^* are the contractions given by (31) evaluated at $z = z_0$. A close examination of (41) indicates that hard inclusions will repell the dislocation while soft ones will attract it. Furthermore, no equilibrium positions exist near the inclusions.

VII. Conclusion

The approach illustrated in the previous sections is completely general and, hence, it may be used to solve other screw dislocation problems in a systematic manner. Furthermore, it indicates the best procedure to be followed in solving edge dislocation problems. The procedure is: First, find general results corresponding to theorems one and two for the case of plane deformation. The results will then yield simple and systematic solutions of edge dislocation problems.

VIII. Acknowledgement

This article is an application of the general results obtained during research supported by the Advanced Research Projects Agency, Department of Defense through Grant No. AF 33 (615)-3110 administered by the Air Force Materials Laboratory.

IX. References

- [1] Smith, E., Int. J. Eng. Sci. **6**, 129 (1968).
- [2] Dundurs, J., in Recent Advances in Engineering Science (Proc. 3d Technical Meeting, Soc. Eng. Sci., Univ. of California, 1965) A. C. Eringen, Ed. (Gordon and Breach, New York, 1967).
- [3] Seims, R., Phys. Kondens. Materie **2**, 1 (1964).
- [4] Eshelby, J. D., J. Appl. Phys. **24**, 176 (1953).
- [5] Kovács, I., Acta Physica Hungarica **15**, 11 (1962).
- [6] Chou, Y. T., Phys. Stat. Sol. **17**, 509 (1966).
- [7] Chou, Y. T., Acta Metallurgica **13**, 1131 (1965).
- [8] Head, A. K., Australian J. Phys. **12**, 278 (1960).
- [9] Head, A. K., Phil. Mag. **44**, 92 (1953).
- [10] Leibfried, G., and Dietze, H. D., Zeits. fur Physik **126**, 790 (1949).
- [11] Dietze, H. D., and Leibfried, G., Statische Versetzungs theorie fur Körper mit freier Oberfläche, Diplomarbeit, Gottingen (1949).
- [12] Louat, N., in Proc. 1st Intern. Conf. on Fracture, Sendai, Japan (1965).
- [13] Milne-Thompson, L. M., Antiplane Elastic Systems (Springer-Verlag, Berlin, 1962).

SUBSONIC, SUPERSONIC, AND TRANSONIC DISLOCATIONS MOVING ON AN INTERFACE SEPARATING TWO MEDIA OF DIFFERENT ELASTIC PROPERTIES

H. M. Berg, J. E. Bloom, H. Ishii, R. H. Marion, D. E. Pease,
D. T. Spreng, J. B. Vander Sande and J. Weertman*

*Materials Science Department and Materials Research Center
Northwestern University
Evanston, Illinois 60201*

This paper examines the problem of a dislocation moving on an interface separating two isotropic elastic media that have differing elastic constants and densities. This problem has application to the phenomenon of diffusionless transformations. Solutions are found for moving screw dislocations, gliding edge dislocations, and climbing edge dislocations. It is assumed that the dislocation velocity lies in either the subsonic, the transonic, or the supersonic velocity region. We have generalized the analysis that was used in a study of the elastic displacements and stress field of subsonic, transonic, and supersonic dislocations moving in an ordinary elastic medium. The results given in the present paper are formally identical to those obtained in that simpler analysis.

Key words: Dislocation dynamics; interface dislocations; supersonic dislocation.

I. Introduction

The problem of a dislocation moving on an interface separating two media of differing elastic properties is interesting from both the theoretical and the practical viewpoint. Diffusionless transformations in crystals probably involve dislocations moving on the interface between transformed and untransformed material. Since the amount of energy released in such transformations may be large, high dislocation velocities are to be expected. In fact, Eshelby [1] has proposed that dislocations may move at supersonic velocities in diffusionless transformations.

* Students and Instructor of Advanced Dislocation Class at Northwestern University.

One of us, Weertman [2], has considered the problem of a discrete screw or gliding edge dislocation moving with a subsonic velocity on an interface between two elastic media of differing physical properties. In the present paper we consider a smeared out dislocation (either screw, gliding edge, or climbing edge dislocation) moving with a *uniform* velocity which may be in the supersonic, transonic, or subsonic velocity range.

The fundamental equations used in our analysis are reviewed in the next section. The derivation of these equations can be found in the review article¹ of Weertman [3] or in the literature cited therein.

II. Review

Let the elastic constants² (Lamé constants) of the two elastic half-spaces be μ_i and λ_i , where $i=1$ refers to the material above the interface and $i=2$ to the material below the interface. Let the density of the two materials be ρ_i . The shear wave velocity c_{i1} is given by the relationship $c_{i1}^2 = \mu_i/\rho_i$ and the longitudinal wave velocity c_{i2} by $c_{i2}^2 = (\lambda_i + 2\mu_i)/\rho_i$. It is assumed that the slower shear wave velocity always occurs in the upper half-space ($c_{11} < c_{21}$).

Assume that the net displacement D across the interface plane is governed by some non-linear periodic force law such as shown in figure 1. That is, at any point on the interface plane the stress required to produce a given net displacement across the plane varies periodically with the net displacement.

The displacement D is equal to $w_1 - w_2$, where w_1 and w_2 are the displacements at the interface in the upper and lower medium, respectively. When the two halfspaces are identical in their properties by symmetry $w_1 = -w_2$. In general, $w_1 \neq -w_2$.

A dislocation density function $B(x)$ is defined by the requirement that $B(x)\delta x$ equal the total strength of the Burgers vectors of all dislocations lying between x and $x + \delta x$ on the interface plane. The distance x is

¹This article discusses the problem of smeared out subsonic, transonic, and supersonic dislocations moving on an interface separating two *identical* elastic half-spaces. The reader may find it helpful to read this review article before considering the more general problem treated in the present paper.

²In this paper the subscripts on any term, say H_{ij} , have the following significance: The first subscript refers to the half-space ($i=1$ for the upper and $i=2$ for the lower half-space). The second subscript refers to the sound velocity upon which the term depends ($j=1$ for the shear wave velocity and $j=2$ for the longitudinal wave velocity). If the term contains only one subscript it refers to the half-space.

measured in a coordinate system moving at the same velocity as the dislocations. The function $B(x)$ also equals the derivative $-dD/dx$, which in turn is equal to $-dw_1/dx + dw_2/dx$.

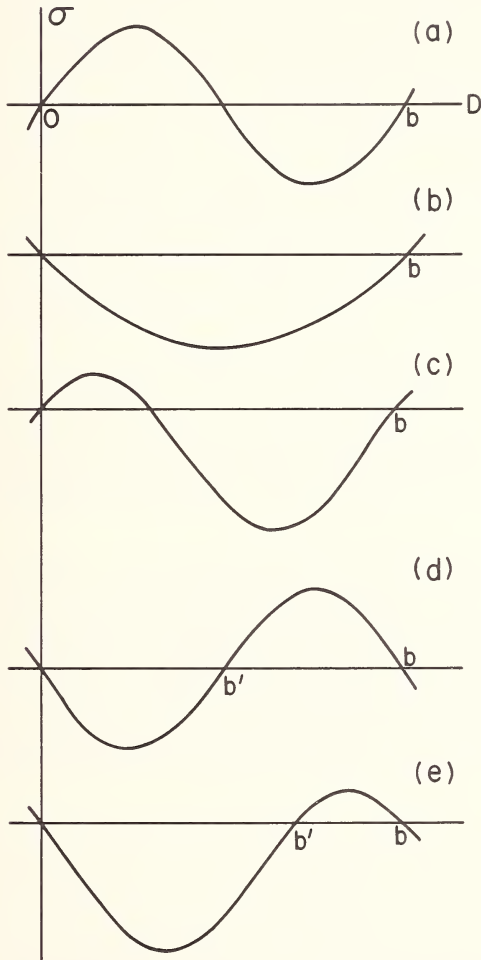


FIGURE 1. Various laws of stress σ versus displacement D . (a) Subsonic. (b) Supersonic. (c) Transonic. (d) Subsonic which starts in unstable equilibrium. (e) Transonic which starts in unstable equilibrium. (Note that laws (d) and (e) are more likely to lead to a supersonic dislocation of partial Burgers vector b' than a subsonic or transonic perfect dislocation of Burgers vector b .)

When the two elastic half-spaces have differing physical properties it is convenient to define two new dislocation density functions,

$$B_1(x) = -dw_1/dx \text{ and } B_2(x) = dw_2/dx.$$

Thus $B(x) = B_1(x) + B_2(x)$. The displacement $D(x)$ is equal to

$$\int_x^{\infty} B(x) dx = \int_x^{\infty} [B_1(x) + B_2(x)] dx$$

and the total Burgers vector b of all the infinitesimal dislocations lying on the interface plane is equal to $\int_{-\infty}^{\infty} [B_1(x) + B_2(x)] dx$.

The displacement field of a moving edge dislocation can be separated into two independent fields: one which involves only the shear wave velocity c_{i1} and another which involves only the longitudinal wave velocity c_{i2} . Therefore the distribution function $B_i(x)$ can be considered to be the sum of two dislocation distribution functions, $B_i(x) = \sum_{j=1}^2 B_{ij}(x)$, where $B_{i1}(x)$ arises from the displacement field which is a function of the shear wave velocity and $B_{i2}(x)$ from the field which is a function of the longitudinal wave velocity. For a screw dislocation $B_{i1}(x) \equiv B_i(x)$ and $B_{i2}(x) \equiv 0$.

Consider a smeared out dislocation which lies parallel to the z -axis and which moves in the x -direction. The existence of a dislocation density $B_{ij}(x)$ will produce on the interface plane ($y=0$ plane) a stress $[\sigma_i(x)]_j$, where σ_i stands for the shear stress $[\sigma_{yz}]_i$ in the case of a screw dislocation, the shear stress $[\sigma_{xy}]_i$ for a gliding edge dislocation, and the tensile or compressive stress $[\sigma_{yy}]_i$ for a climbing edge dislocation.

At any subsonic dislocation velocity V (where $V < c_{ii}$) the stress $[\sigma_i]_j$ is given by

$$[\sigma_i(x)]_j = (\mu_i C_{ij}/\pi) \int_{-\infty}^{\infty} B_{ij}(x') (x-x')^{-1} dx' \quad (1)$$

where $C_{ii} = \beta_i$ for a screw dislocation; $C_{ii} = 2\alpha_i^2/\beta_i$ and $C_{ii} = 2\gamma_i$ for a gliding edge dislocation; and $C_{ii} = 2\beta_i$ and $C_{ii} = 2\alpha_i^2/\gamma_i$ for a climbing edge dislocation. Here $\beta_i^2 = 1 - V^2/c_{ii}^2$; $\gamma_i^2 = 1 - V^2/c_{ii}^2$; and $\alpha_i^2 = 1 - V^2/2c_{ii}^2$.

Equation (1) can be inverted to give

$$B_{ij}(x) = -(1/\pi\mu_i C_{ij}) \int_{-\infty}^{\infty} [\sigma_i(x')]_j (x-x')^{-1} dx'. \quad (2)$$

At any supersonic dislocation velocity ($V > c_{i2}$ for an edge dislocation and $V > c_{i1}$ for a screw dislocation), eqs (1) and (2) are replaced with

$$[\sigma_i(x)]_j = -\mu_i S_{ij} B_{ij}(x) \quad (3)$$

where $S_{i1} = \beta_i^*$ for a screw dislocation; $S_{i1} = -2\alpha_i^2/\beta_i^*$ and $S_{i2} = 2\gamma_i^*$ for a gliding edge dislocation; and $S_{i1} = 2\beta_i^*$ and $S_{i2} = -2\alpha_i^2/\gamma_i^*$ for a climbing edge dislocation. Here $\beta_i^{*2} = -\beta_i^2$ and $\gamma_i^{*2} = -\gamma_i^2$.

For edge dislocations moving at a transonic velocity ($c_{i1} < V < c_{i2}$), eqs (1) and (2) are valid for the dislocation density function B_{i2} and eq (3) is valid for the function B_{i1} .

In the case of edge dislocations, there is an additional traction across the interface plane besides the traction given by eqs (1) and (3). A stress $[\tau_i(x)]_j$ can exist, where τ_i stands for the stress $[\sigma_{yy}]_i$ for gliding edge dislocations and for the stress $[\sigma_{xy}]_i$ for climbing edge dislocations.

The stress τ_i is given by

$$[\tau_i(x)]_j = -(-1)^i \mu_i T_{ij} B_{ij}(x) \quad (4)$$

where $T_{i1} = 2$ and $T_{i2} = 2\alpha_i^2$ for gliding edge dislocations and $T_{i1} = -2\alpha_i^2$ and $T_{i2} = -2$ for climbing edge dislocations. Equation (4) is valid over the entire velocity range ($0 \leq V < \infty$).

III. Screw Dislocations

III.1. Subsonic ($V < c_{11} < c_{21}$)

The shear stress acting on the interface plane must be continuous across it. Thus it can be seen from eqs (1) and (2) that $\mu_1 \beta_1 B_{11}(x) = \mu_2 \beta_2 B_{21}(x)$. From this relationship the following equations are derived easily:

$$\sigma(x) = [(\mu_1 \beta_1 \mu_2 \beta_2)/\pi(\mu_1 \beta_1 + \mu_2 \beta_2)] \int_{-\infty}^{\infty} B(x') (x - x')^{-1} dx' \quad (5)$$

$$B(x) = -[(\mu_1 \beta_1 + \mu_2 \beta_2)/\pi(\mu_1 \beta_1 \mu_2 \beta_2)] \int_{-\infty}^{\infty} \sigma(x') (x - x')^{-1} dx' \quad (6)$$

where $\sigma(x) = \sigma_{yz}(x)$ is the shear stress acting across the interface and $B(x) = B_{11}(x) + B_{21}(x)$.

Equations (5) and (6) can be satisfied by any periodic stress-displacement law, such as is shown in figure 1a, in which the work done per unit distance of dislocation motion, $\mathcal{W} = -\int_0^b \sigma dD$, is equal to zero (see Weertman [3]). A dislocation can move at any arbitrary subsonic dislocation velocity

when such a stress-displacement law exists at the interface. The "width" of a smeared dislocation goes to zero as V approaches c_{11} .

III.2. Supersonic ($V > c_{21} > c_{11}$)

The shear stress on the interface plane in this velocity range may be obtained from eq (3) and the condition that the shear stress is continuous across the interface plane.

$$\sigma(x) = -[(\mu_1 \beta_1^* \mu_2 \beta_2^*) / (\mu_1 \beta_1^* + \mu_2 \beta_2^*)] B(x). \quad (7)$$

Any periodic stress-displacement law (such as that shown in fig. 1b) which has the characteristics that the interface initially is in unstable equilibrium and that the stress does not change sign up to the displacement $D=b$ will satisfy eq (7) (see Weertman [3]). The interface does an amount of work $\mathcal{W} = - \int_0^b \sigma dD > 0$ as a dislocation moves across it. The width of a smeared out dislocation approaches zero as V approaches c_{21} . The dislocation can move at any arbitrary supersonic velocity.

III.3. Transonic ($c_{11} < V < c_{21}$)

Setting the stress given by eq (1) equal to the stress given by eq (3) produces the following equations:

$$\begin{aligned} \sigma(x) = & [(\mu_1 \beta_1^* \mu_2 \beta_2) / \{(\mu_1 \beta_1^*)^2 + (\mu_2 \beta_2)^2\}] [- (1/\mu_1 \beta_1^*) B(x) \\ & + (1/\pi \mu_2 \beta_2) \int_{-\infty}^{\infty} B(x') (x-x')^{-1} dx'] \end{aligned} \quad (8)$$

$$B(x) = - (1/\mu_1 \beta_1^*) \sigma(x) - (1/\pi \mu_2 \beta_2) \int_{-\infty}^{\infty} \sigma(x') (x-x')^{-1} dx'. \quad (9)$$

Equations (8) and (9) are satisfied (see Weertman [3]) by a stress-displacement law (such as that shown in fig. 1c) which has the characteristics that the interface gives up energy as a dislocation moves across it, $\mathcal{W} = - \int_0^b \sigma dD > 0$, and that the interface is in stable equilibrium at the displacement $D=0$. Thus the stress must change sign when D increases from $D=0$ to $D=b$.

A dislocation cannot move at an arbitrary velocity in the transonic region. For example, for the stress-displacement law (see Weertman [3])

$$\sigma = \sigma_0 + (\mu_0/\pi) \log \{(b-D)/D\}, \quad (10)$$

where σ_0 and μ_0 are positive constants, a dislocation can move only at the velocity which satisfies the equation

$$\beta_i^*/\beta_2 = (\mu_2/\mu_1)(\mu_0/\sigma_0). \quad (11)$$

IV. Edge Dislocation

The edge dislocation problem involves the four dislocation distribution functions $B_{ij}(x)$. Four independent equations are required to determine these four functions. Two of these equations are obtained from the requirement that the traction $\sum_{j=1}^2 [\sigma_i(x)]_j$ and the traction $\sum_{j=1}^2 [\tau_i(x)]_j$ be continuous across the interface plane. A third equation is

$$\int_{-\infty}^{\infty} B(x) dx = b,$$

where $B(x) = B_{11}(x) + B_{12}(x) + B_{21}(x) + B_{22}(x)$.

The fourth required equation is obtained by noting that the displacement normal to the displacement D must be continuous across the interface. For gliding edge dislocations, this is the displacement in the y -direction normal to the interface plane; and for climbing edge dislocations, it is the displacement in the x -direction parallel to the interface plane.

Let $[u_i(x)]_j$ represent the displacement on the interface plane which is normal to the displacement D and which is produced by the dislocation distribution functions $B_{ij}(x)$. For $V < c_{i1}$ or $V < c_{i2}$ this displacement is (Weertman [3])

$$[u_i(x)]_j = (G_{ij}/2\pi) \int_{-\infty}^{\infty} B_{ij}(x') \log(x - x')^2 dx' \quad (12)$$

apart from an arbitrary constant term. In this equation $G_{i1} = 1/\beta_i$ and $G_{i2} = \gamma_i$ for gliding edge dislocations and $G_{i1} = -\beta_i$ and $G_{i2} = -1/\gamma_i$ for climbing edge dislocations.

For $V > c_{i1}$ or $V > c_{i2}$ the displacement $[u_i(x)]_j$ is shown easily from results in Weertman [3] to be

$$[u_i(x)]_j = H_{ij} \int_x^{\infty} B_{ij}(x) dx \quad (13)$$

where $H_{i1} = 1/\beta_i^*$ and $H_{i2} = -\gamma_i^*$ for gliding edge dislocations and $H_{i1} = \beta_i^*$ and $H_{i2} = -1/\gamma_i^*$ for climbing edge dislocations.

IV.1. Subsonic ($V < c_{11} < c_{21}$)

The dislocation distribution functions $B_{ij}(x)$ are determined from the four independent equations:

$$\sum_{i,j=1}^2 B_{ij}(x) = B(x), \quad (14a)$$

$$\sum_{i,j=1}^2 \mu_i T_{ij} B_{ij}(x) = 0, \quad (14b)$$

$$\sum_{i,j=1}^2 (-1)^i \mu_i C_{ij} B_{ij}(x) = 0, \quad (14c)$$

$$\sum_{i,j=1}^2 (-1)^i G_{ij} B_{ij}(x) = 0. \quad (14d)$$

From these we find that:

$$\sigma(x) = (\bar{\mu}/\pi) \int_{-\infty}^{\infty} B(x') (x - x')^{-1} dx' \quad (15)$$

and

$$B(x) = -(1/\bar{\mu}\pi) \int_{-\infty}^{\infty} \sigma(x') (x - x')^{-1} dx' \quad (16)$$

where $\sigma(x)$, the stress acting on the interface, is $\sigma_{xy}(x)$ for gliding edge dislocations and $\sigma_{yy}(x)$ for climbing edge dislocations. The constant $\bar{\mu}$ is given by

$$\bar{\mu} = \mu_1 (C_{11} \Delta_{11} + C_{12} \Delta_{12}) / \Delta \quad (17a)$$

where Δ_{11} , Δ_{12} , and Δ are the values of the determinates

$$\Delta = \begin{vmatrix} 1 & 1 & 1 & 1 \\ \mu_1 T_{11} & \mu_1 T_{12} & \mu_2 T_{21} & \mu_2 T_{22} \\ -\mu_1 C_{11} & -\mu_1 C_{12} & \mu_2 C_{21} & \mu_2 C_{22} \\ -G_{11} & -G_{12} & G_{21} & G_{22} \end{vmatrix} \quad (17b)$$

$$\Delta_{11} = \begin{vmatrix} \mu_1 T_{12} & \mu_2 T_{21} & \mu_2 T_{22} \\ -\mu_1 C_{12} & \mu_2 C_{21} & \mu_2 C_{22} \\ -G_{12} & G_{21} & G_{22} \end{vmatrix} \quad (17c)$$

$$\Delta_{12} = \begin{vmatrix} -\mu_1 T_{11} & \mu_2 T_{21} & \mu_2 T_{22} \\ \mu_1 C_{11} & \mu_2 C_{21} & \mu_2 C_{22} \\ G_{11} & G_{21} & G_{22} \end{vmatrix}. \quad (17d)$$

Equations (15) and (16) are valid at any subsonic velocity V for stress-displacement laws which fulfill the requirement that the interface does no work ($\mathcal{W} = \int_0^b \sigma dD = 0$). When $\bar{\mu}$ is a positive quantity a stress-displacement law such as is shown in figure 1a satisfied eqs (15) and (16). Should $\bar{\mu}$ be a negative quantity a stress-displacement law such as is shown in figure 1d is needed to satisfy eqs (15) and (16). This displacement law requires the interface to be in unstable equilibrium at $D=0$. (The law shown in figure 1d is more likely to produce a supersonic partial dislocation than a subsonic perfect dislocation.)

IV. 2. Supersonic ($V > c_{12}$ and c_{22})

For the supersonic dislocations, eqs (14a) and (14b) remain unaltered. In eq (14c) S_{ij} replaces the term C_{ij} and in eq (14d) H_{ij} replaces the term G_{ij} . Equations (15) and (16) are replaced with

$$\sigma(x) = -[\mu_1(S_{11}\Delta_{11} + S_{12}\Delta_{12})/\Delta]B(x) \quad (18)$$

where Δ_{11} , Δ_{12} , and Δ are given by eqs (17b), (17c), and (17d) when C_{ij} is replaced with S_{ij} and G_{ij} with H_{ij} . Solutions of eq (18) exist for stress-displacement laws of the form shown in figure 1b. These laws describe a situation in which the interface does a net amount of work ($\mathcal{W} = -\int_0^b dD > 0$) and the stress does not change sign. Solutions of eq (18) exist for any arbitrary supersonic dislocation velocity V for which $(S_{11}\Delta_{11} + S_{12}\Delta_{12})/\Delta$ is a positive quantity. (When this term is a negative quantity the interface plane absorbs rather than gives up energy.)

IV. 3. Transonic ($c_{11} < V < c_{12}$ or c_{22})

In this velocity region the dislocations are moving faster than the slower shear wave velocity but slower than the faster longitudinal wave velocity. Equations (14a) and (14b) again remain valid. Equation (14c) is replaced with

$$\sum_{i,j=1}^2 (-1)^i \mu_i \left\{ \begin{array}{l} (C_{ij}/\pi) \int_{-\infty}^{\infty} B_{ij}(x') (x-x')^{-1} dx' \\ -S_{ij} B_{ij}(x) \end{array} \right\} = 0 \quad (19)$$

where the upper term in the bracket is used when $V < c_{ij}$ and the lower the lower term is used when $V > c_{ij}$.

Equation (14d) is replaced with

$$\sum_{i,j=1}^2 (-1)^i \left\{ \begin{array}{l} (G_{ij}/\pi) \int_{-\infty}^{\infty} B_{ij}(x') (x-x')^{-1} dx' \\ -H_{ij} B_{ij}(x) \end{array} \right\} = 0 \quad (20)$$

where again the upper term in the bracket is used when $V < c_{ij}$ and the lower term when $V > c_{ij}$.

From the form of eqs (19) and (20) it follows that the functions $B_{ij}(x)$ must have a solution of the form

$$B_{ij}(x) = N_{ij} B(x) + (M_{ij}/\pi) \int_{-\infty}^{\infty} B(x') (x-x')^{-1} dx' \quad (21)$$

where N_{ij} and M_{ij} are constants. If eq (21) is inserted into eqs (4a), (14b), (19), and (20), and use is made of the relationship

$$B(x) \equiv -(1/\pi^2) \int_{-\infty}^{\infty} \int_{-\infty}^{\infty} B(x'') (x'-x'')^{-1} (x-x')^{-1} dx'' dx',$$

four equations are obtained of the form

$$\sum_{i,j} F_{ij} B(x) + \sum_{i,j} F_{ij}^* \int_{-\infty}^{\infty} B(x') (x-x')^{-1} dx' = 0.$$

The quantities F_{ij} and F_{ij}^* are velocity-dependent constants. Equations of this form can hold at any arbitrary point x only if

$$\sum_{i,j} F_{ij} = 0 \text{ and } \sum_{i,j} F_{ij}^* = 0.$$

Thus we find the eight independent linear equations

$$\begin{aligned} \sum_{i,j=1}^2 N_{ij} &= 1; & \sum M_{ij} &= 0; \\ \sum \mu_i T_{ij} N_{ij} &= 0; & \sum \mu_i T_{ij} M_{ij} &= 0; \\ \sum (-1)^i \mu_i \left\{ \begin{array}{l} C_{ij} N_{ij} \\ -S_{ij} M_{ij} \end{array} \right\} &= 0; & \sum (-1)^i \mu_i \left\{ \begin{array}{l} C_{ij} M_{ij} \\ S_{ij} N_{ij} \end{array} \right\} &= 0; \\ \sum (-1)^i \left\{ \begin{array}{l} G_{ij} N_{ij} \\ -H_{ij} M_{ij} \end{array} \right\} &= 0; & \sum (-1)^i \left\{ \begin{array}{l} G_{ij} M_{ij} \\ H_{ij} N_{ij} \end{array} \right\} &= 0 \end{aligned} \quad (22)$$

which determine the eight constants N_{ij} and M_{ij} . Again, the upper term in each bracket is used when $V < c_{ij}$ and the lower term when $V > c_{ij}$.

The stress $\sigma(x)$ (where $\sigma(x)$ is $\sigma_{xy}(x)$ for gliding edge dislocations and $\sigma_{yy}(x)$ for climbing edge dislocations) which acts on the interface plane is given by the equation

$$\sigma(x) = -\mu_1 P B(x) + (\mu_1 R / \pi) \int_{-\infty}^{\infty} B(x') (x - x')^{-1} dx' \quad (23)$$

where

$$P = S_{11} N_{11} + \left\{ \begin{array}{l} C_{12} M_{12} \\ S_{12} N_{12} \end{array} \right\} \quad (24a)$$

and

$$R = -S_{11} M_{11} + \left\{ \begin{array}{l} C_{12} N_{12} \\ -S_{12} M_{12} \end{array} \right\}. \quad (24b)$$

The upper term in each bracket is used when $V < c_{12}$ and the lower term when $V > c_{12}$. Equation (23) can be inverted to give

$$B(x) = [1/\mu_1(P^2 + R^2)] \left[-P\sigma(x) - (R/\pi) \int_{-\infty}^{\infty} \sigma(x') (x - x')^{-1} dx' \right]. \quad (25)$$

When P and R are positive quantities, a stress-displacement law of the type shown in figure 1c can satisfy (23) at some unique velocity. For the stress-displacement law given by eq (10) the velocity must be such that the equation $R/P = \mu_0/\sigma_0$ also is satisfied. If R is a negative quantity and P is positive, a stress-displacement law of the type shown in figure 1e can satisfy eq (23). Again, only at some unique velocity is it possible to satisfy eq (23). (For a stress-displacement law of the form given by eq (10) but with μ_0 in that equation a negative rather than a positive

quantity, the velocity must be such that the same equation $R/P = \mu_0/\sigma_0$ is satisfied.) At velocities where P is a negative constant no solution exists because the interface must absorb rather than give up energy.³

V. Summary

We have shown that the solution of the problem of smeared out dislocations moving on an interface between two media of differing elastic properties is formally the same as the solution for smeared out dislocations moving between two identical elastic half-spaces. If the stress-displacement law is such that the interface cannot give up energy the dislocations move at an arbitrary subsonic velocity, where a subsonic velocity is defined to be any velocity smaller than the smaller shear wave velocity. If the stress-displacement law requires the interface to give up energy and if the stress never changes sign as the displacement changes, the dislocations move at an arbitrary supersonic velocity. A supersonic velocity is defined to be larger than the faster longitudinal wave velocity for edge dislocations and larger than the faster shear wave velocity for screw dislocations. If the stress-displacement law requires the interface to give up energy but the stress changes sign when the displacement is changed, the dislocations move at a unique transonic velocity. A transonic velocity for screw dislocations is larger than the slower shear wave velocity but smaller than the faster shear wave velocity, and a transonic velocity for edge dislocations is larger than the slower shear wave velocity and smaller than the faster longitudinal wave velocity.

VI. Acknowledgement

The research upon which this paper is based was supported in part by the Advanced Research Projects Agency of the Department of Defense through the Northwestern University Materials Research Center.

VII. References

- [1] Eshelby, J. D., Proc. Phys. Soc. (London) **B69**, 1013 (1956).
- [2] Weertman, J., J. Mech. and Phys. Solids **11**, 197 (1963).
- [3] Weertman, J., Mathematical Theory of Dislocations, T. Mura, Ed. (American Society of Mechanical Engineers, New York, 1969) p. 178.

³ When the interface plane gives up energy the supersonic components of the dislocation radiate sound waves that diverge from the interface plane. If the interface plane absorbs energy it is possible to set up a formal dislocation-like solution of the problem in which the supersonic components of the dislocation absorb sound waves that converge on the interface. Such a solution requires the external generation of sound waves at the outer surface of a specimen and is not physically plausible.

Discussion on Papers by A. K. Head, K. Malén, and D. Kuhlmann-Wilsdorf and T. R. Duncan.

GRANATO: I'd like to ask Dr. Malén in what sense he means that the line tension goes negative at reasonable velocities? I would say that those were unreasonable velocities because they are never achieved under ordinary circumstances (for example, for yield stresses at room temperature).

MALÉN: You can get instability already at zero velocity, as Professor Head mentioned. I have only performed the calculation for certain directions, and you can find instability for lower velocities than you get in the isotropic case.

GRANATO: I thought that you implied that it still had to be within 5% and 10% of the speed of sound. My point is that I don't know of any "ordinary" circumstances where you get those speeds.

MALÉN: Yes. But these are more reasonable velocities than in the isotropic case, although I have not shown any very reasonable velocities here. However you can find instability already at zero velocity for some directions; so I suppose you can find more reasonable velocities.

GRANATO: The lowest velocity is zero?

MALÉN: That is well known already, that you can have unstable directions.

TEUTONICO: On the same point, I think it is misleading to compare the dislocation velocities to the transverse velocity. If you take the ratio of the velocity at which you get the instability to the limiting dislocation velocity in the cases you have shown, I think you will find that it is much higher than .9 or .95, because the transverse velocity is not the limiting velocity of dislocations—as you point out.

MALÉN: You are right. But, for instance, for an edge dislocation in lithium, you find the ratio you mention to be 0.6—See my table 1.

TEUTONICO: The ratio of, say, the velocity in lithium at which the instability occurs to the actual limiting velocity (which is about one half of the speed of sound in lithium for that direction) is very close to unity, which makes it even less reasonable.

KOEHLER: One point is that your calculations work for room temperature, is that correct?

MALÉN: Yes. But not for lithium.

KOEHLER: For lithium the instability which is associated with zero velocity occurs at low temperature. Is that correct?

MALÉN: I think that's right.

BESHERS: I would like to address my question to Professor Kuhlmann-Wilsdorf and Dr. Duncan about their paper. They are talking about the separation of close partials in stacking faults. What meaning can you give to the stacking fault energy when the partials are so close together that the cores are overlapping?

KUHLMANN-WILSDORF: This is a very relevant question. I have been aware of the difficulty of assigning a value to the stacking fault energy between close partials for a long time. We have chosen simply to employ the normal value of the stacking fault energy, also, in this case. I believe that the same has been done almost uniformly in the past by other workers in the field and, for want of a better solution, we continued this practice. It is, however, true that this choice involves some ambiguity. Instead, one should calculate from the local atom-atom interaction potentials the local stacking fault energy which is dependent on the actual displacement across the slip plane at the point considered. Very fortunately, the error involved in neglecting the said strain dependence of the stacking fault energy is probably small for the reason that the atomic interaction potentials across the slip plane are presumably far from sinusoidal, being rather flat at the top. Therefore, the error in assuming the stacking fault energy to be independent of strain is comparatively small, as the interaction energy is always near its maximum value.

SAADA: I would like to ask two questions. The first one is to Dr. Malén. Don't you think that the fact that the sound velocity varies with frequency could be in some cases more important than the effect of anisotropy, for example in lithium where the acoustic phonon dispersion curve has a singularity?

MALÉN: I didn't consider the question, and I don't know.

SAADA: The second question was for Professor Head. You pointed out that the stacking fault modifies the modulus locally. I think that the stacking fault is a long range perturbation, so that you don't have a kind of two-phase system, but something more complicated.

HEAD: This is very true, and although the conventional model of a stacking fault is a billiard ball stacking, it certainly relaxes to some extent on either side. It is not just close packing. It still is true that there are some atoms there which are in hexagonal symmetry configurations and the stress and strain field of the dislocation are moving these atoms from a hexagonal basis. Their response will be quite different from

atoms which are in a cubic environment. However, a stacking fault is certainly not a sharp plane, as you say.

BULLOUGH: I would just like to complement Professor Head's remarks. As you will see in the paper by Dr. Englert and myself on copper, using a fairly rigorous interatomic potential, the relaxation around a stacking fault causes the energy per unit area to drop by 15%. There are other points but they will be made in the paper.

HIRTH: Seeing Dr. Malén's picture of an inverse energy plot used to predict an instability criterion reminded me that there was an analogue in dealing with surface energy, and there are two instability criteria in that case. If there is an analogue for the dislocation energies there might possibly be a second criterion there. One criterion is the one that Dr. Malén discussed of having positive curvature in a polar plot, and the other is that in such an inverse Gibbs-Wulff surface energy plot all orientations (including convex ones) lying between points of tangency of the plane fitted on to the inverse Gibbs-Wulff plot are also unstable. So, for example, possibly there would be instability of the second kind for a little region of negative curvature in Malén's plot.

MALÉN: You can find these instability criteria discussed in the analysis of Indenbom and Orlov. (In the appendix of ref. [2] of my paper.) But there is one thing which you have for crystals that does not apply here (e.g. for the Wulff construction): there is a constraint about constant volume that does not exist for a dislocation.

HEAD: I would like to comment on Professor Hirth's comments. We have made a lot of measurements on the unstable angles in β brass where there is quite a large difference between the two instability criteria, and there is no doubt in my mind that all our measurements support the physical correctness of the tangent construction. It includes more directions than given by negative line tension, and the difference can extend to 10 or 15° on either side in these cases.

LOTHE: These two different stability criteria—isn't that just a question of spontaneous instability of the original straight line versus an instability over an activation barrier? Is that right—I mean that you really have to zig-zag it out to get it down into the valley?

HEAD: There are a number of ways of explaining the difference. It is really a problem in the calculus of variations, and it depends on what conditions you impose. You get the negative line tension by considering a state which is close both in position and direction to the straight line. If you remove the constraint of closeness in direction of the line, but are still close in position (that is you now can have a large change in direction,

but zig-zagging so it is always close) you get the second criterion. You get both from the calculus of variations depending on whichever condition you like.

LOTHE: When you are outside the region of negative line tension but you are still in the instability region, starting with an infinite straight line, don't you in some initial stage have to increase the energy to get the dislocation into an unstable position and over into the zig-zag configuration?

HEAD: Not in the ideal case where you can have infinitesimal elements of the dislocation doing anything they like. In a physical case, yes, I guess so, because you have the atomic structure underneath you, but it is not true in the mathematical sense that you ever have to go uphill first in energy. You can always pick a path that goes downhill in energy all the way. I think this is true.

LOTHE: Well, I don't see that, because wouldn't any small initial deformation from the straight state be describable in terms of the curvatures, which again leads to the line tension concept? [At this point Professor Head drew a picture on the board showing how a straight dislocation segment could go downhill in energy to a zig-zag configuration without going uphill first. See fig. 1.] I agree with that.

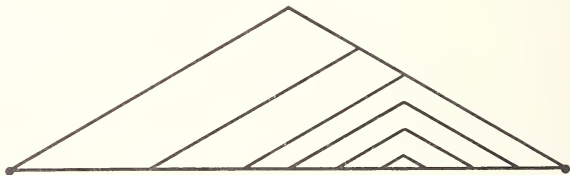


FIGURE 1. Sequence leading from a straight to a zig-zag dislocation configuration.

MALÉN: [Written contribution] I would like to add two comments on Professor Head's zig-zagging dislocations: (1) The analysis by Lothe, Brown, or Indenbom and Orlov (references [2], [13] and [3] of my paper) do not cover this case. It only gives the force on a bent dislocation or on a straight dislocation with a small bow-out. (2) The length of the dislocation is increased and an argument based on energy per unit length for the dislocation thus leads to the conclusion that the zig-zag dislocation has higher energy than both the straight and the bent dislocation.

TEUTONICO: I have done some calculations of line instabilities in hexagonal metals. The difference between the two instability criteria was greatest in thallium. Using the negative curvature criterion, one finds an instability range of approximately 45° near the edge orientation; the double tangent construction gives an instability range of approximately 90° .

INTERNAL STRESS AND THE INCOMPATIBILITY PROBLEM IN INFINITE ANISOTROPIC ELASTICITY

John A. Simmons

*Metallurgy Division
National Bureau of Standards
Washington, D.C. 20234*

and

R. Bullough

*Theoretical Physics Division
A.E.R.E., Harwell
Didcot, Berkshire, England*

Using the language of integral projection operators, the linear elastic distortion field of an infinite anisotropic body is decomposed into its internal and external components. The kernel of the external projection operator is identified as the elastic field due to force dipoles while that of the internal field corresponds to internal distortion fields due to displacement dipoles.

By integration of the projection operator for the internal distortion field, an alternative description for internal distortion fields in terms of dislocations is given. The Mura-Willis formula as well as the distortion field due to a rational dislocation element (in the sense of Eshelby and Laub) for an anisotropic body are then obtained as integrals of the basic displacement dipole kernel for internal distortions.

Further integration of the displacement dipole kernel provides a description of the internal distortion field due to a rational incompatibility element. The general formula for the stress function due to an incompatibility distribution in a general infinite anisotropic body is then given and shown to reduce to the formulation of Kröner for isotropic bodies.

Finally, explicit methods to compute kernels for internal distortions due to incompatibilites are given and discussed.

Key words: Anisotropic elasticity; dislocations; Green's tensor; incompatibility; internal stress; source kernels; stress functions.

I. Introduction

The problem of finding the stress or strain distribution induced by an imposed incompatibility distribution has been solved for isotropic solids

by Kröner using the important method of stress functions [1]. The general anisotropic problem, again using stress functions, was also discussed by Kröner [2] but no useful general solution was found. Eshelby [3] has treated the same question and written a prescription whereby, in principle, one can find a solution to the incompatibility problem using the Green's tensor for anisotropic elasticity, but this prescription is difficult to use. More recently Kunin [4] developed one explicit solution for the general incompatibility problem in an infinite body using operational methods and the Green's tensor. Kunin's solution promises to be useful, but has not been studied in detail.

We present here a general technique for obtaining stress fields, particularly internal stress fields, due to distributions of stress sources in infinite anisotropic elastic bodies.¹ The starting point is a general decomposition method for elastic distortion and stress fields using projection techniques similar to those employed by Kunin [4]. The sources of these elastic fields are identified using integral projection operators whose kernels are fundamental source tensors for force dipole and displacement dipole densities. That part of these elastic fields induced by force dipoles—or, alternately, body forces—is the force induced component, and the part induced by displacement dipoles is the residual, or internal component.

The generation of residual stresses from plastic deformation and “extra matter” is presented as is the physical equivalence of the source kernel approach for residual stresses with Eshelby's stress-free strain ideas [3, 6], which have also been extensively developed by Mura [7, 8] and applied to dislocations in a dynamic formalism. Antisymmetric stresses and disclinations are also touched upon.

The properties of the source kernel for internal distortions are investigated and used to obtain explicit integral representations of source kernels for dislocations and incompatibilities, thus providing an identification of other ways of characterizing the internal distortion or stress fields and several expressions in terms of source functions for computing them. This source tensor approach is shown to contain the Mura-Willis formula [9, 10] in the case of infinite anisotropic bodies as well as Kröner's stress function approach in the case of infinite isotropic bodies. Finally, general source function solutions for stress functions valid in infinite anisotropic bodies are presented and concrete expressions for source kernels solving the incompatibility problem are given in terms of the Green's tensor for anisotropic elasticity.

¹ The more complex problem dealing with sources of internal stress fields in finite bodies is treated elsewhere [5].

II. The Decomposition Theorem

One way of viewing decomposition theorems is in terms of projection operators—a projection operator being any linear operator \mathbf{P} such that $\mathbf{P}^2 = \mathbf{P}$ [11]. We refer to two projection operators, \mathbf{P} and \mathbf{Q} , as being independent if $\mathbf{QP} = \mathbf{PQ} = \mathbf{0}$. Thus, for instance, \mathbf{P} and $(\mathbf{1} - \mathbf{P})$ are always independent and the sum or difference of any two independent projection operators is a projection. The idea of a decomposition theorem, then, is to decompose the identity operator into a sum of independent projection operators, which we may write as $\mathbf{1} = \sum_{n=1}^N \mathbf{P}_i$. When dealing with physical fields, we often recognize each projection operator as identifying that component of the field due to a given physical process. Since the sum of the operators is $\mathbf{1}$ we have an exhaustive decomposition of the field into its component parts. Naturally, it is usually possible to obtain different ways of “looking at” the physical field and it may also be possible to decompose a particular projection operator into independent sub-operators which then give a finer way of looking at the same physical process.

In the case of integral projection operators whose kernel is a source function—or Green’s function—one can often use the Green’s function to identify the physical sources of the field. If one starts with the identity operator which has as its kernel a δ -function of some type,² it is often possible to represent the δ -function kernel in terms of source functions and thus obtain a complete decomposition of a field and identify its physical sources.

As an example, in the static electromagnetic case suppose we consider an arbitrary well behaved vector field \mathbf{v} which we may imagine to be composed of both suitably dedimensionalized electric and magnetic fields. We may then write

$$v_m(\mathbf{r}') = \int \delta_{ml} \delta(\mathbf{r}' - \mathbf{r}) v_l(\mathbf{r}) dV \quad (2.1)$$

where $\delta_{ml} \delta(\mathbf{r}' - \mathbf{r})$ is the kernel of the identity operator. Now, if we introduce the harmonic Green’s function

$$G(\mathbf{r}' - \mathbf{r}) = \frac{1}{4\pi} |\mathbf{r}' - \mathbf{r}|^{-1}, \quad (2.2)$$

which satisfies the equation

$$G_{jj}(\mathbf{r}' - \mathbf{r}) + \delta(\mathbf{r}' - \mathbf{r}) = 0, \quad (2.3)$$

² δ -functions and other kernel functions used in this work are to be understood as generalized functions, or distributions, in the sense of Laurent Schwartz [12, 13].

we may decompose the vector field \mathbf{v} according to Helmholtz theorem [14]:

$$\begin{aligned} v_m(\mathbf{r}') &= \int \delta_{lm} G_{,jj'}(\mathbf{r}' - \mathbf{r}) v_l(\mathbf{r}) dV \\ &= -4\pi \int G_{,m'}(\mathbf{r}' - \mathbf{r}) \rho(\mathbf{r}) dV \\ &\quad + \frac{4\pi}{c} \int \epsilon_{klm} G_{,k'}(\mathbf{r}' - \mathbf{r}) J_l(\mathbf{r}) dV. \end{aligned} \quad (2.4)$$

Here the indices after the comma signify differentiation with respect to the primed or unprimed variables as indicated.

The first equation in (2.4) involves the representation of the identity kernel and the second equation defines two projection operators which serve to define the electrostatic and magnetostatic fields, respectively. Associated to these projection operators, of course, are the field operators that allow one to identify the physical sources—charge and current densities:

$$\rho(\mathbf{r}) \equiv \frac{1}{4\pi} v_{j,j}(\mathbf{r})$$

$$J_l(\mathbf{r}) \equiv \frac{c}{4\pi} \epsilon_{jkl} v_{k,j}(\mathbf{r}).$$

Let us now turn to the problem of the elastic field with sources of internal stress. We consider in detail the decomposition of an arbitrary distortion field $\beta_{mn}(\mathbf{r})$ in the infinite anisotropic body B^∞ . It is a little simpler to obtain decomposition formulas for the stress or strain fields but we choose to consider distortions to make clearer the irrelevance of rotations. We shall indicate, where appropriate, the kernels required for allied decomposition problems.

In the linear elastic continuum, where we do not distinguish between initial and final states, any elastic distortion $\boldsymbol{\beta}$ must satisfy the equations of elastic equilibrium:

$$C_{ijkl} \beta_{kl,j}(\mathbf{r}) + f_i(\mathbf{r}) = 0, \quad (2.5)$$

where $\mathbf{f}(\mathbf{r})$ is the body force at \mathbf{r} and C_{ijkl} are the elastic constants satisfying the relations:

$$C_{ijkl} = C_{jikl} = C_{klij} \quad (2.6a)$$

and, for arbitrary β :

$$C_{ijkl}\beta_{ij}\beta_{kl} > 0, \quad (2.6b)$$

unless $\beta = 0$. Now, given the body force field \mathbf{f} determined by eq (2.5) one can employ the concept of the fundamental Green's tensor solution of the elastic equations to write down a displacement field \mathbf{u}^F whose associated distortion field exactly reproduces the body force field \mathbf{f} : Thus, from the elastic Green's tensor $\mathbf{G}^\infty(\mathbf{r}' - \mathbf{r})$ for B^∞ —which for convenience in this work we denote simply by $\mathbf{G}(\mathbf{r}' - \mathbf{r})$ —defined by:

$$C_{ijkl}G_{mk,lj}(\mathbf{r}' - \mathbf{r}) + \delta_{im}\delta(\mathbf{r}' - \mathbf{r}) = 0 \quad \text{for } \mathbf{r} \text{ in } B^\infty \quad (2.7a)$$

and satisfying the symmetry relations [15]:

$$G_{mn}(\mathbf{r}' - \mathbf{r}) = G_{mn}(\mathbf{r} - \mathbf{r}') = G_{nm}(\mathbf{r}' - \mathbf{r}), \quad (2.7b)$$

one can define \mathbf{u}^F by:

$$\begin{aligned} u_m^F(\mathbf{r}') &\equiv \int G_{mi}(\mathbf{r}' - \mathbf{r})f_i(\mathbf{r})dV \\ &= - \int G_{mi}(\mathbf{r}' - \mathbf{r})C_{ijkl}\beta_{kl,j}(\mathbf{r})dV \\ &= \int G_{mi,j}(\mathbf{r}' - \mathbf{r})C_{ijkl}\beta_{kl}(\mathbf{r})dV, \end{aligned} \quad (2.8)$$

where the last form is obtained by integration by parts assuming $\beta(\mathbf{r}) = 0(|\mathbf{r}|^{-1})$ at infinity. The distortion field β^F associated to \mathbf{u}^F is defined by:

$$\begin{aligned} \beta_{mn}^F(\mathbf{r}') &\equiv u_{m,n'}^F(\mathbf{r}') = \int G_{mi,n'}(\mathbf{r}' - \mathbf{r})f_i(\mathbf{r})dV \\ &= \int G_{mi,n'j}(\mathbf{r}' - \mathbf{r})C_{ijkl}\beta_{kl}(\mathbf{r})dV. \end{aligned} \quad (2.9)^3$$

One can then easily verify, using eqs (2.5), (2.7), and (2.9), that the body forces associated to β^F are the same as those associated to the original

³The reader will note from this equation that we have adopted the convention of adding on differentiated indices to the right. This convention is counter to several recent papers in dislocation theory which seem to stem from the notation of Schouten where the index is added on the left. Although the reader may readily find both types of notation in the dislocation literature, the convention we have adopted is that predominantly followed in other relevant branches of theoretical physics, mathematics and continuum mechanics.

distortion field β , even though the fields β^F and β need not be equal:

$$f_i^F(\mathbf{r}) \equiv -C_{ijkl}\beta_{kl,j}^F(\mathbf{r}) = -C_{ijkl}\beta_{kl,j}(\mathbf{r}) = f_i(\mathbf{r}_0). \quad (2.10)$$

We shall call β^F the force induced component of β .

From the above considerations, one can introduce an integral operator \mathbf{F} , with a kernel \mathbf{F} , which induces the distortion field β^F from β :

$$\beta_{mn}^F = \mathbf{F}(\beta) \equiv \int F_{mnkl}(\mathbf{r}' - \mathbf{r})\beta_{kl}(\mathbf{r})dV, \quad (2.11)$$

where

$$F_{mnkl}(\mathbf{r}' - \mathbf{r}) \equiv C_{ijkl}G_{mi,n'j}(\mathbf{r}' - \mathbf{r}). \quad (2.12)$$

It then follows from eq (2.10) that \mathbf{F} is a projection operator.

Let us now consider the projection operator \mathbf{R}

$$\mathbf{R} \equiv \mathbf{1} - \mathbf{F}, \quad (2.13a)$$

complementary to \mathbf{F} . \mathbf{R} may also be written as an integral operator, so that if we set

$$\mathbf{R}(\beta) = \beta - \mathbf{F}(\beta) \equiv \beta^R, \quad (2.13b)$$

then

$$\beta_{mn}^R(\mathbf{r}') = \int R_{mnkl}(\mathbf{r}' - \mathbf{r})\beta_{kl}(\mathbf{r})dV, \quad (2.14)$$

where the kernel \mathbf{R} is given by

$$R_{mnkl}(\mathbf{r}' - \mathbf{r}) = \delta_{mk}\delta_{nl}\delta(\mathbf{r}' - \mathbf{r}) - C_{ijkl}G_{mi,n'j}(\mathbf{r}' - \mathbf{r}). \quad (2.15)$$

One recognizes from eqs (2.10) and (2.13) that the distortion field β^R has no body force sources, that is

$$C_{ijkl}\beta_{kl,j}^R(\mathbf{r}) = 0. \quad (2.16)$$

Such a field is termed “residual” or “internal.” Any residual distortion field β^R produced by the operator \mathbf{R} is then energetically independent of any force induced distortion field β^F produced by the operator \mathbf{F} ; this means that the interaction energy between two such fields is always null:

$$\int C_{ijkl}\beta_{ij}^F(r)\beta_{kl}^R(\mathbf{r})dV = 0. \quad (2.17)$$

Equation (2.17) follows from equation (2.16) by using integration by parts and the fact that β^F possesses the displacement potential \mathbf{u}^F as given by eqs (2.8) and (2.9).

Finally, we wish to introduce here the kernel S for the residual stress associated to the elastic distortion β :

$$\begin{aligned} S_{mnkl}(\mathbf{r}' - \mathbf{r}) &\equiv C_{mnpq} R_{pqkl}(\mathbf{r}' - \mathbf{r}) \\ &= C_{mnkl} \delta(\mathbf{r} - \mathbf{r}') - C_{mnpq} G_{ijkl} G_{pi,qj}(\mathbf{r}' - \mathbf{r}). \end{aligned} \quad (2.18a)$$

$S_{mnkl}(\mathbf{r}' - \mathbf{r})$ is symmetric in mn and kl and obeys the other symmetry properties:

$$S_{mnkl}(\mathbf{r}' - \mathbf{r}) = S_{mnkl}(\mathbf{r} - \mathbf{r}') = S_{kltm}(\mathbf{r}' - \mathbf{r}) \quad (2.18b)$$

which follow directly from the symmetries of \mathbf{C} and \mathbf{G} .

Thus far, we have thought of β as the elastic distortion field (as though this were a restriction) and eq (2.13) above as providing the decomposition of the elastic distortion field into its force induced and residual components:

$$\beta^F + \beta^R = \beta \quad (2.19a)$$

or, in operator form,

$$\mathbf{F} + \mathbf{R} = \mathbf{1}. \quad (2.19b)$$

But the operator equation (2.19b) together with the general definitions of the kernels \mathbf{F} and \mathbf{R} which in no way restrict β (except to place mild asymptotic restrictions at infinity and weak restrictions on the coefficients of β as generalized functions⁴) indicate that β may be considered as an arbitrary distortion field, so that equations (2.19) provide the sought after decomposition not only of elastic fields but of any distortion field. In this context we may say that *any distortion field may be considered as an elastic distortion field which is acting in the presence of body forces and sources of residual distortion*. The operators \mathbf{R} and \mathbf{F} then decompose β in situ (without reference to any “deformation” from an initial state) into its force induced and residual parts, β^F and β^R . The body forces serving as a source for β^F are then defined by equation (2.5) and the residual component, β^R , is what remains when β^F is removed from β . The sources for β^R at the same “level of integration” as the body force sources of β^F are—as is well-known—dislocations. The relationship of β^R with its dislocation sources is treated in section IV. An alternate, and in some

⁴ It seems sufficient here to assume that the coefficients of β behave as no worse than first distributional derivatives of piecewise smooth locally integrable functions in B^∞ and that these coefficients are $O(|\mathbf{r}|^{-1})$ at infinity.

ways more basic, set of sources for β^F and β^R in terms of dipoles will be discussed in section III.

Decomposition formulas analogous to (2.19) can easily be given for the elastic strain fields or stress fields. Thus, we have the symmetrized⁵ kernels $(F_{mnkl})_{(mn)}$ and $(R_{mnkl})_{(mn)}$, which we denote by (\mathbf{F}) and (\mathbf{R}) , as the source kernels for the decomposition of the elastic strain $e_{mn} \equiv \beta_{(mn)}$:

$$\begin{aligned} e_{mn}(\mathbf{r}') &= e_{mn}^F(\mathbf{r}') + e_{mn}^R(\mathbf{r}') = \int (F)_{mnkl}(\mathbf{r}' - \mathbf{r}) e_{kl}(\mathbf{r}) dV \\ &\quad + \int (R)_{mnkl}(\mathbf{r}' - \mathbf{r}) e_{kl}(\mathbf{r}) dV. \end{aligned} \quad (2.20)$$

To obtain a decomposition formula for the stress, we see that given the stress field $\sigma_{kl}(\mathbf{r})$, which—as will be applied in section III—we do not assume to be necessarily symmetric in k and l , and using $\tilde{\mathbf{C}}$ to denote the inverse elastic constants (elastic compliances), we may use the definition of \mathbf{F} in eq (2.12) and the symmetries of $\tilde{\mathbf{C}}$ and \mathbf{G} to write:

$$\begin{aligned} \beta_{ij}^F(\mathbf{r}') &= \int F_{ijpq}(\mathbf{r}' - \mathbf{r}) \beta_{pq}(\mathbf{r}) dV \\ &= \int F_{ijpq}(\mathbf{r}' - \mathbf{r}) e_{pq}(\mathbf{r}) dV \\ &= \int F_{ijpq}(\mathbf{r}' - \mathbf{r}) \tilde{C}_{pqkl} \sigma_{kl}(\mathbf{r}) dV \\ &= \int (G_{ik,j'l})_{(kl)}(\mathbf{r}' - \mathbf{r}) \sigma_{kl}(\mathbf{r}) dV, \end{aligned} \quad (2.21)$$

so that

$$\begin{aligned} \sigma_{mn}^F(\mathbf{r}') &= C_{mni j} \beta_{ij}^F(\mathbf{r}') \\ &= \int C_{mni j} (G_{ik,j'l})_{(kl)}(\mathbf{r}' - \mathbf{r}) \sigma_{kl}(\mathbf{r}) dV \\ &= \int (F)_{klmn}(\mathbf{r}' - \mathbf{r}) \sigma_{kl}(\mathbf{r}) dV \\ &\equiv \int (F)_{mnkl}^*(\mathbf{r}' - \mathbf{r}) \sigma_{kl}(\mathbf{r}) dV. \end{aligned} \quad (2.22)$$

Then using (2.22), the kernel for the symmetric residual component of the

⁵The symbol (mn) refers to the symmetrization on the indices m and n ; that is $\frac{1}{2}((mn + nm))$.

stress field is obtained from:

$$\begin{aligned}
 \sigma_{mn}^R(r') &= C_{mnij}\beta_{ij}^R(r') \\
 &= \int [(\delta_{mk}\delta_{nl})_{(mn)}\delta(\mathbf{r}' - \mathbf{r}) - (F)_{klmn}(\mathbf{r}' - \mathbf{r})]\sigma_{kl}(\mathbf{r})dV \\
 &= \int (R)_{klmn}(\mathbf{r}' - \mathbf{r})\sigma_{kl}(\mathbf{r})dV \\
 &\equiv \int (R)_{mnkl}^*(\mathbf{r}' - \mathbf{r})\sigma_{kl}(\mathbf{r})dV.
 \end{aligned} \tag{2.23}$$

The kernels $(\mathbf{F})^*$ and $(\mathbf{R})^*$ for the stress representation are thus the “transposes” or adjoints, respectively, of the kernels (\mathbf{F}) and (\mathbf{R}) for the strain representation. Further, it is apparent that no information concerning the antisymmetric part of σ is obtainable using source functions; this indicates the proper decomposition of the stress is into its two symmetric residual and force induced parts together with its antisymmetric part—a decomposition analogous to that of the strain given in section V.

The dependence of the kernel \mathbf{F} on the symmetric part of β also demonstrates the irrelevance of rotations in the linear elastic continuum. One consequence of this fact is that disclinations can produce no new sources of symmetric stress. As will be shown—and is actually clear from the Mura-Willis formula—the rotational component of the residual distortion field β^R is determined by the dislocation density. In a body which has distributions of infinitesimal rotational disclinations, the rotational component of β^R is presumed to be undeterminable and the strain is used as the relevant field. In that case (\mathbf{R}) and (\mathbf{F}) provide the representations of the residual and force induced strain fields. However, since \mathbf{R} and \mathbf{F} themselves exist, being constructed from the Green's tensor only, we can construct distortion fields β^R , β^F , and $\beta = \beta^R + \beta^F$ whose strain fields are exactly the same as when disclinations are presumed present. Put in another way, the rotation is a hidden ignorable variable when the strain is chosen as the physical field.⁶

III. Stress Free Strain and Dipole Densities as the Sources for the Elastic Field

Although in subsequent sections we shall obtain descriptions of sources for the elastic field in terms of dislocations—or incompatibilities—and body forces, the decomposition formula given by (2.19) is in one sense

⁶ The above considerations say nothing about disclinations as sources of antisymmetric stresses. Although we discuss antisymmetric stresses somewhat—in the context of force dipoles, no systematic investigation of this topic is undertaken in this work.

the most basic of decomposition formulas in that the unique kernels \mathbf{R} and \mathbf{F} provide the genesis of all subsequent source kernels.

It seems worthwhile, then, to investigate the physical meaning of \mathbf{F} and \mathbf{R} . These kernels will be shown to be interpretable in terms of elastic fields due to force dipole and displacement dipole sources. These dipole sources can also be thought of as internal boundary conditions, imposed on the body in situ, to which the elastic fields must conform. Further, as seen in later sections, such sources serve to define through differentiation "higher order" source quantities such as body forces, dislocations and incompatibilities.

In this section we shall also discuss the intimately related problem of finding the elastic fields induced in the continuum by externally imposed sources which are themselves representable as force and displacement dipole densities. These can be thought of as imposed on the elastic body in an undeformed state, thereby giving rise to a deformation in which elastic force and displacement dipoles are induced in the body to counteract the imposed dipole fields. As an application of this dipole approach, we shall treat the problem of finding the elastic fields due to stress-free strains plus inhomogeneities and we shall give an explicit solution for a small, inhomogeneous, anisotropic spherical inclusion in an anisotropic matrix.

Consider first the definition of the kernel \mathbf{F} given by (2.12). We wish to show that one way of interpreting $F_{mnkl}(\mathbf{r}' - \mathbf{r})$ is as the kl components of the stress field at \mathbf{r} produced by a force dipole density of type mn at \mathbf{r}' . By a force dipole density we mean here the analogous concept in elastostatics to that employed in electrostatics, that is a distribution through space of pairs of equal and opposite forces.⁷ Given such a pair of forces, \mathbf{f}_0 at $\mathbf{r}' + \delta\mathbf{r}'$ and $-\mathbf{f}_0$ at \mathbf{r}' , the dipole tensor is given by the dyadic product $\frac{1}{2}(\mathbf{f}(\mathbf{r}' + \delta\mathbf{r}') - \mathbf{f}(\mathbf{r}')) \otimes \delta\mathbf{r}' = \mathbf{f}_0 \otimes \delta\mathbf{r}'$. A density of such dipoles distributed throughout space, then, has the dimensions $\mathbf{f} \otimes \delta\mathbf{r}' \otimes dV$, where \mathbf{f} is a covariant force vector, $\delta\mathbf{r}'$ a contravariant position vector, and dV a third order covariant antisymmetric volume density. Deliberately neglecting to distinguish between covariant and contravariant indices,⁸ we may designate such a density by τ_{mndV} , where the first index refers to the force components and the second to the vector components; such a dipole density need not, a priori, be symmetric in its two indices—such symmetry implies the absence of body moments. Since the product of the force magnitude and vector length occurring in τ must remain constant, standard arguments show that in

⁷ cf Kröner [16] for a considerable discussion on dipoles in the elastic continuum.

⁸ These arguments may be made completely rigorous by introducing the Euclidean metric, but if the distinction between contravariant and covariant quantities is retained, the only need for this metric is in discussions of tensor symmetries.

the limit as the vector length goes to zero, the distortion field, $\beta_{ij}(\mathbf{r})$, produced by a singular force dipole density at $\mathbf{r} = \mathbf{r}'$ with coefficients τ_{mn} (thus $\boldsymbol{\tau}(r) = \tau_{mn}\delta(\mathbf{r} - \mathbf{r}')dV$) is just $\tau_{mn}G_{mi,n'j}(\mathbf{r}' - \mathbf{r})$ from which the interpretation of \mathbf{F} directly follows. Additionally, one notes that by treating τdV as a vector density with force coefficients, the divergence theorem for such densities [17] clearly demonstrates that force dipole densities are natural potentials for body force densities. In fact, an equivalent way of writing such a force dipole density is obtained by contracting the contravariant vector $\delta\mathbf{r}$ in $\boldsymbol{\tau}$ with the volume density dV to yield a tensor of the type $\mathbf{f} \otimes \mathbf{dA}$ (where \mathbf{dA} is a covariant antisymmetric area element) whose dimensions and interpretation are identical with that of the general nonsymmetric stress tensor, $\boldsymbol{\sigma}$.

We also introduce the concept of displacement dipole density, energetically conjugate to that of force dipole density mentioned above: We consider a small oriented element of surface $\delta\mathbf{A}$, which can be represented in tensor form as a second order antisymmetric contravariant tensor; and we consider, proceeding in the positive direction across the surface element, a *discontinuity* in displacement, \mathbf{v} ⁹. We then define a displacement dipole as the product of these two tensors, $\mathbf{v} \otimes \delta\mathbf{A}$ and denote this tensor as γ_{ijk} , where $\boldsymbol{\gamma}$ is antisymmetric in the last two indices. Such a displacement dipole can be considered as generating a small dislocation loop around the boundary of $\delta\mathbf{A}$ with Burgers vector \mathbf{v} (but $\boldsymbol{\gamma}$ is *not* the dislocation tensor $\boldsymbol{\alpha}$ for the loop),¹⁰ and such a loop is analogous to a small current loop in magnetostatics. A density of displacement dipoles may then be expressed in the form $\boldsymbol{\gamma} \otimes dV$, or alternatively, by contracting the contravariant area part of $\boldsymbol{\gamma}$ (the second and third indices) with the third order covariant density component dV , we can express the displacement dipole density in the form β_{il} , where the first index of $\boldsymbol{\beta}$ is contravariant and the second index is covariant. The tensor $\boldsymbol{\beta}$, then, has exactly the dimensions of distortion with the interpretation that upon moving a small distance $\delta\mathbf{r}$, one accumulates discontinuities in displacement amounting to $\beta_{il}\delta r_l$; hence displacement dipole densities are equivalent to internally imposed distortions and are closely related to Eshelby's notion of stress-free strains [6].

We have already observed that the elastic stress has the same form as a force dipole density and the distortion has the same form as a displacement dipole density. Thus, it is possible to view elasticity as a theory of force and displacement dipole densities, and the elastic stress-strain

⁹ This discontinuity formulation is an alternate way of treating dipoles. Neglecting the average value of the displacement at $\delta\mathbf{A}$, we could as well have thought of a displacement of $\frac{1}{2}\mathbf{v}$ on the positive side of $\delta\mathbf{A}$ and $-\frac{1}{2}\mathbf{v}$ on the negative side of $\delta\mathbf{A}$.

¹⁰ A discussion of dislocation loops is given by Kroupa [18].

relations then become constitutive relations between displacement dipoles and the symmetric force dipole density they induce in the elastic continuum. This situation is exactly analogous to the dielectric and diamagnetic-paramagnetic medium in electrostatics as has been discussed by Kröner [16, 19].

With this viewpoint of the elastic continuum, one can give to the kernel \mathbf{F} an interpretation using displacement dipoles alternate to that given earlier in terms of force dipoles. Let us consider a singular elastic displacement dipole density at the point \mathbf{r}' , $\beta_{kl}\delta(\mathbf{r} - \mathbf{r}')$, with the associated elastic force dipole density $\tau_{ij}(\mathbf{r})dV = C_{ijkl}\beta_{kl}\delta(\mathbf{r} - \mathbf{r}')$. Then, as previously, the elastic distortion due to this singular force dipole density is

$$\begin{aligned}\beta_{mn}(\mathbf{r}) &= G_{mi, j'n}(\mathbf{r} - \mathbf{r}')C_{ijkl}\beta_{kl} \\ &= G_{mi, n'j}(\mathbf{r}' - \mathbf{r})C_{ijkl}\beta_{kl} \\ &= F_{mnkl}(\mathbf{r}' - \mathbf{r})\beta_{kl}.\end{aligned}$$

Thus, $F_{mnkl}(\mathbf{r}' - \mathbf{r})$ may also be interpreted as the force induced elastic distortion field of type mn at \mathbf{r}' produced by the force dipole equivalents of the displacement dipole density of type kl at \mathbf{r} . A similar dual interpretation of the source kernel \mathbf{R} for residual fields in terms of dipolar sources is also easily obtained.

These interpretations of the physical meaning of the dipolar source kernels have thus far been a way of looking at the elastic fields, themselves, as dipolar fields and of interpreting the projection properties of the kernels so that one can see how each component, force induced and residual, reproduces itself. Let us now turn to an important application of the dipole kernels which will provide another way of thinking about them and at the same time give a direct link to the theory of stress free strains.

We consider externally applied distributions of force dipoles, $\boldsymbol{\sigma}^A$, and displacement dipoles, $\boldsymbol{\beta}^P$, to be imposed upon an undeformed body.¹¹ The body reacts, producing an elastic distortion field $\boldsymbol{\beta}$ and stress field $\boldsymbol{\sigma}$ (which need not be symmetric). To find these elastic fields, we shall make certain assumptions, particularly:

(1) We assume that the applied dipolar fields have the same characteristics as the elastic fields in that they may be superimposed upon the elastic fields. Thus

$$\boldsymbol{\sigma}^A + \boldsymbol{\sigma} = \boldsymbol{\sigma}^T \quad (3.1)$$

¹¹The terminology $\boldsymbol{\beta}^P$ which was called plastic distortion and the relation (3.3) originate with Kröner [20].

and

$$\beta^T + \beta = \beta^T \quad (3.2)$$

where σ^T and β^T represent the total stress and distortion fields, respectively.

(2) The total stress, σ^T , must satisfy the equations of elastic equilibrium.¹² Since σ^T includes both applied and elastic field quantities, it must then be free of body moments and body forces.

(3) The total distortion field must have a displacement potential, i.e., there must exist a displacement field u^T such that

$$\beta_{ij}^T(\mathbf{r}) = u_{i,j}^T(\mathbf{r}). \quad (3.3)^{13}$$

To solve the above problem we begin by examining the consequences of assumption 2. The absence of body moments in σ^T demands that σ^T be symmetric, so that

$$[\sigma]_{mn} \equiv \sigma_{[mn]} = -\sigma_{[mn]}^A \quad (3.4)^{13}$$

and the freedom from body forces is simply expressed by the operator equation

$$\overset{\sigma}{\mathbf{F}}(\sigma^T) = \mathbf{0}. \quad (3.5)$$

Here the operator $\overset{\sigma}{\mathbf{F}}$ is, as always, the force induced projection operator, but the kernel for $\overset{\sigma}{\mathbf{F}}$ must be that for the stress problem as given in (2.22).

Then if one applies the operator $\overset{\sigma}{\mathbf{F}}$ to both sides of equation (3.1), one obtains:

$$\overset{\sigma}{\mathbf{F}}(\sigma) = \sigma^F = -\overset{\sigma}{\mathbf{F}}(\alpha^A). \quad (3.6)$$

¹² We deal throughout this work with a linear continuum in which the distinction between initial and final state is somewhat obscure. However, as regards this postulate, it obviously holds rigorously in the final state configuration rather than the initial state configuration to which it is applied here on the assumption that the strains are small. In those situations where this is not formally correct, such as problems involving singularities, it is sometimes possible to formulate the problem in the final state configuration (or in a corrected initial state formulation) and solve it by iterative methods.

¹³ The symbol $[mn]$ refers to the antisymmetrization on the indices m and n ; that is $\frac{1}{2}((mn - nm))$.

Similarly, employing eqs (3.1) and (2.21), one may write

$$\beta_{mn}^F(\mathbf{r}') = - \int (G_{mi,n'j})_{(ij)} (\mathbf{r}' - \mathbf{r}) \sigma_{ij}^A(\mathbf{r}) dV. \quad (3.7)$$

Equation (3.6) gives the expression for $(\boldsymbol{\sigma})^F$ and (3.7) that for $\boldsymbol{\beta}^F$ in terms of $\boldsymbol{\sigma}^A$; and these force induced fields may be thought of as generated by the “elastic dipole” reaction, $-\boldsymbol{\sigma}^A$, to the applied dipole density, $\boldsymbol{\sigma}^A$. Turning to assumption (3), we observe that for any displacement field \mathbf{u} , eq (2.10) and the uniqueness theorem for classical elasticity [21] imply that

$$\mathbf{F}(u_{i,j}) = u_{i,j} \quad (3.8)^{14}$$

and therefore

$$\mathbf{R}(u_{i,j}) = 0,$$

whence

$$\mathbf{R}(\boldsymbol{\beta}^T) = 0. \quad (3.9)$$

Applying \mathbf{R} to eq (3.2), we thus obtain

$$\mathbf{R}(\boldsymbol{\beta}) = \boldsymbol{\beta}^R = -\mathbf{R}(\boldsymbol{\beta}^P). \quad (3.10)$$

Equation (3.10) provides the desired expression for the residual distortion field, and therefore the residual component of the stress field, from a knowledge of the imposed displacement dipole density. As with the relation between the force induced field and force dipoles, the residual distortion field may be thought of as induced by the elastic displacement dipole reaction, $-\boldsymbol{\beta}^P$, to the applied (or plastic) dipole density, $\boldsymbol{\beta}^P$.

Together with eq (3.7), eq (3.10) completes the solution of the dipole source problem and we can write

$$\boldsymbol{\beta} = \boldsymbol{\beta}^F + \boldsymbol{\beta}^R = \overset{\beta}{\mathbf{F}}(-\boldsymbol{\sigma}^A) + \mathbf{R}(-\boldsymbol{\beta}^P), \quad (3.11)$$

where $\overset{\beta}{\mathbf{F}}$ is the form of the force induced operator whose kernel is given in eq (3.7). Also

$$\boldsymbol{\beta}^T = \boldsymbol{\beta}^P + \boldsymbol{\beta} = \overset{\beta}{\mathbf{F}}(-\boldsymbol{\sigma}^A) + \mathbf{F}(\boldsymbol{\beta}^P) = \mathbf{F}(\boldsymbol{\beta}^P - \tilde{\mathbf{C}}\boldsymbol{\sigma}^A) \quad (3.12)$$

which, from the form of \mathbf{F} , allows us to write down directly the displace-

¹⁴ In finite bodies equation (3.8) would have to be altered to include a possible constant rotation. This physically unimportant rotation is excluded in the infinite body by assuming appropriate asymptotic fall-off of the field $\boldsymbol{\beta}$ at infinity.

ment potential \mathbf{u}^T in eq (3.3):

$$u_m^T(r') = \int G_{mi,j'}(\mathbf{r}' - \mathbf{r}) ((\sigma)_{ij}^A(\mathbf{r}) - C_{ijkl}\beta_{kl}^P(\mathbf{r})) dV. \quad (3.13)$$

Finally,

$$\boldsymbol{\sigma} = \mathbf{C}\boldsymbol{\beta} - [\boldsymbol{\sigma}^A] \quad (3.14)$$

and

$$\boldsymbol{\sigma}^T = \mathbf{C}\boldsymbol{\beta} + (\boldsymbol{\sigma}^A). \quad (3.15)$$

It should be noted from the above solution that the antisymmetric part of the force dipole density field, $\boldsymbol{\sigma}^A$, has no influence on the elastic distortion, which is only affected by the antisymmetric part of the displacement dipole density $\boldsymbol{\beta}^P$. By the same token, the antisymmetric part of the displacement dipole density has no influence on the elastic stress, which is affected only by the antisymmetric part of $\boldsymbol{\sigma}^A$. Thus, only symmetric displacement dipoles—or “stress-free strains” [6]—have any influence on the elastic stress. Such symmetric displacement dipoles can always be considered as a combination of a number of dipoles where the displacements are normal to the dipole surface, so we can think of the sources of residual stress as equivalent to a distribution of prismatic dislocation loops—these loops being mathematically equivalent to displacement dipoles with normal displacements or to what Kröner has called “extra matter” [16].

In formulating the above dipole source problem, it was stated that this problem was directly linked to the problem of stress-free strains discussed by Eshelby [6]. We now wish to make that connection explicit by showing how the above problem can be used to solve the stress-free strain problem where not only extra matter, but also foreign matter—that is, inhomogeneities whose elastic constants differ from that of the matrix—are introduced. It will be seen from this solution that each particle of foreign matter can formally be replaced in the homogeneous continuum by a similar particle of extra matter together with an appropriate force dipole:

1. We imagine cutting out a small volume element from the continuum at the point \mathbf{r} and replacing it by a new piece of material with elastic constants $C_{ijkl} + \Delta C_{ijkl}(\mathbf{r})$ and with a shape related to that of the original by the “stress-free transformation” $\delta_{ij} + \beta_{ij}^P(\mathbf{r})$.

2. We then apply to the detached volume element an elastic deformation $\delta_{ij} - \beta_{ij}^P(\mathbf{r})$ which induces a “plastic” force dipole density $\sigma_{ij}^P(\mathbf{r}) = -(C_{ijkl} + \Delta C_{ijkl}(\mathbf{r}))\beta_{kl}^P(\mathbf{r})$ in the element.

3. If we now replace the strained volume element back in the hole, it again fits perfectly. Performing this process at each point \mathbf{r} (with the possibility that the material is not altered, in which case $\Delta C(r) = 0$, and/or no stress-free transformation is applied, in which case $\beta^P(r) = 0$)

we obtain what we shall call the initial state of the continuum, where the elastic distortion $\beta(\mathbf{r}) = -\beta^p(\mathbf{r})$ and the elastic constants are given by $C_{ijkl} + \Delta C_{ijkl}(\mathbf{r})$. This initial state is clearly not in elastic equilibrium, so that we must have forces throughout the body to hold it in this condition.

4. We now relax any imposed forces and the body undergoes an elastic deformation given by \mathbf{u}^T to reach a final state which is in elastic equilibrium with no body forces present. The stress-free strain problem consists in finding \mathbf{u}^T from which the elastic fields in the final state may easily be derived.

The elastic distortion in the final state is

$$\beta = -\beta^p + \beta^T$$

where

$$\beta_{ij}^T(\mathbf{r}) = u_{i,j}^T(\mathbf{r}).$$

These equations coincide with eqs (3.2) and (3.3) above. The stress in the final state, which we shall call σ^T , is

$$\sigma_{ij}^T(\mathbf{r}) = (C_{ijkl} + \Delta C_{ijkl}(\mathbf{r}))\beta_{kl}(\mathbf{r}) \quad (3.16)$$

and σ^T must satisfy the equations of elastic equilibrium as in assumption (2) of the dipole problem. Let us define

$$\sigma_{ij}(\mathbf{r}) = C_{ijkl}\beta_{kl}(\mathbf{r}) \quad (3.17)$$

and

$$\sigma_{ij}^A(\mathbf{r}) = \Delta C_{ijkl}(\mathbf{r})\beta_{kl}(\mathbf{r}) \quad (3.18)$$

so that eq (3.1) is satisfied. It is now clear that we have satisfied the conditions of the dipole problem with (as seen from eq (3.18)) all foreign matter effects being incorporated into force dipoles situated at the foreign particles, themselves.¹⁵ Further, from the solution of the force dipole problem, it is possible to write down at once an implicit solution for the

¹⁵ This formulation must, of course, be understood as purely formal. In the real, now inhomogeneous material, there are no applied force dipoles and the fields are purely residual. There is thus no interaction energy between the elastic field, β , and the fields induced by any additional *real* applied forces.

general “stress-free transformation” problem. From eq (3.13), noting that σ^A is symmetric,

$$\begin{aligned}
 u_m^T(\mathbf{r}') &= \int G_{mi,j'}(\mathbf{r}' - \mathbf{r}) (\sigma_{ij}^A(\mathbf{r}) - C_{ijkl}\beta_{kl}^P(\mathbf{r})) dV \\
 &= \int G_{mi,j'}(\mathbf{r}' - \mathbf{r}) (\Delta C_{ijkl}(\mathbf{r})\beta_{kl}(\mathbf{r}) - C_{ijkl}\beta_{kl}^P(\mathbf{r})) dV \\
 &= \int G_{mi,j'}(\mathbf{r}' - \mathbf{r}) (C_{ijkl}(\mathbf{r})u_{k,l}^T(\mathbf{r}) - (C_{ijkl} + \Delta C_{ijkl}(\mathbf{r}))\beta_{kl}^P(\mathbf{r})) dV \\
 &= - \int (G_{mi,j'}(\mathbf{r}' - \mathbf{r}) \Delta C_{ijkl}(\mathbf{r}))_{,l} u_k^T(\mathbf{r}) dV \\
 &\quad - \int G_{mi,j'}(\mathbf{r}' - \mathbf{r}) (C_{ijkl} + \Delta C_{ijkl}(\mathbf{r})) \beta_{kl}^P(\mathbf{r}) dV. \tag{3.19}
 \end{aligned}$$

The last two equalities in equation (3.19) follow from (3.2), (3.3) and integration by parts. Equation (3.19) provides a singular integral equation for \mathbf{u}^T which, in general, is very difficult to solve; however, approximating solutions can be obtained in certain instances such as the isolated singular inclusion.

To see a specific application of the above solution, we shall explicitly solve the problem of a small spherical inclusion of foreign material in a matrix. In that instance we take $\beta_{kl}^P(\mathbf{r}) = \beta_{kl}^P \delta(\mathbf{r})$ and $\Delta C_{ijkl}(\mathbf{r}) = \Delta C_{ijkl} \Sigma_a(\mathbf{r})$ where Σ_a is the characteristic, or Heaviside, function of a small ball of radius a . We shall later let the radius of the ball tend to zero. Then (3.19) takes the form

$$\begin{aligned}
 u_m^T(\mathbf{r}') &= -G_{mi,j'}(\mathbf{r}') (C_{ijkl} + \Delta C_{ijkl}) \beta_{kl}^P \\
 &\quad - \int G_{mi,j'l}(\mathbf{r}' - \mathbf{r}) \Delta C_{ijkl} \Sigma_a(\mathbf{r}) u_k^T(\mathbf{r}) dV \\
 &\quad + \int_{\partial\Sigma_a} G_{mi,j'}(\mathbf{r}' - \mathbf{r}) \Delta C_{ijkl} u_k^T(\mathbf{r}) n_l(\mathbf{r}) dS. \tag{3.20}
 \end{aligned}$$

From the form of (3.20), it is clear that the answer will be a perturbation of the leading term on the right side of (3.20) which, because of the known properties of Green's tensor functions, is homogeneous of degree -2 . The displacement, \mathbf{u}^T , must be continuous and we expect it to behave as $|\mathbf{r}|^{-2}$ outside of the sphere and in a fashion not more singular inside the sphere. Consequently the second term on the right side of (3.20) will become

negligible for sufficiently small a and we shall approximate the third term in (3.20) by assuming that $G_{mi,j'}$ is constant over $\partial\Sigma_a$. Then (3.20) becomes:

$$u_m^T(\mathbf{r}') = G_{mi,j'}(\mathbf{r}') (\Delta C_{ijkl} u_{kl}^T - [C_{ijkl} + \Delta C_{ijkl}] \beta_{kl}^P) \quad (3.21)$$

where

$$u_{kl}^T = \lim_{a \rightarrow 0} \int_{\partial\Sigma_a} u_k^T(\mathbf{r}) n_l(\mathbf{r}) dS. \quad (3.22)$$

To obtain the explicit solution for \mathbf{u}^T , we define

$$G_{mnij} \equiv - \int_{\partial\Sigma_a} G_{mi,n}(\mathbf{r}) n_j(\mathbf{r}) dS. \quad (3.23)$$

Since the Green's tensor gradients are homogeneous of degree -2 , G_{mnij} is independent of the radius a and can be obtained directly for general anisotropic media using the Fourier transform $\hat{\mathbf{G}}$ of the Green's tensor:

$$G_{mnij} = \frac{1}{4\pi} \int_{\partial\hat{\Sigma}} k_j k_n \hat{G}_{mi}(\mathbf{k}) d\hat{\Omega}. \quad (3.24)$$

Here the integral of (3.24) is performed over the unit sphere, $\partial\hat{\Sigma}$, of reciprocal space. In the case of the isotropic matrix, G_{mnij} can be more simply evaluated by direct integration:

$$G_{mnij} = \frac{1}{3\mu} \left[\delta_{mi} \delta_{nj} - \frac{1}{10(1-\nu)} (\delta_{ij} \delta_{mn} + \delta_{in} \delta_{jm} + \delta_{im} \delta_{jn}) \right], \quad (3.25)$$

where μ is the shear modulus and ν is Poisson's ratio.

From (3.21), (3.22), and (3.23),

$$u_m^T = -G_{mnij} (\Delta C_{ijkl} u_{kl}^T - [C_{ijkl} + \Delta C_{ijkl}] \beta_{kl}^P), \quad (3.26)$$

which can be written as a matrix equation involving nine by nine matrices where the indices from one to nine run over all pairs of numbers ij , $i = 1, 2, 3$; $j = 1, 2, 3$. Thus u_m^T becomes a vector in this terminology and we write

$$(\mathbf{I} + \mathbf{G}\Delta\mathbf{C}) \mathbf{u}^T = \mathbf{G}(\mathbf{C} + \Delta\mathbf{C}) \boldsymbol{\beta}^P \quad (3.27)$$

from which

$$\mathbf{u}^T = (\mathbf{I} + \mathbf{G}\Delta\mathbf{C})^{-1} \mathbf{G}(\mathbf{C} + \Delta\mathbf{C}) \boldsymbol{\beta}^P \quad (3.28)$$

where \mathbf{I} is the identity matrix and $(\mathbf{I} + \mathbf{G}\Delta\mathbf{C})^{-1}$ is the inverse matrix to

(I + $\mathbf{G}\Delta\mathbf{C}$). The solution to (3.28) together with (3.21) solves the small spherical inclusion problem. Explicit numerical results for an isotropic matrix can be obtained using (3.25) and yield the same results as Eshelby [6].

Finally, it is also interesting to interpret the formula $\mathbf{F} + \mathbf{R} = \mathbf{1}$ in a way involving dipole sources. Let us imagine imposing into the elastic body sources of internal stress described by a distribution $-\beta^P$. We may imagine that the body physically breaks up $-\beta^P$ into its two components, $\mathbf{F}(-\beta^P)$ and $\mathbf{R}(-\beta^P)$. But, since ultimately only $\mathbf{R}(-\beta^P)$ remains (which is what is meant by $-\beta^P$ being a source of residual distortion) the component represented by $\mathbf{F}(-\beta^P)$ must radiate into the body as elastic waves. The net force and dipole contents of $\mathbf{F}(-\beta^P)$ must always be contained in the distribution of elastic waves reverberating throughout the body and the energy of these elastic waves is, of course, the self energy of $\mathbf{F}(-\beta^P)$ plus the amount of heat energy contributed to the body by the applied force fields due to the imposition of $-\beta^P$. This fact and the exact mathematical analogy between point forces in elastostatics and charges in electrostatics suggest that further continuation of the electromagnetic analogy—as summarized by Kröner [19]—into elastodynamics may produce many fruitful ideas.

IV. The Mura-Willis Formula and the Decomposition of the Elastic Distortion Field at the Dislocation Level

In the previous sections we have given and discussed the primitive decomposition of the elastic distortion field into its force induced and residual components in terms of dipole sources. We now wish to develop the decomposition for the infinite body appropriate to sources at one higher level of integration, notably body forces and dislocations. The identification of body forces as sources for the force induced component of the distortion field has already been given in equation (2.9) and this component was seen to be connected through an integration by parts to a distribution of force dipole sources.

There remains, then, only the task of representing the sources of the residual distortion field through an integration process. This representation is already provided in one form by the Mura-Willis formula [9], [10]:

$$\begin{aligned} \beta_{mn}(\mathbf{r}') &= \int G_{mi,n'}(\mathbf{r}' - \mathbf{r}) f_i(\mathbf{r}) dV \\ &+ \int \epsilon_{nsl} C_{ijks} G_{mi,j'}(\mathbf{r}' - \mathbf{r}) \alpha_{kl}(\mathbf{r}) dV, \end{aligned} \quad (4.1)$$

where the dislocation density α is defined by

$$\alpha_{kl}(\mathbf{r}) \equiv \epsilon_{lqp}\beta_{kp,q}(\mathbf{r}), \quad (4.2)^{16}$$

and in an alternate fashion by the concept of rational dislocation element formulated for the isotropic body by Eshelby and Laub [23].

In order, however, to develop this representation in terms of the dipole decomposition (2.19), let us reconsider the kernels \mathbf{R} and \mathbf{S} given by (2.15) and (2.18).

Because of the symmetry of \mathbf{S} and its interpretation as a residual stress kernel, it is not surprising and, in fact, easily verified that \mathbf{S} is divergence free in all four indices:

$$S_{mnkl,m}(\mathbf{r}' - \mathbf{r}) = S_{mnkl,n}(\mathbf{r}' - \mathbf{r}) = S_{mnkl,k}(\mathbf{r}' - \mathbf{r}) = S_{mnkl,l}(\mathbf{r}' - \mathbf{r}) = 0. \quad (4.3)$$

It then follows that, since the symmetrized distortion kernel (\mathbf{R}) is linearly related to \mathbf{S} , (\mathbf{R}) is also divergence free in its last two indices:

$$(R)_{mnkl,l}(\mathbf{r}' - \mathbf{r}) = (R)_{mnkl,k}(\mathbf{r}' - \mathbf{r}) = 0. \quad (4.4)$$

Equation (4.4), only, is needed to discuss the strain decomposition or incompatibility problem. For our present purpose, however, the slightly stronger result that the kernel \mathbf{R} , itself, is divergence free in its last index, that is

$$R_{mnkl,l}(\mathbf{r}' - \mathbf{r}) = 0, \quad (4.5)$$

is required. Equation (4.5) can be verified by direct calculation.

Equation (4.5) implies the existence of a tensor field \mathbf{D} such that $-\mathbf{D}(\mathbf{r}' - \mathbf{r}) \times \nabla_r = \mathbf{R}(\mathbf{r}' - \mathbf{r})$; that is

$$\epsilon_{lqp}D_{mnkp,q}(\mathbf{r}' - \mathbf{r}) = R_{mnkl}(\mathbf{r}' - \mathbf{r}). \quad (4.6)$$

\mathbf{D} is by no means unique but is essentially determined up to a gradient. For instance, one form for \mathbf{D} , which we shall call \mathbf{D}^* , may be obtained

¹⁶ We have here adopted the FS/RH convention of Bilby, Bullough, and Smith [22]. This definition of α is also consistent with the analogous definition in magnetostatics of the current density in terms of the magnetic field.

directly from the definition of \mathbf{R} and the representation of the δ function in terms of the Green's tensor given by eq (2.7):

$$\begin{aligned} R_{mnkl}(\mathbf{r}' - \mathbf{r}) &= \delta_{mk}\delta_{nl}\delta(\mathbf{r}' - \mathbf{r}) - C_{ijkl}G_{mi,n'j}(\mathbf{r}' - \mathbf{r}) \\ &= \epsilon_{lpq}\epsilon_{spn}C_{ijks}G_{mi,jq}(\mathbf{r}' - \mathbf{r}) \\ &= \epsilon_{lpq}[\epsilon_{spn}C_{ijks}G_{mi,j}(\mathbf{r}' - \mathbf{r})]_{,q} \\ &= \epsilon_{lqp}D_{mnkp,q}^*(\mathbf{r}' - \mathbf{r}). \end{aligned}$$

where

$$D_{mnkp}^*(\mathbf{r}' - \mathbf{r}) \equiv \epsilon_{nps}C_{ijks}G_{mi,j}(\mathbf{r}' - \mathbf{r}). \quad (4.7)$$

An alternate form for \mathbf{D} —which we shall denote as \mathbf{D}^∞ —can be constructed by use of the Helmholtz decomposition theorem [14]:

$$\begin{aligned} D_{mnkl}^\infty(\mathbf{r}' - \mathbf{r}) &= \frac{1}{4\pi} \int \epsilon_{lqp}R_{mnkp,q}(\mathbf{r}' - \mathbf{r}'') |\mathbf{r}'' - \mathbf{r}|^{-1} dV \\ &= +\frac{1}{4\pi} \left(\delta_{mk}\epsilon_{nlq}|\mathbf{r}' - \mathbf{r}|_{,q}^{-1} \right. \\ &\quad \left. + \int C_{ijkq}G_{mi,n'j''}(\mathbf{r}' - \mathbf{r}'') \epsilon_{lsq}|\mathbf{r}'' - \mathbf{r}|_{,s''}^{-1} dV'' \right). \quad (4.8) \end{aligned}$$

No matter which form of \mathbf{D} is used, one may employ eq (4.6) and integration by parts to identify dislocations as the sources of residual distortion in B^∞ :

$$\begin{aligned} \beta_{mn}^R(\mathbf{r}') &= \int R_{mnkl}(\mathbf{r}' - \mathbf{r})\beta_{kl}(\mathbf{r}) dV \\ &= \int \epsilon_{lqp}D_{mnkp,q}(\mathbf{r}' - \mathbf{r})\beta_{kl}(\mathbf{r}) dV \\ &= - \int \epsilon_{lqp}D_{mnkp}(\mathbf{r}' - \mathbf{r})\beta_{kl,q}(\mathbf{r}) dV \\ &= \int D_{mnkp}(\mathbf{r}' - \mathbf{r})\alpha_{kp}(\mathbf{r}) dV \quad (4.9) \end{aligned}$$

where $\boldsymbol{\alpha}$ is the dislocation density tensor given in (4.2).

In summary, then, we may extend the basic decomposition formula

(2.19) for general anisotropic bodies with internal strains to include a decomposition at the dislocation level:

$$\begin{aligned}\beta_{mn}(\mathbf{r}') &= \int F_{mnkl}(\mathbf{r}' - \mathbf{r})\beta_{kl}(\mathbf{r})dV + \int R_{mnkl}(\mathbf{r}' - \mathbf{r})\beta_{kl}(\mathbf{r})dV \\ &= \int G_{mi, n'}(\mathbf{r}' - \mathbf{r})f_i(\mathbf{r})dV + \int D_{mnkl}(\mathbf{r}' - \mathbf{r})\alpha_{kl}(\mathbf{r})dV.\end{aligned}\quad (4.10)$$

The second part of eq (4.10) provides the analog in elastostatics of the Helmholtz theorem for vector fields given by eq (2.4). From this expression one can construct β from a knowledge of its dislocation and body force sources. This construction is still valid when these sources occur in sheets or lines which produce singularities or discontinuities in the normal or tangential components of β ; such sources are then considered as distributions, or generalized functions.¹⁷

If we turn to the comparison of equation (4.10) with the previously cited Mura-Willis formula, equation (4.1), it is immediately clear that if the kernel \mathbf{D} is taken to be \mathbf{D}^* as given in equation (4.7), the second part of equation (4.10) provides the Mura-Willis decomposition of the distortion field. On the other hand, if the kernel \mathbf{D} is taken to be \mathbf{D}^∞ , then one has what may be called the rational dislocation decomposition of the distortion field. In order to see this most easily, let us consider the distortion field at \mathbf{r}' , which we may call $\beta^D(\mathbf{r}')$ produced by a rational dislocation element $b_k dl_l$ at \mathbf{r} —as introduced by Eshelby and Laub [23]:

$$\beta_{mn}^D(\mathbf{r}') = D_{mnkl}^\infty(\mathbf{r}' - \mathbf{r}) b_k dl_l \quad (4.11)$$

Equation (4.10) tells us that the superposition of such distortion fields weighted by the dislocation density at each point \mathbf{r} will produce the residual distortion field β^R due to that dislocation density. However, the individual element $b_k dl_l$ is not a physically valid dislocation distribution since it does not close—that is, it is not divergence free in the index l . Thus if we calculate the dislocation density due to β^D , which density must be divergence free, we shall obtain a physically valid dislocation-field which includes the rational dislocation element $b_k dl_l$. If we call such a dislocation density α^D , then from (4.8), (4.11)

$$\alpha_{mn}^D(\mathbf{r}') = b_m dl_l \delta(\mathbf{r}' - \mathbf{r}) - \frac{1}{4\pi} b_m dl_q |\mathbf{r}' - \mathbf{r}|_{,nq'}^{-1}, \quad (4.12)$$

since the integral expression involving \mathbf{G} has a vanishing curl in the second index. Equation (4.12) is exactly the rational dislocation density of Eshelby and Laub.

¹⁷ cf [20].

V. The Incompatibility Problem

In this section we wish to continue the source kernel approach to obtain the solution for the incompatibility problem for internal stresses. The incompatibility η of an arbitrary distortion field β is defined by the relation

$$\eta_{kl}(\mathbf{r}) \equiv -(\epsilon_{kmp}\epsilon_{lnq}\beta_{mn, pq}(\mathbf{r}))_{(kl)} \quad (5.1)$$

$$= -\epsilon_{kmp}\epsilon_{lnq}e_{mn, pq}(\mathbf{r}) \quad (5.2)$$

where the strain $e_{ij}(\mathbf{r})$ is given by

$$e_{ij}(\mathbf{r}) = \frac{1}{2}(\beta_{ij}(\mathbf{r}) + \beta_{ji}(\mathbf{r})). \quad (5.3)$$

In terms of the dislocation density α , (5.1) may be written

$$\eta_{kl}(\mathbf{r}) = (\epsilon_{knq}\alpha_{nl, q}(\mathbf{r}))_{(kl)}. \quad (5.4)$$

The concept of incompatibility as an alternate source of residual stress has been discussed by several authors [3, 20, 24, 25]. In terms of residual distortions, however, since the incompatibility, η , is a function of the strain field, it is clear than η can serve as a source of the residual strain field \mathbf{e}^R only, rather than as a source of the residual distortion field β^R . This means that to formally treat the incompatibility problem, we must provide an alternate decomposition of the total distortion field in which the rotations are separated.

Let us, then, define the projection operator \mathbf{W} with kernel \mathbf{W} which identifies the rotational or antisymmetric components of the distortion field:

$$\mathbf{W}(\beta) \equiv \beta^W \quad (5.5)$$

where

$$\beta_{mn}^W(\mathbf{r}') = \frac{1}{2}(\beta_{mn}(\mathbf{r}') - \beta_{nm}(\mathbf{r}')) = \int W_{mnkl}(\mathbf{r}' - \mathbf{r})\beta_{kl}(\mathbf{r})dV \quad (5.6)$$

and

$$W_{mnkl}(\mathbf{r}' - \mathbf{r}) \equiv \frac{1}{2}(\delta_{mk}\delta_{nl} - \delta_{nk}\delta_{ml})\delta(\mathbf{r}' - \mathbf{r}) \quad (5.7)$$

The kernels \mathbf{W} , (\mathbf{F}) , and (\mathbf{R}) are easily seen to define another set of

independent projection operators decomposing the elastic distortion field according to:

$$\begin{aligned}
 \beta_{mn}(\mathbf{r}') &= \beta_{mn}^W(\mathbf{r}') + e_{mn}^F(\mathbf{r}') + e_{mn}^R(\mathbf{r}') \\
 &= \int W_{mnkl}(\mathbf{r}' - \mathbf{r})\beta_{kl}(\mathbf{r})dV + \int (F)_{mnkl}(\mathbf{r}' - \mathbf{r})\beta_{kl}(\mathbf{r})dV \\
 &\quad + \int (R)_{mnkl}(\mathbf{r}' - \mathbf{r})\beta_{kl}(\mathbf{r})dV \\
 &= \int W_{mnkl}(\mathbf{r}' - \mathbf{r})\beta_{kl}(\mathbf{r})dV + \int (G_{mi,n'})_{(mn)}(\mathbf{r}' - \mathbf{r})f_i(\mathbf{r})dV \\
 &\quad + \int (D_{mnkl})_{(mn)}(\mathbf{r}' - \mathbf{r})\alpha_{kl}(\mathbf{r})dV. \tag{5.8}
 \end{aligned}$$

Equation (5.8) provides a decomposition of the distortion field in terms of the strain and rotation. In view of eq (4.4), however, one notes that there are possible source tensors—which we may designate by **(D)**—such that

$$(D)_{mnkl}(\mathbf{r}' - \mathbf{r}) = (D)_{nmkl}(\mathbf{r}' - \mathbf{r})$$

and

$$\epsilon_{lqp}(D)_{mnkp,q}(\mathbf{r}' - \mathbf{r}) = (R)_{mnkl}(\mathbf{r}' - \mathbf{r}), \tag{5.9}$$

but where

$$\epsilon_{lqp}(D)_{mnkp,q}(\mathbf{r}' - \mathbf{r}) \neq R_{mnkl}(\mathbf{r}' - \mathbf{r}).$$

These source tensors will then produce from α the correct residual strain field, but a distortion field which may differ from β by a rotation field. Such source tensors need not correctly reproduce the original dislocation density α .¹⁸

¹⁸ If we designate

$$\beta_{mn}^{(D)}(\mathbf{r}') \equiv \int (D)_{mnkl}(\mathbf{r}' - \mathbf{r})\alpha_{kl}(\mathbf{r})dV$$

so that

$$\beta^R - \beta^{(D)} \equiv \omega$$

is a pure rotation field, then

$$\alpha_{kl}^{(D)}(\mathbf{r}) \equiv \epsilon_{lqp}\beta_{kp,q}^{(D)}(\mathbf{r})$$

differs from $\alpha_{kl}(\mathbf{r})$ by the curl of the rotation field ω :

$$\alpha_{kl}(\mathbf{r}) - \alpha_{kl}^{(D)}(\mathbf{r}) = \epsilon_{lqp}\omega_{kp,q}(\mathbf{r}).$$

Dislocation fields of the type $\alpha - \alpha^{(D)}$ which have a rotational potential have been called by Mura “imotent dislocation fields” [26].

The second part of eq (5.8), therefore, has the disadvantage that the source field α is not reproduced exactly by the source kernel (\mathbf{D}) for e^R if we use the appropriate defining relation (5.9). On the other hand, as seen from eqs (5.2) and (5.4)

$$\boldsymbol{\eta} = \boldsymbol{\eta}^R,$$

where

$$\eta_{kt}^R(\mathbf{r}) \equiv -\epsilon_{kmp}\epsilon_{lnq}c_{mn,pq}^R(\mathbf{r}), \quad (5.10)$$

so that, as mentioned above, the incompatibility is truly an invariant of residual strain field.

The converse problem is the incompatibility problem, and we shall look for a kernel \mathbf{I} which provides a source kernel for the residual strain in terms of the incompatibility. That is:

$$e_{mn}^R(\mathbf{r}') = \int I_{mnkl}(\mathbf{r}' - \mathbf{r})\eta_{kl}(\mathbf{r})dV. \quad (5.11)$$

Equation (5.11) will then permit an extension of eq (5.8) to include a decomposition in terms of incompatibilities:

$$\begin{aligned} \beta_{mn}(\mathbf{r}') &= \int W_{mnkl}(\mathbf{r}' - \mathbf{r})\beta_{kl}(\mathbf{r})dV + \int (G_{mi,n'})_{(mn)}(\mathbf{r}' - \mathbf{r})f_i(\mathbf{r})dV \\ &\quad + \int I_{mnkl}(\mathbf{r}' - \mathbf{r})\eta_{kl}(\mathbf{r})dV \end{aligned} \quad (5.12)$$

We seek, first, conditions needed to characterize \mathbf{I} . Let us note that since \mathbf{I} operates on $\boldsymbol{\eta}$, which is the symmetric part, only, of $\boldsymbol{\eta}^*$:

$$\eta_{kl}^*(\mathbf{r}) \equiv -\epsilon_{kmp}\epsilon_{lnq}\beta_{mn,pq}(\mathbf{r}), \quad (5.13)$$

it is required that

$$I_{mnpq,t}(\mathbf{r}' - \mathbf{r})\epsilon_{pqt} = 0 \quad (5.14)$$

to permit the substitution of $\boldsymbol{\eta}^*$ for $\boldsymbol{\eta}$ in eq (5.11).

Equation (5.14) is identically satisfied if $I_{mnpq}(\mathbf{r}' - \mathbf{r})$ is symmetric in p and q . However, it can be seen that any kernel \mathbf{I}^* (symmetric or not) obtained using the Mura-Willis kernel \mathbf{D}^* defined in (4.7) also satisfies (5.14) whose generality, therefore, has some use. The construction of

such a kernel \mathbf{I}^* is described in the final section.

To see the necessity of eq (5.14) we set

$$\lambda_t(\mathbf{r}) \equiv \frac{1}{2} \eta_{pq}^*(\mathbf{r}) \epsilon_{pqt} = -\frac{1}{2} \beta_{ij,kl}(\mathbf{r}) \epsilon_{ikp} \epsilon_{jlt} \epsilon_{pqt} = -\frac{1}{2} \alpha_{pp,t}(\mathbf{r}) \quad (5.15)$$

and write for the residual strain field

$$\begin{aligned} e_{mn}^R(\mathbf{r}') &= \int I_{mnpq}(\mathbf{r}' - \mathbf{r}) \eta_{pq}(\mathbf{r}) dV \\ &= \int I_{mnpq}(\mathbf{r}' - \mathbf{r}) \eta_{pq}^*(\mathbf{r}) dV - \int I_{mnpq}(\mathbf{r}' - \mathbf{r}) \epsilon_{pqt} \lambda_t(\mathbf{r}) dV \\ &= \int I_{mnpq}(\mathbf{r}' - \mathbf{r}) \eta_{pq}^*(\mathbf{r}) dV + \int I_{mnpq,t}(\mathbf{r}' - \mathbf{r}) \epsilon_{pqt} \alpha_{kk}(\mathbf{r}) dV \end{aligned}$$

from which the necessity of (5.14) follows. We shall now assume that \mathbf{I} satisfies eq (5.14) and proceed by integrating the right-hand side of eq (5.11) with η replaced by η^* :

$$\begin{aligned} e_{mn}^R(\mathbf{r}') &= \int I_{mnkl}(\mathbf{r}' - \mathbf{r}) \eta_{kl}^*(\mathbf{r}) dV \\ &= - \int I_{mnkl}(\mathbf{r}' - \mathbf{r}) \epsilon_{kps} \epsilon_{lqt} \beta_{pq,st}(\mathbf{r}) dV \\ &= \int I_{mnkl,s}(\mathbf{r}' - \mathbf{r}) \epsilon_{kps} \epsilon_{lqt} \beta_{pq,t}(\mathbf{r}) dV \\ &= - \int I_{mnkl,st}(\mathbf{r}' - \mathbf{r}) \epsilon_{kps} \epsilon_{lqt} \beta_{pq}(\mathbf{r}) dV. \end{aligned} \quad (5.16)$$

From (5.16) we conclude, by comparison with eq (5.8), that $\text{Inc } \mathbf{I} = (\mathbf{R})$, i.e.

$$-I_{mnkl,st}(\mathbf{r}' - \mathbf{r}) \epsilon_{kps} \epsilon_{lqt} = (R)_{mnpq}(\mathbf{r}' - \mathbf{r}). \quad (5.17)$$

By examination of (5.9), (5.10) and (5.17) it is also clear that $-\nabla_{\mathbf{r}} \times \mathbf{I}(\mathbf{r}' - \mathbf{r}) \equiv (\mathbf{D})(\mathbf{r}' - \mathbf{r})$, i.e.,

$$(D)_{mnpq}(\mathbf{r}' - \mathbf{r}) \equiv I_{mnkl,s}(\mathbf{r}' - \mathbf{r}) \epsilon_{kps}, \quad (5.18)$$

defines a dislocation source tensor for the strain field—although such a (\mathbf{D}) cannot be expected to be a satisfactory source kernel for the distortion field. Thus, for our purpose the incompatibility problem will be solved if we can obtain a source kernel \mathbf{I} satisfying equations (5.14) and (5.17). \mathbf{I} , of course, is not unique and each source tensor \mathbf{I} will also provide an expression for a dislocation source tensor (\mathbf{D}) for residual strains.

Two methods are generally available for finding such an \mathbf{I} : the harmonic Eshelby-Eddington approach [3] and the biharmonic approach of Kröner [1].

The Eshelby-Eddington approach follows from the observation that given any tensor field S_{ij} and a tensor field ϕ_{ij} such that $\Delta\phi_{ij}=S_{ij}$ and $\phi_{ij,j}=\phi_{ij}, i=0$, one can find by a short calculation that if $T_{ij}\equiv\phi_{ji}-\phi_{nn}\sigma_{ij}$, then $\text{Inc } \mathbf{T}=\mathbf{S}$.

On the other hand the biharmonic approach says that if one can find a tensor field χ_{ij} such that $\Delta\Delta\chi_{ij}=S_{ij}$ and $\chi_{ij,j}=\chi_{ij,i}=0$, then setting $\mathbf{T}\equiv\text{Inc } \chi$ yields $\text{Inc } \mathbf{T}=\mathbf{S}$ with the additional property here that $T_{ij,j}=T_{ij,i}=0$.

For our present applications we may assume that \mathbf{S} is such that $S_{ij}=S_{ji}$, and $S_{ij,j}=0$.¹⁹ We can then define the appropriate ϕ and χ by setting:

$$\phi_{ij}(\mathbf{r}') = -\frac{1}{4\pi} \int \frac{S_{ij}(\mathbf{r})}{|\mathbf{r}'-\mathbf{r}|} dV \quad (5.19)$$

and

$$\chi_{ij}(\mathbf{r}') = -\frac{1}{8\pi} \int S_{ij}(\mathbf{r}) |\mathbf{r}'-\mathbf{r}| dV. \quad (5.20)$$

The symmetry of $|\mathbf{r}'-\mathbf{r}|$ in \mathbf{r} and \mathbf{r}' and an integration by parts suffice to establish that both ϕ and χ are divergence free.

It should be noted that the biharmonic integral will generally diverge unless $S_{ij}=o(|\mathbf{r}|^{-4})$ —which is not the case for our particular application. However, this difficulty can be overcome in two ways: (1) If \mathbf{T} (which in our case will be the fourth order source tensor I_{mnkl}) is to be reintegrated with another quantity η (in our case, the incompatibility), generalized function theory allows us to interchange the order of integration if η is sufficiently well behaved at ∞ and thereby calculate $\int |\mathbf{r}'-\mathbf{r}| \eta(\mathbf{r}) dV$ first. This approach leads to Kröner's stress function method in infinite isotropy as we shall discuss in detail in the next section, but it does not permit the identification of a source tensor \mathbf{I} . (2) The other approach is to make use of the fact that $\mathbf{T}=\text{Inc } \chi$ and to interchange the order of integration and differentiation—also permitted by generalized function theory—to write:

$$\begin{aligned} T_{ij}(\mathbf{r}') &= \frac{\epsilon_{ikm}\epsilon_{jln}}{8\pi} \int S_{kl}(\mathbf{r}) |\mathbf{r}'-\mathbf{r}|_{,m'n'} dV \\ &= -\frac{1}{4\pi} \int \frac{S_{ij}(\mathbf{r}) - S_{nn}(\mathbf{r})\delta_{ij}}{|\mathbf{r}'-\mathbf{r}|} \\ &\quad - \frac{1}{8\pi} \int S_{kk}(\mathbf{r}) |\mathbf{r}'-\mathbf{r}|_{,ij} dV. \end{aligned} \quad (5.21)$$

¹⁹ Even in the finite body B these formulae hold provided that \mathbf{S} satisfies the additional boundary condition on B :

$$S_{ij}n_j = 0.$$

The second equation follows after a brief calculation and integration by parts using the divergence conditions for \mathbf{S} . This result gives a direct comparison between the Eshelby-Eddington and biharmonic approaches. The first term on the right hand side of (5.21) is the Eshelby-Eddington solution for \mathbf{T} while the second exhibits the incompatibility free term which is required if one desires \mathbf{T} to be divergence free.

If we choose for the tensor $S_{ij}(\mathbf{r})$ the fundamental source tensor $(R)_{mnij}(\mathbf{r}' - \mathbf{r})$, which by (4.4) satisfies the required divergence conditions, then we can write, using the Eshelby-Eddington formula and eq (2.15):

$$I_{mnkl}(\mathbf{r}' - \mathbf{r}) = \frac{1}{4\pi} \left(\frac{\delta_{mn}\delta_{kl} - \delta_{mk}\delta_{nl}}{|\mathbf{r}' - \mathbf{r}|} + (C_{ijkl} - \delta_{kl}C_{ijpp}) \int \frac{G_{mi, n'j''}(\mathbf{r}' - \mathbf{r}'')}{|\mathbf{r}'' - \mathbf{r}|} dV'' \right)_{(mn)} \quad (5.22)$$

The additional terms in the biharmonic solution for \mathbf{I} may also easily be written down. It is clear by construction that the \mathbf{I} given in (5.22) and the corresponding biharmonic expression satisfy eq (5.14) and (5.17) and thus provide acceptable source kernels for the incompatibility problem. We note that, at least in the case of infinite isotropy where these expressions can be explicitly evaluated, the biharmonic solution has a substantially simpler form than does the harmonic. A method for calculating \mathbf{I} is outlined in section VII.

VI. The Stress Function Problem

The technique of stress functions may also be developed using the more general source kernel approach exposed herein: Associated to an incompatibility source tensor \mathbf{I} which gives expressions for the internal strain, we can define a source tensor \mathbf{T} which describes the internal stress field:

$$T_{mnkl}(\mathbf{r}' - \mathbf{r}) \equiv C_{mnrs} I_{rskl}(\mathbf{r}' - \mathbf{r}) \quad (6.1)$$

from which it follows that $\text{Inc } \mathbf{T} = \mathbf{S}$:

$$-\epsilon_{kps}\epsilon_{lqt} T_{mnpq, st}(\mathbf{r}' - \mathbf{r}) = S_{mnkl}(\mathbf{r}' - \mathbf{r}). \quad (6.2)$$

\mathbf{T} is symmetric in both mn and kl when I_{mnkl} is symmetric in kl , but \mathbf{T} is not symmetric with respect to interchange of the pairs mn and kl . From the properties of \mathbf{S} and the manner of construction of \mathbf{I} , it is also clear that \mathbf{T} actually describes an internal stress field ($T_{mnkl, n'}(\mathbf{r}' - \mathbf{r}) = 0$) due to a rational incompatibility of type kl .

Using the integration methods described in the preceding section, one expects it to be possible to integrate \mathbf{T} to find a stress function source tensor Ψ . Thus the biharmonic formula gives

$$\begin{aligned}\Psi_{mnkl}(\mathbf{r}' - \mathbf{r}) = & -\frac{1}{4\pi} \int \frac{T_{mnkl}(\mathbf{r}'' - \mathbf{r}) - T_{ppkl}(\mathbf{r}'' - \mathbf{r})\delta_{mn}}{|\mathbf{r}'' - \mathbf{r}'|} dV'' \\ & - \frac{1}{8\pi} \int T_{ppkl}(\mathbf{r}'' - \mathbf{r}) |\mathbf{r}'' - \mathbf{r}'|_{,m'n'} dV''.\end{aligned}\quad (6.3)$$

The kernel Ψ would then provide a solution to the stress function problem: notably, given an incompatibility distribution η one could write down a stress function tensor due to the incompatibility distribution:

$$\psi_{mn}(\mathbf{r}') = \int \Psi_{mnkl}(\mathbf{r}' - \mathbf{r}) \eta_{kl}(\mathbf{r}) dV,\quad (6.4)$$

so that $\text{Inc } \psi = \sigma^R$, where σ^R is the residual stress field associated to η . Unfortunately, the above stress function source tensor fails to exist in the ordinary sense in the infinite body since the integrals involved diverge in the same way as does the integral of r^{-2} in all space. This difficulty was discussed earlier in the previous section except that here there is no way out except the first approach discussed therein. This allows ψ to still be defined as a generalized function in terms of the “convolution” of two generalized functions, but this process can be made valid only if the distortion field is “zeroey” enough at infinity.

The above source kernel approach to the stress function problem is not the same as that suggested by Kröner and actually solved by him for the isotropic body [1, 2]. Nonetheless, Kröner's isotropic solution may be generalized to the infinite anisotropic body by the techniques developed above. Accordingly, we follow Kröner by introducing (c.f. deWit [27])

$$\chi_{kl}(\mathbf{r}'') = \int |\mathbf{r}'' - \mathbf{r}| \eta_{kl}(\mathbf{r}) dV.\quad (6.5)$$

which satisfies, since η is divergence free, the auxiliary conditions:

$$\chi_{kl,k}(\mathbf{r}) = \chi_{kl,l}(\mathbf{r}) = 0.\quad (6.6)$$

Let us note the following identity for convolutions:

$$\int f(\mathbf{r}' - \mathbf{r}'') g(\mathbf{r}'' - \mathbf{r}) dV'' = \int f(\mathbf{r} - \mathbf{r}'') g(\mathbf{r}'' - \mathbf{r}') dV''.\quad (6.7)$$

where f and g are arbitrary, suitable even functions. Then, applying (6.7)

to (6.3), we may write

$$\begin{aligned}\Psi_{mnkl}(\mathbf{r}' - \mathbf{r}) = & -\frac{1}{4\pi} \int \frac{T_{mnkl}(\mathbf{r}'' - \mathbf{r}') - T_{ppkl}(\mathbf{r}'' - \mathbf{r}') \delta_{mn}}{|\mathbf{r}'' - \mathbf{r}|} dV'' \\ & - \frac{1}{8\pi} \int T_{ppkl}(\mathbf{r}'' - \mathbf{r}') |\mathbf{r}'' - \mathbf{r}|_{,mn} dV''.\end{aligned}\quad (6.8)$$

From (5.21) with the tensor $S_{ij}(\mathbf{r})$ identified with the stress kernel $S_{mnij}(\mathbf{r}' - \mathbf{r})$, we also have

$$\begin{aligned}T_{mnkl}(\mathbf{r}' - \mathbf{r}'') = & -\frac{1}{4\pi} \int \frac{S_{mnkl}(\mathbf{r}' - \mathbf{r}''') - S_{mnqq}(\mathbf{r}' - \mathbf{r}''') \delta_{kl}}{|\mathbf{r}''' - \mathbf{r}''|} dV''' \\ & - \frac{1}{8\pi} \int S_{mnqq}(\mathbf{r}' - \mathbf{r}''') |\mathbf{r}''' - \mathbf{r}''|_{,k''l'} dV'''.\end{aligned}\quad (6.9)$$

Since, by (6.7) and (6.9),

$$T_{mnkl}(\mathbf{r}'' - \mathbf{r}') = T_{mnkl}(\mathbf{r}' - \mathbf{r}''), \quad (6.10)$$

we may now usefully substitute (6.9) directly into (6.8) to obtain:

$$\begin{aligned}\Psi_{mnkl}(\mathbf{r}' - \mathbf{r}) = & -\frac{1}{8\pi} \int [S_{mnkl}(\mathbf{r}' - \mathbf{r}''') - S_{mnqq}(\mathbf{r}' - \mathbf{r}''') \delta_{kl} \\ & - S_{ppkl}(\mathbf{r}' - \mathbf{r}''') \delta_{mn} + S_{ppqq}(\mathbf{r}' - \mathbf{r}''') \delta_{kl} \delta_{mn}] |\mathbf{r}''' - \mathbf{r}| dV''' \\ & - \frac{1}{96\pi} \int [S_{mnqq}(\mathbf{r}' - \mathbf{r}''') - S_{ppqq}(\mathbf{r}' - \mathbf{r}''') \delta_{mn}] |\mathbf{r}''' - \mathbf{r}|^3_{,k'''l'''} dV''' \\ & - \frac{1}{96\pi} \int [S_{ppkl}(\mathbf{r}' - \mathbf{r}''') - S_{ppqq}(\mathbf{r}' - \mathbf{r}''') \delta_{kl}] |\mathbf{r}''' - \mathbf{r}|^3_{,m'''n'''k'''l'''} dV''' \\ & - \frac{1}{2880\pi} \int S_{ppqq}(\mathbf{r}' - \mathbf{r}''') |\mathbf{r}''' - \mathbf{r}|^3_{,m'''n'''k'''l'''} dV'''.\end{aligned}\quad (6.11)$$

Here we have performed one of the volume integrals by using the results

$$\int \frac{dV''}{|\mathbf{r}''' - \mathbf{r}''| |\mathbf{r}'' - \mathbf{r}|} = -2\pi |\mathbf{r}''' - \mathbf{r}|, \quad (6.12)$$

$$\int \frac{|\mathbf{r}'' - \mathbf{r}|_{,m''n''}}{|\mathbf{r}''' - \mathbf{r}''|} dV'' = -\frac{\pi}{3} |\mathbf{r}''' - \mathbf{r}|^3_{,m'''n'''}, \quad (6.13)$$

and

$$\int |\mathbf{r}''' - \mathbf{r}''|_{,m''n''} |\mathbf{r}'' - \mathbf{r}|_{,k''l''} dV'' = -\frac{\pi}{45} |\mathbf{r}''' - \mathbf{r}|^5_{,m'''n'''k'''l'''}; \quad (6.14)$$

these results being understood to be valid in a formal sense, that is they only take on meaning when the result is reintegrated with the second derivative of some well behaved function.

Now to find the stress function ψ given in (6.4), we observe that since η is divergence free, the second and fourth integrals in (6.11) give zero contribution to ψ . In addition, the first integral occurring in (6.11) may be seen by comparison with equation (5.21) to provide the Eshelby-Eddington form for the stress function kernel, Ψ . Therefore, the Eshelby-Eddington formula giving the full generalization to infinite anisotropy of Kröner's isotropic stress function method is:

$$\begin{aligned} \psi_{mn}^{EE}(\mathbf{r}') = & -\frac{1}{8\pi} \int [S_{mnkl}(\mathbf{r}' - \mathbf{r}'') - S_{mnqq}(\mathbf{r}' - \mathbf{r}'')\delta_{kl} \\ & - S_{ppkl}(\mathbf{r}' - \mathbf{r}'')\delta_{mn} + S_{ppqq}(\mathbf{r}' - \mathbf{r}'')\delta_{kl}\delta_{mn}] \chi_{kl}(\mathbf{r}'') dV'' \end{aligned} \quad (6.15)$$

where χ is given by eq (6.5). ψ^{EE} however, does not satisfy the gauge condition

$$\psi_{mn,n}(\mathbf{r}) = \psi_{mn,m}(\mathbf{r}) = 0. \quad (6.16)$$

In order to achieve this gauge condition one must employ the full biharmonic form given in (6.11) by adding to ψ^{EE} the term $\Phi_{,m'n'}(\mathbf{r}')$:

$$\Phi(\mathbf{r}') = -\frac{1}{96\pi} \int [S_{ppkl}(\mathbf{r}' - \mathbf{r}'') - S_{ppqq}(\mathbf{r}' - \mathbf{r}'')\delta_{kl}] \phi_{kl}(\mathbf{r}'') dV''. \quad (6.17)$$

where

$$\phi_{kl}(\mathbf{r}'') \equiv \int |\mathbf{r}'' - \mathbf{r}|^3 \eta_{kl}(\mathbf{r}) dV. \quad (6.18)$$

As a special case we may check this general formulation for an infinite isotropic body. The expression for \mathbf{S} is, from (2.18) and the isotropic Green's tensor:²⁰

²⁰ $G_{ij}(\mathbf{r}) = \frac{1}{16\pi\mu(1-\nu)} [2(1-\nu)\delta_{ij}|\mathbf{r}|_{,pp} - |\mathbf{r}|_{,ij}]$

$$\begin{aligned}
S_{mnpq}(\mathbf{r}) = & \frac{2\nu\mu}{1-\nu} \delta_{mn}\delta_{pq}\delta(\mathbf{r}) + 2\mu(\delta_{mp}\delta_{np}\delta(\mathbf{r}))_{(mn)} \\
& + \frac{\mu}{4\pi} \left[\frac{\nu}{1-\nu} (\delta_{mn}|\mathbf{r}|_{jjpq} + \delta_{pq}|\mathbf{r}|_{jjmn}) \right. \\
& \left. + 2(\delta_{mp}|\mathbf{r}|_{jjnq})_{(mn)(pq)} - \frac{1}{1-\nu} |\mathbf{r}|_{mnpq} \right]. \quad (6.19)
\end{aligned}$$

Substituting (6.19) into (6.15) and (6.17) and using (6.6) and the analogous condition on Φ , notably

$$\Phi_{kl,k}(\mathbf{r}) = \Phi_{kl,l}(\mathbf{r}) = 0, \quad (6.20)$$

we obtain the result

$$\psi_{mn}(\mathbf{r}') = 2\mu \left[\chi_{mn}(\mathbf{r}') + \frac{\nu}{1-\nu} \delta_{mn}\chi_{pp}(\mathbf{r}') \right], \quad (6.21)$$

which is seen to coincide with Kröner's stress function solution [27] in this isotropic case.

VII. Discussion

The question as to how one calculates a dislocation source tensor \mathbf{D} has been discussed in section IV while formulas for the calculation of the incompatibility tensor \mathbf{I} have been presented in section V. We would like to indicate here some perhaps numerically useful techniques for calculating such source tensors in the infinite body. Because of the explicit representation for the dislocation source tensor in terms of the Green's tensor derivatives given by eq (4.7)

$$D_{mnkl}^*(\mathbf{r}' - \mathbf{r}) = \epsilon_{nts} C_{ijks} G_{mi,j}(\mathbf{r}' - \mathbf{r})$$

and because of the similar methods involved in calculating \mathbf{D} and \mathbf{I} , we have chosen to explore only the calculations of the less well-known incompatibility source tensor \mathbf{I} . On the other hand it should be admitted that although defect descriptions in terms of incompatibility avoid ex-

traneous rotational terms, the physical usefulness of the more complex incompatibility source tensor may be open to question. This is particularly true as long as no experimental situations occur in which physical data are given directly in terms of incompatibility sources.

We first present an explicit expression for a dislocation source tensor I^* derived from the dislocation source tensor \mathbf{D}^* and given in terms of easily numerically evaluated integrals of the Green's tensor.

$$I_{mnpq}^*(\mathbf{r}) = \left[C_{ijkl} x_s G_{nk,l}(\mathbf{r}) \epsilon_{pmj} \epsilon_{qis} \ln |\mathbf{r}| + \frac{1}{|\mathbf{r}|^3} \{ \epsilon_{pjma_{jn}} (x_3 x_q - |\mathbf{r}|^2 \delta_{q3}) - \epsilon_{pjmb_{jn}} b_{jn} x_s |\mathbf{r}| \} \right]_{(mn)}. \quad (7.1)$$

Here

$$\begin{aligned} a_{jn}(\theta, \phi) &= \int_0^\phi K_{jn}(\theta, \lambda) d\lambda - \frac{\phi}{2\pi} \int_0^{2\pi} K_{jn}(\theta, \lambda) d\lambda \\ b_{jn}(\theta) &= \frac{1}{2\pi \sin^2 \theta} \int_0^\theta \sin \mu d\mu \int_0^\pi K_{jm}(\mu, \lambda) d\lambda \end{aligned} \quad (7.2)$$

and

$$K_{jn}(\theta, \phi) = |\mathbf{r}| x_i C_{ijkl} G_{nk,l}(\mathbf{r}). \quad (7.3)$$

This result may be derived from the following lemma which will be started without proof:

LEMMA. *Given a vector field \mathbf{v} each of whose components, v_i , is homogeneous of degree -2 such that $\nabla \cdot \mathbf{v}(\mathbf{r}) = 0$ for $\mathbf{r} \neq 0$ and such that*

$$\int |\mathbf{r}| \mathbf{v} \cdot \mathbf{r} dS = 0 \quad (7.4)$$

for any sphere containing the origin, one can write:

$$\nabla \times \mathbf{w} = \mathbf{v} \quad (7.5)$$

and $\mathbf{w} \cdot \mathbf{r} = 0$ for the vector field \mathbf{w} given by:

$$\mathbf{w}(\mathbf{r}) = \mathbf{r} \times \left(\mathbf{v} \ln |\mathbf{r}| - \frac{\mathbf{h}(\Omega)}{|\mathbf{r}|^2} \right), \quad (7.6)$$

where $\mathbf{h}(\Omega)$ is the vector field on the sphere:

$$\mathbf{h}(\theta, \phi) \equiv A(\theta, \phi) \mathbf{n}_\theta + B(\theta) \mathbf{n}_\phi,$$

$$A(\theta, \phi) \equiv \int_0^\phi g(\theta, \lambda) \sin \theta d\lambda - \frac{\phi}{2\pi} \int_0^{2\pi} g(\theta, \lambda) \sin \theta d\lambda,$$

$$B(\theta) = \frac{1}{2\pi \sin \theta} \int_0^\theta d\mu \int_0^{2\pi} g(\mu, \lambda) \sin \mu d\lambda, \quad (7.7)$$

$g(\theta, \phi) \equiv |\mathbf{r}| \mathbf{v} \cdot \mathbf{r}$, and \mathbf{n}_θ and \mathbf{n}_ϕ are the unit normals in the θ and ϕ directions, respectively.

The Eshelby-Eddington formula (5.22) for \mathbf{I} can also be made somewhat more palatable if one integrates by parts and rewrites the expression as

$$I_{mnkl}^{EE}(\mathbf{r}' - \mathbf{r}) = \frac{1}{4\pi} \left(\frac{\delta_{mn}\delta_{kl} - \delta_{mk}\delta_{nl}}{|\mathbf{r}' - \mathbf{r}|} \right. \\ \left. + (C_{ijkl} - \delta_{kl}C_{ijpp}) \int |\mathbf{r}'' - \mathbf{r}|, j^{-1} G_{mi, n'}(\mathbf{r}' - \mathbf{r}'') dV'' \right)_{(mn)}. \quad (7.8)$$

The components of the Green's tensor derivatives in (7.8) are exactly those that must be tabulated in any useful numerically computed Green's function. Also, using the fact that the Green's tensor is homogeneous of degree -1 , it is possible to rotate a spherical coordinate system so that the vector $\mathbf{r}' - \mathbf{r}$ is along the \mathbf{x}_3 axis and carry out the radial integration showing that \mathbf{I} defined by the Eshelby-Eddington formula is homogeneous of degree -1 ; the explicit angular integrals, however, would have to be carried out numerically.

Pending a forthcoming computer program for numerically calculating Green's tensors and their derivatives, important applications can still be made employing the source function approach, since the Fourier transforms for arbitrary anisotropic bodies are readily available as rational polynomials. Thus \mathbf{G} , the Fourier transform of \mathbf{G} is given by:

$$\hat{G}_{ik}(\mathbf{k}) = \tilde{K}_{ik}(\mathbf{k}) \quad (7.9)$$

where $K_{ik}(\mathbf{k}) = C_{ijkl} \mathbf{k}_j \mathbf{k}_l$ and $\tilde{\mathbf{K}}$ represents the inverse matrix to \mathbf{K} . The source function method now provides a powerful technique for calculating the Fourier transforms of internal stress and strain fields, since these fields are obtained in the infinite body as convolutions of the source function kernel with the appropriate distribution of sources of internal stress. Consequently, the Fourier transform of the internal field is merely the product of the Fourier transforms of the source kernel and of the

internal stress source distribution. All the source kernels have themselves been expressed as convolutions on the fundamental tensors \mathbf{R} and \mathbf{S} . The transforms of \mathbf{R} and \mathbf{S} are, however, homogeneous rational polynomials of degree zero in reciprocal space simply obtained from the expressions for the transforms for the Green's tensor, so that it is a practical possibility to calculate the Fourier transform for the fields of many types of both residual and force induced stress fields.

The uses for these transforms have not been thoroughly explored, but their importance to problems such as diffraction is self-evident. Kuriyama [28] for instance has already developed an explicit expression for the scattering matrix elements directly in terms of the Fourier transform of the residual displacement field, whose transform can readily be written down at least for infinitesimal loops.

Another important application for the Fourier transforms of the internal fields is in finding interaction energies. This approach is being investigated by Mura [29, 8]. The general point to note is that Parseval's theorem from Fourier Transform theory tells us that given two functions f and g in three dimensions with Fourier transforms \hat{f} and \hat{g} in reciprocal space, one has the relation

$$\int f^*(\mathbf{r})g(\mathbf{r})dV = \frac{1}{(2\pi)^3} \int \hat{f}^*(\mathbf{k})\hat{g}(\mathbf{k})d\hat{V}, \quad (7.10)$$

where * indicates the complex conjugate. Thus, one can take the integral of the Fourier transform of a plastic strain source field with the transforms of the stress field from another such source to obtain the interaction energy.

For example, if β^{1P} and β^{2P} , are two plastic displacement dipole distributions, the interaction energy of their induced residual stress fields is

$$(2\pi)^{-3} \int \hat{S}_{ijkl}(\mathbf{k}) \hat{\beta}_{ij}^{1P*}(\mathbf{k}) \hat{\beta}_{kl}^{2P}(\mathbf{k}) d\hat{V}. \quad (7.11)$$

This interaction energy, involving only one integral over reciprocal space, may in certain cases be more practical to evaluate than the real space interaction integral.

VIII. Acknowledgements

The authors wish to thank Drs. J. Fong, M. Kuriyama, R. de Wit, and T. Mura for their valuable comments and discussion. Also the first author wishes to thank the United Kingdom Atomic Energy Research Establishment, Harwell, where part of this work was carried out through an arrangement between the UKAERE and the Institute for Materials Research of the National Bureau of Standards.

IX. References

- [1] Kröner, E., Z. Physik **139**, 175 (1954).
- [2] Kröner, E., Z. Physik **141**, 386 (1955).
- [3] Eshelby, J. D., in Solid State Physics **3**, F. Seitz and D. Turnbull, Eds. (Academic Press, New York, 1956) p. 79.
- [4] Kunin, I. A., Supplement to Russian edition of Tensor Analysis for Physicists by J. A. Schouten (Izdatel'stvo "NAUK" Glavnaya Redaktsiya Fiziko-Matematicheskoi Literatury, Moscow, 1965).
- [5] Simmons, J. A., and Bullough, R., to be published.
- [6] Eshelby, J. D., in Progress in Solid Mechanics **II**, I. N. Sneddon and R. Hill, Eds. (North Holland, Amsterdam, 1961) p. 89.
- [7] Mura, T., in Advances in Materials Research **3**, H. Herman, Ed. (John Wiley & Sons, New York, 1968) p. 1.
- [8] Mura, T., in Mathematical Theory of Dislocations, T. Mura, Ed. (ASME, New York, 1969) p. 25.
- [9] Mura, T., Phil. Mag. **8**, 843 (1963).
- [10] Willis, J., Int. J. Engng. Sci. **5**, 171 (1967).
- [11] Halmos, P. R., Finite Dimensional Vector Spaces, (D. Van Nostrand Co., Princeton, N. J., 1958).
- [12] Schwartz, L., Mathematics for the Physical Sciences (Addison-Wesley, Inc., Reading, Mass., 1966).
- [13] Gelfand, I. M., and Shilov, G. E., Generalized Functions, Vol. 1 (Academic Press, New York, 1964).
- [14] Phillips, H. B., Vector Analysis, (John Wiley & Sons, New York, 1933).
- [15] Synge, J. L., The Hypercircle in Mathematical Physics (Cambridge University Press, England, 1957).
- [16] Kröner, E., Arch. Rat. Mech. Anal. **4**, 273 (1960).
- [17] Weyl, H., Space-Time-Matter (Dover, New York, 1922).
- [18] Kroupa, F., Czech. J. Phys. **B12**, 191 (1962).
- [19] Kröner, E., in Theory of Crystal Defects, B. Gruber, Ed. (Academic Press, New York, 1966) p. 215.
- [20] Kröner, E., Kontinumstheorie der Versetzungen und Eigenspannungen (Springer, New York, 1958).
- [21] Sokolnikoff, I. S., Mathematical Theory of Elasticity (McGraw-Hill, New York, 1956).
- [22] Bilby, B. A., Bullough, R., and Smith, E., Proc. Roy. Soc. **A231**, 263 (1955).
- [23] Eshelby, J. D., and Laub, T., Canadian J. Physics **45**, 887 (1967).
- [24] Nabarro, F. R. N., Theory of Crystal Dislocations (Oxford at the Clarendon Press, England, 1967).
- [25] Moriguti, S., Oyo Sugaku Rikigaku **1**, 29 (1947).
- [26] Mura, T., in Mechanics of Generalized Continua, K. Kröner, Ed. (Proc. IUTAM Symp., Freudenstadt-Stuttgart, 1967) (Springer-Verlag, New York, 1968) p. 269.
- [27] deWit, R., in Solid State Physics **10**, F. Seitz and D. Turnbull, Eds. (Academic Press, New York, 1960) p. 249.
- [28] Kuriyama, M., J. Phys. Soc. Japan **23**, 1369 (1967).
- [29] Mura, T., J. Appl. Phys. **40**, 73 (1969).

SERIES REPRESENTATIONS OF THE ELASTIC GREEN'S TENSOR FOR CUBIC MEDIA

D. M. Barnett

*Metallurgy Section
Scientific Research Laboratory
Ford Motor Company
Dearborn, Michigan 48121*

Two representations for the cubic Green's tensor components as power series in the anisotropy factor $\omega = 1 - (c_{11} - c_{12})/2c_{44}$ are developed, and first order corrections of anisotropy to the Green's tensor and to the interaction energy between two "mechanical" point defects are calculated. It is shown that the best successive approximation scheme is that which constructs the zeroth order (isotropic) approximation to the Green's tensor by identifying the Lamé constants λ and μ as $\lambda = c_{12}$, $\mu = c_{44}$.

Key words: Anisotropy; cubic materials; elasticity; Green's tensor.

I. Introduction

The static Green's tensor for an infinite elastic continuum, $G_{il}(\bar{r} - \bar{r}')$, is defined as the i th component of the displacement at \bar{r} produced by a unit force in the l th direction at \bar{r}' ; G_{il} is symmetric in i and l . Closed analytical expressions for G_{il} have been constructed only for materials exhibiting isotropy or transverse isotropy [1, 2].

Knowledge of the Green's tensor and its derivatives allows one to construct the elastic fields of dislocations [2-5] and point defects (represented in a continuum by "crossed double forces without moment" [6, 7]) in linear anisotropic media. An iteration technique devised by Willis [8] utilizes the Green's tensor method to treat the more general case of dislocations in *nonlinear* anisotropic materials. Because both dislocations and point defects play such an important role in the plastic deformation of cubic metals, it is desirable to consider the effect of cubic anisotropy upon $G_{il}(\bar{r} - \bar{r}')$.

The construction of numerical and approximate analytical solutions for the cubic Green's tensor and its derivatives has intrigued several investigators. Lifshitz and Rosenzweig [9] and Eshelby [10] obtained first order

contributions of cubic anisotropy to the Green's tensor and the dilatation associated with three orthogonal sets of double forces, respectively. G_{il} was extracted numerically by Flinn and Maradudin [11] from the long wave limit of the discrete lattice Green's tensor and by Lie and Koehler [12], who followed Fredholm's classical analysis [13]. From their numerical results Lie and Koehler, after conjecturing that a useful expansion in spherical harmonics could not be expected, were able to approximate G_{il} as a double trigonometric series. Bross [14] avoided the cumbersome Fredholm technique and used the more direct Fourier transform approach [15] to derive an expansion for the Green's tensor in terms of cubic harmonics. Although the Bross representation obviously reflects the cubic symmetry of G_{il} , a measure of the effect of anisotropy of the elastic constants is not easily deduced from it.

The present work considers a very natural method for analytically displaying the effect of anisotropy upon $G_{il}(\bar{r} - \bar{r}')$, i.e., the representation of the cubic Green's tensor components as power series in the anisotropy factor

$$w = 1 - \frac{c_{11} - c_{12}}{2c_{44}}$$

(normally $0 \leq w < 1$, although cases in which $w < 0$ exist [16]). Because only three of the quantities c_{11} , c_{12} , c_{44} and w are independent, such expansions may be obtained in several ways. We shall treat the two cases in which the independent elastic variables are taken to be

- (a) w , c_{44} , c_{12}
- (b) w , c_{44} , c_{11} ,

compute first order anisotropy contributions to G_{il} and the dilatation due to three sets of crossed double forces, and compare the results with previous calculations of a similar nature [9, 10].

II. Construction of the Cubic Green's Tensor

The elastic equilibrium equations determining $G_{il\ell}$ for a cubic medium are

$$c_{44}\nabla^2 G_{il} + (c_{12} + c_{44})\partial_i \sum_{j=1}^3 \partial_j G_{jl} - 2c_{44}w\partial_i \partial_l G_{il} + \delta_{il}\delta(\bar{r} - \bar{r}') = 0; \\ i, l = 1, 2, 3. \quad (1)$$

The x_i are cartesian coordinates to which the elastic constants c_{ij} are referred, $\partial_i \equiv \partial/\partial x_i$, δ_{il} is the Kronecker delta, and $\delta(\bar{r} - \bar{r}')$ is the three-

dimensional Dirac delta function. (1) may also be written

$$c_{44}\nabla^2 G_{il} + (c_{11} - c_{44})\partial_i \sum_{j=1}^3 \partial_j G_{jl} + 2c_{44}w\partial_i \left(\sum_{j=1}^3 \partial_j G_{jl} - \partial_l G_{il} \right) + \delta_{il}\delta(\bar{r} - \bar{r}') = 0. \quad (2)$$

An iterative procedure for solving (1) may be developed in the following manner. Taking the Fourier transform of (1) yields

$$\sum_{j=1}^3 \left(\delta_{ij} + \frac{\gamma_{ij}}{\beta} \right) g_{il} = \frac{\delta_{il}}{c_{44}k^2} + 2w(\gamma_i)^2 g_{il} \quad (3)$$

where

$$g_{il}(\bar{k}) = \iiint_{-\infty}^{\infty} e^{i\bar{k} \cdot \bar{r}} G_{il}(\bar{r}) d^3\bar{r} \quad (4)$$

and

$$\begin{aligned} k &= |\bar{k}|, & \gamma_i &= k_i/k, \\ \gamma_{ij} &= \gamma_i \gamma_j, & \beta &= c_{44}/(c_{12} + c_{44}). \end{aligned} \quad \left. \right\} \quad (5)$$

We now write

$$g_{il} = \sum_{n=0}^{\infty} (2w)^n g_{il}^{(n)}, \quad (6)$$

substitute (6) into (3), and compare coefficients of w^n to obtain

$$\sum_{j=1}^3 \left(\delta_{ij} + \frac{\gamma_{ij}}{\beta} \right) g_{il}^{(n)} = (\gamma_i)^2 g_{il}^{(n-1)}, \quad n \geq 1 \quad (7)$$

$$= \frac{\delta_{il}}{c_{44}k^2}, \quad n = 0. \quad (8)$$

Simple matrix algebra inverts (7) and (8) to yield

$$g_{il}^{(n)} = \sum_{j=1}^3 \left(\delta_{ij} - \frac{\gamma_{ij}}{1+\beta} \right) (\gamma_j)^2 g_{jl}^{(n-1)}, \quad n \leq 1 \quad (9)$$

$$g_{il}^{(0)} = \frac{1}{c_{44}k^2} \left(\delta_{il} - \frac{\gamma_{il}}{1+\beta} \right). \quad (10)$$

Let $[Q]$ represent any 3×3 matrix whose elements are Q_{ij} . Using induction and the recursive relation (9), one finds that $[g]$, the Fourier transform of the Green's matrix $[G]$, may be written as

$$[g] = \frac{[M^*]}{c_{44}k^2} \sum_{n=0}^{\infty} (2w)^n ([R][M^*])^n, \quad (11)$$

$$\left. \begin{aligned} M_{ij}^* &= \delta_{ij} - \frac{\gamma_{ij}}{1+\beta} \\ R_{ij} &= \gamma_{ij} (i=j) \\ &= 0 (i \neq j). \end{aligned} \right\} \quad (12)$$

If we started with (2) rather than with (1), an analogous iterative procedure would have yielded

$$[g] = \frac{[M]}{c_{44}k^2} \sum_{n=0}^{\infty} (-2w)^n ([T][M])^n, \quad (13)$$

$$\left. \begin{aligned} M_{ij} &= \delta_{ij} - \frac{\gamma_{ij}}{1+\beta'} \\ \beta' &= c_{44}/(c_{11}-c_{44}) \\ T_{ij} &= \gamma_{ij} - R_{ij}. \end{aligned} \right\} \quad (14)$$

Leibfried [3] and Mura [17] have indicated how the elastic fields of and the interaction energies between dislocations may be expressed as line integrals involving the Fourier transform of G_{il} , so that the first several terms in (11) and (13) could be used to estimate anisotropy effects in such calculations. Equations (11) and (13) may be written in a more compact form, since

$$\sum_{n=0}^{\infty} (2w)^n ([R][M^*])^n = \{[I] - 2w[R][M^*]\}^{-1} \quad (15)$$

$$\sum_{n=0}^{\infty} (-2w)^n ([T][M])^n = \{[I] + 2w[T][M]\}^{-1}, \quad (16)$$

(provided, of course, that the series are convergent), where

$$I_{ij} = \delta_{ij}$$

and -1 denotes the inverse matrix.

The Green's tensor components are obtained from

$$G_{il}(\bar{r}-\bar{r}') = (2\pi)^{-3} \iiint_{-\infty}^{\infty} e^{-i\bar{k}\cdot(\bar{r}-\bar{r}')} g_{il}(\bar{k}) d^3\bar{k}. \quad (17)$$

Following Fourier inversion, our two iterative procedures yield

$$[G] = [G^*] + \frac{1}{8\pi^2 c_{44} |\bar{r}-\bar{r}'|} \sum_{n=1}^{\infty} (2w)^n \int_0^{2\pi} [m^*]([A][m^*])^n d\Psi \quad (18)$$

$$[G] = [G^\circ] + \frac{1}{8\pi^2 c_{44} |\bar{r}-\bar{r}'|} \sum_{n=1}^{\infty} (-2w)^n \int_0^{2\pi} [m]([K][m])^n d\Psi \quad (19)$$

with

$$\left. \begin{aligned} m_{ij}^* &= \delta_{ij} - \frac{a_{ij}}{1+\beta} \\ m_{ij} &= \delta_{ij} - \frac{\alpha_{ij}}{1+\beta'} \\ \alpha_{ij} &= \alpha_i \alpha_j \\ \alpha_1 &= \cos \varphi \cos \theta \cos \Psi - \sin \theta \sin \Psi \\ \alpha_2 &= \cos \varphi \sin \theta \cos \Psi + \cos \theta \sin \Psi \\ \alpha_3 &= -\sin \varphi \cos \Psi \\ A_{ij} &= \alpha_{ij} (i=j) \\ &\quad = 0 (i \neq j) \\ K_{ij} &= \alpha_{ij} - A_{ij}. \end{aligned} \right\} \quad (20)$$

θ and φ are angular spherical coordinates of $\bar{r}-\bar{r}'$, e.g.,

$$x_1 - x'_1 = |\bar{r} - \bar{r}'| \sin \varphi \cos \theta. \quad (21)$$

The matrix $[G^*]$ is given by

$$G_{ij}^* = \frac{1}{8\pi c_{44} (1+\beta) |\bar{r}-\bar{r}'|} \left\{ (2\beta+1) \delta_{ij} + \frac{(x_i - x'_i)(x_j - x'_j)}{|\bar{r}-\bar{r}'|^2} \right\}, \quad (22)$$

and $[G^\circ]$ is the same with β replaced by β' .

It should be mentioned that the reduction of the three-dimensional inversion integral (17) to the one-dimensional integrals (18) and (19) is most easily accomplished by representing the integrand in spherical polar

coordinates in k -space and integrating over $k = |\vec{k}|$ first. This integration yields a delta function (e.g., see [11]), so that in (17) only those unit Fourier wave vectors perpendicular to $\vec{r} - \vec{r}'$ contribute to G_{il} [18]. In fact, α_i is merely the direction cosine between such a vector and the x_i axis expressed in terms of Eulerian angles θ, φ, Ψ .

Using (18) and (19), the first order contribution of cubic anisotropy to the Green's tensor may be determined. To first order in w

$$G_{ij} = \frac{\delta_{ij}}{4\pi c_{44}|\vec{r} - \vec{r}'|} \left\{ 1 + w \left[(1 - n_j^2) + \frac{n_1^2 n_2^2 + n_3^2(1 - n_3^2)}{(1+B)^2} \right] \right\} \\ - \frac{\delta_{ij} - n_i n_j}{8\pi c_{44}(1+B)|\vec{r} - \vec{r}'|} \left\{ 1 + \frac{w}{2} \left[3(2 - n_i^2 - n_j^2) \right. \right. \\ \left. \left. + \frac{5(n_1^2 n_2^2 + n_3^2(1 - n_3^2)) - 5 + (\delta_{ij} + n_i^2 + n_j^2) + C}{(1+B)} \right] \right\} \quad (23)$$

with

$$\left. \begin{aligned} n_i &= \frac{x_i - x_i}{|\vec{r} - \vec{r}'|} \\ B &= \beta \text{ or } \beta' \\ C &= 0 \text{ if } B = \beta \\ &= 4\beta'^2 \text{ if } B = \beta' \end{aligned} \right\} \quad (24)$$

The corresponding first order expansion obtained by Lifshitz and Rosenzweig ([9], eq 2.12) was

$$G_{ij} = \frac{\delta_{ij}}{4\pi c_{44}|\vec{r} - \vec{r}'|} \{ 1 + w(1 - n_j^2) \} \\ - \frac{\delta_{ij} - n_i n_j}{8\pi c_{44}(1+\beta)|\vec{r} - \vec{r}'|} \{ 1 + \frac{3w}{2} (2 - n_i^2 - n_j^2) \}, \quad (25)$$

which, by comparison with (23), is obviously incomplete. Consider Al, Cu, and Li, the three cubic media discussed in [12].

$$\begin{aligned} \text{Al:} \quad w &= 0.180, & \beta &= 0.312, & \beta' &= 0.350 \\ \text{Cu:} \quad w &= 0.687, & \beta &= 0.383, & \beta' &= 0.810 \\ \text{Li:} \quad w &= 0.894, & \beta &= 0.464, & \beta' &= 2.69 \end{aligned}$$

A smaller *relative* first order anisotropy contribution to the Green's tensor components for Al and Cu is obtained by choosing $B = \beta$ and

$C = 0$ in (23) (e.g., the contribution $C/(1 + B)$ when $B = \beta'$ is significant for Cu). In the case of Li, the series (16) and (19) do not converge (note that $C/(1 + B) \sim 8$ for $B = \beta'$): the expansions (15) and (18) are always convergent for $w > 0$ (see Conclusions), although the convergence for lithium is not rapid. This essentially means that $[G^*]$ is a better zeroth order approximation to $[G]$ than is $[G^\circ]$, or that the best choices for the “zeroth order” Lamé constants λ and μ are

$$\mu = c_{44}, \lambda = c_{12}.$$

Choosing $[G^\circ]$ as a zeroth order approximation is equivalent to the identification

$$\mu = c_{44}, \lambda = c_{11} - 2c_{44}.$$

III. Applications to Point Defect Interactions

Consider as a mechanical model for a point defect in a cubic metal three orthogonal sets of double forces without moment, each set being of strength P_1 . The interaction energy between such a “defect” and another of strength P_2 is given by [6, 7]

$$E_{\text{int}} = -P_1 P_2 \partial_i \partial_l G_{il}. \quad (26)$$

In (26) summation over repeated indices is implied so that $\partial_i \partial_l G_{il} = \Delta$, the dilatation associated with three crossed double forces, each of unit strength. Noting that the Fourier transform of Δ is $-k^2 \gamma_i g_{ij} \gamma_j$ and using (11) coupled with the identity

$$m_{ij}^* \alpha_j = \frac{\beta}{1 + \beta} \alpha_i, \quad (27)$$

after some manipulation one can show that

$$\Delta = \frac{1}{c_{44}} \left\{ -\left(\frac{\beta}{1 + \beta}\right) \delta(\bar{r} - \bar{r}') + \frac{1}{8\pi^2} \left(\frac{\beta}{1 + \beta}\right)^2 \sum_{n=1}^{\infty} (2w)^n \nabla^2 \left[\frac{F_n(\theta, \varphi)}{|\bar{r} - \bar{r}'|} \right] \right\}. \quad (28)$$

$F_n(\theta, \varphi)$ is defined by

$$F_n(\theta, \varphi) = \int_0^{2\pi} \int_0^{\pi} \alpha[A]([m^*][A])^{n-1} \hat{\alpha} d\Psi, \quad (29)$$

where $\hat{\alpha}$ is the column vector with components α_i , and α is its transpose (a row vector).

Equation (28) can be simplified somewhat by the decomposition

$$\nabla^2 \left[\frac{F_n(\theta, \varphi)}{|\bar{r} - \bar{r}'|} \right] = -\delta(\bar{r} - \bar{r}') \int_{\Omega} F_n(\theta, \varphi) d\Omega + \frac{1}{|\bar{r} - \bar{r}'|^3} \nabla_s^2 F_n(\theta, \varphi), \quad (30)$$

$$\nabla_s^2 = \frac{1}{\sin \varphi} \frac{\partial}{\partial \varphi} \left(\sin \varphi \frac{\partial}{\partial \varphi} \right) + \frac{1}{\sin^2 \varphi} \frac{\partial^2}{\partial \theta^2}, \quad (31)$$

and Ω is the surface of the unit sphere. (28) may then be rewritten as:

$$\begin{aligned} c_{44}\Delta = & -\left(\frac{\beta}{1+\beta}\right) \left\{ 1 + \frac{1}{8\pi^2} \left(\frac{\beta}{1+\beta}\right) \sum_{n=1}^{\infty} (2w)^n \int_{\Omega} F_n(\theta, \varphi) d\Omega \right\} \delta(\bar{r} - \bar{r}') \\ & + \frac{1}{8\pi^2} \left(\frac{\beta}{1+\beta}\right)^2 \frac{1}{|\bar{r} - \bar{r}'|^3} \sum_{n=1}^{\infty} (2w)^n \Delta_s^2 F_n(\theta, \varphi). \end{aligned} \quad (32)$$

The terms in (32) proportional to $\delta(\bar{r} - \bar{r}')$ do not contribute to the interaction energy (26), but they do yield the only contribution to the *total* volume change associated with the “unit mechanical point defect.” To first order in w ,

$$E_{\text{int}} = P_1 P_2 \left(\frac{\beta}{1+\beta}\right)^2 \frac{15w}{2\pi |\bar{r} - \bar{r}'|^3} \left\{ \frac{1}{5} - \langle n_1^2 n_2^2 + n_3^2 (1 - n_3^2) \rangle \right\} \quad (33)$$

where n_1, n_2, n_3 are direction cosines of the line joining the two defects, i.e., $\bar{r} - \bar{r}'$. Equation (33) is similar to a result obtained previously by Eshelby [6, 10]. Eshelby's approximate technique replaces $\left(\frac{\beta}{1+\beta}\right)$ in (33) by $\frac{c_{11}^0}{c_{11} + 2c_{12}}$, where c_{11}^0 is not uniquely defined, but rather depends upon the choice of “zeroth order” Lamé constants.

Second and third order anisotropy contributions to the interaction energy may be obtained using

$$F_2(\theta, \varphi) = \int_0^{2\pi} \left\{ I_3 - \frac{(I_2)^2}{1+\beta} \right\} d\Psi \quad (34)$$

$$F_3(\theta, \varphi) = \int_0^{2\pi} \left\{ I_4 - 2 \frac{I_2 I_3}{1+\beta} + \frac{(I_2)^3}{(1+\beta)^2} \right\} d\Psi \quad (35)$$

with

$$I_p(\theta, \varphi; \Psi) = \sum_{j=1}^3 \{ \alpha_j(\theta, \varphi; \Psi) \}^{2p}. \quad (36)$$

IV. Conclusions

Two series expansions for the cubic Green's tensor have been derived; the essential difference between the two representations is the manner in which a zeroth order or isotropic approximation is split off from $G_{i\ell}$. The question of convergence of the series (i.e., the validity of eqs (15) and (16) is most easily treated in the following manner.

The expansion (15) is valid provided

$$\left. \begin{aligned} |J^* - 1| &< 1, \\ J^* &= \text{Det} \{ [I] - 2w[R][M^*] \} \end{aligned} \right\} \quad (37)$$

where Det means "determinant of." Now

$$J^* = 1 - 2w \frac{\beta}{1+\beta} + \frac{4w}{1+\beta} (1 + \beta w)(\gamma_1^2 \gamma_2^2 + \gamma_3^2 (1 - \gamma_3^2)) + \frac{4w^2}{1+\beta} (3 - 2w) \gamma_1^2 \gamma_2^2 \gamma_3^2. \quad (38)$$

Since

$$\left. \begin{aligned} 0 &\leq \gamma_1^2 \gamma_2^2 \gamma_3^2 \leq \frac{1}{27} \\ 0 &\leq \gamma_1^2 \gamma_2^2 + \gamma_3^2 (1 - \gamma_3^2) \leq \frac{1}{3} \end{aligned} \right\} \quad (39)$$

if $0 \leq w < 1$, condition (37) is satisfied, and (15) is a valid representation of $G_{i\ell}$.

Similarly the expansion (16) is valid if

$$\left. \begin{aligned} |J - 1| &< 1, \\ J &= \text{Det} \{ [I] + 2w[T][M] \} \end{aligned} \right\} \quad (40)$$

But

$$J = \frac{1 + \frac{1}{\beta}}{1 + \frac{1}{\beta'}} J^*. \quad (41)$$

For lithium, $J \approx 3J^*$, and direction triplets $(\gamma_1, \gamma_2, \gamma_3)$ exist for which (40) is not satisfied, even though (37) is.

Any useful successive approximation scheme of analytically representing the cubic Green's tensor must be based upon a convergent technique. Normally such schemes involve splitting the Voigt constants c_{ij} so that $c_{ij} = c_{ij}^0 + c'_{ij}$ where the c_{ij}^0 satisfy the condition for isotropy. As Eshelby [6] has remarked, "there seems to be no way of arranging that the c'_{ij} shall be convincingly smaller than the c_{ij}^0 ." Indeed, the present calculation indicates that the validity and rate of convergence of such approximations is critically dependent upon the choice of c_{ij}^0 . At the present time identifying the zeroth order Lamé constants for a cubic medium as

$$\lambda = c_{12}, \mu = c_{44}$$

provides the most useful splitting of c_{ij} . Leibfried [3] has proposed a splitting based upon an averaging of the c_{ij} over all possible crystal orientations; the convergence of a successive approximation scheme based upon this technique has yet to be investigated.

V. References

- [1] Kröner, E., Z. Physik **136**, 402 (1953).
- [2] Willis, J. R., Quart J. Mech. and Applied Math. **18**, 419 (1965).
- [3] Leibfried, G., Z. Physik **135**, 23 (1953).
- [4] Hirth, J. P., and Lothe, J., Theory of Dislocations (McGraw-Hill, New York, 1968).
- [5] Mura, T., Proc. Roy. Soc. **A280**, 528 (1964).
- [6] Eshelby, J. D., in Solid State Physics, **3**, F. Seitz and D. Turnbull, Eds., (Academic Press, New York, 1956) p. 79.
- [7] Kröner, E., Arch. Rat. Mech. Anal. **4**, 273 (1960).
- [8] Willis, J. R., Int. J. Engrg. Sci. **5**, 171 (1967).
- [9] Lifshitz, I. M., and Rosenzweig, L. N., Zhur. Eksptl. i Teort. Fiz. **17**, 783 (1947).
- [10] Eshelby, J. D., Acta Met. **3**, 487 (1955).
- [11] Flinn, P. A., and Maradudin, A. A., Annals of Phys. **18**, 81 (1962).
- [12] Lie, K. C., and Koehler, J. S., Adv. in Phys. **17**, 421 (1968).
- [13] Fredholm, I., Acta Math., Stockholm **23**, 1 (1900).
- [14] Bross, H., ZAMP **19**, 434 (1968).
- [15] Zeilon, N., Ark. Mat. **6**, No. 23 (1911).
- [16] Malén, K., Scripta Met. **2**, No. 4, 223 (1968).
- [17] Mura, T., J. App. Phys. **40**, No. 1, 73 (1969).
- [18] Synge, J. L., The Hypercircle in Mathematical Physics (Cambridge Univ. Press, 1957).

SOME PROBLEMS INVOLVING LINEAR DISLOCATION ARRAYS

N. Louat

*Edgar C. Bain Laboratory for Fundamental Research
U.S. Steel Corporation
Research Center
Monroeville, Pennsylvania 15146*

Muskhelishvili's inversion formulae for singular integral equations are shown to be special cases of a more general result which is then employed to deal with two types of problems. In the first we consider the distribution of dislocations in a double periodic array of screw pile-ups in an arbitrary stress field. The second type is concerned with screw pile-ups terminating at phase boundaries, again for arbitrary stress fields.

Key words: Dislocations-elasticity; dislocation pileups; phase boundaries.

I. Introduction

Current practice for the determination of dislocation distribution functions (Leibfried [1]) is to formulate the condition of equilibrium as a singular integral equation and to solve this equation by the inversion procedures of Muskhelishvili [2]. However, there are situations of physical interest which lead to integral equations to which Muskhelishvili's formulae do not apply. The development of analytical techniques applicable to such cases is the prime purpose of this work.

We proceed first to introduce the "path function". By this term is meant a function of a complex variable which defines, in the complex plane, the end points and weight to be accorded each of the lines of integration of the integral equation specified by the problem. We then show how such functions may be employed to invert the relevant singular integral equations.

To illustrate this approach we first obtain Muskhelishvili's results and then consider two other types of problem. In the first we examine the behavior of a doubly periodic array of screw dislocation pileups (or cracks in antiplane strain). In the second we consider pileups which terminate at a phase boundary.

Fundamental Aspects of Dislocation Theory, J. A. Simmons, R. de Wit, and R. Bullough,
Eds. (Nat. Bur. Stand. (U.S.), Spec. Publ. 317, I, 1970).

II. Analysis

Suppose that the dislocations are of screw character, lie parallel to the z -axis, and that they can move only in the x -direction. Suppose further that they lie in the intervals

$$(x_0, y_0) - (x_1, y_0), (x_2, y_0) - (x_3, y_0), \\ (x_0, y_1) - (x_1, y_1), (x_2, y_1) - (x_3, y_1),$$

Let $f(x)$ be the dislocation density at any point in these intervals, with the conventions that $f(x)$ is positive where the dislocations are positive and that a positive dislocation tends to move in the positive x direction under the action of a positive shear stress. Let $g(x)$ represent the applied shear stress.

We obtain the equation of equilibrium from the condition that the total stress must vanish at every point of the array. We obtain

$$\alpha_1 \int_{D_1} f(x) \frac{dx}{x-f} + \alpha_2 \int_{D_2} f(x) \frac{dx}{x-f} + \dots + \alpha_n \int_{D_n} f(x) \frac{dx}{x-f} = -\frac{g(f)}{A} \quad (1)$$

where $A = \mu\lambda/2\pi$. μ is the shear modulus, and λ the displacement of a unit dislocation. Here the weighting factors α_r have the values

$$-1 \leq \alpha_r \leq 1$$

and have been included to allow for situations in which dislocations in different regions are effectively of different strengths. For brevity we write eq (1) in the form

$$\int_D f(x) \frac{dx}{x-t} = -\frac{g(t)}{A} \quad (2)$$

where it is to be understood that integration is to be carried out, with the required weighting, over the union D of line segments $D_1, D_2 - D_n$. We now introduce the path function $k(t)$ of which we, so far, require only that it define the line segments D_r and the weighting factors α_r . Proceeding formally we write

$$\int_D k(t) \frac{dt}{t-y} \int_D f(x) \frac{dx}{x-t} = -\frac{1}{A} \int_D k(t) \frac{dt}{t-y}. \quad (3)$$

We then generalize a result originally due to Hardy [3] to interchange

the order of integration¹ and have

$$\begin{aligned} -\pi^2 C^2 k(y) f(y) + \int_D f(x) dx \int_D k(t) \frac{dt}{(t-y)(x-t)} \\ = -\frac{1}{A} \int_D k(t) g(t) \frac{dt}{t-y} \quad (4) \end{aligned}$$

where C is a constant independent of y . Now substituting for $f(y)$ from eq (4) in eq (2) we have

$$\begin{aligned} \int_D f(y) \frac{dy}{y-u} &= \frac{1}{\pi^2 C^2 A} \int_D \frac{1}{k(y)} \frac{dy}{y-u} \int_D k(t) g(t) \frac{dt}{t-u} \\ + \frac{1}{\pi^2 C^2} \int_D \frac{1}{k(y)} \frac{dy}{y-u} \int_D f(x) dx \int_D k(t) \frac{dt}{(t-y)(x-f)} &= -\frac{g(u)}{A}. \quad (5) \end{aligned}$$

Inverting the first integral of (5) as in (4) we see that a necessary condition for the validity of these procedures is that

$$\begin{aligned} \frac{1}{A} \int_D k(t) g(t) dt \int_D \frac{1}{k(y)} \frac{dy}{(y-u)(t-y)} \\ + \int_D \frac{1}{k(y)} \frac{dy}{y-u} \int_D f(x) dx \int_D k(t) \frac{dt}{(t-y)(x-f)} &= 0. \quad (6) \end{aligned}$$

If this condition is satisfied and if additionally the second term of eq (4) vanishes we have

$$f(y) = \frac{1}{\pi^2 C^2} k(y) \int_D k(t) g(t) \frac{dt}{t-y}. \quad (7)$$

We now seek to define the circumstances under which these two conditions will be satisfied. To this end we examine the contour integrals corresponding to the integrals of (6) which contain the factors $(y-u)^{-1}$ $(t-y)^{-1}$. To begin we consider the characteristics of the contours employed. From our original assumptions as to the nature of a path function we expect that the contour consists of lines traversing the lines of integration twice in opposite directions and of a circle at infinity (vide, fig. 1). A consideration of the contour integrals indicates that towards the satisfaction of (6) we introduce the following additional restrictions on $k(x)$:

(A) $k(z) \rightarrow z^n$ as $z \rightarrow \infty$, with $z = x + iy$ where n is a finite integer, positive, negative or zero.

¹ For the class of functions with which Hardy was concerned $C=1$

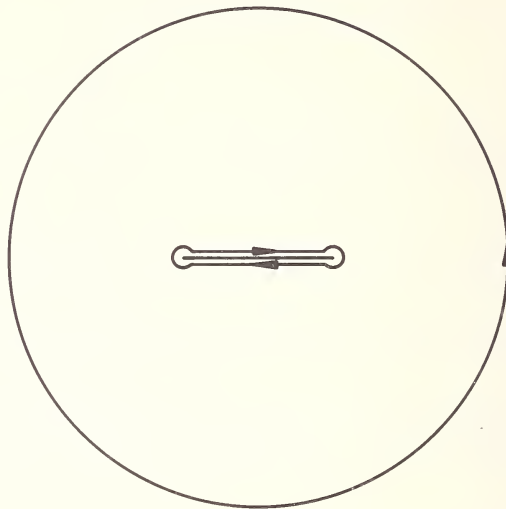


FIGURE 1. Contour traversing of circle at infinity and line of integration.

(B) $k(z)$ and $1/k(z)$ have no poles.

(C) $k(z)/(z-u)(t-z)$ and $1/(k(z)(z-u)(t-z))$ provide no residues when u and t lie on the line of integration.

We have for the following several cases:

(i) $n=0$. Equation (6) is satisfied.

(ii) $n > 0$. The first integral of (6) vanishes whilst the last integral of the second term gives a polynomial of degree $n-1$ in x and y so that (6) reduces to the condition

$$\int_D (a_1y^{n-1} + a_2y^{n-2} - \dots - a_n) \frac{dy}{k(y)(y-u)} = 0 \quad (8)$$

which may be seen to be satisfied if conditions A and B are satisfied.

(iii) $n < 0$. The second term of (6) now vanishes whilst the second part of the first integral leads to a polynomial of degree $n-1$. We then require that

$$\int_D g(t)k(t)(b_1t^{n-1} + b_2t^{n-2} - \dots - b_n) dt = 0. \quad (9)$$

Taking these results with (4) we have:

Case (i), n = 0

$$f(y) = + \frac{1}{\pi^2 C^2 A k(y)} \int_D k(t) g(t) \frac{dt}{t-y}. \quad (10)$$

Case (ii), n > 0

$$f(y) = + \frac{1}{\pi^2 C^2 A k(y)} \int_D k(t) g(t) \frac{dt}{t-y} + \frac{1}{\pi^2 C^2 A k(y)} (C_1^{n-1} + C_2 y^{n-2} + C_n) \quad (11)$$

where the coefficients C_r are arbitrary constants.

Case (iii), n < 0

$$f(y) = \frac{1}{\pi^2 C^2 A k(y)} \int_D k(t) g(t) \frac{dt}{t-y} \quad (12)$$

provided

$$\int_D g(t) k(t) t^s dt = 0 \quad (13)$$

for

$$0 \leq s \leq n-1.$$

It remains to identify the functions $k(z)$. This we shall do for four cases of physical interest in the succeeding sections.

III. The Cases of Muskhelishvili

As a first exercise we shall recover Muskhelishvili's results by considering that $|\alpha_r| = 1$ and that the lines of integration are a finite number of elements of the x -axis. In this case the analysis is not restricted to screw dislocations.

In the absence of an analytic process which will determine $k(z)$ it is necessary to guess this function. However, this process can be rationalized so as to severely restrict the number of possible choices. Thus, we note that $k(z)$ is to define the end points of each of the lines of integration and is to be without poles. Accordingly we consider functions having branch points at the end points of the lines of integration. Again, since the path function must also define the lines of integration we must expect that the branch points are arranged in pairs so that $k(z)$ is single valued with a line of discontinuity between them which is the line of integration. Func-

tions having these properties can be built up by forming products of constituents having any of the forms:

$$\left(\frac{z-a}{z-b} \right)^{1/2}, (z-a)^{1/2}(z-b)^{1/2} \quad \text{or} \quad (z-a)^{-1/2}(z-b)^{-1/2}. \quad (14)$$

Furthermore, functions formed in this way satisfy the requirements A, B, and C so that in these cases (6) is also satisfied. It may also be verified that here the constant C introduced in (4) has the value unity and that the weighting factors $\alpha_r = \pm 1$.

We remark finally that substitution of such functions in equations (10), (11), (12), and (13) leads immediately to the results given by Muskhelishvili.

IV. STACKED ARRAYS

We suppose dislocations to lie in periodic arrays such as that illustrated in figure 2 and that $\alpha_r = \pm 1$. We suppose further that the dislocations are of screw character so that we may follow Louat [3] in his consideration of the same problem and write the equation of equilibrium as

$$a \int_D f(z) \frac{dz}{z-t} = -g(t). \quad (15)$$

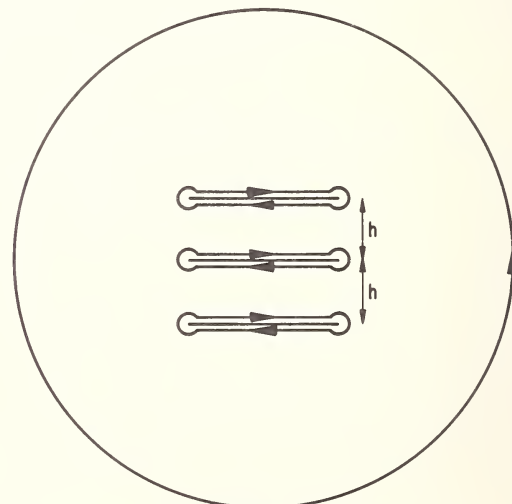


FIGURE 2. Contour for singly periodic dislocation arrays.

Toward the determination of the appropriate path function we recognize that the weighting factors are here the same as in Muskhelishvili's case and so expect that $k(z)$ will be the square root of a periodic function (Period h) having simple zeros and infinities at and only at the ends of the lines of integration. This prescription defines functions in which the algebraic factors of (14) are replaced by hyperbolic sines, e.g., $\sinh(x-a)$. Functions corresponding to the second and third members are acceptable only in pairs since otherwise the number n introduced in section III would be infinite. Thus, we are concerned only with the case $n=0$. With $k(z)$ as defined the only inversion formula applicable is (10) and the results given by Louat (loc. cit.) are immediately available. Additionally, the restriction which he imposes, namely, that $f(z) \equiv f(x)$ on all the lines of integration is seen to be unnecessary.

It remains to remark that for asymmetrical pile-ups the constant C introduced is not one.

V. Periodic Arrays

Proceeding as in the last section we suppose dislocations to lie in the doubly periodic array as illustrated in figure 3 and that $\alpha_r = \pm 1$.

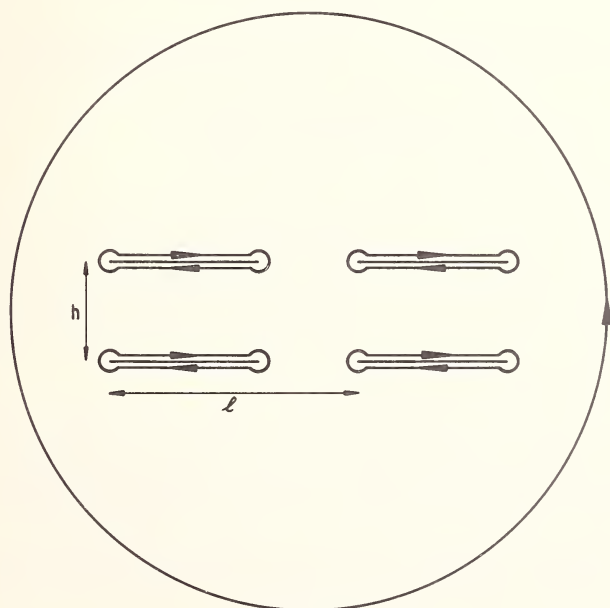


FIGURE 3. Contour for doubly periodic arrays.

We again suppose that dislocations are of screw character and have

$$A \int_D f(z) \frac{dz}{z-t} = -g(t). \quad (16)$$

We now expect that $k(z)$ will be the square root of a doubly periodic function having simple zeros and poles at the ends of the lines of integration. It is then natural to consider Jacobian elliptic functions.

Among such functions the function

$$\underset{\text{Def}}{cn}(z, k)/sn(z, k) \equiv P(z, k) \quad (17)$$

is of particular interest. It is characterized by periods $4K$ in the x -direction and $2K^1$ in the y -direction. K and K^1 are defined by the equations

$$K = \int_0^1 \{(1-x^2)(1-k^2x^2)\}^{1/2} dx \quad (18)$$

and

$$K^1 = \int_0^1 \{(1-x^2)(1-(1-k^2)x^2)\}^{-1/2} dk. \quad (19)$$

$P(z, k)$ has simple zeros at

$$z = (2m+1)K + 2niK^1 \quad (20)$$

and simple poles at

$$z = 2mK + 2niK^1 \quad (21)$$

where m and n are integers or zero. Thus, pole follows zero along lines $y = \text{constant}$.

We now consider the function

$$L(z) \equiv \frac{cn(z-b)K/\ell \cdot cn(z+b)K/e}{sn(z-b)K/\ell \cdot sn(z+b)K/e} - \frac{cn(a-b)K/e \cdot cn(a+b)K/\ell}{sn(a-b)K/e \cdot sn(a+b)K/\ell}. \quad (22)$$

When k is chosen such that $K^1 = hK/\ell$ (vide fig. 3), $L(z)$ is characterized by simple infinities (poles) at and only at

$$z = \pm b + 2ml + 2iuh$$

and simple zeros at and only at

$$z = \pm a + 2ml + 2iuh$$

where m and n are positive or negative integers or zero. It then follows by analogy that $(L(z))^{1/2} = k(z)$ is the required path function.

As in section IV we are restricted to the case $n=0$ and have from (10)

$$f(z) = \frac{1}{\pi^2 AC^2} \left\{ \frac{cn(z-b)K/\ell \cdot cn(z+b)K/\ell}{sn(z-b)K/\ell \cdot sn(z+b)K/\ell} - \frac{cn(a-b)K/\ell \cdot cn(a+b)K/\ell}{sn(a-b)K/\ell \cdot sn(a+b)K/\ell} \right\}^{-1/2}$$

$$\int_D g(t) \left\{ \frac{cn(t-b)K/\ell \cdot cn(t+b)K/\ell}{sn(t-b)K/\ell \cdot sn(t+b)K/\ell} - \frac{cn(a-b)K/\ell \cdot cn(a+b)K/\ell}{sn(a-b)K/\ell \cdot sn(a+b)K/\ell} \right\}^{1/2} \frac{dt}{t-x}. \quad (23)$$

For the case of most interest in which $g(t) = \text{constant} = \sigma$, the integral in (23) may be simplified by taking account of the periodic character of the integral. We obtain

$$\frac{2\sigma}{\ell} \int_{ih}^{2\ell+ih} \left\{ \frac{cn(z-b)K/\ell \cdot cn(z+b)K/\ell}{sn(z-b)K/\ell \cdot sn(z+b)K/\ell} - \frac{cn(a-b)K/\ell \cdot cn(a+b)K/\ell}{sn(a-b)K/\ell \cdot sn(a+b)K/\ell} \right\}^{1/2} = C\sigma. \quad (24)$$

This quantity which we have identified with the constant C introduced in (4) can, it would seem, only be evaluated by numerical means. The number of dislocations in a particular array is similarly difficult to determine and will not be evaluated here.

VI. Screw Dislocation Pileups Adjoining a Phase Boundary

We suppose that screw dislocations lie in the plane $y=0$ and are forced against a barrier at the plane $x=0$ by an applied stress $-g(x)$ and that there is a discontinuity in elastic modulus at that plane. We suppose further that the distribution is unbounded at the end point $x=0$ and bounded at $x=b$.

We take account of the discontinuity in elastic modulus by using the imaging properties of screw dislocations (Head [4]) and write the equation

of equilibrium in the form

$$\alpha \int_{-b}^{-a} f(x) \frac{dx}{x-t} + \int_a^b f(x) \frac{dx}{x-t} = -g(t) \quad (25)$$

with $f(x) = \pm f(-x)$ and for $t > 0$ (26)

$$\alpha = \frac{\mu_1 - \mu_2}{\mu_1 + \mu_2}. \quad (27)$$

μ_1 and μ_2 are respectively the shear moduli for the elastically isotropic and semi-infinite bodies to the left and right of the boundary.

Here the weighting factors are not ± 1 and it is instructive towards the determination of the path function to consider the contour integral

$$\oint \frac{z^{m+1/2}}{(z+b)^{-m}(z-b)^{1/2}} \frac{dz}{z-x}; \quad x > 0, 0 < n < \frac{1}{2} \quad (28)$$

with the contour shown in fig. 4. We find the relation

$$\sin m\pi \int_{-b}^0 \frac{x^{m+1/2}}{(b-x)^m(b-x)^{1/2}} \frac{dx}{x-t} + \int_0^b \frac{x^{m+1/2}}{(b+x)^m(b-x)^{1/2}} \frac{dx}{x-t} = \pi \quad (29)$$

in which the two intervals of integration have been accorded different weighting. This function is not the one we seek since it is not symmetrical as required by (26). However, this result does suggest that the required weighting can be obtained through the presence of a branch point of order m at $z=0$.

It is readily seen from symmetry that there can be no such branch points at $z=\pm b$. For analyticity we then require that the effect introduced on following the contour past the point $z=0$ in one direction be removed on passing it in the opposite direction. We note that this could be achieved if the function were to invert on passing around the end point $z=b$. We now note that the quantity

$$\sqrt{z^2 - b^2} \quad (30)$$

changes sign in following the contour around $z=b$. Accordingly, we consider the equation

$$\left(\frac{B - \sqrt{b^2 - x^2}}{D} \right) = \left(\frac{D}{B + \sqrt{b^2 - x^2}} \right) \quad (31)$$

whence we see that for a branch point to exist at $z=0$, $B=b$, and that $D=x$. We are thus led to the function

$$\left(\frac{b - \sqrt{b^2 - x^2}}{x} \right)^m = \left(\frac{b - \sqrt{b^2 - x^2}}{b + \sqrt{b^2 - x^2}} \right)^{m/2} \quad (32)$$

and thus as matter of preference to the path function

$$k(z) = \left[\frac{b + i\sqrt{z^2 - b^2}}{b - i\sqrt{z^2 - b^2}} \right]^m; \quad 0 \leq m < \frac{1}{2}. \quad (33)$$

Along the lines of integration $k(z)$ the real part of $k(z)$ behaves as required taking the values indicated in figure 4.

With this trial path function we now proceed as before and consider the quantity

$$\bar{f}(z) = -\frac{1}{\pi^2 AC^2} \left(\frac{b - i\sqrt{z^2 - b^2}}{b + i\sqrt{z^2 - b^2}} \right)^m \int_D g(t) \left(\frac{b + i\sqrt{t^2 - b^2}}{b - i\sqrt{t^2 - b^2}} \right) \frac{dt}{t - z}. \quad (34)$$

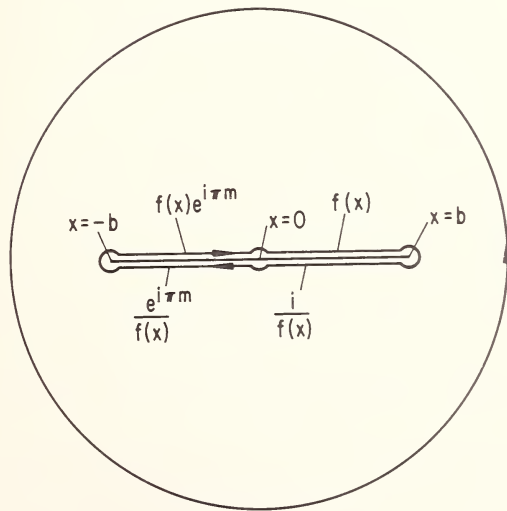


FIGURE 4. Contour for section 5.

$\bar{f}(z)$ is the solution of (25) only in the sense that it is the complex function which when integrated around the circuit D of figure 4 leads to real integrals which satisfy that equation.

For the case $-g(t) = \sigma$ we find in this way that

$$f(x) = \frac{\sigma}{2A \sin m\pi} \left[\left(\frac{b + \sqrt{b^2 - x^2}}{b - \sqrt{b^2 - x^2}} \right)^m - \left(\frac{b - \sqrt{b^2 - x^2}}{b + \sqrt{b^2 - x^2}} \right)^m \right]. \quad (35)$$

This is equivalent to the result given by Tetelman and Barnett [5].

It may be verified by trial that these procedures also give solutions when the applied stress is a function of position.

VII. References

- [1] Leibfried, G., Z. f. Physik **130**, 214 (1951).
- [2] Muskhelishvili, N. I., Some Basic Problems of The Mathematical Theory of Elasticity, (P. Noordhoff, Groningen, Netherlands, 1953).
- [3] Louat, N., Phil. Mag. **8**, 1219 (1963).
- [4] Head, A. K., Phil. Mag. **44**, 92 (1953).
- [5] Barnett, D. M., Tetelman, A. S., J. Mech. Phys. Solids **14**, 329 (1966).

SOME RECENT RESULTS ON DISLOCATION PILEUPS

J. C. M. Li

*Materials Research Center
Allied Chemical Corporation
Morristown, New Jersey 07960*

A few results intended to illustrate the usefulness of orthogonal polynomials and singular integral equations for the problem of dislocation pileups are described. A simple method of solving a few special integral equations is suggested. The usefulness of a Moutier cycle for the calculation of stress concentration is shown.

Key words: Dislocation pileups; Moutier cycle; stress concentrations.

I. Introduction

Eshelby, Frank, and Nabarro [1] showed the usefulness of orthogonal polynomials for the problem of dislocation pileups. In a single-layered, single-ended pileup of n dislocations with the first one locked in position, the rest of the dislocations assume equilibrium positions which are zeros of the first derivative of the n th Laguerre polynomial. Chou [2] found later that, if the locked dislocation has a Burgers vector mb instead of b , the equilibrium positions are then given by the zeros of the $(n-1)$ th generalized Laguerre polynomial of order $2m-1$. Stroh [3] and Chou [2] were both able to use the properties of the polynomials to obtain analytical results for the stress field and strain energy of the pileups.

Leibfried [4], and Head and Louat [5] showed the usefulness of singular integral equations in the problem of pileups. A simple method for obtaining the solution is suggested here for a few special singular integral equations. The force exerted on the locked dislocation is calculated by the application of Moutier's theorem [6].

II. Single-Layered, Double-Ended Pileups Without External Stress

Eshelby, Frank, and Nabarro [1] also solved the following problem: Between two locked dislocations at $(\pm a, o)$, let $n-2$ dislocations of the same Burgers vector assume equilibrium positions without the influence

of any applied stress. The equilibrium positions were found to be the zeros of the first derivative of $(n-1)$ th Legendre polynomial. The force exerted on the locked dislocation is $\pm n(n-1)A/4a$ where

$$A = \mu [b_x^2 + b_y^2 + b_z^2 (1 - \nu)]$$

for an isotropic medium and $A = K_e b_x^2 + K_n b_y^2 + K_s b_z^2$ for an anisotropic medium with μ , ν , K_e , K_n , and K_s all functions of elastic constants. The problem is extended here to determine the effects of locked dislocations with different Burgers vectors. Let $m_1 b$ be the Burgers vector of the locked dislocation at (a, o) and $m_2 b$ be that at $(-a, o)$. Then the equilibrium positions are found to be the zeros of the $(n-2)$ th Jacobi polynomial of orders $2m_1 - 1$ and $2m_2 - 1$. The forces exerted on the locked dislocations are now:

$$\frac{A}{a} \left[\frac{(n-2)(n-3+2m_1+2m_2)+2m_1m_2}{4m_1} \right] \text{ at } (a, o)$$

and

$$-\frac{A}{a} \left[\frac{(n-2)(n-3+2m_1+2m_2)+2m_1m_2}{4m_2} \right] \text{ at } (-a, o).$$

The stress field and energy can all be derived analytically. Results will be sent upon request.

Instead of using discrete dislocations, the same problem can also be solved for continuous distributions of dislocations of infinitesimal Burgers vectors. The relevant integral equation is

$$\int_{-a}^a \frac{f(x)dx}{t-x} = 0 \quad \text{for any } -a < t < a$$

and the solution is

$$f(x) = n/\pi \sqrt{a^2 - x^2}$$

which is obtained by substituting $x = a \sin \theta$ and noting that $d\theta/(t - a \sin \theta)$ integrated from $-\pi/2$ to $\pi/2$ is zero for any $t^2 < a^2$. The strain energy can be obtained by making a cut in the plane of the pileup from $(-a, o)$ to (R, o) , where R is the size of the specimen, applying tractions on the two cut surfaces to maintain the elastic state of the system and reversibly removing the pileup. The result is simply

$$(n^2 A/2) \ln (2R/a).$$

The stress field can be obtained by contour integration and the results agree with those of the case of discrete dislocations for large n .

III. Single-Layered, Double-Ended Pileups with External Stress

This problem is solved for the case of continuous distributions of dislocations with infinitesimal Burgers vectors. The relevant integral equation is

$$A \int_{-a}^a \frac{f(x)dx}{t-x} = \sigma b \quad \text{for any } -a < t < a.$$

A solution for the case in which $f(x)$ is unbounded at both (a, o) and $(-a, o)$ is

$$f(x) = \frac{\sigma b}{\pi A} \frac{\zeta - x}{\sqrt{a^2 - x^2}}$$

where (ζ, o) is a point at which $f(\zeta)$ is zero. This solution can be obtained as before as follows: Since the integral equation is true for any t , it is true for $t = \zeta$. Subtract the two integral equations to obtain an integral which equals zero. Then make a substitution of $x = a \sin \theta$ and remember that $d\theta/(t - a \sin \theta)$ integrated between $-\pi/2$ and $\pi/2$ is zero for any $t^2 < a^2$.

The numbers of dislocations with opposite signs are not equal to each other. They are

$$\frac{\sigma b}{\pi A} \left[\zeta \left(\frac{\pi}{2} \pm \sin^{-1} \frac{\zeta}{a} \right) \pm \sqrt{a^2 - \zeta^2} \right].$$

The net number with one sign is then $\zeta b \sigma / A$. In the case of $\zeta = 0$, the numbers of dislocations with opposite signs are each equal to $\sigma b a / \pi A$.

The strain energy is obtained by making a cut in the plane of the pileup from $(-a, o)$ to (R, o) where R is the size of the specimen, applying tractions on the two cut surfaces to maintain the elastic state of the system, and reversibly removing the pileup. The result is simply

$$\frac{n^2 A}{2} \left(\frac{a^2}{2\zeta^2} + \ln \frac{2R}{a} \right).$$

The force exerted on the locked dislocation can be obtained by using a Moutier cycle: A cut is made in the plane of the pileup from $(-a, o)$ to (R, o) and the pileup is removed as just described. The cut is then made

a little longer, from $(-a - 2\delta a, o)$ to (R, o) , and a new pileup is formed without altering the position of ζ until the applied stress is again σ . Then the locking agent is replaced by an external force and the pileup is reversibly shortened to the original length. The total reversible work for the cycle is zero. This gives the following forces at the locked dislocations:

$$\sigma^2 b^2 (a - \zeta)^2 / 4aA \text{ at } (a, o)$$

and

$$\sigma^2 b^2 (a + \zeta)^2 / 4aA \text{ at } (-a, o).$$

These results are believed to be useful in theories of yielding and fracture.

IV. References

- [1] Eshelby, J. D., Frank, F. C., Nabarro, F. R. N., Phil. Mag. **42**, 351 (1951).
- [2] Chou, Y. T., J. Appl. Phys. **38**, 2080 (1967).
- [3] Stroh, A. N., Proc. Roy. Soc. **A218**, 391 (1953).
- [4] Leibfried, G., Z. Physik **130**, 214 (1951).
- [5] Head, A. K., Louat, N., Austr. J. Phys. **8**, 1 (1955).
- [6] Guggenheim, E. A., Thermodynamics (Interscience, New York, 1949) p. 78.

THE BEHAVIOR OF AN ELASTIC SOLID CONTAINING DISTRIBUTIONS OF FREE AND FIXED DISLOCATIONS

E. Smith

*Department of Metallurgy
University of Manchester
England*

There are many situations in metal physics where the stresses acting on fixed dislocations have an important bearing on a physical phenomenon, and the paper derives a general expression relating these stresses when fixed edge dislocations are contained within an infinite elastic solid in which there are also free edge dislocations that occupy equilibrium positions.

Special cases are considered in detail, particular attention being given to the situation where all the dislocations are of the same type, the free ones having identical Burgers vectors b while there are two fixed dislocations with Burgers vectors pb and qb ; all the dislocations lie in the same plane within an infinite solid. This is the most general model for which the stresses on each dislocation and also the equilibrium positions of the free dislocations may be determined analytically. It is indicated how the model degenerates into all the others that have been discussed analytically in terms of classic polynomial functions.

The results are briefly discussed in relation to the problem of cleavage crack nucleation in crystalline solids.

Key words: Crack nucleation; dislocations-elasticity; internal stresses.

I. Introduction

The inhomogeneous nature of plastic deformation in crystalline solids is intimately associated with many situations in metal physics, and in considering these theoretically, idealized models are often employed and consequently the dislocations are usually assumed to be linear, being either entirely edge or screw in character. In conducting such procedures, the majority of the dislocations in the system are free to move of their own accord, while a limited number are fixed in position by some mechanism.

The free dislocations occupy equilibrium positions such that the total energy of the system is a minimum, and for each equilibrium configuration non-zero stresses act on each fixed dislocation. Such stresses are important in practice since they may be high and consequently play a major role in localized phenomena such as, for example, crack nucleation. This paper gives consideration to the magnitude of these stresses when edge dislocations, all being of the same type, are contained within an infinite solid, and section II derives a general expression relating the stresses acting on the fixed dislocations; some simple special cases are considered in section III.

The most general situation for which these stresses may be determined analytically (section IV) is if there are two fixed dislocations with Burgers vectors pb and qb together with a number of free dislocations of Burgers vector b , all the dislocations lying in the same plane within an infinite solid, which is not subject to an applied stress. The equilibrium positions of the free dislocations are then related to the zeros of the Jacobi polynomials, and it is indicated how the model degenerates into all the others (1-4) that have been discussed analytically in terms of classic polynomial functions. Section V briefly discusses the case where there is an externally applied stress; in this situation, of course, it is impossible to discuss the problem analytically. Finally, the results are discussed in relation to the problem of cleavage crack nucleation, with particular reference to the effect of a free surface on the number of dislocations required for fracture.

II. General Theory

Let an infinite elastically isotropic solid (shear modulus μ and Poisson's ratio v), which is subject to the applied shear stress $p_{xy} = \sigma^A$, contain edge dislocations that are parallel to the z axis and have Burgers vectors parallel to the x -axis (positive dislocations have their associated extra material in the positive y -direction). Moreover suppose that n^L fixed dislocations with Burgers vectors b_i^L are situated at the points L_i , while n^F free dislocations with Burgers vectors b_i^F occupy the equilibrium positions F_i .

The free dislocations occupy equilibrium positions when the total energy of the system is stationary, a situation which corresponds to the requirement that the force acting on each free dislocation is zero. Thus if $p_{xy}(A \rightarrow B)$ is the shear stress at B due to an edge dislocation situated at A , the equilibrium positions of the n^F free dislocations are given by the following set of n^F equations:

$$\sigma^A + \sum_{\substack{j=1 \\ i \neq j}}^{n^F} p_{xy}(F_j \rightarrow F_i) + \sum_{j=1}^{n^L} p_{xy}(L_j \rightarrow F_i) = 0 \quad (1)$$

for $i=1, 2 \dots n^F$. Since the stress at a point (x, y) due to an edge dislocation of Burgers vector b situated at the origin is

$$p_{xy} = Kbx(x^2 - y^2)/(x^2 + y^2)^2$$

where $K = \mu/2\pi(1-v)$, it immediately follows that

$$\left. \begin{aligned} b_i^F p_{xy}(F_j \rightarrow F_i) + b_j^F p_{xy}(F_i \rightarrow F_j) &= 0 & (i \neq j) \\ b_i^L p_{xy}(L_j \rightarrow L_i) + b_j^L p_{xy}(L_i \rightarrow L_j) &= 0 & (i \neq j) \\ b_i^L p_{xy}(F_j \rightarrow L_i) + b_j^F p_{xy}(L_i \rightarrow F_j) &= 0 & (\text{all } i \text{ and } j) \end{aligned} \right\} \quad (2)$$

whereupon multiplication of each of the n^F equations (1) by b_i^F and summing, using relation (2), gives

$$\sigma^A \sum_{i=1}^{n^F} b_i^F + \sum_{i=1}^{n^F} \sum_{j=1}^{n^L} b_i^F p_{xy}(L_j \rightarrow F_i) = 0 \quad (3)$$

The p_{xy} component of shear stress at the site of the fixed dislocation at L_i due to the remaining fixed dislocations, the free dislocations and the applied stress is

$$S_i = \sigma^A + \sum_{j=1}^{n^F} p_{xy}(F_j \rightarrow L_i) + \sum_{\substack{j=1 \\ i \neq j}}^{n^L} p_{xy}(L_j \rightarrow L_i) \quad (4)$$

for $i=1, 2 \dots n^L$. whereupon multiplication of each of the n^L equations (4) by b_i^L and summing, using relations (2) and (3), gives

$$\sum_{i=1}^{n^L} b_i^L S_i = \sigma^A \left[\sum_{i=1}^{n^L} b_i^L + \sum_{i=1}^{n^F} b_i^F \right]. \quad (5)$$

Special cases of this general relationship will be considered in the subsequent sections.

III. Some Simple Special Cases

III.1. One fixed dislocation

If there is a single fixed dislocation with Burgers vector b_i^F together with $(n-1)$ free dislocations, relation (5) gives the shear stress acting

on the fixed dislocation as

$$S_1 = \sigma^A + \frac{\sigma^A}{b_1^L} \sum_{i=1}^{(n-1)} b_i^F \quad (6)$$

reducing, when the $(n-1)$ free dislocations have the same Burgers vector b , to

$$S_1 = \sigma^A + \frac{(n-1)b\sigma^A}{b_1^L}. \quad (7)$$

The validity of this result does not necessarily depend on all the dislocations lying along a single plane but only the existence of an equilibrium situation; its range of application does, however, include the case (with σ and b_1^L both positive, and the fixed dislocation situated at $x=0$, $y=0$) where all the free dislocations are situated on the plane $y=0$ (i.e., along the negative x axis). Relation (7) is then the result derived by Chou [3, 4], and for the special case where $b_1^L=b$, that obtained by Eshelby, Frank and Nabarro [1].

If all the free dislocations occupy equilibrium positions along a single plane (not necessarily that containing the fixed dislocation), the validity of relation (7) is independent of their mode of distribution; thus they may either be discrete as envisaged so far in this paper, be in the form of super-dislocations with Burgers vectors whose sum is $(n-1)b$, or be smeared into a continuous distribution of infinitesimal dislocations with a total Burgers vector $(n-1)b$.

III.2. Two fixed dislocations

If there are two fixed dislocations with Burgers vectors b_1^L and b_2^L together with $(n-2)$ free dislocations, expression (5) shows that the shear stresses S_1 and S_2 acting on the fixed dislocations are related by the equation

$$(b_1^L S_1 + b_2^L S_2) = \sigma^A \left[(b_1^L + b_2^L) + \sum_{i=1}^{(n-2)} b_i^F \right] \quad (8)$$

reducing, when the $(n-2)$ free dislocations have the same Burgers vector b , to

$$(b_1^L S_1 + b_2^L S_2) = \sigma^A [(b_1^L + b_2^L) + (n-2)b]. \quad (9)$$

Again this result does not rely on all the dislocations lying along a single plane, but of course it encompasses the situation where this is the

case. Thus for σ , b_1^L , b_2^L all positive and all the dislocations situated on the plane $y=0$ with the fixed ones at $x=\pm a$, equilibrium configurations exist with the free dislocations contained within the range $-\infty < x < +a$: relation (9) is then true irrespective of how the free dislocations partition themselves between the intervals $-\infty < x < -a$ and $|x| < a$, although the actual magnitudes of S_1 and S_2 are dependent on the method of partitioning.

For the symmetric situation where all the dislocations have the same Burgers vector b , and are situated symmetrically on each of two parallel planes, relation (9) gives the shear stress on each fixed dislocation as $n\sigma^A/2$. This particular model was discussed in detail by Ichikawa and Yokobori [5] (see also Smith [6]), and in this respect the present paper is a generalization of their work; it is important with respect to the problem of cleavage crack nucleation by slip bands. For if it is assumed that nucleation occurs when the stress on a fixed dislocation attains some critical value (see for example Cottrell [7]), the result implies that for a given number of dislocations, the necessary applied shear stress is markedly dependent on the mode of distribution of the dislocations in the slip band; thus the stress required if the dislocations are situated on two planes is twice as large as when they are situated on a single plane.

IV. The Special Case Where the Applied Stress Is Zero, All the Dislocations Are on the Same Plane, Two Being Fixed and the Remainder Having the Same Burgers Vector

A particular case of the model of section III.2. arises when the applied stress is zero, all the dislocations lie along the same plane, two being fixed and the remaining ($n-2$) have the same Burgers vector b ; relation (9) then shows that the stresses S_1 and S_2 on the fixed dislocations are related by the equation

$$b_1^L S_1 + b_2^L S_2 = 0. \quad (10)$$

In this situation the magnitudes of S_1 and S_2 can be determined analytically, together with the equilibrium positions of the free dislocations. This is the most general model for which such an approach is possible, but hitherto the stresses on the fixed dislocations have not been determined, although Head and Thomson [2] have indicated that the equilibrium positions of the free dislocations are related to the zeros of Jacobi polynomials.

Suppose that the ($n-2$) free positive dislocations of Burgers vector b are situated at the points $x=x_i$ ($i=1, 2, \dots, n-2$) along the plane $y=0$, while the fixed dislocations of Burgers vectors $b_1^L = pb$ and $b_2^L = qb$

are situated respectively at $x = -a$, $y = 0$ and $x = +a$, $y = 0$. The free dislocations will be in equilibrium if

$$\sum_{\substack{j=1 \\ i \neq j}}^{n-2} \frac{A}{(x_i - x_j)} + A \left[\frac{p}{(x_i + a)} + \frac{q}{(x_i - a)} \right] = 0 \quad (11)$$

for $i = 1, 2, \dots, (n-2)$, with $A = \mu b / 2\pi(1-v)$; substituting $\lambda_i = x_i/a$ so that the equilibrium positions are represented in dimensionless terms, relations (11) become

$$\sum_{\substack{j=1 \\ i \neq j}}^{n-2} \frac{1}{(\lambda_i - \lambda_j)} + \left[\frac{p}{(\lambda_i + 1)} + \frac{q}{(\lambda_i - 1)} \right] = 0. \quad (12)$$

for $i = 1, 2, 3, \dots, (n-2)$.

Following Eshelby, Frank, and Nabarro [1], and introducing the polynomial $f(\lambda)$ of degree $(n-2)$ and whose zeros are λ_i ($i = 1, 2, \dots, (n-2)$):

$$f(\lambda) = \prod_{i=1}^{n-2} (\lambda - \lambda_i) \quad (13)$$

it immediately follows that $f(\lambda)$ satisfies the differential equation

$$f''(\lambda) + 2 \left[\frac{p}{(\lambda+1)} + \frac{q}{(\lambda-1)} \right] f'(\lambda) + Q(n, \lambda) f(\lambda) = 0 \quad (14)$$

provided that $Q(n, \lambda)$ is chosen so that $f(\lambda)$ has a polynomial solution of degree $(n-2)$ with real and distinct roots, while $Q(n, \lambda)$ does not have a pole at any of these roots. The appropriate value for $Q(n, \lambda)$ is

$$Q(n, \lambda) = \frac{-(n-2)(n-3+2p+2q)}{(\lambda^2 - 1)} \quad (15)$$

when equation (14) reduces to

$$(1 - \lambda^2) f''(\lambda) + 2[(p - q) - (p + q)\lambda] f'(\lambda) + (n-2)(n-3+2p+2q) f(\lambda) = 0. \quad (16)$$

This equation is satisfied by the Jacobi polynomial $P_{n-2}^{(2q-1, 2p-1)}(\lambda)$, whereupon the $(n-2)$ free dislocations occupy the equilibrium positions $x_i = av_i$ the v_i being the $(n-2)$ zeros of $P_{n-2}^{(2q-1, 2p-1)}(v)$.

The p_{xy} component of shear stress at a point $(x, 0)$ (not coincident with the site of a free dislocation) due to the free dislocations is

$$S_F(x) = \sum_{j=1}^{n-2} \frac{A}{(x-x_j)} = \frac{A f'(\lambda)}{a f(\lambda)} \quad (17)$$

with $\lambda = x/a$. Accordingly for the present model

$$S_F(x) = \frac{A}{a} \cdot \frac{\frac{d}{d\lambda} [P_{n-2}^{(2q-1, 2p-1)}(\lambda)]}{P_{n-2}^{(2q-1, 2p-1)}(\lambda)} \quad (18)$$

and, by evaluating this expression and adding the stress due to the fixed dislocation at $x=-a$, the total shear stress on the fixed dislocation at $x=a$ is

$$S(a) = \frac{A[(n-2)^2 + (n-2)(2p+2q-1) + 2pq]}{4qa}. \quad (19)$$

Similarly the total shear stress acting on the fixed dislocation at $x=-a$ is

$$S(-a) = \frac{-A[(n-2)^2 + (n-2)(2p+2q-1) + 2pq]}{4pa}. \quad (20)$$

Expressions (19) and (20) for the stresses on the fixed dislocations clearly satisfy the general relationship (10).

It has been implicitly assumed so far that p and q are both positive, when an equilibrium configuration is possible only if all the free positive dislocations lie between the fixed dislocations. However, if either p or q (but not both) is negative such that $(p+q+n-2) < 0$, equilibrium configurations are possible with all the free dislocations lying respectively in the intervals $x > a$ and $x < -a$, and expressions (19) and (20) are still valid. In such situations the free dislocations are situated where $x_i = av_i$ the v_i still being the $(n-2)$ zeros of the Jacobi polynomial $P_{n-2}^{(2q-1, 2p-1)}(v)$, but with $|v_i| > 1$. When p and q are both negative, no equilibrium configuration is possible.

The results for all the other models (1, 3, 4) that have been discussed analytically will now be deduced, by observing the special properties of Jacobi polynomials. If $p=q=1$, the model reduces to that of n identical

dislocations of Burgers vector b , two of them being fixed at $x=\pm a$, and the free dislocations lie within the range $|x| < a$ being situated at the points $x_i = au_i$, where the u_i are the $(n-2)$ zeros of $P'_{n-1}(u)$, the first derivative of the $(n-1)$ th Legendre polynomial, while the stresses on the locked dislocations are $\pm An(n-1)/4a$; these results have been obtained by Eshelby, Frank, and Nabarro [1]. If $p=q$ and p and a both tend to infinity such that $2Ap/a^2$ equals a constant C , the model becomes that of $(n-2)$ free dislocations subject to the applied stress $-Cx$, and the free dislocations are situated at the points $x_i = w_i(A/C)^{1/2}$ where the w_i are the $(n-2)$ zeros of $H_{n-2}(w)$, the $(n-2)$ th Hermite polynomial, a result that is also in accord with that derived by Eshelby, Frank, and Nabarro [1].

If a new system of co-ordinates is introduced such that $\bar{x} = x + a$ the stress on the fixed dislocation at $\bar{x} = 0$ is given by relation (20), while the free dislocations occupy the positions $\bar{x} = a + av_i$ where the v_i are the $(n-2)$ zeros of the Jacobi polynomial $P_{n-2}^{(2q-1, 2p-1)}(v)$. However, if q and a both tend to infinity in such a way that $Aq/2a$ is equal to σ , the model reduces to that of $(n-2)$ free dislocations of Burgers vector b forced against a fixed dislocation of Burgers vector pb by an applied shear stress $-\sigma$, and the free dislocations occupy the positions $\bar{x}_i = \rho_i A/2\sigma$ the ρ_i being the $(n-2)$ zeros of the generalized Laguerre polynomial $L_n^{(2p-1)}(\rho)$, while relation (20) gives the stress on the fixed dislocation as $-(n-2+p)\sigma/p$. These results agree with those derived by Chou [3, 4] and also with those obtained by Eshelby, Frank, and Nabarro [1] for the special case when $p=1$; in this latter situation the free dislocations are situated at the points $\bar{x}_i = \Psi_i A/2\sigma$ where the Ψ_i are the $(n-2)$ zeros of $L'_{n-1}(\Psi)$ the first derivative of the $(n-1)$ th Laguerre polynomial.

V. Discussion

The previous section discussed the situation where dislocations of Burgers vectors pb and qb are fixed respectively at $x=-a$, $y=0$ and $x=+a$, $y=0$, while $(n-2)$ free dislocations lie along the plane $y=0$, there being no applied stress. If p and q are both positive, all the free dislocations must lie within the interval $|x| < a$, but if either p or q (but not both) is negative such that $(p+q+n-2) < 0$, an equilibrium configuration is possible with all the free dislocations situated outside the interval $|x| < a$; in all cases, however, the stresses on the fixed dislocations are given by expressions (19) and (20).

The situation becomes more complicated when there is an applied shear stress, for the equilibrium positions of the free dislocations are then not given by the zeros of a classic polynomial function, and the stresses on the fixed dislocations cannot be determined analytically. If p and q are

both positive and the applied shear stress is $p_{xy} = \sigma^4 = -\sigma$ where σ is also positive, then writing $\beta = \sigma a/A$ and proceeding as in section IV, it follows that the equilibrium positions of the $(n-2)$ free dislocations are given by $x_i = a\lambda_i$ ($i = 1, 2, \dots, n-2$) where the λ_i are the zeros of the function $f(\lambda)$ satisfying the differential equation

$$f''(\lambda) + 2 \left[\frac{p}{(\lambda+1)} + \frac{q}{(\lambda+1)} - \beta \right] f'(\lambda) + R(n, \lambda) f(\lambda) = 0 \quad (21)$$

provided that $R(n, \lambda)$ is chosen so that $f(\lambda)$ has a polynomial solution of degree $(n-2)$ with real and distinct roots, while $R(n, \lambda)$ does not have a pole at any of these roots. The appropriate value for $R(n, \lambda)$ is

$$R(n, \lambda) = \frac{[\Phi - 2\beta(n-2)\lambda]}{(1-\lambda^2)} \quad (22)$$

when equation (21) reduces to

$$(1-\lambda^2)f''(\lambda) + 2[(p-q) - \beta - (p+q)\lambda + \beta\lambda^2]f'(\lambda) + [\Phi - 2\beta(n-2)\lambda]f(\lambda) = 0 \quad (23)$$

For the special case that arises when $p=q=1$ and all the dislocations in the system have the same Burgers vector, relation (23) reduces to

$$(1-\lambda^2)f''(\lambda) + 2[-\beta - 2\lambda + \beta\lambda^2]f'(\lambda) + [\Phi - 2\beta(n-2)\lambda]f(\lambda) = 0, \quad (24)$$

an equation arising in the theory of the ionised hydrogen molecule [1], and for which there is an extensive literature (see, for example, a recent review by Buckingham [8] on the subject). Introducing a new variable such that $w = (\lambda - 1)$, relation (24) becomes

$$w(w+2)f''(w) + 2[2 + 2w - 2\beta w - \beta w^2]f'(w) + [2\beta(n-2)w + \chi]f(w) = 0. \quad (25)$$

There are clearly $(n-1)$ values of χ for which equation (25) admits of a polynomial solution of degree $(n-2)$, each value of χ corresponding to a certain number of dislocations being contained within the interval $|x| < a$

(i.e., $-2 < w < 0$), the others lying within the range $x > a$ (i.e., $w > 0$). For example, one value of χ corresponds to the case where all the free dislocations lie within the interval $|x| < a$, while another corresponds to the situation where they all lie within the range $x > a$. In all cases $f(w)$ can be expressed in the form

$$f(w) = \sum_{m=0}^{n-2} a_m w^m \quad (26)$$

and since the stress at a point $(x, 0)$ (not coincident with the site of a free dislocation) due to the free dislocations is $Af'(w)/af(w)$, it immediately follows from relations (25) and (26) that the total shear stress on the fixed dislocation at $x = +a$ is

$$S(a) = -\frac{\chi A}{4a} + \frac{A}{2a} - \sigma \quad (27)$$

while that acting on the fixed dislocation at $x = -a$ is

$$S(-a) = \frac{\chi A}{4a} - \frac{A}{2a} - (n-1)\sigma. \quad (28)$$

Expressions (27) and (28) for the stresses on the fixed dislocations clearly satisfy the general relationship (9). From physical considerations it is clear that the greatest value of χ corresponds to the case where all the free dislocations lie in the range $x > a$, whereas the lowest value describes the situation where all the free dislocations lie in the interval $|x| < a$.

The problem therefore resolves itself into determining the values of χ in terms of β , but the general situation for an arbitrary number of free dislocations is beyond the scope of this paper. It will be considered in a subsequent communication when the model is applied to a discussion of the flow stress of a solid containing ordered particles. However, the case where there is a single free dislocation may be immediately discussed, for then $n=3$ and equation (25) gives

$$\chi = 2(\beta - 1) \pm 2(\beta^2 + 1)^{1/2} \quad (29)$$

and the stresses on the fixed dislocations are given by relations (27) and (28) as

$$S(a) = -\frac{A}{a} \left[\frac{(\beta-1)}{2} \pm \frac{(\beta^2+1)^{1/2}}{2} \right] + \frac{A}{2a} - \sigma \quad (30)$$

and

$$S(-a) = \frac{A}{a} \left[\frac{(\beta-1)}{2} \pm \frac{(\beta^2+1)^{1/2}}{2} \right] - \frac{A}{2a} - 2\sigma \quad (31)$$

the positive and negative signs corresponding respectively to the cases where the free dislocation lies within the ranges $x > a$, and $|x| < a$; β is equal to $\sigma a/A$.

The validity of the general expression (5), and consequently its application to the associated special cases, depends on all the dislocations being of the same type and the fact that $p_{xy}(A \rightarrow B)$ equals $-p_{xy}(B \rightarrow A)$, where $p_{xy}(A \rightarrow B)$ is the stress at B due to a dislocation of Burgers vector b situated at A ; as illustrated in section II the latter condition is clearly satisfied when a dislocation lies within an infinite isotropically elastic solid. For the special case where n similar dislocations are forced by an applied shear stress σ^A against the leader (which is assumed to be fixed by some mechanism), the stress acting on it is $n\sigma^A$ (see relation (7)).

The same result is obtained for edge dislocations piled up on a plane parallel to $y=0$, and lying within a semi-infinite solid bounded by the surface $y=0$, provided that their Burgers vectors are parallel to the x axis; in this case the p_{xy} component of shear stress at the point $(x, -h)$ due to a single positive edge dislocation of Burgers vector b situated at $(\lambda, -h)$ is

$$p_{xy} = \frac{\mu b}{2(1-v)} \left[\frac{1}{(x-\lambda)} - \frac{(x-\lambda)}{[4h^2 + (x-\lambda)^2]^2} + \frac{12h^2(x-\lambda)}{[4h^2 + (x-\lambda)^2]^2} - \frac{64h^4(x-\lambda)}{[4h^2 + (x-\lambda)^2]^3} \right] \quad (32)$$

and $p_{xy}(A \rightarrow B) = -p_{xy}(B \rightarrow A)$ provided that A and B lie along the same plane. The same state of affairs exists when dislocations lie along a single plane within an infinite slab with faces parallel to the x axis, provided the Burgers vector of the dislocations is parallel to this axis. However, the $n\sigma^A$ result is not valid when the dislocations have a component of Burgers vector that is normal to the slab faces, or indeed in any situation where $p_{xy}(A \rightarrow B) \neq -p_{xy}(B \rightarrow A)$. Thus assuming that cleavage crack nucleation occurs when the stress on a fixed dislocation attains a critical value (7), it is concluded that crack nucleation in the vicinity of a surface is dependent on the orientation of the slip plane that is responsible for nucleation.

VI. References

- [1] Eshelby, J. D., Frank, F. C., and Nabarro, F. R. N., Phil. Mag. **42**, 351 (1951).
- [2] Head, A. K., and Thomson, P. F., Phil. Mag. **7**, 439 (1962).
- [3] Chou, Y. T., Can. J. Phys. **45**, 559 (1967).
- [4] Chou, Y. T., J. Appl. Phys. **38**, 2080 (1967).
- [5] Ichikawa, M., and Yokobori, T., Rep. Res. Inst. Strength Fracture Materials, Tohoku Univ. **1**, 59 (1965).
- [6] Smith, E., Acta Met. **16**, 313 (1968).
- [7] Cottrell, A. H., in Fracture (University of Melbourne, Butterworth, London 1963) p.1.
- [8] Buckingham, R. A., in Quantum Theory I. (Pure and Applied Physics Textbook). D. R. Bates, Ed. (Academic Press, New York and London 1961) p. 81.

THE ELASTIC INTERACTION BETWEEN GRAIN BOUNDARIES AND SCREW DISLOCATION PILE-UPS

M. O. Tucker*

*Department of Physics
University of Surrey
Guildford, Surrey, England*

The configuration of an array of parallel infinitive straight screw dislocations, in equilibrium under a constant applied stress, and piled-up on a plane inclined to a grain boundary at an arbitrary angle is considered. The model used for the grain boundary is the plane interface between two elastically anisotropic half-spaces welded together. Using this approximation of a continuous distribution of infinitesimal dislocations the integral equation expressing the equilibrium conditions is solved using a Wiener-Hopf technique and approximate expressions are presented for the stresses near to the tip of the array when the dislocations are parallel to orthotropic symmetry axes in each half-crystal.

Key words: Anisotropic elasticity; dislocations-elasticity; dislocation pileups; grain boundaries.

I. Introduction

To investigate the propagation of plastic deformation and the nucleation of fracture at grain boundaries in polycrystalline aggregates, a suitable elastic model of a piled-up group of coplanar dislocations at interfaces is required. The interaction between an infinite straight dislocation and a plane boundary separating two isotropic half-spaces of different elastic constants was derived by Head [1, 2]. However, this analysis can only be applied to boundaries between different materials, or different phases of the same material, and not to grain boundaries. Since the difference in elastic properties of neighbouring grains arises solely from their relative

*Now at Central Electricity Generating Board, Berkeley Nuclear Laboratories, Berkeley, Gloucestershire, England.

orientation, Head's model must then be replaced by two elastically anisotropic half-spaces joined by a plane interface. The solution to this problem, for materials exhibiting the most general elastic anisotropy, has been given by Tucker and Crocker [3] and Tucker [4].

Using the approximation of a continuous distribution of infinitesimal dislocations Barnett [5] obtained the stress field and configuration of a group of coplanar screw dislocations in equilibrium under a constant applied stress, piled-up perpendicular to a plane boundary in an elastically isotropic material. This solution was obtained using an iterative technique based on the inversion theorem of Muskhelishvili [6] for singular integral equations. More recently Chou and Barnett [7] have extended this solution to the case when the materials on either side of the interface are elastically anisotropic, provided that they have high symmetry in the direction of the dislocation line. Kuang and Mura [8] have found by means of a Wiener-Hopf technique the equilibrium distribution of edge dislocations piled-up perpendicular to a plane boundary between two isotropic half-spaces. Their results do not appear in a closed form however, and this prohibits an algebraic determination of the stresses due to the pile-up.

In the present paper the calculation using a Wiener-Hopf technique of the equilibrium distributions of screw dislocations piled-up at angles other than 90° to a plane boundary in an anisotropic solid is discussed. The form of the solution obtained allows the stresses near the tip of the array to be expressed in a simple form.

II. Dislocation-Boundary Interactions in Anisotropic Materials

Tucker [4] has presented exact expressions for the force experienced by one of a pair of infinite straight dislocations, of arbitrary Burgers vector, lying parallel to each other and to a plane boundary in an elastically anisotropic bicrystal. The results are valid for composite materials consisting of two different anisotropic half-spaces which are either welded together or may slip freely relative to one another, and also for a single half-space bounded by a free surface. Since in each case the materials are assumed to exhibit the most general elastic anisotropy, the expressions for the force on the dislocation contain complicated functions of the 21 independent elastic compliance constants s_{ijkl} , and are too lengthy to be included in the present paper. However, the nature of this force may be approximately described in terms of "image" dislocations, provided that the anisotropy of the component materials is not very large.

Consider two dislocations labelled (1) and (2), having Burgers vectors $\mathbf{b}^{(1)}$ and $\mathbf{b}^{(2)}$ respectively, situated on one side of a plane boundary, as shown in figure 1. The force on dislocation (1) in the presence of the boundary is

approximately the same as that due to (2) and to the image dislocations (1') and (2') when the boundary is absent and the solid homogeneous. The Burgers vectors $\mathbf{b}^{(1')}$ and $\mathbf{b}^{(2')}$ of the image dislocations depend upon $\mathbf{b}^{(1)}$ and $\mathbf{b}^{(2)}$ respectively, the elastic properties of the two component half-spaces and the type of boundary joining them.

An elastically anisotropic medium is termed orthotropic if there exists a set of rectangular cartesian axes $0x_i$ such that using the reduced notation s_{12} , s_{13} and s_{23} are the only non-zero off-diagonal elements of the matrix of compliances. If, in the above problem, material (I) is orthotropic and oriented so that the dislocation lines and the boundary are parallel to the axis $0x_3$, the complexity of the solutions to the boundary-value problems is greatly reduced. In particular, when the dislocations are of pure screw type the expressions for the forces they experience may be written in a form resembling those obtained from isotropic theory as given by Head [2], even in the most general case when medium (II) possesses no symmetry elements and therefore the elements s_{ij} are all independent and non-zero.

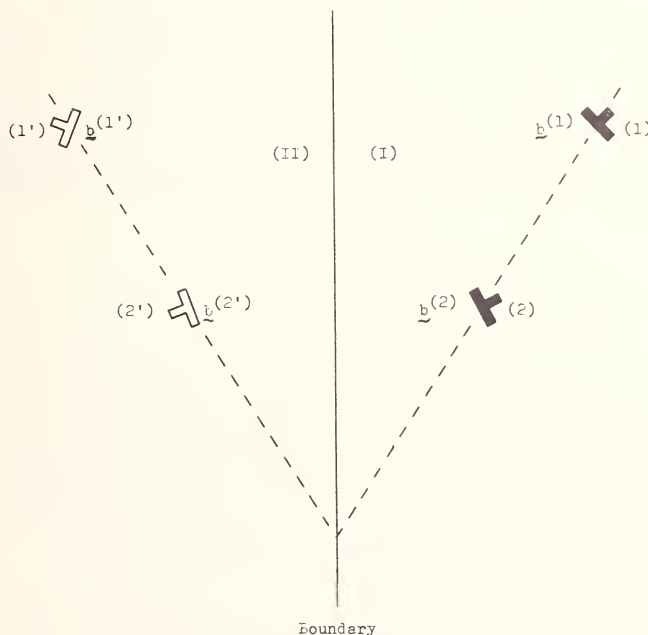


FIGURE 1. The approximate representation of the interaction of one of a pair of dislocations, (1) and (2), of Burgers vectors $\mathbf{b}^{(1)}$ and $\mathbf{b}^{(2)}$ respectively, with a plane boundary separating two elastically anisotropic half-spaces. The undislocated material in region (II) may be replaced by the material in (I) containing image dislocations (1') and (2') of Burgers vectors $\mathbf{b}^{(1')}$ and $\mathbf{b}^{(2')}$.

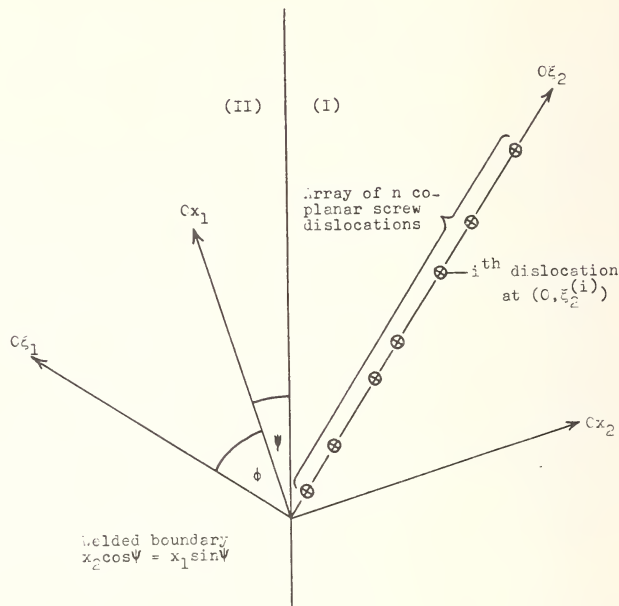


FIGURE 2. The array of n right-hand screw dislocations on the plane $\xi_1=0$ inclined at an angle $(\pi/2-\psi-\phi)$ to the plane of the welded boundary between two elastically anisotropic half-spaces. The i th dislocation of the array cuts the plane of the figure at the point $(0, \xi_2^{(i)})$.

Consider an arbitrary array of n parallel right-hand screw dislocations lying on a single plane inclined at an angle $(\pi/2-\psi-\phi)$ to the welded boundary between two anisotropic half-spaces, as shown in figure 2. In the following analysis quantities pertaining to media (I) and (II) will be indicated by superfixes (I) and (II) respectively. Material (I) is assumed to be orthotropic relative to axes $0x_i$, and the dislocations arrayed on the plane $0\xi_1=0$ and lying parallel to $0\xi_3=0x_3$. If the j th dislocation cuts the $\xi_3=0$ plane at $(0, \xi_2^{(j)})$, then the ξ_2 -component of the force it experiences due to the other $n-1$ dislocations takes the form

$$F_2^{(j)} = (2\pi)^{-1} G^{(I)} b^{(j)} \left\{ \sum_{\substack{k=1 \\ k \neq j}}^n b^{(k)} (\xi_2^{(j)} - \xi_2^{(k)})^{-1} + \frac{1}{2} \sum_{k=1}^n b^{(k)} [K(\xi_2^{(j)} + e^{i2\lambda} \xi_2^{(k)})^{-1} + \bar{K}(\xi_2^{(j)} + e^{-i2\lambda} \xi_2^{(k)})^{-1}] \right\} \quad (1)$$

where

$$\lambda = \frac{1}{2} \arctan \{ 2\eta^{(1)} (\sin \phi \cos \psi + \eta^{(1)2} \cos \phi \sin \psi) \cos(\phi + \psi) \\ \times [\eta^{(1)} \cos^2(\phi + \psi) - (\sin \phi \cos \psi + \eta^{(1)2} \cos \phi \sin \psi)^2] \}^{-1}, \quad (1a)$$

$$\eta^{(\ell)} = [s_{44}^{(\ell)}]^{1/2} [s_{55}^{(\ell)}]^{-1/2} \text{ and } G^{(\ell)} = [s_{44}^{(\ell)} s_{55}^{(\ell)}]^{-1/2}.$$

The constant K , and its complex conjugate \bar{K} , are complicated functions of the elastic compliances of both half-spaces.

III. Dislocations in Equilibrium Under an Applied Stress

To find the equilibrium configuration of n screw dislocations of equal strength b when they are piled-up against the boundary under the action of an applied stress $\sigma_{23} = -\sigma^A$, referred to axes $0\xi_i$, it is convenient to represent the array approximately by a continuous distribution of infinitesimal dislocations whose total Burgers vector between ξ_2 and $\xi_2 + d\xi_2$ is $bg(\xi_2)d\xi_2$, where b is the magnitude of the Burgers vector of a single dislocation in the discrete model. The condition for equilibrium of the array is that the net force acting on every dislocation is zero. By assuming that the frictional stress opposing the motion of the dislocations may be represented by a constant stress $\sigma_{23} = \sigma^F$, from eq (1) the equilibrium conditions may be written

$$\int_0^L g(u) [(\xi_2 - u)^{-1} + \frac{K}{2} (\xi_2 + e^{i2\lambda} u)^{-1} + \frac{\bar{K}}{2} (\xi_2 + e^{-i2\lambda} u)^{-1}] du \\ = 2\pi\sigma [G^{(1)} b]^{-1} \quad (2)$$

where $\sigma = \sigma^A - \sigma^F$ and L is the length of the pileup.

The singular integral equation (2) has been solved [9] using a Wiener-Hopf technique with Mellin transforms for the case when K is real. The solution for $g(\xi_2)$ is a function of the roots α of the equation

$$\cos \pi\alpha + K \cos \lambda\alpha = 0 \quad (3)$$

which in general are infinite in number and may only be obtained numerically. However, in the special cases when $\lambda = \pi pq^{-1}$, where p and q are integers, the roots of equation (3) occur in the form

$$\pm [q(2n+1) \pm \alpha_i] \begin{cases} n=0, 1, 2, \dots \\ i=1, 2, \dots, q \end{cases}$$

where α_i are the q values of α in the range $0 < \alpha_i < q$. The periodicity of α in these cases permits the distribution function $g(\xi_2)$ to be expressed in terms of generalised hypergeometric functions ${}_2F_{2q-1}[(\xi_2/L)^{2q}]$. It is convenient to define the functions

$${}_{2q}T_{2q-1}(a_j; b_i; x) = x^{a_j-1} t_q(a_j; b_i) \\ \times {}_{2q}F_{2q-1} \left[\begin{matrix} (a_j+2i-3)/2q; (a_j+2i-2)/2q; \\ a_j/q; (2q+a_j-b_i)'/2q; (a_j+b_i)'/2q; \end{matrix} x^{2q} \right]$$

where

$$t_q(a_j; b_i) = (2q)^{2-a_j} \Gamma(1-a_j/q) [\Gamma(2-a_j)]^{-1} \\ \times \prod_{\substack{i=1 \\ i \neq j}}^q \{\Gamma[(b_i-a_j)/2q] \Gamma[1-(b_i+a_j)/2q]\}.$$

In the function ${}_{2q}F_{2q-1}$ single terms such as $(a_j+2i-3)/2q$ represent a sequence of q terms obtained by placing $i=1, 2, \dots, q$, and dashes indicate that terms for $i=j$ are omitted. The distribution function may now be written

$$g(\xi_2) = 4\pi\sigma(G^{(1)}b)^{-1} A \sum_{j=1}^q \{{}_{2q}T_{2q-1}(\alpha_j; \alpha_i; \xi_2/L) \\ + {}_{2q}T_{2q-1}(2q-\alpha_j; \alpha_i; \xi_2/L)\}, \quad (4)$$

where

$$A = (2\pi)^{-2q} \prod_{i=1}^q \{\Gamma[(1+2q-\alpha_i)/2q] \Gamma[(1+\alpha_i)/2q]\}.$$

In the limiting case when $\lambda=0$, corresponding to a pile-up perpendicular to the plane boundary, eq (4) reduces to

$$g(\xi_2) = 2\sigma(G^{(1)}b\gamma)^{-1} \sinh[2\pi^{-1} \sin^{-1} \gamma \cosh^{-1}(L/\xi_2)],$$

where $\gamma = [(1-K)/2]^{1/2}$, which is the result previously obtained by Barnett [5]. The number of dislocations, n , contained in the pile-up is given by

$$n = \int_0^L g(\xi) d\xi = 2\sigma L (G^{(1)}b)^{-1} (4\pi)^{1-q} q A \left\{ \prod_{i=1}^q \sin(\pi\alpha_i/2q) \right\}^{-1}.$$

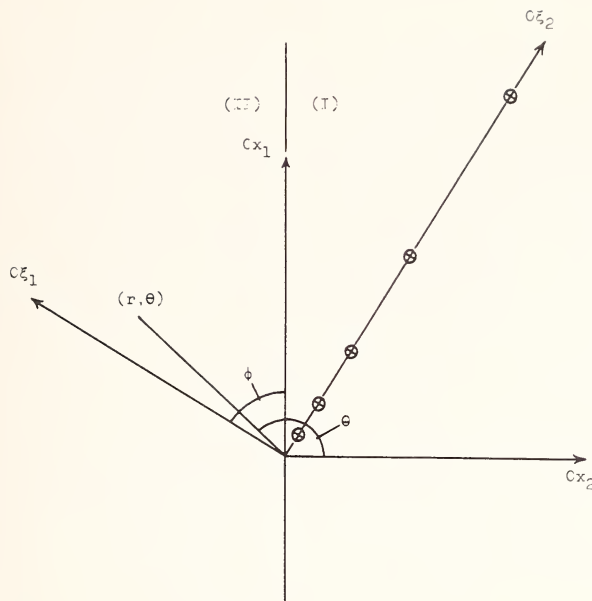


FIGURE 3. Schematic illustration of the array of screw dislocations in equilibrium under constant applied stress, in the example discussed in Section III, showing the relationship between the rectangular cartesian axes $0\xi_i$, $0x_i$ and the cylindrical polar coordinates (r, θ, z) .

To illustrate how the stresses in the vicinity of the leading dislocation may be calculated consider the simple case of two semi-infinite materials (I) and (II) whose elastic constants have orthotropic form referred to the same set of axes $0x_i$, and which are welded together along the plane $x_2=0$. The dislocations are distributed on the plane $\xi_1=0$, which is inclined to the plane $x_1=0$ at an angle ϕ , as shown in figure 3. The value of λ is obtained by placing $\psi=0$ in eq (1a). The solution to this problem for $\phi=0$ has been obtained by Chou and Barnett [7].

Using the system of cylindrical polar coordinates $r, \theta, z (= x_3)$ the stresses at points (r, θ) in medium (II) due to a single screw dislocation at $(0, \xi_2)$ may be most simply expressed in terms of the functions

$$R = rP(\theta)P(\phi)^{-1}$$

and

$$\begin{aligned} \zeta = \arctan\{ & [\eta^{(II)} \cos \phi \sin \theta - \eta^{(I)} \sin \phi \cos \theta] \\ & \times [\cos \phi \cos \theta + \eta^{(I)} \eta^{(II)} \sin \phi \sin \theta]^{-1} \} \end{aligned}$$

where

$$P(\theta) = [\cos^2 \theta + \eta^{(II)^2} \sin^2 \theta]^{1/2},$$

$$P(\phi) = [\cos^2 \phi + \eta^{(I)^2} \sin^2 \phi]^{1/2}.$$

Clearly $R=r$ and $\zeta=\theta-\phi$ when the materials are isotropic. If

$$\cos \delta = (\cos^2 \theta - \eta^{(II)^2} \sin^2 \theta) P(\theta)^{-1},$$

$$\sin \delta' = (1 - \eta^{(II)^2}) \sin \theta \cos \theta P(\theta)^{-1},$$

$$\cos \beta = (\cos \theta \cos \phi - \eta^{(I)} \eta^{(II)} \sin \theta \sin \phi) P(\phi)^{-1}$$

and $\sin \beta' = (\sin \theta \cos \phi - \eta^{(I)} \eta^{(II)} \cos \theta \sin \phi) P(\phi)^{-1}$, then

$$\sigma_{rz} = G^{(I)} b (2\pi)^{-1} (1+K) [R \cos \delta - \xi_2 \cos \beta] [\xi_2^2 - 2\xi_2 R \cos \zeta + R^2]^{-1}$$

$$\sigma_{\theta z} = -G^{(I)} b (2\pi)^{-1} (1+K) [R \sin \delta' - \xi_2 \sin \beta'] [\xi_2^2 - 2\xi_2 R \cos \zeta + R^2]^{-1}$$

where

$$K = [G^{(II)} - G^{(I)}] [G^{(II)} + G^{(I)}]^{-1}.$$

The stress component σ_{rz}^* due to the entire pileup is calculated from the integral

$$\sigma_{rz}^* = \int_0^L \sigma_{rz}(\xi_2) g(\xi_2) d\xi_2$$

and a similar expression holds for $\sigma_{\theta z}^*$. Although the forms of the resultant stresses are complicated, near to the tip of the array, where $r \ll L$, they are given by

$$\begin{aligned} \sigma_{rz}^* \sim & S(R/L)^{\alpha_1-1} \{ \cos \delta \sin [(\alpha_1-1)(\pi-\zeta)] \\ & - \cos \beta \sin [\alpha_1(\pi-\zeta)] \} (\sin \zeta \sin \pi \alpha_1)^{-1} + C_1 \end{aligned} \quad (5a)$$

$$\begin{aligned} \sigma_{\theta z}^* \sim & -S(R/L)^{\alpha_1-1} \{ \sin \delta' \sin [(\alpha_1-1)(\pi-\zeta)] \\ & - \sin \beta' \sin [\alpha_1(\pi-\zeta)] \} (\sin \zeta \sin \pi \alpha_1)^{-1} + C_2 \end{aligned} \quad (5b)$$

where

$$S = 2\pi\sigma(1+K)At_q(\alpha_1; \alpha_i).$$

α_1 is the smallest of the roots α_i , and C_1 and C_2 are functions of ϕ and θ , but independent of r .

Discussion

The stresses ahead of a blocked slip band vary with r , the distance from the leading dislocation, as r^{-m} , where the value of m depends on the size and the elastic nature of the obstacle. If it is simply a fixed dislocation $m = 1/2$, whereas if it is a plane boundary m is a function not only of the elastic constants of the materials each side of the boundary, as shown by Barnett [5], but also of the inclination of the slip band to the boundary, as demonstrated by eqs (5a) and (5b) in the present paper.

The solutions presented above are of use in deciding whether a slip band will initiate plastic deformation in the adjacent grain or nucleate fracture by coalescence of the leading dislocations. Furthermore the solutions apply to a stationary crack loaded in anti-plane strain and can be used to formulate a criterion for the propagation of fracture in the adjacent grain. Cracks and slip bands inclined at small angles to the boundary can induce intergranular fractures and grain boundary sliding, particularly at high temperatures, and the present paper provides for the first time a realistic model suitable for investigating these effects.

V. Acknowledgements

The author wishes to thank Dr. A. G. Crocker for his continued help and encouragement, and the Ministry of Technology for their financial support of this work.

VI. References

- [1] Head, A. K., Phil. Mag. **44**, 92 (1953).
- [2] Head, A. K., Proc. Phys. Soc. **B66**, 789 (1953).
- [3] Tucker, M. O., and Crocker, A. G., in Mechanics of Generalized Continua (Proc. IUTAM Symposium, Freudenstadt-Stuttgart, 1967), E. Kröner, Ed. (Springer-Verlag, Berlin 1968) p. 286.
- [4] Tucker, M. O., Phil. Mag. **19**, 1141 (1969).
- [5] Barnett, D. M., Acta Met. **15**, 589 (1967).
- [6] Muskhelishvili, N. I., Singular Integral Equations (P. Noordhoff, N. V., Groningen, 1953).
- [7] Chou, Y. T., and Barnett, D. M., phys. stat. sol. **21**, 239 (1967).
- [8] Kuang, J. G., and Mura, T., J. Appl. Phys. **39**, 109 (1968).
- [9] Tucker, M. O., to be published (1969).

Discussion on Papers by J. A. Simmons and R. Bullough, and D. M. Barnett.

BULLOUGH: We observe that Lie and Koehler can get an accurate representation in trigonometric series for the cubic Green's tensor—even for lithium—in a very few number of terms.¹ We can replace their trigonometric functions by spherical harmonics and the same number of finite terms is still required. Having done that, one is then in a position to calculate a very beautiful closed expression for the incompatibility source tensor. I am sure you didn't fail to recognize the beauty of the final slide of Dr. Simmons' talk.²

KOEHLER: The convergence difficulty associated with the spherical harmonic series can be clarified as follows: If one converts the double Fourier series into spherical harmonics the ϕ terms are similar, but the θ dependence gives difficulty. For given ϕ dependence (say $\cos 4\phi$) the coefficient associated with a given $P_n^m(\cos \theta)$ contains contributions from *all terms* of the double Fourier series associated with $\cos 4\phi$. Thus, for example, the coefficient of $P_4^4(\cos \theta)$ includes contributions from the terms $\cos 4\phi, \cos 4\phi \cos 2\theta, \cos 4\phi \cos 4\theta, \cos 4\phi \cos 6\theta$, etc. Since lower order double Fourier series terms give contributions, it is not surprising that convergence of the spherical harmonic expansion is bad (see E. Hobson, Theory of Spherical and Ellipsoidal Harmonics, p. 147, Cambridge University Press, 1931).

BULLOUGH: I'm afraid I don't understand your point. I merely replaced the trigonometric terms in your series by spherical harmonics; it's exactly the same series.

KRÖNER: I have one comment on Dr. Barnett's paper and one on Dr. Simmons' paper. I do not know any theory in mathematics which states that any function can be better developed in terms of spherical harmonics than in trigonometrical series or power series. I think it depends on the circumstances, so I can believe that in some situations the double trigonometric series are better than the spherical harmonics, but I am quite sure that the spherical harmonics are better in other situations. Also, I would like to say that in the spherical harmonics expansion which was used by Burgers and in my first paper, one should use, of course, only the spherical harmonics of cubic symmetry in this case, and then

¹ Lie, K.-H. C., and Koehler, J. S., Adv. in Phys., **17**, 421 (1968).

² This slide gives an expression for the spherical harmonic expansion of the incompatibility source tensor in terms of a spherical harmonic expansion of the elastic Green's tensor. See Simmons, J. A., and Bullough, R., Theory of Defects and Stress Sources in Linear Anisotropic Elasticity, to be published.

it is exactly the same series as used by Professor Bross which he called cubical harmonics. This is my comment on Dr. Barnett's paper.

Concerning the paper of Drs. Simmons and Bullough, I worked on this incompatibility problem in 1954 and I was very interested in your paper. [At this point Professor Kröner went to the board and gave a brief exposition of his techniques as contained in the papers: *Z. für Phys.*, **139**, 175 (1954); **141**, 386 (1955).] I can derive your results in such a way: Consider the sixth-order differential operator $f(\nabla) \equiv \det(c_{ijkl}\partial_j\partial_l)$ where c_{ijkl} is the Hookean tensor of elasticity. Let us introduce a sixth-order stress function tensor ψ_{kl} from which the stress tensor σ_{ij} is derived by using a certain tensorial differentiation of sixth order: $\sigma_{ij} = X_{ijkl}(\nabla)\psi_{kl}$. We can determine $X_{ijkl}(\nabla)$ in such a way that the equations $\partial_k\psi_{kl} = 0$, $\partial_i\sigma_{ij} = 0$ and $f(\nabla)\nabla^2\psi_{kl} = \eta_{kl}$ hold simultaneously. Here η_{kl} is the incompatibility tensor.

By using the well-known Fourier representation of the Green's function of the last equation, it can easily be shown that this function gives rise to the solution of Simmons and Bullough.

In the last equation, the incompatibility problem has two parts: the elastic part represented by $f(\nabla)$ and the harmonic part represented by ∇^2 . It seems to me that considerable complications implied by the operator $f(\nabla)\nabla^2$ may be avoided if ∇^2 can be removed in such a way that the resulting equation is $f(\nabla)\chi_{kl} = \eta_{kl}$ where χ_{kl} is now a fourth-order stress-function tensor.

I have proved in my 1955 paper mentioned earlier and rederived just now in a different manner that the indicated simplification is, in fact, possible in the case of cubic symmetry. It is also possible for the two-dimensional problem of any symmetry. Since Indenbom and Orlov succeeded in representing the three-dimensional Green's function through the whole set of two-dimensional Green's functions (one with respect to each direction in space), it appears quite feasible to assume that the combined elastic-harmonic problem can be reduced to a purely elastic one in three dimensions for any symmetry.

SIMMONS: If I understand your comments correctly, you're pointing out that one form of our incompatibility source tensor T can be written down from a sixth-order differential operator acting on $\int U(\mathbf{r}' - \mathbf{r})|\mathbf{r}'|^{-1}dV$, which is the Green's function of $f(\nabla)\nabla^2$ when U is the Green's function of $f(\nabla)$, and that's quite right. You would then like to get rid of the ∇^2 and do the incompatibility problem with just the operator $f(\nabla)$ by means of a hypothetical fourth order differential operator, which I'll call Y_{ijkl} , so that $\text{Inc}_{ijkl}\tilde{C}_{klmn}Y_{mnpq} = \delta_{ip}\delta_{jq}f(\nabla)$, where \tilde{C} are the elastic compliances. I agree that it would be nice if your hypothesis were correct and one could remove the harmonic component from the incompatibility source tensor, but I don't think this is likely to be true in general. The reason the

harmonic integral occurs has nothing to do with the elastic constants or the Green's tensor. The harmonic integral arises from inverting the incompatibility operator which is very closely related, as you know, to the Laplacear operator. In fact, you can see in our paper that if one wishes to obtain a stress from the plastic distortion β^P rather than the incompatibility η , then you don't need the harmonic integral part; it only arises when inverting the incompatibility operator.

So, it's not clear what symmetry properties the elastic constants have to have to satisfy your hypothesis that ∇^2 can be absorbed into $f(\nabla)$, but I think they're quite strong. Anyway, it's possible to test your guess, which I note is more general than that in your 1955 paper, by comparing it with a general expression for our source tensor \mathbf{T} —but the algebra is very messy.

However, I'd like to make another, slightly more general point, and that is that when dealing with such complex functions as the function U you have mentioned, which essentially have to be computed numerically, or in power series, differentiation is much more difficult than integration. Writing down a quantity like the Green's tensor components or the source tensor \mathbf{T} as high order derivatives is no help. It's much better to deal with direct representations of these quantities, preferably in integral form. This is what we have tried to do and I'm not sure that high order stress functions, whose use we have deliberately avoided, will ever have any practical utility for general anisotropy.

ESHELBY: May I add a separate comment. There is one class of problems which you can do, because you can find the anisotropic Green's tensor ever so easily, namely when $C_{44} = -C_{12}$. I thought of this, and I know a lot of other people have too, but I thought it was too bogus for publication. I used to be impressed by some of the results got by the lattice dynamics people for the interaction of point defects, but then I discovered that their lattice model was just the one which in the continuum limit goes over into the particular elastic solid I'm talking about. I believe it is called the Rosenstock-Newell model. Now, is this fair, and does any material approximate to it? Professor Maradudin, would you like to comment? Is he here? No,³ well, it is a pity because it could keep people in business for years; having done the whole of three-dimensional elasticity for isotropy you could do it all again for this anisotropic material. It is true that iron pyrites have a negative C_{12} , but it is not nearly negative enough to cancel the C_{44} . I have hopes that some other materials with the same rather odd cubic crystal structure might do it, maybe platinum arsenide. I do wish someone would measure those elastic constants.

³ Professor Maradudin did comment the following day. See p. 250.

II LATTICE THEORIES

Chairman:

R. BULLOUGH

ONE-ELECTRON THEORIES OF COHESION ON ION-PAIR POTENTIALS IN METALS

N. W. Ashcroft

*Laboratory of Atomic and Solid State Physics
Cornell University
Ithaca, New York 14850*

The single particle picture of cohesion in metals is briefly reviewed in the light of modern knowledge of their band structures. Periodic components in the electron density distributions (intimately connected with the same band structures) are important in the determination of the effective potential between ions.

In simple metals, defined to be those with tightly bound core states, the net binding of the metallic state is basically a remnant of a competition between kinetic (Pauli principle) and Madelung energies of ostensibly free conduction electrons. Various corrections (for correlation, for exchange, etc.) must be included, and the Madelung energy (which is normally appropriate to a uniform electron gas in a Coulomb lattice of point ions) can be modified as necessary for departures from Coulomb's law. Terms in the total energy also arise from periodic variations in conduction electron density; for perfect lattices these are naturally dependent on the ionic arrangement and will vary in importance from crystal structure to crystal structure. Electronic density variations arising from disorder (e.g. distributions of defects) also introduce corrections into total energy.

The structurally dependent terms in the total energy can be evaluated to second order in the pseudopotential: to this same order the *total* energy may be written as a sum over pair potentials between ions whose form is quite straight forward to evaluate. As with many inter-atomic potentials, the ion-ion potentials demonstrate "hard-core" effects at small separation, and are rather weak at large distances.

Extending the simple theory to transition metals or metals exhibiting additional band structure more akin to itinerant narrow-band behavior, can be carried through by incorporating Born-Mayer interactions between tight binding atomic states. This procedure is, of course, only valid in situations where the Bloch method itself is applicable. While the core-core exchange term approximated by the Born-Mayer interaction is quite small in the simple metals it is appreciable for metals like Cu, Ag and Au, and in fact is basically responsible for fixing the equilibrium den-

sity. Its addition to the otherwise "simple-metal" like ion pair potentials modifies the behavior at short range.

Key words: Band structure; cohesion; core-core interactions; electron density; interatomic; one-electron potentials; pseudopotentials.

I. Introduction

In spite of particularly difficult problems connected with the determination of the actual single-particle periodic potential of a crystal, theories of band structures of solids¹ have progressed to a point now where first principles calculations can give reasonable predictions of a variety of properties. Approaches which are somewhat less than "first principles" such as the pseudopotential method are also generally highly successful in accounting for properties explicitly related to the Fermi surface. Extending the method to energies away from the Fermi energy (such as occur in optical properties) requires, in general, a knowledge of the energy dependence of the pseudopotential. Calculations of the total ground state energy of a metal by this method have not been numerous enough to decide whether or not it is an unqualified success, although on balance it looks as though, at least for simple metals it is quite promising. Since the simple metals are in great measure, free electron like, the use of the method really lies in its ability to provide corrections to large electron gas terms.

Almost without exception lattice theories of cohesion in metals have been formulated in the independent particle approximation. The effective electron-ion potential seen by a single electron (which results from this approximation) is well known to be partly nonlocal. The nonlocal contribution, or the exchange part, can be traced back to the requirements of antisymmetry in the many electron trial wave functions. Slater's [2] famous " $\rho^{1/3}$ " approximation to this term (and subsequent refinements of the numerical factors [3]) renders the single particle problem more tractable by providing a completely local potential to work with. But, the valence-valence exchange is only one contribution to the potential. The others, including the basic Hartree potential, valence-core exchange, core-core exchange and so on, must also be calculated. The work of Herman [1] and co-workers has shown that with remarkable care the separate terms

¹ For a summary of the various methods available see Ref. [1].

can all be included with fair precision. However, band structures calculated with these potentials still require slight modification to match easily identifiable experimentally determined points.² Frequently the aim is to take the derived band structures and their associated potentials and use the knowledge to calculate other properties of the solid. Along these lines it often makes good sense to avoid the first principles determination of the potential and to extract it (or its matrix elements) once and for all from experiment and use them in subsequent calculations. This is very much the approach of the pseudopotential method: here however pseudopotential matrix elements rather than real potential matrix elements are determined and the subsequent calculations must be performed in a consistent manner with pseudowave functions rather than the real valence states.

In the next section we shall expand on this in the context of binding and pair interactions in simple metals. However, before we do it is worth pointing out here that the pseudo-potential method runs into difficulties³ for metals with sets of valence states which are neither compact and tight-bindinglike or are completely itinerant and free-electronlike. The *d*-states fall into this category for metals in the transition series. Although they have, in most cases, been approximated by Bloch tight binding states the widths of the resulting *d*-bands somewhat negate the initial starting assumptions. Against this however is the fact that many qualitative features of transition metals (the specific heats trends for example) are reasonably well accounted for in form.

In the transition metals the role of the *d*-states in mechanical properties is far from passive: the opposite is true for the corresponding core electrons in simple metals. Indeed by a simple metal we mean one in which core electrons play a minor role. Their core states are tightly bound and as a consequence have large ionization energies. Nonsimple (including transition) metals have characteristically small ionization energies for electrons in *d*-shells. Electrons in the *d*-band contribute to the total ground state energy of the metal and its volume derivatives. Electrons in tightly bound simple metal core bands also contribute, but since the core wave-function overlap only little, their share—the core-core exchange term (or Born-Mayer term)—is small. It becomes progressively larger however, as the core size increases in relation to the atomic volume (and indeed may be large enough in some cases to cause ordered electronic states such as ferromagnetism and antiferromagnetism). This is exactly the situation in the transition metals if we view them from the tight binding

² As is done for example in interpreting the optical properties of the semiconductors.

³ See however, Ref. [4].

approach. But if the core electrons are becoming more loosely bound then we have in addition to core-core repulsion terms and possible covalent effects the familiar attractive terms arising from the fluctuating dipole or van der Waals attraction. These are, of course, modified by the presence of the interacting gas of *s*-derived electrons: consider the usual semiclassical argument leading to the r^{-6} attractive force. A fluctuation of electron charge density at one atom produces a dipole of strength p and at a distance r away a field of roughly p/r^3 . In turn this field induces a dipole of strength $\alpha p/r^3$ (α is the core electronic polarizability) in an atom at r and in combination the two dipoles attract with an energy proportional to r^{-6} . If we proceed to include the effects of *s*-electrons, then the fields which induce dipoles must be reduced by screening. The potential of the induced dipole is of order r^{-2} and this is reduced to $r^{-2}e^{-\lambda r}$ in a Thomas-Fermi approximation. The polarizing field is thus proportional to $r^{-3}e^{-\lambda r}\{1+\lambda r\}$ and we expect in this crude approximation a potential behaving as $r^{-6}e^{-\lambda r}\{1+\lambda r\}$.⁴ If we go beyond the tight binding approach we expect substantial deviations from this form. As it is, it merely accounts for the leading term in the interaction between closed shell atoms and we have no guarantee that when working to specified accuracy the total potential energy of a collection of N atoms can be written solely in terms of two-body potentials. In a similar way we may expect *d*-electron exchange and correlation to be screened, a point we return to briefly in section III.

II. Simple Metals: Cohesion

In both this and the section on the transition metals we will find it convenient to express total energies as functions of ionic rather than electronic densities or separations. While the latter is commonly used in simple metals the lack of a clear cut valence in many of the transition metals forces one to use ion densities which are unequivocal. Linear dimensions will be given in atomic units ($a_0=0.529 \text{ \AA}$) and energies in Rydbergs (13.59 eV). The total energy is to be regarded as the internal energy; terms arising from configurational entropy are generally small.

Immediately after the introduction of Fermi-Dirac statistics and their application by Sommerfeld to the free electron gas, Frenkel [5] suggested that the basic mechanism operating in cohesion is a competition between the kinetic energy of confinement (of free noninteracting electrons in the metal) and the potential energy they have as negatively charged

⁴ Because of the existence of a sharp Fermi surface we expect asymptotic oscillations of the Ruderman-Kittel type in the interaction.

particles in the field of positively charged ions. Using Wigner and Seitz's [6] original idea⁵ that on average one atomic volume Ω (approximated by a sphere of radius r_o : $4/3\pi r_o^3 a_o^3 = \Omega$) holds a neutralizing complement of Z valence electrons, we can imagine the metal to be constructed, in the simplest approximation by an array of neutral slightly overlapping spheres. These have only weak multipole type interactions with each other so that the energy in this *uniform sphere approximation* is the total of kinetic and potential energies required to build up each sphere: The kinetic energy (expressed Rydbergs per ion) is

$$U_{KE} = Z^{5/3} (2.21) / r_o^2 \quad (1)$$

and elementary electrostatics gives the potential energy of the sphere of constant density in the field of a *point ion* is (again in Rydbergs/ion)

$$U_{PE} = -\frac{1.8Z^2}{r_o} \quad (2)$$

The combination of (1) and (2) exhibits a minimum when $r_o = 2.45/Z^{1/3}$ which at least indicates that polyvalent metals may be more tightly bound than monovalent metals, but does not in any way account for the striking density trends within isovalent series. This calculation is performed within the so-called Hartree approximation. The constant electron density is appropriate to a many electron wave function which is simply a product of single particle wave functions (these being just plane waves). No information on the spatial correlation of electrons one with another can of course be present in this wave function which neglects their mutual Coulomb interactions. Nor is any account taken that the total product trial wave function should at least be antisymmetrized to properly represent a collection of Fermions. Thus in calculating (2) which includes the electrostatic energy of the *uniform* cloud of electrons, it is necessary to incorporate the fact that two electrons with parallel spins are forbidden by Pauli exclusion from approaching each other arbitrarily close (which constant particle density assumes is possible). The Coulomb energy of closely spaced electrons with parallel spins (and equal charge) is thus reduced; hence by allowing for this *exchange* term (2) in fact becomes more negative. The exchange correction is [8]

$$U_{ex} = -\frac{0.916}{r_o} Z^{4/3}. \quad (3)$$

⁵ For an expanded review on this section the reader is referred to the article by H. Brooks, Ref. [7].

To this we must also account for the fact that in an interacting electron gas, electrons with antiparallel spins tend to avoid each other because of the strong Coulomb repulsion between them (present also, of course, between electrons with parallel spins). Again contributions to (2) arising from electrons at small separation are reduced and the total becomes more negative still due to correlations by an amount⁶

$$U_{\text{cor}} = -(0.115 - 0.031 \ln(r_o/Z^{1/3}))Z \quad (4)$$

At this point exchange and correlation corrections to the elementary uniform sphere approximation gives, for point ions,

$$U = Z^{5/3} \left(\frac{(2.21)}{r_o^2} - \frac{1.8Z^2}{r_o} - \frac{0.916Z^{4/3}}{r_s} \right) - (0.115 - 0.031 \ln r_o/Z^{1/3})Z \text{ Rydbergs/atom} \quad (5)$$

and again it is clear isovalent metals are erroneously predicted to have the same equilibrium densities.

To proceed from here we can first correct for the fact that the uniform sphere approximation leads to small overlaps between neighboring spheres. A direct calculation of the energy of a *lattice* of point ions in a uniform electron gas (the *Madelung energy* first calculated for a metal by Fuchs [9]) shows that the energy is remarkably close to (2); i.e.,

$$U_{PE} = \frac{-1.792Z^2}{r_o}. \quad (6)$$

Actually (6) depends on the ionic arrangement but only weakly: as we have given it (6) is accurate to 3 places for each of the structures f.c.c., b.c.c. and h.c.p. Indeed, for a *liquid* metal the term is changed only by a small amount to $\frac{-1.73Z^2}{r_o}$ [10] which indicates its lack of sensitivity to extreme changes in structure. Thus (5) is replaced by

$$U = Z^{5/3} \left(\frac{(2.21)}{r_o^2} - \frac{1.792Z^2}{r_o} - \frac{0.916}{r_o} Z^{4/3} \right) - (0.115 - 0.031 \ln r_o/Z^{1/3})Z \quad (7)$$

where again, we emphasize that the calculation is for *point* ions.

⁶ This result is due to Pines and Nozieres [8] and differs only slightly from other correlation corrections.

The next step is to relax the restraint of *point* ions to a physically more meaningful situation. We replace point ions by ions with characteristic atomic sizes. These sizes are, of course, determined principally by the core electrons and in introducing their presence in a physical way we concurrently introduce more terms in the energy. One of these we can dispose of immediately: the core functions of the ions overlap slightly and produce a Born-Mayer or core-core exchange interaction. For the simple metals we may neglect this term but will return to it in connection with the transition metals. We shall also neglect any effects arising from the polarizability of the ion cores.

Far more important is the effect of the extended ion on valence electron wave functions and on the potential that the valence electrons experience. At large electron-ion separations a single electron will surely see a potential of the type $-Ze^2/r$. But for small separations the deviations from this form are marked. In the one-electron picture we are now confronted with the difficulties in calculating the potential alluded to in the Introduction. Terms like valence-core exchange contributions which now arise (and for reasons similar to those outlined for valence-valence exchange) are difficult to estimate with accuracy. In a careful calculation of the binding energy of Al, Kleinman [11] estimated the uncertainties of about 0.2 Ry/ion.⁷

One other effect of extended ion cores is the following: For point ions we can, in principle, consider a uniform density of conduction electrons throughout the crystal. But in the presence of ion cores the valence wave functions are only sensibly flat in the interstitial regions. Within the ion core the charge density in valence wave functions is certainly *not* uniform. In fact, we know that since the valence states are one group of eigenstates of the crystal Hamiltonian, they are orthogonal to the other class, the core states trapped in the deep crystalline potential.

But it is now known that although the single particle potentials may be strong, the resulting band structure may be surprisingly free-electronlike. The simple reasons for this are (a) the mobility of the conduction electrons and their ability to reduce the total self consistent potential by screening. (b) the fact that where the one-electron potential is strongest (i.e., near the ion) the valence electrons are forbidden from entering. Pauli exclusion by the core states already there considerably reduces the efficacy of the potential. It is therefore possible to describe the band structure by a weak periodic pseudopotential providing we use, in a consistent manner, linear combinations of plane waves to represent the pseudowave function.⁸

⁷ But nevertheless arrived at a final cohesive energy within 0.01 Ry of the observed value.

⁸ For a discussion of cohesion in terms of phase shifts, see Ref. [12]. Note also that the normalization of the pseudowave function may result in the use of a small effective charge correction on the ions as discussed in reference [13].

The essential aspects of pseudopotential theory [13] can be summarized as follows. Let the one electron self consistent real potential be $V(\mathbf{r})$. We can distinguish between two classes of states, valence $|\Psi^v\rangle$ and core $|\Psi^c\rangle$ satisfying

$$\left(-\frac{\hbar^2}{2m}\nabla^2 + V(\mathbf{r})\right) |\Psi^v\rangle = \epsilon^v |\Psi^v\rangle \quad (8)$$

and

$$\left(\frac{\hbar^2}{2m}\nabla^2 + V(\mathbf{r})\right) |\Psi^c\rangle = \epsilon^c |\Psi^c\rangle \quad (9)$$

(Since the Hamiltonian is periodic each state may be labeled by Bloch wavevector \mathbf{k} and the superscripts v and c are taken to include this.)

If we define a projection operator

$$P = \sum_c |\Psi^c\rangle \langle \Psi^c|$$

then it follows that the operator

$$-\frac{\hbar^2}{2m}\nabla^2 + V(\mathbf{r}) + PO \quad (10)$$

has precisely the same *valence* eigenspectrum as

$$-\frac{\hbar^2}{2m}\nabla^2 + V(\mathbf{r})$$

i.e.,

$$\left(-\frac{\hbar^2}{2m}\nabla^2 + (V(r) + PO)\right) |\phi^v\rangle = \epsilon^v |\phi^v\rangle \quad (11)$$

The only requirement on the *arbitrary operator* O is that it have the translation group of the lattice.⁹ For different choices of O we naturally generate different forms of wave functions $|\phi^v\rangle$ but for each the energy is unchanged. The main observation is that whereas plane wave matrix elements of $V(r)$ may be slowly convergent, the elements of $V_{ps} = V(r)$

⁹ So that the same Bloch wavevector labels the states of (11). By taking O as a simple function ($O = -V$ for example) or as an operator diagonal in core states ($O = \epsilon - H$) the pseudo-Hamiltonian is assured to be Hermitian.

$+PO$ are much more quickly convergent. Hence, a secular equation derived from using a plane wave basis $\left(-\frac{\hbar^2}{2m} + V_{ps}\right)$ can represent the band structure and yet be of much lower order than a secular equation based on (8).

In many practical applications of the method one simplifies V_{ps} to a local form and deduces its local matrix elements from experiment, typically Fermi surface data. Corresponding to this choice the pseudowave function is now the sum of a few plane waves. To apply the method to the problem of cohesion we observe that the energy terms can easily be calculated for a weak pseudopotential for a *single* plane wave representing the pseudowave function. A single plane wave deposits electron charge uniformly: corrections to the inherent periodic variations in charge density will follow in a moment.

We imagine that on each lattice site we place an ion with a “bare” electron-ion pseudopotential $v(r)$. We can write this as

$$v(r) = \frac{-Ze^2}{r} + \Delta(r) \quad (12)$$

where $\Delta(r)$ is the difference between the point ion potential and the pseudopotential

$$\Delta(r) = \frac{Ze^2}{r} + v(r) \quad (13)$$

In a constant background of charge deposited by one plane wave the potential energy for the point ion part is just the Madelung term

$$U_{PE} = \frac{-1.792}{r_0} Z^2.$$

But there is also a term coming from the correction $\Delta(r)$. Since the electron density is n_e this is (per ion)

$$\Delta U_{PE} = \frac{1}{N} \int_{\text{crystal}} (n_e d\mathbf{r}) \sum_i \Delta(\mathbf{r} - \mathbf{r}_i)$$

where i labels the ion sites. Thus

$$\begin{aligned}\Delta U_{PE} &= \frac{Z}{\frac{4}{3}\pi r_0^3} \int_{\text{crystal}} d\mathbf{r} \Delta(\mathbf{r}) = \frac{Z}{\frac{4}{3}\pi r_0^3} \lim_{k \rightarrow 0} \int d\mathbf{r} e^{ik \cdot \mathbf{r}} \Delta(\mathbf{r}) \\ &= \frac{Z}{\frac{4}{3}\pi r_0^3} \lim_{k \rightarrow 0} \left\{ \frac{4\pi Z e^2}{k^2} + v_k \right\} \quad (14)\end{aligned}$$

where v_k is the Fourier transform of the local unscreened pseudopotential. We may write this as

$$\Delta U_{PE} = \frac{\alpha Z^2}{r_0^3} \text{ Rydbergs} \quad (15)$$

with

$$\alpha = \frac{3}{4\pi} \lim_{k \rightarrow 0} \left\{ \frac{8\pi}{k^2} \frac{v_k}{Z} \right\}$$

if v_k is measured in atomic units. For uniform electron density, the total energy per ion is

$$U = \frac{2.21}{r_0^2} Z^{5/3} - \frac{1.792 Z^2}{r_0} - \frac{0.916}{r_0} Z^{4/3} - (0.115 - 0.031 \ln r_0/Z^{1/3}) Z + \frac{\alpha Z^2}{r_0^3} \quad (16)$$

and we now have a term which explicitly depends on the properties of the ion and may therefore be expected to change even in isovalent series.

The final correction we shall consider is that arising from periodic variations in electron density, a manifestation of the electronic band structure. These are most easily thought of by considering a general arrangement of ions at positions r_i . The effect of electron-ion interactions (as described by the pseudopotential) is surely to cause nonuniformities in electron density. We have ignored this in calculating the terms in (16); but as we now see the nonuniform distribution of electrons introduces additional terms into the total energy. The argument is as follows: consider a volume $d\mathbf{r}$ of the solid in which $n_i(\mathbf{r})d\mathbf{r}$ ions are present, $n_i(\mathbf{r})$ being the local ion density. Because the ions interact with the electrons, they will induce at a point \mathbf{r}' an induced charge density in the electron gas a charge density $\rho_{\text{ind}}(\mathbf{r}')$. The energy of interaction between the electrons induced in $d\mathbf{r}'$ at \mathbf{r}' and the ions in $d\mathbf{r}$ at \mathbf{r} is

$$n_i(\mathbf{r})d\mathbf{r} \rho_{\text{ind}}(\mathbf{r}')d\mathbf{r}' v(\mathbf{r} - \mathbf{r}')$$

where, again, $v(\mathbf{r} - \mathbf{r}')$ is the local pseudopotential. The total energy per ion is thus (allowing for double counting)

$$U_{BS} = \frac{1}{2} \frac{1}{N} \int n_i(\mathbf{r}) d\mathbf{r} \int d\mathbf{r}' v(\mathbf{r} - \mathbf{r}') \rho_{\text{ind}}(\mathbf{r}') \quad (17)$$

which we may simplify by introducing the Fourier transforms

$$U_{BS} = \frac{1}{2N} \sum_{k \neq 0} n_i(k) v_k \rho_{\text{ind}}(-k) \quad (18)$$

where BS refers to “band structure.”

We may calculate $\rho_{\text{ind}}(-k)$ by noting that Poisson’s equation gives

$$\rho_{\text{ind}}(-k) = \left(\frac{1}{\epsilon_k} - 1 \right) (k^2 v_k / 8\pi) n_i(k) \quad (19)$$

(again working in atomic units). Here ϵ_k is the wave number dependent dielectric constant and may be taken for an interacting electron gas [8] as

$$\epsilon_x = 1 + \frac{f(x)}{(\pi a_0 k_F) x^2}; \quad x = k/2k_F$$

with

$$f(x) = \left\{ \frac{1}{2} + \frac{1-x^2}{4x} \ln \left| \frac{1+x}{1-x} \right| \right\} g(x)$$

where $g(x)$ is a correction for exchange.¹⁰

Collecting (18) and (19) we get

$$U_{BS} = \frac{1}{2N} \sum_{k \neq 0} n_i(k) n_i(-k) \frac{k^2}{8\pi} v_k \left(\frac{1}{\epsilon_k} - 1 \right) \quad (20)$$

and since a *perfect solid* $\rho_k = N\delta_{k,K}$ where K is a reciprocal lattice vector, we find

$$U_{BS} = - \left(\frac{Z}{3\pi^2} \right) \sum_K \frac{f(x_K)}{(x_K)^4 [1 + 0.166 r_0 f(x_K) / Z^{1/3} x_K^2]} \left(\frac{v(x_K)}{v^c(x_K)} \right)^2 \text{ (Ryd/ion)} \quad (21)$$

¹⁰ For $0 < k < 2k_F$ this is a factor of order 1.

where $v^c(k) = 8\pi/k^2$. However, in a solid with defects (assumed at equilibrium), or in a disordered solid the expression must be modified. If we define the average structure ¹¹ by

$$S(k) = \frac{1}{N} \langle n_i(k) n_i(-k) \rangle \quad (22)$$

as is usual then (20) becomes

$$U_{BS} = -\frac{4Z^2}{\pi^2} \int_0^\infty dx S(x) \frac{f(x)}{x^2 + 0.166r_0 f(x) Z^{-1/2}} \left(\frac{v(x)}{v^c(x)} \right)^2 \quad (23)$$

(note that $f(x) \sim x^{-2}$ as $x \rightarrow \infty$).

This is precisely what one would write down for the band structure energy of a liquid metallic system for which (22) is recognized as the static structure factor. For a highly defected solid the contribution from structure will lie between (21) and (23) with concomitant changes in the Madelung energy. It is clear from (23) that the importance of the structural term is quite sensitive to the valence, a result that will remain true for disordered or defected metals.

If we keep to perfect solids then (21) is easily evaluated when the pseudopotential is known [10]. The binding energies of several simple metals (the heat of sublimation plus the characteristic ionization energy sums) are given in table 1. These figures are obtained by actually eliminating α with the zero pressure condition $(dU/dr_0)_{eqm} = 0$ and using the observed densities. The elastic constants may also be computed by taking appropriate derivatives ¹² of the total energy. It is found [10] that the band structure term (21) has relatively little effect in monovalent metals but gives a large contribution in the polyvalent metals.

¹¹ For example by taking ensemble averages over microscopic regions of the solid containing statistically large numbers of atoms.

¹² The compressibility K at $T \sim 0$ is given by $\frac{1}{K} = -V \frac{\partial P}{\partial V}$ or in terms of n_i and U it is

$$\frac{1}{K} = n_i \frac{\partial}{\partial n_i} \left\{ n_i^2 \frac{\partial U}{\partial n_i} \right\}.$$

TABLE 1. *Theoretical and Experimental binding energies (in Ry/atom) of metals calculated using the pseudopotential method. (Ref. [10]).*

	$-U^{\text{th}}$	$-U^{\text{exp}}$
Li	0.564	0.511
Na	0.454	0.460
K	0.383	0.390
Rb	0.344	0.366
Cs	0.318	0.345
Mg	1.72	1.78
Zn	2.20	2.10
Al	4.23	4.14
Pb	6.20	7.16

III. Simple Metals: Ion-Ion Potentials

We may use arguments very similar to those used in the calculation of the ground state energy to obtain expressions for the effective interaction between two simple metal ions.¹³ First we imagine the ions to be separated by a distance \mathbf{r} and situated in an electron gas of uniform density. Then if \mathbf{r} is large enough that the Born-Mayer potential may be neglected, the interaction of the ions is simply expressed by Coulomb's law:

$$\phi_c = Z^2 e^2 / r$$

or

$$\phi_c(k) = 4\pi Z^2 e^2 / k^2. \quad (23)$$

Next, we allow one of the ions to induce (via the electron-ion interaction) a charge fluctuation $\rho_{\text{ind}}(\mathbf{r}')$ at \mathbf{r}' . In an element $d\mathbf{r}'$ located there we find induced charge $\rho_{\text{ind}}(\mathbf{r}') d\mathbf{r}'$ which in the pseudopotential field of the other ion gives an energy contribution:

$$d\phi_{ei} = d\mathbf{r}' \rho_{\text{ind}}(r') v(\mathbf{r} - \mathbf{r}') \\ \text{or a total } \phi_{ei}(\mathbf{r}) = \int d\mathbf{r}' \rho_{\text{ind}}(\mathbf{r}') v(\mathbf{r} - \mathbf{r}'). \quad (24)$$

¹³ A discussion of pair potentials in simple metals may also be found in Ref. [13].

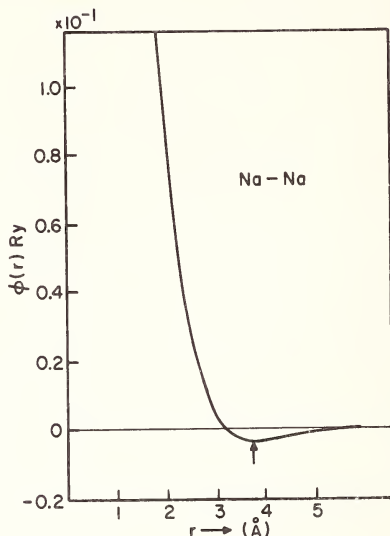


FIGURE 1. Pair interactions between two sodium ions. Energy is measured in Rydbergs and separation in Å. The arrow indicates the nearest neighbor distance observed in the b.c.c. phase.

Thus the “electron-ion” contribution to the ion pair potential is

$$\phi_{ei}(k) = \rho_{\text{ind}}(k) v_k$$

and again, by Poisson’s equation, the charge induced by a single ion is

$$\rho_{\text{ind}}(k) = \left(\frac{1}{\epsilon_k} - 1 \right) \frac{k^2 v_k}{8\pi}$$

hence

$$\phi_{ei}(k) = \left(\frac{1}{\epsilon_k} - 1 \right) \frac{k^2}{8\pi} v_k^2$$

The total potential between two ions is thus (in atomic units)

$$\phi = \phi_c + \phi_{ei} = \frac{2Z^2}{r} + \frac{V}{8\pi^3} \int dk e^{ik \cdot r} \left(\frac{1}{\epsilon_k} - 1 \right) \frac{k^2}{8\pi} v_k^2. \quad (25)$$

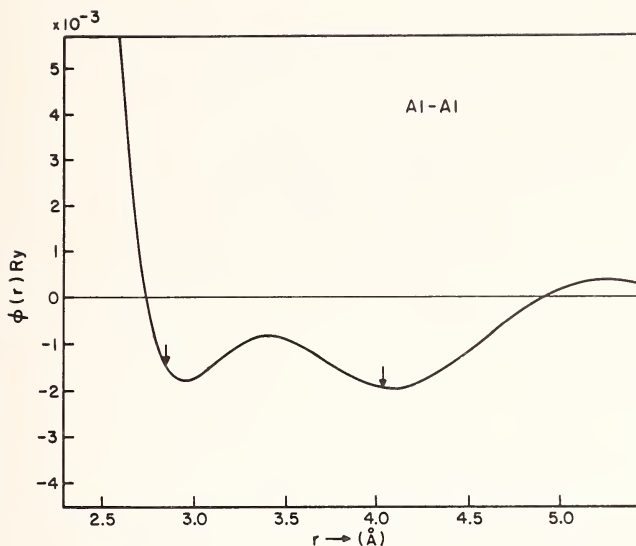


FIGURE 2. Pair interactions between two aluminum ions. Again energy is measured in Rydbergs and separation in Å. The arrows indicate first and second nearest neighbor positions.

We may observe that (25) does not simply lead to the total energy of the metal by summing over pair potentials. Summing over (25) in the presence of the neutralizing background in fact leads to the band structure term, and the Madelung energy term, but does not account for the electron gas terms. Thus the pair potentials may in fact be regarded as set relative to an overall potential term fixed by structure independent contributions. Within this limitation and within the limitations of linear response theory which we have been using, the total energy of the metal must be constructed from the sum of pair potentials. Since the energy depends on *volume* as well as ion-ion separation the conditions under which the Cauchy relations are satisfied are not met.

Pair potentials calculated using (25) are shown in figures 1 and 2 and are valid for the normal pressure densities of the metals. The screened pseudopotentials used in their calculation have been deduced from Fermi surface data and are shown in figures 3 and 4. As found by other authors [14] these are all characterized by steeply rising repulsive parts and much weaker attractive regions. The position of the crossover (which we may take as a measure of the effective ionic size) depends somewhat on the pseudopotential and on the degree of its nonlocality. For very large separa-

tions, the asymptotic form of the potentials exhibit oscillatory behavior (Friedel oscillations) arising from the existence of a logarithmic singularity in the dielectric function [15].

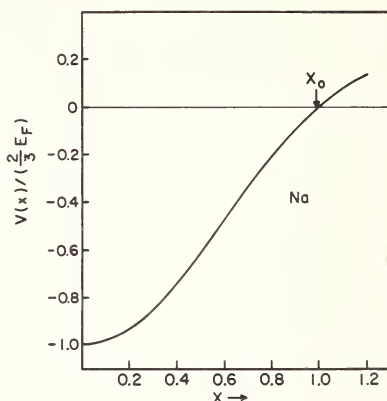


FIGURE 3. Fourier transform of the effective screened electron-ion interaction in metallic Na. Wave vectors are measured in units of $2k_F$ ($x = k/2k_F$) and energies in units of $(2/3) E_F$.

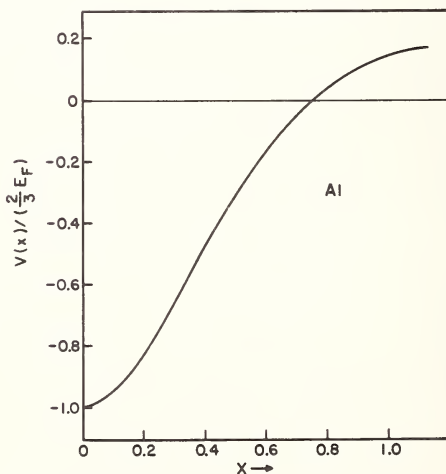


FIGURE 4. Fourier transform of the effective screened electron-ion interaction in Al. Again wave vectors are measured in units of $2k_F$ ($x = k/2k_F$) and energies in units of $(2/3) E_F$.

IV. Transition Metals

Compared with the simple metals we have been discussing the band structures of the transition metals are considerably more complex [16]. Certain features, however, do appear to be common in a great many cases. Recent first principles band structure calculations in a number of metals indicate that on the whole the basic results can be summarized in terms of a nearly free-electronlike structure with an overlap of d -states, the latter forming a system of comparatively narrow bands. This is indicated schematically in figure 5. To calculate the ground state energy of the metal we need, of course, to sum the single particle energies of the electrons in the bands and to finally incorporate the potential energy terms. This is an extremely difficult procedure and we are forced to resort to a somewhat more simplistic approach.

Early estimates of the form of the d -bands relied heavily on the Bloch tight binding method [17] (ignoring the possible mixing with s -derived electrons). The resulting bands, often 2–3 V wide suggest that the perturbations to the atomic states are substantial. Nevertheless the method has produced qualitative success in its description of various properties and lately has been combined with the pseudopotential method [18] in an attempt to incorporate the s -derived parts of the band structure.

Proceeding within the framework of the tight binding approach we may extend the methods outlined in sections II and III to include an estimate of the contribution of d -electron states to both cohesion and ion pair potentials. For neutral atoms in close proximity we normally expect two basic terms to appear in the mutual interaction viz, the repulsive

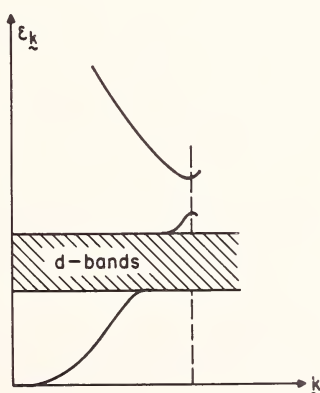


FIGURE 5. Schematic representations of s -derived and d -derived electron bands in transition metals.

core-core exchange interaction and the attractive fluctuating dipole interaction.¹⁴ The same basic terms may be expected to occur in the interactions between reasonably compact *d*-states situated on the ions of transition metals. (These were first quantitatively discussed in the problem of cohesion by Fuchs [9] in connection with copper.) But since we now have in addition the possibility of the presence of *s*-derived electrons, certain physical differences are bound to occur. As outlined in I the polarization field set up by fluctuations in the *d*-electron system are screened, hence if the atomic states remain compact the van der Waals type of interaction common in covalent systems will be considerably weakened. In a similar way, calculating the Born-Mayer with screened exchange would appear to lead to a weakened repulsive interaction. But these expectations will be partly offset by the fact that in the condensed metallic state the *d* states are more extended than they are in isolated ions. Again, an *a priori* calculation of the form of the modified potential is difficult. But since we are not concerned here with large changes in volume (and hence in ion-ion separation) we can express the Born-Mayer and screened van der Waals potential over a limited range in terms of the (*m*, *n*) form:

$$\begin{aligned}\phi_{dd} &= C \left[\left(\frac{\sigma}{r} \right)^m - \left(\frac{\sigma}{r} \right)^n \right] \\ &= \phi_{\min} \left[\left(\frac{\sigma}{r} \right)^m - \left(\frac{\sigma}{r} \right)^n \right] \left[\left(\frac{m}{n} \right)^{\frac{n}{n-m}} - \left(\frac{m}{n} \right)^{\frac{m}{n-m}} \right]^{-1}\end{aligned}\quad (26)$$

where ϕ_{\min} is the minimum value of the potential function and $r=\sigma$ is where ϕ_{dd} vanishes. Here the r^{-m} and r^{-n} terms may be interpreted as the leading powers originating in an expansion of the core-core and fluctuating dipole contributions to the pair energy. Because of the screening action we expect *m* and *n* to differ from the familiar empirical values of 12 and 6. We put

$$R = \rho r_o$$

where *R* is the nearest neighbor distance (in f.c.c. $\alpha^3 = \frac{4\sqrt{2}\pi}{3}$, in b.c.c.

¹⁴ Suggested to contribute a large term to the cohesive energy (Ref. [19]).

$\alpha^3 = 3\pi$). Then the energy per particle resulting from ϕ_{dd} is

$$\begin{aligned} U_{dd} &= \frac{C}{2} \left[\left(\frac{\sigma}{R} \right)^m \sum_i \frac{1}{y_i^{-m}} - \left(\frac{\sigma}{R} \right)^n \sum_j \frac{1}{y_j^n} \right] \\ &= \frac{C}{2} \left[\left(\frac{\sigma}{R} \right)^m A_m - \left(\frac{\sigma}{R} \right)^n A_n \right] \end{aligned} \quad (27)$$

where y_i is defined in terms of the interionic spacing r_i by

$$y_i = r_i/R.$$

TABLE 2. Values of the lattice sums $A_m = \sum_i y_i^{-m}$ taken from reference [20].

(m, n)	BCC	FCC
	A_m	A_m
4	22.64	25.34
5	14.76	16.97
6	12.25	14.45
7	11.05	13.36
8	10.36	12.80
9	9.89	12.49
10	9.56	12.31
11	9.31	12.20
12	9.11	12.13
13	8.95	12.09
14	8.82	12.06
15	8.70	12.04

The lattice sums n have been tabulated for cubic metals by Jones and Ingham [20] and some of their values for various n are reproduced in table 2. Writing (27) as

$$U_{dd} = \left(\frac{C}{2} \right) \left[\beta^{-m} \left(\frac{\sigma}{r_o} \right)^m A_m - \beta^{-n} \left(\frac{\sigma}{r_o} \right)^n A_n \right]$$

(with $\beta r_o = R$) we find that the total energy per ion is (with C expressed in Rydbergs)

$$U = Z^{5/3} \frac{(2.21)}{r_o^2} - \frac{1.792Z^2}{r_o} - \frac{0.916}{r_o} Z^{4/3} - (0.115 - 0.031 \ln r_o/Z^{1/3}) Z \\ + \frac{\alpha}{r_o^3} - U_{BS} - \frac{C}{2} \left[\beta^{-m} \left(\frac{\sigma}{r_o} \right)^m A_m - \beta^{-n} \left(\frac{\sigma}{r_o} \right)^n A_n \right] \text{Ry/ion.} \quad (28)$$

As with the band structure term U_{BS} in the simple metals, the contribution U_{dd} has a very pronounced effect on the values of the derivatives of U and is thus quite important in determining the equilibrium separation and the elastic constants.¹⁵ Note that in computing the zeroth Fourier component of the energy we must include the influence of the d -states on the effective potential seen by the s -electrons. This term can also be eliminated by using the zero pressure condition.

Some idea of the relative importance of the d -electrons may be obtained by ignoring U_{BS} and the correlation terms. In this approximation the equilibrium energy density is

$$U = \frac{Z^{5/3} 2.21}{3r_o^2} - \frac{1.792Z^2 + 0.916Z^{4/3}}{1.5r_o} - \frac{C}{2} \left[\left(\frac{m}{3} - 1 \right) \left(\frac{A_m}{\beta^m} \right) \left(\frac{\sigma}{r_o} \right)^m \right. \\ \left. - \left(\frac{n}{3} - 1 \right) \frac{A_n}{\beta^n} \left(\frac{\sigma}{r_o} \right)^n \right]$$

where the strength parameter C is typically $\lesssim 0.1$ Ry. From

$$\frac{1}{K} = n_i \frac{\partial}{\partial n_i} \left[n_i^2 \frac{\partial U}{\partial n_i} \right]$$

or its equivalent at equilibrium

$$\frac{1}{K_o} = \frac{1}{12\pi r_o a_o^3} \frac{d^2 U}{dr_o^2} \Big|_{\text{eq}}$$

¹⁵ But its absolute contribution to the cohesive energy at observed densities may still be small. In the noble metals whose d -band widths are ~ 3 eV, there is some evidence that U_{dd} has only a minor effect on the overall cohesive energy, Ref. [21].

we may extract the compressibility K_o i.e.,

$$\frac{1}{K_o} = \frac{1}{12\pi r_o^3 a_o^3} \cdot \left[\frac{-Z^{5/3} 2.21}{0.5 r_o^2} + \frac{1.792 Z^2 + 0.916 Z^{4/3}}{0.5 r_o} \right. \\ \left. + \frac{C}{2} \left\{ m(m-3) \left(\frac{A_m}{\beta^m} \right) \left(\frac{\sigma}{r_o} \right)^m - n(n-3) \left(\frac{A_n}{\beta^n} \right) \left(\frac{\sigma}{r_o} \right)^n \right\} \right]$$

For fairly large values of m and n the constants A_m and A_n approach the coordination numbers appropriate to the given lattice [see table 2]. It is therefore apparent that even with C as low as $\lesssim 0.1$ Ry the core-core exchange term may represent a sizable contribution to K provided, of course, that $\sigma \sim r_o$. In the case of the simple metals we have seen that the ionic separation is much larger (typically more than a factor of two) than the ionic diameter. It follows that $(\sigma/r_o)^m \ll 1$ and this more than compensates the factor $m(m-3)A_m$. But for the transition metals the ions are “touching” in the sense that typical values of the ionic diameter are very close to the interionic spacing. Although we cannot hope to include the details of band structure (including the important $s-d$ hybridization) in a model of this simplicity, it does demonstrate, however, the fact that to put the analysis on a firmer footing a more thorough treatment of the d -states (including a discussion of their self-consistent band structure) is required.

As to the form of the pair potential, to eq (25) we must now add the core-core exchange term.¹⁶ Thus in the approximation of tight binding the ion-ion interaction in transition metals may be approximated by

$$\phi = \frac{V}{8\pi^3} \int d\mathbf{k} e^{i\mathbf{k} \cdot \mathbf{r}} \frac{8\pi z^2 e^2}{k^2} \left[1 + \left(\frac{v(k)}{v^c(k)} \right)^2 \left(\frac{1}{\epsilon_k} - 1 \right) \right] + C \left[\left(\frac{\sigma}{r} \right)^m - \left(\frac{\sigma}{r} \right)^n \right].$$

The determination of the effective pseudopotential $v(k)$ presents a problem: in some cases [14] it can be estimated from transport properties of the metal if the d bands are totally contained below the Fermi energy and the states there are principally s -like. In others it may be obtained from combined tight-binding plane-wave interpolations to the band structure [18]. The coefficients of the core-core contribution may be obtained, in principle from calculations of the energy arising from the effective exchange changes [22] associated with the tight binding states. This has been carried through for the noble metals by Hafemeister [23].

¹⁶This again assumes that pair forces dominate the contributions to the total energy of a collection of atoms.

V. Acknowledgement

Supported in part by the Advanced Research Projects Agency through the Materials Science Center at Cornell, MSC Report #1147.

VII. References

- [1] For a summary of the various methods available see Methods in Computational Physics **8**, Energy Bands of Solids (Academic Press, 1968).
- [2] Slater, J. C., Phys. Rev. **81**, 385 (1951).
- [3] Gaspar, R. Acta Phys. Hung. **3**, 263 (1954); Tong, B. Y. and Sham, L. J., Phys. Rev. **144**, 1 (1966).
- [4] Harrison, W., Phys. Rev. **181**, 1036 (1969); Moriarty, J., Phys. Rev. (1970) (to appear); Fong, C. Y., and Cohen, M. L., Phys. Rev. Letters **24**, 306 (1970).
- [5] Frenkel, J., Z. Physik **49**, 31 (1928).
- [6] Wigner, E. P., and Seitz, F., Phys. Rev. **43**, 804 (1933).
- [7] Brooks, H., Trans. AIME **227**, 546 (1963).
- [8] Pines, D., and Nozieres, P., The Theory of Quantum Liquids **I** (W.A. Benjamin, New York, 1966).
- [9] Fuchs, K., Proc. Roy. Soc. **A151**, 585 (1935). The result for HCP Structures is due to W. Kohn and D. Scheeter and is quoted in W. J. Carr, Jr., Phys. Rev. **122**, 1437 (1961).
- [10] Ashcroft, N. W., and Langreth, D., Phys. Rev. **155**, 682 (1967).
- [11] Kleinman, L., Phys. Rev. **146**, 472 (1966).
- [12] Hayes, T. M., and Young, W. H., Phil. Mag. **18**, 965 (1968).
- [13] Harrison, W., Pseudopotentials in the Theory of Metals (W. A. Benjamin, New York, 1966).
- [14] Ashcroft, N. W. and Langreth, D. C., Phys. Rev. **159**, 500 (1967).
- [15] Langer, J. S. and Vosko, S. H., J. Phys. Chem. Solids **12**, 196 (1959).
- [16] Mott, N. F., Adv. Phys. (Phil. Mag. Suppl.) **13**, 325 (1964).
- [17] Fletcher, G. C., Proc. Phys. Soc. **A65**, 192 (1952); Asdente, M. and Friedel, J., Phys. Rev. **124**, 384 (1961); **126**, 2762 (1962).
- [18] Mueller, F. M., Phys. Rev. **153**, 659 (1967); Hodges, L., Ehrenreich, H., and Lang, N. N. D., Phys. Rev. **152**, 5051 (1966).
- [19] Friedel, J., Proc. Phys. Soc. **B65**, 769 (1952); and by Mott, N. F., and Stevens, K. W. H., Phil. Mag. **2**, 1364 (1957).
- [20] Jones, J. E., and Ingham, A. E., Proc. Roy. Soc. **107**, 636 (1925).
- [21] Cubanov, A. I., and Nikulin, V. K., Phys. stat. sol. **17**, 815 (1966); Brown, J. S., Phys. stat. sol. **31**, 297 (1969).
- [22] Dick, B. G., and Overhauser, A. W., Phys. Rev. **112**, 90 (1958).
- [23] Hafemeister, D. W., J. Phys. Chem. Solids **30**, 117 (1969).

Discussion on Paper by N. W. Ashcroft.

CHANG: Some interesting results were encountered in our search for the simple pairwise ion-ion potential for the transition metals employing the Born-Mayer potential plus the attractive potential, subject to the conditions that: First, the calculated cohesive energy must equal the experimental value. Second, the lattice energy is a minimum at the equilibrium separation corresponding to the experimental lattice parameters. We have found that the attractive term is of the Van der Waals type of power six, invariably, for all the transition metals—whether it is b.c.c., f.c.c. or h.c.p.—whose *d*-shells are more than half filled. From this we feel that there may be a simplification in getting a pairwise ion-ion potential for the transition metals.

ASHCROFT: What I was trying to point out is this: If one ignores for the moment the *s-d* hybridization, which is a difficult problem as you already know, putting in the *s*-electrons in a manner which has been successful up to now, at least gives you a method for getting some of the powers, let us say, of the attractive part of the potential.

GEHLEN: How sensitive are the potentials that you get to the choice of the bare potential? The potentials that one obtains using neutron diffraction patterns from liquids are often quite different from pseudopotentials. They do not necessarily have a pronounced minimum in the vicinity of the equilibrium lattice parameter. In some cases that minimum is on the positive side of the energy axis. Frequently, they do not have Friedel oscillations. Is it possible to bring pseudopotentials and “liquid” potentials in agreement by varying the bare potential? Do you see what I mean?

ASHCROFT: I see precisely what you mean. I think by liquid theories you mean the measurements of the structure factor which are done in *k*-space, up to a few wiggles, and then subsequently Fourier transformed into real space. Then the potentials are extracted from, let us say, the “Percus-Yevick,” or “Born-Green” theories of the liquid state.

GEHLEN: Yes, let me point out that Dr. J. E. Enderby and I¹ have solved the Born-Green equation in reciprocal space. That eliminates most of the tedious corrections that have to be brought to the data when one works in real space.

ASHCROFT: Providing, of course, that you believe in the superposition approximation at high density. I think the answer here is that if one takes

¹ Enderby, J. E., and Gehlen, P. C., *J. Chem. Phys.*, **51**, 547 (1969).

Fundamental Aspects of Dislocation Theory, J. A. Simmons, R. de Wit, and R. Bullough, Eds. (Nat. Bur. Stand. (U.S.), Spec. Publ. 317, I, 1970).

potentials like these and works the other way, that is, if I take a calculated pair potential—and we have done this—then feed that into the three equations for the radial distribution function, and then make adjustments on the potential, the differences in $s(k)$, (the static structure factor), are extremely difficult to see. Therefore, I think the question really is: With what sort of confidence can you extract those potentials working the other way when the data you are dealing with has got experimental error in it in the first place?

GEHLEN: Let me ask the question like this: Assuming that from the liquid data you get a potential with a minimum on the positive side of the energy axis, could you use the pseudopotential theory in reverse and obtain a bare potential that is realistic?

ASHCROFT: I guess again it depends what you want to do with them, but I don't think I would expect unrealistic ones. As you probably know, the screening is different in the band structure case from what it is in the ion-ion response case, but I don't think the differences will be large.

BULLOUGH: Actually, I think the structure factor data at low q is most unreliable.

ASHCROFT: I am delighted to hear you say it, but one can appreciate why. It is a very difficult experimental region to work in.

GEHLEN: It is correct that the structure factor data is least well known at low q . However, for liquid lead, at least, it is not possible to generate a potential that looks like a pseudopotential even if you assume extremely large errors in the data.

SAADA: I would like to ask two questions. The first is about your potential $V(k)$. In the simple metals you can calculate it from different approximations, but in complicated metals like copper or the transition metals you don't calculate it. You take it from experimental measurements.

ASHCROFT: In fact, in most cases we take it from experiment. But in the case of copper, for example, what you would interpret $w(q)$ is here the pseudopotential in the presence of this itinerant set of d -states.

SAADA: I don't understand how you can calculate it that way because then the difference in energy between d -states and s -states is not large enough because of mixing. I don't understand how you can de-mix them.

ASHCROFT: Are you familiar with the work of Mueller, Ehrenreich and company?²

SAADA: Not very much.

ASHCROFT: Perhaps this is best discussed privately, but let me tell you the way we did it. If you go to liquid copper, the d -bands are known to be

² c.f. Ref. [18] of previous paper.

completely contained beneath the Fermi surface and it's only through the symmetry at the particular point l in the face centered cubic structure that they cause significant d -like contributions to the wave function at the Fermi energy. If you remove the symmetry, on the average, by melting it, then the wave function becomes more s -like on the Fermi surface. So what we have done is to extract this potential here by just applying simple s -wave transport theory. Then we argue that part of it is in fact the potential for the s -electrons in the presence of the d -electrons.

BULLOUGH: What I am intrigued to know is whether the potential you got for aluminum gives a good agreement with the phonon dispersion data.

ASHCROFT: Well, the calculations we have done for the dispersion relation in aluminum, I think, can only be described as sort of quasi-good. There is a very difficult problem in the polyvalent metals because the electron-ion contribution to the dynamic matrix swamps the basic Coulomb lattice contribution and the thing you are left with is very sensitive to what you put in, for example, for the dielectric function. We have been using simple diagonal form in the calculations we did, for example, on the alkali metals, and I am just worried that if one did a better job of calculating the dielectric constant by putting in the band structure, this could swing the results quite a bit. The potential we have in aluminum seems to be reasonably good in other respects; I think it is a computational difficulty one has in doing the lattice spectrum, and I just really don't know the answer to your question.

LOCALIZED VIBRATION MODES ASSOCIATED WITH SCREW DISLOCATIONS

A. A. Maradudin

*Department of Physics
University of California
Irvine, California 92664*

The dispersion relation for the one-dimensional continuum of localized modes associated with a screw dislocation is obtained in the long wavelength limit, as a function of the wave vector parallel to the dislocation line. The result has the form $\omega^2(q) = s^2q^2 - \omega_0^2 \exp(-\text{const.}/q)$ where s is the speed of sound for transverse acoustic waves, and ω_0 is a typical Brillouin zone boundary frequency.

Key words: Dislocation-phonon interactions; dispersion relations; lattice dynamics; localized modes.

The problem with which I will be concerned in this paper is that of determining the frequencies of localized vibration modes associated with a screw dislocation in a solid, and the conditions necessary for the occurrence of such exceptional modes. Localized modes are modes whose frequencies lie outside the ranges allowed the normal modes of a perfect crystal, in which, because they lie in a stop band for the crystal, the atomic displacements decrease exponentially with increasing distance from the line of the defect. In the case of a (straight) dislocation a crystal retains its periodicity in the direction parallel to the dislocation line. A one-dimensional continuum of localized modes can appear, for which the displacement pattern in each such mode is wavelike parallel to the defect and decays exponentially in directions perpendicular to the line of the dislocation. Such modes are labeled by the component of the wave vector parallel to the defect. One of our problems will be to find the dispersion relation between the frequency of the localized mode and the wave vector component parallel to the dislocation line.

This problem has been studied previously by Lifshitz and Kosevich [1]. Oversimplified though their formulation of this problem is, and despite qualitative differences between their results and those to be reported here, this work reflects the essence of the problem, and has a heuristic value for all work which follows it, including this one.

Although the basic equations which underlie this work were originally derived on the basis of a lattice theory of the kind used previously to study the core structure of discrete screw dislocations [2], the integral equations which arise in the theory appear to be analytically solvable only in the long wavelength limit. Consequently, because elasticity theory is the long wavelength limit of lattice theory, and because it is probably much more familiar to those interested in dislocations than is lattice dynamics, I have formulated the problem I wish to discuss from the start in the language of continuum theory rather than in the language of lattice dynamics.

The starting point for our discussion are the equations of motion of an arbitrary nonlinear elastic continuum [3]

$$\rho \frac{\partial^2 \mathbf{u}}{\partial t^2} = \operatorname{div}_x \left(\frac{\rho}{\rho_0} \mathbf{J} \frac{\partial \Phi}{\partial \eta} \tilde{\mathbf{J}} \right). \quad (1)$$

In these equations $u_r(a_1, a_2, a_3; t)$ is the r -Cartesian component of the displacement field expressed as a function of the coordinates (a_1, a_2, a_3) of a point in the undeformed medium;

$$x_r = a_r + u_r(\mathbf{a}) \quad (2)$$

is the position of the point \mathbf{a} in the deformed body; the elements of the matrix \mathbf{J} are given by

$$J_{rs} = \delta_{rs} + \frac{\partial u_r}{\partial a_s}; \quad (3)$$

the elements of the Lagrangian strain tensor are defined by

$$\eta_{rs} = \frac{1}{2} \left\{ \frac{\partial u_r}{\partial a_s} + \frac{\partial u_s}{\partial a_r} + \sum_t \frac{\partial u_t}{\partial a_r} \frac{\partial u_t}{\partial a_s} \right\}; \quad (4)$$

the mass density in the deformed medium ρ is related to the mass density in the undeformed medium ρ_0 by

$$\rho = |\mathbf{I} + 2\boldsymbol{\eta}|^{-1/2} \rho_0; \quad (5)$$

and finally, the strain energy Φ can be expanded in powers of the strain

parameters according to

$$\Phi = \frac{1}{2} \sum_{ijkl} C_{ijkl} \eta_{ij} \eta_{kl} + \frac{1}{6} \sum_{ijklmn} C_{ijklmn} \eta_{ij} \eta_{kl} \eta_{mn} + \dots \quad (6)$$

where the $\{C_{ijkl}\}$, $\{C_{ijklmn}\}$, . . . are the second, third, . . . , order elastic constants, respectively.

The substitution of eqs (2)–(6) into eq (1), together with some algebraic manipulations, yields the following nonlinear wave equations for the determination of the displacement field,

$$\rho_o \frac{\partial^2 u_r}{\partial t^2} = \sum_{skl} C_{rskl} \frac{\partial^2 u_k}{\partial a_s \partial a_l} + \sum_{sklmn} D_{rsklmn} \frac{\partial^2 u_k}{\partial a_s \partial a_l} \frac{\partial u_m}{\partial a_n}, \quad (7)$$

where only the leading nonlinear terms on the righthand side of this equation have been retained. The coefficients D_{rsklmn} are given by

$$D_{rsklmn} = C_{rsklmn} + C_{rsln} \delta_{km} + C_{lsmn} \delta_{rk} + C_{nskl} \delta_{rm} + C_{rlmn} \delta_{sk} - C_{rsmn} \delta_{kl}. \quad (8)$$

Although the $\{D_{rsklmn}\}$ do not have the symmetry properties of the third order elastic constants under the interchange of indices or pairs of indices, from the transformation properties of the elastic constants under the operations of the point group of the crystal, it follows that the $\{D_{rsklmn}\}$ transform as the components of a sixth rank tensor,

$$D_{rsklmn} = \sum_{\rho\sigma\kappa\lambda\mu\nu} S_{\rho} S_{s\sigma} S_{k\kappa} S_{l\lambda} S_{m\mu} S_{n\nu} D_{\rho\sigma\kappa\lambda\mu\nu}, \quad (9)$$

where S is a 3×3 real, orthogonal matrix representative of the operations of the crystal point group. In particular, if the crystal point group is one of the cubic point groups, it follows that the only nonvanishing elements of D_{rsklmn} are those for which each subscript, 1, 2, or 3, appears an even number of times.

We now express $\mathbf{u}(\mathbf{a}; t)$ as the sum of a static displacement field $\mathbf{v}(\mathbf{a})$, describing the screw dislocation, and a dynamic displacement field $\xi(\mathbf{a}; t)$, describing the vibrations of the elastic medium about the dislocated configuration,

$$\mathbf{u}(\mathbf{a}; t) = \mathbf{v}(\mathbf{a}) + \xi(\mathbf{a}; t). \quad (10)$$

In substituting eq (10) into eqs (7), we linearize the latter by retaining only terms of first order in $\xi(\mathbf{a}; t)$ on the righthand side,

$$\rho_0 \frac{\partial^2 \xi_r}{\partial t^2} = \sum_{skl} C_{rskl} \frac{\partial^2 v_k}{\partial a_s \partial a_l} + \sum_{sklmn} D_{rsklmn} \frac{\partial^2 v_k}{\partial a_s \partial a_l} \frac{\partial v_m}{\partial a_n} \\ + \sum_{skl} C_{rskl} \frac{\partial^2 \xi_k}{\partial a_s \partial a_l} + \sum_{sklmn} D_{rsklmn} \left(\frac{\partial^2 v_k}{\partial a_s \partial a_l} \frac{\partial \xi_m}{\partial a_n} + \frac{\partial v_m}{\partial a_n} \frac{\partial^2 \xi_k}{\partial a_s \partial a_l} \right). \quad (11)$$

The equilibrium condition for the dislocated medium is obtained by equating to zero the time independent terms on the righthand side of this equation

$$0 = \sum_{skl} C_{rskl} \frac{\partial^2 v_k}{\partial a_s \partial a_l} + \sum_{sklmn} D_{rsklmn} \frac{\partial^2 v_k}{\partial a_s \partial a_l} \frac{\partial v_m}{\partial a_n} + \dots \quad (12)$$

The equations of motion of the dislocated crystal are therefore found to be

$$\rho_0 \frac{\partial^2 \xi_r}{\partial t^2} = \sum_{skl} C_{rskl} \frac{\partial^2 \xi_k}{\partial a_s \partial a_l} + \sum_{mn} T_{rmn}(\mathbf{a}) \frac{\partial \xi_m}{\partial a_n} + \sum_{skl} T_{rskl}(\mathbf{a}) \frac{\partial^2 \xi_k}{\partial a_s \partial a_l} \quad (13)$$

where

$$T_{rmn}(\mathbf{a}) = \sum_{skl} D_{rsklmn} \frac{\partial^2 v_k}{\partial a_s \partial a_l} \quad (14a)$$

$$T_{rskl}(\mathbf{a}) = \sum_{mn} D_{rsklmn} \frac{\partial v_m}{\partial a_n}. \quad (14b)$$

For a screw dislocation with its Burgers vector directed along the a_3 -axis, the displacement field $\mathbf{v}(\mathbf{a})$ has only an a_3 component, which is a function only of a_1 and a_2 ,

$$\mathbf{v}(\mathbf{a}) = (0, 0, v_3(a_1, a_2)). \quad (15)$$

The equation determining $v_3(a_1, a_2)$ in a medium of cubic symmetry, with the coordinate axes along the cube axes, or in an isotropic medium, in the linear approximation is

$$C_{44} \left(\frac{\partial^2 v_3}{\partial a_1^2} + \frac{\partial^2 v_3}{\partial a_2^2} \right) = 0, \quad (16)$$

which possesses the solution

$$v_3(a_1, a_2) = \frac{b}{2\pi} \tan^{-1} \frac{a_2}{a_1}, \quad (17)$$

where b is the magnitude of the Burgers vector. It follows, therefore, that

for this case

$$\begin{aligned} T_{rmn}(a_1, a_2) = & [D_{r131mn} - D_{r232mn}] \frac{b}{2\pi} \frac{2a_1 a_2}{(a_1^2 + a_2^2)^2} \\ & + [D_{r231mn} + D_{r132mn}] \frac{b}{2\pi} \frac{a_2^2 - a_1^2}{(a_1^2 + a_2^2)^2} \end{aligned} \quad (18a)$$

$$T_{rskl}(a_1, a_2) = D_{rskl32} \frac{b}{2\pi} \frac{a_1}{(a_1^2 + a_2^2)} - D_{rskl31} \frac{b}{2\pi} \frac{a_2}{(a_1^2 + a_2^2)}. \quad (18b)$$

Because $T_{rmn}(\mathbf{a})$ and $T_{rskl}(\mathbf{a})$ are independent of a_3 , it follows that the solutions of eqs (13) can be chosen to have the form

$$\xi(\mathbf{a}; t) = \xi_0(a_1, a_2) e^{iq a_3} e^{-i\omega t}. \quad (19)$$

In what follows we will expand the amplitude vector $\xi_0(a_1, a_2)$ in a double Fourier series

$$\xi_0(a_1, a_2) = \sum_{k_1 k_2} \hat{\xi}(k_1, k_2) e^{i(k_1 a_1 + k_2 a_2)}, \quad (20)$$

where ($i=1, 2$)

$$k_i = \frac{2\pi n_i}{L} \quad n_i = 0, \pm 1, \pm 2, \pm 3, \dots, \quad (21)$$

and $L^3 = V$ is the normalization volume for the medium.

When the solution given by eqs (19) and (20) is substituted into eqs (13), and use is made of the orthogonality of the complex exponentials, the equation for $\xi_r(k_1, k_2)$ takes the form

$$\sum_s C_{rs}(k_1 k_2; q; \omega^2) \hat{\xi}_s(k_1 k_2) = i \sum_s \sum_{k'_1 k'_2} T_{rs}(k_1 k_2; k'_1 k'_2; q) \hat{\xi}_s(k'_1 k'_2). \quad (22)$$

The matrix $\mathbf{C}(\mathbf{k}_{||}; q; \omega^2)$ ($\mathbf{k}_{||} = (k_1, k_2)$) has the following form for an isotropic elastic continuum

$$\mathbf{C}(\mathbf{k}_{||}; q; \omega^2) = \begin{pmatrix} (\lambda + 2\mu)k_1^2 + \mu k_2^2 & (\lambda + \mu)k_1 k_2 & (\lambda + \mu)k_1 q \\ & + \mu q^2 - \rho_0 \omega^2 & \\ (\lambda + \mu)k_1 k_2 & (\lambda + 2\mu)k_2^2 + \mu k_1^2 & (\lambda + \mu)k_2 q \\ & + \mu q^2 - \rho_0 \omega^2 & \\ (\lambda + \mu)k_1 q & (\lambda + \mu)k_2 q & (\lambda + 2\mu)q^2 + \mu(k_1^2 + k_2^2) \\ & & - \rho_0 \omega^2 \end{pmatrix} \quad (23)$$

where λ and μ are the Lamé constants for the medium. The elements of the matrix $T(\mathbf{k}_{||}; \mathbf{k}'_{||}; q)$, which are singular at the point $\mathbf{k}_{||} = \mathbf{k}'_{||}$, will not be presented here in full; only the elements actually required will be introduced at the appropriate point in the calculation.

The inverse of the matrix $\mathbf{C}(\mathbf{k}_{||}; q; \omega^2)$ has a very simple form,

$$C_{rs}^{-1}(\mathbf{k}_{||}; q; \omega^2) = \frac{1}{\rho_0} \left\{ \frac{e_r e_s}{c_l^2(k_1^2 + k_2^2 + q^2) - \omega^2} + \frac{\delta_{rs} - e_r e_s}{c_l^2(k_1^2 + k_2^2 + q^2) - \omega^2} \right\} \quad (24)$$

where

$$c_l^2 = (\lambda + 2\mu)/\rho_0 \quad c_t^2 = \mu/\rho_0, \quad (25a)$$

and

$$\mathbf{e} = \frac{(k_1, k_2, q)}{(k_1^2 + k_2^2 + q^2)^{1/2}}. \quad (25b)$$

The integral equation (22) can be rewritten as

$$\hat{\xi}_r(\mathbf{k}_{||}) = i \sum_{st} \sum_{\mathbf{k}'_{||}} C_{rs}^{-1}(\mathbf{k}_{||}; q; \omega^2) T_{st}(\mathbf{k}_{||}; \mathbf{k}'_{||}; q) \hat{\xi}_t(\mathbf{k}'_{||}). \quad (26)$$

Since the kernel of this homogeneous integral equation is pure imaginary and singular, it is convenient to transform this equation into one with a real, nonsingular kernel. If we separate $\hat{\xi}(\mathbf{k}_{||})$ into its real and imaginary parts,

$$\hat{\xi}(\mathbf{k}_{||}) = \hat{\xi}^{(1)}(\mathbf{k}_{||}) + i\hat{\xi}^{(2)}(\mathbf{k}_{||}), \quad (27)$$

and substitute eq (27) into eq (26) we obtain the pair of real equations

$$\hat{\xi}^{(1)}(\mathbf{k}_{||}) = - \sum_{st} \sum_{\mathbf{k}'_{||}} C_{rs}^{-1}(\mathbf{k}_{||}; q; \omega^2) T_{st}(\mathbf{k}_{||}; \mathbf{k}'_{||}; q) \hat{\xi}^{(2)}(\mathbf{k}'_{||}) \quad (28a)$$

$$\hat{\xi}^{(2)}(\mathbf{k}_{||}) = \sum_{st} \sum_{\mathbf{k}'_{||}} C_{rs}^{-1}(\mathbf{k}_{||}; q; \omega^2) T_{st}(\mathbf{k}_{||}; \mathbf{k}'_{||}; q) \hat{\xi}^{(1)}(\mathbf{k}'_{||}). \quad (28b)$$

Thus, knowing one of the functions $\hat{\xi}^{(1)}(\mathbf{k}_{||})$ or $\hat{\xi}^{(2)}(\mathbf{k}_{||})$, the other can be obtained by quadratures. Combining eqs (28a) and (28b) we find that $\hat{\xi}^{(1)}(\mathbf{k}_{||})$ is the solution of the equation

$$\hat{\xi}^{(1)}(\mathbf{k}_{||}) = - \sum_s C_{rs}^{-1}(\mathbf{k}_{||}; q; \omega^2) \sum_t \sum_{\mathbf{k}'_{||}} V_{st}(\mathbf{k}_{||}; \mathbf{k}'_{||}; q; \omega^2) \hat{\xi}^{(1)}(\mathbf{k}'_{||}) \quad (29)$$

where

$$V_{st}(\mathbf{k}_{||}; \mathbf{k}'_{||}; q; \omega^2) = \sum_{mn} \sum_{\mathbf{k}''_{||}} T_{sm}(\mathbf{k}_{||}; \mathbf{k}''_{||}; q) \times C_{mn}^{-1}(\mathbf{k}''_{||}; q; \omega^2) T_{nt}(\mathbf{k}''_{||}; \mathbf{k}'_{||}; q). \quad (30)$$

Equation (30) is in the canonical form for determining the displacement field in a perturbed crystal.

The solution of the set of coupled homogeneous integral equations (30) is in progress. Here, in order to simplify the analysis, we solve an approximate form of these equations which bears the same relation to the exact equations that the Rosenstock-Newell-Montroll-Potts (RNMP)⁴ model of a simple cubic lattice with nearest neighbor central and non-central force interactions bears to a more realistic model: we approximate the matrices $\mathbf{C}(\mathbf{k}_{||}; q; \omega^2)$ and $T(\mathbf{k}_{||}; \mathbf{k}'_{||}; q)$ by their diagonal elements only. By so doing we neglect the coupling between the a_1 -, a_2 -, and a_3 -components of the displacement field. It is known from the results of lattice dynamical calculations based on the RNMP model that this kind of approximation yields qualitatively correct results for many quantities of physical interest.

In the sense that after formulating it exactly only an approximate version of this problem will be solved exactly here, what follows represents work in progress. Nevertheless, the treatment described here provides valuable guidelines to the solution of the exact problem, which will be summarized later, and is free from the inessential complications which attend the solution of a matrix integral equation.

With this approximation, the equation determining $\hat{\xi}^{(1)}(\mathbf{k}_{||})$ becomes

$$\hat{\xi}^{(1)}(\mathbf{k}_{||}) = -\frac{1}{\rho_0} \frac{1}{c_\ell^2 k^2 + c_t^2 k_2^2 + \Omega^2} \sum_{\mathbf{k}'_{||}} V_{11}(\mathbf{k}_{||}; \mathbf{k}'_{||}; q; \omega^2) \hat{\xi}^{(1)}(\mathbf{k}'_{||}), \quad (31)$$

where we have put $\Omega^2 = c_t^2 q^2 - \omega^2 > 0$, and where

$$V_{11}(\mathbf{k}_{||}; \mathbf{k}'_{||}; q; \omega^2) = \frac{1}{\rho_0} \frac{(bq)^2}{L^4} \sum_{\mathbf{k}''_{||}} \frac{U(\mathbf{k}_{||}; \mathbf{k}''_{||}) U(\mathbf{k}''_{||}; \mathbf{k}'_{||})}{c_\ell^2 k_1'^2 + c_t^2 k_2'^2 + \Omega^2} \\ \equiv \frac{1}{\rho_0} \frac{(bq)^2}{L^2} K(\mathbf{k}_{||}; \mathbf{k}'_{||}; \Omega), \quad (32)$$

where

$$U(\mathbf{k}_{||}; \mathbf{k}'_{||}) = \frac{Ak'_1(k_2 - k'_2) + B(k_1 - k'_1)(k_2 - k'_2) - C(k_1 - k'_1)k'_2}{(k_1 - k'_1)^2 + (k_2 - k'_2)^2}, \quad (33)$$

with

$$\begin{aligned} A &= D_{111331} + D_{131131} = 2C_{166} + C_{44} \\ B &= D_{113113} - D_{123213} = C_{166} - C_{456} \\ C &= D_{121332} + D_{131232} = 2C_{456} + 2C_{44}. \end{aligned} \quad (34)$$

Equation (31) therefore takes the form

$$\hat{\xi}_1^{(1)}(\mathbf{k}_{||}) = -\left(\frac{b}{\rho_0 L}\right)^2 \frac{q^2}{c_\ell^2 k_1^2 + c_t^2 k_2^2 + \Omega^2} \sum_{\mathbf{k}'_{||}} K(\mathbf{k}_{||}; \mathbf{k}'_{||}; \Omega) \hat{\xi}_1^{(1)}(\mathbf{k}'_{||}). \quad (35)$$

With the approximations made, the equations for $\hat{\xi}_2^{(1)}(\mathbf{k}_{||})$ and $\hat{\xi}_3^{(1)}(\mathbf{k}_{||})$ have exactly the same structure and will not be discussed further here.

To obtain the dispersion relation connecting Ω with q from the integral equation (35), we use the fact that we are working in the long wavelength limit together with the fact that the numerator of the expression on the righthand side of eq (35) is already proportional to q^2 , to set k_1 and k_2 equal to zero in the function $K(\mathbf{k}_{||}; \mathbf{k}'_{||}; \Omega)$. The omitted terms are of higher than the second order in k_1 , k_2 , and q . The integral equation we must solve is therefore

$$\hat{\xi}_1^{(1)}(\mathbf{k}_{||}) = -\left(\frac{b}{\rho_0 L}\right)^2 \frac{q^2}{c_\ell^2 k_1^2 + c_t^2 k_2^2 + \Omega^2} \sum_{\mathbf{k}'_{||}} K(\mathbf{0}; \mathbf{k}'_{||}; \Omega) \hat{\xi}_1^{(1)}(\mathbf{k}'_{||}). \quad (36)$$

This equation is a homogeneous integral equation with a separable kernel. The condition that it have a nontrivial solution is that

$$1 = -\left(\frac{b}{\rho_0}\right)^2 q^2 \frac{1}{L^2} \sum_{\mathbf{k}_{||}} \frac{K(\mathbf{0}; \mathbf{k}_{||}; \Omega)}{c_\ell^2 k_1^2 + c_t^2 k_2^2 + \Omega^2}, \quad (37)$$

and this equation is the dispersion relation connecting Ω with q .

In solving this equation we will set $c_\ell = c_t = s$, a step which greatly simplifies the integrals over angles without changing any of the qualitative features of the result. In fact, this step leads to a denominator of the form obtained in the full matrix Green's function formulation of this problem. It is convenient to convert the sum over $\mathbf{k}_{||}$ into an integral, with the result that

$$1 = -\frac{1}{4\pi^2} \left(\frac{bq}{\rho_0}\right)^2 \int_{-K_0}^{K_0} dk_1 \int_{-K_0}^{K_0} dk_2 \frac{K(\mathbf{0}; \mathbf{k}_{||}; \Omega)}{s^2 k_{||}^2 + \Omega^2}. \quad (38)$$

We have cut off the integrals at values of the wave vector components of the order of the reciprocal of a lattice spacing, $K_0 \cong 1/a_0$. Such a cutoff arises naturally in a lattice theory, where the allowed values of the wave vector are restricted to lie inside the first Brillouin zone for the crystal, but it must be imposed explicitly, from without, in a continuum theory.

We now go over to polar coordinates, and obtain the equation

$$-\left(\frac{2\pi\rho_0}{bq}\right)^2 = \int_0^{K_0} dk \frac{k \langle K(0; k; \Omega) \rangle}{s^2 k^2 + \Omega^2}, \quad (39)$$

where

$$\langle K(\mathbf{0}; k; \Omega) \rangle = \int_0^{2\pi} d\theta K(\mathbf{0}; k \cos \theta, k \sin \theta; \Omega). \quad (40)$$

An explicit expression for $K(\mathbf{0}; \mathbf{k}_{||}; \Omega)$ is

$$\begin{aligned} K(\mathbf{0}; \mathbf{k}_{||}; \Omega) &= (-A + B + C) \frac{1}{L^2} \sum_{\mathbf{k}'_{||}} \frac{k'_1 k'_2}{k'^2 + k'^2} \frac{1}{c_\ell^2 k'^2 + c_\ell^2 k'^2 + \Omega^2} \\ &\times \frac{B k'_1 k'_2 - (B + C) k'_1 k'_2 + (A - B) k_1 k'_2 + (-A + B + C) k_1 k_2}{(k'_1 - k_1)^2 + (k'_2 - k_2)^2} \\ &= K(\mathbf{0}; -\mathbf{k}_{||}; \Omega). \end{aligned} \quad (41)$$

Rewriting this expression as an integral in polar coordinates we obtain

$$\begin{aligned} K(0; k; \Omega) &= \frac{(-A + B + C)}{4\pi^2} \int_0^{K_0} dk' \frac{k'}{s^2 k'^2 + \Omega^2} \\ &\times \int_0^{2\pi} \frac{d\theta}{k'^2 + k^2 - 2k'(k_1 \cos \theta + k_2 \sin \theta)} \\ &\times [B k'^2 \cos^2 \theta \sin^2 \theta + (A - B) k' k_1 \cos \theta \sin^2 \theta \\ &- (B + C) k' k_2 \cos^2 \theta \sin \theta + (-A + B + C) k_1 k_2 \cos \theta \sin \theta]. \end{aligned} \quad (42)$$

If we make the changes of variables

$$\theta - \alpha = \varphi \quad (43)$$

where

$$\cos \alpha = \frac{k_1}{k} \equiv \hat{k}_1 \quad \sin \alpha = \frac{k_2}{k} \equiv \hat{k}_2, \quad (44)$$

and $k' = kz$, we can re-express $K(\mathbf{0}; \mathbf{k}; \Omega)$ as

$$\begin{aligned} K(\mathbf{0}; \mathbf{k}; \Omega) = & \frac{(-A+B+C)}{4\pi^2 s^2} \int_0^{\xi(sK_0/\Omega)} dz \frac{z}{z^2 + \xi^2} \int_0^{2\pi} \frac{d\varphi}{1+z^2 - 2z \cos \varphi} \\ & \times \{Bz^2 [\hat{k}_1^2 \hat{k}_2^2 \cos^4 \varphi + (\hat{k}_1^4 - 4\hat{k}_1^2 \hat{k}_2^2 + \hat{k}_2^4) \cos^2 \varphi \sin^2 \varphi + \hat{k}_1^2 \hat{k}_2^2 \sin^4 \varphi] \\ & + (A-B)z [(\hat{k}_1^4 - 2\hat{k}_1^2 \hat{k}_2^2) \cos \varphi \sin^2 \varphi + \hat{k}_1^2 \hat{k}_2^2 \cos^3 \varphi] \\ & - (B+C)z [(\hat{k}_2^4 - 2\hat{k}_1^2 \hat{k}_2^2) \cos \varphi \sin^2 \varphi + \hat{k}_1^2 \hat{k}_2^2 \cos^3 \varphi] \\ & + (-A+B+C)\hat{k}_1^2 \hat{k}_2^2 (\cos^2 \varphi - \sin^2 \varphi)\} \end{aligned} \quad (45)$$

where $\xi = \Omega/sk$. To evaluate the integrals over φ we break up the range of z into two intervals $(0, 1)$ and $(1, \xi(sK_0/\Omega))$. When this is done, and the average of $K(\mathbf{0}; \mathbf{k}; \Omega)$ over the angle θ defined by $\hat{k}_1 = \cos \theta$, $\hat{k}_2 = \sin \theta$ is carried out according to eq (40), it is found that the former interval makes no contribution, and we obtain

$$\begin{aligned} \langle K(0; k; \Omega) \rangle = & \frac{(-A+B+C)}{8s^2} \int_1^{\xi(sK_0/\Omega)} dz \frac{z}{z^2 + \xi^2} \left\{ B + \frac{(A-B-C)}{z^2} \right\} \\ = & \frac{(-A+B+C)}{8s^2} \left\{ \frac{B}{2} \ln \frac{\left(1 + \frac{s^2 K_0}{\Omega^2}\right) \xi^2}{1 + \xi^2} \right. \\ & \left. - \frac{(A-B-C)}{2\xi^2} \ln \frac{\left(1 + \frac{\Omega^2}{s^2 K_0^2}\right)}{1 + \xi^2} \right\}. \end{aligned} \quad (46)$$

The dispersion relation (39) takes the following form when eq (46) is substituted into it,

$$\begin{aligned} -\left(\frac{2\pi\rho_0}{bq}\right)^2 = & \frac{(-A+B+C)}{8s^4} \int_{(\Omega/sK_0)}^{\infty} d\xi \frac{1}{\xi(1+\xi^2)} \\ & \times \left\{ \frac{B}{2} \ln \frac{\left(1 + \frac{s^2 K_0^2}{\Omega^2}\right) \xi^2}{1 + \xi^2} - \frac{(A-B-C)}{2\xi^2} \ln \frac{\left(1 + \frac{\Omega^2}{s^2 K_0^2}\right)}{1 + \xi^2} \right\}. \end{aligned} \quad (47)$$

It is convenient to break up the integration range into two intervals, $((\Omega/sK_0), 1)$ and $(1, \infty)$. Since the limits in the latter range are independent of Ω , the only dependence on Ω from this integration comes from the explicit dependence of the integrand on Ω . Denoting this integral by

I_2 , we have

$$\begin{aligned} I_2 = & \frac{B}{2} \ln \left(1 + \frac{s^2 K_0^2}{\Omega^2} \right) \int_1^\infty d\xi \frac{1}{\xi(1+\xi^2)} \\ & - \frac{(A-B-C)}{2} \ln \left(1 + \frac{\Omega^2}{s^2 K_0^2} \right) \int_1^\infty d\xi \frac{1}{\xi^3(1+\xi^2)} \\ & + \int_1^\infty d\xi \frac{1}{\xi(1+\xi^2)} \left\{ \frac{B}{2} \ln \frac{\xi^2}{1+\xi^2} - \frac{(A-B-C)}{2\xi^2} \ln \frac{1}{1+\xi^2} \right\}. \end{aligned} \quad (48)$$

The integrals over ξ all converge to give numerical coefficients, and we see that in the limit as $\Omega \rightarrow 0$, I_2 is dominated by

$$I_2 \sim \frac{B}{2} \ln \frac{s^2 K_0^2}{\Omega^2} \int_1^\infty \frac{d\xi}{\xi(1+\xi^2)} = - \left(\frac{B}{2} \ln 2 \right) \ln \frac{\Omega}{s K_0}. \quad (49)$$

The contribution from the range $((\Omega/s K_0), 1)$ will be denoted by I_1 , and is given by ($a = \Omega/s K_0$)

$$\begin{aligned} I_1 = & \frac{B}{2} \ln \frac{1+a^2}{a^2} \int_a^1 \frac{1}{\xi(1+\xi^2)} - \frac{(A-B-C)}{2} \ln (1+a^2) \\ & \int_a^1 \frac{d\xi}{\xi^3(1+\xi^2)} + \frac{B}{2} \int_a^1 d\xi \frac{1}{\xi(1+\xi^2)} \ln \frac{\xi^2}{1+\xi^2} \\ & + \frac{(A-B-C)}{2} \int_a^1 d\xi \frac{\ln (1+\xi^2)}{\xi^3(1+\xi^2)}. \end{aligned} \quad (50)$$

In the limit as $a \rightarrow 0$, I_1 is dominated by the contributions from the first and third integrals which yield the result that

$$\begin{aligned} I_1 = & - \frac{B}{2} \ln \frac{a^2}{1+a^2} (-\ln a) + \frac{B}{2} (-(\ln a)^2) + 0(\ln a) \\ = & + B(\ln a)^2 - \frac{B}{2} (\ln a)^2 + 0(\ln a) \\ = & \frac{B}{2} \left(\ln \frac{\Omega}{s K_0} \right)^2 + 0 \left(\ln \frac{\Omega}{s K_0} \right) \end{aligned} \quad (51)$$

Consequently, in the limit as $\Omega \rightarrow 0$, the dispersion relation becomes

$$-\left(\frac{2\pi\rho_0}{bq} \right)^2 = \frac{(-A+B+C)}{8s^4} \frac{B}{2} \ln \left(\frac{\Omega}{s K_0} \right)^2. \quad (52)$$

Thus, if $B(-A+B+C) < 0$, we obtain

$$\left(\frac{2\pi\rho_0}{bq}\right)^2 = \frac{B(A-B-C)}{16s^4} \left(\ln \frac{\Omega}{sK_0}\right)^2 \quad (53)$$

or

$$\Omega = sK_0 e^{-\frac{8\pi s^2 \rho_0}{[B(A-B-C)]^{1/2}} \frac{1}{bq}}, \quad (54)$$

which can be rewritten as

$$\omega^2 = s^2 q^2 - s^2 K_0^2 e^{-\frac{16\pi s^2 \rho_0}{[B(A-B-C)]^{1/2}} \frac{1}{bq}}. \quad (55)$$

The result obtained by Lifshitz and Kosevich differs from the above result in that the second term on the righthand side has the stronger dependence on q , $\exp(-\text{const.}/q^2)$. This is a consequence of the proportionality of the righthand side of their dispersion relation to the first power of $\ln(\Omega/sK_0)$ rather than on the second, as here. This in turn is due to the fact that their phenomenological approach to the problem does not predict that the kernel of the homogeneous integral equation for the Fourier coefficient of the displacement field is pure imaginary, which fact leads to a more complicated real integral equation to solve than considered by Lifshitz and Kosevich.

What clues does this simplified calculation give us which will help in the solution of the complete matrix integral equation? The more important is that only those terms which are logarithmically divergent as $\Omega \rightarrow 0$ need to be retained on the righthand side of eq (29). This means that in the expression for the Green's function matrix $C_{rs}^{-1}(\mathbf{k}_{||}, q; \omega^2)$ only the contribution from the transverse branches needs to be kept. It is only this part which gives rise to a logarithmic singularity as the frequency ω approaches $c_l q$, the bottom of the band of unperturbed acoustic modes from which the localized modes appear. It also means that in the kernel $V_{st}(\mathbf{k}_{||}; \mathbf{k}'_{||}; q; \omega^2)$ of the integral equation (29) for the real part of the Fourier coefficient of the displacement amplitude only the terms which are explicitly proportional to q^2 , i.e., are independent of k_1 and k_2 , need to be retained. The terms which are proportional to powers of k_1 and k_2 other than the zeroeth do not lead to divergences as $\Omega \rightarrow 0$. These two approximations have the consequence of uncoupling the equations for the a_1 , a_2 , and a_3 components of $\hat{\xi}^{(1)}(\mathbf{k}_{||})$. The dispersion relations associated with $\hat{\xi}_1^{(1)}(\mathbf{k}_{||})$ and $\hat{\xi}_2^{(1)}(\mathbf{k}_{||})$ are the same and differ from that associated with $\hat{\xi}_3^{(1)}(\mathbf{k}_{||})$. The discussion of the exact solution will be published elsewhere.

Acknowledgement

This work was supported by the Air Force Office of Scientific Research, Office of Aerospace Research, U.S.A.F., under AFOSR Grant No. 68-1448, technical report No. 69-11. The author would also like to thank Academician V. M. Tuchkevich for the hospitality extended him at the A. F. Ioffe Physico-Technical Institute, where this work was carried out, and would also like to thank the University of California, Irvine, and the U.S. National Science Foundation for travel grants.

References

- [1] Lifshitz, I. M., and Kosevich, A. M., Reports on Progress in Physics **29**, 217 (1966).
- [2] Maradudin, A. A., J. Phys. Chem. Solids **9**, 1 (1958).
- [3] See, for example, Murnaghan, F. D., Finite Deformation of an Elastic Solid (John Wiley & Sons, New York, 1951).

THE METHOD OF LATTICE STATICS

J. W. Flocken and J. R. Hardy

*Behlen Laboratory of Physics
University of Nebraska
Lincoln, Nebraska 68508*

The formalism of the method of lattice statics for treating the lattice distortions and the formation and interaction energies associated with a defect in a crystal is presented in detail. This approach is based on the Fourier transformation of the set of direct space equilibrium equations to reciprocal space. This results in a set of decoupled equations which can be explicitly solved for the Fourier amplitudes of the displacement field which can then be found by Fourier inversion. A similar approach is used to obtain Fourier transformed expressions for the relaxation and interaction energies associated with the defect.

The solution of the equations of lattice statics for the Fourier amplitudes in the limit of small wave vectors gives expressions for the displacement field identical to those obtained from the theory of continuum elasticity.

Results are presented of recent applications of the method of lattice statics to find the formation energies of Schottky pairs in certain alkali halides. Strain field displacements, relaxation energies and interaction energies associated with vacancies in Na and K are given.

Lattice statics in its asymptotic form has been used to find the displacement field far from cubic point defects and double force defects in a number of metals. Displacement profiles about vacancies in Na and K and about a double force defect in Cu are shown. A comparison of the exact lattice statics results to asymptotic results along a $\langle 111 \rangle$ direction in K shows that the elastic limit is only attained at about the 19th or 20th neighbor position from the defect.

Key words: Computer simulation; Kansaki method; lattice statics; point defects; Schottky pairs.

I. Introduction

In this paper we propose to give a review of the method of lattice statics for treating the distortions produced by lattice defects in a variety

Fundamental Aspects of Dislocation Theory, J. A. Simmons, R. de Wit, and R. Bullough, Eds. (Nat. Bur. Stand. (U.S.), Spec. Publ. 317, I, 1970).

of crystals. We shall review the work that has been carried out to date and present some typical results which the method has produced. At present, such calculations as have been carried out, have been confined largely to point imperfections, although the method can also be applied to dislocations.

The basic problem one is faced with when studying the behavior of crystal defects can ultimately be reduced in most cases to the need to compute the displacement field and, in the case of ionic crystals, the dipole field which are produced by the defect. Once these fields are known, it is then in principle possible to proceed to calculate such quantities as the formation energy of the defect, and the interaction energies between defects. More generally, one can tackle the problems which one faces when one is considering the scattering of some wavelike disturbance (e.g., x rays or electrons) when defects are present.

In the past the methods that have been used for tackling these problems have been of what we may describe as a semidiscrete character. By this phrase, we mean that in these calculations a certain region about the defect itself, which we call Region I is treated on a discrete basis, whereas the remainder of the lattice is regarded as a continuum; in the case of metals this would be an elastic continuum and in the case of ionic crystals, the continuum would be both elastic and dielectric.

One of the most crucial results that has come out of the sequence of investigations being reviewed in this paper is the impracticality of this type of approach. The reason for this can be stated very concisely. We have found in our calculations that in order to obtain any satisfactory account of the defect behavior, it is generally necessary to consider an impossibly large Region I. When one does this, the number of equilibrium equations involved in determining the displacements and polarizations becomes extremely large and complex. Moreover, one is also faced with the problem of matching the discrete atomic displacements and polarizations calculated in Region I to their continuum counterparts in Region II. This has been discussed by a number of authors [1-4], and it is probably fair to say that there is, at least at present, no satisfactory solution to this problem. Moreover, this type of approach lacks aesthetic appeal. What is needed is some means of tackling these problems which does not introduce this dichotomy between the two regions, but which enables one to make the transition between the two in a continuous manner. The method of lattice statics provides such an approach; moreover, it is a natural and logical extension to the consideration of static distortions in crystal lattices of the concepts which have been used so extensively in studying their dynamical behavior. Even in the semidiscrete type of calculations, it is natural, when carrying out the computations, to exploit to the full point symmetry of the defect. Thus, it is also logical to

proceed to the final state and exploit in defect calculations the translational symmetry of the lattice, and this is something which, it would appear, is beyond the scope of the semidiscrete methods.

The basic idea of lattice statics is very simple; since we are concerned with the displacement and polarization fields produced by the defect, once we accept the need to exploit the transitional symmetry of the lattice, then the logical way of determining these is to Fourier decompose both. One then finds that the equilibrium equations in direct space assume a much simpler form in reciprocal space [5], a fact which is particularly marked in the case of ionic crystals [6], or any crystal where the interatomic forces are of long range. Furthermore, it is apparent from our investigations [7-10] that the existence of long range forces renders the use of brute force relaxation calculations extremely unreliable. This is a point which we shall demonstrate explicitly later on.

Once one has the Fourier amplitudes of the displacement and polarization fields, one can then proceed to back transform and thus obtain the real space quantities. If one is concerned with such parameters as, for example, the relaxation energy, there is no need to carry out this explicit back transformation. The crucial point is that the Fourier amplitudes are as good a set of generalized coordinates as the Cartesian coordinates of the atomic displacements themselves. Thus, if one is computing a relaxation energy, which is effectively a sum of (forces) \times (displacements), in reciprocal space, this transforms very simply into the corresponding product of generalized forces and Fourier amplitudes. In the case of ionic crystals, this second sum is very much simpler to work out than it would be to carry out the direct space sums by brute force. Indeed, it is unlikely that the second alternative is feasible since the sums involved are only conditionally convergent.

We shall begin our description of the method by describing the way in which one applies lattice statics to the case of a point defect in a monoatomic lattice, and, at present, our considerations are restricted to lattices possessing cubic symmetry. However, this is not a fundamental limitation.

We shall then proceed to outline the manner in which one treats ionic crystals by essentially the same method; only the appropriate equilibrium equations become more complicated and one has to recognize the fact that the ions in such a crystal have essentially six degrees of freedom rather than three in that as well as displacing, they can also polarize. Throughout these calculations, we shall use the harmonic approximation to describe the energy of the distorted perfect lattice. This is certainly valid in regions of the crystal well removed from the defect, where the displacements and polarizations are small. In the vicinity of the defect, this approximation becomes somewhat more suspect: however, one can

still handle the problem using our technique, the only modification is that the equations become more complex.

Next, we shall proceed to discuss the problem of computing the interaction energy between pairs of defects. In this instance, we shall restrict ourselves to the interaction between pairs of defects in nonionic materials, although the work has been carried to the point where it is possible to see how these results can be extended to deal with the analogous problem for charged point defects in ionic materials.

In these sections we shall be concerned with the exact solutions of the equations. In the next section, we shall proceed to discuss the way in which one can show how the theory of lattice statics goes over smoothly and logically into the standard results of continuum elasticity when one is considering such problems as the displacements of atoms which are far removed from the defect. Moreover, the methods used in the lattice statics calculation are such that it is then possible to obtain the exact Green's functions for the solution of the elasticity problem presented by a point inclusion in an anisotropic elastic medium. We believe our method provides the most direct and elegant way of explicitly computing the appropriate displacement field.

The approach that we use is equivalent to the lattice Green's function method [11] which is essentially the method of lattice statics formulated in a slightly different way; the Green's function is by definition the response of atom a to unit force applied to atom b , and this is essentially what we work out in the course of the lattice statics calculations.

In the final section we shall briefly mention the limitations on the methods we are using in the case of metals, in so far as these are imposed by our present imprecise knowledge of the interaction between the atoms of the host lattice, and the interaction between the defect and the atoms of the host lattice. These limitations are limitations which are imposed by the present status of the theory of metals. When these limitations are removed, the method of lattice statics will provide a means of calculating the appropriate displacement fields, etc. in a precise manner.

II. Application of Lattice Statics to an Isolated Point Defect in a Cubic Material

The basic equation can be set up by considering the lattice to be distorted, but still perfect, hence the change in lattice energy is, within the harmonic approximation, given by the usual expression

$$\Delta U = \frac{1}{2} \sum_{\ell\ell'} \sum_{\alpha\beta} \xi(\ell_\alpha) \left(\frac{\partial^2 U}{\partial \xi(\ell_\alpha) \partial \xi(\ell_\beta)} \right)_0 \xi(\ell_\beta) \quad (1)$$

where $\xi(\ell_\alpha)$ is the α th Cartesian component of the displacement of the ℓ th atom. If we now introduce the defect, then there is an additional term in this equation such that it now assumes the form

$$\Delta U = \sum_{\ell} \psi(|\mathbf{r}^\ell + \xi^\ell|) + \frac{1}{2} \sum_{\ell' \ell' \alpha \beta} \xi(\ell_\alpha) \left(\frac{\partial^2 U}{\partial \xi(\ell_\alpha) \partial \xi(\ell_\beta)} \right)_0 \xi(\ell_\beta) \quad (2)$$

The first term in this equation represents the interaction energy between the defect and the atoms of the host lattice. \mathbf{r}^ℓ is the perfect lattice position vector of the ℓ th atom. In order to determine the minimum energy configuration, one now minimizes this energy with respect to displacements, ξ and thus obtains

$$F(\ell_\alpha) \equiv -\frac{\partial \psi}{\partial \xi(\ell_\alpha)} (|\mathbf{r}^\ell + \xi^\ell|) = \sum_{\ell' \beta} \left(\frac{\partial^2 U}{\partial \xi(\ell_\alpha) \partial \xi(\ell_\beta)} \right)_0 \xi(\ell_\beta) \quad (3)$$

Where $F(\ell_\alpha)$ is seen to be the α th component of the force exerted by the defect on the ℓ th atom, at its relaxed position. At this stage we make the transformation to reciprocal space by introducing normal coordinates, \mathbf{Q}^q , defined by

$$\xi^\ell = \frac{1}{N} \sum_{\mathbf{q}} \mathbf{Q}^q e^{i \mathbf{q} \cdot \mathbf{r}^\ell} \quad (4)$$

The sum is over the N allowed wave vectors, \mathbf{q} , in the first Brillouin zone. On substituting this equation back into the previous equation, we obtain

$$F(\ell_\alpha) = \frac{1}{N} \sum_{\ell' \beta} \sum_{\mathbf{q}} \left(\frac{\partial^2 U}{\partial \xi(\ell_\alpha) \partial \xi(\ell_\beta)} \right)_0 Q(\ell'_\beta) e^{i \mathbf{q}' \cdot \mathbf{r}^{\ell'}}$$

Multiplying both sides of this equation by $e^{-i \mathbf{q} \cdot \mathbf{r}^\ell}$ and summing over ℓ , we obtain

$$\begin{aligned} \sum_{\ell} F(\ell_\alpha) e^{-i \mathbf{q} \cdot \mathbf{r}^\ell} &= \frac{1}{N} \sum_{\ell' \beta} \sum_{\mathbf{q}} \left(\frac{\partial^2 U}{\partial \xi(\ell_\alpha) \partial \xi(\ell'_\beta)} \right)_0 Q(\ell'_\beta) e^{i \mathbf{q}' \cdot \mathbf{r}^{\ell'}} e^{-i \mathbf{q} \cdot \mathbf{r}^\ell} \\ &= \frac{1}{N} \sum_{\ell' \beta} \sum_{\mathbf{q}} Q(\ell'_\beta) \left(\frac{\partial^2 U}{\partial \xi(\ell_\alpha) \partial \xi(\ell'_\beta)} \right)_0 e^{-i \mathbf{q}' \cdot (\mathbf{r}^\ell - \mathbf{r}^{\ell'})} e^{-i(\mathbf{q} - \mathbf{q}') \cdot \mathbf{r}^\ell}. \end{aligned}$$

Since the expression $e^{-i\mathbf{q}' \cdot (\mathbf{r}^\ell - \mathbf{r}^{\ell'})}$ has translational symmetry, we may take ℓ as being the zeroth cell. Then

$$\sum_{\ell} F(\ell) e^{-i\mathbf{q} \cdot \mathbf{r}^{\ell}} = \frac{1}{N} \sum_{\ell'} \sum_{\beta \mathbf{q}} \left(\frac{\partial^2 U}{\partial \xi(\ell) \partial \xi(\ell')} \right)_0 Q(\beta) e^{i\mathbf{q}' \cdot \mathbf{r}^{\ell'}} \\ \times \sum_{\ell} e^{-i(\mathbf{q} - \mathbf{q}') \cdot \mathbf{r}^{\ell}}.$$

The sum $\sum_{\ell} e^{-i(\mathbf{q} - \mathbf{q}') \cdot \mathbf{r}^{\ell}}$ must vanish unless $\mathbf{q} - \mathbf{q}'$ is a reciprocal lattice vector and since \mathbf{q} and \mathbf{q}' are constrained to lie in the first Brillouin zone, $\mathbf{q} = \mathbf{q}'$ and

$$\sum_{\ell} F(\ell) e^{-i\mathbf{q} \cdot \mathbf{r}^{\ell}} = \sum_{\ell} \sum_{\beta \mathbf{q}} \left(\frac{\partial^2 U}{\partial \xi(\ell) \partial \xi(\ell')} \right)_0 Q(\beta) e^{i\mathbf{q} \cdot \mathbf{r}^{\ell'}}$$

Now define

$$F(\alpha) \equiv \sum_{\ell} F(\ell) e^{-i\mathbf{q} \cdot \mathbf{r}^{\ell}}$$

and

$$V(\alpha\beta) \equiv \sum_{\ell} \left(\frac{\partial^2 U}{\partial \xi(\ell) \partial \xi(\ell')} \right)_0 e^{i\mathbf{q} \cdot \mathbf{r}^{\ell'}}$$

then

$$F(\alpha) = \sum_{\beta} V(\alpha\beta) Q(\beta). \quad (5)$$

And it can now be seen that we have decoupled the original matrix of direct space equilibrium equations into a set of 3 by 3 independent matrix equations, one for each allowed wave vector in the Fourier series. At this point, it is necessary to define the procedure for selecting these allowed wave vectors. This we do by imposing periodic boundary conditions across the faces of a supercell containing N primitive cells and having the same symmetry as the primitive unit cell. In this way, we are

effectively treating the problem of an infinite superlattice of defects having the same lattice structure as that of the host crystal. One then solves eq (5) by simple matrix inversion and thereby obtains a Fourier amplitude for each of the allowed wave vectors. Finally one sums the Fourier series given by (4) and obtains as many of the direct space displacements as one requires. However, because of the choice of the allowed wave vectors, we are effectively imposing artificial constraints on the resultant displacements. In order that these constraints be not serious, it is necessary to restrict our calculations to the determination of the displacements of atoms which are still well removed from the supercell boundary. One has a good criterion of the validity of the displacements by examining the way in which they change as one increases the density of the sample of wave vectors, since in the limit $N \rightarrow \infty$, they should be independent of N . In most of the calculations described here, the wave vector sample density was that appropriate to a supercell containing 64,000 primitive cells. One does encounter some difficulty at the later stage when one is concerned with ascertaining at what point the computed displacements attain those predicted by continuum elasticity or lattice statics in its limiting form. However, these difficulties can be surmounted.

Once one has the displacements, then by simple substitution one can obtain the relaxation energy which is defined as the difference in the energy of the imperfect lattice before and after relaxation. Thus, in terms of our present notation, the relaxation energy can be written

$$E_R = \psi(|\mathbf{r}' + \tilde{\boldsymbol{\xi}}'|) - \psi(|\mathbf{r}'|) + \frac{1}{2} \tilde{\boldsymbol{\xi}} \mathbf{V} \tilde{\boldsymbol{\xi}}$$

The last term in this expression is just the matrix form of the ΔU given in eq (1).

The above expression can be simplified by expanding $\psi(|\mathbf{r}' + \tilde{\boldsymbol{\xi}}'|)$ in a power series in $\tilde{\boldsymbol{\xi}}$. This leads to the expression

$$E_R = \tilde{\boldsymbol{\xi}} \frac{\partial \psi(r')}{\partial \tilde{\boldsymbol{\xi}}} + \frac{1}{2} \tilde{\boldsymbol{\xi}} \frac{\partial^2 \psi(r')}{\partial \tilde{\boldsymbol{\xi}} \partial \tilde{\boldsymbol{\xi}}} \tilde{\boldsymbol{\xi}} + \frac{1}{2} \tilde{\boldsymbol{\xi}} \mathbf{V} \tilde{\boldsymbol{\xi}}$$

But at equilibrium,

$$\mathbf{V} \tilde{\boldsymbol{\xi}} = \frac{-\partial \psi(r')}{\partial \tilde{\boldsymbol{\xi}}} - \frac{\partial^2 \psi(r')}{\partial \tilde{\boldsymbol{\xi}} \partial \tilde{\boldsymbol{\xi}}} \tilde{\boldsymbol{\xi}}$$

hence

$$\frac{1}{2} \tilde{\boldsymbol{\xi}} \frac{\partial \psi(r')}{\partial \tilde{\boldsymbol{\xi}}} + \frac{1}{2} \tilde{\boldsymbol{\xi}} \frac{\partial^2 \psi(r')}{\partial \tilde{\boldsymbol{\xi}} \partial \tilde{\boldsymbol{\xi}}} \tilde{\boldsymbol{\xi}} = -\frac{1}{2} \tilde{\boldsymbol{\xi}} \mathbf{V} \tilde{\boldsymbol{\xi}}$$

and

$$E_R = \frac{1}{2} \tilde{\xi} \frac{\partial \psi(r^\ell)}{\partial \tilde{\xi}}$$

or, since

$$\frac{-\partial \psi(r^\ell)}{\partial \xi} = \mathbf{F}_0^\ell \text{ we may write}$$

$$E_R = -\frac{1}{2} \sum_{\ell \alpha} F_0(\ell) \xi(\ell)_\alpha \quad (6)$$

where the subscript 0 indicates that the forces are to be evaluated in the unrelaxed configuration. One then simply substitutes into this equation the appropriate forces and displacements.

This equation is written in direct space. We are however, perfectly free to write it in the following form

$$E_R = -\frac{1}{2} \sum_{\alpha q} F(\bar{q}) Q(q)_\alpha.$$

Thus one can see there is no need, if one is merely interested in the relaxation energy, to actually compute the appropriate displacements. In the case of a lattice in which the interatomic forces are short range, and the defect forces are also of short range, then there is no particular merit of one method over the other, and it is, on balance, probably simpler to use the direct space expression. However, in the case of an ionic crystal to which the above equations cannot be applied directly without modification, it is only feasible to compute the relaxation energy by using the Fourier transformed expression.

This technique has been applied to various defects in a variety of materials; vacancies in copper and aluminum were treated by Bullough and Hardy [7], and we have examined the behavior of an interstitial copper atom in a copper host lattice [8] and vacancies in the sequence of alkali metals [9]. In the present review, we will illustrate the type of results obtained by describing those for vacancies in Na and K. In the case of these materials, it has been established by pseudopotential theory [12, 13], and also by direct measurements of the phonon dispersion curves [14], that the interatomic forces are relatively long range and extend out at least as far as fifth neighbors. Moreover, these metals have a body-centered structure which is relatively more open than the face-centered structure, and one expects that the computed displacements are likely to be more marked, as is indeed the case.

In tables I and II, we show the results computed using two different sets of interatomic force constants, and it should be mentioned that the force constants used are such that one can regard the lattice as being held together by pair-wise central potentials under tension. This is the view to which one is led by pseudopotential theory.

In the case of vacancies, to a first approximation at least, it is logical to regard the defect-lattice forces as being the negatives of those exerted by the removed atom. However, it will be observed that in the eq (3), the forces involved are those evaluated at the relaxed position. In order to allow for this, at least partially, we take the vacancy lattice force as being equal to

$$\mathbf{F}^\ell = \frac{\partial \psi(r)}{\partial \xi} \Big|_{\mathbf{r}^\ell} + \tilde{\xi}^\ell \frac{\partial^2 \psi(r)}{\partial \xi \partial \tilde{\xi}} \Big|_{\mathbf{r}^\ell} \quad (7)$$

where we have expanded each force to first order in the lattice displacement. The beauty of this approach is that we can solve the problem entirely in the terms of the first and second derivatives of the appropriate potentials, which in turn we can extract from the neutron dispersion curves or from the pseudopotential calculations, and we do not need to have any explicit knowledge of the overall form of the interatomic potential. For more sophisticated calculations, this is not true; if the relaxations are large, then the higher order terms in the foregoing expansion will be important.

It will be observed that the results obtained, using the two sets of potentials are drastically different. The computed displacements for the two different potentials are very different, even though both give reasonably good fits to the measured dispersion curves. This is typical of this sequence of calculations and reflects the sensitivity of the force constants to the slightest displacement of the interatomic potential curve.

We have also computed the relaxation energies which are shown in table III, the method used in this case being the simple summation of (force) \times (displacement) over the atoms in direct space.

The actual generalized forces and the elements of the $\mathbf{V}^{(-q)}$ matrix are somewhat complex and will not be given in detail here since they have appeared elsewhere [8].

One particular point with regard to the calculated displacements that is worthy of comment, is the manner in which they fall off along a $\langle 1, 1, 1 \rangle$ direction. At large distances, it can be shown that the displacements of atoms along a given direction fall off inversely as the square of the distance from the defect and it appears that the asymptotic region has been reached at the third or fourth neighbor position along $\langle 1, 1, 1 \rangle$;

TABLE Ia. Displacements for Na using ref. [12] force constants

Neighbor (L_1, L_2, L_3)	Displacement components of neighbors around a vacancy (units of 2a)			$ \xi \{L_1^2 + L_2^2 + L_3^2\}$ + indicates outward relaxation - indicates inward relaxation
	ξ_1	ξ_2	ξ_3	
111	-0.02935	-0.02935	-0.02935	-0.1525
200	0.013180	0.0	0.0	+0.1272
220	-0.009550	-0.009550	0.0	-0.1080
222	-0.01434	-0.01434	-0.01434	-0.2980
311	0.004580	0.001854	0.001854	+0.05805
331	-0.004977	-0.004977	-0.000528	-0.1341
333	-0.007660	-0.007660	-0.007660	-0.3582
400	0.001954	0.0	0.0	+0.03127
420	0.0005935	0.0002243	0.0	+0.01269
422	0.001156	-0.0003015	-0.0003015	+0.02957
440	-0.003064	-0.003064	0.0	-0.1387
442	-0.002949	-0.002949	-0.0006096	-0.1517
444	-0.004261	-0.004261	-0.004261	-0.3542
511	0.001027	0.00001615	-0.00001615	+0.02773
531	-0.0006627	-0.0002428	-0.0001838	-0.01091
533	-0.0001422	-0.0008395	-0.0008395	-0.05144
551	-0.001968	-0.001968	-0.0002138	-0.1424
555	-0.002492	-0.002492	-0.002492	+0.3237
600	0.0008190	0.0	0.0	+0.02949
620	0.0005104	0.0000950	0.0	+0.02080
622	0.0004182	-0.0001857	-0.0001857	+0.02173
640	-0.0002477	-0.0003623	0.0	-0.02282

however, this is spurious, since as we shall show later, the true asymptotic region is not attained until the 18th or 19th neighbor.

III. Point Defects in Ionic Crystals

In this section we want to consider the way in which the formalism can be extended to deal with charged point defects in ionic crystals. In this case, one has to consider in addition to the ionic displacements, their dipole moments. In order to carry out the calculations and set up the analogy of the $V^{(-q)}$ matrix, one needs a particular model for the interatomic potential of the perfect crystal, and in the case of the alkali halide crystals, we use the deformation dipole model. For this model the change in energy for the distorted perfect lattice can be written in the following form [15]

TABLE Ib. Displacements for Na using ref. [13] force constants

Neighbor (L_1, L_2, L_3)	Displacement components of neighbors around a vacancy (units of $2a$)			$ \xi \{L_1^2 + L_2^2 + L_3^2\}$ + indicates outward relaxation - indicates inward relaxation
	ξ_1	ξ_2	ξ_3	
111	-0.05536	-0.05536	-0.05536	-0.2877
200	0.05402	0.0	0.0	+0.2161
220	-0.01596	-0.01596	0.0	-0.1806
222	-0.02992	-0.02992	-0.02992	-0.6219
311	0.007334	0.002605	0.002605	+0.09029
331	-0.009074	-0.009074	-0.0003475	-0.24401
333	-0.01711	-0.01711	-0.01711	-0.8002
400	0.006850	0.0	0.0	+0.1096
420	0.0006615	0.0002765	0.0	+0.01435
422	0.001964	-0.001135	-0.001135	+0.06088
440	-0.006183	-0.006183	0.0	-0.2798
442	-0.005769	-0.005769	-0.0007287	-0.2949
444	-0.01007	-0.01007	-0.01007	-0.8369
511	0.002659	0.0001093	0.0001093	+0.07191
531	-0.0002236	-0.0004190	-0.0002624	-0.01899
533	-0.0003968	-0.002076	-0.002076	-0.1274
551	-0.004180	-0.004180	-0.0003472	-0.3020
555	-0.006149	-0.006149	-0.006149	-0.7988
600	0.002216	0.0	0.0	+0.07979
620	0.001133	0.0003535	0.0	+0.04746
622	0.001287	-0.0003556	-0.0003556	+0.06079
640	-0.0005497	-0.0006650	0.0	-0.04487

$$Y = 1/2 \tilde{\xi}(\mathbf{R} - \mathbf{H})\xi - 1/2 \tilde{\mu}' \mathbf{U}\mathbf{H}\xi - 1/2 \tilde{\xi}\mathbf{H}\mathbf{U}\mu' - 1/2 \mu' \mathbf{U}\mathbf{H}\mathbf{U}\mu' + 1/2 \mu\alpha^{-1}\mu$$

where

$$\mu' = \mu + \tilde{\mathbf{S}}\xi. \quad (8)$$

In this equation, ξ and μ are the column matrices of the displacements and dipole moments, respectively. \mathbf{R} and $-\mathbf{H}$ are matrices of force constants referring to the closed shell repulsions and the monopole-monopole interactions respectively. α and \mathbf{U} are matrices defined by

$$\alpha_{k\lambda} = \alpha_\lambda \delta_{k\lambda}$$

and

$$U_{k\lambda} = e_\lambda^{-1} \delta_{k\lambda}$$

TABLE IIa. Displacements for K using ref. [14] force constants

Neighbor (L_1, L_2, L_3)	Displacement components of neighbors around a vacancy (units of $2a$)			$ \xi \{L_1^2 + L_2^2 + L_3^2\}$ + indicates outward relaxation - indicates inward relaxation
	ξ_1	ξ_2	ξ_3	
111	-0.02551	-0.02551	-0.02551	-0.1326
200	0.02281	0.0	0.0	+0.09122
220	-0.005896	-0.005896	0.0	-0.06671
222	-0.01260	-0.01260	-0.01260	-0.2619
311	0.002400	0.0007299	0.0007299	+0.02874
331	-0.003783	-0.003783	0.00004181	-0.1017
333	-0.006968	-0.006968	-0.006968	-0.3259
400	0.002072	0.0	0.0	+0.03316
420	0.0001854	0.00004645	0.0	+0.003730
422	0.0007030	-0.0007538	0.00007538	-0.03065
440	-0.002671	-0.002671	0.0	-0.1209
442	-0.002461	-0.002461	-0.0003672	-0.1260
444	-0.004010	-0.004010	-0.004010	-0.3334
511	0.0008795	-0.0001315	-0.0001315	+0.02427
531	-0.0001071	-0.0002534	-0.0001537	-0.01103
533	-0.0002461	-0.0009812	-0.0009817	-0.06063
551	-0.001787	-0.001787	-0.0001904	-0.1293
555	-0.002423	-0.002423	-0.002423	-0.3147
600	0.0008520	0.0	0.0	+0.03067
620	0.0004091	0.00003843	0.0	+0.01643
622	0.0003890	-0.0002758	-0.0002758	+0.02424
640	-0.0002238	-0.0003387	0.0	-0.02111

where α_λ and e_λ^{-1} are, respectively the polarizability and monopole charge of ion λ . Equation (8) is written in matrix form and the significance of this is that the various terms are either $6N$ by $6N$ matrices or $6N$ column vectors. We have not yet Fourier transformed. The various terms in this equation are fairly easily understandable; essentially they describe the short range repulsion, the displacement dipole-displacement dipole interaction, the displacement dipole-electronic dipole interaction, the electronic dipole-electronic dipole interaction, and the self energy of the polarization dipoles. $S\xi$ is the contribution to the electronic dipole moment, due to the deformation dipoles; those dipoles which are induced on the ions by the short range force, and we restrict them to negative ions only. It will be observed that the self-energy term refers only to the

TABLE IIb. Displacements for K using ref. [13] force constants

Neighbor (L_1 , L_2 , L_3)	Displacement components of neighbors around a vacancy (units of $2a$)			$ \xi \{L_1^2 + L_2^2 + L_3^2\}$ + indicates outward relaxation - indicates inward relaxation
	ξ_1	ξ_2	ξ_3	
111	-0.09013	-0.09013	-0.09013	-0.4684
200	0.09355	0.0	0.0	+0.3742
220	-0.02678	-0.02678	0.0	-0.3030
222	-0.05186	-0.05186	-0.05186	-1.078
311	0.01200	0.005335	0.005335	+0.1559
331	-0.01532	-0.01532	-0.0007852	-0.4118
333	-0.03094	-0.03094	-0.03094	-1.447
400	0.01531	0.0	0.0	+0.2450
420	0.001003	0.0004748	0.0	+0.02220
422	0.003270	-0.001434	-0.001434	+0.09237
440	-0.01080	-0.01080	0.0	-0.4888
442	-0.01005	-0.01005	-0.001036	-0.5128
444	-0.01888	-0.01888	-0.01888	-1.569
511	0.05452	0.0008155	0.0008155	+0.1505
531	-0.0003738	-0.0004552	-0.0003732	-0.02418
533	-0.0006812	-0.003463	-0.003463	-0.2126
551	-0.007550	-0.007550	-0.0004523	-0.5450
555	-0.01188	-0.01188	-0.01188	-1.5435
600	0.00455	0.0	0.0	+1.638
620	0.002211	0.0009362	0.0	+0.09603
622	0.002904	-0.0001848	-0.0001848	+0.1283
640	-0.0009978	-0.0008832	0.0	-0.06929

TABLE III. Relaxation energies associated with a single vacancy in Na and K (eV)

	Na(Ref. [12])	Na(Ref. [13])	K(Ref. [14])	K(Ref. [13])
E_R	-0.045	-0.177	-0.031	-0.339

polarization dipoles since the self-energy of the deformation dipoles is included in the first term which describes the change in the overlap repulsive energy. When the defect is present, one has an additional term of the following form

$$W = W_0 - \tilde{\mathbf{E}}\boldsymbol{\mu} - \tilde{\mathbf{E}}\mathbf{U}^{-1}\boldsymbol{\xi} - \tilde{\mathbf{E}}\mathbf{S}\boldsymbol{\xi} - \tilde{\mathbf{V}}\boldsymbol{\xi} \quad (9)$$

which represents the interaction between the defect and the distorted perfect lattice. For other than first neighbors this force is purely electrostatic in origin. One now proceeds to minimize the energy and thereby obtains the following equations for the dipoles and displacements

$$-\frac{\partial X}{\partial \mu_\lambda} = (\alpha^{-1} - \mathbf{U}\mathbf{H}\mathbf{U})\boldsymbol{\mu} - \mathbf{U}\mathbf{H}(\mathbf{I} + \mathbf{U}\mathbf{S})\boldsymbol{\xi}$$

$$-\frac{\partial X}{\partial \xi_\lambda} = [\mathbf{R} - (\mathbf{I} + \mathbf{S}\mathbf{U})\mathbf{H}(\mathbf{I} + \mathbf{U}\mathbf{S})]\boldsymbol{\xi} - (\mathbf{I} + \mathbf{S}\mathbf{U})\mathbf{H}\mathbf{U}\boldsymbol{\mu}$$

where X represents the energy of the distorted host lattice plus the interaction between the defect and the host lattice. It is then possible to eliminate either one or the other and obtain an expression for either the dipole moment or the displacement separately. When one does this, one obtains

$$\begin{aligned} \boldsymbol{\mu} = & \mathbf{C}^{-1}\alpha[\mathbf{I} + \mathbf{U}\mathbf{H}(\mathbf{I} + \mathbf{U}\mathbf{S})\mathbf{M}^{-1}\mathbf{U}^{-1}(\mathbf{I} + \mathbf{U}\mathbf{S})\mathbf{C}^{-1}]\mathbf{E} \\ & + \mathbf{C}^{-1}\alpha\mathbf{U}\mathbf{H}(\mathbf{I} + \mathbf{U}\mathbf{S})\mathbf{M}^{-1}\mathbf{V} \end{aligned} \quad (11)$$

and

$$\mathbf{M}\boldsymbol{\xi} = \mathbf{U}^{-1}(\mathbf{I} + \mathbf{U}\mathbf{S})\mathbf{C}^{-1}\mathbf{E} + \mathbf{V},$$

where

$$\begin{aligned} \mathbf{M} = & [\mathbf{R} - (\mathbf{I} + \mathbf{S}\mathbf{U})\mathbf{H}\mathbf{U}\mathbf{C}^{-1}\mathbf{U}^{-1}(\mathbf{I} + \mathbf{U}\mathbf{S})], \\ \mathbf{C} = & \mathbf{I} - \alpha\mathbf{U}\mathbf{H}\mathbf{U}, \end{aligned}$$

and \mathbf{V} contains the closed-shell interactions. One can then write the energy stored in the perfect lattice at equilibrium in the following form

$$Y_{\min} = 1/2 [\tilde{\mathbf{E}}(\mathbf{S}\mathbf{U} + \mathbf{I})\mathbf{U}^{-1}\boldsymbol{\xi}_{\min} + \mathbf{V}\boldsymbol{\xi}_{\min} + \tilde{\mathbf{E}}\boldsymbol{\mu}_{\min}]$$

and it can then be readily shown that, if we consider the forces between the defect and the lattice ions to be evaluated at the *unrelaxed* position, the relaxation energy assumes the following form

$$\begin{aligned} E_{\text{Relax}} = & -1/2 [\tilde{\mathbf{V}}\boldsymbol{\xi}_{\min} + \tilde{\mathbf{E}}(\mathbf{I} - \alpha\mathbf{U}\mathbf{H}\mathbf{U})^{-1}(\mathbf{U}^{-1} + \tilde{\mathbf{S}})\boldsymbol{\xi}_{\min} \\ & + \mathbf{E}(\mathbf{I} - \alpha\mathbf{U}\mathbf{H}\mathbf{U})^{-1}\alpha\mathbf{E}]. \end{aligned} \quad (13)$$

All these equations are perfectly general, and it is then very simple to Fourier transform them. The transformed equations for the Fourier amplitudes of $\boldsymbol{\xi}$ and $\boldsymbol{\mu}$ have exactly the same form except that all of the matrices and vectors are understood as Fourier transformed. Similarly, in eq (12) for the relaxation energy, one also has the appropriate Fourier amplitudes appearing, and in addition, one must sum over all allowed wave vectors.

Numerical computations of Schottky pair formation energies have been made using this zero-order approximation for a sequence of alkali halides and some typical numbers are shown below in table IV, together with the appropriate experimental values. In these calculations the model used for the perfect lattice cohesive energy was a simple Born-Mayer model with overlap repulsions restricted to first neighbors, the appropriate force constants being determined by the lattice equilibrium condition and the compressibility.

TABLE IV. *Schottky pair formation energies, Es for certain alkali halides*

Crystal	$E_s (N \rightarrow \infty)$	E_s (Ref. [16])	E_s (experimental)
LiF	1.878	1.797	2.68
LiCl	1.203	1.075	2.12
NaCl	1.851	1.841	2.12
NaI	1.372	1.347	1.68
KCl	1.976	2.052	2.22
KI	1.648	1.719	
RbCl	1.907		
RbI	1.655	1.798	

The agreement between theory and experiment is quite good for materials like NaCl and KCl although there is a tendency for the theoretical values to be on the low side. Further investigations have been made in which the relaxation energy and the formation energy are computed, allowing for the effect of relaxation on the forces exerted on the first neighbors of the defect. The results are significantly modified and at present, we do not have the final values.

IV. The Strain Field Interaction Energies Between Point Imperfections

The basic theory of this has been discussed in the original paper by Hardy and Bullough [17] where they were able to show that the interaction energy between two similar point defects in a nonionic material can be written in the following form

$$E = + \frac{\partial \psi_a}{\partial \xi} \xi_b^o \quad (14)$$

where $-\frac{\partial \psi_a}{\partial \xi}$ is the force array due to a defect at "a" and ξ_b^o is the displacement field due to a single defect at "b", and this can be transformed into

reciprocal space to give the following result

$$E = -\frac{1}{N} \sum_{\mathbf{q}} \mathbf{F}_a^{-\mathbf{q}} (\mathbf{V}^{-\mathbf{q}})^{-1} \mathbf{F}_b^{\mathbf{q}} \cos (\mathbf{q} \cdot \mathbf{R}) \quad (15)$$

where \mathbf{R} is the interdefect separation vector.

This result is not exact insofar as a power series expansion has been made in the displacements produced by defect a in the vicinity of defect b and vice versa, and only the first order term retained. At large distances, this will certainly be a good approximation and it should be reasonably reliable even at small distances.

In addition to this strain field interaction, one must, in the case of defects that are close neighbor pairs, allow for the direct interaction between the two defects arising from the fact that the second defect may be within the range of the interatomic potential due to the first. We do not propose to discuss this correction in the present work since its esti-

TABLE V. *Interaction energies between (0, 0, 0) and (L_1, L_2, L_3) vacancy pairs in K (eV)*

(L_1, L_2, L_3)	(Ref. [14] force constants)	(Ref. [13] force constants)
111	0.007347	0.01820
200	-0.01833	-0.2271
220	0.01068	0.1642
222	0.007609	0.08182
311	-0.008440	-0.1220
331	0.002673	0.06419
333	0.004180	0.05641
400	0.001627	0.03249
420	-0.0001429	-0.01371
422	-0.002843	-0.05564
440	0.001324	0.02389
442	0.001286	0.02860
444	0.002193	0.03572
511	-0.0005115	-0.006659
531	-0.0003331	-0.005499
533	-0.001164	-0.02660
551	0.0008796	0.01551
555	0.001174	0.02162
600	-0.0005711	-0.003343
620	-0.0001328	-0.002266
622	-0.0002636	-0.005262
640	-0.0002645	-0.004214

mation requires more knowledge of the interatomic potential. Our main concern is with the strain field interaction. At large distances, it was shown in [17] that in an isotropic material the interaction given by equation (15) falls off as R^{-5} . Moreover, this interaction is a direct consequence of lattice theory and cannot be extracted from elastic continuum theory, although Siems [18], in a recent paper, has pointed out that one can get part of the interaction by a multipole expansion of the force associated with the defect. However, this is a somewhat inconsistent procedure since the effect of lattice periodicity on the $\mathbf{V}^{(-q)}$ matrix is of the same order, and they must both be included to give a consistent result.

In tables V and VI we show the computed interaction energies for vacancy pairs in the alkali metals at various interdefect spacings. The most significant result is that it appears that the second nearest neighbor configuration is the most stable, irrespective of the interatomic potential one considers.

TABLE VI. *Interaction energies between (0, 0, 0) and (L_1, L_2, L_3) vacancy pairs in Na (eV)*

(L_1, L_2, L_3)	(Ref. [12] force constants)	(Ref. [13] force constants)
111	0.006282	0.01535
200	-0.01502	-0.09935
220	0.01471	0.07420
222	0.007983	0.04176
311	-0.01262	-0.05420
331	0.007007	0.02778
333	0.004059	0.02614
400	0.003882	0.01005
420	-0.003006	-0.007106
422	-0.004393	-0.02306
440	0.002631	0.01110
442	0.002959	0.01231
444	0.002311	-0.01544
511	-0.0001439	-0.002690
531	-0.001022	-0.003057
533	-0.001809	-0.01025
551	0.001442	0.006827
555	0.001288	0.008915
600	-0.0005302	-0.002725
620	-0.0002979	-0.001129
622	-0.0002615	-0.002177
640	-0.0004292	-0.001862

V. Asymptotic Displacements Obtained by Lattice Statics

The equations of lattice statics as applied up to the present have been exact and no approximations have been made. However, if one looks at the Fourier series in eq (4) and considers the displacements far from the defect, then one can see that it is likely that this will be dominated by the contribution arising from the small wave vectors. In this limit, the expression for the Fourier amplitude can be written

$$\mathbf{Q}^q = K \times$$

$$\begin{pmatrix} C_0 q^4 + C_1 q_1^2 q^2 + C_2 q_2^2 q_3^2 & q_1 q_2 (C_3 q^2 + C_4 q_3^2) & q_1 q_3 (C_3 q^2 + C_4 q_2^2) \\ q_1 q_2 (C_3 q^2 + C_4 q_3^2) & C_0 q^4 + C_1 q_2^2 q^2 + C_2 q_1^2 q_3^2 & q_2 q_3 (C_3 q^2 + C_4 q_1^2) \\ q_1 q_3 (C_3 q^2 + C_4 q_2^2) & q_2 q_3 (C_3 q^2 + C_4 q_1^2) & C_0 q^4 + C_1 q_3^2 q^2 + C_2 q_2^2 q_1^2 \end{pmatrix} \times \begin{pmatrix} q_1 \\ q_2 \\ q_3 \end{pmatrix} \quad (16)$$

where, for the alkali metals,

$$K = -4i \left\{ \frac{2F^{(1)}}{\sqrt{3}} + F^{(2)} + 2\sqrt{2} F^{(3)} + 2\sqrt{11} F^{(4)} + \frac{4}{\sqrt{3}} F^{(5)} \right\}.$$

Here the $F^{(n)}$ are the direct space forces exerted by the defect on its n th neighbor shell. The coefficients in the matrix in the right-hand side of eq (16) can be directly identified with various linear combinations of the elastic constants. This identification is essentially the same as that made in the method of long waves when one is considering the dynamics of the crystal lattice. Thus when we write the equation for the displacements in the asymptotic limit, we obtain the following form:

$$\xi(\ell) = \frac{G}{(2\pi)^3} \int \int \int \frac{q_1 \{Eq^4 + Fq_1^2 q^2 + Hq_2^2 q_3^2\} \sin (\mathbf{q} \cdot \mathbf{r}^\ell) d^3 q}{\{Dq^6 + Bq^2(q_1^2 q_2^2 + q_2^2 q_3^2 + q_3^2 q_1^2) + Aq_1^2 q_2^2 q_3^2\}} \quad (17)$$

where $G = iKa$ and where it can be seen clearly that the integral is dominated by the contribution from $\mathbf{q} \sim 0$. We now use the device originally introduced by Kanzaki [5] of transforming to polar coordinates in reciprocal space with the polar axis along the same direction as that along which one

is interested in computing displacements in direct space. Thus we obtain

$$\xi(\ell_1) = -\frac{G}{(2\pi)^3} \frac{\partial}{\partial r_1} \int \int \int f_1(\cos \theta, \phi) \cos(qr^\ell \cos \theta) dq d(\cos \theta) d\phi, \quad (18)$$

where $f(\cos \theta, \phi)$ is some function of direction only. We can now carry out the integration on q by extending the limit to infinity and introducing a convergence factor $e^{-\epsilon q}$, and taking the limit as ϵ tends to zero, a procedure justified by Duffin [19], and we thus obtain:

$$\xi(\ell_1) = -\frac{G}{2\pi^2} \frac{\partial}{\partial r_1} \int_{-1}^1 \int_0^{2\pi} \frac{f_1(\cos \theta, \phi)}{r^\ell} \delta(\cos \theta) d(\cos \theta) d\phi \quad (19)$$

where the $\int_0^\infty dr$ has given us the delta function in $\cos \theta$.

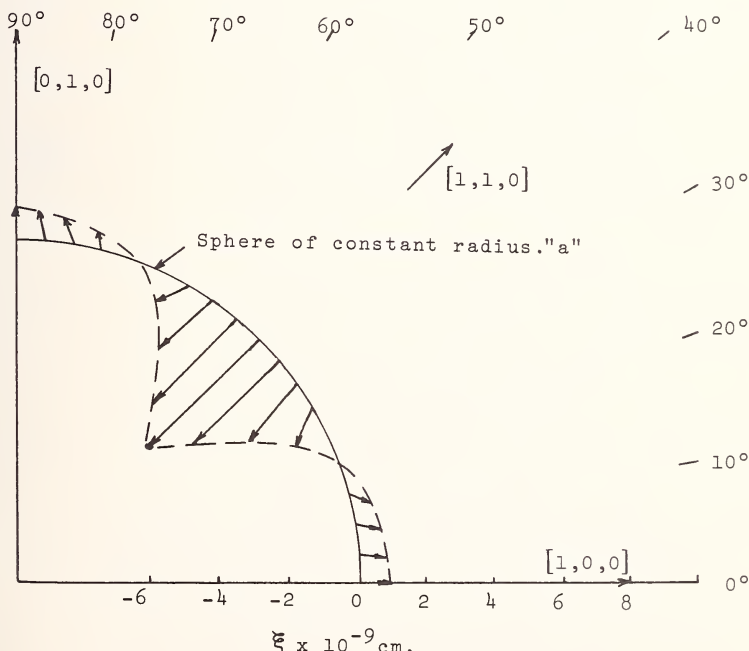


FIGURE 1. Displacement profile in the first quadrant of the $(0, 1, 1)$ plane about a vacancy in Na. Force constants used are those given in Ref. [12], $G = -1.263 \times 10^{-12}$ dyne cm, and $a = 2.14$ Angstroms.

We now carry out the θ integration and thus obtain

$$\xi(\ell) = -\frac{G}{2\pi^2} \frac{\partial}{\partial r(\ell)} \int_0^{2\pi} \frac{f_1(0, \phi)}{r^\ell} d\phi. \quad (20)$$

The last integration over ϕ cannot be done analytically for an anisotropic material for a general direction. However, this integral may readily be evaluated numerically for any given direction after the differentiations with respect to the components of r^ℓ in the integrand have been carried out. In the figures 1 through 4 we show the results of these calculations for Na and K and since one can see from eq (20) that the displacements fall off inversely as the square of the distance from the defect, we have chosen to plot these displacements in terms of the distortion of a sphere of constant radius about the defect. One can see the influence of lattice anisotropy.

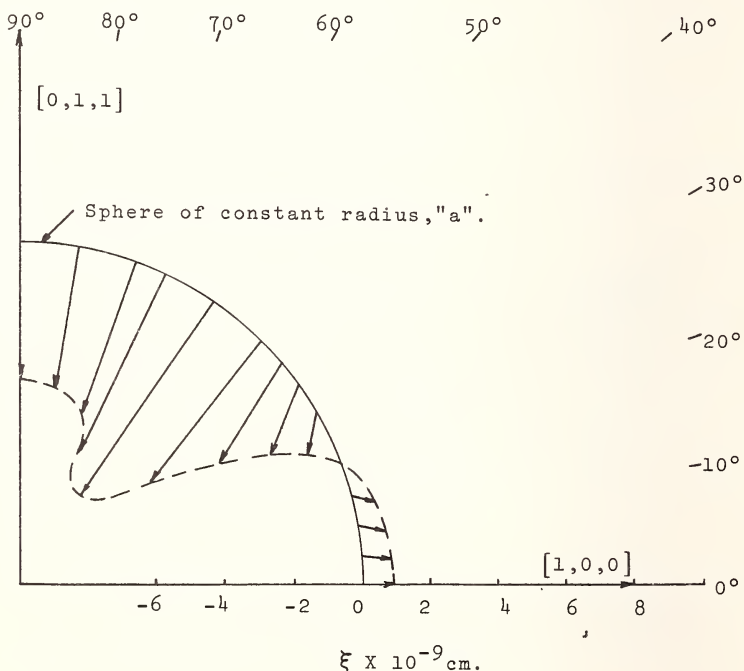


FIGURE 2. Displacement profile in the first quadrant of the $(0, \bar{1}, 1)$ plane about a vacancy in Na. Force constants used are those given in Ref. [12], $G = -1.263 \times 10^{-12}$ dyne cm, and $a = 2.14$ Angstroms.

The asymptotic value of $|\xi|r^2$ for any given direction in a crystal is a constant for a truly elastic medium. By plotting the values of $|\xi|r^2$ obtained from exact lattice statics for various directions, we may observe the way in which the lattice statics results approach the elastic limit as the distance from the defect increases. Such a plot is shown in figure 5 for a $\langle 111 \rangle$ direction in K . The lattice statics results in this case were obtained using a supercell containing 512,000 host atoms. Even so, the effects of other defects in the superlattice become dominant beyond \sim the (28, 28, 28) neighbor and give rise to the rapid increase in the curve observed beyond this point. It is quite obvious, however, that the elastic limit is not reached in this case until one is at least 18 or 19 neighbors from the defect.

In these calculations the strength of the defect is taken to have some arbitrary value and the displacements for any real defect can be obtained by appropriately scaling the displacement contours for the defect strength.

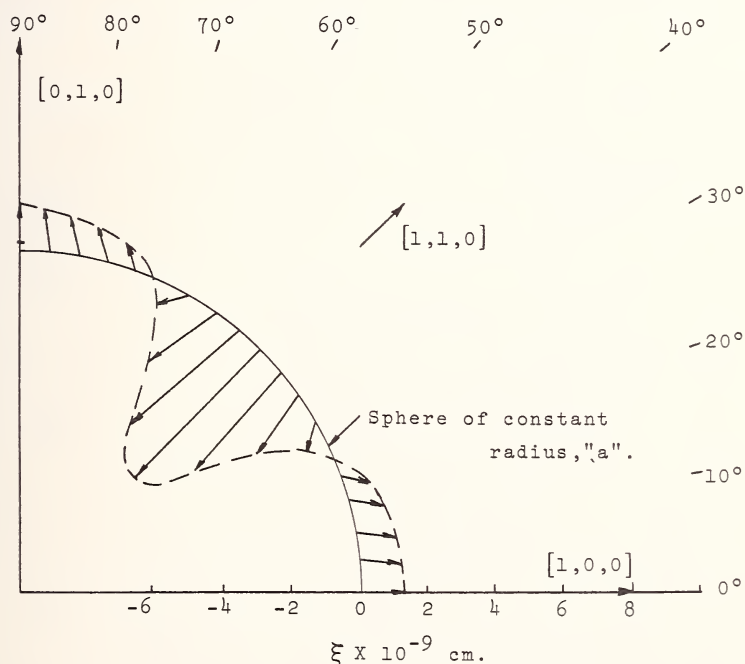


FIGURE 3. Displacement profile in the first quadrant of the $(0, 0, 1)$ plane about a vacancy in K . Force constants used are those given in Ref. [14], $G = -9.756 \times 10^{-13}$ dyne cm, and $a = 2.665$ Angstroms.

These results can also be extended to defects which do not have cubic symmetry. In particular, we [10] have considered defects in Cu and Al which can be regarded as double forces in the lattice and the appropriate displacement contours for Cu are shown in the figures 6 and 7.

As regards actually determining the elastic strength of the defect, the method of lattice statics provides an exact prescription for doing this [20]. We observed in eq (16) that the limiting form for the generalized force is directly expressed in terms of the interatomic forces exerted by the defect on its various neighbors and this provides an exact identification of the strength parameter which appears in the equations of continuum elasticity $G = \sum_{\alpha} F(\alpha) \cdot r(\alpha)$. It can also be shown, as one would expect, that this strength parameter is the same as that which determines the lattice dilatation due to the introduction of the defect. The actual proof of this result is quite lengthy, and it transpires that this volume change in both equations is given by $\Delta V = \frac{G}{\kappa}$, where κ is the bulk modulus. In order to obtain this result, one has to allow for the dilatation of the im-

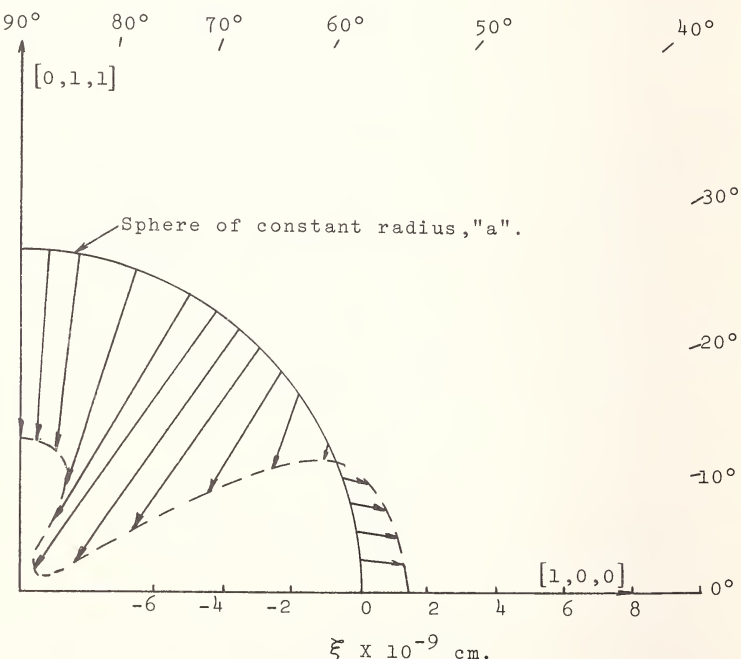


FIGURE 4. Displacement profile in the first quadrant of the $(0, \bar{1}, 1)$ plane about a vacancy in K. Force constants used are those given in Ref. [14], $G = -9.756 \times 10^{-13}$ dyne cm, and $a = 2.665$ Angstroms.

perfect lattice and then minimize the total energy of the system with respect to this dilatation.

One can now evaluate the macroscopic volume changes which we expect for vacancies in Na and K, and the results are shown in table VII. It will be observed that the two sets of force constants we have used lead to very different results. When one adds to the values in the table one atomic volume, in order to obtain the total formation volume, since the removed atom is assumed to be placed on the surface, one obtains for the second potential a negative activation volume for the vacancy formation which would certainly seem to be unphysical.

TABLE VII. *Dilatations associated with a single vacancy in Na and K*

[ΔV is given in atomic volumes]

	Na (Ref. [12])	Na (Ref. [13])	K (Ref. [14])	K (Ref. [13])
ΔV	-0.696	-1.82	-0.322	-1.61

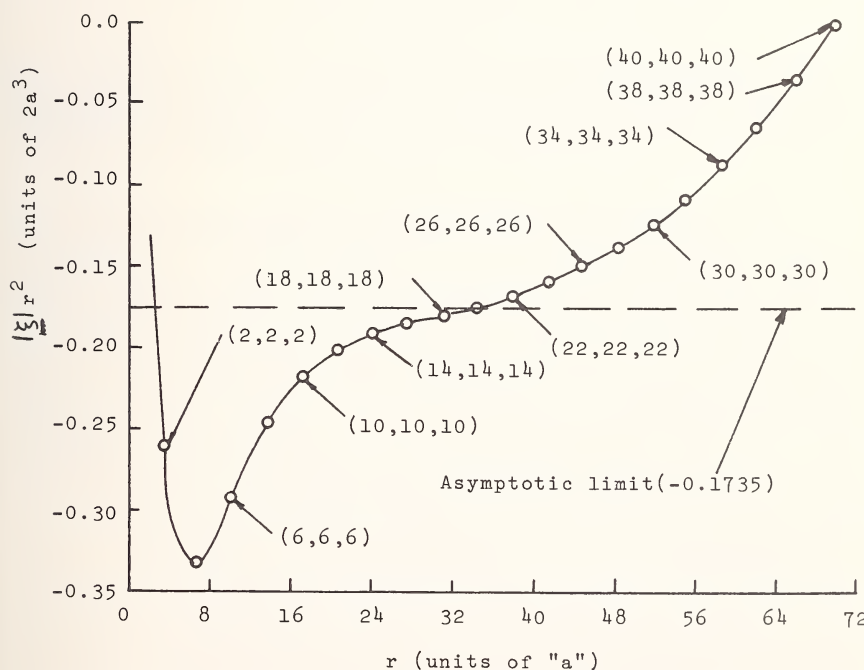


FIGURE 5. $|\xi|r^2$ calculated from exact lattice statics as a function of distances r from the defect along $\langle 111 \rangle$ in K. The dotted line shows the elastic limit predicted by the asymptotic theory.

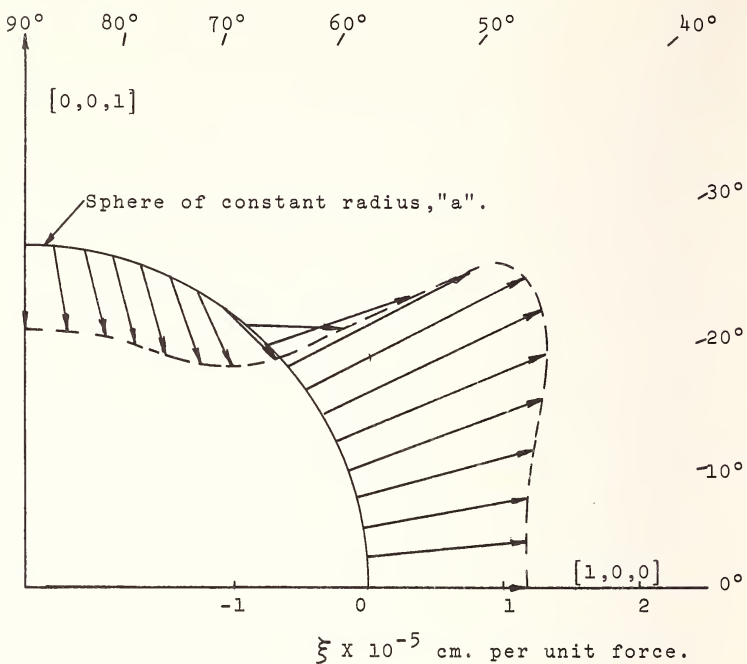


FIGURE 6. Displacement profile in the first quadrant of the $(0, 0, 1)$ plane about a unit single double force along $\langle 100 \rangle$ in Cu. Here $a = 1.805$ Angstroms, $C_{11} = 1.70 \times 10^{12}$ dynes/cm 2 , $C_{12} = 1.23 \times 10^{12}$ dynes/cm 2 , $C_{44} = 0.75 \times 10^{12}$ dynes/cm 2 , and $G = 3.61 \times 10^{-8}$ dyne cm.

VI. Discussion of the Interatomic Potentials Used

We shall restrict this discussion to the interatomic potentials used in the case of metals. In our discussion there, we have followed the spirit of the pseudopotential approach in that we have regarded the lattice energy as composed of a sum of pair-wise interactions plus a volume dependent term. Because of the existence of this second term, the pair-wise interaction term itself does not have to be in overall equilibrium. The only overall requirement is that the first derivative of the total energy with respect to volume be zero. Whether this is, in fact, satisfied for the various potentials that we have used is somewhat questionable. Pseudopotential calculations are usually made at fixed volume and in any attempt to establish whether or not the total lattice energy is minimal, one runs into the difficulty of computing the volume dependent term which is highly sensitive to the manner in which one includes the exchange and correlation energy of the electron gas.

Even without considering this limitation one is gravely concerned by the difference in the force constants that are obtained by the two different

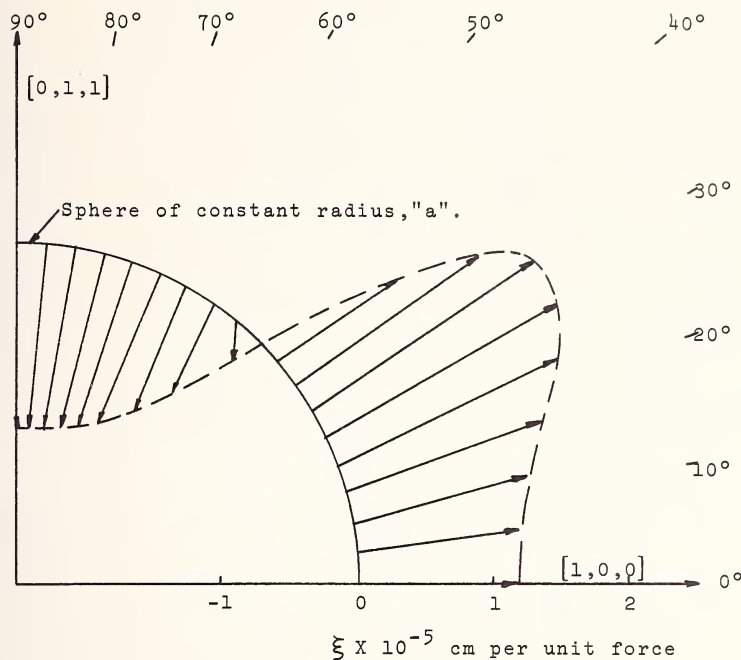


FIGURE 7. Displacement profile in the first quadrant of the $(0, \bar{1}, 1)$ plane about a unit single double force along $[100]$ in Cu. Here $a = 1.805$ Angstroms, $C_{11} = 1.70 \times 10^{12}$ dynes/cm 2 , $C_{12} = 1.23 \times 10^{12}$ dynes/cm 2 , $C_{44} = 0.75 \times 10^{12}$ dynes/cm 2 , and $G = 3.61 \times 10^{-8}$ dyne cm.

pseudopotentials used for Na and K. Moreover, there exists a whole range of calculations of the pseudopotentials for the alkali metals in addition to those we used [21, 22], and the associated force constants are very different. The main problem is that the oscillations in the effective interionic potential, particularly near first and second neighbor sites are very violent. This is because the maxima and minima, in particular the first minimum in this region are very sharp, thus any slight change in the form factors

$$\Omega_0^{-1} \int e^{-i(\mathbf{k} + \mathbf{q}) \cdot \mathbf{r}} W(r) e^{i\mathbf{k} \cdot \mathbf{r}} d\tau \quad (22)$$

(where \mathbf{k} is the free electron wave vector) used in the calculation, or for that matter, any modification in the form of the effective dielectric screening function, particularly for large \mathbf{k} vectors can produce violent changes in the force constants by making very slight displacements of the minima and maxima.

At present there is, as far as we know, no clear cut solution to this problem, but certainly such a solution must be found before the results

of calculations, such as we have been making are even remotely reliable. One can fall back on the procedures which have been used by Johnson [23] and also by Girifalco and Weizer [24] of using a heuristic potentials of relatively short range, and this approach has its merits when one is dealing with materials like iron or copper where one hopes that the interatomic potentials are genuinely short range, and confined to first and second neighbor interactions. However, for the alkali metals, or materials like aluminum, it is clear that such short range potentials are not reliable. Moreover, even a Morse potential is of somewhat dubious use since it too has a long range tail which however, does not have any oscillations as one believes the interatomic potential should have.

A more fundamental limitation of the approach that one is using in the present calculations for metals, is that we have, in the case of vacancies, regarded the vacant lattice site as being equivalent to a negative interatomic potential acting at that site. This procedure has been questioned and, it is probably invalid. The reason for this is that for the assumption to be valid, it is necessary that the electron gas does not redistribute itself in the presence of the vacancy, and this is certainly untrue and as Seeger [25] has pointed out, it is highly questionable as to whether or not one can regard the vacancy as a weak perturbation on the electron gas. At large distances this approximation is presumably valid, but in the immediate vicinity of the defect, there would seem to be good reason for regarding it as extremely questionable. These are the problems which must be resolved before the calculations of lattice distortion, formation energies, etc. by any technique are to be really definitive. However, our basic point with regard to the superiority of the method of lattice statics for the computation of lattice configurations about defects still holds.

VII. Acknowledgement

This work was supported in part by the A.E.C. through L.R.L., Livermore, Calif.

VIII. References

- [1] Mott, N. F., and Littleton, M. J., Trans. Faraday Soc. **34**, 485 (1938).
- [2] Seeger, A., and Mann, E., J. Phys. Chem. Solids **12**, 326 (1959).
- [3] Bennemann, K. H., and Tewordt, L., Z Naturforsch **15a**, 772 (1960).
- [4] Johnson, R. A., and Brown, E., Phys. Rev. **127**, 446 (1962).
- [5] Kanzaki, H., J. Phys. Chem. Solids **2**, 24 (1957).
- [6] Hardy, J. R., J. Phys. Chem. Solids **15**, 39 (1960).
- [7] Bullough, R., and Hardy, J. R., Phil. Mag. **17**, 833 (1968).
- [8] Flocken, J. W., and Hardy, J. R., Phys. Rev. **175**, 919 (1968).
- [9] Flocken, J. W., and Hardy, J. R., Phys. Rev. **177**, 1054 (1969).

- [10] Flocken, J. W., and Hardy, J. R. (to be published).
- [11] Flinn, P. A., and Maradudin, A. A., Annals of Phys. **18**, 81 (1962).
- [12] Shyu, W. M., Brust, D., and Fumi, F. G., J. Phys. Chem. Solids **28**, 717 (1967).
- [13] Shyu, W. M., and Gaspari, G. D., Phys. Rev. **163**, 667 (1967).
- [14] Cowley, R. A., Woods, A. D. B., and Dolling, G., Phys. Rev. **150**, 487 (1966).
- [15] Hardy, J. R., and Lidiard, A. B., Phil. Mag. **15**, 825 (1967).
- [16] Boswarva, I. M., and Lidiard, A. B., Phil. Mag. **17**, 805 (1967).
- [17] Hardy, J. R., and Bullough, R., Phil. Mag. **15**, 237 (1967).
- [18] Seims, R., Phys. Stat. Sol. **30**, 645 (1968).
- [19] Duffin, R. J., Duke Math. J. **20**, 233 (1953).
- [20] Hardy, J. R., J. Phys. Chem. Solids **29**, 2009 (1968).
- [21] Mayer, A., Young, W. H. and Dicky, J. M., J. Phys. C. (Proc. Phys. Soc.) **1**, 486 (1968).
- [22] Torrens, I. M. and Gerl, M., Solid State Communications **1**, 263 (1968).
- [23] Johnson, R. A., Phys. Rev. **134**, A1329 (1964).
- [24] Girifalco, L. A., and Weizer, V. G., J. Phys. Chem. Solids **12**, 260 (1960).
- [25] Seeger, A., in Calculations of the Properties of Vacancies and Interstitials, Nat. Bur. Stand. Misc. Publ. No. 287 (Government Printing Office, Wash., D.C., 1966).

Discussion on Papers by A. A. Maradudin, and J. W. Flocken and J. R. Hardy.

ASHCROFT: Do you regard your theory as a $T=0$ theory, Professor Hardy? . . . You minimize with respect to the internal energy rather than the free energy.

HARDY: Yes, we're doing it for $T=0$. The thing is, we're in enough trouble as it is.

ELBAUM: This is a question for Professor Maradudin: I would think that for a defect, such as a dislocation, with a fairly long range strain field prime physical interest would be in modes of large wave vector values rather than in the long wave length limit. Would you agree with that?

BULLOUGH: I hardly think he will agree.

MARADUDIN: If one thinks of two dimensional defects, it's Rayleigh waves that are physically important. Here, the only thing that's really of any great interest, I think, is the long wave length limit, because the dispersion of Rayleigh waves is, at this time, anyway, experimentally unmeasurable, and I suspect that probably any corrections to the long wave results obtained, say, for the localized modes about a dislocation are probably unmeasurable also. If you come up with any idea of how to do it, I would be very interested.

ELBAUM: No, I don't have any idea of how to do it. I was expecting a comment from you that perhaps there is a way. I appreciate the algebraic difficulty. It's only a question of projecting what would appear to me intuitively as the more interesting case physically: That is the case of the short wave length modes — away from $q=0$.

MARADUDIN: Well, I guess I'm not even convinced that they are the more interesting case, and I would also have to rely, unfortunately, on the pragmatic argument that in this case the analysis would be extremely difficult, particularly starting from the lattice point of view.

SIMMONS: This question is directed to Professor Maradudin. As I understand it, you used the perturbation method in non-linear elasticity to find the dynamic normal modes for a screw dislocation. But, because of the fact that in the linear solution you have an infinity at the core (since you have basically a distributional, or generalized function, solution) whereas in the non-linear case you cannot obtain such a solution without a complete divergence everywhere throughout the whole of three-space, it seems highly questionable that you can use any kind of a perturbation procedure without first of all starting out with an already

well-defined, assumed core position where you have a finite static solution from which you perturb. In other words, I'm perturbed about your perturbation.

MARADUDIN: As far as the equations of motion are concerned, it's true I have linearized them about the solution of the static equations which define the equilibrium positions. I then did make the further approximation of using as the static displacement field not the solution of the non-linear problem, but the solution of the linear equations: the standard arc-tangent solution. The basis for this was simply the heuristic continuity argument that, if it is really true that linear elasticity theory gives a reasonable description of the dislocated configuration—although I know that non-linear equations can have solutions which don't pass continuously into the solutions of the linear equation when the non-linearity tends to zero—still and all, I argued on the basis of the physical argument that, since the linear equations do apparently describe many features of the dislocation problem satisfactorily, that whatever the significant difference is between the static displacement field calculated by some kind of solution of the non-linear field equations and the solution obtained from the linear equations, one presumably passes continuously into the other as the anharmonic or non-linearity tends to zero—for example, as the third order elastic constants or the D -parameters tend to zero. This being the case, then, since I'm substituting the static displacement field into terms in my dynamic equations of motion which are already proportional to the non-linearity, that is, to the third order elastic constants, then to substitute in a better approximation than that obtained from the linear theory would be to include higher order anharmonic corrections than I have worked with up to this point.

KRÖNER: When we speak of dispersion in long and short waves we have to say long and short compared to what. I think this is a question here. It is not long compared to the lattice parameter because there was no lattice parameter in your calculation. The only length I can imagine is the decay length perpendicular to the dislocation. I would say the dispersion can be noticed as long as a wave length is not too long compared to this length. Now the question is: How long is this length with which we have to compare the wave length to say that it is a short wave or a long wave limit.

MARADUDIN: Well this is always a disagreeable feature of the continuum approach, because a crystal after all has a built-in cutoff in the lattice parameter. Had I started with, for example, the equations of motion in which I expand the displacement amplitudes in terms of the eigenvectors and eigenfrequencies of the undislocated crystals then all of my sums would have been confined to the first Brillouin zone. This automati-

cally provides a large k -cutoff on the sums so that there are no divergence difficulties and then the relevant length becomes simply the lattice parameter. In the continuum case the length is not clear. I didn't show the last slide for example on which I've actually worked out what the displacement field is, because it is not terribly illuminating, given in terms, as it is, of exponential integrals and things of that sort.

KRÖNER: Well, I think it must depend on the ratio of the third and second order constants.

MARADUDIN: Yes.

SCHOECK: I have a question for Professor Hardy. You calculated the interaction between point defects. Now it is known that if we use isotropic elastic continuum theory the only interaction we get between centers of dilatation is due to image fields. I wonder, therefore, how the use of periodic boundary conditions affects your results. Do you think if you would assume free boundaries you would get an additional term?

HARDY: No, I don't think the boundary conditions have got anything to do with the issue. The r^{-6} interaction is that induced in the continuum case. The origin of our r^{-5} term in the isotropic case is essentially twofold: It arises a) from the dispersion of the lattice waves and b) from the finite extent of the force array. In fact, Mr. Flocken worked out the equations for an anisotropic medium where you get an r^{-3} interaction. So I don't think this is a surface effect.

BULLOUGH: The surface effect causes a constant interaction.

HARDY: Yes, that's right.

TEODOSIU: I should like to discuss the paper by Professor Maradudin. Professor Seeger and I studied the elastic non-linear problem which was the starting point of this paper and we also considered static and uniformly moving dislocations and superimposed displacement fields. Now in linearizing this problem at least two small parameters appear: One is the gradient of the superimposed displacement field and the other is the magnitude of the distortion produced by the dislocations. We have shown that the linearized system of equations strongly depends on the relative magnitude of these two small parameters. Now it seems to me that in the paper by Maradudin, such a hypothesis was also tacitly used, that is to say, if the order of magnitude of the elastic distortion is proportional to ϵ then the order of magnitude of the gradient of the superimposed displacement is proportional to ϵ^2 . Only in this case, it seems to me, is this linearization valid. Is that true? That is my question.

MARADUDIN: I'm afraid that I cannot answer yes or no. I think that there is one thing though that perhaps it is well to keep in mind, namely in the

long wave length limit, where things vary slowly, the gradient is going to be proportional to the first power of the wave vector of the vibrating field of the crystal, and by going to sufficiently long wave lengths I presume I can make that gradient small compared to the gradient of the static displacement field.

BEN-ABRAHAM: Professor Kröner asked my first question, but it induces another one. What happens when the localized modes start to overlap?

MARADUDIN: Overlap with what?

BEN-ABRAHAM: With each other. I've got two dislocations coming very near and the localized modes start to overlap.

MARADUDIN: It is the same thing that happens whenever impurity levels overlap. Here it is a little bit different from the case of localized modes associated with an isolated impurity in which you just get, say, a delta function peak in the frequency spectrum. Here you have a one dimensional continuum, so you actually have a band—an impurity mode band—in the case of a single dislocation. When you have several and they are close enough to overlap, then obviously you will have distortion of this impurity band—it may merge in some different way with the bottom of the acoustic continuum of the undeformed crystal. But, beyond such a qualitative result, no one has looked at quite such a complicated problem.

BEN-ABRAHAM: I'm mainly interested in the following: If we have a lot of dislocations, whether you think it's possible, if localized modes overlap, to form a new phonon spectrum. Is that sound?

MARADUDIN: Certainly. In addition once the dynamic or vibrational displacement fields of the dislocations overlap, you will have an additional force or energy of interaction between two dislocations that is over and above the interaction that comes just from their static displacement fields.

BULLOUGH: Could I suggest at the prompting of Dr. Simmons that perhaps Professor Eshelby would like to put his question on the Rosenstock-Newell model now? The question of whether the Rosenstock-Newell model has any physical significance.¹

ESHELBY: I didn't really want to ask the question.

BULLOUGH: Well, don't, then!

AUDIENCE: General laughter.

¹ See p. 175.

MARADUDIN: I'll be happy to answer it.

BULLOUGH: Will you answer the imaginary question? (laughter). I would like to know.

MARADUDIN: The chief difficulty here is not any difficulty associated with the elastic constants. I think that the real difficulty with the Rosentock-Newell model is that it's not rotationally invariant. This is nowhere, I think, more dramatically highlighted than in the book by Kittel on Solid State Theory,² where on something like two successive pages by calculating the elastic constants either from the long wave length limit or from static deformation theory he gets two different results. This is simply a reflection of the lack of rotational invariance in the model. But for many purposes the dependence on rotational invariance is a refinement, which, while desirable, is not essential to get physically meaningful results. You may still calculate, for example, frequencies of localized modes—of certain kinds of surface modes—frequency spectra, thermodynamic properties of crystals, and so forth, all of which are qualitatively and even quantitatively reliable despite the lack of rotational invariance.

ESHELBY: Well, now I *would* like to ask the question.

AUDIENCE: General laughter.

ESHELBY: The point I want to make is that, if $C_{12} = -C_{44}$ then the Green's function can be written down as essentially the solution of Laplace's equations for a point source which is squeezed differently in the x , y , and z directions. You can do anything you can do in isotropic elasticity—there is a wealth of things waiting to be done—but there is no material I know that is remotely like such a solid. It isn't this mysterious rotational invariance that worries me, but the fact that it isn't approached by any known material, which is a kind of irritation. I was just hoping perhaps someone knows of such a material. If I, like the lattice boys, could persuade myself that this was sufficiently unbogus to inflict on the public, then I could have thousands of students doing thousands of Ph.D. theses on it. I hoped someone would come up with a crystal that did satisfy the condition; there is no reason why there shouldn't be one; C_{12} is negative for iron pyrites, but not nearly negative enough to satisfy $C_{12} = -C_{44}$. Of course, the ideal thing is the thing which Dr. Bullough had which satisfied Cauchy's relations, was isotropic, and had the Rosentock-Newell relations; but strictly speaking that is impossible.

BULLOUGH: He's slandering me, you know!

² Kittel, C., Introduction to Solid State Physics (John Wiley and Sons, New York, 1966).

AUDIENCE: Laughter.

BULLOUGH: This particular lattice was constructed to permit an analytic demonstration of an effect; it was certainly not intended to model a physical substance.

MARADUDIN: I'm prepared to defer to Professor Eshelby's memory, but is the condition that $C_{12} = -C_{44}$ a consequence of the static or the dynamic calculation of the elastic constants for the Rosenstock-Newell model?

ESHELBY: The history of this is that if one puts $C_{12} = -C_{44}$, the equations for a cubic material become remarkably simple and you can do all of these things. Also, the x , y and z displacements are uncoupled and this, I understand, is one of the features of the Rosenstock-Newell model. That's why I say that $C_{12} = -C_{44}$ is the Rosenstock-Newell elastic solid. I may be wrong there.

MARADUDIN: Well, I think that it may be a situation where one implies to the other, but not conversely.

ESHELBY: Yes, I'm just saying that I understand that the lattice people use crystal lattices, which in the continuum or long wave length limit have $C_{12} = -C_{44}$. Can they produce one physically—a pound of it?

AUDIENCE: General laughter.

HARDY: The answer to Professor Eshelby's question—or an answer—is: I can construct for you, or go into the lab and make for you,—at least I could if I were a practical man—a model which had these properties. I would merely take a simple cubic lattice with nearest neighbor springs and then I would stretch it uniformly in each direction and in such a way that the force constants come out right. This you could do and then you can get a Rosenstock-Newell lattice. Whether, in fact, it will be possible to supply this pressure, say by the pressure of the electron gas in some hypothetical metal, I don't know. But that's the sort of physical way in which one can produce a model like this.

ESHELBY: Well, what I'm really asking is can you put a lot of this sort of stuff on the market?

AUDIENCE: Applause.

BULLOUGH: On that note we must adjourn the discussion.

EFFECT OF ZERO-POINT MOTION ON PEIERLS STRESS

H. Suzuki

*Department of Physics
Faculty of Science
University of Tokyo
Bunkyo-ku, Tokyo, Japan*

Calculations of the Peierls stress hitherto made are criticized and the following conclusions are obtained. The significant difference in Peierls stress between different materials arises mainly from the difference in crystal structures. The Peierls stress is necessarily high in a rectangular lattice where atoms just above and below the slip plane face each other, while in the lattices where the atoms face alternately along the slip plane it is of the order of one percent of that in the rectangular lattice. The Peierls stress in the body-centered cubic crystal is, however, rather high for a screw dislocation owing to the screw structure of this crystal with the axes parallel to [111] direction. The calculated Peierls stresses are several times of those expected from experiments. The zero-point motion decreases the calculated Peierls stress through two mechanisms. The one is the difference in frequency spectrum of a dislocation line at the bottom of the potential valley and at the top of the potential hill. The other is due to the change in spring constants of atom pairs around the dislocation through anharmonicity.

Key words: Anharmonicity; dislocations in lattices; Peierls stress; zero point motion.

I. Introduction

The calculation of the force required to move a dislocation in an otherwise perfect crystal is one of the most important problems in dislocation theory. This force was first calculated by Peierls [1] and later re-calculated by Nabarro [2], and so it is called the Peierls or Peierls-Nabarro stress. The calculation has been revised by several workers, especially using computers in recent years. As the accuracy of the calculation increases, the calculated Peierls stress appears too high compared with those of experiments.

Fundamental Aspects of Dislocation Theory, J. A. Simmons, R. de Wit, and R. Bullough, Eds. (Nat. Bur. Stand. (U.S.), Spec. Publ. 317, I, 1970).

The discrepancy between the calculation and experiments may arise from inadequate models connecting the Peierls stress with the temperature dependence of flow stress, with the low-temperature yield stress, and also with the Bordoni peak. The major origin of the discrepancy, however, seems to be in the method of calculation of the Peierls stress itself. It is widely recognized that the selection of suitable pairwise potential between atoms is extremely difficult in metals. There seems, however, a more serious defect in usual calculations of the Peierls stress—that is, disregard of the lattice vibration, especially of the zero-point motion.

A part of the effect of zero-point motion was discussed by Suzuki [3] in the calculation of the Peierls stress of a screw dislocation in a body-centered cubic crystal using the string model. There is also another mechanism contributing to the Peierls stress from the zero-point motion through the change in frequency spectrum of lattice vibration due to the anharmonicity around the dislocation.

In this paper, previous calculations of Peierls stress are criticized and then the importance of zero-point motion is discussed using a simple model of a screw dislocation in a body-centered cubic crystal.

II. Peierls-Nabarro Approximation

Suppose a simple rectangular lattice with interatomic distance b along the slip plane, taken to be in the x direction, and with interatomic distance a along the y axis vertical to the slip plane. Cut the lattice at a slip plane and rejoin after a displacement by $b/2$. Let now the upper half undergo a compressive displacement $u_+(x)$ and the lower half an expansive displacement $u_-(x)$ so that registry is re-established at large distances, or $u_+(\infty) = -u_-(\infty) = b/4$. A relative displacement function is defined by the relation.

$$\phi = b/2 + u_+ - u_- \approx b/2 + 2u_+(x - \alpha b) \quad (1)$$

where αb denotes the position of the center of the dislocation. Any row of atoms bordering the slip plane is subjected to two forces:

(1) Forces from the material in the own half-crystal; these are treated on the basis of elasticity theory.

(2) Forces from the other half crystal, particularly from the atoms bordering the half crystal. The x component of this force σ_{xy} is a periodic function of ϕ with the period b and is assumed to be given by the relation

$$\sigma_{xy} = -\frac{\mu b}{2\pi a} \sin \frac{2\pi\phi}{b} = \frac{ub}{2\pi a} \sin \left(\frac{4\pi\mu}{b} \right) \quad (2)$$

per unit area, where μ is the shear modulus of the lattice, and u is written for u_+ .

In equilibrium these forces balance, and we have

$$\sigma_{xy} = \frac{\mu}{\pi(1-\nu)} \int_{-\infty}^{\infty} \frac{du}{dx'} \frac{dx'}{x-x'} \quad (3)$$

where ν is Poisson's ratio. An appropriate solution of the above equation turns out to be

$$u(x) = -\frac{b}{2\pi} \tan^{-1} \left\{ \frac{2(1-\nu)(x-\alpha b)}{a} \right\} \quad (4)$$

for u .

By integrating eq (2), the interaction potential or the misfit energy per a row of atoms per unit length of dislocation

$$V(x) = \frac{\mu b^3}{4\pi^2 a} \left(1 + \cos \frac{2\pi\phi}{b} \right) \quad (5)$$

is obtained. Assuming that the elastic strain energies in both half crystals are independent of the position of the dislocation, αb , the part of the dislocation energy that depends on α is correctly given by the sum of the potential (5) for each row of atoms.

Peierls and Nabarro took one half the sum of the values of this potential evaluated at positions of each of the atom rows adjoining the slip plane. Above the slip plane rows have $x=nb$ and below the slip plane $x=(n+1/2)b$, where $n=0, \pm 1, \pm 2, \dots$. Accordingly for the dislocation energy one obtains

$$\begin{aligned} E &= \frac{\mu b^3}{8\pi^2 a} \sum_{m=-\infty}^{\infty} \left[1 + \cos \left\{ 2 \tan^{-1} \left(\frac{1}{2} m - \alpha \right) \left(\frac{b}{\zeta} \right) \right\} \right] \\ &= \frac{\mu b \zeta^2}{\pi^2 a} \sum_{m=-\infty}^{\infty} [4(\zeta/b)^2 + (m-2\alpha)^2]^{-1} \end{aligned} \quad (6)$$

where $\zeta=a/2(1-\nu)$, and $n=m/2$. The sum is given in the form

$$E \approx \frac{\mu b^2}{4\pi(1-\nu)} [1 + 2 \cos 4\pi\alpha \exp(-4\pi\zeta/b)]. \quad (7)$$

As a result the shear stress required to move a dislocation (Peierls stress) is

$$\tau_p = \frac{2\mu}{1-\nu} \exp(-4\pi\zeta/b). \quad (8)$$

The quantity 2ζ means the width of the dislocation where the misfit between the atoms above and below the slip plane is considerably large, namely, $b/4 \leq \phi \leq 3/4b$. Equation (8) indicates that the Peierls stress depends on the dislocation width exponentially.

III. Criticism and Revision of Peierls-Nabarro Model

Peierls [1] and Nabarro [2] summed the misfit energies for the displacements at the positions separated by $b/2$ as shown in eq (6). Meanwhile, Kuhlman-Wilsdorf [5] did it for the displacements at the positions separated by b , and obtained the result essentially included in the expression of the total misfit energy

$$E = \frac{\mu b^2}{4\pi(1-\nu)} [1 + 2 \cos 2\pi\alpha \exp(-2\pi\zeta/b)] \quad (9)$$

instead of eq (7), or

$$\tau_p = \frac{\mu}{1-\nu} \exp(-2\pi\zeta/b) \quad (10)$$

instead of eq (8). Comparing eqs (7) and (9) or (8) and (10), it is easily seen that the Peierls stress differs remarkably between two cases, which differ in the distance of atoms in the summation of misfit energy to each other.

Peierls and Nabarro took the distance of $b/2$, because they started from an artificial undeformed crystal in which a half crystal was displaced by $b/2$ along the slip plane as mentioned in section II. It is, however, evident in a rectangular lattice that the summation of eq (6) must be done over the misfit energies for the relative displacement ϕ between the facing atoms at the distance b at least in the region far from the dislocation center.

Huntington [6] carried out the summation satisfying the above mentioned requirement. He expressed the displacement of atoms as a function of the displaced position of atoms, namely,

$$u(x') = u[x + u(x)]. \quad (11)$$

He summed the misfit energies for the displacement $u(x')$ and obtained considerably higher Peierls stress than the eq (8).

The displacement of each atom, however, had been calculated as a function of the initial position of atom but not of the displaced position in the elasticity theory. The relative position of the atoms just above and below the slip plane is denoted by $x'_+ - x'_- = u_+(x) - u_-(x) + \text{const.}$, but not by $u_+(x'_+) - u_-(x') = u_+[x + u_+(x)] - u_-[x + u_-(x)] + \text{const.}$ Here the terms of *const.* denote the rigid displacement of the half crystal above the slip plane relatively to the other half crystal. Therefore, the procedure by Huntington is not correct, and the summation¹ satisfying the above-mentioned requirement is simply to take the distance b . As a result the Peierls stress for the rectangular lattices is given by eq (10).

On the other hand, in lattices where atoms face alternate along the slip plane, the misfit energy of a row of atoms at x just above the slip plane depends almost equally upon the positions of rows at $x - b/2$ and $x + b/2$ just below the slip plane. The total misfit energy, therefore, obtained by summing over the misfit energies of rows of atoms for the displacement at the positions separated by $b/2$. Finally we obtain eq (8) as the Peierls stress in lattices with atoms facing alternatively along slip plane.

Assuming $\nu = 1/3$ and $a = b$, one obtains the quantity about $2.4 \times 10^{-4} \mu$ for the Peierls stress in lattices with atoms facing alternately along slip plane. Meanwhile the Peierls stress in the rectangular lattices is about $5.2 \times 10^{-2} \mu$ from eq (10). The difference between these two quantities explains naturally the difference in the Peierls stress between covalent crystals and metals. The atoms just above and below the slip plane face each other in the diamond lattice which is typical of covalent crystals, while the atoms face alternatively along the slip plane in metals. The hydrogen bonded crystals belong to the former group, and ionic crystals such as alkali and silver halides belong to the latter group. The Peierls stress in covalent crystals such as germanium and silicon is supposed to be of the order of 100 Kg/mm², while that in face-centered cubic metals is of the order of or less than 1 Kg/mm².

The force-displacement relation (2) assumed by Peierls and Nabarro is of course too simple. Forman, Jaswon, and Wood [7] modified this relation so as to decrease the restoring force for large displacement while keeping it constant for small displacement. The weaker the restoring force for large displacement, the wider is the dislocation. The Peierls stress decreases remarkably with the decrease of the restoring force. The sinusoidal law (2), however, is a rather good approximation for the shearing displacement along slip plane as discussed in section V. The Peierls stresses obtained from eqs (8) and (10) do not seem to be modified in the order of magnitude.

¹This summation is correct approximately for edge dislocations. However, the adequacy of this summation is easily seen for screw dislocations provided that the distance between rows of atoms parallel to the screw dislocation is substituted for the atomic distance b .

IV. Numerical Computations on Atomic Configurations and Peierls Stress of Dislocations

Peierls' approximation is of course very crude to calculate the core structure. It is the next step to calculate the position of each atom assuming a pairwise potential between atoms. The interatomic potential, however, is difficult to define, especially in metal crystals. In the case of ionic crystals and in inert gas crystals, the nature of the interatomic force is rather well understood and approximated by a central force which depends only upon the distance between atoms or ions. The core structures of edge and screw dislocations in NaCl crystal were calculated by Huntington, Dickey, and Thomson [8]. Kurosawa [9] calculated the Peierls stress for an edge dislocation in an ionic crystal.

Some calculations have been carried out for metals assuming appropriate potentials. In the case of face-centered cubic metals Cottrill and Doyama [10, 11] used Morse potential which is given by

$$\phi(r_{ij}) = D[\exp\{-2\alpha(r_{ij} - r_0)\} - 2 \exp\{-\alpha(r_{ij} - r_0)\}]. \quad (12)$$

They demonstrated that a perfect dislocation dissociates spontaneously into two half dislocations connected by stacking fault.

Core structure of a screw dislocation in body-centered cubic metals are discussed by Chang [12], Bullough and Perrin [13], and Suzuki [3]. The former two assumed interatomic potential shown in table I, while the last used a simplest form of potential between closest-packed atomic rows which are parallel to the Burgers vector. According to Chang's calculation [12], a screw dislocation $a/2$ [111] dissociates symmetrically

TABLE I. Interatomic potential used for iron. $\phi(r)$ is in eV and r is in Angstroms.

R. Chang [12, 14]

$$\begin{aligned}\phi(r) &= -0.15614r^4 + 0.815729r^3 + 1.24594r^2 - 12.2404r + 16.0183 \\ &\quad (2.40 < r \leq 3.3894) \\ &= 34.0878r^4 - 327.9263r^3 + 1184.7172r^2 - 1905.7946r + 1152.0160 \\ &\quad (r \leq 2.40)\end{aligned}$$

R. Bullough and R. C. Perrin [13]

$$\begin{aligned}\phi(r) &= -2.195976(r - 3.097910)^3 + 2.70406r - 7.436448 \\ &\quad 1.9 \leq r \leq 2.4 \\ &= -0.639230(r - 3.115829)^3 + 0.477871r - 1.581570 \\ &\quad 2.4 \leq r \leq 3.0 \\ &= -1.115035(r - 3.066403)^3 + 0.466892r - 1.547967 \\ &\quad 3.0 \leq r \leq 3.44\end{aligned}$$

into three partials $a/6$ [111] on three {110} planes with faults of one atomic distance width as shown in figure 1, where each circle indicates a [111] atomic row normal to the plane of the figure and the numerals in the circles denote the positions of atoms in the unit of $b/3$. Here b is the distance between atoms in the [111] atomic row. Suzuki [3] obtained the same core structure by a very simple calculation, in which the interaction potential between [111] atomic rows was given by a sinusoidal function of relative displacement of atomic rows and no relaxation was allowed in other directions than the dislocation line. Meanwhile, Bullough and Perrin [13] reported asymmetric dissociation, using the potential in table I.

In the calculation of the Peierls stress for a dislocation in a discrete lattice, one must be careful to specify the position of the dislocation and to correct the interaction energy between the dislocation and the surface of the model crystal. These two points are not very important in the calculation of the position of atoms around the dislocation. Some of the calculations of the Peierls stress hitherto made seem to be incorrect because of ignoring these two points.

The most reliable calculation of the Peierls stress is due to Kurosawa [9]. His calculation is for an edge dislocation in NaCl type crystal, of which the slip plane is (110) and the Burgers vector is a [1 $\bar{1}$ 0]. The interionic

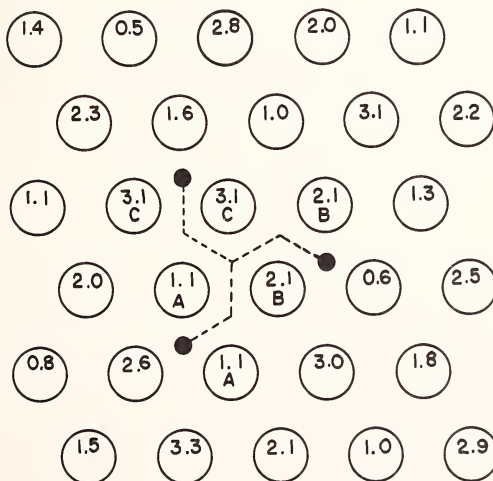


FIGURE 1. Atom arrangement of screw dislocation in b.c.c. iron viewed along the dislocation line. The dislocation $a/2$ [111] dissociates into three partials with the Burgers vector $a/6$ [111]. The stacking faults are shown by broken lines. (Based on the calculation by Chang [12])

potentials are assumed to be

$$-\frac{e^2}{r} + \frac{\alpha_M e^2 \rho}{6a^2} \exp [-(r-a)/\rho] \quad (13)$$

between ions of the opposite sign, and

$$e^2/r \quad (14)$$

between ions of the same sign, where α_M is the Madelung constant, and a is the lattice constant.

In the case of edge dislocation on (110) plane in NaCl type crystal, the straight rows of ions parallel to the dislocation line are rigid and the displacements are only in its normal direction. The potentials between the rows of ions are given by

$$\phi(r) = \frac{4e^2}{a} K_0 \left(\frac{\pi r}{a} \right) \quad (15)$$

for like rows, and

$$\phi(r) = -\frac{4e^2}{a} K_0 \left(\frac{\pi r}{a} \right) + \frac{\alpha_M e^2 \rho}{6a^2} \exp \left\{ -\frac{(r-a)}{\rho} \right\} \quad (16)$$

for unlike rows, per length of a . Here $K_0(z)$ is the Bessel function of order zero with imaginary argument.

In the calculation of the Peierls stress Kurosawa divided the crystal into two regions C and D . In the region C the positions of rows of ions are independent variables, while in the region D the displacement of each row of ions (δx , δy) is given by

$$(\delta x, \delta y) = (u(x_i - \xi, y_i) - u(x_i, y_i) + \sigma y_i, v(x_i - \xi, y_i) - v(x_i, y_i)), \quad (17)$$

where $u(x_i - \xi, y_i)$ and $u(x_i, y_i)$ are the x -components displacement of row of ions at (x_i, y_i) due to the edge dislocation at $(\xi, 0)$ and at $(0, 0)$, respectively, $v(x_i - \xi, y_i)$ and $v(x_i, y_i)$ are the y -components of the same quantity, and σy_i is the displacement by homogeneous shear in the x -direction. At first regarding σ and ξ as independent variables he calculated the positions of rows of ions in the region D by means of (17). Next he calculated the equilibrium positions of rows of ions in the region C under the boundary condition given by the positions of rows of ions in the region D . If σ and ξ are properly taken each other, all rows of ions are force free. Otherwise the rows in D , particularly the rows in the vicin-

ity of the boundary of C , are not in equilibrium. Correct combinations of σ and ξ are searched for by this criterion. He adopted the moment

$$M = \sum_i F_{ix} y_i \quad (18)$$

as the equilibrium criterion, where F_{ix} is the x -component of the force acting on i -th row, and the summation is taken over the region D . Then the relations between σ and ξ were calculated as shown in figure 2. The maximum strain σ corresponds to the ratio of the Peierls stress to the shear modulus μ . The Peierls stress was about $2 \sim 6 \times 10^{-3}\mu$ as shown in figure 3. The calculation by Kurosawa is for rather a small number of rows of ions due to the limitation of the capacity of computer, but he took into account correctly the boundary condition.

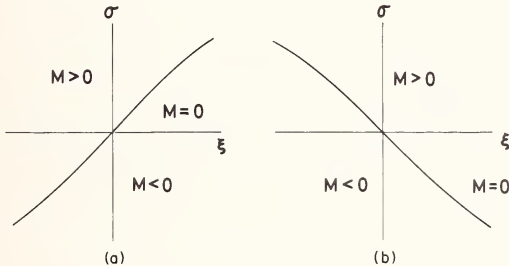


FIGURE 2. Illustrations of the relations between M , σ , ξ , the state of $M=0$ corresponds to the minimum energy of the dislocation in the left figure and to the maximum in the right one. (After Kurosawa [9])

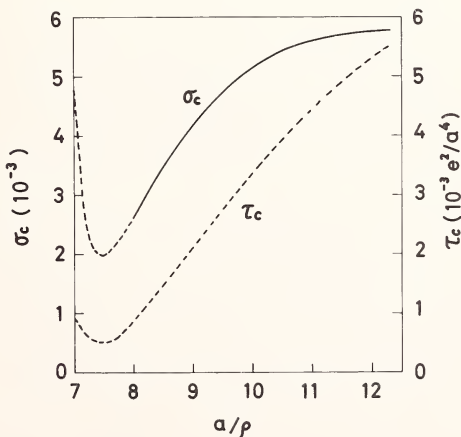


FIGURE 3. The critical yield strain σ_c and stress τ_c as a function of a/ρ . (After Kurosawa [9])

V. Peierls Stress for a Screw Dislocation in a Body-Centered Cubic Crystal

The Peierls stress of a screw dislocation in a body-centered cubic crystal is considerably higher than a face-centered cubic crystal. Chang [12] obtained a value of Peierls stress comparable with observation, while Suzuki [3] obtained a value of about ten times of that. However, Chang assumed that the energy of a screw dislocation is a periodic function of its position with the period of $\sqrt{6} a$ for the motion along $\{110\}$ plane, where a is the lattice parameter. It is, however, evident that a perfect body-centered cubic crystal is invariant for the translation $a/2[111]$. The component of this translation normal to the dislocation line is $\sqrt{2}/3a$. The energy of a screw dislocation must be identical at positions of this separation, provided that we neglect the interaction with the crystal surface. Chang obtained, however, different values of potential energy of dislocation at positions separated by $\sqrt{2}/3a$. His estimation of Peierls stress was based on this energy change, so it is reasonable to suppose that the Peierls stress differs considerably from his result if the calculation is carried out correctly.

The Peierls stress of a screw dislocation in a body-centered cubic crystal was calculated for a simple potential in the previous paper [3]. Then the calculation was continued for a different potential given by the following expression

$$\phi_{ij} = A \left[\cos \left(2\pi \frac{z_i - z_j}{b} \right) - \alpha \cos \left(4\pi \frac{z_i - z_j}{b} \right) \right] \quad (19)$$

where

$$A = \frac{\mu b^2}{2\sqrt{3}\pi^2(1-4\alpha)} \quad (20)$$

Here z_i, z_j are the coordinates of atoms in the i th and j th atomic rows, b the magnitude of Burgers vector, μ the shear modulus, and α a constant. In order to have only one maximum and minimum of potential energy during one atomic distance displacement, the value of α must be limited in the range

$$-1/4 < \alpha < 1/4. \quad (21)$$

The relations between ϕ_{ij} versus $(z_i - z_j)/b$ are shown in figure 4 for various values of α . The values of ϕ_{ij} is denoted in the unit of μb^2 and the zero is taken at the value of ϕ_{ij} for $z_i - z_j = b/3$. The curves differ from each other so markedly for different values of α , especially for the values larger than 0.2.

The interaction energies between neighbouring two [111] rows of atoms are also calculated from the pairwise potential used by Chang

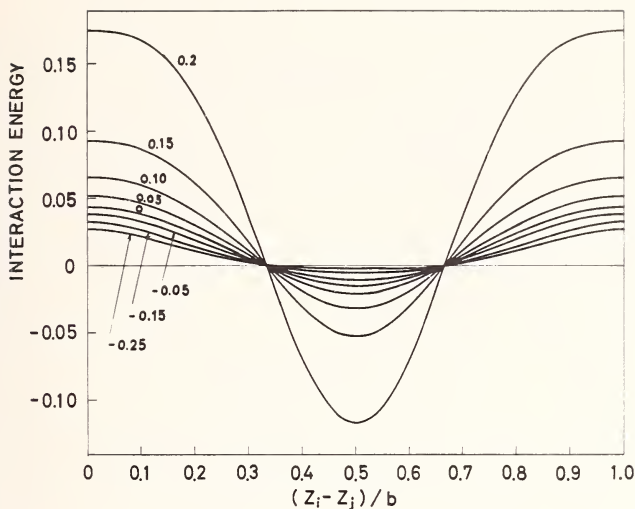


FIGURE 4. Interaction energy between two [111] rows of atoms calculated from eq (19) for various values of α , which are denoted by numerals on each curve. The energy is shown in the unit of μb^2 , and the zero of the energy is taken as the energy between the rows in the perfect crystal configuration.

[12, 14] and Johnson [15] or Bullough and Perrin [13]. The curves are calculated for different distances between rows of atoms and shown in figures 5 and 6. From these curves we can obtain the interaction energies under the conditions of no force in the direction normal to the row of atoms, and also of suitable force in that direction compatible with strain of the surrounding material.

The interaction energy denoted by eq (19) may be a good approximation of the effective interaction energy allowing the relaxation in the direction normal to the row of atoms if the value of α is selected appropriately. Comparing figure 4 with figures 5 and 6, it is evident that the possible interaction potential is given by eq (19) for the values of α between -0.1 and 0.05.

The potential energy of a screw dislocation was calculated for the position of atoms evaluated by isotropic elastic theory. The model crystal was composed of 380 arrays of [111] atom rows.

The energy of the dislocation was also calculated, locating the dislocation at different positions which would satisfy the translational symmetry if the crystal had infinite size. The difference in these energies give the interaction energy between the crystal surface and the dislocation and used for the correction of the potential energy of the dislocation by interpolation.

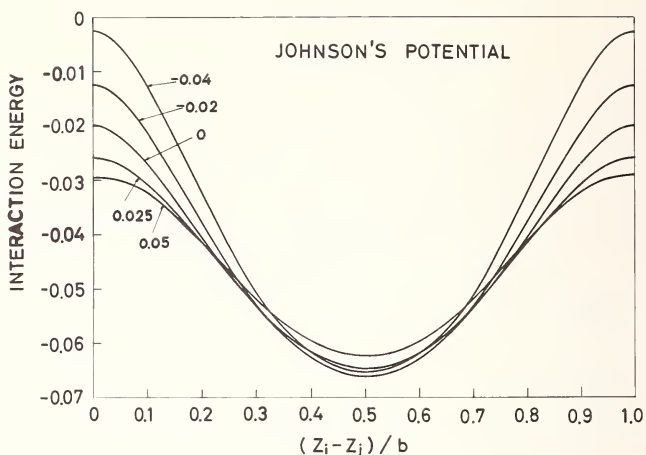


FIGURE 5. Interaction energy between two [111] rows of atoms calculated from Johnson's pairwise potential. The numerals on each curve mean the difference of the distance between the rows from its equilibrium value. The unit of energy is μb^2 .

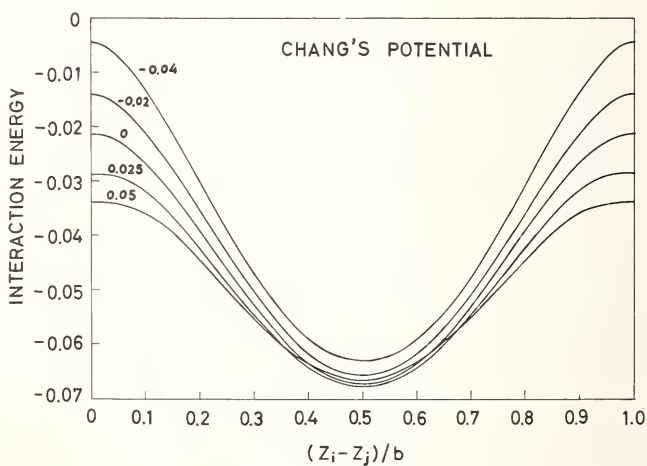


FIGURE 6. Interaction energy between two [111] rows of atoms calculated from Chang's pairwise potential.

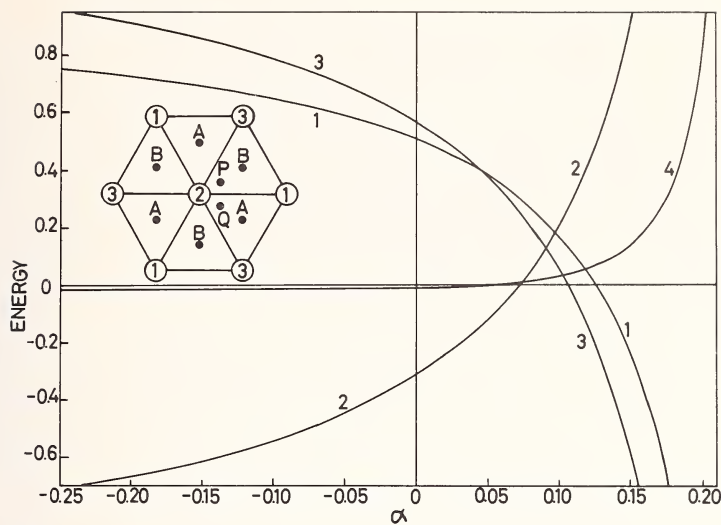


FIGURE 7. Various energy differences plotted against α . The triangle net shows atom arrangement of body-centered cubic crystal viewed along [111] direction. A number in the circle shows the position of an atom in each [111] atom row in the unit of one third of the atomic distance. The unit of energy is $\mu_0 b^2 / 2 \sqrt{3} \pi^2$.

- Curve 1: The potential energy difference between P and A .
- Curve 2: The potential energy difference between Q and B .
- Curve 3: The potential energy difference between B and A .
- Curve 4: The zero-point energy difference between P and A .

Figure 7 denotes the difference of potential energy of a screw dislocation between at some representative positions. The relative height of potential energy between the triangle A and B is reversed when the value of α increases beyond 0.106.

The equipotential curves for $\alpha=0$ is shown in figure 8. The map of these curves changes considerably if α increases more than 0.07. Centers of both kinds of triangles A and B are the positions of potential minimum for $0.07 < \alpha < 0.125$. Then the dislocation moves passing the line connecting the centers of neighbouring triangles. The plausible values of α for actual body-centered cubic crystals are less than 0.05, and correspond to the potential map shown in figure 8.

The magnitude of the Peierls stress is estimated from the potential energy difference between the stable and saddle points. In the region of plausible values of α , the Peierls stress is about 0.05μ and is larger by one order of magnitude than that expected from experiments as already mentioned in a previous paper (Suzuki [3]). The discrepancy may decrease by employing more suitable potential between atoms and allowing full relaxation of the position of atoms. The high Peierls potential for

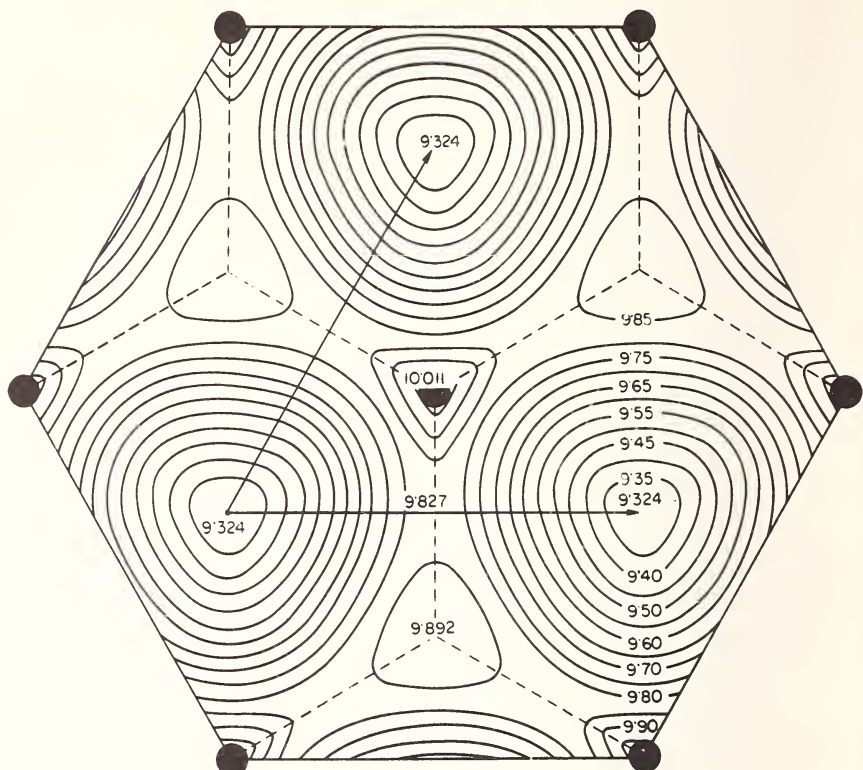


FIGURE 8. Potential energy of a screw dislocation in a body-centered cubic crystal for the interaction energy of $\alpha=0$. Filled circles indicate the positions of rows of atoms. The numerals in the figure indicate the energy in the unit of $\mu_0 b^2/2 \sqrt{3}\pi^2$.

a screw dislocation in a body-centered cubic crystal arises, however, from the geometry of the crystal as discussed in the previous paper. The above-mentioned calculation indicates that the height of Peierls potential does not change significantly over wide range of the value of α . The decrease of the potential energy due to the relaxation in the direction of the rows of atoms is only about twenty percent of the Peierls potential itself.

It must also be mentioned that the most plausible calculation of Peierls stress by Kurosawa on ionic crystals with NaCl type structure is several times larger than the values expected from experiments. We can, therefore, conclude that the discrepancy between the calculations and the experiments can not be removed completely only by the calculation in which the positions of atoms are determined by minimizing the total potential energy of the crystal and the Peierls stress is defined as the maximum value of the derivative of the total potential energy differentiated by the position of the dislocation.

VI. Zero-Point Energy of a Vibrating Dislocation

Kuhlmann-Wilsdorf [5] has arrived at almost the same conclusion in the previous section because the core energy change during the motion of dislocation must be less than 10^{-4} of the core energy itself if the Peierls stress is less than 1 Kg/mm². She introduced the concept of the uncertainty in the position of dislocation and pointed out a possibility to decrease the Peierls stress. Her concept of the uncertainty in the dislocation position is based on the uncorrelated motion of atoms in the crystal, but the motion of atoms at very low temperature is in the ground state and necessarily correlated. At high temperatures, the motion of each atom becomes to be uncorrelated, but we must use free energy including the entropy which may reverse the discussion based only upon the potential energy.

The present author [3] pointed out that the zero-point energy of dislocation line is less at the top of the potential hill than at the bottom of potential valley, so the Peierls stress decreases by the zero-point motion. The previous calculation, however, for straight dislocation. Then we would like to estimate the zero-point energy at the saddle point during the formation of a double kink.

The vibration of a dislocation about the saddle point configuration of the formation of double kink has been discussed by Celli, Kabler, Nino-miya, and Thomson [16] and by Seeger and Schiller [17]. Celli et al. especially discussed the localized and the translation modes associated with the double kink. We will discuss the effect of zero point motion based on their treatment.

For simplicity assume the Peierls potential made up of pieces of parabolas,

$$\begin{aligned}
 \text{I} \quad E(x) &= Px^2/2 && \text{for } |x| < a/4 \\
 \text{II} \quad E(x) &= Pa^2/8 - P(x-a/2)^2/2 && \text{for } a/4 < x < 3a/4 \\
 \text{III} \quad E(x) &= P(x-a)^2/2 && \text{for } |x-a| < a/4
 \end{aligned} \tag{22}$$

The equation of motion of the dislocation under external stress, τ , is

$$\begin{aligned}
 M \frac{\partial^2 x}{\partial t^2} &= T \frac{\partial^2 x}{\partial z^2} - \frac{dE(x)}{dx} + \tau b \\
 &= T \frac{\partial^2 x}{\partial z^2} - Px + \tau b && \text{in regions I and III} \\
 &= T \frac{\partial^2 x}{\partial z^2} + P(x-a/2) + \tau b && \text{in region II}
 \end{aligned} \tag{23}$$

where M is the mass of the dislocation per unit length, and T is the line tension of the dislocation.

Since the effect of zero-point motion is to decrease the effective Peierls stress, the saddle point configuration of the double kink formation must be wider than that determined only by the potential energy consideration. However, for simplicity we neglect the difference between these two configurations.

Let

$$x = x_0 + \xi e^{i\omega t} \quad (24)$$

where x_0 is the static solution denoting the saddle point configuration. The time independent equation of motion for the small oscillation about the saddle point is then

$$\begin{aligned} T \frac{d^2\xi}{dz^2} + (M\omega^2 - P)\xi &= 0 && \text{in region I and III} \\ T \frac{d^2\xi}{dz^2} + (M\omega^2 + P)\xi &= 0 && \text{in region II} \end{aligned} \quad (25)$$

At the boundary between different regions the value of ξ and $d\xi/dz$ must be continuous, and the following relation must be satisfied

$$T \left(\frac{d^2\xi}{dz^2} \right)_{z=z_1}^I - P\xi^I(z_1) = T \left(\frac{d^2\xi}{dz^2} \right)_{z=z_1}^{II} + P\xi^{II}(z_1) \quad (26)$$

The most important are the modes with the frequencies below than ω_0 , where $\omega_0 = \sqrt{P/M}$. As discussed in detail by Celli et al. there are two translational modes associated with the double kink. The one is a longitudinal motion of the double kink in which both members of kink move in opposite direction, tending to expand or contract the double kink. The other is the translational motion of the double kink. In this mode both sides of the double kink move in the same direction, and their net separation is not changed during the vibration. The two translational modes are newly introduced by the formation of double kink.

There is no localized mode with the frequency below than ω_0 other than the translational modes provided that the saddle point configuration is determined by static equilibrium condition.

For the vibrational frequency above ω_0 , dislocation segments in both regions vibrate as if those are independent segments of straight dislocations with suitable boundary conditions. The difference between the zero-point energy between the infinitely straight dislocation approximation, and in the case of double kink formation is then shown schematically in figure 9.

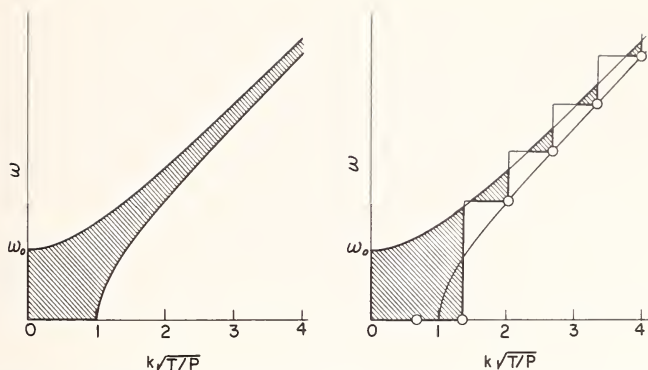


FIGURE 9. The zero-point energy difference between the infinite straight string model (a), and the finite length string model with the Debye cutoff (b).

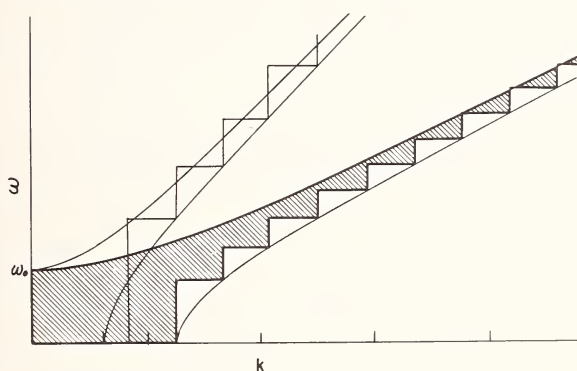


FIGURE 10. The effect of the widening of the double kink on the zero-point energy difference in the finite length string model with the Debye cutoff.

In the infinitely straight dislocation approximation, the relations between ω and k at the bottom of the potential valley and at the top of the potential hill are shown by smooth curves, respectively, while in the case of double kink there are only discrete points. The zero-point energy in the infinitely straight dislocation approximation is proportional to the shaded area bounded by the two smooth curves and coordinate axes in the figure (a), while in the double kink the difference is proportional to the area shaded in the figure (b).

It is easily seen from these figures that the approximation of infinitely straight dislocation overestimates the effect of zero-point motion. However, it must be mentioned that if the width of double kink at the saddle point increases, the frequencies change as shown in figure 10, and the effect of zero-point motion increases considerably, approaching to infinite length approximation. Then the zero-point energy has the effect of decreasing the Peierls potential itself in the calculation of the static equilibrium of the saddle point configuration.

VII. Change in Zero-Point Energy Due to Anharmonicity

As mentioned in the previous section, the Peierls potential decreases by the zero-point motion of dislocation. The amount of decrease, however, is only about ten per cent of the Peierls potential in body-centered cubic transition metals. Thus the zero-point motion of a dislocation line is not enough to explain the discrepancy between the calculation and observation. However, it must be mentioned that the zero-point motion of a dislocation line bears only a part of the change in the zero-point energy caused by the formation of a dislocation. A more important effect may take place through the anharmonicity of the crystal.

It is very difficult to evaluate the change in frequency spectrum of lattice vibration due to the change in force constant of each atomic row pair around a dislocation. Then we estimate the average change in shear modulus of the model crystal. The shear modulus along the atomic row is assumed to be proportional to the average of force constants between atomic rows, namely

$$\mu = K \sum_{i,j} \frac{\partial^2 \phi_{ij}}{\partial z^2} = -K \frac{4\pi^2}{b^2} A \sum_{i,j} \left[\cos \left(2\pi \frac{z_i - z_j}{b} \right) - 4\alpha \cos \left(4\pi \frac{z_i - z_j}{b} \right) \right] \quad (27)$$

where

$$A = \frac{\mu_0 b^2}{2\sqrt{3}\pi^2(1-4\alpha)}, \quad K = \frac{1}{\sqrt{3}N}. \quad (28)$$

Here N is the number of atomic rows in the model crystal, μ_0 is the shear modulus of the perfect model crystal in the direction [111]. Putting

$$\bar{W}(\alpha) = 2 \sum_{ij} \left[\cos \left(2\pi \frac{z_i - z_j}{b} \right) - 4\alpha \cos \left(4\pi \frac{z_i - z_j}{b} \right) \right], \quad (29)$$

we have

$$\frac{\mu}{\mu_0} = \frac{\bar{W}(\alpha)}{3N(1-4\alpha)}. \quad (30)$$

If the change in shear modulus is very small,

$$\frac{\Delta\omega}{\omega} \approx \frac{1}{2} \frac{\Delta\mu}{\mu_0}. \quad (31)$$

We have calculated the shear modulus change for the shear in the direction [111]. Taking [111] direction as z axis, the shear moduli C_{44} and C_{55} change according to eq (30). Another independent shear modulus

C_{66} may change in the same sense with C_{44} and C_{55} , but we neglect the change. Then the frequency of 4/9 of the total normal modes changes according to eqs (30) and (31). Using Debye approximation, the change in zero-point energy per unit length dislocation due to the anharmonicity is given by the relation

$$\begin{aligned}\Delta E_0 &= \frac{1}{2} \hbar \sum_n \Delta \omega_n \\ &= \frac{\hbar \omega_D}{12b} \frac{\Delta \bar{W}(\alpha)}{1 - 4\alpha}\end{aligned}\quad (32)$$

where ω_D is the Debye frequency of the lattice vibration, $\Delta \bar{W}(\alpha)$ is the difference of $\bar{W}(\alpha)$ between two specified positions of the dislocation.

If we assume the value ω_D , the relative difference of zero-point energy between two positions is obtained. The curve 4 in figure 7 shows the difference, ΔE_0 , between the saddle point P and the position A assuming the Debye temperature of the crystal to be 300 K. It must be noticed that ΔE_0 increases very rapidly with increasing α , and the magnitude is comparable with the potential energy difference in the region $0.10 < \alpha < 0.15$. Of course the values of α in this range do not seem to appear in real crystal. The change in zero-point energy given by eq (32) may be negligible in the real crystal. It must, however, be mentioned that the energy change (32) is the possible least value, and the actual value must be larger than this. If the calculation of zero point energy difference due to the change in force constants between rows of atoms were carried out correctly, the effect mentioned in the previous section must be included in the calculation.

VIII. Conclusions

In this paper the calculations of the Peierls stress hitherto made are criticized and the following conclusions are obtained.

a. The Peierls-Nabarro approximation may provide rather a good answer for the Peierls stress problem if the summation of the misfit energy is carried out correctly. Peierls' and Nabarro's result is for the lattices where the atoms face alternately along the slip plane, while the result by Kuhlman-Wilsdorf is for the lattices in which the atoms face each other along the slip plane. Significant difference between two results explains the different Peierls stresses between metals and covalent crystals.

b. The Peierls stress in the body-centered cubic crystal is necessarily high for a screw dislocation due to the crystal structure itself.

c. The Peierls stress depends strongly upon the crystal structure, but only weakly upon the details of the interaction potential between atoms.

d. The calculated Peierls stress ignoring the lattice vibration seems to be considerably higher than those expected from experiments.

e. The change of zero-point energy depending on the position of dislocation appears to be the most plausible origin of the discrepancy between the calculation and observation, but the quantitative discussion on this effect is extremely difficult.

IX. References

- [1] Peierls, R. E., Proc. Phys. Soc. London **52**, 34 (1940).
- [2] Nabarro, F. R. N., Proc. Phys. Soc. London **59**, 236 (1947).
- [3] Suzuki, H., in Dislocation Dynamics, A. R. Rosenfield, et al. Eds. (McGraw-Hill, New York, 1968) p. 679.
- [4] Cottrell, A. H., Dislocations and Plastic Flow of Crystals (Oxford Univ. Press, London, 1953).
- [5] Kuhlmann-Wilsdorf, D., Phys. Rev. **120**, 773 (1960).
- [6] Huntington, H. B., Proc. Phys. Soc. London **B68**, 1043 (1955).
- [7] Forman, A. J., Jaswon, M. A., and Wood, J. K., Proc. Phys. Soc. London **A64**, 156 (1951).
- [8] Huntington, H. B., Dickey, J. E., and Thomson, R., Phys. Rev. **100**, 1117 (1955); **113**, 1696 (1959).
- [9] Kurosawa, T., J. Phys. Soc. Japan **19**, 2096 (1964).
- [10] Cotterill, R. M. J., and Doyama, M., Phys. Rev. **145**, 465 (1966).
- [11] Doyama, M. and Cotterill, R. M. J., Phys. Rev **150**, 448 (1966).
- [12] Chang, R., Phil. Mag. **16**, 1021 (1967).
- [13] Bullough, R., and Perrin, R. C., in Dislocation Dynamics A. R. Rosenfield, et. al, Eds. (McGraw-Hill, New York, 1968) p. 175.
- [14] Chang, R., and Graham, L. J., Phys. Stat. Sol. **18**, 99 (1966).
- [15] Johnson, R. A., Phys. Rev. **134**, 1329 (1964).
- [16] Celli, V., Kabler, M., Ninomiya, T., and Thomson, R., Phys. Rev. **131**, 58 (1963).
- [17] Seeger, A., Schiller, P., in Physical Acoustics, IIIA, W. P. Mason Ed. (Academic Press, New York, 1966) p. 361.

POINT DEFECTS AND DISLOCATIONS IN COPPER

A. Englert,* H. Tompa

*Union Carbide European Research Associates
95, Rue Gatti de Gamond
Brussels 18, Belgium*

and

R. Bullough

*Theoretical Physics Division
A.E.R.E., Harwell
Didcot, England*

A new pair potential for copper has been constructed from a set of ten interpolated cubic polynomials. The form of the potential is such that at short range it agrees with the usual Born-Mayer repulsive potential and is in satisfactory agreement with the available phonon dispersion data and the observed stacking fault energy and vacancy formation energy for copper. The potential has been used to study the atomic configuration associated with various point and line defects in copper. In particular, because of its fit to the stacking fault energy, it provides a consistent result for the degree and nature of the dissociation to be expected for an edge dislocation in copper.

Key words: Computer simulation; copper; dislocation structure; pair-potential; point defects.

I. Introduction

Many physical phenomena depend on the detailed atomic configuration associated with point and line defects; thus, for example, the ductility of a metal is closely related to the atomic configuration in the dislocation cores. Also the various aging processes, involving the migration to and subsequent strong interactions between point defects and dislocations are dominated by the interactions arising from the long range configuration fields of the defects. These and many other important problems

*Visiting Research Associate, Harwell, Summer 1968.

Fundamental Aspects of Dislocation Theory, J. A. Simmons, R. de Wit, and R. Bullough, Eds. (Nat. Bur. Stand. (U.S.), Spec. Publ. 317, I, 1970).

cannot even be discussed until we have some estimate of the relevant atomic configurations.

At the present time the only feasible way to obtain an estimate of the atomic configuration associated with a defect as topologically complicated as a dislocation is to assume that the atomic interactions can be adequately described by a relatively simple two body potential. The required configuration can then be obtained by an iterative procedure with the aid of a large high speed digital computer. Such a procedure has been followed in several recent investigations [1, 2, 3] and will be followed in the present work. In section II we describe the physical basis and the construction procedure for the two body potential. A particular feature of the potential is its oscillatory form, which has arisen by carefully matching it to the pertinent phonon dispersion data and the observed stacking fault energy for copper. This potential is used, in section III, to obtain the energies and atomic configurations associated with a vacancy, a divacancy, an intrinsic stacking fault and finally an edge dislocation. The relation of the present results to previous relevant theoretical results and their possible physical significance will be discussed.

II. The Pair Potential for Copper

The total potential consists of two parts: a volume dependent potential and a pairwise potential; the former simulates the cohesive energy arising from the free electron gas and the latter describes the ion-ion interactions which arise via polarization of the electron gas. In this work we shall ignore local changes in the volume dependent potential which probably occur in regions where the atomic configuration is far from perfect, and suppose that the effective interatomic forces can always be adequately described by the appropriate derivatives of the pair potential.

This model, though obviously open to criticism, has the distinct advantage over the simple central force models [2] with no volume term, that it does not erroneously enforce the Cauchy relations between the elastic constants.

The pair potential $V(r)$ is constructed from a set of 10 interpolated cubic polynomials (a so called "spline function") and extends up to the third neighbour separation in the perfect copper lattice at which point it is arbitrarily set to zero with zero slope and curvature. At interatomic distances less than the first neighbour separation in the perfect lattice the potential was carefully matched to the Born-Mayer repulsive potential

$$V(r) = A \exp [-\rho(r - r_0)/r_0]$$

with the constants $A = 0.051$ eV, $\rho = 13$ Å and $r_0 = 2.551$ Å as determined by Vineyard et al. [4] from radiation damage experiments. The spline function may be represented by the equation

$$V(r) = A_K(r - r_K)^3 + B_K(r - r_K)^2 + C_K(r - r_K) + D_K$$

where K runs from 1 to 10 and r_K are the interatomic separations at which adjacent cubics are joined (with continuous first and second derivatives); such points are usually referred to as knots. The numerical coefficients A_K , B_K , C_K and D_K have been determined by ensuring that $V(r)$ satisfies the above criteria at each end of its range together with the following data:

- (i) The pair potential plus the volume dependent potential should lead to a stable face-centred cubic copper lattice with the correct lattice spacing of 3.608 Å.
- (ii) The derivatives dV/dr and d^2V/dr^2 of the pair potential should have values at the first and second neighbour equilibrium spacings that are consistent with the axially symmetric force constants for copper. The latter have been computed by Bullough and Hardy [5] who fitted a harmonic lattice model to the elastic constants and to the phonon dispersion data of Sinha [6]. If $\alpha_i = 2 \frac{d^2V}{dr^2}(r_i)$ and $\beta_i = \frac{2}{r_i} \frac{dV}{dr}(r_i)$, with $i = 1$ or 2, are the axially symmetrical force constants at $r_1 = 2.551$ Å and $r_2 = 3.608$ Å and the elastic constant values [7] $C_{11} = 1.67$, $C_{12} = 1.23$, $C_{44} = 0.75$ are adopted then we find, from Bullough and Hardy [5]:

	$r_1(2.551\text{\AA})$	$r_2(3.608\text{\AA})$
$\frac{dV}{dr}(r_i)$	-0.573	0.0294×10^{-4} dynes
$\frac{d^2V}{dr^2}(r_i)$	3.349	-0.0559×10^4 dynes/cm.

- (iii) The pair potential should lead to a vacancy formation energy E_f^v that is in good agreement with the most recent experimental value value of 1.14 ± 0.06 eV [8]. In fact we have, for the face-centered cubic lattice:

$$E_f^v = 6 V(r_1) + 3 V(r_2) - E_r^v$$

where $V(r_1)$ and $V(r_2)$ are the interaction energies at the first and second neighbour distances respectively and E_r^v is the relaxation energy as-

sociated with the vacancy. This last (correction) quantity can only be obtained when the pair potential has been fixed and the numerical procedure for estimating E_f^v will be described in the next section.

However, we know from previous experience that E_f^v rarely exceeds 10 percent of the total E_f^v and thus we simply adjusted the spline potentials $V(r_1)$ and $V(r_2)$ so that the contribution of the pair potential exceeded the experimental value of E_f^v by 10 percent. The result of the subsequent accurate relaxation, which will be described in the next section, lead to a theoretical E_f^v value of 1.09 eV which is sufficiently close to the experimental value.

(iv) Finally, the pair potential should lead to the experimentally observed intrinsic stacking fault energy of about 70 ergs/cm²[9]. If e_s

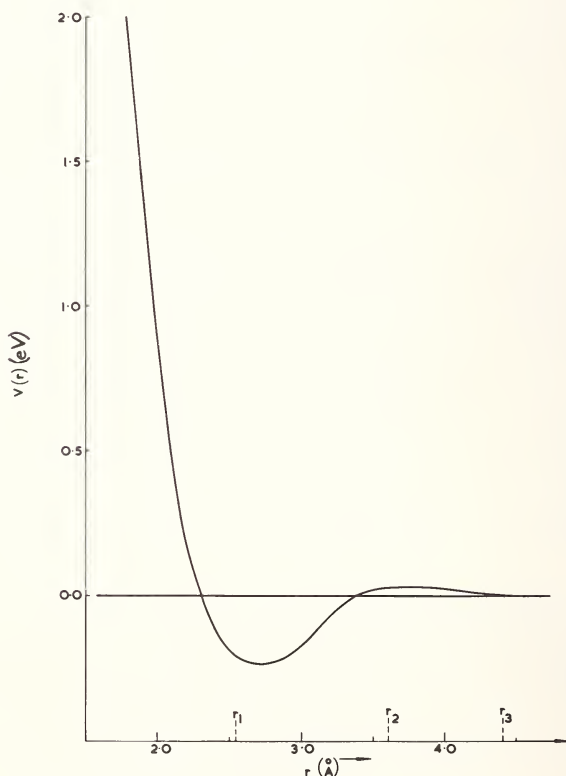


FIGURE 1. The pair potential for copper in electron volt units, r_1 , r_2 , and r_3 are the first, second and third neighbour spacings.

is the stacking fault energy per atom in the {111} plane then we have

$$e_s = 2V(r_s) - e_r$$

where $V(r_s)$ is the interaction energy at the particular separation $r_s = [8/3]^{1/2}r_1$ and e_r is the energy change per atom due to relaxations from the perfect stacking fault configuration. The procedure for calculating e_r and some detailed results are given in the next section. Again it was necessary to fit the potential value at r_s to a fault energy larger in magnitude than the observed value in order to compensate for its eventual reduction by relaxation. In fact to obtain satisfactory agreement with the experimental value of 70 ergs/cm² we set the unrelaxed value to 80 ergs/cm².

These criteria can be satisfied with a certain choice of the positions of the knots; the final positions r_K and the corresponding numerical values of the coefficients A_K, B_K, C_K, D_K are given in table 1; the units of the coefficients are such that $V(r)$ is expressed in electron volts with r and r_K in Angstrom units. The rather interesting oscillatory form of the potential shown in figure 1 has arisen as a direct consequence of the enforced stacking fault condition (iv) above, and such consistency with stacking fault energy data, is, of course, of paramount importance if we wish to use the potential to study the core configuration of a dislocation.

TABLE 1. *The coefficients of the pair potential for copper, given by a spline function consisting of 10 cubic equations*

$$V(r) = A_K(r - r_K)^3 + B_K(r - r_K)^2 + C_K(r - r_K) + D_K$$

each valid for $r_K \leq r \leq r_{K+1}$. V is in eV and r_K in Å.

K	$r_K(\text{\AA})$	A_K	B_K	C_K	D_K
1	1.	-667.9458	1081.8838	-628.5649	138.1100
2	1.5	-49.0449	79.9655	-47.6408	10.8050
3	2.0	-3.2382	6.3981	-4.4591	0.8453
4	2.551	-0.258148	1.045285	-0.357854	-0.210930
5	3.061199	-2.221407	0.650164	0.507164	-0.155699
6	3.341810	1.507669	-1.219882	0.347295	-0.011272
7	3.607658	-0.080144	-0.017445	0.018353	0.023168
8	4.209149	2.186182	-0.162063	-0.089620	0.010455
9	4.311190	-1.575972	0.507171	-0.054405	0.001945
10	4.418461	0.0	0.0	0.0	0.0

Several applications of this potential are discussed in the next section.

III. Atomic Configurations Around Defects in Copper

The atomic configuration associated with each defect was obtained by simulating the particular defect in an appropriate atomic assembly, or crystallite, of face-centred cubic copper. The free atoms adjacent to the defect were allowed to find their minimum potential energy configuration by what is now a standard dynamical relaxation procedure [10]. In every case investigated the dynamical relaxation procedure resulted in a satisfactory rate of convergence to the desired minimum potential energy configuration.

As we have discussed in the previous section the single vacancy and the intrinsic stacking fault were each necessarily studied in the course of actually constructing the potential $V(r)$. For the vacancy a cube assembly of atoms bounded by $\{100\}$ crystallographic planes was used. With the vacancy located at the centre of the cube, twelve shells of neighbours, or 248 atoms, were treated as independent particles and the atoms in the boundary layer of the cube were held fixed. The minimum energy configuration under the potential $V(r)$, corresponded to a vacancy formation energy of

$$E_f^v = 1.09 \text{ eV},$$

and was obtained after 65 preliminary relaxation sweeps through an assembly of half the linear size followed by 55 relaxation sweeps through the complete assembly. The displacements of the atoms in successive shells around the vacancy are shown in figure 2. In this figure the circles (joined by a curve) indicate the radial displacements in units of r_1 , the first neighbour distance.

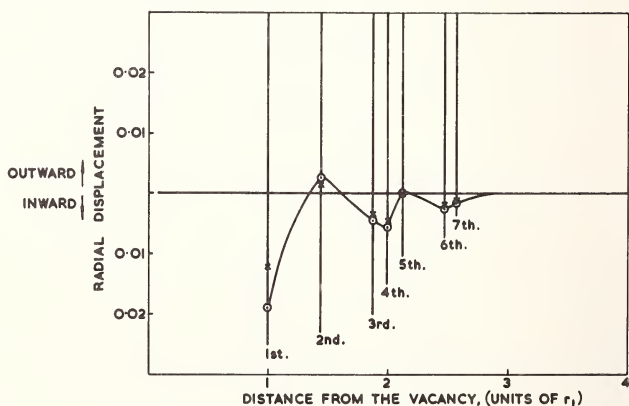


FIGURE 2. Displacements of atoms in successive shells around the vacancy in units of r_1 , the 1st neighbour distance.
 \odot , the results of the present calculation using $V(r)$.

X , the corresponding results of Bullough and Hardy using a harmonic lattice model.

We also show by crosses the displacements predicted by Bullough and Hardy [5] around a vacancy using a harmonic lattice model for copper. Apart from the 1st neighbour displacements the two sets of results are in very close agreement. We see that the 1st, 3rd, 4th, 6th and 7th neighbours all move inwards towards the vacancy and the 2nd neighbour moves outward; the 5th neighbour also has a very small outward displacement. The disagreement on the 1st neighbour displacements between this work and the harmonic lattice calculation is to be expected and indicates the magnitude of the error in adopting a simple harmonic lattice model in very close proximity to the defect.

To obtain the relaxation energy and associated atomic configuration of an intrinsic stacking fault we constructed a parallelepiped of atoms consisting of 40 closed-packed (111) planes bounded by the appropriate orthogonal {112} and {110} faces. Periodic boundary conditions were imposed across all the bounding faces and each (111) plane contained four atoms. An intrinsic stacking fault was introduced across one of the (111) planes near the middle of the parallelepiped and the entire assembly was allowed to dynamically relax under the potential $V(r)$. The only displacement which occurs was that of an entire (111) plane in the orthogonal [111] direction. The magnitude of the numerical computation was considerably reduced by taking advantage of the obvious symmetry across the fault plane. The relaxation energy was found to be surprisingly large; thus an ideal geometrical stacking fault energy of 79.8 ergs/cm² dropped to 70.5 ergs/cm² after complete relaxation.

The actual displacements of the adjacent (111) planes are shown in figure 3 and we see that for the potential $V(r)$ the sets of (111) planes

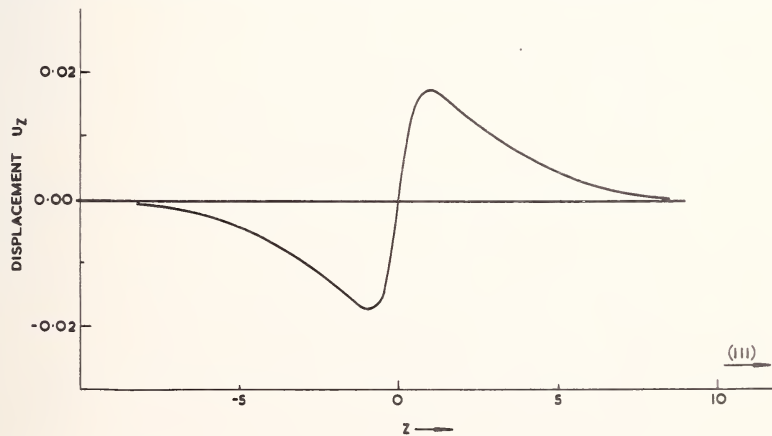


FIGURE 3. The displacements of the adjacent close-packed planes parallel to an intrinsic fault, in the [111] direction orthogonal to the fault. The displacements u_z are all away from the fault (at $z=0$) and are given in units of r_1 , the 1st neighbour distance. The relaxed stacking fault energy is 70.5 ergs/cm².

on either side of the fault each move *away* from the fault plane; the distance between the two neighbouring planes across the fault exceeded the corresponding distance in the unrelaxed configuration by almost 2 percent. The sense of this displacement is related to the sign of the stacking fault energy. Similar relaxations have been performed for various types of potentials and only when the potential was such that the corresponding fault energy was negative did the adjacent planes show a relaxation towards the fault.

The cubic array of atoms used to simulate the single vacancy has also been used to study the divacancy. In particular by removing two neighbouring atoms at the centre of the assembly and then relaxing the remaining atoms into their minimum potential energy configuration we obtained an estimate of the divacancy binding energy

$$E_B^{2v} = -0.31 \pm 0.01 \text{ eV}$$

which is in very good agreement with some previous theoretical estimates,¹ [11, 12, 13]. Unfortunately due to contamination difficulties, for which copper is infamous, a reliable experimental value cannot be quoted.

The core structure and dissociation of an edge dislocation in this "copper" lattice is being studied in some detail and we shall report some of our results for this defect which justify several interesting conclusions but also emphasize the need for further careful investigation. To study the dislocation a parallelepiped with $(\bar{1}10)$, (111) , and $(11\bar{2})$ faces containing 2700 freely interacting atoms was constructed. The assembly was only six layers thick in the $[11\bar{2}]$ direction and as extensive as possible in the other two directions. To enable a straight edge dislocation (parallel to the $[11\bar{2}]$) to be studied we impose periodic boundary conditions across the two $(11\bar{2})$ faces, and the dislocation is then introduced through the centre of the $(11\bar{2})$ planes by moving the atoms to their anisotropic elastic positions with the elastic singularity (the dislocation "line") placed midway between two appropriate (111) layers. The boundary atoms in the $(\bar{1}10)$ and (111) surfaces of the parallelepiped are then held in the above elastic positions and the remaining internal atoms are allowed to find the configuration with lowest potential energy (subject to the boundary displacement constraints) by the dynamical relaxation procedure. By using simple linear anisotropic elasticity and a constant stacking fault energy of 70 ergs/cm² it can easily be shown

¹This value is *not* in good agreement with the divacancy binding energy obtained by Bullough and Hardy. This poor agreement further emphasizes the danger of using a harmonic model in regions very close to defects.

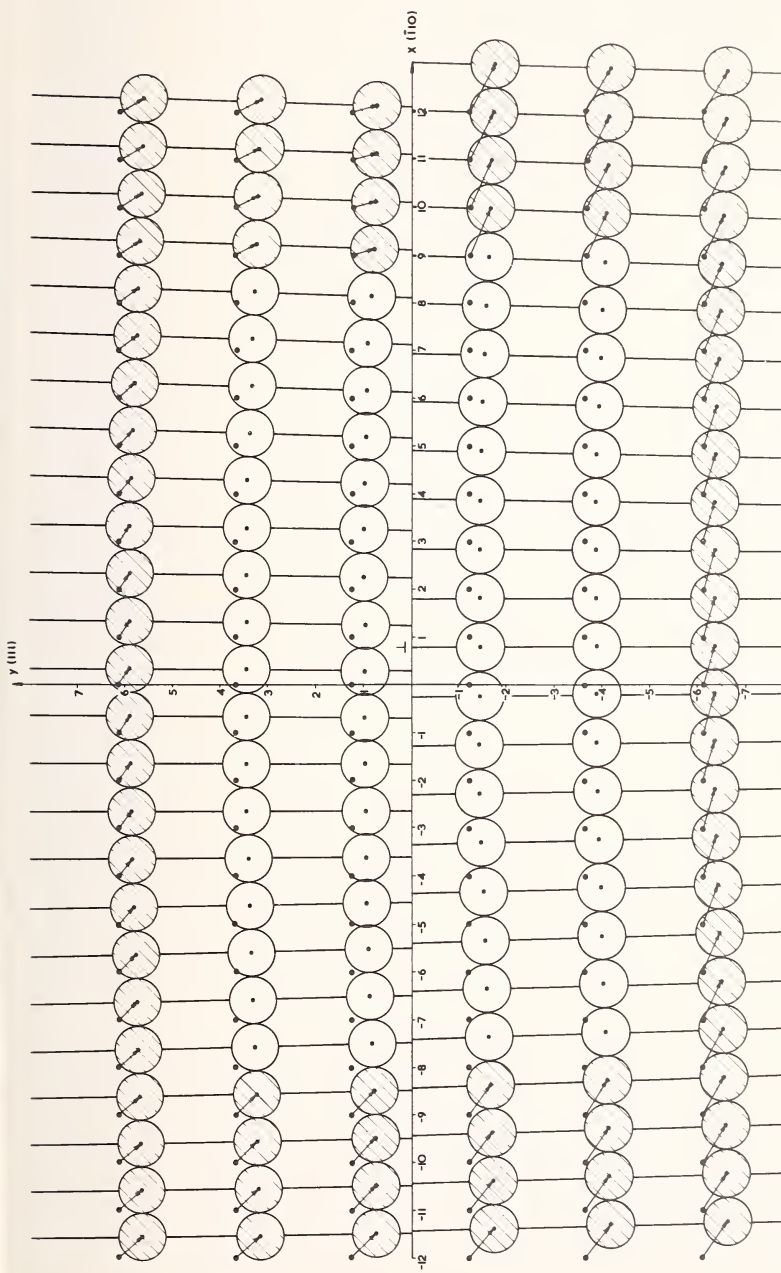


FIGURE 4. A $(11\bar{2})$ projection of the atoms, originally in a perfect $(11\bar{2})$ crystallographic plane, surrounding a positive edge dislocation in copper. The (x, z) plane is the slip plane and is situated midway between two (111) layers. The centre of the dissociated dislocation is indicated by the usual dislocation symbol. \odot represent the atomic positions in the perfect face centred cubic lattice; \circ represent the final dislocated positions. The final positions have been enclosed by circles that would display the close packed nature of the perfect lattice and the held (elastically dislocated) border atoms are identified by hatching.

that the equilibrium separation of the two elastic partials defining the above edge dislocation will be almost $8b$, where b is the magnitude of the total Burgers vector (the nearest neighbour distance). Since we expect that the extent of dissociation in our lattice model will be of comparable magnitude it was very soon clear that we could not study this dissociation dislocation without the partials getting rather close to the surfaces. The total number of mobile atoms in any numerical relaxation procedure is strictly limited by considerations of computer storage and speed. To obtain the precise equilibrium separation of the two partials in our model we had to proceed as follows.

The anisotropic elastic solution for a pair of parallel partial elastic dislocations which together constitute the anisotropic elastic model for a dissociated edge dislocation was obtained for arbitrary separation of the partials. This, rather complex solution, was used to fix the boundary conditions corresponding to three possible partial separations of $4b$, $6b$, and $8b$. The internal atoms were completely relaxed for each of these possibilities and the final potential energies were computed. The boundary constraints were such that the partials in the lattice always remained at the separations defined by the surface atom positions (the initial elastic solution) but the final potential energies of the three possibilities were *not* equal. The $4b$ energy was greater than either the $6b$ or $8b$ whereas the $8b$ energy was only slightly greater than the $6b$.

The final configuration for the $6b$ case is shown in figure 4. This figure shows the atomic configuration adopted by the atoms that were in one of the $(11\bar{2})$ crystallographic planes; for clarity the atoms originally in the other five $(11\bar{2})$ planes have been omitted. The perfect lattice positions and the final dislocation positions are both indicated; also we show the border atoms held in their anisotropic elastic positions (hatched). The centre of the faulted region is indicated by the usual dislocation symbol and the two cores on either side can be clearly seen. It is also apparent from this projection that the atoms above the slip-plane (the x , z axis) are under a high compressive strain whereas the atoms below the slip plane are under a high tensile strain.

We also note that the usual concept of a dissociated dislocation consisting of two partials separated by a region of *constant* stacking fault is in this case fallacious. The cores are so wide that their misfit spreads almost completely across the fault and even in the $8b$ nominal separation case there is only $2b$ of genuine perfect fault. It follows that the misfit energy, rather than the stacking fault energy will be the energy controlling quantity and thus explains the almost identical energies of the $6b$ and $8b$ nominal separations. Such relative insensitivity certainly suggests, for instance, that stacking fault energy estimates based on equilibrium node measurements may be rather questionable.

It is intended to extend this work by obtaining a quantitative estimate of the diffusivity in the fault and core regions and also to obtain the spatial variation of the binding energy of point defects to such a dissociated dislocation.

IV. References

- [1] Englert, A., and Tompa, H., *J. Phys. Chem. Solids*, **21**, 306 (1961); and *Ibid*; **24**, 1145 (1963).
- [2] Cotterill, R. M. J., and Doyama, M., *Phys. Rev.* **145**, 465 (1966).
- [3] Bullough, R., and Perrin, R. C., in *Dislocation Dynamics* (Proc. Battelle Inst. Mat. Science Colloquium—Harrison 1967) A. R. Rosenfield et al., Ed. (McGraw-Hill Book Co. New York, 1968) p. 175.
- [4] Gibson, J. B., Goland, A. N., Milgram, M., and Vineyard, G. H., *Phys. Rev.* **120**, 1229 (1960).
- [5] Bullough, R., and Hardy, J. R., *Phil. Mag.* **17**, 833 (1968).
- [6] Sinha, S. K., *Phys. Rev.* **143**, 422 (1966).
- [7] Overton, V. C., and Goffney, J., *Phys. Rev.* **98**, 969 (1965).
- [8] Wright, P., and Evans, J. H., *Phil. Mag.* **13**, 521 (1966).
- [9] Jøssang, T., and Hirth, J. P., *Phil. Mag.* **13**, 657 (1966).
- [10] Bullough, R., and Perrin, R. C., *Proc. Roy. Soc. A* **305**, 541 (1968).
- [11] Johnson, R. A., *Phys. Rev.* **152**, 629 (1966).
- [12] Bartlett, J. H., and Dienes, G. J., *Phys. Rev.* **89**, 848 (1953).
- [13] Seeger, A., and Bross, H., *Z. Physik*, **145**, 161 (1956).

ATOMISTIC CALCULATIONS OF DISLOCATIONS IN SOLID KRYPTON

M. Doyama

*Argonne National Laboratory and
University of Tokyo, Japan*

and

R. M. J. Cotterill

*Argonne National Laboratory and
The Technical University of Denmark
Lyngby, Denmark*

The elastic continuum theory treatment usually fails near the core of dislocations. Atomic calculations of edge and screw dislocations in solid krypton were carried out using a pairwise potential. In rare gases, the electron redistribution of the electron density is small, thus, this method is useful in studying the properties of dislocation cores.

Key words: Atomic calculation; interatomic potential; krypton.

I. Introduction

The elastic-continuum treatment of dislocations in solids has always suffered from difficulties associated with the dislocation core. The stress due to a dislocation, derived by this method, becomes infinite at the center of the dislocation. It is clear that such a singularity does not occur in a real solid. This difficulty is usually overcome by treating separately that part of the solid which lies inside a small cylindrical core whose axis is the dislocation line and the radius of which is r_c , say. This part is referred to as the dislocation core, where the linear elastic theory is said to break down. This procedure is, of course, unsatisfactory in estimating the energy and the atomic configuration within the core.

The difficulties associated with these points can be successfully overcome by the use of an atomistic model. In this model the interaction

potential between atoms was assumed by a central force function. Discrete atomic positions were obtained by minimizing the energy of the crystal containing a dislocation. The interaction potentials in metals are not well understood and the problem of the redistribution of the electron density in metals with lattice defects is difficult. In the previous treatment this redistribution of the electron density was ignored. In solid rare gases, however, it should be small and this method is particularly suitable for these solids. In this paper the energies and atomistic configurations of dislocations in solid krypton were calculated with the aid of the Argonne CDC 3600 digital computer and processed with a HITAC 5020E digital computer. The pairwise interaction between atoms was represented by a truncated Morse potential function.

II. Interaction Potential Function

In the present calculations the interaction energy between atoms was represented by a Morse function, a central-force function. The interaction energy $E(r_{ij})$ of a pair of atoms is then given by

$$E(r_{ij}) = D \{ \exp [-2\alpha(r_{ij} - r_0)] - 2 \exp [-\alpha(r_{ij} - r_0)] \}$$

where r_{ij} is the distance between the two atoms, D is the dissociation energy of the pair, r_0 is the equilibrium separation distance of the two atoms, and α is a constant which is effectively a measure of the "hardness" of the interaction. The energy of any atom in the crystal is then E_i , where $E_i = \sum_{j=1}^{i=J} E(r_{ij})$. Here J is the number of atoms in the sphere of influence.

J is related by a geometrical factor to the distance over which the interaction extends. The values of the constants must, of course, depend upon J . If J were 12 (i.e., of only nearest neighbors interact) then r_0 would be equal to the nearest-neighbor distance. In variational calculations of the type used here, the successive relaxations of atoms are rather time consuming even when the latest computers are employed; so it becomes impracticable to consider long range interactions. Moreover, one cannot be certain that the field of an atom is still adequately described by a Morse function at distance greater than a few nearest-neighbor distances. One would expect screening effects from other atoms to modify the field. In the work described here the potential was truncated at $\sqrt{9.4}$ nearest-neighbor distances and the constants were $r_0 = 4.1063 \text{ \AA}$, $\alpha = 1.3125 \text{ \AA}^{-1}$, $D = 0.0158135 \text{ eV}$. The energy of sublimation, the bulk modulus and the lattice constant were used to determine these constants. An additional constraint was that the Born stability criteria have to be satisfied.

III. Method of Computation

A. EDGE DISLOCATIONS

The edge dislocation examined in this study lies along a $\langle 112 \rangle$ direction. The slip plane is a $\{111\}$ plane. Its Burgers vector was of the type $(a_0/2)\langle 110 \rangle$. The six different resolved atomic positions (Elasto-atomic) of the atoms are given by the linear elastic continuum theory. The atomic configurations and the energy of the complete edge dislocation can be obtained by minimizing the energy of each atom, restricting the displacement perpendicular to the edge dislocation line.

Starting with the atomistic positions of the complete edge dislocation, the atomic configuration and the energy of dissociated edge dislocation can be also obtained by minimizing the energy of the crystal, relaxing each atom three dimensionally.

B. SCREW DISLOCATIONS

The screw dislocation investigated in this paper lies along a $\langle 110 \rangle$ direction. Its Burgers vector was therefore of the $(a_0/2)\langle 110 \rangle$ type. There are just two nonequivalent types of plane normal to a $\langle 110 \rangle$ direction in the fcc lattice. The positions of atoms of the elasto-atomic screw dislocation were fed into the computer. The atomic configuration of the complete screw dislocation was obtained by relaxing the atoms parallel to the screw dislocation. After this treatment, the atomic configuration of the dissociated screw dislocation was obtained by relaxing the atoms three dimensionally.

IV. Results

A. EDGE DISLOCATION

The atomic configuration of a complete edge dislocation in solid krypton could be obtained by relaxing the atoms perpendicular to the dislocation, thus preventing the dissociation into the Heidenreich-Shockley partial dislocations. After the atomic configuration of a complete edge dislocation was obtained, the atoms are relaxed three dimensionally. If the complete edge dislocation is in a metastable state it would not be dissociated into partials. The results showed, however, this is not the case. This means that the complete edge dislocation is not metastable but unstable: it split into a pair of Heidenreich-Shockley partial dislocations with no thermal activation energy. Figure 1 is the view looking down onto the slip plane for the dissociated edge dislocation. It shows the position of atoms in the $\{111\}$ plane immediately below the slip plane (circles), and the $\{111\}$ plane immediately above the slip plane (triangle). The dissociation can easily be distinguished by observing the figure from either side at a low angle. The energies of the elasto-atomic, com-

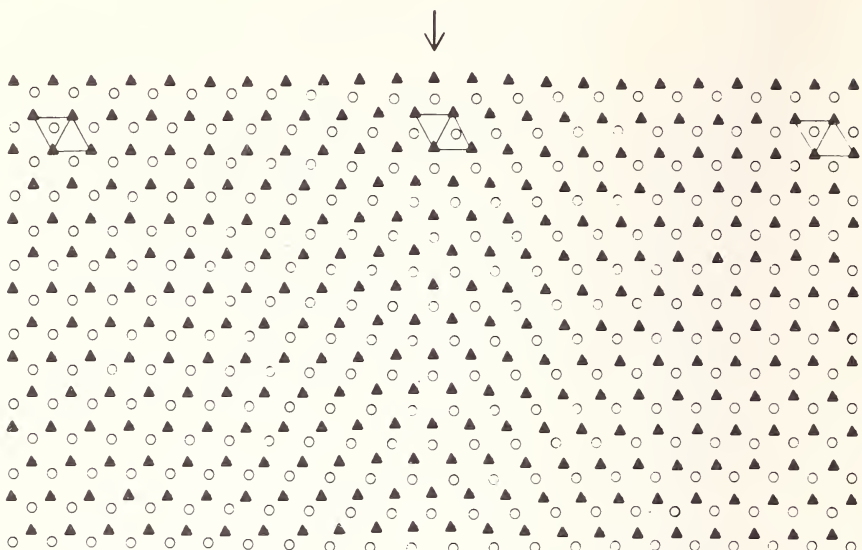


FIGURE 1. Positions of atoms in two $\{111\}$ planes, one above, \blacktriangle , and one below, \circ , the slip plane of a dissociated edge dislocation. The region of stacking fault which separates partial dislocations can easily be distinguished by observing the figure from either side at a low angle.

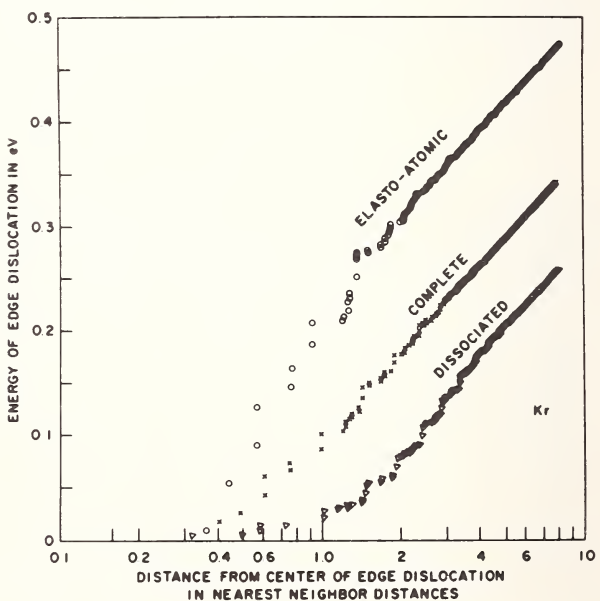


FIGURE 2. Energy within a given radius as a function of that radius as measured from the center of an edge dislocation.

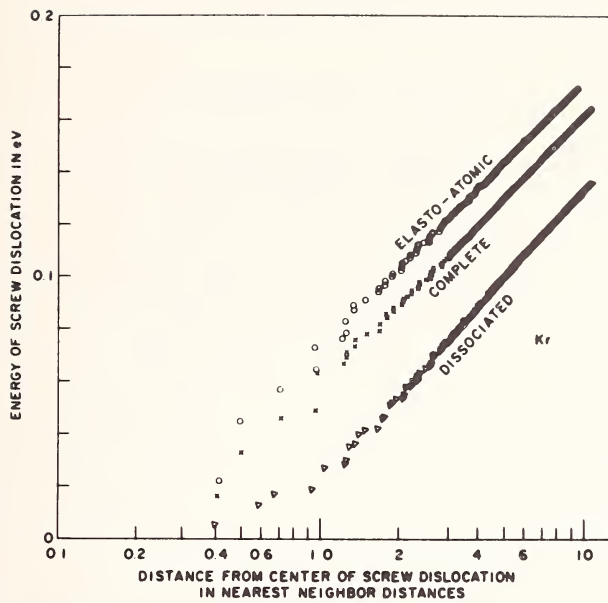


FIGURE 3. Energy within a given radius as a function of that radius as measured from the center of a screw dislocation.

plete and dissociated edge dislocation are plotted as a function of radius in figure 2.

B. SCREW DISLOCATION

It was also found that the complete screw dislocation was unstable and it split into a pair of Heidenreich-Shockley partials with no thermal activation energy. The energies of the elasto-atomic, the complete, and the dissociated screw dislocations are shown in figure 3.

V. Conclusions

Atomistic calculations of dislocations in solid rare gases can be obtained using a pairwise potential. In these solids, the redistribution of the electron density is not so important, thus this method is particularly useful. The atomic properties of the core can be studied in this way, and the method also has potential utility in the study of other defect problems such as jogs and the interactions between impurities, vacancies, or interstitials and dislocations.

A LATTICE THEORY MODEL FOR PEIERLS-ENERGY CALCULATIONS

A. Hölzler and R. Siems

*Institut für Theoretische Physik C, Technische Hochschule
Aachen, West Germany*

A lattice theory model for a screw dislocation is discussed which is similar to that of Maradudin. For the forces between neighbouring rows of atoms, however, a sinusoidal, not a linear, dependence of their relative displacements is assumed throughout the whole lattice. The displacements are expanded about the elastic theory values. The conditions of equilibrium then yield a system of linear equations for the deviations of the displacements from the elastic theory values, which is solved by an iteration procedure making use of Green's Function for a plane square lattice. For a number of points in the vicinity of the source point and for points in certain symmetry directions simple exact analytical expressions for the latter are derived, for points at larger distances an asymptotic expansion is given. The displacements thus obtained are then used to calculate the energies of the dislocation at the position of minimum energy and at the saddle point and their difference, the Peierls energy, by direct summation of the interaction energies of neighbouring pairs of atoms.

Key words: Computer simulation; Green's tensors; interatomic potential; lattice studies; Peierls energy; screw dislocation.

I. Introduction

In Maradudin's lattice theory model of a screw dislocation [1] the following assumptions are made concerning the displacements and the interatomic forces:

- (1) Only displacements parallel to the dislocation line are allowed.
- (2) Only forces between neighbouring rows of atoms are considered.
- (3) These forces are assumed to depend linearly on the relative displacements of the rows.

The equilibrium displacements and energies are calculated for two positions I and II of the dislocation line, corresponding to stable and unstable equilibrium (fig 1). The energy difference is the Peierls energy.

Due to assumptions (1) and (3) the calculated energies will be too large: Admitting radial displacements will allow the system to lower its energy,

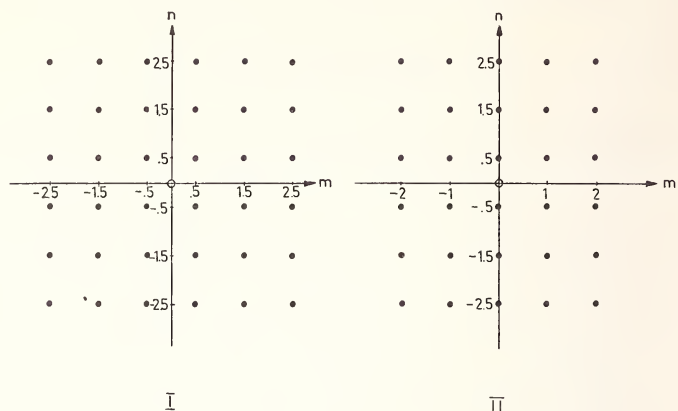


FIGURE 1. Projection of the lattice onto a plane perpendicular to the dislocation line. Open circles: Center of the dislocation. The figure shows two equilibrium positions of the dislocation: Configurations I and II.

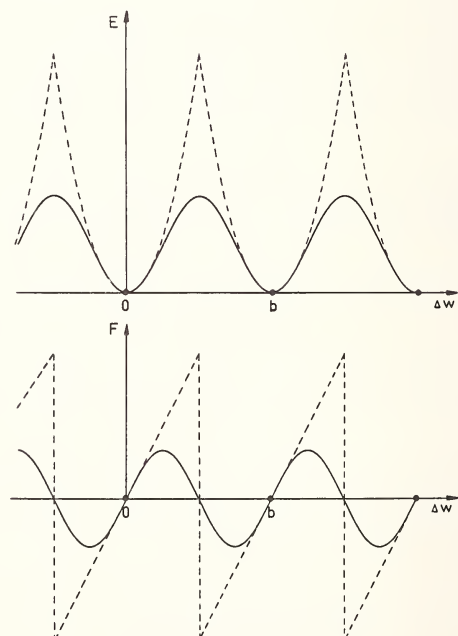


FIGURE 2. Interaction energy E and Force F versus relative displacement Δw of neighbouring rows of atoms. Dots: Equilibrium positions. Broken lines: Linear force law and parabolic energy law. Full lines: Sinusoidal force and energy laws.

and replacing the linear force law by a more realistic one with smaller forces for large displacements (fig 2) will also decrease the energy. These energy decreases are expected to be larger for the high energy configuration (II), i.e., the Peierls energy will be lowered. The largest contribution to a force law correction of the energy will come from the pair of atom rows at positions $(0, 1/2)$, $(0, -1/2)$ in situation II (fig 1). Maradudin calculated the displacements already under the assumption of zero force between these two rows, and Celli [2] determined the energy change corresponding to a sinusoidal force law for these two rows (the force laws for all other bonds being linear). If one applies Maradudin's energy formulas and Celli's correction to a $[001]$ dislocation in a cubic crystal (for which the projections in figures 1, I and 1, II form a square lattice with equal force constants for vertical and horizontal bonds) one obtains a negative value for the energy difference $E^{\text{II}} - E^{\text{I}}$. This might be due to the fact that, after Celli's correction is performed, the largest remaining relative displacements occur in situation I, so that an introduction of sinusoidal force laws for all bonds would mainly decrease E^{I} and thus make $E^{\text{II}} - E^{\text{I}}$ positive again.

In the present paper such a model with a sinusoidal force law for all bonds is considered. The equilibrium equations are set up and solved and from the displacements the Peierls energy is calculated. The force laws are similar to those used by Suzuki [3] for a $[111]$ dislocation in a bcc crystal.

II. Lattice Theory Model With Sinusoidal Force Law

A $[001]$ screw dislocation in a simple, b.c. or f.c. cubic lattice is considered. The projection of the atoms of the undisturbed crystal onto the (001) plane yields a square lattice in this plane (see fig 3). The dislocation is supposed to move parallel to most densely packed planes which are depicted by broken lines in figure 3. Assumptions (1) and (2)

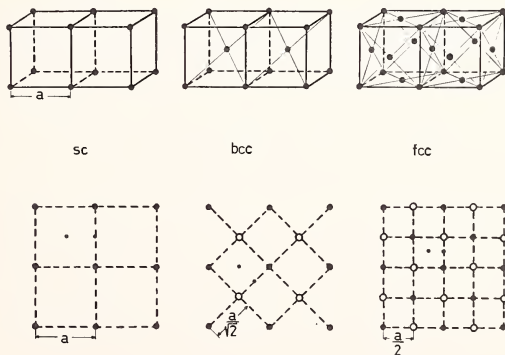


FIGURE 3. S.c., b.c.c., and f.c.c. lattices. The lower parts of the figure show the projection of atoms onto the (001) -plane. Broken lines: Most density packed planes.

are not changed. Instead of assumption (3), however, a sinusoidal dependence of the forces between neighbouring rows of atoms on their relative displacements is assumed: The force exerted by the row at position $\mu' = (m', n')$ on its neighbour at position $\mu = (m, n)$ is:

$$F_{\mu\mu'} = -B(2\pi)^{-1} \sin [2\pi(w_\mu - w_{\mu'})/b] \quad (1)$$

where w_μ is the displacement of the row μ and B/b is the force constant. The interaction energy of these two rows is

$$\delta E_{\mu\mu'} = bB(4\pi^2)^{-1} \{1 - \cos [2\pi(w_\mu - w_{\mu'})/b]\} \quad (2)$$

(the zero of energy has been chosen in such a way as to make the energy of the undeformed lattice zero).

The equilibrium conditions are then, with $Z_{\mu\mu'} = 1$ or 0 for $|\mu - \mu'| = 1$ or $\neq 1$ respectively:

$$\sum_{\mu'} Z_{\mu\mu'} \sin [2\pi(w_\mu - w_{\mu'})/b] = 0. \quad (3)$$

We want the dislocation solution of this system of equations. From the symmetry of the arrangements of atom rows in figures 1,I and 1,II it follows that the isotropic elastic theory solution

$$w_\mu = b \cdot (2\pi)^{-1} \phi_\mu = b(2\pi)^{-1} \operatorname{arctg} (n/m) \quad (4)$$

is the correct solution of eq (3) for the rows $(0, n)$, $(m, 0)$, (m, m) , $(m, -m)$ in situation I and for the rows $(0, n)$, $(m, 0)$ in situation II. It is hoped, and this hope is borne out by the results of our calculations, that the elastic solution (4) is a good approximation also for the rows between these symmetry directions. So, in order to facilitate the solution of (3), this system is linearized by an expansion about the elastic theory displacements:

$$w_\mu = b(2\pi)^{-1} (\phi_\mu + \eta_\mu).$$

Keeping only the lowest orders in η one obtains from eq (3) the linearized equations

$$\sum_{\mu'} Z_{\mu\mu'} \{(\eta_\mu - \eta_{\mu'}) \cos (\phi_\mu - \phi_{\mu'}) + \sin (\phi_\mu - \phi_{\mu'})\} = 0 \quad (5)$$

The neglected terms are smaller by factors of order η^2 .

III. Solution of the Equilibrium Equations by an Iteration Method

Introducing linear operators L and l defined by

$$(L\eta)_{\mu} = \sum_{\mu'} Z_{\mu\mu'} (\eta_{\mu} - \eta_{\mu'}) \quad (6)$$

$$(l\eta)_{\mu} = \sum_{\mu'} Z_{\mu\mu'} (\eta_{\mu} - \eta_{\mu}) [1 - \cos (\phi_{\mu} - \phi_{\mu'})] \quad (7)$$

and the inhomogeneity term

$$I_{\mu} = \sum_{\mu'} Z_{\mu\mu'} \sin (\phi_{\mu} - \phi_{\mu}) \quad (8)$$

the equilibrium conditions may be written in shorthand notation:

$$(L - l)\eta = I \quad (9)$$

with the solution

$$\eta = (L - l)^{-1}I = (1 - L^{-1}l)^{-1}L^{-1}I \quad (10)$$

$(L - l)^{-1}$ is the Green's function operator of the system (9) and L^{-1} that of the simpler system

$$L\eta = I \quad (11)$$

or, in components: $\sum_{\mu'} Z_{\mu\mu'} (\eta_{\mu} - \eta_{\mu'}) = I_{\mu}$.

The factors $\{1 - \cos (\phi_{\mu} - \phi_{\mu'})\}$ in $l\eta$ are smaller than 1. With a few exceptions they are even smaller than 0.14. The handling of these exceptional bonds will be discussed below. Expanding the right-hand side of eq (10) one obtains successive approximations, in analogy to Born's series:

$$\eta = L^{-1}I + L^{-1}lL^{-1}I + \dots$$

or

$$\eta = \eta^0 + \eta^1 + \dots \quad (12)$$

with

$$\eta^n = L^{-1}l\eta^{n-1}.$$

We define Green's function $G_{\mu\mu'}$ of the problem (11) by the equations

$$\sum_{\mu'} Z_{\mu\mu'} (G_{\mu\mu''} - G_{\mu'\mu''}) = \delta_{\mu\mu''} \text{ and } G_{00} = 0.$$

Simple exact expressions for Green's function $G_{\mu'\mu''} = G_{\mu'-\mu''} \equiv G_\mu$ of the problem (11) were obtained [4] for

- (a) points μ in the vicinity of (00).
- (b) points $\mu = (m, m), (m, m+1), (m, m+2), (m, m+3)$ with arbitrary (integral) m . For example

$$G_{\mu=(m,m)} = - (1/\pi) \left[1 + \sum_{k=0}^m (2k-1)^{-1} \right]$$

with $m \geq 0$.

For large $|\mu|$ an approximate expression for Green's function is [4]:

$$G_\mu^\infty = - (2\pi)^{-1} \{ \gamma + 1.5 \ln 2 + \ln r \} + (24\pi r^2)^{-1} \cos 4\theta$$

with $\mu = r (\cos \theta, \sin \theta)$.

The terms $\eta^0 = L^{-1}I$, $\eta^1 = L^{-1}l\eta^0$ in eq (12) are calculated successively:

$$\eta_\mu^0 = \sum_{\mu'} G_{\mu-\mu'} I_{\mu'} \quad \eta_\mu^1 = \sum_{\mu'} G_{\mu-\mu'} (l\eta^0)_{\mu'}$$

The sum is carried out explicitly for rows μ' within a circle of radius R centered at the dislocation and is replaced by an integration for rows μ' outside of this circle.

Actually the factors $\{1 - \cos(\phi_\mu - \phi_{\mu'})\}$ in eq (7) (c.f. eq (6)) are rather large for the bonds

$$(3/2, 1/2) - (3/2, -1/2) : .2$$

in situation I, noting that $(1/2, 1/2) - (1/2, -1/2)$ does not occur since $\eta_{1/2, 1/2} = \eta_{1/2, -1/2} = 0$, and for the bonds

$$(1, 1/2) - (1, -1/2) : .4$$

$$(0, 1/2) - (1, 1/2) : .553$$

in situation II, noting that $(0, 1/2) - (0, -1/2)$ does not occur since $\eta_{0, 1/2} = \eta_{0, -1/2} = 0$.

Therefore, to improve the convergence of the series in eq (12), the expression $l\eta$ (eq (7)) was split up into two parts, one of which ($l_1\eta$) contained only these bonds, while the other ($l_2\eta$) contained all the others. The Green's function corresponding to the set of equations

$$(L - l_1)\eta = I$$

was calculated [4]; it can be expressed in terms of the Green functions

$G_{\mu, \mu'}$ of eq (11). The values η_μ are then obtained, in the same way as explained before, from eqs (12) where now, however, L^{-1} is replaced by $(L - l_1)^{-1}$ and l by l_2 .

The resulting values of η are shown in table 1.

TABLE 1a. *The values of $\eta_{m,n}$ for Sit. I. ($\eta_{n,m} = -\eta_{m,n}$)*

$m \backslash n$	1/2	3/2	5/2	7/2	9/2
1/2	0	-0.04257	-0.01638	-0.00629	-0.00279
3/2	0.04257	0	-0.01023	-0.00765	-0.00486
5/2	.01638	.01023	0	-0.00486	-0.00354
7/2	.00629	.00765	.00328	0	-0.00153
9/2	.00279	.00486	.00354	.00153	0
11/2	.00122	.00282	.00284	.00188	.00080

TABLE 1b. *The values of $\eta_{m,n}$ for Sit. II.*

$m \backslash n$	1/2	3/2	5/2	7/2	9/2
1	0.12415	0.01747	0.00043	-0.00114	-0.00086
2	.04671	.02669	.00870	.00219	.00030
3	.01648	.01873	.01087	.00508	.00218
4	.00672	.01136	.00923	.00587	.00341
5	.00327	.00696	.00701	.00554	.00375

IV. Energy Calculations

The energy of the dislocated crystal was calculated by direct summation of the energies (eq (2)) stored in the nearest neighbour bonds. For bonds at larger distances from the dislocation line the summation was replaced by an integration. To ensure a good convergence of the Peierls energy sums, the energy differences of corresponding bonds in situations I and II (e.g.,

$$\delta E_{(2, 1/2)(2, -1/2)}^{\text{II}} - 1/2(\delta E_{(3/2, 1/2)(3/2, -1/2)}^{\text{I}} + \delta E_{(5/2, 1/2)(5/2, -1/2)}^{\text{I}})$$

were formed first, and then the summation of these differences was performed.

One thus obtains for the Peierls energy

$$E_p = E^{\text{II}} - E^{\text{I}} = 0.20 bB / (4\pi^2) = 0.0050 Gb^2$$

(with $B = Gb$) as compared to the value following from Maradudin's model (for a square lattice) with Celli's correction:

$$E^{\text{II}} - E^{\text{I}} = -0,47 bB / (4\pi^2) \approx -0,012 Gb^2.$$

Assuming a sinusoidal Peierls potential our value for the Peierls stress is

$$\sigma_p = \pi E_p / (b^2) = 0,016 G.$$

V. Acknowledgement

We thank Professor G. Leibfried for stimulating discussions.

VI. References

- [1] Maradudin, Alexei A., J. Phys. Chem. Solids, **9**, 1 (1959).
- [2] Celli, V., J. Phys. Chem. Solids, **19**, 100 (1961).
- [3] Suzuki, H., In Dislocation Dynamics, A. R. Rosenfield, et al., Eds. (McGraw-Hill, New York, 1968) p. 679.
- [4] Hötzler, A., and Siems, R., to be published.

THE INTERACTION BETWEEN A SCREW DISLOCATION AND CARBON IN BODY-CENTERED CUBIC IRON ACCORDING TO AN ATOMIC MODEL

R. Chang

*Science Center
North American Rockwell Corporation
Thousand Oaks, California 91360*

The interaction energy between carbon and a screw dislocation in body-centered cubic iron near the core regions of the dislocation was calculated atomistically using a pair-wise interatomic potential matching the elastic properties of the material. In order to avoid the use of the iron-carbon potential, it was assumed that the iron-carbon octahedron of the Johnson configuration (2 iron atoms separated by $1.225 a_0$ in the [100] direction and 4 iron atoms separated by $0.958 a_0$ in the (100) plane, a_0 being the lattice parameter) remains undistorted whether it is present in a perfect or a defective lattice. Our first calculations yield, depending on site location, binding energies varying from 0.04 to 0.55 eV.

Key words: Carbon in iron; computer simulation; dislocation-interstitial interaction; interatomic potentials; lattice defects.

An understanding of the interaction between dislocations and impurity atoms in crystalline solids based on first principles should be an important step toward the development of the fundamental aspects of dislocation theory. The interaction between a screw dislocation and interstitial impurities such as carbon in body-centered cubic iron is a timely subject of interest to material scientists.

The apparent success of the application of pseudo-potentials to studies of the material properties of simple metals and semiconductors suggests that the same approach can be used to investigate the dislocation behavior of crystalline solids. The crux of the problem is the availability of rigorous and realistic interatomic potentials. This is indeed fortunate since the pseudopotential method implies that, at constant volume, an effective two-body potential, combining the structure- and volume-dependent parts of the ion-ion, ion-electron and electron-electron potentials, can be used [1]. The

Fundamental Aspects of Dislocation Theory, J. A. Simmons, R. de Wit, and R. Bullough,
Eds. (Nat. Bur. Stand. (U.S.), Spec. Publ. 317, I, 1970).

volume-dependent but structure-independent parts of the potentials can be excluded since at constant volume they contribute a constant energy term independent of the details of the atom configurations.

For transition metals, however, the construction of an effective two-body potential via the pseudo-potential method is not yet possible. If the potential could be constructed some other way so as to avoid quantum-mechanical considerations, it might not be too bad, as a first order approximation, to treat all metals alike. We therefore choose to express the two-body potential empirically in power series of the interatomic separation and match the potential with the elastic properties of the material. Explicit relationships exist between a two-body interatomic potential and the second and third order elastic constants for b.c.c. metals [2]. The interatomic potential so constructed for b.c.c. iron is used in this study. The details of obtaining this potential from experimental elastic constants data have been discussed by the author elsewhere [3].

The detailed core structures of a screw dislocation in b.c.c. iron (Burgers vector along [111]) studied by the author using the two-body Fe-Fe potential have been published [4]. Further investigation of the interaction of a screw dislocation and carbon in b.c.c. iron cannot be carried out without the availability of an Fe-C potential. An approximate Fe-C potential has been proposed by Johnson [5] in his investigation of the motional activation energy of an interstitial carbon atom in b.c.c. iron. Johnson reported that the six iron atoms in the immediate vicinity of an octahedrally situated carbon atom are separated by $1.225 a_0$ for the two iron atoms in the [100] direction and by $0.958 a_0$ for the four iron atoms in the (100) plane, a_0 being the lattice parameter. Since Johnson's Fe-C potential is at best semiquantitative, we choose to circumvent the existing difficulty in our approach by assuming that the Fe-C octahedron (composed of six iron atoms and one carbon atom of Johnson's configuration) remains undistorted whether it is present in a perfect or a defective b.c.c. iron lattice. The Fe-C octahedron is then placed at various sites of the b.c.c. iron crystallite containing a screw dislocation (Burgers vector along [111]) and the equilibrium positions and energies of all the iron atoms surrounding the Fe-C octahedron are searched according to our Fe-Fe interatomic potential. The binding energy E_i between a screw dislocation and a carbon atom located at site "i" is given by

$$E_i = e_i^d - e_i^p, \quad (1)$$

where e_i^d is the total energy of the dislocated crystallite containing N iron atoms and one carbon atom at site "i" (at fixed volume) minus the energy of the same dislocated crystallite without the carbon atom, and e_i^p is the

total energy of a perfect crystallite containing N iron atoms. Since the Fe-C octahedron is assumed to remain unchanged whether it is present in a perfect or dislocated lattice, the energy contribution from Fe-C interaction (which according to Johnson's potential is short range and concerns only the six iron atoms of the Fe-C octahedron) cancels according to eq (1). We hope to arrive in this manner at a reasonable estimate of the binding energy E_i regardless of the details of the Fe-C potential.

Since our relaxation of the iron atoms is carried out at constant volume while the insertion of a carbon atom in both the dislocated and perfect lattices gives rise to a change in volume, a dilatation correction to both e_i^d and e_i^p in eq (1) is required.

Two methods of estimating the interaction energy E_i according to eq (1) were used. In the fixed boundary method, the energy of all 720 atoms (30 atom planes each containing 24 atoms along the screw dislocation line outlined by the rectangle abcd in fig. 1) was monitored. The volume

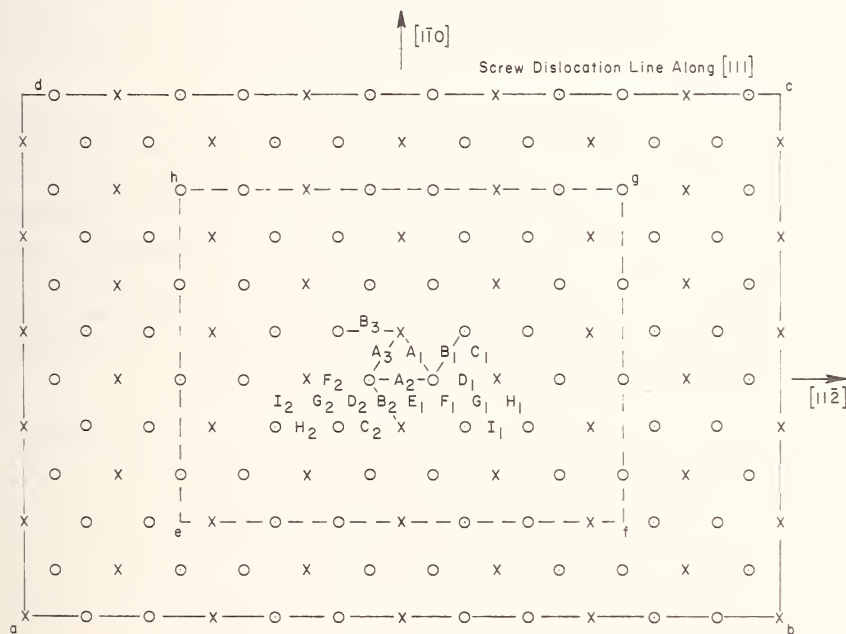


FIGURE 1. Projections of atoms (pertaining to three atom planes or one repeat distance) on $\{111\}$ plane along the screw dislocation line. Boundary abcd (30 atom planes along screw dislocation line) and boundary eghf (12 atom planes along screw dislocation line) represent, respectively, the lattice volume used in the fixed boundary method and the moving boundary method. Capital letters indicate the octahedral positions where the carbon atom is located (nearly midway along the dislocation line); subscript numerals indicate the three equivalent sites around the screw dislocation core outlined by $A_1A_2A_3$.

change of the assemblage of atoms was estimated from the relaxed atom positions of the surface atoms along the three Cartesian axes and corrections for the interaction energies were estimated from the volume change according to the interatomic potential [3]. In the moving boundary method, the energy of those atoms within the dotted rectangle efgh in figure 1 and the inner 12 atom planes along the screw dislocation line was monitored. Since the surfaces outlined by the rectangle efgh and the two end boundaries (between the ninth and tenth atom planes and between the 21st and 22nd atom planes along the screw dislocation line) were moving during the relaxational procedures, any energy change associated with the volume change was taken care of by the moving boundaries; therefore no energy correction was necessary. The moving boundary method yielded directly the screw dislocation-carbon interaction energy while the fixed boundary method suffered inaccuracies inherent in the energy corrections due to volume changes. It is believed that the accuracy can be further improved by using larger crystallite dimensions. The crystallite size used in this study was chosen as a compromise between accuracy and excessive costs in computer time. The CDC 6600 computer was used entirely in this investigation.

A total of eleven octahedral sites shown in figure 1 (lying nearly midway along the dislocation line) were investigated. The screw dislocation-carbon interaction energies corresponding to these sites are compiled in table I. Four of the sites, A₁, C₁, D₁, and E₁, yield negative interaction energies. Site G₁ (and corresponding site G₂) yields a maximum binding energy of about 0.5 eV. This value is about 0.2 to 0.25 eV smaller than that estimated by Cochardt, Schoeck, and Wiedersich [6] from linear elasticity calculations. Reasons for the possible discrepancy have already been discussed by Hirth and Cohen [7] and by Schoeck [8].

TABLE I. Screw dislocation-carbon interaction energy according to the atomic model

Octahedral position (see fig. 1)	E_i , Interaction energy, eV	
	Fixed boundary method	Moving boundary method
A ₁	< 0	< 0
B ₁	0.26	0.04
C ₁	< 0	< 0
D ₁	< 0	< 0
E ₁	< 0	< 0
F ₁	Not Estimated	0.25
G ₁	Not Estimated	0.52
G ₂	Not Estimated	0.59
H ₁	Not Estimated	0.41
H ₂	0.42	0.47
I ₁	0.41	0.33

Acknowledgement

The author wishes to thank Dr. H. Wiedersich, North American Rockwell Corporation, Science Center, for his help in the formulation of equation (1).

References

- [1] Harrison, W. A., *Pseudo-Potentials in the Theory of Metals* (W. A. Benjamin Press, 1966).
- [2] Coldwell-Horsfall, R. A., *Phys. Rev.* **129**, 22 (1963).
- [3] Chang, R., and Graham, L. J., in *Calculations of the Properties of Vacancies and Interstitials*, Nat. Bur. Stand., Misc. Publ. No. 287 (Government Printing Office, Wash. D.C., 1966), p. 53.
- [4] Chang, R., *Phil Mag* **16**, 1021 (1967).
- [5] Johnson, R. A., Dienes, G. J., and Damask, A. C., *Acta Met.* **12**, 1215 (1964).
- [6] Cochardt, A. W., Schoeck, G., and Wiedersich, H., *Acta Met.* **3**, 533 (1955).
- [7] Hirth, J. P., and Cohen, M., *Scripta Met.* **3**, 107 (1969).
- [8] Schoeck, G., *Scripta Met.* **3**, 239 (1969).

THE STRUCTURE OF THE $\langle 111 \rangle$ SCREW DISLOCATION IN IRON

P. C. Gehlen, G. T. Hahn, and A. R. Rosenfield

*Metal Science Group
Battelle Memorial Institute
Columbus, Ohio 43201*

The concept of a dissociated $a/2 \langle 111 \rangle$ screw dislocation has been invoked to explain the slip behavior in b.c.c. materials and particularly the asymmetry of the critical resolved shear stress. No direct experimental evidence of dissociation has been obtained, but the idea has received some albeit conflicting support from discrete lattice calculations of the atomic positions in the core. Chang, using isotropic elasticity for α -iron, found that the dislocation core has three very narrow intrinsic faults. These three faults are symmetric with respect to the screw axis. Bullough and Perrin, on the other hand, found that the screw is split with faults on two $\{112\}$ planes belonging to the zone of the screw axis. The misfit is spread over a distance of about $3b$. On the third $\{112\}$ plane no splitting was found to occur.

In view of these discrepancies, the calculations were repeated for anisotropic and isotropic elastic boundary conditions and with different interatomic potentials. Excellent agreement was found with Chang's configuration even though a volume expansion term was added to the displacements associated with the dislocation.

It was shown that the final configuration is strongly dependent on the position of the dislocation line with respect to the lattice and at least two metastable positions were found. Even though the atomic arrangement is quite different, their energy is not more than 0.1 eV larger than the energy of the stable one.

Using the Johnson potential unmodified for long-range electronic effects, the dislocation was found to have the following characteristics: core radius, 4-5.5 Å; core energy, 0.20-0.25 eV per atomic plane; and an effective hole radius of 1.35 Å.

It was shown that the final configurations are rather insensitive to the model size and to the boundary conditions used.

Key words: Computer simulation; dislocation core structure; interatomic potentials; iron.

We have calculated the atomic positions in and around the core of the $a/2 \langle 111 \rangle$ screw dislocation in α -iron. This dislocation is of great interest because it appears to play a dominant role in the deformation behavior of body-centered-cubic transition metals. The computational procedure is essentially the same as used for the [001] (100) edge [1]. In particular, the Johnson [2] potentials were used along with a modified version of the GRAPE [3] computer program and anisotropic boundary conditions [4]. Particular care was taken with specifying the boundary conditions since our calculations suggest that an improper choice could lead to spurious results. In addition, a radial dilatation term suggested by Hirth [5], was included.¹ This expansion, discussed by Seeger and Haasen [6] arises from second order elasticity effects and was omitted in all previous lattice calculations. Its physical basis lies in the observed change of lattice parameter of cold worked metals during subsequent annealing [7]. Considerable precautions were taken to avoid metastable configurations.

This calculation is of particular interest because two previous studies for the same dislocation show significant differences. Bullough and Perrin [8] found that the screw dislocation was dissociated on two {112} planes 60° apart, while the misfit was quite narrow on the third {112} plane parallel to the dislocation line. Chang, on the other hand [9], found that the core was quite narrow and retained a threefold symmetry with respect to the dislocation line.

The configuration that we have generated is very similar to the one generated by Chang and the slight differences can definitely be attributed to the fact that Chang used isotropic boundary conditions and his own anharmonic potential [10] (which is slightly different from the Johnson potential), while neglecting the volume expansion mentioned above.

The position of the screw axis with respect to the b.c.c. lattice had an important influence on the core configuration. Suzuki [11] has pointed out that if the dislocation line is made equivalent to one of the $\langle 111 \rangle$ screw triads, two different core configurations can be found. This was confirmed by this study: two metastable configurations were found, the one with the lowest energy corresponding to the triad with the same sense as the dislocation itself (in our case both left handed).

The stable configuration was generated starting with the lower energy metastable configuration and destroying the threefold symmetry on pur-

¹In the isotropic case, Hirth has suggested that the additional radial displacement, u_r is given by: $u_r = \frac{b^2}{2\pi r}$, where b is the Burgers vector and r the distance from the dislocation line. Since the corresponding formula for the anisotropic case is not available, this one was used.

pose (say by displacing only one atom near the core). However, after relaxation the symmetry was restored. It is rather surprising that the potential energies of the stable and metastable configurations did not differ by more than 0.1 eV per repeat distance (i.e., 3 atomic planes).

Even very close to the core, the metastable configurations can be roughly approximated by using the elastic displacement equations. However, the deviations from the elastic positions are considerable for the stable configuration.

The dislocation can be characterized by several conventional parameters which are obtained from a plot of dislocation energy versus the logarithm of distance from the dislocation. The dislocation energy has two components—a structure dependent and a volume dependent term. The structure dependent term can be calculated by pairwise summing of the bond energies throughout the crystal (assuming the volume is constant). The volume dependent term cannot be evaluated accurately and was estimated by either treating a non-expanded configuration or else by using an expanded perfect b.c.c. lattice as reference state. The results obtained by these two independent methods are in good agreement. At large distances from the dislocation, the energy versus log distance curve is a straight line whose slope is in excellent agreement with the slope calculated using elasticity theory. At small distances the following values can be easily ascertained from the curve: if the Johnson potential II [2] (unmodified for long-range electronic effects) is used

$$\text{Core radius} = 4 - 5.5 \text{ \AA}, 1.6 - 2.2 \mathbf{b}$$

$$\text{Core energy} = 0.20 - 0.25 \text{ eV/atomic plane}$$

$$\text{Effective hole radius} = 1.35 \text{ \AA}, \text{ or } \mathbf{b}/1.8$$

These results are consistent with other theoretical predictions (e.g., Hirth and Lothe [12]).

Subsidiary calculations show that the same core configurations are obtained independently of whether isotropic or anisotropic elasticity is used to specify the boundary conditions and that the model contains a sufficiently large number of atoms for convergence on the correct configuration.

Currently, the $a/2 \langle 111 \rangle$ screw dislocation is being studied using a potential developed by Bullough and Perrin [13]. This potential is very different from the Johnson potential since it includes third nearest neighbor interactions (only second neighbors for the Johnson potentials) and contains a large positive potential energy between second and third neighbors. It is not known at the present time whether or not the configuration is sensitive to the change-over to this potential and these results with

the details of the present investigation will be presented in the near future.

Acknowledgement

We are grateful to the Office of Naval Research for support of this research.

References

- [1] Gehlen, P. C., Rosenfield, A. R., and Hahn, G. T., *J. Appl. Phys.* **39**, 5246 (1968).
- [2] Johnson, R. A., *Phys. Rev.* **145**, 423 (1966).
- [3] Gibson, J. B., Goland, A. N., Milgram, M., and Vineyard, G. H., *Phys. Rev.* **120**, 1229 (1960).
- [4] Hirth, J. P., and Gehlen, P. C., *J. Appl. Phys.* **40**, 2177 (1969).
- [5] Hirth, J. P., private communication.
- [6] Seeger, A., and Haasen, P., *Phil. Mag.* **3**, 470 (1958).
- [7] Crussard, C., and Aubertin, F., *Rev. Met. Paris* **46**, 356 (1949).
- [8] Bullough, R., and Perrin, R. C., *Dislocation Dynamics*, Rosenfield, Hahn, Bement, and Jaffee, Eds. (McGraw-Hill Book Co., New York, 1968) p. 175.
- [9] Chang, R., *Phil. Mag.* **16**, 1021 (1967).
- [10] Chang, R., and Graham, L. T., in *Calculation of the Properties of Vacancies and Interstitials*, Nat. Bur. Stand. Misc. Publ. No. 287 (Government Printing Office, Wash., D.C., 1966) p. 53.
- [11] Suzuki, H., *Dislocation Dynamics*, Rosenfield, Hahn, Bement, and Jaffee, Eds., (McGraw-Hill Book Co., New York, 1968) p. 679.
- [12] Hirth, J. P., and Lothe, J., *Theory of Dislocations* (McGraw-Hill, New York, 1968).
- [13] Bullough, R., and Perrin, R. C., private communication.

Discussion on Papers by H. Suzuki, A. Hözlér and R. Siems, R. Chang, and P. C. Gehlen et al.

BEN-ABRAHAM: I would like to comment on the papers by Professor Suzuki, by Drs. Doyama and Cotterill, and by Drs. Hözlér and Siems, which are very much alike. Three years ago a student of mine, Joseph M. Ya'eli, made a very similar calculation for copper and aluminum and also for a simple cubic lattice. He used what he called an elasto-static approximation in which he divided the crystal into cells, took the elastic values for the displacement at the actual lattice points, and then instead of integrating, he summed them up. That method made it possible to apply simple anisotropic elasticity, yet still account for the discreteness of the lattice. I must say he got very similar results as were here presented by Professor Suzuki. He also compared his results with results available at that time by Drs. Cotterill and Doyama¹ and others. I wish to point out that the result of this calculation was that the minimum energy position is neither configuration I nor configuration II, but rather a point on the diagonal. [See fig. 1 in the paper by A. Hözlér and R. Siems, and fig. 1 of this discussion.] I wish to point out that the value of this approximation is that it is very simple indeed, so that you can save a lot of computer time as compared with more sophisticated calculations. At the same time, you can fare much better than by elasticity at estimating core energies. So, it's something workable for everyday use. Thank you.

SIEMS: We also considered this type of approximation. We assigned to any row of atoms that displacement which a dislocation in a continuous elastic medium would produce at the same position. Summing up the corresponding interaction energy yields a Peierls energy differing by about 30% from the value calculated in our paper.

HIRSCH: I'd like to report on some calculations made by Vitek recently. He also has calculated the configurations of the atoms around a screw dislocation in a bcc metal using the Johnson type potentials, but giving lower misfit energies on the {112} planes. These calculations were done in collaboration with Dr. Perrin in Dr. Bullough's group. The results of the calculations so far show that the dislocation tends to be dissociated on {112} planes by very small amounts and the dissociation has three-fold symmetry. In that respect, I believe, it differs from Dr. Chang's dissociated model.

¹ Cotterill, R. M. J., and Doyama, M., Phys. Letter 13, 110 (1964); Phys. Letters 14, 79 (1965).

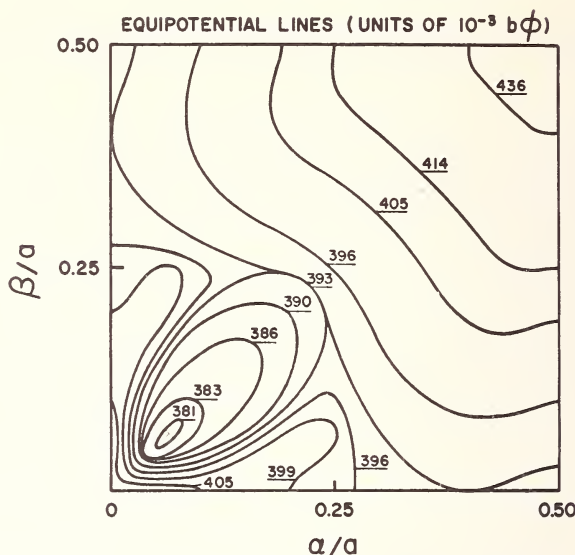


FIGURE 1. Location of energy minimum for a screw dislocation in a simple orthorhombic lattice, according to Ya'eli.

KUHLMANN-WILSDORF: As we all know, the Peierls stress is the derivative of the dislocation core energy as a function of position. For symmetry reasons, this function has to have extrema at the two symmetrical positions, *i.e.* the two extrema we saw on the slides. If now there is a minimum of the energy, as Dr. Ben-Abraham pointed out, on the 45° line, that gives four extrema to the curve per periodicity interval. Did I misunderstand, or do you seriously think there are four extrema?

BEN-ABRAHAM: I don't blindly believe in those calculations, but I do believe that they tell us that the crystal symmetry isn't conserved around the dislocation, and therefore, there is no good reason why what is a symmetric position in a perfect crystal should be a symmetric position in a dislocated crystal. On the other hand, it also implies what Professor Suzuki showed us, that the dislocation would dissociate at least locally in terms of one or two Burgers vectors. I don't think we have a way to see whether the difference is half an Ångstrom or something like that.

HIRTH: I would like to comment on boundary conditions that are used for many of the atomic calculations. Professor Haasen, in collaboration with Professor Seeger, calculated some time ago that a dislocation line produces an area expansion ΔA of the order of b^2 . This estimate is supported by measurements of volume changes accompanying cold-working of a crystal. Professor Nabarro has discussed the elastic implications which would indicate that this corresponds to a biaxial dilatation around

the dislocation with a radial displacement field of the type $\Delta A / 2\pi r$. This field should vary with r until the distance from the core is about $5b$ or $10b$ and then become uncertain because of non-linear effects. However, in putting the boundary conditions on the large cells of atoms to carry out atomic calculations, the usual procedure is to apply only the displacement field of the dislocation itself. It would seem that in many cases the dilatational displacement field could also be appreciable at the boundary. Because of the high sensitivity quantities such as stacking fault energy to hydrostatic compression this could conceivably significantly affect deduced dislocation dissociations and stacking fault energies.

BULLOUGH: Any comment on this point?

GEHLEN: For the dislocation configurations presented here, we have used the correction that Professor Hirth mentioned. Some of the configurations were generated with different proportionality constants in the expression for the dilatation term. This should affect the value of the stacking fault energy and hence the splitting of the dislocation, if any. However, since the core configuration remains unchanged when the value of the proportionality constant is increased, one may postulate that the core is not split.

BULLOUGH: It depends whether the core configuration is dominated by the Peierls width or by stacking fault energy.

GEHLEN: But it seems to me that the stacking fault energy as well as the Peierls energy would be affected in similar ways when the dilatation field is altered.

ARSENAULT: I have two questions for Professor Suzuki: 1) Did you calculate the Peierls stress of an edge dislocation? 2) By manipulation of your potential or splitting it into two parts, could you get the Peierls stress of an edge greater than that for a screw?

SUZUKI: I have calculated the Peierls stress only for screw dislocations. I haven't obtained any numerical results for edge dislocations. I think for the rather qualitative estimate using the Peierls-Nabarro approximation, the Peierls stress for an edge dislocation is rather smaller than for a screw dislocation in the b.c.c. crystal.

SCHOECK: I have a question for Professor Siems. You assume in the primitive lattice that the center of the dislocation is in the interspace between two lattice planes. Could you not put the center also in a row of atoms, and if you do so would this not reduce the energy since the center row is then not displaced at all and the next atoms nearest to the center which are displaced are further away?

SIEMS: The situation where the center of the dislocation coincides with a row of atoms can be treated in the same way as the cases discussed in the paper. An estimate of the resulting energy (taking only rows in the vicinity of the dislocation into account) indicates, however, that the resulting energy is higher than the energy of the situations discussed in the paper.

ELBAUM: I just wanted to ask Professor Suzuki on the matter of the comparison he has made with experimental results on the Peierls-Nabarro stress: What experimental results are you referring to?

SUZUKI: In the case of body-centered cubic crystals, I referred to the values obtained by Professor Conrad,² who estimated the Peierls-Nabarro stress by extrapolating the flow stress to 0 °K and analyzing the temperature dependence and the strain rate sensitivity of the flow stress. Meanwhile, in the case of face centered cubic crystals, I don't know a reliable value for the Peierls stress as determined by experiment. It is possible that we give the Peierls stress of the order of 1/kg/mm or less. This value may not contradict all observations.

² Conrad. H., in *The Relation Between the Structure and Mechanical Properties of Metals* (Her Majesty's Stationery Office, London, 1963) p. 476.

III DISLOCATION-PHONON INTERACTIONS

Chairman:

J. LOTHE

EIGENFREQUENCIES IN A DISLOCATED CRYSTAL

T. Ninomiya

*Department of Physics
University of Tokyo
Tokyo, Japan*

Dynamical theories of dislocation vibration and interactions with phonons are surveyed. Eigenfrequencies of lattice vibrations in a crystal containing a straight dislocation are calculated by using Lagrangian formalism. It is found that there is one eigenfrequency of dislocation vibration (wave number κ) in each of the intervals of the normal mode frequencies of $k_z = \kappa$ in a perfect lattice. It is also found that there is a band of localized dislocation vibration below the phonon band. The mean squared amplitude of the dislocation vibration is determined by the localized mode for an edge dislocation and by the resonance modes for a screw dislocation. Phonon scattering by the fluttering mechanism is next treated by using the above results and the conditions of resonance scattering is given. Finally, the effect of the Peierls potential and the vibration of a dislocation dipole are discussed. In the Appendices the problem of quantization of dislocation vibration and the extension of the above theories to a case of translational motion are briefly described.

Key words: Dislocation-phonon interactions; dislocation vibration; internal friction; localized modes.

I. Introduction

A dislocation in a crystal scatters phonons to give thermal resistivity. For a dislocation which makes translational motion, the scattering results in a frictional force acting on the dislocation. Two mechanisms of the dislocation-phonon interactions have been considered based on treatments of dislocation in an elastic continuum. One is the scattering due to large strains around a dislocation because of the anharmonicity in the crystal potential. In connection with thermal conductivity at low temperatures, this mechanism was first investigated by Klemens [1] and reviewed by Carruthers [2]. These theories have predicted too small thermal resistivity due to dislocations compared with the experiments in alkali halides

(Sproull et al., [3]). Recently Bross et al. [4] have studied this mechanism to explain thermal resistivity in copper alloys and have extended their calculations to the cases of dislocation arrays. The frictional force on a dislocation by this mechanism has been given by Mason [5] for a straight dislocation and by Seeger and Engelke [6] for a kink.

The other mechanism of phonon scattering comes from the ease of dislocation motion. Forced oscillation of a dislocation by an incident phonon results in phonon emission and gives the scattering of the incident phonon. This mechanism is called fluttering. Dynamic response of a dislocation to an external force is quite often treated by assuming that the dislocation has a line tension and an effective mass (the string model). Although this model makes the problem quite easy to treat mathematically, the concepts of the line tension and the effective mass have rather important defects for general use. Essential points of the criticisms to this model are the following:

(1) The interactions between dislocation segments are of long range and it is not clearly shown how good approximation the line tension is.

(2) For a dynamic problem, the long-range nature of the interactions necessitates taking into account retardation in propagation of the strain around a dislocation.

(3) From the field-theoretical point of view, the dislocation mass is given by the self-force, as was shown by Eshelby [7] and Kosevich [8]. Then, as in the line tension, the above points of criticism must be considered for the mass, too.

Actually it has been shown by Laub and Eshelby [9] and by Ninomiya and Ishioka [10] that, for a sinusoidal displacement of an oscillating dislocation, the effective line tension and the effective mass can be defined including the effects of both the long-range interaction and the retardation. These are, however, dependent on the wavelength and the frequency. That is, one cannot use a single line tension or a mass for an arbitrary motion of the dislocation.

The kink model is superior to the string model in the respect that the kink mass can be defined for an arbitrary motion (Ninomiya and Ishioka [10]). When one deals with a chain of kinks, however, one must take into account the long-range nature of the kink-kink interactions and their retardation. Then, the problem becomes quite similar to that in the string model.

There is another defect which is common to the string model and the kink model. The existence of a dislocation does not change the degrees of freedom of the crystal, because the number of atoms in the crystal is not changed by introduction of the dislocation. On the other hand, the assumption of the dislocation mass increases the degrees of freedom. One must remember that the effective mass is entirely determined by the self-

force; that is, the dislocation has no eigen-mass (Ninomiya and Ishioka [10]).

The above described objections to the use of the effective mass and the line tension suggest necessity of developing a general theory of dislocation dynamics without using these concepts. On the basis of the Peierls model of a dislocation, Nabarro [11] calculated the response of a straight and rigid dislocation to a phonon by balancing the stress on the slip plane. Eshelby [7] treated motion of a kink by considering the self-force. Recently, Ninomiya [12] has tried general treatments of dislocation vibrations in an elastic continuum.

In the present paper the problems of dislocation vibration in an isotropic and elastic continuum are surveyed. General treatments of dislocation motion start with the expressions of the elastic and kinetic energies of the elastic body in terms of dislocation field and phonon field and use Lagrangian formalisms. The retardation in the strain propagation is taken into account by the phonon field. Lattice vibrations in a dislocated crystal are first treated along this line. Knowledge of the eigen-frequencies of the lattice vibrations then gives directly the scattering cross-section of a phonon by the fluttering mechanism.

Of course, these treatments of dislocation vibration in an elastic continuum are not valid near the Debye frequency. The vibration of a dislocation in a lattice was first investigated by Kratochvil [13] for the one-dimensional (Frenkel-Kontorova) model. Calculations of the vibration in a three-dimensional lattice have been done by Litzman and Kunc [14]. They studied the modes localized around an edge dislocation in a simple cubic crystal in which the x , y , and z components of the displacements are uncoupled. Although the present calculations for an elastic continuum are considered to be complementary to their results, direct comparisons between these calculations are not easy. The reason is that, in the calculations done for the cubic lattice, the effects of anharmonicity and of dislocation fluttering are mixed. Lengelar and Ludwig [15], Lifshitz and Kosevich [16], and Brown [17] have also treated the lattice vibration in a crystal containing a one-dimensionally extended defect. Their models are, however, concerned with the linear array of impurity atoms, and the physical relation to dislocations seems to the present author not very clear, although it is expected that such an array may reflect some characters of the dislocation core.

Dynamic theories for continuous distribution of dislocations are not described in the present paper, because these will be treated in the session of dynamic field theories.

In section II the equations of motion for vibrations in the crystal with a straight dislocation are presented by using a Lagrangian formalism. In section III the eigen-frequencies of the lattice vibrations are obtained

for the modes accompanied or not accompanied with dislocation vibration. The change in the state density by introduction of the dislocation is also given. In section IV the mean squared amplitude of the dislocation vibration is discussed. It is found that for an edge dislocation the localized modes make the largest contribution to the amplitude and for a screw dislocation the amplitude is determined almost entirely by the resonance modes. Section V is devoted to the problem of phonon scattering by the fluttering mechanism. This becomes the extension to general cases of the work by Nabarro. The condition of resonance scattering for oblique incidence of a phonon on a dislocation is given. The next section (section VI) treats the effects of the Peierls potential on the dislocation vibration and phonon scattering. Finally the case of a dislocation dipole is discussed (sections VII and VIII). In Appendix C the quantization of the dislocation vibration is done and in Appendix D the energies of an elastic body in which a dislocation makes translational motion in addition to infinitesimal vibrations are given for future extension to calculations of frictional force. Appendix E gives a brief comparison of the theoretical and experimental determinations of the contribution of fluttering to thermal conductivity.

II. Dislocation Energies and Equations of Motion

In the present work, we will treat infinitesimal vibration of a straight dislocation in an isotropic and elastic continuum.

Let us take the xz plane as the slip plane and consider that the dislocation is along the z axis. The displacement $\xi(z)$ of the dislocation from an equilibrium position (a straight configuration) is expanded in a Fourier series

$$\xi(z) = \sum_{\kappa} \xi(\kappa) e^{i\kappa z}. \quad (1)$$

The elastic field around the moving dislocation is different from that around a static dislocation with the same configuration, because of retardation in the strain propagation as stated in the introduction. The displacement, strain and stress are decomposed into two components as follows:

$$u_i = u_i^s + u_i^d \quad (\text{displacement}),$$

$$e_{ij} = e_{ij}^s + e_{ij}^d \quad (\text{strain}),$$

and

$$p_{ij} = p_{ij}^s + p_{ij}^d \quad (\text{stress}).$$

u_i^s is the static displacement corresponding to an instantaneous configuration of the dislocation. u_i^d is a deviation from the static displacements and will be called dynamical one. Since the relative displacement b across

the slip plane is given by the static displacement, the dynamical displacement is continuous even across the slip plane. The superscripts “*s*” and “*d*” attached to the strain and the stress represent similar meanings. This splitting of the elastic field is convenient for treating the dislocation-phonon interactions, because the dynamic field becomes just a phonon field if we have no dislocations.

For the dislocation displacement given by eq (1) the static displacement has a following form

$$u_i^s = \sum_{\kappa} f_i(x, y : \kappa) e^{i\kappa z} \xi(\kappa) + u_{i0}^s. \quad (2)$$

The explicit formula of $f_i(x, y : \kappa)$ is obtained by integrating the displacements due to infinitesimal dislocation loops and is given in Appendix A. u_{i0}^s is the displacement when the dislocation displacement is zero.

The dynamic displacement u_i^d can be expressed with the superposition of plane waves in an isotropic elastic continuum:

$$u_i^d = \sum_{\mathbf{k}, s} q(\mathbf{k}, s) e_i(\mathbf{k}, s) e^{i\mathbf{kr}}, \quad (3)$$

where *s* stands for the mode of the wave (transverse or longitudinal) and *e* is the polarization vector.

The kinetic energy of the body containing the dislocation is

$$\begin{aligned} T = & \frac{\rho}{2} \int \sum_i (\dot{u}_i^s + \dot{u}_i^d)^2 dv = \frac{\rho V}{2} \sum_{\mathbf{k}, s} \dot{q}(\mathbf{k}, s) \dot{q}^*(\mathbf{k}, s) \\ & + \rho L \sum_{\kappa} \sum_{k, s} \sum_i \left[\int f_i^*(x, y : \kappa) e^{i(k_x x + k_y y)} dx dy \right] e_i(\mathbf{k}, s) \dot{q}(\mathbf{k}, s) \dot{\xi}^*(\kappa) \\ & + \frac{\rho L}{2} \sum_{\kappa} \sum_i \left[\int f_i(x, y : \kappa) f_i^*(x, y : \kappa) dx dy \right] \dot{\xi}(\kappa) \dot{\xi}^*(\kappa). \end{aligned} \quad (4)$$

Here, we have considered the energy in the cube $L^3 = V$ and chosen a cyclic boundary condition. Σ^{κ} means the summation over the modes which have the wave vector $k_z = \kappa$. Let us write briefly as follows:

$$B_i(k, \kappa) = \rho L \int f_i^*(x, y : \kappa) e^{i(k_x x + k_y y)} dx dy, \quad (5a)$$

and

$$m(\kappa) = \rho L \sum_i \int f_i(x, y : \kappa) f_i^*(x, y : \kappa) dx dy = \frac{1}{\rho V} \sum_{\mathbf{k}} \sum_i B_i(\mathbf{k}, \kappa) B_i^*(\mathbf{k}, \kappa). \quad (5b)$$

In an isotropic continuum, we have (Appendix A)

$$\sum_i B_i(\mathbf{k}, \kappa) e_i(\mathbf{k}, s) = -\frac{i\mu L}{c_s^2 k^2} [(\mathbf{e}\mathbf{b})(\mathbf{k}\mathbf{n}) + (\mathbf{b}\mathbf{k})(\mathbf{e}\mathbf{n})], \quad (6)$$

where \mathbf{n} is the unit vector perpendicular to the slip plane and

$$c_s = c_t \text{ or } c_l,$$

according as the wave is transverse or longitudinal. Let us define $\varphi(\mathbf{k}, s)$ by

$$\varphi(\mathbf{k}, s) = -i[(\mathbf{e}\mathbf{b})(\mathbf{k}\mathbf{n}) + (\mathbf{b}\mathbf{k})(\mathbf{e}\mathbf{n})],$$

then we have

$$\sum_i B_i(\mathbf{k}, \kappa) e_i(\mathbf{k}, s) = \frac{\mu L}{c_s^2 k^2} \varphi(\mathbf{k}, s) = \frac{\mu L}{\omega_0^2(\mathbf{k}, s)} \varphi(\mathbf{k}, s), \quad (7)$$

where $\omega_0(\mathbf{k}, s)$ is the frequency for the wave (\mathbf{k}, s) in a perfect crystal.

The elastic energy is given by

$$\begin{aligned} E &= \frac{1}{2} \int \sum_{i,j} p_{ij} e_{ij} dv \\ &= \frac{1}{2} \sum_{i,j} \int p_{ij}^d e_{ij}^d dv + \frac{1}{2} \sum_{i,j} \int [p_{ij}^d e_{ij}^s + p_{ij}^s e_{ij}^d] v + \frac{1}{2} \sum_{i,j} \int p_{ij}^s e_{ij}^s dv \\ &= E_d + E_{ds} + E_s. \end{aligned} \quad (8)$$

The elastic energy of the dynamical field E_d is written as

$$E_d = \frac{1}{2} \rho V \sum_{\mathbf{k}, s} \omega_0^2(\mathbf{k}, s) q(\mathbf{k}, s) q^*(\mathbf{k}, s) \quad (9)$$

by using eq (3).

The interaction term E_{ds} between the dynamical and static fields is found to vanish as follows:

$$\begin{aligned} E_{ds} &= \sum_{i,j} \int p_{ij}^s e_{ij}^d dv \\ &= \sum_{i,j} \left[\int_{\Sigma} p_{ij}^s u_i^d ds_j - \int p_{ij}^s u_i^d dv \right], \end{aligned} \quad (10)$$

where the first term is the integral over the surface of the volume V . This term vanishes because of the cyclic boundary condition. The second

term is also zero because

$$\sum_j p_{ij,j}^s = 0.$$

Thus, there are no elastic interactions between the dynamical and the static fields. We have the interactions between these fields via the kinetic energy as seen in eq (4).

Here, we must notice that, when we consider the interactions between static dislocations, the force acting on the dislocation is derived from the elastic interaction energy to be

$$df_k = \epsilon_{kjm} b_i p_{ij} dl_m, \quad (11)$$

where dl is the dislocation segment. Since the dislocation has no elastic interactions with the dynamical field, we have no direct reason to expect that a force exerted on a dislocation by a phonon is also given by eq (11).

Next we must find an explicit expression of the static elastic energy E_s as a function of the dislocation displacements. The dislocation can be regarded as an assembly of infinitesimal hair-pin dislocations. Let us first consider the energy of two hair-pin dislocations (fig. 1). As shown by Eshelby [18], the static elastic energy can be written in the form of a surface integral:

$$E_s = \frac{1}{2} \sum_{i,j} \int p_{ij}^s \epsilon_{ij}^s dv = \frac{1}{2} \sum_{i,j} b_i \left[\int_{S_1} p_{ij}^s ds_j + \int_{S_2} p_{ij}^s ds_j \right]. \quad (12)$$

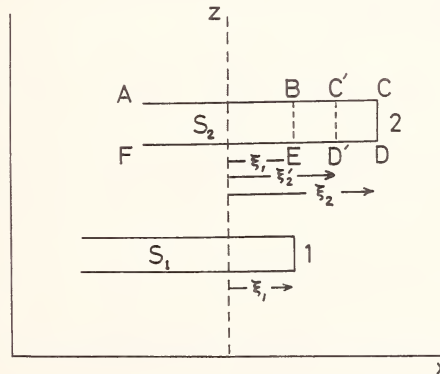


FIGURE 1. The static elastic energy is considered for two hair-pin dislocations. (see text)

The stress p_{ij}^s is the sum of the stresses due to each hair-pin dislocation:

$$p_{ij}^s = p_{ij}^{s1}(x, y, z; \xi_1) + p_{ij}^{s2}(x, y, z; \xi_2).$$

Displacement of an isolated hair-pin dislocation in the x direction does not result in the change in a static self energy, if the interaction with the surface of the body is neglected:

$$\sum_{i,j} b_i \int_{S_1} p_{ij}^{s1} ds_j = \text{const.},$$

and

$$\sum_{i,j} b_i \int_{S_2} p_{ij}^{s2} ds_j = \text{const.}$$

The static elastic energy is dependent on ξ_1 and ξ_2 through the interaction energy between the hair-pin dislocations 1 and 2.

$$E_s = \text{const.} + \frac{1}{2} \sum_{i,j} b_i \int_{S_1} p_{ij}^{s2} ds_j + \frac{1}{2} \sum_{i,j} b_i \int_{S_2} p_{ij}^{s1} ds_j. \quad (13)$$

The second term of eq (13) is evaluated as follows. At first we decompose the hair-pin dislocation 2 into the loops $ABEF$ and $BCDE$ (fig. 1). The interaction of the loop $ABEF$ with the hair-pin dislocation 1 is dependent on neither ξ_1 nor ξ_2 . Next we consider the interaction of an infinitesimal dislocation loop $d\xi'_2 \cdot dz_2$ located at $C'D'$ with the dislocation 1. The interaction energy is given as

$$\text{const. } d\xi'_2 dz_2 dz_1 - \frac{1}{2} \sum_i b_i P_{iy} (z_2 - z_1) d\xi'_2 \cdot dz_2 \cdot (\xi'_2 - \xi_1) dz_1,$$

where $P_{ij}(z_2 - z_1) d\xi'_2 dz_2$ is the stress due to the loop $d\xi'_2 dz_2$ at the head of the hair-pin dislocation 1. Therefore, the interaction energy of the loop $BCDE$ with the dislocation 1 is

$$\begin{aligned} \text{const. } dz_1 dz_2 \int_{\xi_1}^{\xi_2} d\xi'_2 - \frac{1}{2} \sum_i b_i P_{iy} (z_2 - z_1) dz_1 dz_2 \int_{\xi_1}^{\xi_2} (\xi'_2 - \xi_1) d\xi'_2 \\ = \text{const. } dz_1 dz_2 (\xi_2 - \xi_1) - \frac{1}{4} \sum_i b_i P_{iy} (z_2 - z_1) dz_1 dz_2 (\xi_2 - \xi_1)^2. \end{aligned}$$

Summing these energies, we have

$$\begin{aligned} \frac{1}{2} \sum_{i,j} b_i \int_{S_1} p_{ij}^{s2} ds_j = \text{const.} + \text{const. } (\xi_2 - \xi_1) dz_1 dz_2 \\ - \frac{1}{4} \sum_i b_i P_{iy} (z_2 - z_1) \cdot (\xi_2 - \xi_1)^2 dz_1 dz_2. \quad (14) \end{aligned}$$

When we consider all the hair-pin dislocations, the static elastic energy is obtained by integrating eq (14) over z_1 and z_2 . If the dislocation displacement is given by eq (1), the energy is

$E_s = \text{const.}$

$$+ \frac{L}{2} \sum_{\kappa} \xi(\kappa) \xi^*(\kappa) \left[\frac{1}{2} \int_{-\infty}^{\infty} \sum_i b_i P_{iy}(z) (\exp i\kappa z - 2 + \exp -i\kappa z) dz \right]. \quad (15)$$

The integral in the brackets is explicitly evaluated in Appendix A and, here, is written briefly as

$$\kappa^2 T(\kappa) = \frac{1}{2} \int_{-\infty}^{\infty} \sum_i b_i P_{iy}(z) (\exp i\kappa z - 2 + \exp -i\kappa z) dz. \quad (16)$$

Throughout this work, we consider that the core width of the dislocation is zero and shall impose a Debye cut-off, if necessary, to avoid the difficulty of infinity associated with the core.

From the Lagrangian $L = T - E$, we obtain the equations of motion:

$$\ddot{q}^*(\mathbf{k}, s) + \omega_0^2(\mathbf{k}, s) q^*(\mathbf{k}, s)$$

$$+ \frac{1}{\rho V} \sum_i B_i(\mathbf{k}, \kappa = k_z) e_i(\mathbf{k}, s) \ddot{\xi}^*(\kappa) = 0, \quad (17)$$

and

$$\sum_{\mathbf{k}, s} \sum_i B_i(\mathbf{k}, \kappa) e_i(\mathbf{k}, s) \ddot{q}(\mathbf{k}, s) + m(\kappa) \ddot{\xi}(\kappa) + L \kappa^2 T(\kappa) \xi(\kappa) = 0. \quad (18)$$

Multiplying eq (17) by $\sum_j B_j^*(\mathbf{k}, \kappa) e_j^*(\mathbf{k}, s)$, summing over the modes whose wave vector has the z component $k_z = \kappa$, and comparing the resultant equation with eq (18), we finally obtain

$$\kappa^2 T(\kappa) \xi(\kappa) = \mu \sum_{\mathbf{k}, s} \varphi(\mathbf{k}, s) q(\mathbf{k}, s). \quad (19)$$

Here we have used the conditions

$$\sum_s e_i(\mathbf{k}, s) e_j^*(\mathbf{k}, s) = \delta_{ij}.$$

Substitution of eq (19) for eq (17) eliminates the dislocation coordinate $\xi(\kappa)$:

$$\varphi^*(\mathbf{k}, s) \ddot{q}^*(\mathbf{k}, s) + \omega_0^2(\mathbf{k}, s) \varphi^*(\mathbf{k}, s) q^*(\mathbf{k}, s)$$

$$+ g(\kappa) \frac{\varphi(\mathbf{k}, s) \varphi^*(\mathbf{k}, s)}{\omega_0^2(\mathbf{k}, s)} \sum_{\mathbf{k}', s'} \varphi^*(\mathbf{k}', s') \ddot{q}^*(\mathbf{k}', s') = 0, \quad (20)$$

where

$$g(\kappa) = \frac{\mu^2 L}{\rho V \kappa^2 T(\kappa)} \quad \text{and} \quad k_z = \kappa.$$

The third term of eq (20) gives the interaction between phonons via the vibration of the dislocation. It is clear from the term that there is no interaction between phonons which have different k_z . This fact of course agrees with physical intuition for a defect extended in one dimension.

III. Eigenfrequencies of Lattice Vibration in a Dislocated Crystal

In this section the eigenfrequencies of stationary states are obtained from eq (20). For a stationary state eq (20) is

$$\{\omega_0^2(\mathbf{k}, s) - \omega^2\}\varphi^*(\mathbf{k}, s)q^*(\mathbf{k}, s)$$

$$= g(\kappa) \frac{\omega^2}{\omega_0^2(\mathbf{k}, s)} \varphi(\mathbf{k}, s)\varphi^*(\mathbf{k}, s) \sum_{\mathbf{k}', s'}^{\kappa} \varphi(\mathbf{k}', s')q(\mathbf{k}', s'). \quad (20')$$

There are two cases of the stationary states. One is accompanied with dislocation vibration and the other is not. The former case is:

$$\text{Case 1.} \quad \sum_{\mathbf{k}', s'}^{\kappa} \varphi^*(\mathbf{k}, s)q^*(\mathbf{k}, s) \neq 0.$$

In this case we have

$$\begin{aligned} & \sum_{\mathbf{k}', s'}^{\kappa} \varphi^*(\mathbf{k}, s)q^*(\mathbf{k}, s) \\ &= g(\kappa) \sum_{\mathbf{k}, s}^{\kappa} \frac{\omega^2}{\omega_0^2(\mathbf{k}, s)} \cdot \frac{\varphi(\mathbf{k}, s)\varphi^*(\mathbf{k}, s)}{\omega_0^2(\mathbf{k}, s) - \omega^2} \sum_{\mathbf{k}, s}^{\kappa} \varphi^*(\mathbf{k}, s)q^*(\mathbf{k}, s). \end{aligned} \quad (21)$$

The eigenfrequencies are determined by the condition

$$\begin{aligned} F(\omega^2) &= 1 - g(\kappa) \sum_{\mathbf{k}, s}^{\kappa} \frac{\omega^2}{\omega_0^2(\mathbf{k}, s)} \cdot \frac{\varphi(\mathbf{k}, s)\varphi^*(\mathbf{k}, s)}{\omega_0^2(\mathbf{k}, s) - \omega^2} \\ &= 1 + g(\kappa) \sum_{\mathbf{k}, s}^{\kappa} \frac{\varphi(\mathbf{k}, s)\varphi^*(\mathbf{k}, s)}{\omega_0^2(\mathbf{k}, s)} - g(\kappa) \sum_{\mathbf{k}, s}^{\kappa} \frac{\varphi(\mathbf{k}, s)\varphi^*(\mathbf{k}, s)}{\omega_0^2(\mathbf{k}, s) - \omega^2} \\ &= 0. \end{aligned} \quad (22)$$

If the eigenfrequencies of the lattice vibration modes of $k_z = \kappa$ in a perfect

crystal are $\omega_{01}, \omega_{02}, \dots, \omega_{0i}, \dots, \omega_{0m}$ ($\omega_{01} < \omega_{02} < \dots < \omega_{0m}$), including both the longitudinal and transverse modes. $F(\omega^2)$ changes with the frequency ω^2 as shown schematically in figure 2. Therefore, we have one eigenfrequency in the dislocated crystal in each of the frequency intervals for the perfect crystal. That is, the number of the eigenstates accompanied with dislocation vibration is equal to the number of the levels of different frequency in the perfect crystal. There is one and only one state which lies between zero and the lowest frequency for the perfect lattice ($\omega_{01} = c_l \kappa$). This frequency is out of the unperturbed frequency band and gives a localized state.

The above discussions are valid for all possible values of κ . Therefore, the localized states accompanied with dislocation vibration actually form a band as shown in figure 3. $F(\omega^2)$ is evaluated in Appendix B.

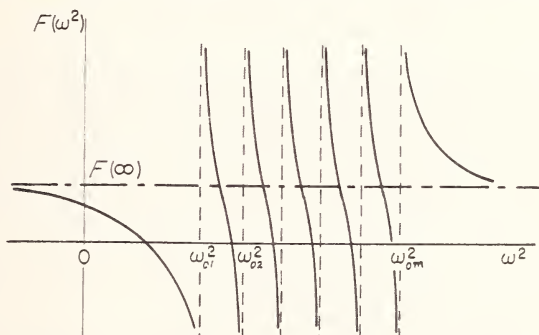


FIGURE 2. A plot of $F(\omega^2)$. The intersections of the curve with the ω^2 -axis give the eigen-frequencies.

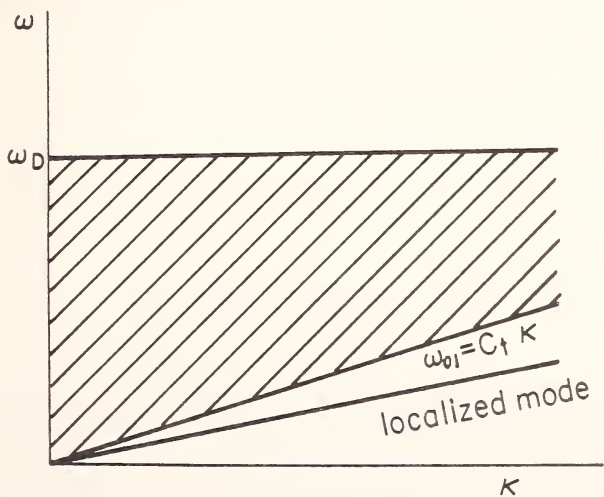


FIGURE 3. The phonon frequency band in a dislocated crystal. The localized modes are accompanied with dislocation vibration.

For an edge dislocation, the frequency of the localized mode is given

$$\frac{\omega^2}{c_l^2 \kappa^2} = \frac{2 \left(\frac{c_t}{c_l} \right)^2}{1 + \left(\frac{c_t}{c_l} \right)^4}, \quad (23)$$

in the limit of the long wavelength along the dislocation ($\kappa/k_D \ll 1$). For a screw dislocation the localized states exist very near the edge of the phonon band.

Case 2:

The second case is that given by the condition

$$\sum_{\mathbf{k}, s} \varphi^*(\mathbf{k}, s) q^*(\mathbf{k}, s) = 0. \quad (24)$$

As seen in eq (19), this condition implies that the dislocation does not vibrate. In this case the eigenfrequencies are the same as those in the perfect lattice. Let us assume that the frequency ω_{0i} is n_i -fold degenerate in the perfect crystal. Then, the modes with the frequency ω_{0i} in the dislocated crystal is $(n_i - 1)$ -fold degenerate because of the condition (24).

The total number of the lattice vibration modes in a dislocated crystal is thus the same as that for a perfect crystal.

Now, let us return to the case of dislocation vibration (Case 1) and discuss the change in the state density due to the vibration of a dislocation. As shown by Maradudin et al. [19], the change in the state density $\delta G(\omega^2, \kappa)$ is given by

$$\delta G(\omega^2, \kappa) = \frac{1}{\pi} \operatorname{Im} \frac{\partial}{\partial \omega^2} \ln F(\omega^2 - i\epsilon). \quad (25)$$

If we write as

$$\kappa^2 T(\kappa) F(\omega^2 - i\epsilon) = F_1(\omega^2) + iF_2(\omega^2),$$

then we have

$$\delta G(\omega^2, \kappa) = \frac{1}{\pi} \frac{\partial}{\partial \omega^2} \arctan \frac{F_2(\omega^2)}{F_1(\omega^2)}. \quad (26)$$

Since the present treatment for an elastic continuum are not valid near the Debye frequency, we shall discuss the state density in the region of frequency much smaller than the Debye frequency. $F_1(\omega^2)$ and $F_2(\omega^2)$ for a screw dislocation in this region are shown schematically in figure 4 (see Appendix B). The change in the state density obtained from eq (26) is plotted in figure 5. At the point (L) of the localized state we have the

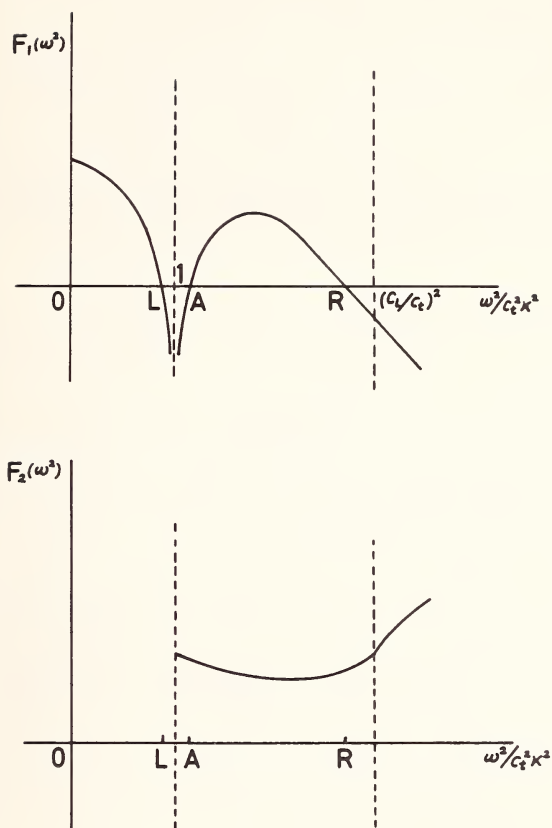


FIGURE 4. A plot of $F_1(\omega^2)$ and $F_2(\omega^2)$. (schematic)

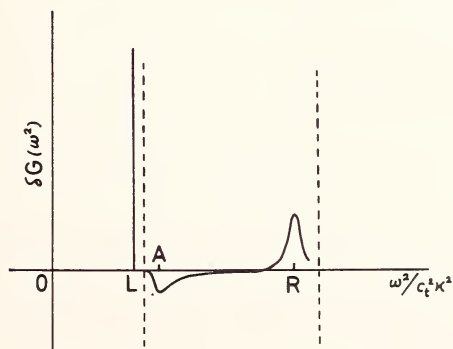


FIGURE 5. Change in the state density in the range of frequency much smaller than the Debye frequency. (schematic)

δ function. We also have the increase of the state density at the resonance point (R) which satisfies

$$F_1(\omega^2) = 0 \quad \text{and} \quad \frac{\partial F_1}{\partial \omega^2} < 0.$$

On the other hand, we have a decrease of the state density at the anti-resonance point (A) which satisfies

$$F_1(\omega^2) = 0 \quad \text{and} \quad \frac{\partial F_1}{\partial \omega^2} > 0.$$

For an edge dislocation, we have neither resonance nor anti-resonance points, although there is a localized state. The increase in the state density at the localized state is compensated with slight decreases over a wide frequency range.

IV. Mean Squared Amplitude of Dislocation Vibration

In this section the mean squared amplitude of dislocation vibration is calculated. The purpose of the calculation is to find which vibrational mode makes the largest contribution to the vibration of the dislocation.

Let us assume that the state l is accompanied with the dislocation vibration with the amplitude ξ_l . The displacement of the dislocation is, then,

$$\xi(z) = \sum_l \xi_l \exp(i\omega_l t + i\kappa_l z). \quad (27)$$

The mean squared amplitude is

$$\langle \xi(z) \xi^*(z) \rangle = \sum_l \xi_l \xi_l^* \quad (28)$$

where the averaging has been taken over both the dislocation length and time.

From eq (17) the amplitude $q_l(\mathbf{k}, s)$ of the dynamical displacement for the state l is given by

$$\{\omega_0^2(\mathbf{k}, s) - \omega_l^2\} \varphi(\mathbf{k}, s) q_l(\mathbf{k}, s) = \frac{\mu L}{\rho V} \frac{\omega_l^2}{\omega_0^2(\mathbf{k}, s)} \varphi(\mathbf{k}, s) \varphi^*(\mathbf{k}, s) \xi_l. \quad (29)$$

The elastic energy of the state l is

$$\begin{aligned} E &= \frac{\rho V}{2} \sum_{k,s} \omega_0^2(\mathbf{k}, s) q_l(\mathbf{k}, s) q_l^*(\mathbf{k}, s) + \frac{L}{2} \kappa^2 T(\kappa) \xi_l(\kappa) \xi_l^*(\kappa) \\ &= \frac{L}{2} \kappa^2 T(\kappa) \left[F(\omega_l^2) - \omega_l^2 \frac{\partial F(\omega_l^2)}{\partial \omega^2} \right] \xi_l \xi_l^* \\ &= -\frac{L}{2} \kappa^2 T(\kappa) \omega_l^2 \frac{\partial F(\omega_l^2)}{\partial \omega^2} \xi_l \xi_l^*. \end{aligned} \quad (30)$$

The last form of eq (30) was obtained, because $F(\omega_l^2) = 0$. The kinetic energy, of course, is equal to the elastic energy:

$$T_l = E_l. \quad (31)$$

Therefore, if some modes have very small value of $\partial F(\omega_l^2)/\partial \omega^2$, these modes are expected to make large contribution to the mean squared amplitude. $F(\omega^2)$ is explicitly evaluated in Appendix B after Dawber and Elliott [20] and for the in-band modes we obtain

$$\begin{aligned} \frac{\partial F(\omega^2)}{\partial \omega^2} &= -\frac{\pi m \nu(\omega^2)}{\text{Im } F(\omega^2 - i\epsilon)} |F(\omega^2 - i\epsilon)|^2 \\ &= -\frac{\pi m \nu(\omega^2)}{\kappa^2 T(\kappa) F_2(\omega^2)} [F_1^2(\omega^2) + F_2^2(\omega^2)], \end{aligned} \quad (32)$$

where $m \nu(\omega^2)$ is the density of the frequency levels $\omega_{01}^2, \omega_{02}^2, \dots, \omega_{0i}^2, \dots, \omega_{0m}^2$. From eqs (30), (31), and (32) we have

$$\xi_l \xi_l^* = \frac{E_l + T_l}{\pi L \omega_l^2 m \nu(\omega_l^2)} \cdot \frac{F_2(\omega_l^2)}{F_1^2(\omega_l^2) + F_2^2(\omega_l^2)}. \quad (33)$$

For the localized mode we have

$$\xi_l \xi_l^* = \frac{E_l + T_l}{L \omega_l^2 \left(-\frac{\partial F_1}{\partial \omega^2} \right)}, \quad (34)$$

because

$$\kappa^2 T(\kappa) F(\omega^2) = \kappa^2 T(\kappa) F(\omega^2 - i\epsilon) = F_1(\omega^2)$$

in the frequency region which is out of the phonon band.

The mean squared amplitude is, then,

$$\langle \xi(z)\xi^*(z) \rangle = \frac{L}{2\pi} \int d\kappa \left[\int d\omega^2 m\nu(\omega^2) \xi \xi^* + \frac{E_l + T_l}{L\omega_l^2 \left(-\frac{\partial F_1}{\partial \omega^2} \right)} \right], \quad (35)$$

where the first term in the brackets is the contribution from the in-band modes and the second term from the localized mode. At high temperature $\Theta (\gg \Theta_D)$

$$E_l + T_l = k_B \Theta$$

and, therefore,

$$\langle \xi(z)\xi^*(z) \rangle = \frac{k_B \Theta}{2\pi} \int d\kappa \left[\frac{1}{\pi} \int \frac{1}{\omega^2} \cdot \frac{F_2}{F_1^2 + F_2^2} d\omega^2 + \frac{1}{\omega_l^2 \left(-\frac{\partial F_1}{\partial \omega^2} \right)} \right]. \quad (36)$$

By using the formulas of $F_1(\omega^2)$ and $F_2(\omega^2)$ given in Appendix B, we can roughly estimate these contributions for the long wavelength modes ($\kappa \ll k_D$). In the case of an edge dislocation, the contribution of the localized mode is

$$\frac{1}{\omega_l^2 \left(-\frac{\partial F_1}{\partial \omega^2} \right)} \approx \frac{1}{\kappa^2 T(\kappa)}$$

and that of the in-band modes is

$$\frac{1}{\pi} \int \frac{1}{\omega^2} \cdot \frac{F_2}{F_1^2 + F_2^2} d\omega^2 \approx \frac{1}{10\kappa^2 T(\kappa)}.$$

Therefore, the mean squared amplitude of the edge dislocation is almost determined by the localized modes.

For a screw dislocation the contributions from the in-band modes are larger because as shown in figure 4 we have the resonance point at which $F_1(\omega^2) = 0$.

$$\frac{1}{\pi} \int \frac{1}{\omega^2} \cdot \frac{F_2}{F_1^2 + F_2^2} d\omega^2 \approx \frac{1}{\kappa^2 T(\kappa)}.$$

Most of the contributions come from the modes in the vicinity of the resonance point. The mode localized around the screw dislocation has

not a large amplitude, because the mode is quite near the band edge and $\partial F_1/\partial\omega^2$ is large.

Finally we must notice that, although eq (36) is obtained under the condition $\Theta \gg \Theta_D$, this equation is valid even at fairly low temperatures for the long wavelength modes ($\kappa \ll k_D$), because the mean squared amplitude is almost determined by either the localized mode or the resonance modes, which have the eigenfrequencies much smaller than the Debye frequency.

V. Scattering of Phonons

As was stated in the introduction, the problem of phonon scattering has a close connection with the problem of finding eigen states. In this section scattering of phonons by the fluttering mechanism is discussed in a rather general way compared with Nabarro.

We start again with eq (20') for a stationary scattering problem. If the incident wave is a plane wave, we expect that the solution has a form of the plane wave plus out-going waves. Thus, for the incident wave ${}^0q^*(\mathbf{k}_0, s_0)$ the scattered wave ${}^s q^*(\mathbf{k}, s)$ is given by

$$\begin{aligned} \varphi^*(\mathbf{k}, s) [{}^0q^*(\mathbf{k}, s)\delta_{kk_0}\delta_{ss_0} + {}^s q^*(\mathbf{k}, s)] &= \varphi^*(\mathbf{k}, s) {}^0q^*(\mathbf{k}, s)\delta_{kk_0}\delta_{ss_0} \\ &+ g(\kappa) \frac{\omega^2}{\omega_0^2(\mathbf{k}, s)} \cdot \frac{\varphi(\mathbf{k}, s)\varphi^*(\mathbf{k}, s)}{\omega_0^2(\mathbf{k}, s) - \omega^2 + i\epsilon} \\ &\times \sum_{\mathbf{k}', s'}^K \varphi^*(\mathbf{k}', s') [{}^0q^*(\mathbf{k}', s')\delta_{k'k_0}\delta_{s's_0} + {}^s q^*(\mathbf{k}', s')], \end{aligned} \quad (37)$$

where

$$\omega^2 = \omega_0^2(\mathbf{k}_0, s_0) \quad \text{and} \quad \kappa = k_{0z} (= z \text{ component of } \mathbf{k}_0).$$

This equation leads to

$$\begin{aligned} \varphi^*(\mathbf{k}, s) {}^s q^*(\mathbf{k}, s) &= \frac{g(\kappa)}{F(\omega^2 - i\epsilon)} \cdot \frac{\omega^2}{\omega_0^2(\mathbf{k}, s)} \cdot \\ &\frac{\varphi(\mathbf{k}, s)\varphi^*(\mathbf{k}, s)}{\omega_0^2(\mathbf{k}, s) - \omega^2 + i\epsilon} \varphi^*(\mathbf{k}_0, s_0) {}^0q^*(\mathbf{k}_0, s_0). \end{aligned} \quad (38)$$

The lattice displacement of the scattered wave is

$$\begin{aligned} u_i(\mathbf{r}) &= \sum_{k,s}^{\kappa} q^*(\mathbf{k}, s) e_i(\mathbf{k}, s) e^{-i\mathbf{kr}} \\ &= \frac{g(\kappa)}{F(\omega^2 - i\epsilon)} \varphi^*(\mathbf{k}_0, s_0) q^*(\mathbf{k}_0, s_0) \\ &\quad \times \sum_{k,s}^{\kappa} \frac{\omega^2}{\omega_0^2(\mathbf{k}, s)} \cdot \frac{\varphi(\mathbf{k}, s) e_i(\mathbf{k}, s)}{\omega_0^2(\mathbf{k}, s) - \omega^2 + i\epsilon} e^{-i\mathbf{kr}}. \end{aligned} \quad (39)$$

The asymptotic expression for the scattered wave, when $r' = (x^2 + y^2)^{1/2}$ is very large, is obtained by using the method of stationary phase (Ludwig [21]).

$$\begin{aligned} u_i(\mathbf{r}) &= \frac{i\mu\varphi^*(\mathbf{k}_0, s_0) q^*(\mathbf{k}_0, s_0)}{2(2\pi)^{1/2}\kappa^2 T(\kappa)F(\omega^2 - i\epsilon)} \\ &\quad \times \sum \frac{c_t^2}{c_s^2} \cdot \frac{1}{(k'r')^{1/2}} \varphi(\mathbf{k}, s) e_i(\mathbf{k}, s) \exp\left(-ik'r' - ik_z z + \frac{i\pi}{4}\right). \end{aligned} \quad (40)$$

The wave number of the scattered wave is determined from the conservation of the energy:

$$c_s k = c_{s0} k_0,$$

and

$$k' = (k^2 - \kappa^2)^{1/2}$$

with

$$\kappa = k_{0z} \quad \text{and} \quad k_y/k_x = y/x.$$

When we consider the energy flow, we can define the scattering width (the scattering cross section per unit length) for an infinitely long dislocation as follows: the differential scattering width is

$$\epsilon_0 dw = \epsilon_s r' d\theta \quad (41)$$

when the energy is scattered to the θ direction in the xy plane. Here ϵ_0 and ϵ_s are the incident and the scattered energy flux respectively. From eq (40)

$$dw = \frac{\mu^2 \varphi(\mathbf{k}_0, s_0) \varphi^*(\mathbf{k}_0, s_0) d\theta}{8\pi\kappa^4 T^2(\kappa) F(\omega^2 - i\epsilon) F^*(\omega^2 - i\epsilon)} \sum_s \frac{c_s}{c_{s0}} \cdot \frac{c_t^4}{c_s^4} \varphi(\mathbf{k}, s) \varphi^*(\mathbf{k}, s) \frac{1}{k'} \cdot \frac{1}{k'^2}. \quad (42)$$

The total scattering width is, after integrating dw over θ ,

$$w = \frac{b^2 \mu^2 \varphi(\mathbf{k}_0, s_0) \varphi^*(\mathbf{k}_0, s_0)}{8\kappa^4 T^2(\kappa) F(\omega^2 - i\epsilon) F^*(\omega^2 - i\epsilon)} \left[\frac{c_t^4}{c_{s0}^3 c_t} \frac{1}{k_0^2} \{ \beta_x^2 k_t'^3 + 4\beta_z^2 \kappa^2 k_t' \} \right. \\ \left. + \frac{c_t}{c_{s0}} \left\{ \beta_x^2 k_t' + \beta_z^2 \frac{\kappa^2}{k_t'} \right\} + \frac{c_t^3}{c_{s0}^3} \frac{1}{k_0^2} \left\{ \beta_x^2 \kappa^2 k_t' + \beta_z^2 \frac{(k_t'^2 - \kappa^2)^2}{k_t'} \right\} \right], \quad (43)$$

where

$$k_t' = \left[\left(\frac{c_{s0} k_0}{c_t} \right)^2 - \kappa^2 \right]^{1/2}, \quad k_t' = \left[\left(\frac{c_{s0} k_0}{c_t} \right)^2 - \kappa^2 \right]^{1/2},$$

and

$$\beta = \frac{\mathbf{b}}{b}.$$

The explicit form of $F(\omega^2 - i\epsilon)$ is given in Appendix B. When the real

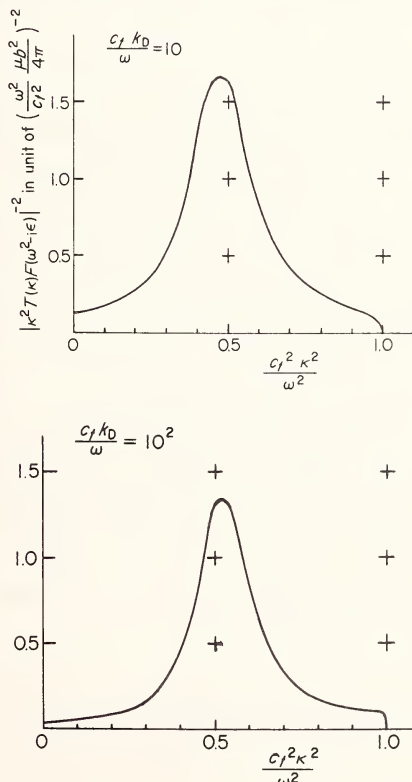


FIGURE 6. A plot of $|\kappa^2 T(\kappa) F(\omega^2 - i\epsilon)|^{-2}$ for a screw dislocation in an isotropic medium as a function of κ . $(c_t/c_l)^2$ is assumed to be 1/3 (Cauchy relation).

part of F becomes zero, we have the resonance scattering of phonons. This condition is satisfied for a transverse phonon incident obliquely on a screw dislocation. The value of $\{\kappa^4 T^2(\kappa) F(\omega^2 - i\epsilon) F^*(\omega^2 - i\epsilon)\}^{-1}$ for a screw dislocation is plotted in figure 6 as a function of the incidence angle, that is, as a function of κ .

When we deviate far from the resonance point, the order of magnitude of the total scattering width is, for $k_0 b \ll 1$,

$$w \approx \frac{2\pi^2}{k_0 \left\{ \ln \left| \frac{\omega^2}{c^2} - \kappa^2 \right| \frac{1}{k_D^2} \right\}},$$

which agrees with the result of Nabarro for $\kappa=0$ (normal incidence).

When we consider a transverse phonon incident on a screw dislocation in parallel, the scattering cross section becomes infinity, because $k'_i=0$. We, however, have no physical trouble, because in this case the scattering angle is zero.

VI. Dislocation Vibration in a Peierls Potential

The treatments of the dislocation vibration discussed in the preceding sections were based on the continuum model of the elastic body. Taking the lattice discreteness into account will be necessary for some problems of dislocation motion. Dislocation vibration near the Debye frequency is of course such a case. Besides, in the case of dislocation the lattice discreteness leads to the existence of the Peierls potential and, therefore, low frequency vibrations of a dislocation will also be affected by the discreteness. In this section we shall consider the effect of the Peierls potential on the dislocation vibration just by adding the potential to the above treatments. We confine ourselves to the infinitesimal vibration in the potential. Then the potential is approximated to be parabolic. Generally, the kinetic energy may also be influenced with the lattice discreteness. But, here, we consider only the effect of Peierls potential.

Let us consider that the displacement of the dislocation is given by eq (1). The Peierls potential energy is

$$E_p = \frac{P}{2} \int \xi^2(z) dz = \frac{PL}{2} \sum_{\kappa} \xi(\kappa) \xi^*(\kappa). \quad (45)$$

The effect of the Peierls potential on the lattice vibration is, therefore, obtained just by replacing $\kappa^2 T(\kappa)$ in the preceeding sections by $\kappa^2 T(\kappa) + P$.

The eigenfrequencies accompanied with dislocation vibration are determined with the condition

$$\frac{P}{\kappa^2 T(\kappa)} + 1 - \frac{\mu^2 L}{\rho V \kappa^2 T(\kappa)} \sum_{k,s}^{\kappa} \frac{\omega^2}{\omega_0^2(\mathbf{k}, s)} \cdot \frac{\varphi(\mathbf{k}, s) \varphi^*(\mathbf{k}, s)}{\omega_0^2(\mathbf{k}, s) - \omega^2} = 0, \quad (46)$$

differing from eq (22) by the constant term $P/\kappa^2 T(\kappa)$. Seeing figure 2, we easily know that there is again one eigenstate in each interval of the eigenfrequencies for a perfect crystal, and below the phonon band we always have a localized vibration of the dislocation for every possible value of κ , although the eigenfrequencies increase with increasing magnitude of the Peierls potential.

The scattering cross section of a phonon is rather largely affected by the Peierls potential, especially at low frequencies. The total scattering width is again given by eq (43) with $\kappa^2 T(\kappa)$ replaced by $\kappa^2 T(\kappa) + P$. Such a replacement results in change in the condition of resonance scattering. In order to obtain a rather rough but more intuitive estimation about the change, we will consider the scattering of a phonon with a frequency much smaller than the Debye frequency. Let us define $F_P(\omega^2)$ by $F(\omega^2)$ with $\kappa^2 T(\kappa)$ replaced by $\kappa^2 T(\kappa) + P$. In this frequency range,

$$\{\kappa^2 T(\kappa) + P\} F_P(\omega^2 - i\epsilon)$$

is roughly but briefly expressed as

$$\{\kappa^2 T(\kappa) + P\} F_P(\omega^2 - i\epsilon) \approx m(\omega_p^2 - \omega^2) + \kappa^2 T + i \frac{m}{10} \omega^2, \quad (47)$$

by neglecting ω or κ dependence of the logarithmic terms in eq (B. 9) and putting these terms constant (m and T). Here, ω_p^2 is defined by $P = m\omega_p^2$ and the imaginary term gives only the order of magnitude. If dislocations are randomly oriented, we must use the cross section averaged over the incident angle:

$$\bar{w} = \frac{1}{2k_0} \int_{-k_0}^{k_0} w(\kappa) d\kappa. \quad (48)$$

Since the κ dependence of the cross section $w(\kappa)$ is given almost by $|\{\kappa^2 T(\kappa) + P\}^2 F_P(\omega^2 - i\epsilon) F_P^*(\omega^2 - i\epsilon)|^{-1}$, we use a following approximate formula of $w(\kappa)$ to evaluate eq (48):

$$w(\kappa) \approx \frac{b^4 \mu^2 \kappa_0^3}{8\{\kappa^2 T(\kappa) + P\}^2 F_P(\omega^2 - i\epsilon) F_P^*(\omega^2 - i'\epsilon)}. \quad (49)$$

Here, we have used

$$\varphi(k_0, s_0)\varphi^*(k_0, s_0) \sim k_0^2 b^2,$$

and put the terms in the brackets in eq (43) equal to k_0 . Then, the averaged cross section \bar{w} for a transverse phonon is given by

$$\begin{aligned}\bar{w} &= \frac{\mu^2 b^4}{8T^2} \cdot \frac{1}{k_0} \int_0^1 \frac{dx}{(x^2 - \alpha)^2 + \beta^2} \\ &\approx \frac{1}{8k_0} \int_0^1 \frac{dx}{(x^2 - \alpha)^2 + \beta^2},\end{aligned}\quad (50)$$

where

$$\alpha = \frac{mc_t^2}{T} \left(1 - \frac{\omega_p^2}{\omega^2} \right)$$

and

$$\beta = \frac{mc_t^2}{10T}.$$

mc_t^2/T has a value of about 0.5 and 1.5 for a screw and an edge dislocation respectively.

The integral in eq (52) changes with the frequency ω^2 as follows:

$$I(\alpha) = \int_0^1 \frac{dx}{(x^2 - \alpha)^2 + \beta^2}.$$

Case 1: $\omega \gg \omega_p$

$$\begin{aligned}I(\alpha) &\sim 40 \text{ for a screw dislocation,} \\ &\sim 0.5 \text{ for an edge dislocation.}\end{aligned}$$

Case 2: $\omega \sim \omega_p$

$I(\alpha)$ has a sharp peak at this frequency. The peak height is

$$\begin{aligned}I(\alpha) &\sim \beta^{-3/2} \sim 90 \text{ (screw),} \\ &\sim 18 \text{ (edge),}\end{aligned}$$

and the peak width is

$$(\omega^2 - \omega_p^2) \equiv \pm \beta \omega^2.$$

Case 3: $\omega \ll \omega_p$

$$\begin{aligned} I(\alpha) &\sim 2\omega^4/\omega_p^4 \text{ (screw),} \\ &\sim \omega^4/4.5\omega_p^4 \text{ (edge).} \end{aligned}$$

The large difference of the cross section between the screw and edge dislocations at high frequencies (Case 1) is due to the existence of resonance scattering for oblique incidence of a transverse phonon on the screw dislocation. Below the frequency ω_p (Case 3), the scattering cross section rapidly decreases with decreasing frequency as ω^3 .

For an edge dislocation the following approximate formula of the cross section can be used in all ranges of frequencies:

$$\bar{w} = \frac{c_t}{16} \cdot \frac{\omega^3}{(\omega^2 - \omega_p^2)^2 + \beta^2 \omega^4}. \quad (51)$$

The above discussions, of course, are not limited to the Peierls potential. If a dislocation is surrounded with impurity atmospheres, the dislocation feels an effective potential for an infinitesimal vibration. Kusunoki and Suzuki [22] have applied eq (51) to lattice thermal conductivity data in Cu-Al alloy.

VII. Energies of a Crystal Containing Many Parallel Dislocations

So far we have treated an isolated dislocation in a crystal. In this section energies of a crystal containing many parallel dislocations and equations of motion are obtained and in the next section the equations are applied to a dislocation dipole.

Let us consider that dislocations are parallel to the z axis and the position of the d th dislocation is denoted by (x_d, y_d) . The displacement $\xi_d(z)$ of the dislocation is again expanded in a Fourier series

$$\xi_d(z) = \sum_{\kappa} \xi_d(\kappa) e^{i\kappa z}. \quad (52)$$

The static displacement of the elastic field is, then,

$$u_i^s = \sum_{\kappa} \sum_d f_i(x - x_d, y - y_d; \kappa; b_d) e^{i\kappa z} \xi_d(\kappa) + u_{i0}^s \quad (53)$$

The kinetic energy of the body is given by

$$\begin{aligned}
T = & \frac{\rho V}{2} \sum_{k,s} \dot{q}(\mathbf{k}, s) \dot{q}^*(\mathbf{k}, s) \\
& + \sum_d \sum_{\kappa} \sum_{k,s}^{\kappa} \frac{\mu L \varphi_d(\mathbf{k}, s)}{\omega_0^2(\mathbf{k}, s)} e^{i(k_x x_d + k_y y_d)} \dot{q}(\mathbf{k}, s) \dot{\xi}_d^*(\kappa) \\
+ & \frac{1}{2\rho V} \sum_{d,d'} \sum_{\kappa} \sum_{k,s}^{\kappa} \frac{\mu^2 L^2 \varphi_{d'}(\mathbf{k}, s) \varphi_d^*(\mathbf{k}, s)}{\omega_0^4(\mathbf{k}, s)} e^{i\{k_x(x_{d'} - x_d) + k_y(y_{d'} - y_d)\}} \dot{\xi}_d(\kappa) \dot{\xi}_{d'}^*(\kappa),
\end{aligned} \tag{54}$$

where $\varphi_d(k, s)$ is $\varphi(k, s)$ for the d th dislocation.

The elastic energy is obtained by following the same way as in section II. The energy of the static field is

$$E_s = \text{const.} - \frac{1}{4} \sum_{d,d'} \sum_i b_{di} \int dz_d dz_{d'} P_{iy}(z_{d'} - z_d; d, d'; b_{d'}) [\xi_d(z_d) - \xi_{d'}(z_{d'})]^2, \tag{55}$$

where $P_{ij}(z_{d'} - z_d; d, d'; b_d)$ is the stress at the d th dislocation due to an infinitesimal dislocation loop on the d' th dislocation. When the dislocation displacements are given by eq (52),

$$\begin{aligned}
E_s = & \text{const.} + \frac{L}{2} \sum_d \sum_{\kappa} \kappa^2 T_d(\kappa) \xi_d(\kappa) \xi_d^*(\kappa) \\
& - \frac{L}{2} \sum_{\substack{d, d' \\ (d+d')}} \sum_{\kappa} \xi_d(\kappa) \xi_{d'}^*(\kappa) \left[\frac{1}{2} \int_{-\infty}^{\infty} \sum_i b_{di} P_{iy}(z; d, d'; b_d) dz \right. \\
& \quad \left. + \frac{1}{2} \int_{-\infty}^{\infty} \sum_i b_{d'i} P_{iy}(z; d', d; b_d) dz \right. \\
& \quad \left. + \frac{L}{2} \sum_{\substack{d, d' \\ (d+d')}} \sum_{\kappa} \xi_d(\kappa) \xi_{d'}^*(\kappa) \left[\frac{1}{2} \int_{-\infty}^{\infty} \sum_i b_{di} P_{iy}(z; d, d'; b_{d'}) e^{-i\kappa z} dz \right. \right. \\
& \quad \left. \left. + \frac{1}{2} \int_{-\infty}^{\infty} \sum_i b_{d'i} P_{iy}(z; d', d; b_d) e^{i\kappa z} dz \right] \right] \\
= & \text{const.} + \frac{L}{2} \sum_d \sum_{\kappa} \kappa^2 T_d(\kappa) \xi_d(\kappa) \xi_d^*(\kappa) \\
& + \frac{L}{2} \sum_{\substack{d, d' \\ (d+d')}} \sum_{\kappa} \xi_d(\kappa) \xi_{d'}^*(\kappa) \left[\frac{\mu^2 L \sum_{k,s}^{\kappa=0} \varphi_{d'}(\mathbf{k}, s) \varphi_d^*(\mathbf{k}, s)}{\rho V} \right. \\
& \quad \times e^{i\{k_i(x_{d'} - x_d) + k_y(y_{d'} - y_d)\}} \left. \right]
\end{aligned}$$

$$\begin{aligned}
& -\frac{L}{2} \sum_{d, d'} \sum_{\kappa} \xi_d(\kappa) \xi_{d'}^*(\kappa) \left[\frac{\mu^2 L}{\rho V} \sum_{\mathbf{k}, s} \frac{\varphi_{d'}(\mathbf{k}, s) \varphi_d^*(\mathbf{k}, s)}{\omega_0^2(\mathbf{k}, s)} \right. \\
& \quad \times e^{i\{k_x(x_{d'} - x_d) + k_y(y_{d'} - y_d)\}} \left. \right], \quad (56)
\end{aligned}$$

where we have used the results obtained in Appendix A to arrive at the final expression.

The third term of eq (56) shows that in a many-dislocation system the apparent line tension changes by

$$\frac{\mu^2 L}{\rho V \kappa^2 T_d(\kappa)} \sum_{d' (\mathbf{k}, s)}^{\kappa=0} \frac{\varphi_{d'}(\mathbf{k}, s) \varphi_d^*(\mathbf{k}, s)}{\omega_0^2(\mathbf{k}, s)} e^{i\{k_x(x_{d'} - x_d) + k_y(y_{d'} - y_d)\}}.$$

The elastic energy of the dynamical field is, of course, given by eq (9). From the Lagrangian $L = T - E$, we obtain the equations of motion:

$$\ddot{q}^*(\mathbf{k}, s) + \omega_0^2(\mathbf{k}, s) q^*(\mathbf{k}, s) + \frac{\mu L}{\rho V} \sum_d \frac{\varphi_d(\mathbf{k}, s)}{\omega_0^2(\mathbf{k}, s)} e^{i\{k_x x_d + k_y y_d\}} \ddot{\xi}_d^*(\kappa) = 0, \quad (57)$$

and

$$\begin{aligned}
& \sum_{\mathbf{k}, s}^{\kappa} \frac{\mu L \varphi_d(\mathbf{k}, s)}{\omega_0^2(\mathbf{k}, s)} e^{i\{k_x x_d + k_y y_d\}} \ddot{q}(\mathbf{k}, s) \\
& + \frac{1}{\rho V} \sum_{d'} \sum_{\mathbf{k}, s}^{\kappa} \frac{\mu^2 L^2 \varphi_d(\mathbf{k}, s) \varphi_{d'}^*(\mathbf{k}, s)}{\omega_0^2(\mathbf{k}, s)} e^{i\{k_x(x_d - x_{d'}) + k_y(y_d - y_{d'})\}} \ddot{\xi}_{d'}(\kappa) \\
& + L \kappa^2 T_d(\kappa) \left[1 + \frac{\mu^2 L}{\rho V \kappa^2 T_d(\kappa)} \sum_{d'}^{\kappa=0} \sum_{\mathbf{k}, s} \frac{\varphi_{d'}(\mathbf{k}, s) \varphi_d^*(\mathbf{k}, s)}{\omega_0^2(\mathbf{k}, s)} \right. \\
& \quad \times e^{i\{k_x(x_{d'} - x_d) + k_y(y_{d'} - y_d)\}} \left. \right] \xi_d(\kappa) \\
& - L \sum_{d'} \frac{\mu^2 L}{\rho V} \sum_{\mathbf{k}, s}^{\kappa} \frac{\varphi_{d'}^*(\mathbf{k}, s) \varphi_d(\mathbf{k}, s)}{\omega_0^2(\mathbf{k}, s)} e^{i\{k_x(x_d - x_{d'}) + k_y(y_d - y_{d'})\}} \xi_{d'}(\kappa) = 0. \quad (58)
\end{aligned}$$

The equation corresponding to eq (9), which gives the force balance at the dislocations, is

$$\begin{aligned} & \kappa^2 T_d(\kappa) \left[1 + g_d(\kappa) \sum_{d'}^{\kappa=0} \sum_{\mathbf{k}, s} \frac{\varphi_{d'}(\mathbf{k}, s) \varphi_d^*(\mathbf{k}, s)}{\omega_0^2(\mathbf{k}, s)} e^{i(k_x(x_{d'} - x_d) + k_y(y_{d'} - y_d))} \right] \xi_d^*(\kappa) \\ & - \kappa^2 T_d(\kappa) g_d(\kappa) \sum_{\substack{d' \\ (= d)}}^{\kappa} \sum_{\mathbf{k}, s} \frac{\phi_{d'}(\mathbf{k}, s) \phi_d^*(\mathbf{k}, s)}{\omega_0^2(\mathbf{k}, s)} e^{i(k_x(x_{d'} - x_d) + k_y(y_{d'} - y_d))} \xi_{d'}^*(\kappa) \\ & = \mu \sum_{\mathbf{k}, s}^{\kappa} \varphi_d^*(\mathbf{k}, s) q^*(\mathbf{k}, s) e^{-i(k_x x_d + k_y y_d)}. \end{aligned} \quad (59)$$

Although these equations are general for parallel dislocations, it is usually difficult to find eigenvibrations of many-dislocation systems except in some special cases. In the next section we shall treat an edge dislocation dipole as one of the simple cases.

VIII. Vibrations of an Edge Dislocation Dipole

In ionic crystals, many dislocation dipoles have been found by Johnston and Gilman [23] to be produced by plastic deformation. Therefore, it will be of interest to calculate the eigenfrequencies of a dislocation dipole and its cross section of phonon scattering as an application of the equations obtained in section VII.

In this section we treat an edge dislocation dipole in the equilibrium configuration (fig. 7). Equation (59) now becomes

$$\begin{aligned} & \kappa^2 T(\kappa) \left[1 - g(\kappa) \sum_{\mathbf{k}, s}^{\kappa=0} \frac{\omega(\mathbf{k}, s) \varphi^*(\mathbf{k}, s)}{\omega_0^2(\mathbf{k}, s)} e^{2ia(k_x + k_y)} \right] \xi_1^*(\kappa) \\ & + \kappa^2 T(\kappa) g(\kappa) \sum_{\mathbf{k}, s}^{\kappa} \frac{\varphi(\mathbf{k}, s) \varphi^*(\mathbf{k}, s)}{\omega_0^2(\mathbf{k}, s)} e^{2ia(k_x + k_y)} \xi_2^*(\kappa) \\ & = \mu \sum_{\mathbf{k}, s}^{\kappa} \varphi^*(\mathbf{k}, s) q^*(\mathbf{k}, s) e^{ia(k_x + k_y)} \end{aligned} \quad (60a)$$

and

$$\begin{aligned} & \kappa^2 T(\kappa) \left[1 - g(\kappa) \sum_{\mathbf{k}, s}^{\kappa=0} \frac{\varphi(\mathbf{k}, s) \varphi^*(\mathbf{k}, s)}{\omega_0^2(\mathbf{k}, s)} e^{-2ia(k_x + k_y)} \right] \xi_2^*(\kappa) \\ & + \kappa^2 T(\kappa) g(\kappa) \sum_{\mathbf{k}, s}^{\kappa} \frac{\varphi(\mathbf{k}, s) \varphi^*(\mathbf{k}, s)}{\omega_0^2(\mathbf{k}, s)} e^{-2ia(k_x + k_y)} \xi_1^*(\kappa) \\ & = -\mu \sum_{\mathbf{k}, s}^{\kappa} \varphi^*(\mathbf{k}, s) q^*(\mathbf{k}, s) e^{-ia(k_x + k_y)}. \end{aligned} \quad (60b)$$

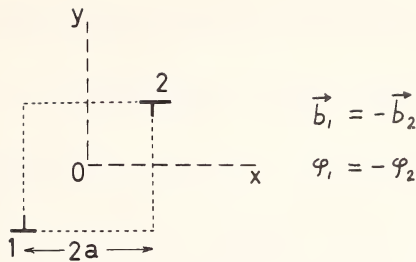


FIGURE 7. Dislocation dipole.

For an edge dislocation, it is easily shown that

$$\varphi(-k_x, -k_y, \kappa, s)\varphi^*(-k_x, -k_y, \kappa, s) = \varphi(k_x, k_y, \kappa, s)\varphi^*(k_x, k_y, \kappa, s) \quad (61)$$

and, therefore, we have

$$\sum_{k,s}^{\kappa} \frac{\varphi\varphi^*(\mathbf{k}, s)}{\omega_0^2(\mathbf{k}, s)} e^{2ia(k_x+k_y)} = \sum_{k,s}^{\kappa} \frac{\varphi\varphi^*(\mathbf{k}, s)}{\omega_0^2(\mathbf{k}, s)} e^{-2ia(k_x+k_y)}.$$

Let us define $\psi(a, \kappa)$ by

$$\psi(a, \kappa) = - \sum_{k,s}^{\kappa} \frac{\varphi\varphi^*(\mathbf{k}, s)}{\omega_0^2(\mathbf{k}, s)} \cos 2a(k_x+k_y). \quad (62)$$

Then, eqs (60a) and (60b) give

$$\{1 + g(\kappa)\psi(a, 0) + g(\kappa)\psi(a, \kappa)\}\{\xi_1^*(\kappa) - \xi_2^*(\kappa)\} = \frac{2\mu}{\kappa^2 T(\kappa)} A, \quad (63a)$$

and

$$\{1 + g(\kappa)\psi(a, 0) - g(\kappa)\psi(a, \kappa)\}\{\xi_1^*(\kappa) + \xi_2^*(\kappa)\} = \frac{2i\mu}{\kappa^2 T(\kappa)} B, \quad (63b)$$

where we have defined A and B by

$$A = \sum_{k,s}^{\kappa} \varphi^*(\mathbf{k}, s) q^*(\mathbf{k}, s) \cos a(k_x+k_y) \quad (64a)$$

and

$$B = \sum_{k,s}^{\kappa} \varphi^*(\mathbf{k}, s) g^*(\mathbf{k}, s) \sin a(k_x+k_y), \quad (64b)$$

respectively. Substitution of these equations for eq (57), gives

$$\varphi^*(\mathbf{k}, s)q^*(\mathbf{k}, s) = 2g(\kappa) \frac{\omega^2}{\omega_0^2(\mathbf{k}, s)} \cdot \frac{\varphi\varphi^*(\mathbf{k}, s)}{\omega_0^2(\mathbf{k}, s) - \omega^2} \\ \times \left[\frac{A \cos a(k_x + k_y)}{1 + g(\kappa)\psi(a, 0) + g(\kappa)\psi(a, \kappa)} + \frac{B \sin a(k_x + k_y)}{1 + g(\kappa)\psi(a, 0) - g(\kappa)\psi(a, \kappa)} \right] \quad (65)$$

for a stationary vibration. Multiplying eq (65) by $\cos a(k_x + k_y)$ or $\sin a(k_x + k_y)$ and summing over the modes whose wave vector has $k_z = \kappa$, we obtain

$$\left\{ 1 - \frac{2g(\kappa)}{1 + g(\kappa)\psi(a, 0) + g(\kappa)\psi(a, \kappa)} \sum_{\mathbf{k}, s}^{\kappa} \frac{\omega^2}{\omega_0^2} \cdot \frac{\varphi\varphi^*(\mathbf{k}, s)}{\omega_0^2 - \omega^2} \cos^2 a(k_x + k_y) \right\} A \\ = \frac{2g(\kappa)B}{1 + g(\kappa)\psi(a, 0) - g(\kappa)\psi(a, \kappa)} \sum_{\mathbf{k}, s}^{\kappa} \frac{\omega^2}{\omega_0^2} \cdot \frac{\varphi\varphi^*(\mathbf{k}, s)}{\omega_0^2 - \omega^2} \\ \times \sin a(k_x + k_y) \cos a(k_x + k_y) \quad (66a)$$

or

$$\left\{ 1 - \frac{2g(\kappa)}{1 + g(\kappa)\psi(a, 0) - g(\kappa)\psi(a, \kappa)} \sum_{\mathbf{k}, s}^{\kappa} \frac{\omega^2}{\omega_0^2} \cdot \frac{\varphi\varphi^*(\mathbf{k}, s)}{\omega_0^2 - \omega^2} \sin^2 a(k_x + k_y) \right\} B \\ = \frac{2g(\kappa)A}{1 + g(\kappa)\psi(a, 0) + g(\kappa)\psi(a, \kappa)} \sum_{\mathbf{k}, s}^{\kappa} \frac{\omega^2}{\omega_0^2} \cdot \frac{\varphi\varphi^*(\mathbf{k}, s)}{\omega_0^2 - \omega^2} \\ \times \sin a(k_x + k_y) \cos a(k_x + k_y). \quad (66b)$$

If we use eq (61), eq (66a) and eq (66b) are easily found to be zero. Eigenstates are classified into three cases:

Case 1. $A \neq 0, B = 0$ ($\xi_2^*(\kappa) = -\xi_1^*(\kappa)$: symmetric)

In this case the eigenfrequencies are determined by the condition

$$F_+(\omega^2) = 1 + g(\kappa)\psi(a, 0) + g(\kappa)\psi(a, \kappa) \\ - 2g(\kappa) \sum_{\mathbf{k}, s}^{\kappa} \frac{\omega^2}{\omega_0^2} \cdot \frac{\varphi\varphi^*(\mathbf{k}, s)}{\omega_0^2 - \omega^2} \cos^2 a(k_x + k_y) \\ = F(\omega^2) + g(\kappa)\psi(a, 0) \\ - g(\kappa) \sum_{\mathbf{k}, s}^{\kappa} \frac{\varphi\varphi^*(\mathbf{k}, s)}{\omega_0^2 - \omega^2} \cos 2a(k_x + k_y) \\ = 0. \quad (67)$$

Case 2. $A=0, B \neq 0$ ($\xi_2^*(\kappa) = \xi_1^*(\kappa)$: antisymmetric)

The condition to determine the eigenfrequencies is

$$\begin{aligned}
 F_-(\omega^2) &= 1 + g(\kappa)\psi(a, 0) - g(\kappa)\psi(a, \kappa) \\
 &\quad - 2g(\kappa) \sum_{\mathbf{k}, s}^{\kappa} \frac{\omega^2}{\omega_0^2 - \omega^2} \frac{\varphi\varphi^*(\mathbf{k}, s)}{\omega_0^2 - \omega^2} \sin^2 a(k_x + k_y) \\
 &= F(\omega^2) + g(\kappa)\psi(a, 0) + g(\kappa) \sum_{\mathbf{k}, s}^{\kappa} \frac{\varphi\varphi^*(\mathbf{k}, s)}{\omega_0^2 - \omega^2} \cos 2a(k_x + k_y) \\
 &= 0. \tag{68}
 \end{aligned}$$

Both these cases are accompanied with dislocation vibration. As in an isolated dislocation (section III), in each case we have one eigenfrequency in each interval of the eigenfrequencies in the perfect crystal. We also have a localized state below the phonon band for each κ .

Case 3. $A=B=0$ ($\xi_1^*(\kappa) = \xi_2^*(\kappa) = 0$)

Lattice vibrations in this case are not accompanied with dislocation vibration. The eigenfrequencies are the same as those in the perfect crystal.

Scattering of a phonon by an edge dislocation dipole can be treated along the same line as by an isolated dislocation. The fundamental equation is obtained from eq (65) as

$$\begin{aligned}
 \varphi^*(\mathbf{k}, s)[\ddot{q}^*(\mathbf{k}, s)\delta_{kk_0}\delta_{ss_0} + \ddot{q}^*(\mathbf{k}, s)] &= \varphi^*(\mathbf{k}, s)\dot{q}(\mathbf{k}, s)\delta_{kk_0}\delta_{ss_0} \\
 &\quad + 2g(\kappa) \frac{\omega^2}{\omega_0^2 - \omega^2 + i\epsilon} \left[\frac{\cos a(k_x + k_y)}{1 + g\psi(a, 0) + g\psi(a, \kappa)} \right. \\
 &\quad \times \sum_{\mathbf{k}' s'}^{\kappa} \varphi^*(\mathbf{k}', s') \{ \dot{q}^*(\mathbf{k}', s')\delta_{k' k_0}\delta_{s' s_0} + \dot{q}^*(\mathbf{k}', s') \} \cos a(k'_x + k'_y) \\
 &\quad + \frac{\sin a(k_x + k_y)}{1 + g\psi(a, 0) - g\psi(a, \kappa)} \sum_{\mathbf{k}' s'}^{\kappa} \varphi^*(\mathbf{k}', s') \{ \dot{q}^*(\mathbf{k}', s')\delta_{k' k_0}\delta_{s' s_0} \\
 &\quad \left. + \dot{q}^*(\mathbf{k}', s') \} \sin a(k'_x + k'_y) \right].
 \end{aligned}$$

After a little calculation, we have

$$\begin{aligned} \varphi^*(\mathbf{k}, s) \dot{q}^*(\mathbf{k}, s) &= 2g(\kappa) \frac{\omega^2}{\omega_0^2 - \omega^2 + i\epsilon} \varphi^*(\mathbf{k}_0, s_0) \dot{q}^*(\mathbf{k}_0, s_0) \\ &\times \left[\frac{\cos a(k_{0x} + k_{0y}) \cos a(k_x + k_y)}{F_+(\omega^2 - i\epsilon)} + \frac{\sin a(k_{0x} + k_{0y}) \sin a(k_x + k_y)}{F_-(\omega^2 - i\epsilon)} \right]. \end{aligned} \quad (70)$$

By using the calculation given in Appendix B, we can estimate roughly the scattering behaviors of a phonon as a function of the frequency. If the frequency is much smaller than the Debye frequency,

$$\begin{aligned} \operatorname{Re} \kappa^2 T(\kappa) F_+(\omega^2 - i\epsilon) &\approx -m\omega^2 + \kappa^2 T + \frac{\mu b^2}{4\pi} \left(1 - \frac{c_l^2}{c_t^2} \right) \frac{1}{2a^2} \\ &- \frac{\mu^2 L}{\rho V} \sum_{\mathbf{k}, s}^{\kappa} \frac{\varphi \varphi^*(\mathbf{k}, s)}{\omega_0^2 - \omega^2 + i\epsilon} \cos 2a(k_x + k_y), \end{aligned} \quad (71a)$$

and

$$\begin{aligned} \operatorname{Re} \kappa^2 T(\kappa) F_-(\omega^2 - i\epsilon) &\approx -m\omega^2 + \kappa^2 T + \frac{\mu b^2}{4\pi} \left(1 - \frac{c_l^2}{c_t^2} \right) \frac{1}{2a^2} \\ &+ \frac{\mu^2 L}{\rho V} \sum_{\mathbf{k}, s}^{\kappa} \frac{\varphi \varphi^*(\mathbf{k}, s)}{\omega_0^2 - \omega^2 + i\epsilon} \cos 2a(k_x + k_y). \end{aligned} \quad (71b)$$

When the phonon frequency is high enough so that

$$m\omega^2 \gg \frac{\mu b^2}{4\pi} \left(1 - \frac{c_l^2}{c_t^2} \right) \frac{1}{2a^2},$$

we have

$$\kappa^2 T(\kappa) F_+(\omega^2 - i\epsilon) \approx \kappa^2 T F_-(\omega^2 - i\epsilon) \approx -m\omega^2 + \kappa^2 T.$$

Then the magnitude of the scattering cross section is about the same as that for an isolated dislocation, although for a dipole we have a remarkable angular dependence due to the coefficients $\cos a(k_{0x} + k_{0y}) \cos a(k_x + k_y)$ and $\sin a(k_{0x} + k_x) \sin a(k_x + k_y)$.

If the phonon frequency is low so that

$$\operatorname{Re} \kappa^2 T(\kappa) F_+(\omega^2 - i\epsilon) \approx \frac{\mu b^2}{4\pi} \left(1 - \frac{c_l^2}{c_t^2} \right) \frac{1}{a^2},$$

$$\operatorname{Re} \kappa^2 T(\kappa) F_-(\omega^2 - i\epsilon) \approx -m\omega^2 + \kappa^2 T,$$

and $a|k| \ll 1$, then the scattering behavior is almost same as that for a dislocation in the parabolic potential (section VI).

IX. Appendix A. Static Strain Around a Dislocation and Static Line Tension

In this appendix the static strain around a dislocation and the static line tension are calculated.

Let us consider a dislocation along the z -axis. When the displacement of the dislocation is given by

$$\xi(z) = \xi(\kappa) e^{i\kappa z}. \quad (\text{A1})$$

the static displacement field in an elastic body is easily obtained by using the Green's function (de Wit, [24]):

$$\begin{aligned} u_i^s(x, y, z) &= b_m c_{mjk} n_j \int_{-\infty}^{\infty} U_{ki,l}(x, y, z-z') \xi(\kappa) e^{i\kappa z'} dz' \\ &= \xi(\kappa) e^{i\kappa z} \left[b_m c_{mjk} n_j \int_{-\infty}^{\infty} U_{ki,l}(x, y, z-z') e^{i\kappa(z-z')} d(z-z') \right]. \end{aligned} \quad (\text{A2})$$

Here, U_{ki} is the Green's tensor function and n is the unit vector perpendicular to the slip plane. We have used the convention that a repeated suffix is to be summed over x, y, z and suffices following comma denote differentiation. It is now convenient to use the Fourier transform of the Green's function.

$$\begin{aligned} \bar{U}_{ki}(k) &= \int U_{ki}(r) e^{-ikr} dr \\ &= \frac{1}{\mu} \left(\frac{\delta_{ki}}{k^2} - \frac{1}{2(1-\nu)} \frac{k_k k_i}{k^4} \right). \end{aligned} \quad (\text{A3})$$

By using

$$c_{mjk} = \lambda \delta_{mj} \delta_{kl} + \mu (\delta_{mk} \delta_{jl} + \delta_{ml} \delta_{jk})$$

and $b_i n_i = 0$, we obtain

$$f_i^*(x, y; \kappa) = -i\mu \left(\frac{1}{2\pi} \right)^2 b_m n_j \int dk_x dk_y \{ \bar{U}_{mi} k_j + \bar{U}_{ji} k_m \} e^{-ik_x x - ik_y y} \quad (\text{A4})$$

and

$$B_i(\mathbf{k}, \kappa) = -i\mu\rho L b_m n_j \{ \bar{U}_{mikj} + \bar{U}_{jikm} \}$$

$$= -i \frac{\mu L}{c_t^2 \kappa^2} \left[b_i(\mathbf{n}\mathbf{k}) + n_i(\mathbf{b}\mathbf{k}) - \frac{1}{(1-\nu)k^2} (\mathbf{b}\mathbf{k})(\mathbf{n}\mathbf{k}) k_i \right]. \quad (\text{A5})$$

Then, the relation

$$(c_t/c_l)^2 = (1-2\nu)/2(1-\nu)$$

gives the following simple formula

$$\sum_i B_i(\mathbf{k}, \kappa) e_i(\mathbf{k}, s) = -i \frac{\mu L}{c_s^2 \kappa^2} [(\mathbf{e}\mathbf{b})(\mathbf{k}\mathbf{n}) + (\mathbf{b}\mathbf{k})(\mathbf{e}\mathbf{n})], \quad (\text{A6})$$

where $c_s = c_t$ or c_l according as the mode is transverse or longitudinal.

Next the static line tension defined by eq (16) is calculated by using eq (A4). Imposing the Debye cut-off, we have

$$\begin{aligned} T(\kappa) &= \frac{\mu b_x^2}{4\pi} \left\{ \frac{1-2\nu}{2(1-\nu)} \ln \frac{k_D^2}{\kappa^2} + 1 - \frac{1}{4(1-\nu)} \frac{\kappa^2}{k_D^2} \right\} \\ &\quad + \frac{\mu b_z^2}{4\pi} \left\{ \frac{1+\nu}{2(1-\nu)} \left(\ln \frac{k_D^2}{\kappa^2} - 1 \right) + \frac{1}{1-\nu} \frac{\kappa^2}{k_D^2} \right\}. \end{aligned} \quad (\text{A7})$$

Similar calculations are necessary to treat a many-dislocation system (eq (56)). In this appendix another expression of the integral

$$\frac{1}{2} \int_{-\infty}^{\infty} \sum_{i,j} b_{d i} n_j P_{ij}(z; d, d' : \mathbf{b}_{d'}) e^{-i\kappa z} dz$$

is derived. From the definition of $P_{ij}(z; d, d' : \mathbf{b}_{d'})$ we have

$$\begin{aligned} &\int_{-\infty}^{\infty} P_{ij}(z; d, d' : \mathbf{b}_{d'}) e^{-i\kappa z} dz \\ &= -\frac{i\mu}{\rho V} \sum_k [\bar{B}_i(\mathbf{k}, \kappa : d') k_j + \bar{B}_j(\mathbf{k}, \kappa : d') k_i] e^{\{ik_x(x_{d'}-x_d) + ik_y(yd'-yd)\}}. \end{aligned} \quad (\text{A8})$$

We then have

$$\begin{aligned}
& b_{di}B_i(\mathbf{k}, \kappa : d') k_j n_j + b_{di}k_i B_j(\mathbf{k}, \kappa : d') n_j \\
&= \sum_s B_i(\mathbf{k}, \kappa : d') e_i(\mathbf{k}, s) [(\mathbf{b}_{d'}\mathbf{e})(\mathbf{kn}) + (\mathbf{b}_d\mathbf{k})(\mathbf{en})] \\
&= -i \sum_s \frac{\mu L \varphi_{d'}(\mathbf{k}, s) \varphi_d^*(\mathbf{k}, s)}{\omega_0^2(k, s)}.
\end{aligned}$$

Therefore, the integral is written as

$$\begin{aligned}
& \frac{1}{2} \int_{-\infty}^{\infty} \sum_{i,j} b_{di} n_j P_{ij}(z : d, d' : \mathbf{b}_{d'}) e^{-i\kappa z} dz \\
&= -\frac{\mu^2 L}{\rho V} \sum_{k,s} \frac{\varphi_{d'}(\mathbf{k}, s) \varphi_d^*(\mathbf{k}, s)}{\omega_0^2(\mathbf{k}, s)} e^{\{ik_x(x_{d'}-x_d) + ik_y(y_{d'}-y_d)\}}. \quad (\text{A9})
\end{aligned}$$

X. Appendix B. Evaluation of $F(\omega^2)$, $F(\omega^2 - i\epsilon)$, etc.

Appendix B is devoted to the evaluation of $F(\omega^2)$ in relation to the problems of localized states and phonon scattering.

$$F(\omega^2) = 1 - g(\kappa) \sum_{k,s} \frac{\omega^2}{\omega_0^2(\mathbf{k}, s)} \cdot \frac{\varphi(\mathbf{k}, s) \varphi^*(\mathbf{k}, s)}{\omega_0^2(\mathbf{k}, s) - \omega^2}. \quad (\text{B1})$$

For the localized states, the summation can be replaced by an integral if the number of atoms in the crystal is large. When we deal with the in-band frequencies, $F(\omega^2)$ is evaluated after Dawber and Elliott [20]:

$$F(\omega^2) = \operatorname{Re} F(\omega^2 - i\epsilon) + \operatorname{Im} F(\omega^2 - i\epsilon) \cot \pi p(\omega^2), \quad (\text{B2})$$

where $p(\omega^2)$ is the value which satisfies

$$\omega_0^2(p) - \omega^2 = 0. \quad (\text{B3})$$

By differentiation

$$\begin{aligned}
\frac{\partial F(\omega^2)}{\partial \omega^2} &= \operatorname{Re} \frac{\partial}{\partial \omega^2} F(\omega^2 - i\epsilon) + \operatorname{Im} \frac{\partial}{\partial \omega^2} F(\omega^2 - i\epsilon) \cot \pi p(\omega^2) \\
&\quad - \pi \operatorname{Im} F(\omega^2 - i\epsilon) \{1 + \cot^2 \pi p(\omega^2)\} \frac{dp}{d\omega^2}.
\end{aligned} \quad (\text{B4})$$

Because of (B3)

$$\frac{dp}{d\omega^2} = \frac{1}{d\omega_0^2/dp} = m\nu(\omega^2)$$

where $m\nu(\omega^2)$ is the state density of the frequency levels in a perfect crystal. If the number of atoms in a crystal is infinity, $m\nu(\omega^2)$ also goes

to infinity. Therefore, we must keep only the third term of eq (B4). Since the value of $\cot \pi\rho(\omega^2)$ is given by $F(\omega^2) = 0$, we finally obtain eq (32).

Thus, the evaluation of $F(\omega^2)$ is obtained after the evaluation of $F(\omega^2 - i\epsilon)$, which is also used in the problems of phonon scattering. To make the calculation, the summation is replaced by an integral:

$$F(\omega^2 - i\epsilon) = 1 - g(\kappa) \sum_s \left(\frac{L}{2\pi} \right)^2 \iint \frac{\omega^2}{\omega_0^2} \cdot \frac{\varphi\varphi^*}{\omega_0^2 - \omega^2 + i\epsilon} dk_x dk_y. \quad (\text{B5})$$

In the case of an isotropic elastic continuum with a Debye cut-off, we have

$$F(\omega^2 - i\epsilon) = 1 - g(\kappa) \sum_s \left(\frac{L}{2\pi} \right)^2 \int_{\kappa}^{k_D} \frac{\omega^2 k dk}{\omega_0^2(\omega_0^2 - \omega^2 + i\epsilon)} \left[\int \varphi\varphi^* d\theta \right], \quad (\text{B6})$$

where

$$\tan \theta = \frac{k_y}{k_x}$$

and

$$\omega_0^2(k, s) = c_s^2 k^2.$$

For longitudinal waves we have

$$\int \varphi\varphi^* d\theta = \frac{\pi b^2}{k^2} [\beta_x^2(k^2 - \kappa^2)^2 + 4\beta_z^2 \kappa^2(k^2 - \kappa^2)], \quad (\text{B7})$$

and for transverse waves with polarization s_1 and s_2

$$\sum_{s_1 s_2} \int \varphi\varphi^* d\theta = \frac{\pi b^2}{k^2} [\beta_x^2(k^4 - \kappa^4) + \beta_z^2(k^4 - 3\kappa^2 k^2 + 4\kappa^4)]. \quad (\text{B8})$$

The integration over k is straightforward and

$$\begin{aligned} \kappa^2 T(\kappa) F(\omega^2 - i\epsilon) &= \omega^2 \frac{\rho b^2}{4\pi} \left[\beta_x^2 \left\{ \frac{1}{2} \ln \left| \frac{\omega^2 - \kappa^2}{c_t^2} \right| + \frac{1}{2} (c_t)^4 \ln \left| \frac{\omega^2 - \kappa^2}{c_t^2 - k_D^2} \right| \right\} \right. \\ &\quad \left. + \beta_z^2 \frac{1}{2} \ln \left| \frac{\omega^2 - \kappa^2}{c_t^2 - k_D^2} \right| \right] + \kappa^2 \frac{\mu b^2}{4\pi} \left[\beta_x^2 \left\{ -\frac{c_t^2}{c_l^2} \ln \left| \frac{\omega^2 - \kappa^2}{c_l^2} \right| \right. \right. \\ &\quad \left. \left. + \frac{1}{2} (c_l)^4 \ln \left| \frac{\omega^2 - \kappa^2}{c_l^2 - k_D^2} \right| \right\} \right. \\ &\quad \left. + \beta_z^2 \frac{1}{2} \ln \left| \frac{\omega^2 - \kappa^2}{c_l^2 - k_D^2} \right| \right] \end{aligned}$$

$$\begin{aligned}
& + \frac{1}{2} + \frac{1}{2} \left(\frac{c_t^2}{c_l} \right)^2 - \frac{1}{2} \frac{\kappa^2 c^2}{\omega^2} \ln \frac{\left| \frac{\omega^2}{c_l^2} - \kappa^2 \right|}{\left| \frac{\omega^2}{c_l^2} - k_D^2 \right|} \cdot \frac{\left| \frac{\omega^2}{c_l^2} - k^2 \right|}{\left| \frac{\omega^2}{c_l^2} - \kappa^2 \right|} \Bigg\} + \beta_z^2 \left\{ -\frac{3}{2} \ln \frac{\left| \frac{\omega^2}{c_l^2} - \kappa^2 \right|}{\left| \frac{\omega^2}{c_l^2} - k_D^2 \right|} \right. \\
& \quad \left. + 2 \left(\frac{c_t}{c_l} \right)^2 \ln \frac{\left| \frac{\omega^2}{c_l^2} - \kappa^2 \right|}{\left| \frac{\omega^2}{c_l^2} - k_D^2 \right|} + \frac{1}{2} + 2 \frac{\kappa^2 c_l^2}{\omega^2} \ln \frac{\left| \frac{\omega^2}{c_l^2} - \kappa^2 \right|}{\left| \frac{\omega^2}{c_l^2} - k_D^2 \right|} \cdot \frac{\left| \frac{\omega^2}{c_l^2} - k_D^2 \right|}{\left| \frac{\omega^2}{c_l^2} - \kappa^2 \right|} \right\} \\
& + i\pi \frac{\mu b^2}{4\pi} \left\{ \beta_x^2 \left\{ \frac{1}{2} \left(\frac{\omega^2}{c_l^2} - \frac{\kappa^4 c_l^2}{\omega^2} \right) H \left(\frac{\omega}{c_l} - |\kappa| \right) + \frac{1}{2} \frac{c_l^2}{\omega^2} \left(\frac{\omega^2}{c_l^2} - \kappa^2 \right)^2 H \left(\frac{\omega}{c_l} - |\kappa| \right) \right\} \right. \\
& \quad \left. + \beta_z^2 \left\{ \frac{1}{2} \left(\frac{\omega^2}{c_l^2} - 3\kappa^2 + \frac{4\kappa^4 c_l^2}{\omega^2} \right) H \left(\frac{\omega}{c_l} - |\kappa| \right) + \frac{2\kappa^2 c_l^2}{\omega^2} \left(\frac{\omega^2}{c_l^2} - \kappa^2 \right) H \left(\frac{\omega}{c_l} - |\kappa| \right) \right\} \right\}, \tag{B9}
\end{aligned}$$

where

$$\begin{aligned}
H(x) &= 1 \text{ if } x > 0 \\
&= \frac{1}{2} \quad = 0 \\
&= 0 \quad x < 0 \text{ or } \omega > \omega_D.
\end{aligned}$$

$F(\omega^2)$ for localized states is same as eq (B9) without the imaginary terms.

Other functions which have been defined in section VIII for the problems of dislocation dipole are calculated quite similarly to $F(\omega^2 - i\epsilon)$ except that for these functions we need not the Debye cut-off because of a finite separation of a dislocation dipole.

$$\begin{aligned}
& \sum_{k,s}^{\kappa} \frac{\varphi(\mathbf{k}, s)\varphi^*(\mathbf{k}, s)}{\omega_0^2(\mathbf{k}, s) - \omega^2 + i\epsilon} \cos 2a (k_x + k_y) \\
& = \frac{L^2 b^2}{4\pi \omega^2} \left[\beta_t^4 \Phi_1(2\sqrt{2}a\beta_t) - \beta_t^2 \Phi_1(2\sqrt{2}a\beta_t) - \frac{\omega^2}{c_l^2} \beta_t^2 \Phi_2(2\sqrt{2}a\beta_t) \right] \\
& \quad - i\pi \frac{L^2 b^2}{4\pi} \frac{1}{2\omega^2} \beta_t^2 [J_0(2\sqrt{2}a\beta_t) + J_+(2\sqrt{2}a\beta_t)] H \left(\frac{\omega^2}{c_l^2} - \kappa^2 \right) \\
& \quad - i\pi \frac{L^2 b^2}{4\pi} \frac{1}{2\omega^2} \left[\left(\frac{\omega^4}{c_l^4} - \kappa^4 \right) J_0(2\sqrt{2}a\beta_t) - \beta_t^4 J_+(2\sqrt{2}a\beta_t) \right] H \left(\frac{\omega^2}{c_l^2} - \kappa^2 \right). \tag{B10}
\end{aligned}$$

where

$$\beta_t^2 = \frac{\omega^2}{c_l^2} - \kappa^2$$

and

$$\beta_l^2 = \frac{\omega^2}{c_l^2} - \kappa^2.$$

Φ_1 and Φ_2 are defined by

$$\begin{aligned}\Phi_1(x) &= \frac{\pi}{2} \{N_0(|x|) + N_4(|x|)\}, & \text{if } x^2 > 0 \\ &= -\{K_0(|x|) + K_4(|x|)\}, & \text{if } x^2 < 0\end{aligned}\quad (\text{B.11})$$

and

$$\begin{aligned}\Phi_2(x) &= \pi N_0(|x|) & \text{if } x^2 > 0 \\ &= -2K_0(|x|) & \text{if } x^2 < 0,\end{aligned}\quad (\text{B.12})$$

where N_i and K_i are Neumann and modified Bessel functions respectively. $\psi(a, \kappa)$ is obtained just by letting ω tend to zero in eq (B.10).

$$\begin{aligned}g(\kappa)\psi(a, \kappa) &= \frac{1}{T(\kappa)} \cdot \frac{\mu b^2}{4\pi} \left[2K_0(2\sqrt{2}a\kappa) \right. \\ &\quad \left. + \left(1 - \frac{c_l^2}{c_l^2}\right) \left(2\sqrt{2}a\kappa + \frac{4}{2\sqrt{2}a\kappa}\right) K_1(2\sqrt{2}a\kappa) \right] \quad (\text{B.12})\end{aligned}$$

and

$$g(\kappa)\psi(a, 0) = \frac{1}{\kappa^2 T(\kappa)} \frac{\mu b^2}{4\pi} \left(1 - \frac{c_l^2}{c_l^2}\right) \frac{1}{2a^2}. \quad (\text{B.13})$$

XI. Appendix C. Quantization of Dislocation Vibration

In this appendix it is discussed how to quantize a system of phonons and a dislocation.

The kinetic and elastic energies of an elastic body containing a vibrating dislocation have been given by eqs (4), (9), and (15). The formulas seem to imply that this system is an assembly of phonons and dislocation oscillators which interact through the second term of the kinetic energy.

If we follow a usual process of quantization, however, we meet a difficulty, because all $\partial L/\partial \dot{q}(k, s)$ and $\partial L/\partial \dot{\xi}(\kappa)$ are not independent. This is easily seen as follows. From the Lagrangian we have

$$\frac{\partial L}{\partial \dot{q}(\mathbf{k}, s)} = \rho V \dot{q}^*(\mathbf{k}, s) + \sum_i B_i(\mathbf{k}, \kappa = k_z) e_i(\mathbf{k}, s) \dot{\xi}^*(\kappa), \quad (\text{C.1})$$

and

$$\frac{\partial L}{\partial \dot{\xi}(\kappa)} = \sum_i \sum_{\mathbf{k}, s} B_i^*(\mathbf{k}, \kappa) e_i(\mathbf{k}, s) \dot{q}^*(\mathbf{k}, s) + m(\kappa) \dot{\xi}^*(\kappa). \quad (\text{C.2})$$

If we multiply (C.1) by $\sum_j B_j^*(\mathbf{k}, \kappa) e_j(\mathbf{k}, s)/\rho V$ and sum over the phonon modes of $k_z = \kappa$, we reach eq (C.2). This difficulty comes from the problem of the degree of freedom described in the introduction. Thus, quantization of the dislocation vibration becomes possible after elimination of the coordinates of dislocation displacements. The elimination is done by using eq (19). Let us introduce new variables $Q(\mathbf{k}, s)$ defined by

$$Q^*(\mathbf{k}, s) = \varphi^*(\mathbf{k}, s) q^*(\mathbf{k}, s)$$

$$+ g(\kappa) \frac{\varphi(\mathbf{k}, s)\varphi^*(\mathbf{k}, s)}{\omega_0^2(\mathbf{k}, s)} \sum_{\mathbf{k}'s'}^{\kappa} \varphi^*(\mathbf{k}', s') q^*(\mathbf{k}', s'). \quad (\text{C.4})$$

Then, the kinetic and elastic energies are given as

$$T = \frac{\rho V}{2} \sum_{\mathbf{k}, s} \frac{\dot{Q}(\mathbf{k}, s)\dot{Q}^*(\mathbf{k}, s)}{\varphi(\mathbf{k}, s)\varphi^*(\mathbf{k}, s)}, \quad (\text{C.4})$$

and

$$E = \frac{\rho V}{2} \sum_{\mathbf{k}, s} \frac{\omega_0^2(\mathbf{k}, s) Q(\mathbf{k}, s) Q^*(\mathbf{k}, s)}{\varphi(\mathbf{k}, s)\varphi^*(\mathbf{k}, s)} - \frac{\rho V}{2} \sum_{\kappa} \lambda(\kappa) g(\kappa) \left\{ \sum_{\mathbf{k}, s}^{\kappa} Q(\mathbf{k}, s) \right\} \left\{ \sum_{\mathbf{k}, s}^{\kappa} Q^*(\mathbf{k}, s) \right\} + E_0, \quad (\text{C.5})$$

where

$$\lambda^{-1}(\kappa) = 1 + g(\kappa) \sum_{\mathbf{k}, s} \frac{\varphi(\mathbf{k}, s)\varphi^*(\mathbf{k}, s)}{\omega_0^2(\mathbf{k}, s)}.$$

The system is now an assembly of harmonic oscillators with the mutual interactions given by the second term of the elastic energy eq (C.5) and is easily quantized in the usual way.

XII. Appendix D. Translational Motion of a Dislocation

In the main text, infinitesimal vibrations of a dislocation have been treated. A dislocation in metals and ionic crystals can move beyond the atomic distance and, in order to treat the frictional force acting on a dislocation by phonons, we must develop a dynamic theory for a translational motion over the atomic distances.

In this appendix we do not develop a general theory but only give the expressions of the energies for a straight dislocation which makes translational motion in addition to infinitesimal vibrations.

The displacement of the dislocation in the x -direction is given by

$$\xi(z) = \xi_0 + \sum_{\substack{\kappa \\ (\neq 0)}} \xi(\kappa) e^{i\kappa z}, \quad (\text{D.1})$$

where ξ_0 is the coordinate for the translational motion. We never restrict ourselves to a uniform movement (constant velocity). The lattice displacement is, then,

$$u_i^s = \sum_{\kappa} f_i(x - \xi_0, y : \kappa) e^{i\kappa z} \xi(\kappa) + u_{i0}^s(x - \xi_0, y) \quad (\text{D.2})$$

and

$$u_i^d = \sum_{\mathbf{k}, s} q(\mathbf{k}, s) e_i(\mathbf{k}, s) e^{i\mathbf{k} r}.$$

The time derivative of u_i^s is

$$\dot{u}_i^s = \sum_{\kappa} f_i(x - \xi_0, y : \kappa) e^{i\kappa z} \dot{\xi}(\kappa) - \dot{\xi}_0 \sum_{\kappa} \frac{\partial f_i}{\partial x} e^{i\kappa z} \xi(\kappa) - \dot{\xi}_0 \frac{\partial u_{i0}^s}{\partial x},$$

where

$$\frac{\partial u_{i0}^s}{\partial x} = - \lim_{\kappa \rightarrow 0} f_i(x_1 - \xi_0, y : \kappa).$$

The elastic energy is given by

$$E = \frac{\rho V}{2} \sum_{\mathbf{k}, s} \omega_0^2(\mathbf{k}, s) q(\mathbf{k}, s) q^*(\mathbf{k}, s) + \frac{L}{2} \sum_{\kappa} \kappa^2 T(\kappa) \xi(\kappa) \xi^*(\kappa) + E_0, \quad (\text{D.3})$$

because the translational motion does not change the elastic energy of the static field. The kinetic energy is

$$T = \frac{\rho}{2} \int \sum_i (\dot{u}_i^d + \dot{u}_i^s) (\dot{u}_i^d + \dot{u}_i^s) dv. \quad (\text{D.4})$$

From the Lagrange equations of motion, we have

$$\xi(\kappa) = \frac{\mu}{\kappa^2 T(\kappa)} \sum_{\mathbf{k}, s} \varphi(\mathbf{k}, s) q(\mathbf{k}, s) e^{i\mathbf{k} x} \xi_0, \quad (\text{D.5})$$

which corresponds to eq (19). For the coordinate ξ_0 , we have, after some

calculations,

$$\sum_{\kappa} \sum_{\substack{\mathbf{k}, s \\ (\neq 0)}}^{\kappa} k_x \varphi^*(\mathbf{k}, s) e^{-ik_x \xi_0} \xi(\kappa) q^*(\mathbf{k}, s) - i \sum_{\substack{\kappa=0 \\ \mathbf{k}, s}}^{\kappa=0} \varphi^*(\mathbf{k}, s) q^*(\mathbf{k}, s) e^{-ik_x \xi_0} = 0. \quad (\text{D.6})$$

Since we have assumed the vibration is infinitesimal, the first term can be neglected and the eq (D.6) becomes

$$\sum_{\substack{\kappa=0 \\ \mathbf{k}, s}}^{\kappa=0} \varphi^*(\mathbf{k}, s) q^*(\mathbf{k}, s) e^{-ik_x \xi_0} = 0. \quad (\text{D.7})$$

To get the correct degree of freedom, we must eliminate some variables by using eqs (D.5) and (D.7). We eliminate $\xi(\kappa)$ ($\kappa \neq 0$) and introduce new variables

$$R(\mathbf{k}, s) = e^{-ik_x \xi_0} \left[\varphi(\mathbf{k}, s) q(\mathbf{k}, s) e^{ik_x \xi_0} + g(\kappa) \frac{\varphi \varphi^*}{\omega_0^2} \sum_{\mathbf{k}', s'}^{\kappa=0} \varphi(\mathbf{k}', s') q(\mathbf{k}', s') e^{ik'_x \xi_0} \right].$$

Then, the kinetic and elastic energies are

$$\begin{aligned} T = & \frac{\rho V}{2} \sum_{\kappa} \sum_{\substack{\mathbf{k}, s \\ (\neq 0)}}^{\kappa} \frac{\dot{R} \dot{R}^*(\mathbf{k}, s)}{\varphi \varphi^*(\mathbf{k}, s)} + \frac{\rho L}{2} \left[\int \frac{\partial u_{i0}^s}{\partial x} \cdot \frac{\partial u_{i0}^s}{\partial x} dx dy \right] \dot{\xi}_0^2 \\ & + \frac{\rho V}{2} \sum_{\mathbf{k}, s}^{\kappa=0} \dot{q}(\mathbf{k}, s) \dot{q}^*(\mathbf{k}, s) \\ & + \dot{\xi}_0 \sum_{\mathbf{k}, s}^{\kappa=0} B_i(\mathbf{k}, \kappa=0) e_i(\mathbf{k}, s) e^{ik_x \xi_0} \dot{q}(\mathbf{k}, s), \end{aligned} \quad (\text{D.8})$$

and

$$\begin{aligned} E = & \frac{\rho V}{2} \sum_{\kappa} \sum_{\substack{\mathbf{k}, s \\ (\neq 0)}}^{\kappa} \omega_0^2(\mathbf{k}, s) \frac{RR^*(\mathbf{k}, s)}{\varphi \varphi^*(\mathbf{k}, s)} \\ & - \frac{\rho V}{2} \sum_{\kappa} \lambda(\kappa) g(\kappa) \left[\sum_{\mathbf{k}, s}^{\kappa} R(\mathbf{k}, s) e^{ik_x \xi_0} \right] \left[\sum_{\mathbf{k}', s'}^{\kappa} R^*(\mathbf{k}', s') e^{-ik'_x \xi_0} \right] \\ & + \frac{\rho V}{2} \sum_{\mathbf{k}, s}^{\kappa=0} \omega_0^2(\mathbf{k}, s) q(\mathbf{k}, s) q^*(\mathbf{k}, s) + E_0. \end{aligned} \quad (\text{D.9})$$

As for the modes of $\kappa=0$, ξ_0 cannot be eliminated easily and we eliminate $q(\mathbf{k}_1, s_1)$ by using eq (D.7), where

$$\mathbf{k}_1 = (0, k_{1y}, 0).$$

We further eliminate $q(-\mathbf{k}_1, s_1) = q^*(\mathbf{k}_1, s_1)$ and introduce a new variable ν defined by

$$\varphi q(\mathbf{k}_1, s_1) - \varphi^* q^*(\mathbf{k}_1, s_1) = 2iv.$$

If the dislocation velocity ξ_0 is much smaller than the sound velocity, the energies are quadratic of these variables except ξ_0 :

$$\begin{aligned} T = & \frac{\rho V}{2} \sum_{\substack{\kappa \\ (\neq 0)}} \sum_{\mathbf{k}, s} \frac{\dot{R}\dot{R}^*(\mathbf{k}, s)}{\varphi\varphi^*(\mathbf{k}, s)} + \frac{\rho L}{2} \left[\int \frac{\partial u_{i0}^s}{\partial x} \frac{\partial u_{i0}^{s*}}{\partial x} dx dy \right] \dot{\xi}_0^2 \\ & + \frac{\rho V}{2} \sum_{\mathbf{k}, s}^{\kappa=0'} \dot{q}(\mathbf{k}, s) \dot{q}^*(\mathbf{k}, s) + \rho V \frac{1}{\varphi\varphi^*(\mathbf{k}_1, s_1)} \dot{v}^2 \\ & + \frac{\rho V}{4} \frac{1}{\varphi\varphi^*(\mathbf{k}_1, s_1)} \sum_{\mathbf{k}, s}^{\kappa=0'} \sum_{\mathbf{k}', s'}^{\kappa=0'} \varphi(\mathbf{k}, s) \varphi^*(\mathbf{k}', s') \dot{q}(\mathbf{k}, s) \dot{q}^*(\mathbf{k}', s') e^{i(k_x - k'_x)\xi_0} \\ & + \mu L \dot{\xi}_0 \sum_{\mathbf{k}, s}^{\kappa=0'} \frac{\varphi(\mathbf{k}, s)}{\omega_0^2(\mathbf{k}, s)} \dot{q}(\mathbf{k}, s) e^{ik_x \xi_0}, \\ & - \mu L \dot{\xi}_0 \frac{1}{\omega_0^2(\mathbf{k}_1, s_1)} \sum_{\mathbf{k}, s}^{\kappa=0'} \varphi(\mathbf{k}, s) \dot{q}(\mathbf{k}, s) e^{ik_x \xi_0}, \end{aligned} \quad (\text{D.10})$$

where Σ' means the summation over the modes except (\mathbf{k}_1, s_1) and $(-\mathbf{k}_1, s_1)$. The elastic energy is

$$\begin{aligned} E = & \frac{\rho V}{2} \sum_{\substack{\kappa \\ (\neq 0)}} \sum_{\mathbf{k}, s} \omega_0^2(\mathbf{k}, s) \frac{RR^*(\mathbf{k}, s)}{\varphi\varphi^*(\mathbf{k}, s)} \\ & - \frac{\rho V}{2} \sum_{\substack{\kappa \\ (\neq 0)}} \lambda(\kappa) g(\kappa) \left[\sum_{\mathbf{k}, s}^{\kappa} R(\mathbf{k}, s) e^{ik_x \xi_0} \right] \left[\sum_{\mathbf{k}', s'}^{\kappa} R^*(\mathbf{k}', s') e^{-ik'_x \xi_0} \right] \\ & + \frac{\rho V}{2} \sum_{\mathbf{k}, s}^{\kappa=0'} \omega_0^2(\mathbf{k}, s) q(\mathbf{k}, s) q^*(\mathbf{k}, s) + \frac{\rho V \omega_0^2(\mathbf{k}_1, s_1)}{\varphi\varphi^*(\mathbf{k}_1, s_1)} v^2 \\ & + \frac{\rho V}{4} \frac{\omega_0^2(\mathbf{k}_1, s_1)}{\varphi\varphi^*(\mathbf{k}_1, s_1)} \sum_{\mathbf{k}, s}^{\kappa=0'} \sum_{\mathbf{k}', s'}^{\kappa=0'} \varphi(\mathbf{k}, s) \varphi^*(\mathbf{k}', s') q(\mathbf{k}, s) q^*(\mathbf{k}', s') e^{i(k_x - k'_x)\xi_0}. \end{aligned} \quad (\text{D.11})$$

From the equations (D.10) and (D.11) we find that, when a dislocation makes translational motion, we have an inelastic scattering of a phonon and the momentum transfer to the dislocation.

Detailed discussions will be given elsewhere.

XIII. Appendix E. Thermal Conductivity

The present theory of phonon scattering by the fluttering mechanism has been applied to thermal conductivity and compared with recent data on deformed LiF by Takayoshi Suzuki of the University of Tokyo. In this appendix the results of the comparisons are briefly described. (Details will soon be published by him elsewhere.)

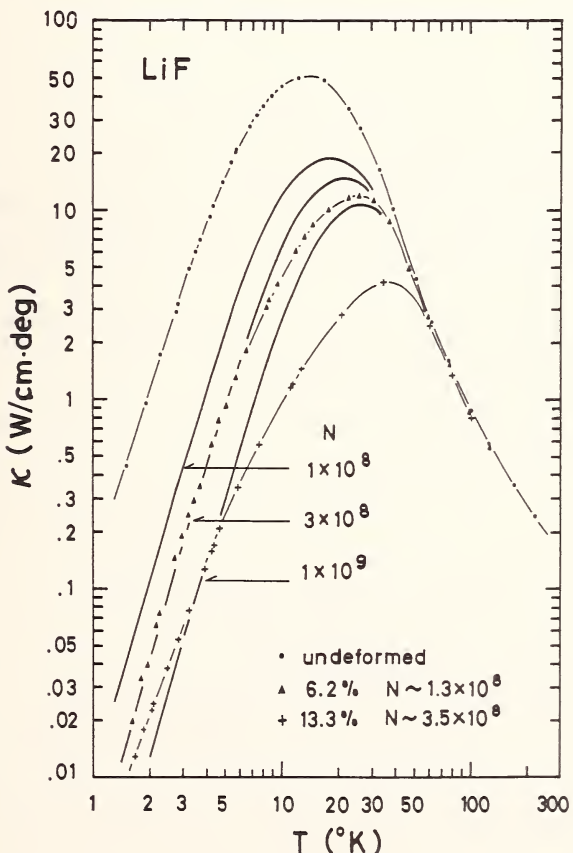


FIGURE 8. Thermal conductivity in deformed LiF crystals. Solid lines show the curves calculated on the basis of the fluttering mechanism.

The lattice thermal conductivity is given by the following equation:

$$K = \frac{k_B}{2\pi^2} \left(\frac{k_B T}{\hbar} \right)^3 \langle v^{-1} \rangle \int_0^{O/T} \tau_R \frac{x^4 e^x}{(e^x - 1)^2} dx.$$

$\langle v^{-1} \rangle$ is an appropriately averaged sound velocity, τ_R is the total relaxation time and $x = h\omega/kT$. Here the effect of normal processes is neglected.

The experimental results by T. Suzuki are shown in figure 8 with the calculated curves which are given by the solid lines. A specimen was compressed by 6.2 percent by single glide. For the crystal the agreement between the experiment and the theory is fairly good within a factor of three. The other specimen compressed by 13.3 percent shows a weaker temperature dependence on the lower temperature side of the peak than the previous specimen. This may be due to the existence of many dislocation dipoles produced by double glide.

XIV. References

- [1] Klemens, P. G., Proc. Phys. Soc. **A68**, 1113 (1955).
- [2] Carruthers, P., Rev. Mod. Phys. **33**, 92 (1961).
- [3] Sproull, R. L., Moss, M., and Weinstock, H., J. Appl. Phys. **30**, 334 (1959); Ishioka, S., and Suzuki, H., Phys. Soc. Japan **18**, Suppl. II, 93 (1963); Taylor, A., Albers, H. R., and Pohl, H. O., J. Appl. Phys. **36**, 2270 (1965); Moss, M., J. Appl. Phys. **36**, 3308 (1965).
- [4] Bross, H., Seeger, A., and Haberkorn, R., Phys. Stat. Sol. **3**, 1126 (1963); Gruner, P., Z. Naturforsch. **20a**, 1626 (1965); Bross, H., Z. Physik. **189**, 33 (1966); Gruner, P., and Bross, H., Phys. Rev. **172**, 583 (1968).
- [5] Mason, W. P., J. Appl. Phys. **35**, 2779 (1964).
- [6] Seeger, A., and Engelke, H., in Dislocation Dynamics, A. R. Rosenfield et al., Eds. (McGraw-Hill, 1968) p. 623.
- [7] Eshelby, J. D., Proc. Roy. Soc. **A266**, 222 (1962).
- [8] Kosevich, A. M., Soviet Physics-JETP **16**, 455 (1963); Soviet Physics-USPEKHI **7**, 837 (1965).
- [9] Laub, T., and Eshelby, J. D., Phil. Mag. **14**, 1285 (1966).
- [10] Ninomiya, T., and Ishioka, S., J. Phys. Soc. Japan **23**, 361 (1967).
- [11] Nabarro, F. R. N., Proc. Roy. Soc. **A209**, 278 (1951).
- [12] Ninomiya, T., J. Phys. Soc. Japan **25**, 830 (1968).
- [13] Kratochvil, J., Czech. J. Phys. **14B**, 328 (1964).
- [14] Litzman, O., and Kunc, K., J. Phys. Chem. Solids **26**, 1825 (1965).
- [15] Lengeler, B., and Ludwig, W., J. Phys. Chem. Solids **1**, Suppl. 439 (1965).
- [16] Lifshitz, I. M., and Kosevich, A. M., Rep. Prog. Phys. **29**, 217 (1966).
- [17] Brown, R. A., Phys. Rev. **156**, 692, 889 (1967).
- [18] Eshelby, J. D., Solid State Physics, **3**, Seitz and Turnbull, Eds. (Academic Press, New York, 1956) p. 79.
- [19] Maradudin, A. A., Montroll, E. W., and Weiss, G. H., Solid State Physics, Supplement 3 (Academic Press, New York, 1963).
- [20] Dawber, P. G., and Elliott, R. J., Proc. Roy. Soc. **A273**, 222 (1963).

- [21] Ludwig, W., *Erg. exak. Naturwiss.*, Vol. 43 (Springer-Verlag, Berlin, 1967).
- [22] Kusunoki, M., and Suzuki, H., *J. Phys. Soc. Japan* **26**, 932 (1969).
- [23] Johnston, W., and Gilman, J. J., *J. Appl. Phys.* **31**, 632 (1961).
- [24] de Wit, R., *Solid State Physics*, **10**, Seitz and Turnbull, Eds. (Academic Press, New York, 1960) p. 254.

Note added in proof:

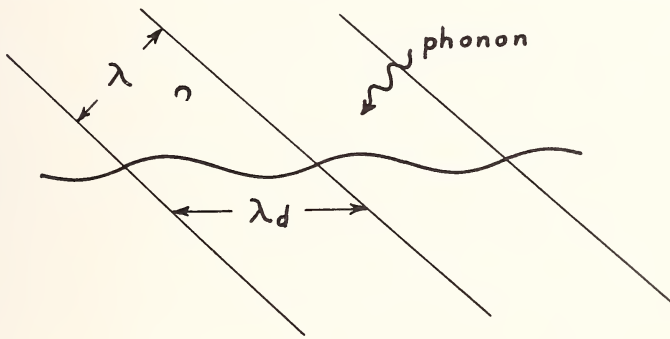
Pegel has also treated the vibration of parallel dislocations using the Kosevich equations. Explicit results are obtained for the vibrations without phonon emission, that is, for the localized modes. [Habilitations schrift, Technische Universität, Dresden 1968. phys. stat. sol. **29**, K133 (1968)]

Recently, Stenzel has given the equation of motion of a dislocation starting from the expression of the strain field in Kröner's form, and discussed the vibration of a pinned dislocation in detail. [Phys. stat. sol. **34**, 351, 365 (1969)]

Discussion on Paper by T. Ninomiya.

GRANATO: Could you amplify your remarks about the angular dependence of the incident phonons?

NINOMIYA: The angular dependence of the scattering cross section is largely determined by the denominator of the formula for the cross section (Eqs 43 and B9 of my paper). The square root of the denominator can be rewritten as $\kappa^2 T(\kappa) F(\omega - i\epsilon) = -m\omega^2 + \kappa^2 T + \text{imaginary part}$, where m and T are only weakly dependent on the frequency ω and the wave number κ . Therefore, the cross section is a function of the incident angle on a dislocation. [See fig. 1.] Resonance scattering occurs when the real part of the denominator is zero and this condition is satisfied at an angle around 40° for a transverse phonon incident on a screw dislocation.



$$\lambda = \frac{2\pi C_t}{\omega} \quad \lambda_d = \frac{2\pi}{\kappa}$$

FIGURE 1. Illustrating Ninomiya's reply to Granato.

ELBAUM: On the subject of the influence of dislocations on the thermal conductivity, you pointed out that there is only a small discrepancy between the predictions of the calculation and experiment, but I noticed that the curve which is labeled "undeformed" only reaches a maximum conductivity of 50 or so watt units. Now, I wonder whether the calculation is relative to that curve or rather to what is known to be the thermal conductivity of lithium fluoride at the maximum when the crystal is isotopically pure, etc., and which is more nearly at 200 or 250 watt units, which would make, of course, the discrepancy much larger.

SUZUKI: I will answer the question of Professor Elbaum. The thermal conductivity of 200 or 250 watt/cm · °K is for a perfect crystal of isotopically

pure lithium fluoride, but the experimental values referred to by Professor Ninomiya are for ordinary lithium fluoride. These values for undeformed crystals are the highest hitherto obtained from ordinary crystals. The dislocation density measured by etch pits was 4.9×10^5 cm $^{-2}$ in the undeformed crystals, so that the effect of dislocations is negligible compared with surface or isotopic scattering. The scattering due to isotopes is proportional to the fourth power of the phonon frequency and decreases the thermal conductivity in the temperature range around its peak or at higher temperatures than the peak. The thermal conductivity in the low temperature region, where we compared the measurements with the calculation, is hardly affected by isotopes. Therefore, we believe the discrepancy between the measurement and the calculation is almost the same even if we were to use isotopically pure crystals.

NINOMIYA: [Written Contribution] The theoretical curves shown in figure 8, Appendix E, of my paper include the effects of isotope scattering and surface scattering beside the effect of dislocations. The process of fitting theoretical curves to the experiments was as follows: (1) The effect of isotopes has been investigated by Berman and Brock.¹ Because Dr. T. Suzuki used the specimens as cleaved, the surface scattering was determined to get the best fit to the experiments for an undeformed natural crystal, by assuming that in this crystal the relaxation time is determined by the isotope and the surface scattering as well as phonon-phonon scattering. (2) The theoretical curves for deformed crystals were obtained just by adding the effects of dislocation fluttering to the reciprocal of the relaxation time.

GRUNER: You showed a peak in the frequency spectrum and I cannot quite understand why you then get a very smooth temperature dependence in the conductivity in the low temperature range. This should give rise to a dent or something like that.

NINOMIYA: The condition of the resonance scattering is given as a function of both the frequency and the wavelength along the dislocation. Therefore, resonance occurs for all frequencies.

GRUNER: Then this holds for moving dislocations, but not for stationary dislocations?

NINOMIYA: Yes, not for stationary dislocations.

WEINER: Does your calculation procedure give you the shape of the localized mode, that is, how far does it extend?

NINOMIYA: I have not made exact calculations of how far it extends. It depends on the frequency difference of the localized mode from the bot-

¹ Proc. Roy. Soc. (London) A289, 46 (1965).

tom of the phonon band with the same wavelength along the dislocation. For an edge dislocation the frequency of the localized mode is about two-thirds that of the bottom of the phonon band. The calculation may not be difficult, although I cannot answer now.

[Written contribution] The localized mode has an asymptotic form of $r^{-1} \exp [-r(\kappa^2 - \omega^2/c_s^2)^{1/2}]$, where r is the distance from the dislocation. The extent of the localization, therefore, is given by $(\kappa^2 - \omega^2/c_s^2)^{-1/2}$, which is about $1.3\kappa^{-1}$ for an edge dislocation.

GRANATO: Which effects do you think should be more important for physical properties, the fluttering effects or the anharmonic effects? For example, do you get a T^4 or T^2 temperature dependence?

NINOMIYA: I think that at lower temperatures the fluttering mechanism is dominant. As you know, the Cornell group first presented the thermal conductivity data with T^2 dependence, which suggested an anharmonic effect despite the large disagreement in magnitude. But their recent data have given the steeper dependence. As shown in figure 8 of my paper, the specimen compressed by single slip shows a T^3 to T^4 dependence and there is good agreement with the fluttering theory. If a crystal is deformed by double slip, it is considered to contain many dislocation dipoles and, in such a case, the thermal conductivity has been found to have the T^2 to T^3 dependence. Therefore, it is likely that such weak dependence comes from the fluttering effect of dislocation dipoles.

PHONON SCATTERING BY DISLOCATIONS AND ITS INFLUENCE ON THE LATTICE THERMAL CONDUCTIVITY AND ON THE DISLOCATION MOBILITY AT LOW TEMPERATURES

P. P. Gruner

*Boeing Scientific Research Laboratories
P.O. Box 3981
Seattle, Washington 98124*

On account of the large strains associated with dislocations, the superposition principle is violated. The resulting scattering of phonons limits the lattice thermal conductivity and leads to a friction force which acts on moving dislocations. The phonon-dislocation interaction is treated with non-linear continuum theory. Terms up to the third order in the strains are retained in the Taylor expansion of the elastic energy density. These third order terms contain the phonon-dislocation interaction and the normal three-phonon interactions. In the case of thermal conductivity, the transport problem is solved with the variational method which leads to a system of linear equations for the phonon occupation numbers. The coefficients of this system of equations contain all the information on the scattering mechanisms. The influence on the thermal conductivity of special dislocation configurations such as piled-up dislocations and dislocation dipoles will be discussed.

It will be shown that the friction force which acts on moving dislocations on account of the anharmonicity can be obtained from quantities that are known from the calculations of the phonon conductivity. A one to one correspondence between friction force and thermal resistance exists, however, only if the dislocation velocity is small compared with the sound velocity and if all parts of the dislocation move with the same velocity.

Key words: Dislocation mobility; dislocation-phonon interactions; nonlinear elasticity; phonons; thermal conductivity.

I. Introduction

In the neighborhood of a dislocation, the lattice is heavily strained. Hence, physical properties like mass density, interatomic forces, etc., deviate in the disturbed region from those of other parts of the crystal

Fundamental Aspects of Dislocation Theory, J. A. Simmons, R. de Wit, and R. Bullough, Eds. (Nat. Bur. Stand. (U.S.), Spec. Publ. 317, I, 1970).

which do not contain defects. On account of these deviations, phonons which travel through the disturbed regions are scattered. This interaction between the phonons and the dislocation strain field limits the lattice thermal conductivity. It also hampers the mobility of moving dislocations.

The influence of the scattering of phonons by lattice defects on the thermal conductivity was first investigated by Klemens [1]. Comprehensive articles on the theory of the thermal resistance by lattice defects have also been presented by Carruthers [2] and by Ziman [3].

Klemens found that the phonon scattering cross sections of various defects are characteristic functions of the phonon wavelength. In the case of the scattering by the strain field of a single dislocation, the scattering cross section is inversely proportional to the phonon wavelength. On account of the sensitivity of the spectral distribution of the phonons to the temperature at low temperatures, the wavelength dependence of the scattering cross section is reflected in the temperature dependence of the lattice thermal conductivity. For this reason, it is possible to distinguish different classes of defects by means of lattice thermal conductivity measurements. The scattering by single dislocations, for example, leads to a quadratic temperature dependence.

In those cases in which the defects are sufficiently far apart from each other or/and randomly distributed, they act as isolated scatterers: the scattering is incoherent. The combined scattering probability is then simply additively composed of the single scattering probabilities. This is also the case when the crystal contains several kinds of defects (dislocations, impurities, vacancies, etc.), as long as they are thus far apart from each other so that their strain fields do not overlap significantly. The additivity of the scattering probabilities leads, at least qualitatively, to the additivity of the reciprocal phonon relaxation times.

Callaway [4] has, based on the additivity of the reciprocal relaxation times, treated the thermal conductivity in crystals which contain several classes of defects. He also could include in his calculations the normal three-phonon processes by using the fact that these processes do not change the total momentum of the phonon gas. A justification of the Callaway theory has been given by Krumhansl [5].

If the temperature is thus low that the dominant phonon wavelength is comparable with the distances between the defects then the defects cannot be regarded as single scatterers. The combined scattering probability is no longer equal to the sum of the single probabilities. In this case the various phases of the scattered waves must be taken into account; the scattering is then partly coherent, partly incoherent. This leads to a structure factor in the scattering probability which is characteristic for a particular arrangement of the defects. Two kinds of dislocation arrangements shall be considered here, the pile-up of dislocations of

the same sign and the edge dislocation dipole configuration. It is readily seen that these configurations must, at sufficiently low temperatures, lead to different temperature dependencies of the thermal conductivity. In the case of the pile-up, the thermal resistance is increased in comparison with the resistance of single dislocations. The dipole configuration, on the other hand, leads to a decrease of the resistance. The calculations outlined in the next sections show that the arrangement of the dislocations is also reflected in a characteristic temperature dependence of the thermal conductivity.

We confine the following calculations to low temperatures. Here, the wavelengths of the phonons are large in comparison with the lattice parameter. The interaction between the phonons and the defects can then be treated by continuum theory. In order to describe the scattering of the phonons by defects, it is necessary to employ nonlinear continuum theory, i.e., we must take into account, in the Taylor expansion of the elastic energy, also terms which are of higher than second order in the strains. For convenience, we restricted ourselves to the lowest degree of the nonlinearity and retained only third order terms. In order to avoid difficulties which arise from the fact that the displacement field of a dislocation is multivalued, a formulation, given by Bross¹ [6], for the elastic energy density of a continuum which contains self-stresses has been used. The essential feature of this formulation is that the interaction between the lattice waves and the defects can be represented in terms of strains alone rather than in terms of displacements. The main advantage of the continuum approach over an atomistic treatment is that the third order elastic constants are known for a variety of materials, whereas it is difficult to get reliable experimental values for the anharmonic force constants. The approximation which is often made, the replacement of the anharmonic force constants by a single parameter, the Grüneisen constant, is avoided in this approach.

The third-order terms in the elastic energy contain as well the phonon-defect interaction as the normal three-phonon processes. The latter processes conserve both the energy and the quasi-momentum of the phonon gas and are, therefore, as has been shown by Peierls [7], not capable of establishing a stationary state. Nevertheless, the normal processes play an important role for the establishment of a stationary state if the phonons are in addition scattered by momentum nonconserving processes, i.e., by defects. This will be demonstrated later for the case in which the phonons interact with the strain field of edge dislocation dipoles. It turns out that without the help of the normal processes the scattering of long wavelength phonons by dipoles is not strong enough to produce a nonvanishing thermal resistance.

¹ Reference [6] will be referred to by I.

The Boltzmann equation which governs the distribution function of the phonons in the stationary state is solved by means of the variational method which has been described in I. We restrict ourselves here to a brief discussion of this method. From Boltzmann's integral equation an expression can be derived which is essentially equal to the density of entropy production. This expression contains implicitly a quantity $\mathbf{X}(\mathbf{k}, j)$ which measures the deviations of the phonon occupation numbers in the stationary state from those in the state of thermal equilibrium. The unknown vector function $\mathbf{X}(\mathbf{k}, j)$ is then replaced by the series expansion

$$\mathbf{Z}(\mathbf{k}, j) = \sum_{r=0}^{\infty} \sum_{n=1}^{\infty} \sum_{m=-n}^n \mathbf{Z}(j, m, n, r) [\hbar\omega(\mathbf{k}, j)]^r Y_{nm}^{(\theta, \phi)}. \quad (\text{I.1})$$

Here, \mathbf{k} is the wave vector, j is a polarization index, $\omega(\mathbf{k}, j)$ is the frequency of the vibration mode $\{\mathbf{k}, j\}$, and \hbar is Planck's constant divided by 2π . Y_{nm} are spherical harmonics. The spherical coordinates of the wave vector are k , θ , and ϕ . The variation of the density of entropy production with respect to the expansion coefficients $\mathbf{Z}(j, m, n, r)$ leads to the following system of linear equations for those coefficients

$$\sum_{\nu'} M(\nu, \nu') \mathbf{Z}(\nu') = \mathbf{N}(\nu). \quad (\text{I.2})$$

The index ν represents the set of indices (j, m, n, r) . The vector $\mathbf{N}(\nu)$ arises from the diffusion part of the Boltzmann equation and has the form²

$$\mathbf{N}(\nu) = -(KT)^{-1} \sum_{\mathbf{k}} \overline{\overline{N}}(\mathbf{k}) + 1 \overline{\overline{N}}(\mathbf{k}) [\hbar\omega(\mathbf{k})]^{r+1} \mathbf{v}(\mathbf{k}) Y_{nm}(\theta, \phi) \quad (\text{I.3a})$$

With the phonon distribution of the thermal equilibrium

$$\overline{\overline{N}}(\mathbf{k}) = \{ \exp [\hbar\omega(\mathbf{k})/KT] - 1 \}^{-1}. \quad (\text{I.3b})$$

All information on the scattering mechanisms is contained in the matrix M which is essentially given by integrals over transition probabilities. Since the explicit form is rather lengthy, we represent M in the appendix. Each kind of defects is represented by a characteristic matrix. The total matrix M is given by the sum of the single matrices. Finally,

² We denote from now on the mode $\{k, j\}$ simply by $\{k\}$. $\mathbf{v}(\mathbf{k})$ is the sound velocity of mode $\{k\}$.

the tensor of the thermal conductivity can be written³

$$\kappa = - (TV_0)^{-1} \sum_{\nu} \mathbf{N}(\nu) \mathbf{Z}(\nu). \quad (I.4)$$

It should be noted that this treatment allows fully for the polarizations of the lattice waves. The approach cannot account for umklapp-processes. Yet, these processes are unimportant in deformed crystals at low temperatures where the dominant contribution to the thermal resistance arises from phonon scattering by dislocations. Since we are interested in the thermal resistance at temperatures which are well below the Debye temperature, it is justified to assume that the dispersion relations of the continuum theory can be used.

In section II, we shall give a brief discussion of the formal theory. Section III contains the application of the theory to special dislocation arrangements and calculated results for the thermal resistance. In section IV, the theoretical results shall be compared with experiments. The relationship between the thermal resistance of resting dislocations and the retarding force which acts on account of the phonon scattering on slowly moving dislocations is treated in section V.

II. Formal Theory

The calculation of the phonon-defect interaction begins with the elastic energy density, Ψ , of the lattice vibrations in a body which contains self-stresses. This energy density depends, as has been shown in I, in the case of an isotropic continuum only on the strains and not on the displacements if all quantities are referred to the coordinate system of the self-stressed state. This is, as has already been mentioned, important in view of the fact that the displacement field of a dislocation is multivalued. The density, Ψ , consists of mixed products between the defect strains and the strains which result from the lattice vibrations. Those mixed terms give rise to the phonon-defect interaction. We retain in the energy density only terms up to the third order in the strains.⁴ Among these third-order terms are also terms which contain only the strains of the elastic waves. The latter terms lead to normal three-phonon processes. Including the kinetic energy density and employing standard methods for the quantization of fields, the Hamiltonian of the elastic waves can be written in the form

$$H = H_0 + H_{\text{Def.}} + H_{\text{NP.}} \quad (\text{II.1})$$

³ V_0 is the volume of the crystal.

⁴ It is consistent with this approximation, as shown in I, to insert in the mixed products only those defect strains which have been calculated with linear elasticity theory.

H_0 is the Hamiltonian of the noninteracting phonon gas and is given by

$$H_0 = \sum_{\mathbf{k}} \hbar\omega(\mathbf{k}) \{a^+(\mathbf{k})a(\mathbf{k}) + 1/2\}. \quad (\text{II.2})$$

The quantities a^+ and a are creation and annihilation operators, respectively. The phonon-defect interaction is contained in $H_{\text{Def.}}$, which can formally be written as

$$H_{\text{Def.}} = \sum_{\mathbf{k}, \mathbf{k}'} V_1(\mathbf{k}, \mathbf{k}') a^+(\mathbf{k}) a(\mathbf{k}') + \dots \quad (\text{II.3a})$$

where the coefficients V_1 describe the coupling between the vibrational modes, represented by their wave vectors \mathbf{k} and their polarization vectors $\mathbf{e}(\mathbf{k})$, and the defects which are represented by the Fourier transforms, $\tilde{\epsilon}$, of their strain fields. A typical element of V_1 has the form

$$V_1 = A_1(\mathbf{e} \cdot \mathbf{k})(\mathbf{e}' \cdot \mathbf{k}') \tilde{\epsilon}(\mathbf{g}) + \dots \quad (\text{II.3b})$$

A_i are linear combinations of elastic constants. Their definition is given in I. Numerical values of the A_i are listed in table 1 for copper and magnesium oxide. The coefficients V_1 vanish, unless

$$\mathbf{k} + \mathbf{k}' + \mathbf{g} = 0. \quad (\text{II.3c})$$

The last equation expresses the fact that the momentum of the phonons is changed in collisions with the defects. A typical term in the operator H_{NP} which describes the creation of two phonons with wave vectors

TABLE 1. *Material constants of copper and magnesium oxide*

	Copper ^a	Magnesium oxide ^b
Elastic constants in 10^{12} [dyn/cm ²].....	$\begin{cases} A_1 & 0.994 \\ A_2 & -0.936 \\ A_3 & -4.58 \\ A_4 & 12.16 \\ A_5 & -15.60 \end{cases}$	$\begin{array}{l} 1.71 \\ -2.68 \\ -5.67 \\ 15.21 \\ -11.85 \end{array}$
Mass density in [g/cm ³].....	8.9	3.58
Burgers vector in [Angstrom].....	2.56	2.98

^a After reference [27].

^b Calculated with the help of reference [28] from anisotropic elastic constants [29].

\mathbf{k} and \mathbf{k}' and the annihilation of a third phonon with \mathbf{k}'' has the form

$$H_{NP} = \sum_{\mathbf{k}, \mathbf{k}', \mathbf{k}''} V_2(\mathbf{k}, \mathbf{k}', \mathbf{k}'') a^+(\mathbf{k}) a^+(\mathbf{k}') a(\mathbf{k}'') + \dots \quad (\text{II.4a})$$

The coupling coefficient is in this case composed of terms which contain triple products of wave and polarization vectors.

The coefficients V_2 vanish, unless

$$\mathbf{k} + \mathbf{k}' + \mathbf{k}'' = 0. \quad (\text{II.4b})$$

This has the consequence that the quasi-momentum of the phonon gas cannot be destroyed by the normal processes.

On account of the coupling of the vibration modes, described by the interaction operators, $H_{\text{Def.}}$ and H_{NP} , phonons are exchanged between the vibration modes. This leads to a rate of change of the average numbers of phonons, $\bar{N}(\mathbf{k})$, in mode $\{\mathbf{k}\}$ which can be represented by⁵

$$\begin{aligned} \dot{\bar{N}}(\mathbf{k}) = & \sum W(\mathbf{k}, -\mathbf{k}') [\bar{N}(\mathbf{k}') - \bar{N}(\mathbf{k})] \\ & + \sum W(\mathbf{k}, \mathbf{k}', -\mathbf{k}'') [(\bar{N}(\mathbf{k}) + 1)(\bar{N}(\mathbf{k}') + 1)\bar{N}(\mathbf{k}'')] \\ & - \bar{N}(\mathbf{k})\bar{N}(\mathbf{k}')(\bar{N}(\mathbf{k}'') + 1)] \\ & + \text{two similar expressions.} \end{aligned} \quad (\text{II.5})$$

The first sum in eq (II.5) represents the increase per unit time of the average number of phonons in mode $\{\mathbf{k}\}$ which results from the phonon-defect interaction. The coefficient $W(\mathbf{k}, -\mathbf{k}')$ is the probability rate for the scattering of a phonon from mode $\{\mathbf{k}\}$ into mode $\{\mathbf{k}'\}$. For static defects one finds:

$$W(\mathbf{k}, -\mathbf{k}')_{\text{stat.}} = w(\mathbf{k}, -\mathbf{k}') \delta\{\omega(\mathbf{k}) - \omega(\mathbf{k}')\} \quad (\text{II.6a})$$

with

$$w = 2\pi [(2\pi)^3/V_0\rho_0]^2 |V_1(\mathbf{k}, -\mathbf{k}')|^2 [\omega(\mathbf{k})\omega(\mathbf{k}')]^{-1}. \quad (\text{II.6b})$$

The δ -function in eq (II.6a) reveals that the energy of the phonons is conserved in collisions with static defects. The remainder of eq (II.5) yields the change of the phonon occupation numbers which is due to the normal processes. The explicit expression for $W(\mathbf{k}, \mathbf{k}', -\mathbf{k}'')$ has been given in I. We note here merely that the energy of the phonon gas is also conserved in three-phonon collisions, i.e., $W(\mathbf{k}, \mathbf{k}', -\mathbf{k}'')$ vanishes.

⁵ The complete form of eq (II.5) can be found in I.

unless

$$\omega + \omega' - \omega'' = 0. \quad (\text{II.7})$$

The influence of the normal processes on the thermal conductivity shall be subsequently discussed in connection with phonon scattering by dislocation dipoles.

We shall, in section V, study the relationship between thermal resistance and the retarding force which acts on a moving dislocation on account of the anharmonicity. The simplest case for a comparison of mobility and thermal resistance is that of a straight dislocation which moves with constant velocity. In other cases where not all parts of the dislocation have the same speed, the comparison is more involved. Let a screw dislocation, oriented parallel to the z direction, move with constant speed \bar{v} in x direction. The displacement in an isotropic and infinitely extended continuum is then

$$u_z = (b/2\pi) \tan^{-1} [y\gamma/(x - \bar{v}t)], \quad u_x = u_y = 0 \quad (\text{II.8a})$$

with

$$\gamma = [1 - (\bar{v}/v_T)^2]^{1/2}. \quad (\text{II.8b})$$

Here, v_T is the velocity of the transversal sound waves and b is the magnitude of the Burgers vector. It is straightforward to derive from eq (II.8a) the Fourier transforms of the strain tensor components. One finds

$$\tilde{\epsilon}_{13}(\mathbf{g}) = (ib/(8\pi)^{1/2})\delta(g_z) \exp(-ig_x\bar{v}t)g_y/(g_x^2\gamma^2 + g_y^2) \quad (\text{II.9a})$$

and

$$\tilde{\epsilon}_{23}(\mathbf{g}) = -(ib/(8\pi)^{1/2})\delta(g_z) \exp(-ig_x\bar{v}t)\gamma^2g_x/(g_x^2\gamma^2 + g_y^2). \quad (\text{II.9b})$$

All the other tensor components are zero. If we are interested in the thermal resistance which results from a resting screw dislocation then we use in eq (II.3b) the Fourier components (II.9a and b) for $\bar{v} = 0$. Substitution, on the other hand, of eqs (II.9a and b) with $\bar{v} \neq 0$ into eq (II.3b) leads to a time dependent coefficient V_1 and hence to a time dependent perturbation operator $H(t)_{\text{Def}}$. A standard time dependent perturbation treatment yields that, in case of the uniformly moving dislocation, the probability rate, $W(\mathbf{k}, -\mathbf{k}')$, has the form

$$W(\mathbf{k}, -\mathbf{k}')_{\text{moving}} = w(\mathbf{k}, -\mathbf{k}')_{\text{moving}} \delta\{\omega(\mathbf{k}) - \omega(\mathbf{k}') - (k_x - k'_x)\bar{v}\}. \quad (\text{II.10})$$

If $\bar{v}/v_T \ll 1$ then

$$w(\mathbf{k}, -\mathbf{k}')_{\text{moving}} = w(\mathbf{k}, -\mathbf{k}') + \text{terms of the order of } (v/v_T)^2 \quad (\text{II.11})$$

with $w(\mathbf{k}, -\mathbf{k}')$ being defined in eq (II.6b).

Aside from the velocity dependence of w_{moving} , eq (II.6a) and eq (II.10) differ in the argument of their δ -functions. This difference expresses the fact that in collisions with moving dislocations not only the momentum but that, in contrast to the static case, also the energy of the phonon changes.

One aspect in which the calculations of the lattice thermal conductivity differ from those of the friction force, should already be noted here. A heat current arises from the deviations of the distribution $\bar{N}(\mathbf{k})$ from the thermal equilibrium distribution $\bar{\bar{N}}(\mathbf{k})$. A retarding force on the moving dislocation resulting from phonon scattering can, on the other hand, already be obtained in the case where the phonon gas stays in thermal equilibrium. In order that the phonons remain in thermal equilibrium, the average time between successive collisions of phonons with the moving dislocation must be large in comparison with the phonon relaxation time. This condition is fulfilled if the dislocation velocity is small with respect to the sound velocity, which is assumed to be the case in the following treatment of the friction force.

III. The Influence of Dislocation Arrangements on the Phonon Conductivity

It has already been mentioned that the concept of individual scatterers is only valid as long as the phonon wavelengths are small in comparison with the distances between the defects. At low temperatures, however, this condition is often not fulfilled. Here, the scattering probability is not only a function of the wave vector, it depends also on the spatial distribution of the defects. We mentioned in the introduction that the defect strains which are to be inserted in the elastic energy density ψ are, in the approximation of the third-order elasticity theory, those which were calculated with normal elasticity theory. The combined strain field of the various defects can, therefore, be obtained by linear superposition of the single defect strains.

In the first case, we consider a series of n closely spaced dislocations of the same signs (pile-up) along the x axis which are parallel to the z direction. The following consideration holds as well for edge dislocation pile-ups as for screw dislocation pile-ups if we insert for the single strains, ϵ_s , either the strains of an edge dislocation or of a screw dislocation, respectively. The total strain field, expressed in the single strains, is

$$\epsilon_P(\mathbf{r}) = \sum_{\nu=1}^n \epsilon_S(\mathbf{r} - \mathbf{i}_x x_\nu). \quad (\text{III.1})$$

The vector \mathbf{i}_x is a unit vector in the direction of the positive x axis, x_ν denotes the position of the ν th dislocation.

The strain field of two parallel edge dislocations of opposite signs (dipole configuration), on the other hand, is given by

$$\epsilon_D(\mathbf{r}) = \epsilon_S(\mathbf{r}) - \epsilon_S(\mathbf{r} - \mathbf{R}). \quad (\text{III.2})$$

Here, ϵ_S , denotes the strain of a single edge dislocation. For convenience, we let again the dislocations be parallel to the z axis. It is assumed that one of the dislocations is situated at $\mathbf{r}=0$ and the second one at $\mathbf{r}=\mathbf{R}$, where \mathbf{R} lies in the x, y -plane. The minus sign in eq (III.2) arises on account of the opposite signs of the two dislocations. From eqs (III.1 and III.2), we find the Fourier transforms of the strains:

$$\tilde{\epsilon}_P(\mathbf{g}) = \tilde{\epsilon}_S(\mathbf{g}) \sum_{\nu=1}^n \exp(-ig_x x_\nu) \quad (\text{III.3a})$$

and

$$\tilde{\epsilon}_D(\mathbf{g}) = \tilde{\epsilon}_S(\mathbf{g}) [1 - \exp(-ig \cdot \mathbf{R})]. \quad (\text{III.3b})$$

The probability rate, $W_{\text{stat.}}(\mathbf{k}, -\mathbf{k}')$, depends, according to eqs (II.3b) and (II.6b), on the absolute square of the Fourier transforms of the strains. The exponential factors in eqs (III.3a and III.3b) give rise to structure factors in the scattering probabilities. Let $W_s(\mathbf{k}, -\mathbf{k}')$ be the probability rate that a phonon of mode $\{\mathbf{k}\}$ is scattered into mode $\{\mathbf{k}'\}$ on account of the interaction of the phonons with a single dislocation, then the probabilities for the combined scattering are

$$W_P = W_s \sum_{\nu=1}^n \sum_{\nu'=1}^n \exp(-ig_x(x_\nu - x_{\nu'})) \quad (\text{III.4a})$$

and

$$W_D = W_s \cdot 2[1 - \cos(g \cdot \mathbf{R})]. \quad (\text{III.4b})$$

The vector \mathbf{g} is, according to eq (II.3c) and eq (II.6a), equal to the difference of the wave vectors \mathbf{k} and \mathbf{k}' .

Equations (III.4a) and (III.4b) show that the arrangement of the dislocations is unimportant if the distances between the dislocations are large in comparison with the phonon wavelengths. We find in this case that

$$W_P = nW_S \quad (\text{III.5a})$$

and

$$W_D = 2W_S. \quad (\text{III.5b})$$

Hence, the thermal resistance is in this case given by the sum of the single resistances. Deviations from the additivity of the resistances occur if $R/\lambda \lesssim 1$ (λ : phonon wavelength). This is the case at sufficiently low temperatures. For $g_x(x_\nu - x_{\nu'}) \rightarrow 0$, the probability W_P approaches the value $n^2 W_S$. Hence, with decreasing temperature the resistance of the pile-up increases with respect to the resistance which is due to isolated dislocations. The opposite result is obtained for the dipole configuration. Here, one finds that if $\mathbf{g} \cdot \mathbf{R} \rightarrow 0$ then $W_D \rightarrow W_S(\mathbf{g} \cdot \mathbf{R})^2$. The thermal resistance decreases in this case with decreasing separation of the two dislocations. This is due to the fact that the smaller the distance between the dislocations of opposite signs is, the more the strain fields of the two single dislocations cancel each other.

On account of the decrease in scattering strength the life times of the phonon states which are limited by the phonon-dipole interaction increase rapidly with increasing phonon wavelength. This would, without the help of other scattering mechanisms, lead to a divergence of the conductivity for small frequencies.

A quite similar situation arises in the case of phonon scattering by point defects. There, the singularity in the conductivity for $\omega \rightarrow 0$ arises from the rapid drop of the strains with increasing distance r from the defect center (strain $\sim 1/r^3$). However, on account of the normal three-phonon processes which, in any case, must be included the divergence can be removed, as was shown in a previous paper [8]. Although, the normal processes do not limit the thermal conductivity by themselves, they are important if the phonons are in addition scattered by lattice defects in that they govern the frequency dependence of the stationary state phonon distribution at the lowest frequencies. It has been shown [9] that interactions between three phonons which belong to the same polarization branch govern the frequency dependence of the mean phonon life times at small frequencies. The life times were in these cases found to be proportional to ω^{-1} . Using this result, it follows from Boltzmann's transport equation that the deviations of the occupation numbers, $\bar{N}(\mathbf{k})$, from the equilibrium distribution, $\bar{\bar{N}}(\mathbf{k})$, must be independent of the frequency for $\omega \rightarrow 0$. This fact has already been used in eq (I.1), where we started the expansion with a frequency independent term ($r=0$).

We should note that, if we take into account boundary scattering, the expansion (I.1) begins with a term which is linear in ω .⁶ In both

⁶If boundary scattering is included then the frequency dependence of $\bar{N}(\mathbf{k})$ is, for $\omega \rightarrow 0$, determined by this scattering mechanism.

cases in which $\mathbf{Z}(\mathbf{k}, j)$ is either proportional to ω^1 or to ω^0 , the singularity in the conductivity is removed. This holds as well in the case of point defects as it does for dislocation dipoles.

The explicit calculations of matrices M of the system of eqs (I.2) are rather lengthy. They have been presented elsewhere.⁷ Here, we confine ourselves only to a few remarks on the symmetry properties of M . The strain resulting from a straight dislocation is, according to linear isotropic continuum theory, independent of the coordinate parallel to the dislocation line. Hence, elastic waves which travel in the direction of the dislocation line will not be scattered. The wave vector component which is parallel to the dislocation line is, therefore, conserved. Hence, we find in both cases, pile-ups and dipoles, in which we considered the dislocations to be oriented parallel to the z -axis that the z -component of the wave vector \mathbf{k} is equal to the z -component of the wave vector \mathbf{k}' . This has the consequence that some of the elements of the matrix M are linearly dependent on each other, in such a way that the determinant of the matrix $M(j, 0, 1, r; j', 0, 1, r')$ vanishes. The component κ_{zz} of the conductivity tensor is therefore infinite.

In the case of the three-phonon interactions a similar relation between the elements of the matrix M yields that the determinant of M vanishes identically. This is a consequence of the fact that energy and quasi-momentum of the phonon gas are conserved in normal three-phonon processes. Hence, if the phonons were only scattered by normal processes, eq (I.2) had no solution. This result expresses the fact that a stationary state of the phonon gas cannot be established by normal processes alone.

Numerical values of the thermal resistance have been given in earlier papers for screw dislocation pile-ups [10] and edge dislocation dipoles [11] for various dislocation arrangements. Bross [12] discussed the asymptotic behaviour of the resistance of dislocation groups for cases in which the distances between the dislocations are not too small. The dependence of the scattering strength of a special defect configuration on the product $R\omega$ yields that the thermal conductivity is a function of RT . Below a certain value of RT which depends on the dislocation arrangement the resistance of a group of dislocations differs from the resistance of the single dislocations. In the case, phonon scattering by pile-ups, the thermal resistance increases below that value. On the other hand, a decrease of the resistance occurs for decreasing RT in the case of phonon scattering by dipoles. For distances R of only a few Burgers units and for temperatures in the neighbourhood of the temperature of liquid helium, the resistance due to dipole becomes temperature independent.

⁷ Gruner [10, 11], Bross [12].

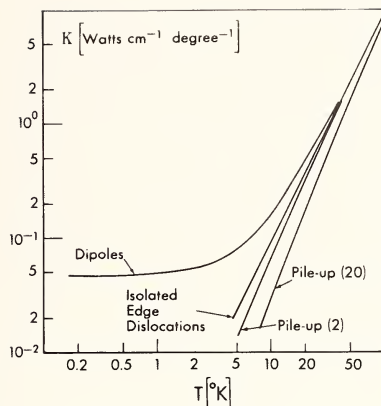


FIGURE 1. Influence of dislocation arrangements on the lattice thermal conductivity in copper (theory). Dislocation density is in all cases $5.12 \cdot 10^{10} \text{ cm}^{-2}$.

Isolated dislocations: random distribution of edge dislocations.

Dipoles: $R = 10 \text{ b}$.

Pile-up (2): $R = 10 \text{ b}$, 2 edge dislocations per group.

Pile-up (20): nearest neighbour distance $R = 10 \text{ b}$, 20 edge dislocations per group.

The magnitude of the resistance is in this temperature region proportional to the second power of R . Figure 1 gives a few examples for the influence the arrangement of edge dislocations has on the thermal conductivity. The average conductivity, defined by $\kappa = (\kappa_{xx}^{-1} + \kappa_{yy}^{-1})^{-1}$, has been calculated with the material constants of copper. The distance between the two dislocations of a dipole was assumed to be equal to 10 Burgers units. That distance has also been used for the separation of nearest neighbour dislocations in the pileups. The pileups contain 20 respectively 2 edge dislocations of the same signs which are parallel to each other and which have all the same Burgers vector. The total number of dislocation lines per cm^2 is in all four cases equal to $5.12 \cdot 10^{10}$. As figure 1 shows, the increase of the thermal resistance, in case of phonon scattering by closely spaced dislocations of the same signs, depends, apart from the dislocation separation, also on the number of dislocations in the group. Furthermore, the change in conductivity, at the lowest temperatures, is more pronounced for the dipole configuration than it is for a group of two dislocations of the same signs. This is due to the low frequency behaviour of the structure factors (III.4a and III.4b). The scattering cross section for pileups has the same frequency dependence for large ω as it has for $\omega \sim 0$; only its magnitude is changed. The frequency dependence of the scattering cross-section of dipoles, however, differs by a factor ω^2 from that one for isolated dislocations, when $\omega \rightarrow 0$.

We shall, in section IV, compare the theory with measurements of the thermal conductivity in ionic single crystals. While in undeformed metals

the lattice thermal conductivity is, at temperatures below the temperature of the conductivity maximum, governed by the phonon-electron interaction, the thermal conductivity is in electrical non-conductors at the lowest temperatures limited by the scattering of phonons at the crystal surfaces (boundary scattering). A rigorous treatment of the boundary effect would require us to solve the transport equation with proper boundary conditions which must be imposed on the phonon distribution. Since this is a rather difficult problem, we used the phenomenological approach which is based on the experimental evidence that at lowest temperatures the phonon mean free path, Λ , is, in pure crystals with rough surfaces, independent of the phonon frequency and approximately equal to the diameter of the crystal. Hence, if boundary scattering is dominant, the relaxation time of the phonon gas does not depend on the frequency of the phonons. This leads then to the well known T^3 -dependence of the thermal conductivity. In order to include the boundary effect in our studies, we had to find the corresponding matrix M . It is possible to construct this matrix for boundary scattering in such a way that it leads to the same expression for the thermal conductivity as it is obtained if a frequency independent relaxation time is used. Taking the definition of the matrix M for phonon scattering by defects (A.1) and assuming that the scattering is elastic and isotropic, we find

$$M(j, m, n, r; j', m', n', r') = -(-1)^m \delta^{jj'} \delta_{m', -m} \delta_{n', m} \\ \times [V_0(KT)^{r+r'+3}/(h^3 v_f^2 \Lambda)] (r+r'+2)! \zeta(r+r'+2). \quad (\text{III.6})$$

ζ denotes the Riemannian Zeta-function. Inserting eq (III.6) into eq (I.2) and solving for Z yields, with the help of eq (I.4), the thermal conductivity

$$\kappa = (1/3) C_v \bar{v}_s \Lambda \quad (\text{III.7a})$$

with

$$\bar{v}_s = \sum (1/v_j)^2 / \sum (1/v_j)^3. \quad (\text{III.7b})$$

C_v is the specific heat per unit volume.

Assuming that eq (III.6) is also valid if the phonons are in addition scattered by lattice defects, we calculated the thermal conductivity in case of the combined scattering of phonons by edge dislocation dipoles, normal processes, and boundaries. The calculation, in this case performed with the material constants of magnesium oxide (table 1), renders the results of figure 2. All curves were obtained with $\Lambda = 0.3$ cm. Curves 1 through 3 were calculated for a dislocation density of 4.10^{10} lines per cm^2 . The dislocation density in cases 4 and 5 is 4.10^9 lines/ cm^2 . Curves 1 and 4 represent cases in which the dislocations are regarded as individual

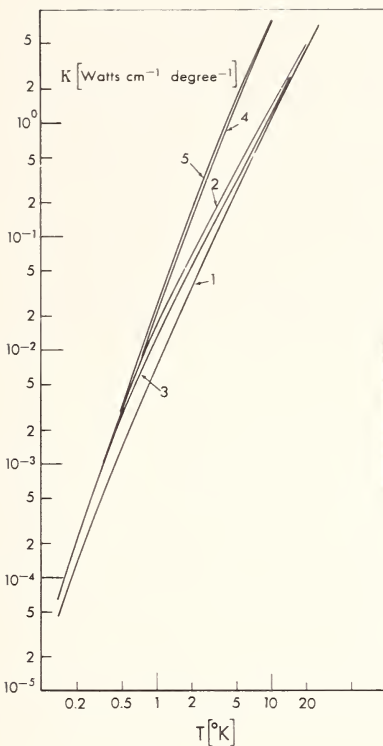


FIGURE 2. Thermal conductivity in magnesium oxide, limited by boundary effect, by edge dislocations, and by normal processes (theory). Mean free path, limited by boundary scattering, $\Lambda=0.3$ cm.

Curve 1: $N_S = 4 \cdot 10^{10} \text{ cm}^{-2}$, random distribution of dislocations.

Curve 2: $N_D = 2 \cdot 10^{10} \text{ cm}^{-2}$, $R = 20$ b (dipole configuration).

Curve 3: $N_D = 2 \cdot 10^{10} \text{ cm}^{-2}$, $R = 35$ b (dipole configuration).

Curve 4: $N_S = 4 \cdot 10^9 \text{ cm}^{-2}$, random distribution of dislocations.

Curve 5: $N_D = 2 \cdot 10^9 \text{ cm}^{-2}$, $R = 35$ b (dipole configuration).

scatterers-isolated dislocations. Proceeding from low temperatures to high temperatures, the transition from the T^3 regime (boundary scattering) to the T^2 regime (scattering from single dislocations) is here monotonous. Curves 2 and 3 were obtained for the case in which the dislocations are arranged in pairs (dipoles). The distances R between the two dislocations of a dipole are $20b$ and $35b$ for case 2 and 3, respectively.

The effect, the dipole configuration has on the conductivity is such that, in the temperature region where dislocations govern the temperature dependence, the slope of the conductivity curve is reduced (smaller than 2). In the low temperature region, however, where boundary scattering dominates, the tendency toward the T^3 -dependence of the conductivity is, in cases 2 and 3, more pronounced than it is in case 1. A pronounced

effect of the dipoles, leading to an inflection point which separates the T^2 region from the T^3 region, is only found if the dipole density is sufficiently high or the width of the crystal is large. Otherwise, as a comparison of curve 5 with curve 4 shows, the arrangement of the dislocations influences only the magnitude of the conductivity but does not lead to an inflection point. If an inflection point cannot be found in the experiment, the contribution of the dipoles to the thermal resistance can only be studied with the help of a curve fitting procedure, provided that Λ is known. Furthermore, the measured curve should exhibit a region where $\kappa \sim T^2$, so that the total number of dislocations can be estimated fairly accurate.

IV. Comparison of the Theory With Experiments and Discussion

In pure metals, the electronic contribution to the thermal conductivity at low temperatures is one to two orders of magnitude larger than the contribution by phonons. It is, therefore, difficult to separate the two components. In dilute alloys, however, the electronic part is considerably reduced on account of the scattering of the electrons by the solute atoms. In this case, it is then possible to separate both contributions, as has been shown by Hulm [13], Berman [14], Esterman et al. [15], and others. The influence of plastic deformation on the thermal conductivity has been studied by Esterman et al., Kemp et al. [16], and by Lomer and Rosenberg [17] in silver alloys and in copper alloys. Since we are here mainly interested in the influence the arrangement of dislocations has on the thermal conductivity, we shall restrict the discussion to measurements which indicate that the dislocation configuration affects the thermal conductivity.

Recently, Zeyfang [18] found deviations from the T^2 -dependence of the lattice thermal conductivity after strong plastic deformation which can be attributed to groups of dislocations of the same signs. He deformed Cu-Ga single crystals in tension in intervals of various temperatures between 4 and 293 K. After each deformation interval, the thermal conductivity was measured between 1.3 and 25 K. In stage I of deformation, the lattice thermal conductivity varied as T^2 between 1.3 and 10 K. In stage II and III, however, it was found that κ varied, at sufficiently low temperatures, stronger than with the second power of the temperature.

The T^2 -dependence of the conductivity indicates that the dislocations act as individual scatterers and that, hence, the average distance between them was in stage I larger than the dominant wavelength of the phonons. In this case, the total resistance of the dislocations is equal to the sum of the single resistances. Bross et al. [19] calculated, on the basis of the theory outlined above, the resistance of a single edge dislocation which is oriented

parallel to the z direction and which has a Burgers vector parallel to the x axis. For a dislocation density of N lines/cm 2 , the components of the resistance tensor are, in the case of copper, given by

$$\rho_{xx} = 6 \cdot 10^{-9} NT^{-2} [\text{cm degree Watt}^{-1}] \quad (\text{IV.1a})$$

and

$$\rho_{yy} = 15.2 \cdot 10^{-9} NT^{-2} [\text{cm degree Watt}^{-1}] \quad (\text{IV.1b})$$

Using that part of the conductivity curve where $\kappa \propto T^2$, Zeyfang calculated with the help of eqs (IV.1a and IV.1b) the dislocation density N which he then compared with measurements of N that were obtained by electron transmission microscopy. The values which he found with the former technique were about 5 times larger than those obtained with the latter one. The eqs (IV.1a and IV.1b) were derived with values of the third-order elastic constants which had been measured at room temperature. Salama et al. [20] showed that the room temperature data of the third-order constants are about 2 times smaller than those which one measures at helium temperatures. Taking this into account, the ratio between the values of N which have been determined by the two techniques is further reduced, probably by a factor of 2 to 3.

Figure 3 shows Zeyfang's measurements of the lattice thermal conductivity of Cu-4 at percent Ga. The measured points, denoted by (d), were obtained for a specimen which had been deformed at 293 K up to the beginning of stage III. The magnitude of the conductivity in the undeformed specimen (measured points denoted by (u)) is, in the linear part of the curve (T^2 -dependence), governed by the phonon-electron interaction. While for weak deformation (stage I) κ was found to vary as T^2 (not represented in fig. 3), the conductivity of the strongly deformed specimen departs from the T^2 -dependence in a manner which indicates the presence of groups of dislocations of the same signs. Zeyfang compared also in this case the experimental and the theoretical results. He used Bross' [12] approximate formulae for the resistance change on account of the dislocation arrangement and calculated for a group of N_g parallel edge dislocations, separated by not too small distances, the relative change in resistance $\Delta\rho/\rho_0$. He found

$$\Delta\rho/\rho_0 \sim (38/TN_g) \sum_{i \neq i'} b/R_{ii'} \quad (\text{IV.2})$$

$R_{ii'}$ is the distance between the i th and the i' th dislocation and ρ_0 is the resistance of N_g single dislocations. Good agreement between theory (curve 1) and the measurements of the deformed crystal (d) is obtained for $N_g = 20$ and $R_{ii'} = 35b |i - i'|$.

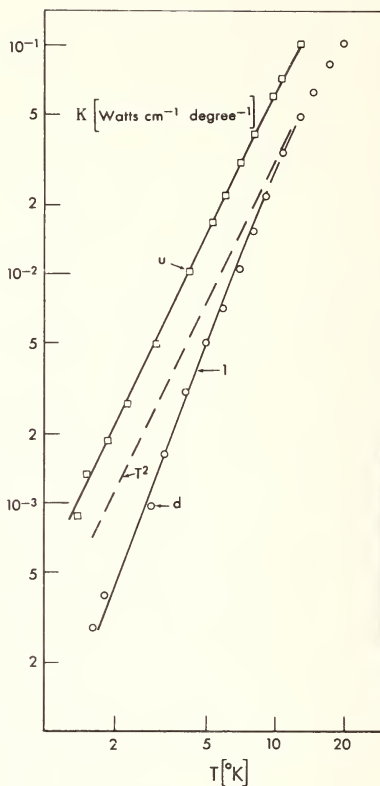


FIGURE 3. Lattice thermal conductivity in Cu-4 percent Ga after reference [18].

Curve u: undeformed specimen (experimental).

Curve d: deformed specimen (experimental).

Curve l: 20 equidistant ($R=35$ b) edge dislocations per group (theory).

Whereas in metals the experiments and the theory agree fairly well, larger differences between the calculated and the measured results seem to be the rule in ionic crystals. The effect of plastic deformation on the thermal conductivity of ionic crystals has been studied by Sproull et al. [21], Moss [22, 23], and Taylor et al. [24]. It was observed that the thermal conductivity decreases strongly with deformation. But, in contrast to the case of metals, the number of dislocations obtained from measurements of the thermal conductivity differ in ionic crystals often by several orders of magnitude from those which are obtained by other techniques. It has been suggested that part of the discrepancies might be due to special dislocation arrangements which scatter phonons stronger than randomly distributed dislocations do. This argument holds, however, only if the dislocations are arranged in groups which consist of closely spaced dislocations of the same signs; the dipole configuration would

lead to a reduction in scattering strength. Yet, an increase in scattering strength by a factor of hundred or even more on account of dislocation grouping is unlikely. The suggestion was made that etch pit counts are not necessarily representative for the number of dislocations if the dislocation density is high. Comparison of etch pit counts and counts of dislocation lines from electron transmission micrographs of deformed magnesium oxide lend some support to this argument. The number of etch pits was here found to be smaller by a factor of 5 than the number that was obtained from counts of dislocation lines.

It was argued that vacancies or vacancy aggregates which are generated during plastic deformation might account for the discrepancies. However, the annealing studies of Taylor et al. in NaCl seem to rule out that possibility.

Apart from the fact that the magnitude of the measured conductivity is too small to yield agreement between etch pit counts and the number of dislocations obtained from the lattice thermal conductivity, Taylor et al. found in several deformed alkali halides deviations from the T^2 -dependence of the conductivity. Furthermore, the temperature dependence of the conductivity in a NaCl crystal which they deformed in compression showed below some 5 K a stronger tendency towards the T^3 -dependence (boundary scattering) than was found in the same specimen after being annealed for 15 min at 355 °C. While the temperature dependence changed considerably (tended towards T^2), the magnitude of the conductivity increased only slightly in the temperature region where the phonon scattering by dislocations is mainly incoherent. Hence, the total number of dislocations could not have changed much during annealing. This was also confirmed by etch pit counts. A possible explanation was that during deformation groups of closely spaced dislocations of the same signs might have been formed. These lead to a stronger temperature dependence than T^2 at the lowest temperatures. It is likely that during annealing the distances between the dislocations had become larger in which case the dislocations act more as individual scatterers rather than as an ensemble.

Figure 4 shows the measured thermal conductivity (full circles, curve (ex)) of magnesium oxide single crystals which had been deformed by bending up to, approximately, an outer fiber strain of 2 percent. Etch pit counts yielded a maximum density of $2 \cdot 10^8$ pits/cm². Transmission electron micrographs revealed that the majority of the dislocations formed elongated loops (dipoles). The smallest observable distance between the two branches of a loop was estimated to be 50 Burgers units. The number of dislocation lines was estimated from the micrographs to be 10^9 lines/cm². Between 6 and 15 K, curve (ex) in figure 4 exhibits the T^2 -dependence of the conductivity. Below 6 K, a gradual transition towards the T^3 -dependence occurs. One of the reasons why an inflection point

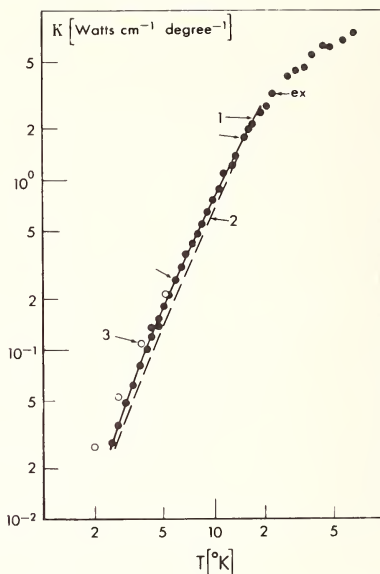


FIGURE 4. Thermal conductivity in magnesium oxide.

Curve ex: deformed crystal (experimental).

Curve 1: dipole configuration (theory). $N_D = 2.45 \cdot 10^{10} \text{ cm}^{-2}$, $\Lambda = 0.0366 \text{ cm}$, $R = 20 \text{ b}$.

Curve 2: random distribution (theory). $N_S = 4 \cdot 9 \cdot 10^{10} \text{ cm}^{-2}$, $\Lambda = 0.0366$.

Curve 3: dipole configuration (theory). $N_D = 2.45 \cdot 10^{10} \text{ cm}^{-2}$, $\Lambda = 0.3 \text{ cm}$, $R = 20 \text{ b}$.

cannot be seen is that the mean free path Λ which is limited by boundary scattering and which had been determined from the conductivity of the undeformed specimen was found to be only some 12 percent of the specimen width. This unexpected small value of Λ might be the consequence of phonon scattering by internal macroscopic boundaries. A subsequent investigation with the light microscope revealed inclusions of rectangular shape which were probably formed during crystal growth. No change in the thermal conductivity of the undeformed and chemically polished crystal could be found after the specimen surfaces had been sandblasted. This indicates again that the external surfaces did not limit Λ . The data, represented in curve (1), have been calculated with the following parameters: Dipole density, $N_D = 2.45 \cdot 10^{10} \text{ cm}^{-2}$; mean free path, $\Lambda = .0366 \text{ cm}$; dipole separation, $R = 20 \text{ b}$.

Curve (2) shows the calculated thermal conductivity ($\Lambda = .0366$) for the case of randomly distributed dislocations. The density of the dislocations was here taken to be $N_S = 2N_D$. Results, obtained with $R = 20 \text{ b}$, $N_D = 2.45 \cdot 10^{10} \text{ cm}^{-2}$ and $\Lambda = 0.3 \text{ cm}$, which is approximately equal to the width of the crystal, are shown by open circles (curve (3)).

The dislocation density which has been used to fit the experimental data at around 15 K is at least by a factor 50 larger than the density which was obtained from line counts. The discrepancy between theory and experiment seems to be somewhat smaller for MgO than it is for other ionic crystals where the number of dislocations has been estimated from the number of etch pits. The comparison of the fitted curve (1) with the results which were obtained with the same total number of dislocations but for a random distribution (curve (2)) shows that around 4 K the deviation between curves (1) and (2) is largest. At higher and lower temperatures both curves tend to join each other. Curve (ex) could not be fitted by taking into account phonon scattering by isolated dislocations and boundaries, only. The experimental data are much better represented by curve (1). This seems to indicate the influence of the dipole configuration on the thermal conductivity. It is hoped that further measurements of the conductivity in stronger deformed MgO crystals which are free from internal boundaries will lead to a more conclusive result.

Several reasons for the lack of agreement between the theoretical and the measured thermal conductivity in ionic crystals have been listed, such as dislocation arrangements, determination of the dislocation density with etch pit counts, etc. But these reasons can hardly account for the whole disparity. It is probable that the extension of the theory to the anisotropic case might improve the situation. A further improvement may be obtained by taking into account the temperature dependence of the third-order elastic constants.

V. The Relationship Between Dislocation Mobility and Thermal Resistance

Seeger and Engelke [25] calculated the retarding force which acts upon a moving kink on account of the anharmonic interaction between the strain field of a dislocation and the phonons. They used the fact that the negative rate of momentum change of the phonon gas must be equal to the force which tends to slow down the moving dislocation. If Umklapp-processes can be neglected—which is the case if the temperature is sufficiently low—then the quasi-momentum of a phonon, $\hbar\mathbf{k}$, can be identified with the ordinary momentum of a particle. The total momentum of the phonon gas is given by

$$\mathbf{p} = \sum \hbar\mathbf{k}N(\mathbf{k}). \quad (\text{V.1})$$

$N(k)$ is here the number of phonons in the vibrational mode $\{k\}$. On account of the interactions between the moving dislocation and the elastic waves, phonons are interchanged between the various modes. This leads to variations of the occupation numbers $N(\mathbf{k})$. Avoiding

difficult many-body calculations, which were necessary in order to obtain the time dependence of the phonon numbers, Seeger and Engelke confined their investigations to the calculation of the mean retarding force. We shall also follow this approach and shall, furthermore, restrict the comparison between the mobility and the thermal resistance to the case of straight dislocations. The average force can be written as

$$\mathbf{f} = - \sum \hbar \mathbf{k} \dot{\bar{N}}(\mathbf{k}). \quad (\text{V.2})$$

Neglecting the normal three-phonon interaction, one can express the average force, according to eqs (II.5) and (II.10), by

$$\begin{aligned} \mathbf{f} = & - \sum \hbar \mathbf{k} w(\mathbf{k}, -\mathbf{k}')_{\text{moving}} \delta\{\omega(\mathbf{k}) - \omega(\mathbf{k}') - (\mathbf{k} - \mathbf{k}') \cdot \bar{\mathbf{v}}\} \\ & \times [\bar{N}(\mathbf{k}') - \bar{N}(\mathbf{k})]. \end{aligned} \quad (\text{V.3})$$

The direction of the dislocation velocity, $\bar{\mathbf{v}}$, is here arbitrary. This is why the scattering probability used in eq (V.3) differs slightly from eq (II.10).

We shall now assume that the time the dislocation needs to travel a distance of the order of the phonon mean free path is large in comparison with the phonon relaxation time. This is the case if the dislocation velocity, \bar{v} , is small with respect to the sound velocity, v_s . The phonon distribution is then, on the average, equal to the distribution of the thermal equilibrium.

In this approximation, the normal processes, which we already neglected in eq (V.3), do not contribute to $\dot{\bar{N}}(\mathbf{k})$.

If we neglect terms of higher order than v/v_s in the force and define the tensor of friction, η , by

$$\mathbf{f} = -\eta \cdot \bar{\mathbf{v}}, \quad (\text{V.4a})$$

we obtain from eq (V.3)

$$\eta = (\hbar^2/KT) \sum \mathbf{k} W(\mathbf{k}, -\mathbf{k}')_{\text{stat.}} [\bar{N}(\mathbf{k}) + 1] \bar{N}(\mathbf{k}) (\mathbf{k} - \mathbf{k}'). \quad (\text{V.4b})$$

η is a symmetric tensor as can readily be verified by using the fact that

$$W(\mathbf{k}, -\mathbf{k}')_{\text{stat.}} = W(\mathbf{k}', -\mathbf{k})_{\text{stat.}}. \quad (\text{V.4c})$$

In order to write eq (V.4b) in terms which are known from the calculations of the thermal conductivity, we express the wave vector, \mathbf{k} , by the frequency, $\omega(\mathbf{k}, j)$, and spherical harmonics, $Y_{nm}(\theta, \phi)$. This yields

$$\mathbf{k} = \sum_{m=-1}^1 \xi(j, m) \hbar \omega(\mathbf{k}, j) Y_{1m}(\theta, \phi) \quad (\text{V.5a})$$

with

$$\xi(j, m) = (2\pi/3)^{1/2} (\hbar v_j)^{-1} \left\{ \begin{array}{l} \delta_{m, 1} - \delta_{m, -1} \\ (\delta_{m, 1} + \delta_{m, -1})/i \\ 2^{1/2} \delta_{m, 0} \end{array} \right\}. \quad (\text{V.5b})$$

Inserting eq (V.5a) into eq (V.4b) and using the expression (A.1) for the matrix M , the friction tensor takes the form

$$\eta = -\hbar^2 \sum_{\substack{j j' \\ m m'}} \xi(j, m) M(j, m, 1, 1; j', m', 1, 1) \xi(j', m'). \quad (\text{V.6})$$

Equation (V.6) shows that, for small dislocation velocities, the friction coefficient can be obtained from the same matrix M which has been used for the calculation of the thermal resistance. From eq (I.2) and (I.4) we find a similar expression for the thermal conductivity which reads

$$\kappa = - (TV_0)^{-1} \sum_{\nu \nu'} \mathbf{Z}(\nu) M(\nu, \nu') \mathbf{Z}(\nu'). \quad (\text{V.7})$$

Whereas ξ is given in eq (V.5b), the vector quantities \mathbf{Z} must be obtained by solving the system of equations (I.2).

Equation (V.6) is valid for any shape of the dislocation line if all parts of the dislocation have the same velocity $\bar{\mathbf{v}}$. We consider now the special case of a straight dislocation which moves perpendicular to its line. Let the dislocation line be parallel to the z axis. In the case of an edge dislocation we let the Burgers vector \mathbf{b} be in the direction of the positive x axis. For a screw dislocation we take \mathbf{b} in the positive z direction. Since the probability rate, $W(\mathbf{k}, -\mathbf{k}')_{\text{stat.}}$, remains in both cases invariant under the transformation $k_x \rightarrow -k_x$ and $k_y \rightarrow -k_y$, the matrix M vanishes unless $m + m'$ is even.

Taking also into account that the friction force has no component in the direction of the dislocation lines, η can be written in the following form:

$$\eta = \bar{\eta}_i \delta_{ik} \quad (\text{V.8a})$$

with

$$\bar{\eta}_1 = -(4\pi/3) \sum_{jj'} [M(j, j'; 1, 1) - M(j, j'; 1, -1)] / (v_j v_{j'}), \quad (\text{V.8b})$$

$$\bar{\eta}_2 = (4\pi/3) \sum_{jj'} M(j, j'; 1, -1) / (v_j v_{j'}), \quad (\text{V.8c})$$

$$\bar{\eta}_3 = 0, \quad (\text{V.8d})$$

and

$$M(j, j'; m, m') = M(j, m, 1, 1; j', m', 1, 1). \quad (\text{V.8e})$$

Numerical values for the matrix M were obtained for edge and screw dislocations by Bross et al. [19, 26] with the material constants of copper. With the help of those results we calculated the following friction coefficients:⁹

$$\bar{\eta}_1 \text{ screw/edge} = E_L b L T / (v_L \Theta) \cdot \alpha^{\text{screw/edge}} \quad (\text{V.9a})$$

with the energy density of the longitudinal phonons

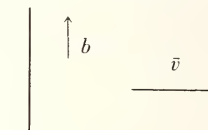
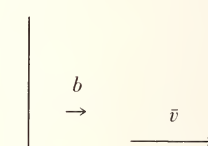
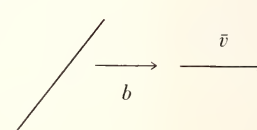
$$E_L = \pi^2 K^4 T^4 / (30 \hbar^3 v_L^3). \quad (\text{V.9b})$$

α^{screw} and α^{edge} are listed in table 2. L is the length of the dislocation.

The retarding force which acts on the screw dislocation is larger than that one which is felt by an edge dislocation. This result is consistent with the results that were obtained from calculations of the thermal conductivity which yielded $\kappa_{xx}^{\text{edge}} > \kappa_{xx}^{\text{screw}}$.

In order to compare these findings with the results obtained by Seeger and Engelke for the moving kink, we calculated the friction force for a mixed straight dislocation of length L , the orientation of which is shown in figure 5. Considering the mixed dislocation as being composed of a screw dislocation and an edge dislocation and applying a simple coordinate

TABLE 2. Coefficients α of eqs (V.9a) and (V.12b) for copper

	α
Screw dislocation	 4.599×10^3
Edge dislocation	 3.040×10^3
Mixed dislocation ($W/a >> 1$)	 4.599×10^3

⁹ Θ is the Debye temperature.

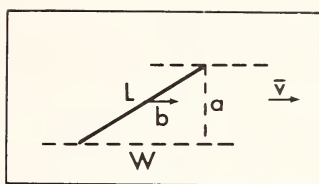
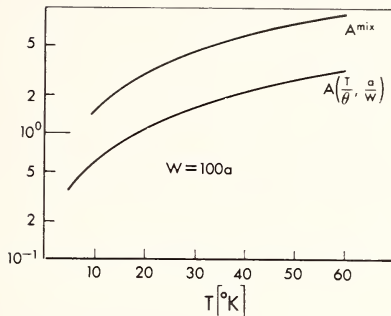


FIGURE 5. Mixed dislocation (schematic).

FIGURE 6. Coefficients A^{mix} and $A(T/\Theta, w/a)$ from eqs (V.12a) and (V.13), respectively, versus temperature.

transformation, the friction coefficient for the mixed dislocation, $\bar{\eta}^{\text{mix}}$, can be represented in terms of $\bar{\eta}_1^{\text{screw}}$ and $\bar{\eta}_1^{\text{edge}}$. Here, $\bar{\eta}^{\text{mix}}$ is defined by

$$f_r = -\bar{\eta}^{\text{mix}} \bar{v}, \quad (\text{V.10})$$

where f_r is the force component in the negative direction of the velocity. We find

$$\bar{\eta}^{\text{mix}} = (E_L b L T / v_L \Theta) (1 + (w/a)^2)^{-2} \{ (w/a)^2 \alpha^{\text{screw}} + \alpha^{\text{edge}} \}. \quad (\text{V.11})$$

We can now compare $\bar{\eta}^{\text{mix}}$ with the results which Seeger and Engelke obtained for the flat kink if we assume that the temperature is such that the dominant wavelength of the phonons is small in comparison with the length of the kink segment. This is the case if $T w / (a \Theta) \gg 1$. For $w/a \gg 1$, eq (V.11) yields

$$\bar{\eta}^{\text{mix}} \sim (E_L b a / v_L) A^{\text{mix}} \quad (\text{V.12a})$$

with

$$A^{\text{mix}} = T a / (w \Theta) \alpha^{\text{mix}} \quad \text{and} \quad \alpha^{\text{mix}} \sim \alpha^{\text{screw}}. \quad (\text{V.12b})$$

In the case of the kink it was found:

$$\bar{\eta}^{\text{kink}} = (E_L b a / v_L) A(T/\Theta, a/w), \quad (\text{V.13})$$

where $A(T/\Theta, a/w)$ is given in reference [25].

In figure 6, we plotted both A^{mix} and $A(T/\Theta, a/w)$ for $w/a=100$. In the temperature region where A^{mix} and $A(T/\Theta, a/w)$ can be compared, i.e., above some 30 K, A^{mix} is larger than $A(T/\Theta, a/w)$ by a factor of roughly 2.7. This is probably due to the fact that Seeger and Engelke took only into account the interaction between the dislocation and the longitudinal phonons, whereas in $\bar{\eta}^{\text{mix}}$ also the scattering of transversal waves is contained.

VI. Appendix

The variational method which has been discussed in the introduction leads to the following expressions for the matrices M . In case of phonon scattering by lattice defects, M is given by:

$$\begin{aligned} & -KTM(j, m, n, r; j', m', n', r') \\ &= \sum_{k, k', j''} W(\mathbf{k}, j; -\mathbf{k}', j'') [\bar{N}(\mathbf{k}, j) + 1] \bar{N}(\mathbf{k}', j'') (\hbar\omega(\mathbf{k}, j))^r \cdot Y_{nm}(\theta, \phi) \\ & \times \{ \delta^{jj'}(\hbar\omega(\mathbf{k}, j)) r' Y_{n'm'}(\theta, \phi) - \delta^{jj''}(\hbar\omega(\mathbf{k}', j'')) r' Y_{n'm'}(\theta', \phi') \}. \end{aligned} \quad (\text{A.1})$$

The matrix for normal three-phonon processes has the form:

$$\begin{aligned} & -KTM(j, m, n, r; j', m', n', r') \\ &= \sum_{\substack{k, k', k'' \\ j'', j'''}} W(-\mathbf{k}, j; \mathbf{k}', j''', \mathbf{k}'', j'') [\bar{N}(\mathbf{k}, j) + 1] \bar{N}(\mathbf{k}', j''') \bar{N}(\mathbf{k}'', j'') \\ & \times (\hbar\omega(\mathbf{k}, j))^r Y_{nm}(\theta, \phi) \cdot \{ \delta^{jj'}(\hbar\omega(\mathbf{k}, j)) r' Y_{n'm'}(\theta, \phi) \\ & - 2\delta^{jj'''}(\hbar\omega(\mathbf{k}', j'')) r' Y_{nm}(\theta', \phi') \} + \text{two similar terms.} \end{aligned} \quad (\text{A.2})$$

VII. References

- [1] Klemens, P. G., in Solid State Physics, **7**, F. Seitz and D. Turnbull, Eds. (Academic Press Inc., New York, 1958) p. 1.
- [2] Carruthers, P., Rev. Mod. Phys. **33**, 92 (1961).
- [3] Ziman, J. M., in Electrons and Phonons, N. F. Mott, E. O. Bullard, and D. H. Wilkinson, Eds. (Clarendon Press, Oxford, 1960).
- [4] Callaway, J., Phys. Rev. **113**, 1046 (1960).
- [5] Krumhansl, J. A., Proc. Phys. Soc. **85**, 921 (1965).
- [6] Bross, H., Phys. Status Solidi **2**, 481 (1962).
- [7] Peierls, R. E., in Quantum Theory of Solids, N. F. Mott and E. C. Bullard, Eds. (Clarendon Press, Oxford, England, 1955).

- [8] Gruner, P., *Phys. status solidi* **12**, 679 (1965).
- [9] Bross, H., Gruner, P., and Kirschenmann, P., *Z. Naturforsch.* **20a**, 1611 (1965).
- [10] Gruner, P., *Z. Naturforsch.* **20a**, 1626 (1965).
- [11] Gruner, P. and Bross, H., *Phys. Rev.* **172**, 583 (1968).
- [12] Bross, H., *Z. Physik* **189**, 33 (1966).
- [13] Hulm, J. K., *Proc. Phys. Soc.* **A64**, 207 (1951).
- [14] Berman, R., *Phil. Mag.* **42**, 642 (1951).
- [15] Esterman, I. and Zimmermann, J. E., *J. Appl. Phys.* **23**, 578 (1952).
- [16] Kemp, W. R. G., Klemens, P. G., Tainsh, R. J., and White, G. K., *Acta Met.* **5**, 303 (1957).
- [17] Lomer, J. N. and Rosenberg, H. M., *Phil. Mag.* **4**, 467 (1959).
- [18] Zeyfang, R., *Phys. status solidi* **24**, 221 (1967).
- [19] Bross, H., Seeger, A. and Haberkorn, R., *Phys. status solidi* **3**, 1126 (1963).
- [20] Salama, K. and Alers, G., *Bull. Am. Phys. Soc.* **12**, 305 (1967).
- [21] Sproull, R. L., Moss, M. and Weinstock, H., *J. Appl. Phys.* **30**, 334 (1959).
- [22] Moss, M., *J. Appl. Phys.* **36**, 3308 (1965).
- [23] Moss, M., *J. Appl. Phys.* **37**, 4168 (1966).
- [24] Taylor, A., Albers, H. R. and Pohl, R. O., *J. Appl. Phys.* **36**, 2270 (1965).
- [25] Seeger, A. and Engelke, H., in *Dislocation Dynamics*, A. R. Rosenfield et al., Eds. (McGraw-Hill Book Company, New York, 1968) p. 623.
- [26] Bross, H., Seeger, A. and Gruner, P., *Annalen der Physik* **11**, 230 (1963).
- [27] Seeger, A. and Buck, O., *Z. Naturforsch.* **15a**, 1056 (1960).
- [28] Bross, H., *Z. Physik* **175**, 345 (1963).
- [29] Bogardus, E. H., *J. Appl. Phys.* **36**, 2504 (1965).

PHONON SCATTERING BY COTTRELL ATMOSPHERES

P. G. Klemens

*Department of Physics and Institute of Materials Science
University of Connecticut
Storrs, Connecticut 06268*

The formation of Cottrell atmospheres can change the scattering of phonons by dislocations and in some cases substantially enhance the lattice thermal resistivity due to dislocations. The strength of the atmospheres can be changed by annealing. This changes thermal conductivity values at high temperatures first, since diffusion through shorter distances is involved. The diffusion coefficient can be determined by means of such annealing studies.

Key words: Cottrell atmospheres; mechanical properties; phonon scattering; thermal resistivity.

Metallic alloys have generally an appreciable lattice component of thermal conductivity at low temperatures. This component is sensitive to lattice imperfections which scatter phonons. In particular, dislocations can reduce the lattice components at very low temperatures, while randomly distributed point defects tend to be important at somewhat higher temperatures [1]. The reason is that dislocations scatter phonons because of the relatively long-range strain field surrounding them, while the perturbation due to point defects is only of short range. Long-wave phonons are thus more sensitive to dislocations, short-wave phonons to point defects.

If point defects are not randomly distributed, but with spatial correlation, then the scattering of phonons is related to the appropriate Fourier coefficients of the spatial correlation function; the theory for phonon scattering [2] is then analogous to the theory of small angle scattering of x rays by correlated solute atoms.

To explain an apparent dependence of the phonon scattering cross section of dislocations on solute content, which had been observed by Charsley et al. [3] in Cu-Al alloys, it was proposed that Cottrell atmospheres of Al about dislocations reinforce the anharmonic scattering of phonons by the strain field [4]. The argument used may be recapitulated as follows.

Fundamental Aspects of Dislocation Theory, J. A. Simmons, R. de Wit, and R. Bullough, Eds. (Nat. Bur. Stand. (U.S.), Spec. Publ. 317, I, 1970).

The fractional change in phonon velocity due to a dilatation Δ is given by

$$\delta v/v = -\gamma \Delta(r) \quad (1)$$

where γ is the Grueneisen constant, and Δ can be regarded as a function of position. The dilatation causes an inhomogeneous solute distribution; the change in solute concentration in the limit of small dilatations is given by

$$\delta c/c = \alpha(VK/kT_0)\Delta(r) \quad (2)$$

where V is the atomic volume, αV is the excess of the atomic volume of the solute over that of the parent metal, K is the bulk modulus, k the Boltzmann constant and T_0 the temperature at which the atmosphere attained equilibrium. While (2) does not hold near the dislocation core, it holds at a distance of a phonon wavelength, which is the most important region for phonon scattering. If we now assume that the presence of solute atoms change the local value of the phonon velocity, and that this change is related to the concentration by

$$\delta v/v = \beta c \quad (3)$$

it follows that the total change in phonon velocity, due to anharmonicity and the atmosphere, is given by

$$\delta v/v = -(\gamma + \gamma')\Delta(r) \quad (4)$$

where

$$\gamma' = -\alpha\beta(VK/kT_0)c \quad (5)$$

and where c is the average solute concentration. Since the total scattering is proportional to $(\gamma + \gamma')^2$, anharmonic scattering is enhanced if γ' is positive. This requires that a solute atom should be larger than the parent metal (positive α) and at the same time heavier (hence negative β); alternatively the atom may be smaller and lighter. The other combinations result in negative values of γ' and thus in a reduction of the phonon scattering cross section.

This model leads to the prediction that Al atmospheres around dislocations in Cu-Al enhance the scattering of phonons and thus the lattice thermal resistivity due to dislocation; the enhancement factor should be about 3 for an 8 percent alloy. There should be several alloy systems showing a similar effect, for example in Cu-Au the presence of 3 percent Au should double the dislocation scattering.

It has been assumed so far that the solute atoms had an opportunity to arrange themselves into their equilibrium positions. After plastic deforma-

tion, when dislocations are torn from their original positions and new dislocations are formed, the solute atoms must diffuse through distances of the order of hundreds of Angstroms to form the atmospheres, for this is the distance (comparable to the phonon wavelength) within which most of the dislocation scattering occurs. To explain the observed enhancement one must conclude that this diffusion has occurred between the time of deformation and the time of measurement in Cu-Al, even though the temperature of the sample did not exceed room temperature significantly. One would expect diffusion of Al in Cu to be extremely slow at room temperature, and one may perhaps expect to find aging effects in the lattice thermal conductivity due to a slow formation of the atmospheres. Another possibility, which would account for atmosphere formation more satisfactorily, is that diffusion of solutes near dislocations is substantially enhanced during and immediately after the deformation process, because vacancies are created during deformation and are thus present for a short time in concentrations well in excess of the equilibrium concentrations which normally determine the diffusivity. On that model the atmospheres form instantaneously.

We note that γ' is inversely proportional to T_0 , the temperature at which equilibrium was attained. In many systems it may be possible to choose an annealing temperature high enough for ordinary diffusion to occur, but low enough to avoid the removal of dislocations. Under such circumstances it should be possible to decrease γ' by a known fraction, and observe a corresponding increase in the lattice thermal conductivity. Furthermore, this change would not be instantaneous, and by following the rate of change as a function of annealing time, it should be possible to determine the diffusion coefficient.

We can put this on a quantitative basis by noting that the diffusion problem can be solved best in terms of the Fourier coefficients of the concentrations, while the phonon scattering problem requires a knowledge of the same Fourier coefficients. Let $c_0(r)$ be the new equilibrium concentration and $c'(r)$ the departure from it, so that $c = c_0 + c'$. The diffusion equation is

$$\frac{\partial c'}{\partial t} - D \nabla^2 c' = 0 \quad (6)$$

where D is the diffusion coefficient. Expressing $c'(r)$ in terms of Fourier coefficients of wave vector q , each component changes with time according to

$$c'(q) \propto e^{-t/\tau} \quad (7)$$

where

$$1/\tau = Dq^2. \quad (8)$$

At temperature T , the dominant phonons contributing to the thermal conductivity have a wave vector

$$q \approx 4aT/\theta \quad (9)$$

where a^3 is the atomic volume and θ the Debye temperature. The change in thermal conductivity at temperature T after annealing at temperature T_0 for a time t may be thus written as

$$\frac{\delta K(T)}{\delta K_0(T)} = 1 - e^{-t/\tau} \quad (10)$$

where δK_0 is the change in thermal conductivity induced by annealing until the new equilibrium has been reached. The characteristic time τ is given by

$$\frac{1}{\tau} = D(T_0) \left(\frac{4T}{a\theta} \right)^2 \quad (11)$$

and this time depends on the temperature T at which the thermal conductivity is measured. At higher measuring temperatures the important phonons are of shorter wavelength, the corresponding Fourier components of the concentration are also shorter, and equilibrium is attained more quickly. It should be possible to anneal for a time such that the new equilibrium of the thermal conductivity is reached at higher temperatures but not at lower temperatures. It should then be possible to determine the diffusion coefficient at the annealing temperature by using eqs (10) and (11). Since diffusion occurs through distances of the order of hundred Angstroms, this method of determining diffusion coefficients may have advantages over the conventional methods at relatively low annealing temperatures.

Acknowledgement

Research sponsored by the Air Force Office of Scientific Research under Grant No. AF-AFOSR-68-1517.

References

- [1] Klemens, P. G., in Solid State Physics, **7**, F. Seitz and D. Turnbull, Eds. (Academic Press, New York, 1958) p. 1.
- [2] Klemens, P. G., in Non-Crystalline Solids, by V. D. Frechette, Ed. (John Wiley & Sons, Inc., New York, 1960) p. 508.
- [3] Charsley, P., Salter, J. A. M., and Leaver, A. D. W., Physica status solidi **25**, 531 (1968).
- [4] Klemens, P. G., J. Appl. Phys. **39**, 5304 (1968).

Discussion on Papers by P. Gruner and P. G. Klemens.

NABARRO: Is it really correct to concentrate attention on the sound velocity or should one rather concentrate on the acoustical impedance?

KLEMENS: I don't know. I have always considered the theory as a perturbation theory and it should come to the same thing if you do it right, but maybe I haven't done it right.

BESHERS: Professor Klemens, you didn't really discuss what is probably the most interesting case of a Cottrell atmosphere formed by the interstitial atoms in a b.c.c. metal. These apparently form fairly completely at room temperature or even low temperature in the case of hydrogen. Would you expect, then, to see large effects?

KLEMENS: The conditions which have to be met to see the effect are several: You must have a reasonable concentration of these impurities, at least a few percent; they must form Cottrell atmospheres; and they must change the velocity of sound effectively. Hydrogen might not meet the last condition.

BESHERS: In what volume must the concentration be reasonable? And within what distance of the dislocation, because you get terrific concentration factors during segregation.

KLEMENS: I am only considering the long range tail end of the Cottrell atmospheres, not things that mechanical people consider. But the effect is proportional to the average concentration of impurities, and the average concentration must be of the order of a few percent.

GRANATO: I have a question for Dr. Gruner, who interprets the increase in the temperature dependence to a higher than T^2 dependence to be evidence for dipoles, but how do you know that it isn't the fluttering mechanism?

GRUNER: I said that a temperature dependence of the conductivity which is stronger than T^2 can arise from phonon scattering by closely spaced dislocations of equal sign: the scattering by dipoles leads to a decrease in the slope of the conductivity curve. I should think that in metals, where the anharmonicity mechanism predicts the right order of magnitude of the conductivity, one is on the safe side if the increase in temperature dependence with increasing deformation is assumed to arise from phonon scattering by dislocation groups. If fluttering were the dominant mechanism, then one would expect that a deviation from the T^2 dependence should also be present at lower degrees of deformation. This is not the case in Zeyfang's results.¹ As to ionic crystals, I think. a

¹ Zeyfang, R., Phys. Stat. Sol. **24**, 221 (1967).

decision on the relative importance of fluttering or dislocation arrangement cannot be made as long as there is still a large discrepancy between theory and experiment concerning the magnitude of the conductivity.

BULLOUGH: [To Professor Klemens] Your theory probably isn't appropriate for carbon in iron, because presumably the impurities have to form Maxwell-Boltzmann atmospheres—not Cottrell atmospheres. A Cottrell atmosphere isn't an atmosphere; it describes local precipitation at the dislocation core.

KLEMENS: I don't know the distinction between the two, but I have used an exponential distribution—which I suppose is a Maxwell-Boltzmann atmosphere—then approximated the exponential by one plus the next term, because I was in the region of small strains about 100 Å away from the dislocation core. Does that answer your question?

BULLOUGH: Yes, it's just the name Cottrell *atmosphere* that I do not like.

KLEMENS: You object to that?

BULLOUGH: Yes.

KLEMENS: I apologize.

AUDIENCE: General laughter.

SUZUKI: I would like to comment on Dr. Gruner's and Professor Klemens' talks. Kusunoki and I² have measured the thermal conductivity of copper-aluminum alloys and obtained almost the same results as Zeyfang's data¹ on copper-gallium alloys. We explained the data as resonant scattering of vibrating dislocations in Cottrell atmospheres and obtained positive agreement. I am wondering whether Dr. Zeyfang's data agree with the predictions of Dr. Gruner.

GRUNER: With a reasonable choice of the distances between the dislocations and the number of the dislocations within a group, the theory and Zeyfang's measurements agree rather well as to magnitude and temperature dependence.

KLEMENS: I think that I have only considered the anharmonic scattering and the atmosphere reinforcement. I think that one would be very bold to claim resonance effects have no effect in these alloys until one has made really quantitative calculations and quantitative measurements with a number of dislocations determined separately and then a measurement which would look at the effect of atmospheres. I think that the atmosphere mechanism that I have presented is only a theoretical mechanism and nothing more.

² Kusunoki, M., and Suzuki, H., J. Phys. Soc. Japan **26**, 932 (1969).

DRAZZING FORCES ON MOVING DEFECTS BY STRAIN-FIELD PHONON SCATTERING

A. Seeger and H. Engelke

Max-Planck-Institut für Metallforschung

Institut für Physik

and

*Institut für Theoretische und Angewandte Physik der Universität
Stuttgart, Germany*

An expression for the dragging force on a uniformly moving defect by scattering of phonons at its strain-field has been derived using nonlinear elasticity theory. The quantization procedures and the formulation of the master equation for the phonon distribution follow the techniques developed in the theory of heat conductivity. Numerical calculations have been performed for kinks in screw dislocations in copper. A comparison with numerical results obtained in the theory of heat conductivity shows quite good agreement. The formalism developed should prove useful also for calculations of the electron drag on dislocations in metals.

Key words: Dislocation drag; dislocation-phonon interactions; electroresistivity; kink motion; phonon scattering.

The lattice heat resistance of defects in crystals is produced by the anharmonic forces between the atoms. These forces cause the scattering of thermal lattice waves at the strain fields of the defects and also bring about dragging forces when the defects are moved through the crystal.

The formalism of the theory of lattice heat conductivity at low temperatures [1] has been applied to derive an expression for this dragging force in the case of uniformly moving defects.

The starting point of this calculation is the Hamiltonian for the lattice waves, which may be written in the following way

$$H = H_0 + H_1(t), \quad (1)$$

where

$$H_0 = \sum_{\mathbf{k}, j} \hbar \omega_{\mathbf{k}}^j \left(\mathbf{a}_{\mathbf{k}}^{+j} \mathbf{a}_{\mathbf{k}}^j + \frac{1}{2} \right) \quad (2)$$

represents an infinite set of uncoupled quantized linear harmonic oscillators.

Fundamental Aspects of Dislocation Theory, J. A. Simmons, R. de Wit, and R. Bullough, Eds. (Nat. Bur. Stand. (U.S.), Spec. Publ. 317, I, 1970).

tors. $\hbar\omega_{\mathbf{k}}$ is the energy of a phonon with wave-vector k and polarisation index j , $a^{+j}_{\mathbf{k}}$ and $a^j_{\mathbf{k}}$ are the creation and annihilation operators. The operator

$$H_1(t) = \sum_{\mathbf{k}, \mathbf{k}'} \{ H'_1 \exp [i(k_z + k'_z)\bar{v}t] + H''_1 \} \quad (3)$$

gives rise to an interaction (coupling) between the oscillators in two-phonon processes and is due to the presence of a defect moving with constant (average) velocity \bar{v} in z -direction. Here k_z and k'_z are the z -components of the wave-vectors \mathbf{k} and \mathbf{k}' of the phonons created and destroyed during the interaction described by the term $a^{+j}_{\mathbf{k}} a^{j'}_{\mathbf{k}'}$ in H_1 . H''_1 represents the effect of the non-moving part of the defect. Both H'_1 and H''_1 are time-independent operators, explicit forms of which may be derived from the theory of heat conductivity.

Since Umklapp processes can be shown to be unimportant in the present treatment, we may identify the quasi-momentum of a phonon with the ordinary momentum. This means that the change of the momentum \mathbf{p} of the phonon gas in such a process is given by $\hbar(\mathbf{k} - \mathbf{k}')$. According to actio-reactio the defect causing this transition undergoes an opposite change in its momentum, and the force f exerted on the defect is given by

$$f = -\frac{\partial \mathbf{p}}{\partial t}. \quad (4)$$

If $N_{\mathbf{k}}^j$ denotes the occupation number of the oscillator $\{j, \mathbf{k}\}$, then the total momentum of the phonon gas is given by

$$\mathbf{p} = \sum_{j, \mathbf{k}} \hbar \mathbf{k} N_{\mathbf{k}}^j. \quad (5)$$

The calculation of the occupation numbers $N_{\mathbf{k}}^j$ as a function of time would require the solution of a complicated many-body problem. It is expedient to introduce the average occupation numbers $\bar{N}_{\mathbf{k}}^j$ according to

$$\bar{N}_{\mathbf{k}}^j = \sum_{\nu} N_{\mathbf{k}}^j P(\nu; \bar{v}; t), \quad (6)$$

where the summation extends over all eigenstates ν of the unperturbed Hamiltonian H_0 . The conditional probability

$$P(\nu; \bar{v}; t) \equiv P(\dots, N_{\mathbf{k}}^j, \dots, \dots, \bar{N}_{\mathbf{k}}^j, \dots, t)$$

gives the probability of finding at time t the occupation numbers $N_{\mathbf{k}}^j$ if the perturbation was switched on at $t=0$ and if the occupation numbers

at that time were \bar{N}_k^j . By averaging eqs (4) and (5) and inserting eq (6), the following expression for the z-component of the mean force on the moving defects is obtained:

$$\bar{f}_z = \sum_{j, k} \sum_{\nu} \hbar k_z N_k^j \dot{P}(\nu; \tilde{\nu}; t). \quad (7)$$

The conditional probability $P(\nu; \tilde{\nu}; t)$ obeys the master equation

$$\dot{P}(\nu; \tilde{\nu}; t) = \sum_{\nu''} \{W(\nu, \nu'')P(\nu'', \tilde{\nu}) - W(\nu'', \nu)P(\nu, \tilde{\nu})\}, \quad (8)$$

where the sum extends over all intermediate states ν'' and $W(\nu, \nu'')$ is the transition probability from state ν'' to ν . Inserting eq (8) into (7) gives the final expression for the mean force \bar{f}_z on the moving defect in terms of $W(\nu, \nu'')$. With only slight alterations this expression is valid also for other Bose-type excitations. The intermediate states ν'' correspond to the creation of one additional phonon (${}_k^j$) and the annihilation of one phonon (${}_k^{j'}$), since only two-phonon processes are considered and the simultaneous creation or annihilation of two phonons is excluded by energy conservation reasons. The summation over ν necessary in order to obtain the average \bar{f}_z [eq (7)] requires averages over triple products of the occupation numbers. Within the framework of the present approximation, we may replace these averages by the products of the averages of the occupation numbers.

If we assume that before switching on the perturbation the phonons were in thermal equilibrium, i.e., that the average occupation numbers were (K =Boltzmann's constant)

$$\bar{N}_k^j = \bar{\bar{N}}_k^j \equiv \{\exp [\hbar \omega_k^j / KT] - 1\}^{-1}, \quad (9)$$

we obtain as the final result for the average force (ρ_0 =density of the ideal crystal)

$$\begin{aligned} \bar{f}_z = & -\frac{\pi}{\rho_0^2} \cdot \sum_{j, j'} \int \left| \frac{\hbar(k_z - k'_z)}{\omega_k^j \omega_{k'}^{j'}} \right| \left| V'{}_{1-kk'}^{jj'} + V'{}_{2-kk'}^{jj'} \right|^2 \cdot (\bar{\bar{N}}_{k'}^{j'} - \bar{\bar{N}}_k^j) \\ & \times \delta(\omega_k^j - \omega_{k'}^{j'} - (k_z - k'_z)v) d\tau_k d\tau_{k'}. \end{aligned} \quad (10)$$

The matrix elements $V'{}_{i-kk'}^{jj'}$ are proportional to the Fourier-transformed time-dependent strain components of the moving defect and are familiar from the theory of heat conductivity.

Formula (10) has been applied to a slowly moving ($V \ll c_1$, c_1 =velocity of longitudinal waves) flat (kink width w large compared with Peierls dis-

tance a) dislocation kink in copper in the limitation to longitudinal-longitudinal-transitions of phonons ($j=1, j'=1$). By introducing the energy density of the longitudinal phonons, E_1 , one obtains the following result:

$$\bar{f}_z^{(11)} = A \left(\frac{T}{\theta}, \frac{a}{w} \right) ab \frac{E_1}{c_1} \quad (11)$$

(θ = Debye temperature, b = dislocation strength).

The factor A is a function of temperature and kink width and is plotted in figure 1. It shows a slight temperature dependence and increases with decreasing kink width. The line denoted by Eshelby is the corresponding value of A predicted by Eshelby's treatment of the flutter mechanism for longitudinal waves only.

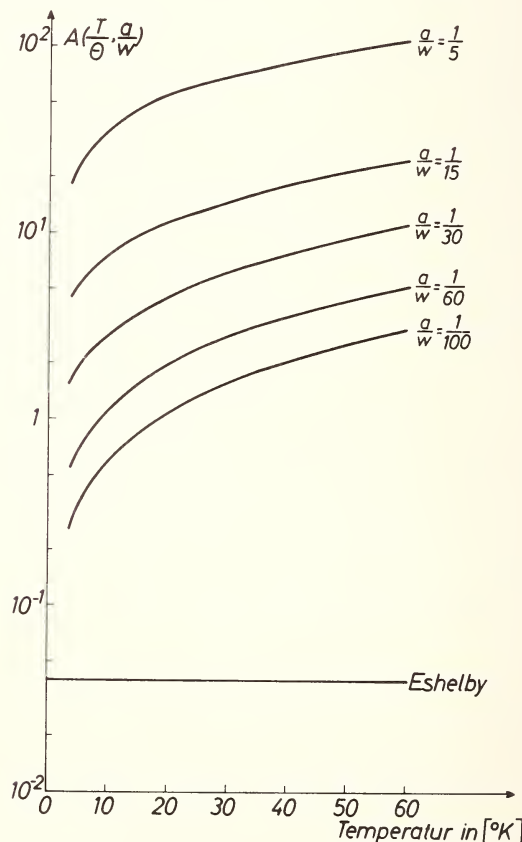


FIGURE 1

The scattering of phonons at a kink may be approximated by the scattering at a suitable mixture of straight edge and screw dislocations if the predominant phonon wavelength is short compared with the kink width. In this case a frictional force may be calculated using heat conductivity results. This has been done by P. Gruner [3]. The factor A obtained in this way, taking $w/a = 100$, has the same temperature-dependence as the corresponding factor in figure 1 but is 2.7 times larger than this. Since in Gruner's calculation all transition types are considered whereas we have only taken into account longitudinal transitions this result looks quite reasonable.

Equation (7) may also be applied to calculate a dragging force on moving dislocations due to the scattering of *electrons*. The calculation runs along similar lines as calculations of the electrical resistance of dislocations (see for example [4]).

Holstein [5] has calculated a dragging force (assuming free electrons) by means of the change of energy per unit time instead of momentum. Both procedures seem to give identical results in the approximation of free electrons. The case of Bloch-electrons undergoing Bragg-reflection needs further investigation.

References

- [1] Bross, H., Phys. Stat. Sol. **2**, 481 (1962).
- [2] Seeger, A., and Engelke, H., in Dislocation Dynamics, A. R. Rosenfield et al., Eds. (McGraw-Hill Book Co., New York, 1968).
- [3] Gruner, P., These Proceedings.
- [4] Seeger, A., and Bross, H., Z. Naturforschg. **15a**, 663 (1960).
- [5] Tittmann, B. R., and Bömmel, H. E., Phys. Rev. **151**, 178 (1966).

THERMAL ENERGY TRAPPING BY MOVING DISLOCATIONS

J. H. Weiner

*Division of Engineering
Brown University
Providence, R. I. 02912*

The steady motion of a dislocation along a piece-wise harmonic Frenkel-Kontorowa model is considered. For suitable model parameters there is one localized mode associated with either the stable or unstable dislocation configuration and the remaining modes are non-localized or extended. Because of the piece-wise harmonic character of the model, the set of normal modes of the system changes at discrete instants of time, referred to as transition times, as the dislocation moves along the chain. In particular, the localized modes must move along with the dislocation position and we refer to the localized mode momentum and energy as the dislocation momentum and energy respectively. The particle momentum and energy due to the sum of the extended modes is termed thermal.

At the transition times, it is necessary to expand atomic velocities in terms of the new set of modes appropriate to the forthcoming state of the crystal. It is found that a coordination effect exists between the transition times and the thermal motion such that on the average over many transitions, thermal momentum in the direction of the dislocation motion is transferred to the dislocation momentum.

Key words: Computer simulation; dislocation-phonon interaction; Frenkel-Kontorowa model.

I. Introduction

One of the inherent aspects of the steady motion of a dislocation is that it involves the successive progression, in its core, from one stable equilibrium configuration to an adjacent one. This applies to the case of the motion of the dislocation as a straight line, so that it moves from Peierls valley to Peierls valley, or to a kink moving along a dislocation line through successive "kink Peierls valleys." We wish to study the effect of this particular aspect of the process on the interaction of dislocation motion with the thermal motion of the atoms in the crystal. In order to do so we

Fundamental Aspects of Dislocation Theory, J. A. Simmons, R. de Wit, and R. Bullough, Eds. (Nat. Bur. Stand. (U.S.), Spec. Publ. 317, I 1970).

utilize a simple model that focuses upon it, namely a modified Frenkel-Kontorowa model. This model may be thought of as representing either the motion of a straight dislocation or a kink along the dislocation (Sanders, [1]). The modification of the Frenkel-Kontorowa model consists in taking the substrate potential as piecewise quadratic so that the forces are piecewise linear. We may say then that the model includes only the "essential anharmonicity" necessary to permit the dislocation to move from one equilibrium position to an adjacent one.

Much of the work we are going to describe has been presented previously (Weiner, [2], [3]). Here we have attempted to make clearer the physical ideas involved, and to estimate the magnitude of the effect observed. It has also proved possible to simplify and at the same time make more general the probability discussion of [3].

II. Dislocation Motion in a Linear Chain

The modified Frenkel-Kontorowa model consists of a linear chain of mass points with mass m interconnected by linear springs and with equilibrium spacing b . In addition to the linear springs, each of the atoms is subjected to a constant force σ , representing an applied stress and to a periodic (with period b) substrate potential $U(x)$ which is continuous and piecewise quadratic (fig. 1). The horizontal line in this figure (hereafter referred to as the transition line) separates the portions of the potential surface with positive and negative curvature. An atom above this line is referred to as a weak-bond atom; one below, as a strong-bond atom. The equilibrium configurations of this model have been studied by Kratochvil and Indenbom [4] and by Weiner and Sanders [5]. As shown there, for a suitable range of model parameters, the stable equilibrium solution has one weak bond while the unstable equilibrium solution has two weak bonds.

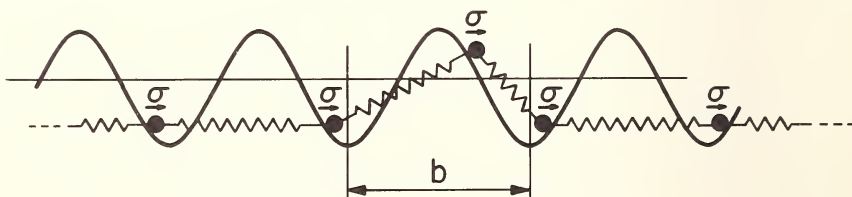


FIGURE 1. Modified Frenkel-Kontorowa model. Potential wells and peaks (separated in figure by horizontal line) are parabolic.

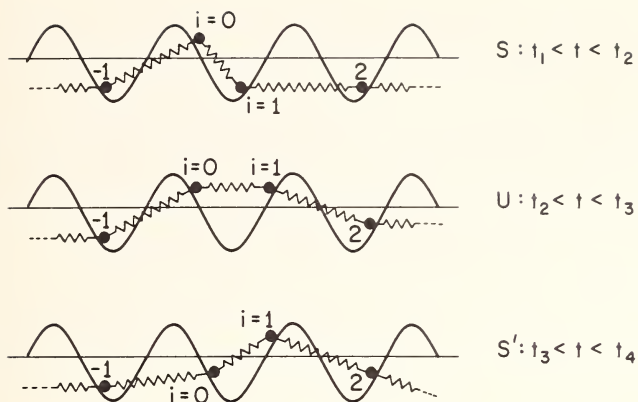


FIGURE 2. Sequence of atom positions during dislocation motion.

We next consider the steady motion of such a dislocation down the chain so that the successive states of the chain, denoted by S , U , S' , U' , . . . etc., have $1, 2, 1, 2, \dots$ weak bonds as in figure 2. Note that the term state as used here denotes only the specification of the weak-bonded atoms and leaves free the displacement of all atoms consistent with that specification. During the successive intervals of time for which each state exists, the equations of motion may be written in the form:

$$m\ddot{q}_i^S + \sum_j S_{ij} q_j^S = \sigma; \quad t_1 < t < t_2 \quad (2.1a)$$

$$m\ddot{q}_i^U + \sum_j U_{ij} q_j^U = \sigma; \quad t_2 < t < t_3 \quad (2.1b)$$

etc.

where q_i^S is the displacement of the i th atom from its equilibrium position under zero stress in the S state, that is when the atom $i=0$ is the only weak-bonded atom, and similarly q_i^U is the atomic displacement measured from the zero-stress position in the U state. The potential energy matrices S_{ij} , U_{ij} , . . . are constant during each time interval because of the piecewise linear nature of the model forces.

Let λ_α^S , $\alpha=0, 1, 2, \dots$ be the eigenvalues of the matrix S_{ij} with associated unit eigenvectors $a_{\alpha j}^S$ where the eigenvalues are ordered in increasing magnitude and $a_{\alpha j}^S$ is the displacement of the j th atom in the α mode. We also introduce the normal coordinates:

$$Q_\alpha^S = \sum_j a_{\alpha j}^S q_j^S \quad (2.2a)$$

so that

$$q_j^S = \sum_{\alpha} a_{\alpha j}^S Q_{\alpha}^S. \quad (2.2b)$$

The analogous notations are employed during successive time intervals with the superscript changed to U, S' , etc. In terms of normal coordinates, the equations of motion, eqs (2.1), may be written:

$$m\ddot{Q}_{\alpha}^S + \lambda_{\alpha}^S Q_{\alpha}^S = \sigma \sum_i a_{\alpha i}^S; \quad t_1 < t < t_2 \quad (2.3a)$$

$$m\ddot{Q}_{\alpha}^U + \lambda_{\alpha}^U Q_{\alpha}^U = \sigma \sum_i a_{\alpha i}^U; \quad t_2 < t < t_3 \quad (2.3b)$$

— — — — etc.

As shown in [2], for a suitable range of parameter values there will be a single localized mode a_{0i}^S in the S state corresponding to $\lambda_0^S > 0$, and a single localized mode a_{0i}^U in the U state corresponding to $\lambda_0^U < 0$. Attention is restricted here to this range of parameters. The importance of the localized modes for the atomic displacements in the vicinity of the dislocation has been emphasized previously (see Bjork [6] and Krumhansl [7]). The argument, which applies of course to any of the states, S, U, \dots etc., is as follows:

The set of eigenvectors $a_{\alpha i}$ are both orthonormal and complete; that is,

$$\sum_j a_{\alpha j} a_{\beta j} = \delta_{\alpha \beta} \quad (2.4a)$$

$$\sum_{\alpha} a_{\alpha j} a_{\alpha k} = \delta_{jk}. \quad (2.4b)$$

In this latter relation, let $j = k$, then

$$\sum_{\alpha \neq 0} (a_{\alpha j})^2 = 1 - (a_{0j})^2. \quad (2.5)$$

But since a_{0j} is a mode localized near the dislocation, it follows from the orthonormality relation that $(a_{0j})^2 \approx 1$ for j near the dislocation and that therefore

$$\sum_{\alpha \neq 0} (a_{\alpha j})^2 \ll 1 \text{ for } j \text{ near the dislocation.}$$

That is, even if all modes are equally energized, the localized modes have the major effect on the atomic displacements and velocities in the vicinity of the dislocation. Furthermore, in contrast to the extended modes, the localized modes a_{0i}^S and a_{0i}^U do not change sign with i so that the stress σ produces a non-zero forcing term for them in eqs (2.3).

In view of the previous considerations, it appears reasonable to refer to that part of the atomic velocity due to the localized mode as the directed portion of its velocity namely

$$\begin{aligned} V_i^S &= a_{0i}^S \dot{Q}_0^S, & t_1 < t < t_2 \\ V_i^U &= a_{0i}^U \dot{Q}_0^U, & t_2 < t < t_3 \\ &\quad \text{--- --- --- etc.} \end{aligned} \quad (2.6)$$

and to the remaining portion of its velocity

$$\begin{aligned} v_i^S &= \sum_{\beta \neq 0} a_{\beta i}^S \dot{Q}_\beta^S, & t_1 < t < t_2 \\ v_i^U &= \sum_{\beta \neq 0} a_{\beta i}^U \dot{Q}_\beta^U, & t_2 < t < t_3 \\ &\quad \text{--- --- --- etc.} \end{aligned} \quad (2.7)$$

as the thermal or random portion of its velocity. Note that from this viewpoint the notion of what constitutes the thermal portion of the atomic velocity is redefined at each transition. We also will refer to the momentum of the dislocation as proportional to \dot{Q}_0^S in the *S* state, to \dot{Q}_0^U in the *U* state, etc. It is clear that \dot{Q}_0^S or \dot{Q}_0^U will vary somewhat as solutions to forced harmonic oscillator equations (eqs (2.3)), but this variation whose relative magnitude decreases for higher dislocation velocities is not of primary concern to us. Rather, we are concerned here with the question of the transfer of thermal momentum, that due to v_i , to the dislocation momentum. Because of the piecewise harmonic character of the model, there can be such momentum transfer only at the transition times and it is this we consider next.

Since $q_i^S(t)$ and $q_i^U(t)$ differ only in their fixed reference points, it follows that $\dot{q}_i^S = \dot{q}_i^U(t)$. Therefore,

$$\begin{aligned} \dot{Q}_0^U(t_2) &= \sum_i a_{0i}^U \dot{q}_i^U(t_2) = \sum_i a_{0i}^U \dot{q}_i^S(t_2) \\ &= \sum_i a_{0i}^U a_{0i}^S \dot{Q}_0^S(t_2) + \sum_{i,\beta} a_{0i}^U a_{\beta i}^S \dot{Q}_\beta^S \end{aligned}$$

or, by use of eq (2.7),

$$\dot{Q}_0^U(t_2) = \sqrt{B} \dot{Q}_0^S(t_2) + \sum_i a_{0i}^U v_i^S(t_2) \quad (2.8)$$

where $\sqrt{B} = \sum_i a_{0i}^U a_{0i}^S$ and $0 < \sqrt{B} < 1$ since a_{0i}^U and a_{0i}^S are like oriented but distinct unit vectors. Equation (2.8) may be interpreted as follows: At the end of the S state period, the dislocation possesses momentum proportional to $\dot{Q}_0^S(t_2)$. Not all of this momentum can be transferred to the localized mode in the U state because the mode shapes a_{0i}^S and a_{0i}^U differ somewhat. This imperfect transfer is given by the first term $\sqrt{B} \dot{Q}_0^S(t_2)$. That portion of the directed velocity $V_i^S(t_2)$ that cannot be accommodated in the mode a_{0i}^U appears at the start of the next time interval $t_2 < t < t_3$ as a wave packet of thermal velocity v_i^T . This represents the dissipated mechanical energy appearing as heat. At the same time, some of the thermal motion $v_i^S(t_2)$ present at the end of the S interval is now assigned to \dot{Q}^U as seen by the second term of eq (2.8). This represents the transfer of thermal momentum to dislocation momentum.

The decomposition of the same atomic velocity distribution in terms of two different complete sets of modes at the time of transition t_2 is shown schematically in figure 3. Of course the point of the new decomposition is that during the U state, the U modes are the appropriate ones and there will be no further interaction between directed and thermal velocity, as defined in figure 3(b), during the U state, that is for $t_2 < t < t_3$. It is noted in figure 3 that the thermal velocity at the end of an interval, in this case the S interval, is represented as relatively uniform; whereas at the start of an interval, in this case the U interval, there is a local concentration or wave packet in the thermal velocity v_i^T due to the rejected portion of the directed velocity V_i^S . The reason for this difference is that

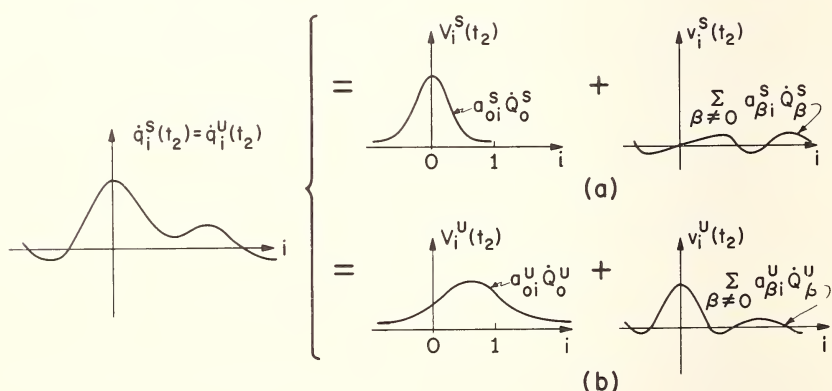


FIGURE 3. Decomposition of atomic velocities into directed (V_i) and thermal (v_i) components at the time of transition from state S to state U according to (a) S normal modes and (b) U normal modes.

the thermal velocity is the sum of extended modes which may be represented by travelling waves. Therefore the wave packet will disperse during the succeeding interval if it is long enough, i.e., if the dislocation is not moving too rapidly. Alternatively if the temperature level is sufficiently high, the perturbation in the thermal velocity distribution produced by the rejected wave packet will be relatively small and may be neglected even if time for its dispersion is not allowed.

Therefore we wish to examine the transfer of thermal momentum to dislocation momentum at a typical transition, say S to U as shown in figure 3, under the assumption that at the end of the S interval the extended modes, Q_β^S , $\beta \neq 0$, correspond to thermal equilibrium at temperature T . (Hereafter it is understood that the subscript β has the range $\beta > 0$.) For this purpose, it will be convenient to think of an ensemble of models of the type described, all in state S with identical values of $Q_0^S(t)$, but with values of $\dot{Q}_0^S(t)$, $Q_\beta^S(t)$, $\dot{Q}_\beta^S(t)$, which vary randomly over the members of the ensemble. The ensemble mean $\langle Q_\beta^S(t) \rangle$ is prescribed to correspond to a given dislocation velocity, while in accordance with the assumption of thermal equilibrium for the extended modes, $Q_\beta^S(t)$, $\dot{Q}_\beta^S(t)$ are independent normally distributed random variables with zero means and

$$\langle (Q_\beta^S(t))^2 \rangle = kT/\lambda_\beta^S, \quad \langle (\dot{Q}_\beta^S(t))^2 \rangle = kT/m. \quad (2.9)$$

It is seen from the definition of $v_i^S(t)$, eq (2.7), that

$$\langle v_i^S(t) \rangle = \sum_{\beta} a_{\beta i}^S \langle \dot{Q}_\beta^S(t) \rangle = 0. \quad (2.10)$$

Therefore if the transition from S to U occurred at the same time for all members of the ensemble, eq (2.8) would yield the result that the ensemble average of thermal momentum transfer to dislocation momentum was zero. However, this is not the case. A typical member of the ensemble will undergo a transition from the S state to the U state at a time τ when atom 1 crosses the transition line (see fig. 2) or equivalently when q_1^S reaches the critical value d_1^S . That is, the transition time τ is given by the equation

$$q_1^S = a_{01}^S Q_0^S(\tau) + \sum_{\beta} a_{\beta 1}^S Q_\beta^S(\tau) = d_1^S \quad (2.11)$$

and it is clear that τ will vary over the ensemble, since the values of $Q_\beta^S(t)$ do so. The appropriate ensemble average to evaluate the thermal momentum transfer is therefore $\langle v_1^S(\tau) \rangle_{\tau}$ where the subscript τ is used to emphasize that τ varies over the ensemble. In the next section it is shown that because (for the S to U transition) τ is determined by the motion of the $j=1$ atom, $\langle v_1^S(\tau) \rangle_{\tau} > 0$.

III. Coordination Effect

Since this discussion deals exclusively with the $j=1$ atom for the chain in the S state, we simplify the notation by dropping the subscript 1 and superscript S . We are dealing then with an ensemble of particles with random independent positions $q(t)$ and velocities $\dot{q}(t)$, where $\dot{q}(t)$ is normally distributed with means $\langle \dot{q}(t) \rangle = V(t)$ and mean square deviation $\langle (\dot{q}(t) - V)^2 \rangle = \alpha^2$ a specified constant. The transition time τ is defined for each member of the ensemble by the equation

$$q(\tau) = d.$$

What is desired is

$$\langle v(\tau) \rangle_\tau = \langle \dot{q}(\tau) - V(\tau) \rangle_\tau.$$

If $V(t)$ has only small variation in a time interval comparable to the dispersion in the transition times, then it is possible to replace $V(t)$ by a suitably chosen constant value. This assumption leads to a stationary probability distribution $p(q, \dot{q})$ defined for the phase space of the particle ensemble.

Instead of computing the average $\dot{q}(t)$ over the set of all members of the ensemble at the time τ when each member crosses the line $q=d$, we may expect intuitively to obtain the same result by averaging the velocity over those members of the ensemble which are at $q=d$ at an arbitrary instant of time, say $t=0$. However, since we are dealing with a continuous probability distribution, the probability or fraction of elements of the ensemble precisely at $q=d$ at a given instant is zero. Kac and Slepian [8] have indicated how this difficulty is to be circumvented. The average velocity is first taken over all those members of the ensemble which cross $q=d$ in the time interval $0 < t < \delta$ with $\dot{q} > 0$ (since we are interested only in those crossing from the left), and the limit as $\delta \rightarrow 0$ is taken only after this average is computed.¹

In order for a particle to cross as stated, it must, to first order in δ , lie in the region $d - \dot{q}\delta < q < d$, $\dot{q} > 0$. The fraction, f_δ , of the total ensemble in this region is

$$f_\delta = \int_0^\infty d\dot{q} \int_{d-\dot{q}\delta}^d p(q, \dot{q}) dq \quad (3.1)$$

and therefore the normalized probability distribution for averaging over

¹This type of limit is termed by Kac and Slepian as a conditional probability in "the horizontal window sense" (a term based on their orientation of the space-time axes for the plotting of a sample path $q(t)$). The calculation which they give ([8], p. 1217) for the time average for a single sample function indicates that this is the proper type of limit for the process under consideration here.

this subset is $p(q, \dot{q})/f_\delta$. The desired velocity average, $\langle \dot{q}(\tau) \rangle_\tau$, is then

$$\begin{aligned}\langle \dot{q}(\tau) \rangle_\tau &= \lim_{\delta \rightarrow 0} \frac{\int_0^\infty \dot{q} d\dot{q} \int_{d-\dot{q}\delta}^d p(q, \dot{q}) dq}{\int_0^\infty d\dot{q} \int_{d-\dot{q}\delta}^d p(q, \dot{q}) dq} \\ &= \frac{\int_0^\infty \dot{q}^2 p(\dot{q}) d\dot{q}}{\int_0^\infty \dot{q} p(\dot{q}) d\dot{q}}\end{aligned}\quad (3.2)$$

where use has been made of the fact (which follows from the assumption of thermal equilibrium of the extended modes) that q and \dot{q} are independent random variables.

If next the normal distribution for $p(\dot{q})$ (with mean V and variance α^2) is used, we find

$$\langle v(\tau) \rangle_\tau = \langle \dot{q}(\tau) \rangle_\tau - V = \frac{\alpha^2 \left(1 + \operatorname{erf} \frac{V}{\alpha\sqrt{2}} \right)}{V \left(1 + \operatorname{erf} \frac{V}{\alpha\sqrt{2}} \right) + \sqrt{\frac{2}{\pi}} \alpha e^{-V^2/2\alpha^2}}. \quad (3.3)$$

a result which indicates that the particle has a tendency to cross a prescribed barrier when it is going faster than its average velocity. This may be understood intuitively since the particle travels a greater distance when it is going faster than its average velocity than when it is going slower. Two approximations to $\langle v(\tau) \rangle_\tau$ may be derived from eq (3.3) for small and large values of α/V .

$$\langle v(\tau) \rangle_\tau \sim \alpha^2/V \quad \text{for} \quad (\alpha/V) \ll 1 \quad (3.4)$$

$$\langle v(\tau) \rangle_\tau \sim \sqrt{\frac{\pi}{2}} \alpha \quad \text{for} \quad (\alpha/V) \gg 1$$

We can now return to the question of the average magnitude of thermal momentum transferred to the dislocation momentum at the transition from one state to another. For an S to U transition, for example, it is seen from eq (2.8) that the value of this momentum is

$$\sum_i a_{0i}^U \langle v_i^S(\tau) \rangle_\tau.$$

It has been just shown that $\langle v_i^S(\tau) \rangle_\tau > 0$ because the $j=1$ atom determines τ . In the absence of such a requirement it appears reasonable

to assume² that $\langle v_j^S(\tau) \rangle_\tau = 0$ for $j \neq 0$. The transfer of thermal momentum to the dislocation momentum is then

$$a_{01}^U \langle v_1^S(\tau) \rangle_\tau > 0 \quad (3.5)$$

with $\langle v_1^S(\tau) \rangle_\tau$ computed by means of eq (3.3). Therefore, due to the coordination effect, the thermal momentum transferred aids the dislocation motion.

IV. Discussion

We have seen that, for the idealized one-dimensional model here considered, and under the assumptions made, there is a transfer of some thermal momentum to the dislocation at each step of its motion with the thermal momentum in the same direction as, and therefore additive to, the dislocation momentum. In effect, then, the dissipative mechanisms acting during the steady motion of the dislocation must account not only for the energy input by the applied stress driving the dislocation, but also for the thermal energy input due to the coordination effect. The general qualitative features of this process have been verified by computer simulation of this model for a particular set of parameters, [3].

We wish next to make a rough estimate of the relative magnitudes of the thermal and stress energy input for this model. In order to motivate the choice of numerical values for the model, we visualize a large planar parallel set of such chains forming the slip plane of a cubic crystal with lattice parameter b , and containing a dislocation. The substrate potential represents the action of the lower half of the crystal on the atoms of the slip plane, while the effect of the upper half is represented by an applied force σb^2 to each atom, where σ is the applied shear stress.

Consider a particular chain and assume that the motion is highly localized, i.e., only one atom with directed velocity in the stable state. In the absence of a coordination effect let its velocity be V . If, because of the coordination effect this velocity is increased to $V + v$, this corresponds to an energy addition E_C (per atom and atomic step) due to the coordination effect of

$$E_C = m(Vv + v^2/2).$$

The stress energy input E_σ per atom when it moves one atomic spacing, b , is

² It should be noted, as demonstrated by the computer simulation studies of [3] that this assumption is made less critical because of the localized nature of a_{0i}^U .

$$E_\sigma = \sigma b^3.$$

The ratio of interest is therefore

$$\frac{E_C}{E_\sigma} = \left[\frac{mV^2}{\sigma b^3} \right] \left[\frac{v}{V} + \frac{1}{2} \left(\frac{v}{V} \right)^2 \right].$$

We estimate the magnitude of v from eqs (3.4) for $\langle v(\tau) \rangle_\tau$. If we set $\alpha^2 = kT/m$, then for either of the two limiting conditions considered in these equations,

$$\frac{E_C}{E_\sigma} \sim \frac{kT}{\sigma b^3}.$$

The magnitude of the coordination effect in this model should be reduced from the above estimate by two effects not yet included:

(1) The mean square of the thermal velocity is less (by a factor of $(1 - a_{0i}^2)$) than kT/m in the vicinity of the dislocation because of the presence of a localized mode. This is a direct consequence of the completeness condition, eqs (2.4b) and (2.5).

(2) The thermal momentum transferred is given by eq (3.5), so that the value of $\langle v(\tau) \rangle_\tau$ must be multiplied by the appropriate localized mode component. The precise reduction produced by these two effects depends on the model parameters, but we may estimate its magnitude as 0.1, so that

$$\frac{E_C}{E_\sigma} \sim 0.1 \frac{kT}{\sigma b^3}.$$

In view of the highly idealized nature of the model, it clearly would be unjustified to extrapolate directly from its behavior to that of real crystals, and it is not clear at present to what extent one can expect thermal energy trapping in more realistic models. Two questionable characteristics of the present model are the requirement of a localized mode in the stable state and the piecewise harmonic character of the potential. It may be worth noting that the absence of these two characteristics does not rule out *a priori* the possibility of some thermal energy trapping, although with reduced effectiveness. For one can expect that the unstable mode, corresponding as it does to a negative eigenvalue, will be localized. If it comes into existence as an essentially uncoupled mode through the large excursion of a single atom there may be a coordination effect operative. There could then be some thermal energy trapping during the unstable portion of the motion, with loss of localized energy from the core during the period between unstable states when there is no localized mode available.

V. Acknowledgements

It is a pleasure to thank Professor J. R. Rice for directing my attention to the method of Kac and Slepian, and Professor J. Lothe for helpful correspondence.

This research was supported by U.S. Air Force Office of Scientific Research under Grants Nos. AF-AFOSR-228-67 and AFOSR 69-1738.

VI. References

- [1] Sanders, W. T., Phys. Rev. **154**, 654 (1967).
- [2] Weiner, J. H., Phys. Rev. **136**, A863 (1964).
- [3] Weiner, J. H., Phys. Rev. **139**, A442 (1965).
- [4] Kratochvil, J., and Indenbom, V. L., Czech. J. Phys. **13**, 814 (1963).
- [5] Weiner, J. H., and Sanders, W. T., Phys. Rev. **134**, A1007 (1964).
- [6] Bjork, R. L., Phys. Rev. **105**, 456 (1957).
- [7] Krumhansl, J. A., J. Appl. Phys. Suppl. **33**, 307 (1962).
- [8] Kac, M., and Slepian, D., Ann. Math. Stat. **30**, 1215 (1959).

Discussion on Papers by A. Seeger and H. Engelke, and J. H. Weiner.

ESHELBY: May I refer to something in Mr. Engelke's curve. I've convinced myself that the curve marked "Eshelby" ought to be raised about a decade. It's not a mistake on anybody's part, mind you, but I got the impression that he hasn't given it the most favorable interpretation possible. That's just a little publicity!

What I really wanted to say: Could Mr. Engelke say something about how he got the H_1 -curve?

ENGELKE: The operator H_1 describes two-phonon processes; it contains the Fourier transform of the time dependent part of the dislocation strain field.

ESHELBY: That's fed in for ordinary uniform motion; is that right?

ENGELKE: Yes, we have considered explicitly a uniformly moving dislocation configuration. To get the Fourier transform of the strain field we started from the following equations derived by Bross:

$$\operatorname{div} \sigma = \dot{s}_0,$$

where the total displacement field s_0 consists of an elastic and a plastic part:

$$s_0 = s_0^{el} + s_0^{pl}.$$

THOMSON: This is a question both to Mr. Engelke and Professor Weiner. I am disturbed about the use of the momentum conservation law. A phonon doesn't represent actual physical momentum, it's a special kind of "crystal" momentum. On the other hand when a dislocation moves, that is a *real* momentum, and I believe there may be a subtlety here: I wonder if you've thought about how one can put down the momentum conservation in the way you did, although it's dimensionally correct. I wonder, for example, if in Professor Weiner's calculations there is a direct conservation law in the sense of the transfer of phonon momentum directly into the dislocation? Does that really work out in the simple minded way?

WEINER: In the calculations I did there is an interaction between the dislocation momentum, which is represented by the localized mode momentum, and the phonon or thermal motion momenta only at the discrete times of transition. In between these times there is no interaction at all; that is between transition times there is scattering of the thermal motion because of the perturbation of force constants, but there is no net momentum transfer to the localized mode. So it does raise the sort of

question that you've mentioned. Between transition times the momentum transfer takes place between the thermal modes themselves with none transferred to the dislocation momentum.

THOMSON: You mean it doesn't transfer physical momentum to the dislocation?

WEINER: Not at any time except the transition time, because after all, the localized mode is a normal mode of the system. If you write the equation of motion for the localized mode, it is a completely uncoupled equation. There is nothing on its right hand side that says anything about the thermal motion, so there couldn't be any transfer. The only kind of interaction that takes place is at the transition times, and thus what seems to play the predominant role is this coordination effect.

THOMSON: I'm a little puzzled then. Does this mean that thermal motion is interacting with local modes of the dislocation, but that the translational mode is peculiarly de-coupled from this thermal agitation?

WEINER: The localized mode does interact with the thermal motion, but only at discrete instants of time at which transitions from one state to another occur.

THOMSON: How much transfer gets from the thermal motion into the translational motion of the dislocation?

WEINER: This is something that would be statistically determined by the sort of picture that I've given you. If we said that kinetic energy of the thermal motion is of the order of kT , then energy of that order is transferred to the dislocation modes.

NABARRO: I want to ask whether the localized mode is localized in the locality where the dislocation is moving.

WEINER: If the dislocation is moving down the chain and the atom $i = 0$ (fig. 2 of my paper) is the only atom on a hill of the substrate, then the localized mode S is appropriate and it is centered on and localized about the $i = 0$ atom. When atom $i = 1$ crosses the transition line there are two atoms on substrate hills. Then the S mode is no longer relevant and the appropriate localized mode is the U mode which is symmetrical about the position mid-way between atoms 0 and 1. So the localized mode sort of jumps along.

KRÖNER: I would like to ask Professor Weiner: In the state U you have two atoms that are loosely bound. Do you have two localized modes then?

WEINER: This depends on the parameters of the model. It is easy for this model to calculate the localized modes and to see how many one has, and

the conditions for it, etc. You can choose the parameters in such a way that you have only one localized mode in both cases. You can also choose the parameters such that, as you say, you would have two localized modes in the case of the two weak bonded atoms. In order to keep the whole picture as simple as possible I restricted myself to the case where you have only one localized mode in each case. That was for simplicity, but certainly that leaves questions to be answered: namely it is not clear what happens to this sort of process when you do have more localized modes. This raises other questions that have to be looked at.

BRAILSFORD: I would just like to suggest that there may be an analogy here between the motion of the defect and that of a small polaron in insulating crystals. With regard to Mr. Engelke's paper, would either he or Professor Eshelby remind us of the different ingredients in their two models?

ENGELKE: [Written contribution] The two calculations are similar only with respect to the use of field-theory. They consider different interactions between the moving defect and the surrounding elastic medium. In the case of Eshelby, the ordinary radiation damping arises already in a linear treatment, while in our case the effect comes from non-linear elastic interactions. The difference between the two mechanisms may be seen most clearly at zero temperature where the Eshelby mechanism gives a contribution to the dragging force but not the anharmonic interaction, which depends on phonons being thermally excited.

THOMSON: Dr. Hobart just pointed out to me, concerning my previous question, that there is a difficulty in transferring the calculation of Professor Weiner into the momentum conservation rule for a dislocation in a three-dimensional crystal. The reason is that the substrate can absorb an infinite amount of momentum. It is not necessary in that case, I believe, to have a strict conservation law. But I'm still puzzled about the three-dimensional case. It does seem to me that we are dealing with two kinds of momenta.

LOTHE: I think Professor Eshelby could clarify this matter.

ESHELBY: First of all you have the ordinary momentum of the continuum, shall we say, and you also have the quasi-momentum, or pseudomomentum, or crystal momentum, or bogus momentum—it doesn't matter what you call it—which is given to you by field theory (I've been reading this book on field theory, you see). In fact, there is a law that says that the difference between these quantities is a constant provided a certain surface integral, surrounding the region you are interested in, is zero. There are two cases in which it is zero. One, if you can surround what you are interested in by an enormous surface upon which nothing happens, and

two—this is more to the point—if you have periodic boundary conditions. Then, in any time interval, the change of ordinary momentum and the change of quasi-momentum are equal. So, apart from a constant difference which doesn't matter, they are identical, so you can use one in place of the other.

While I'm up here—I don't know if Dr. Brailsford got the point—let me say that what I did was to treat a kink which flutters as it goes along and scatters phonons nearly exactly like an electron sliding along a wire (an insulated wire) scatters photons. Mine was flutter and Mr. Engelke's was the interaction due to non-linear elasticity and they are additive or competitive—so that it isn't the same calculation done two different ways, it's two different ones. I'm just plugging the fact that mine's a bit bigger than stated, because I was irritated with that picture with "Eshelby" like this: [At this point Dr. Eshelby held his hand about one foot from the floor.]

AUDIENCE: General laughter.

DISLOCATION RESONANCE

J. A. Garber and A. V. Granato

*Department of Physics
University of Illinois
Urbana, Illinois 61801*

At low temperatures in insulators and superconductors, only reradiation of elastic waves should limit dislocation resonance. This effect has been calculated using Eshelby's expression for the reradiation. It is found that the resonance is very sharp, and still persists even when a random distribution of dislocation segment lengths is assumed.

Key words: Dislocation damping; dislocation resonance; internal friction.

The vibrating string model [1, 2] has been useful in rationalizing dislocation damping measurements. This model predicts that pinned dislocation line segments of the order of one micron in length will have resonances typically at about 10⁹ Hz.

Comparisons of theory and experiment have shown that this resonance is normally overdamped by the viscous drag of the dislocation-phonon and dislocation-electron interaction so that the dislocation inertia cannot be measured. In the absence of these processes (low temperatures in insulators or superconductors), only dislocation reradiation of elastic waves should limit the resonance. This effect has been calculated using Eshelby's [3] expression for the reradiation.

The results found in this way for the decrement as a function of frequency are given in figure 1. The decrement Δ is normalized by the factor $\Omega\Delta_0\Lambda L^2$ and the frequency ω by the resonant frequency $\omega_0(\nu = \omega/\omega_0)$. Here Ω is an orientation factor taking into account the fact that only the resolved shear stress in the slip plane is effective; $\Delta_0 = 8Gb^2/\pi^3C$ where G is the shear modulus, \mathbf{b} the Burgers vector, C is the tension, Λ is the dislocation density and L is the average dislocation loop length. The measurement frequency is ω and the resonant frequency ω_0 is given by $\omega_0 = \pi(C/A)^{1/2}/L$, where A is the dislocation mass per unit length.

If all loops have the same length the thin curve is obtained, showing that the resonance is very sharp. If a random distribution of loop lengths is assumed, the resonance is broadened out somewhat, but remains

Fundamental Aspects of Dislocation Theory, J. A. Simmons, R. de Wit, and R. Bullough, Eds. (Nat. Bur. Stand. (U.S.), Spec. Publ. 317, I, 1970).

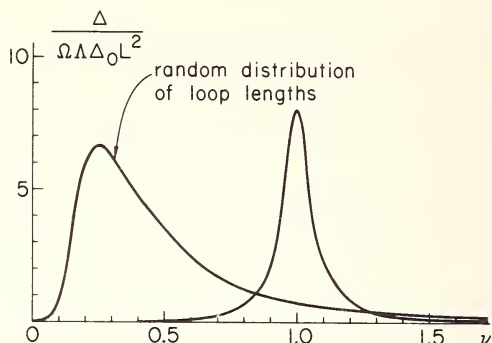


FIGURE 1. Decrement as a function of frequency. The effect of a random distribution of loop lengths is to broaden out the otherwise extremely sharp resonance. The decrement and frequency have been normalized by values given in the text.

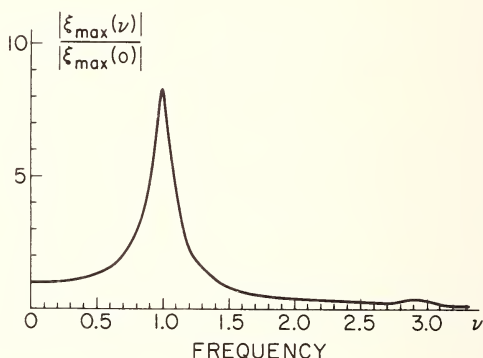


FIGURE 2. The maximum displacement ξ of a dislocation loop as a function of frequency. The maximum displacement has been normalized to the value obtained for low frequencies.

quite narrow. The magnitude of the decrement at the maximum is much larger than is the case for a resonance overdamped by phonon and electron scattering. Also the frequency dependence of the decrement is different and goes as ω^2 for $\omega \ll \omega_0$.

Near the resonance the dislocation displacement increases sharply. The maximum value of the displacement ξ_{\max} as a function of normalized frequency is given in figure 2. The displacement amplitude has been normalized to the maximum value at low frequencies. Although the amplitude increases by a factor of 8.3, the maximum displacement is still small compared to the loop length for typical ultrasonic strain amplitudes. Thus nonlinear effects resulting from changes in dislocation tension with displacement can be safely neglected. The displacement at the

third harmonic increases somewhat over the background value but is still small compared to that at the fundamental resonant frequency.

Experiments to check the calculations using ultrasonic attenuation and thermal resistivity measurements are in progress. A more extended account of the calculations including modulus changes and finite temperatures will be given later.

References

- [1] J. S. Koehler, in *Imperfections in Nearly Perfect Crystals* (John Wiley & Sons, Inc., New York, 1952) p. 197.
- [2] A. V. Granato and K. Lücke, *J. Appl. Phys.* **27**, 583 (1956).
- [3] J. D. Eshelby, *Proc. Roy. Soc. (London)* **A266**, 222 (1962).

DISLOCATION RADIATION

R. O. Schwenker and A. V. Granato

*Department of Physics
University of Illinois
Urbana, Illinois 61801*

Thin walls of mobile dislocations have been produced. These can be excited to emit macroscopic plane sound waves. Calculations have been made to predict the properties of the reradiated waves on the basis of a vibrating string model which neglects dislocation interactions. Measurements of the relative modulus change $\Delta G/G$ and the decrement Δ (real and imaginary part of the response) as a function of frequency permit a check of the Kramers-Kronig dispersion relations. In addition, measurements of the amplitude of the reradiated wave provide another check since the amplitude is proportional to $[(\Delta G/G)^2 + (\Delta/\pi)^2]^{1/2}$.

Key words: Dislocation radiation; dispersion relations; internal friction.

Thin walls of mobile dislocations have been produced. These can be excited to emit macroscopic plane waves. The amplitude of the radiated plane waves can be measured in addition to the decrement Δ and the relative modulus change $\Delta G/G$. We give here the relation between these quantities.

A schematic representation of the paths taken by the incident and reradiated waves in a crystal containing a thin dislocation wall is given in figure 1. For definiteness and to correspond with an experimental arrangement actually used, the $Z=0$ plane is taken to be the slip plane and the y direction is the slip direction. The wall width W is here supposed to be small compared to a sound wavelength λ . For an incident shear ultrasonic wave polarized in the y direction [110], the dislocations in the boundary oscillate in phase.

A plane wave solution for the displacement V for the radiated wave with the required properties for small and large distances from the distances from the dislocation wall is

$$V = b \Lambda W \bar{\xi} \exp [-i(kZ + \omega t)] \quad (1)$$

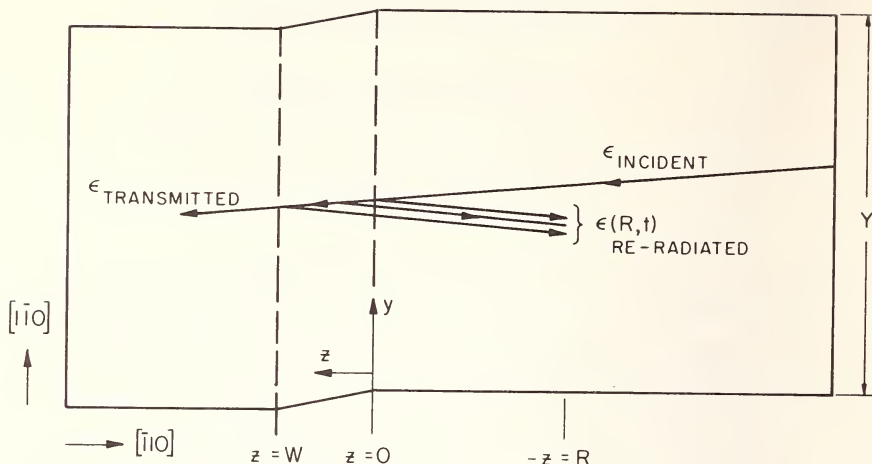


FIGURE 1. A schematic representation of the paths taken by incident and reradiated sound waves in a crystal containing a thin mobile dislocation wall.

where b is the Burgers vector, Λ the dislocation density, $\bar{\xi}$ the average dislocation displacement amplitude, k the propagation vector, and ω the frequency of the ultrasonic wave. This satisfies the wave equation and reduces to the proper displacement field $V = b\Lambda\bar{\xi}W \exp(-i\omega t)$ for $d \ll Z \ll \lambda/2\pi$, where d is the spacing between dislocations in the wall.

The reradiated strain wave amplitude is given by $|\epsilon_{rr}| = |\partial V / \partial Z| = b\Lambda\bar{\xi}Wk$. The incident elastic wave amplitude is given by $|\epsilon_{in}| = \sigma_0/G$, where σ_0 is the stress amplitude and G is the shear modulus. The ratio of the reradiated strain amplitude to the incident strain amplitude is then given by

$$\left| \frac{\epsilon_{rr}}{\epsilon_{in}} \right| = \frac{bG\Lambda W\bar{\xi}(\omega)}{\sigma_0 v} \omega \quad (2)$$

where v is the velocity of the incident sound wave. The frequency dependence of the ratio then depends on the product of the (frequency-dependent) dislocation displacement $\bar{\xi}(\omega)$ and the first power of the frequency.

For the displacement $\bar{\xi}(\omega)$, we have taken the relation given by Granato and Lücke [1] for the vibrating string model

$$\bar{\xi} = \frac{b\sigma_0}{A} \frac{8}{\pi^2} \left[\frac{(\omega_0^2 - \omega^2) - i\omega d}{(\omega_0^2 - \omega^2) + (\omega d)^2} \right] \quad (3)$$

where A is the dislocation mass per unit length, $\omega_0 = \pi(C/A)^{1/2}/L$, C

is the dislocation tension, $d = B/A$ and B is the viscous drag constant.

But this can also be expressed in terms of the measurable quantities Δ and $\Delta G/G$ by using the definitions of the decrement and measured modulus change:

$$|\bar{\xi}| = \frac{\sigma_0}{\Lambda G b} \left| \frac{\Delta G}{G} - i \frac{\Delta}{\pi} \right|. \quad (4)$$

Thus, substituting (4) into (2), we obtain

$$\left| \frac{\epsilon_{rr}}{\epsilon_{in}} \right| = \frac{W\omega}{v} \left[\left(\frac{\Delta G}{G} \right)^2 + \left(\frac{\Delta}{\pi} \right)^2 \right]^{1/2}. \quad (5)$$

This relation is general, and does not depend on the model used for the displacement ξ .

For the string model of an overdamped resonance, Δ and $\Delta G/G$ (also taking into account a random distribution of loop lengths) are given as functions of frequency in figure 2. The curves are normalized by the dimen-

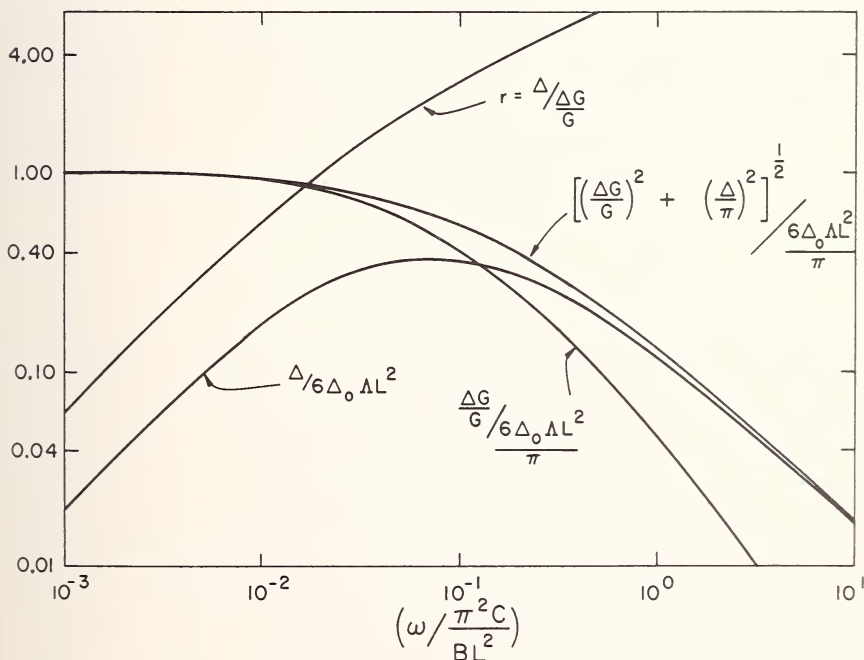


FIGURE 2. The values predicted by the vibrating string model for the decrement, the modulus change, the ratio of the decrement to the modulus change, and the dislocation displacement for an exponential distribution of loop lengths versus the frequency of the exciting elastic wave.

sionless quantity $6\Delta_0\Lambda L^2$, where $\Delta_0 = 8Gb^2/\pi^3C$. The ratio $r = \Delta/(\Delta G/G)$ is a useful curve for determining the (normalized) frequency since it is a monotonic function of frequency.

Measurements of the frequency dependence of the relative modulus change $\Delta G/G$ and the decrement Δ correspond to the real and imaginary part of the response of the system and permit a check of the Kramers-Kronig dispersion relations. But here, in addition, measurements of the amplitude of the reradiated wave provide another check since the amplitude is proportional to $[(\Delta G/G)^2 + (\Delta/\pi)^2]^{1/2}$.

An analysis of experimental results verifies this relationship. Dislocation interactions are found to be unimportant since the measured amplitudes are as large as those possible in the absence of such interactions. At 10 MHz, the reradiated amplitude is typically several percent of the exciting stress amplitude. The direct scattering loss (reradiation) is not always negligible compared to the indirect scattering loss (viscous phonon scattering), contrary to assumptions previously made implicitly.

Reference

- [1] A. V. Granato and K. Lücke, J. Appl. Phys. **27**, 583 (1956).

THE ANHARMONIC PROPERTIES OF VIBRATING DISLOCATIONS

C. Elbaum and A. Hikata

*Department of Physics
Brown University
Providence, R.I. 02912*

The anharmonic properties of vibrating dislocations are discussed in terms of the nonlinear stress-strain relation and of the higher harmonics of an ultrasonic wave generated when an initially sinusoidal wave propagates in a solid containing (mobile) dislocations. The treatment takes account of both lattice and dislocation contributions to the anharmonic behavior of the solid.

Estimates of the amplitude of the harmonics (these estimates have been confirmed experimentally) indicate that the lattice and dislocation components are comparable for the second harmonic and that the dislocation component is much larger than the lattice component for the third harmonic. Therefore, by investigating the third harmonic, it is possible to obtain detailed information on dislocation dynamics, without the complications of the lattice contribution.

Key words: Anharmonic properties; dislocation dynamics; ultrasonics.

I. Introduction

When a sinusoidal ultrasonic wave of a given frequency and of sufficient amplitude is introduced into a nonlinear or anharmonic solid, the fundamental wave will distort as it propagates, so that the second, third, and higher harmonics of the fundamental frequency will be generated. In many solids the nonlinearity of the stress-strain relation (deviation from Hooke's law) may arise from two causes. One is the anharmonicity of the lattice which is a characteristic of all solids, and the other is the contribution of the nonlinear part of the stress-strain relation for dislocation displacement; this cause applies to solids in which glide motion of dislocations is produced by small stresses, i.e., to most metals. The remainder of this discussion refers to the cases for which both contributions are present.

The dislocation contribution to the generation of second harmonics in high-purity aluminum single crystals was demonstrated experimentally

[1, 2]. For the generation of the second harmonic the stress-strain relation must of course be nonlinear, as well as not symmetric with respect to displacement gradients. In the case of dislocations, therefore, the displacement from the equilibrium position should be different for equal positive and negative values of stress. This condition may be achieved, for example, by applying a static bias stress in addition to the ultrasonic wave, assuming that the dislocations are straight at the outset. The static bias stresses usually required for this purpose are in the range 10^5 – 10^6 dyn/cm²; these stresses have no measurable effect on the coefficients of the anharmonic terms of the lattice [1–4].

In the case of the third harmonic, however, the condition of nonsymmetry is not required. A symmetric (nonlinear) stress-strain relation is sufficient; in other words, the bias stress is no longer necessary for dislocations to generate the third harmonic. In the case of the second harmonic, the lattice contribution and the dislocation contribution were found to be of comparable magnitude. Thus, in order to study experimentally either lattice or dislocation anharmonicity it is necessary to separate the two effects. On the other hand, the lattice contribution to the third harmonic is found to be a factor of 10 or more smaller than the dislocation contribution to the third harmonic (the dislocation contribution is comparable for the second and the third harmonic). Therefore, by investigating the third harmonic, it should be possible to obtain detailed information on dislocation motion under stress without the complications of the lattice contribution.

II. Equation of Motion

When a stress wave is propagated along a solid containing dislocations, the dislocations will oscillate causing additional local displacement and strain in the solid. If one denotes the longitudinal displacement of an infinitesimal element of a solid in the x direction by u , then

$$u = u_l + u_d,$$

where u_l is the displacement of the lattice, and u_d is the displacement due to the dislocation motion. The one-dimensional form of the equation of motion for the displacement u in the x direction is given by

$$\rho \frac{\partial^2 u}{\partial t^2} = \rho \frac{\partial^2}{\partial t^2} (u_l + u_d) = \frac{\partial \sigma}{\partial x}, \quad (1)$$

where ρ is the density of the undeformed material, σ is the applied stress, and t denotes time. It is convenient to use the differentiated

form (with respect to x) of eq (1)

$$\rho \frac{\partial^2}{\partial t^2} \left(\frac{\partial u_l}{\partial x} + \frac{\partial u_d}{\partial x} \right) = \frac{\partial^2 \sigma}{\partial x^2}. \quad (2)$$

Thus, the problem is now reduced to expressing $\partial u_l/\partial x$ and $\partial u_d/\partial x$ as a function of stress σ and to solve eq (2) with respect to σ . In the present case, however, a sinusoidal wave of frequency ω is introduced at one end of the specimen (at $x=0$). As the wave propagates, the wave form will be distorted due to the nonlinearity of the solid. Therefore, at a distance x , the stress σ should be expressed in terms of the harmonics of the fundamental wave, i.e.,

$$\begin{aligned} \sigma = A_0 + A_1 \cos(\omega t - kx) + A_2 \cos 2(\omega t - kx - \delta_2) \\ + A_3 \cos 3(\omega t - kx - \delta_3), \end{aligned} \quad (3)$$

where A_0 is a static bias stress, A_1 , A_2 , and A_3 are the amplitudes of the fundamental, the second, and the third harmonic waves, respectively, $2\delta_2$ and $3\delta_3$ are the phase angles of the second and the third harmonics relative to the fundamental wave, respectively, and k is the wave vector. It is assumed here that dispersion is negligible. The boundary conditions are

at $x=0$,

$A_1 = A_{10}$ (the amplitude of the induced fundamental wave),

$A_2 = A_3 = 0$.

Since the nonlinearity considered here is not expected to be large, one can assume that

$$A_2, A_3 \ll A_1.$$

Thus, if one expresses both sides of eq (2) in terms of the harmonics, a comparison of the sine and cosine terms of the corresponding frequencies will provide sets of equations which determine the amplitudes of the harmonics.

A. EXPRESSION FOR $\partial u_l/\partial x$

The one-dimensional relation between stress σ and displacement gradient $\partial u_l/\partial x$ of a solid, correct to the square terms is given by [5]

$$\sigma = E_1 \frac{\partial u_l}{\partial x} + a \left(\frac{\partial u_l}{\partial x} \right)^2. \quad (4)$$

Where E_1 is the second-order elastic constant and a is a combination of the second- and third-order elastic constants. Thus,

$$\begin{aligned} \frac{\partial u_l}{\partial x} = & \frac{1}{E_1} \sigma - \frac{a}{E_1^3} \sigma^2 + \dots = \frac{A_0}{E_1} - \frac{a}{E_1^3} \left(A_0^2 + \frac{A_1^2}{2} \right) \\ & + \left[\frac{A_1}{E_1} - \frac{a}{E_1^3} (2A_0A_1 + A_1A_2 \cos 2\delta_2) \right] \cos (\omega t - kx) \\ & - \left(\frac{a}{E_1^3} A_1A_2 \sin 2\delta_2 \right) \sin (\omega t - kx) + \left[\frac{A_2}{E_1} \cos 2\delta_2 \right. \\ & \left. - \frac{a}{E_1^3} (2A_0A_2 \cos 2\delta_2 + \frac{A_1^2}{2}) \right] \cos 2(\omega t - kx) \\ & + \left[\frac{A_2}{E_1} \sin 2\delta_2 - \frac{a}{E_1^3} 2A_0A_2 \sin 2\delta_2 \right] \sin 2(\omega t - kx) \\ & + \left[\frac{A_3}{E_1} \cos 3\delta_3 - \frac{a}{E_1^3} (2A_0A_3 \cos 3\delta_3 + A_1A_2 \cos 2\delta_2) \right] \cos 3(\omega t - kx) \\ & + \left[\frac{A_3}{E_1} \sin 3\delta_3 - \frac{a}{E_1^3} (2A_0A_3 \sin 3\delta_3 + A_1A_2 \sin 2\delta_2) \right] \sin 3(\omega t - kx). \quad (5) \end{aligned}$$

B. EXPRESSION FOR $\partial u_d / \partial x$

The linear case of small-amplitude dislocation oscillations under the influence of an externally applied oscillatory stress was treated, using the vibrating string analogy, by Koehler [6] and later by Granato and Lücke [7]. In these treatments [6, 7] the line energy is assumed to be independent of the position and orientation of a dislocation. In fact, however, even in an isotropic material, the line energy of an edge dislocation differs significantly from that of a screw dislocation [8–11]. It follows that, in general, the line energy of a bowed-out dislocation (under an external stress) is not constant along the dislocation line. In the case of an anisotropic solid, the energy difference between edge and screw dislocations could be quite large as pointed out by Foreman [9], and deWit and Koehler [10].

The present study is concerned with nonlinear effects for which the assumption of small displacement amplitudes does not apply. Under such conditions, one has to take into account the effects of both the variation of the line energy along dislocations and the higher order terms in $(\partial \xi / \partial \eta)$ (for definitions of ξ and η see fig. 1).

In order to obtain the equation of motion of dislocations, one has to establish first the differential equation determining the equilibrium con-

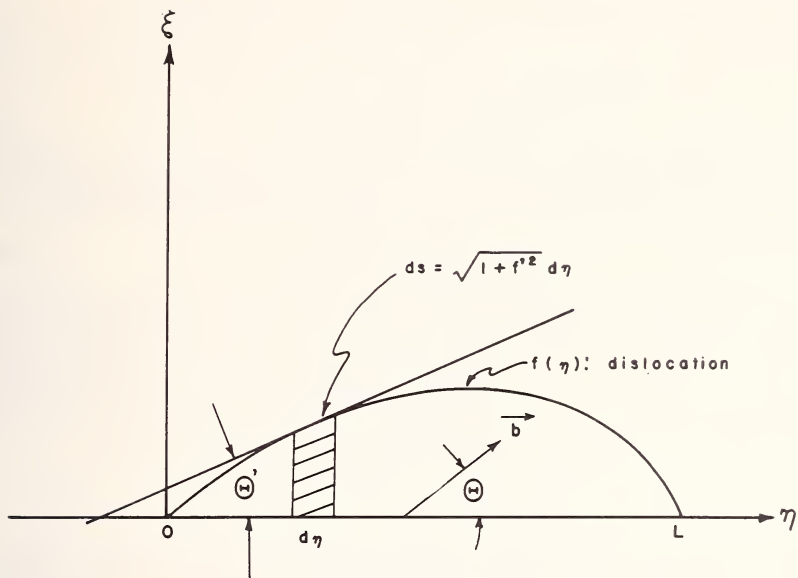


FIGURE 1. Bowed-out dislocation $\xi = f(\eta)$. η axis coincides with the straight-line configuration of the dislocation before bowing out. \mathbf{b} , Burgers vector.

figuration of dislocations under the influence of a static stress. For this purpose, we follow the calculation carried out by Leibfried [11] and extend it to the nonlinear case by retaining the higher order terms of $(\partial \xi / \partial \eta)$ in the expansion of the energy expression [see eqs (10) and (11)].

The line energy of a dislocation (per unit length) in an isotropic material is given by

$$W_e = \frac{\mu b^2}{4\pi} \frac{1}{1-\nu} \ln \frac{R}{R_c} \quad (6)$$

for edge dislocations and

$$W_s = (\mu b^2 / 4\pi) \ln (R/R_c) \quad (7)$$

for screw dislocations. Here μ is the shear modulus, ν is Poisson's ratio, b is the absolute value of the Burgers vector, R_c is an effective core radius (in the order of b), and R is an effective external radius. Typically, R/R_c is about 10^4 and the logarithm therefore is in the order of 10. Since W is only logarithmically dependent on R/R_c the exact value of R/R_c is usually considered to be of minor importance.

In the string model, a line segment ds of a dislocation line has an energy $U_L ds$ with

$$U_L = W_e(b_\perp^2/b^2) + W_s(b_{\parallel}^2/b^2) = W_e(1 - m \cos^2 \theta). \quad (8)$$

Here, b_\perp and b_{\parallel} are the components of the Burgers vector \mathbf{b} perpendicular and parallel to the segment, θ is the angle between \mathbf{b} and ds , and

$$m = (W_e - W_s)/W_e. \quad (9)$$

In the following we will refer to a straight dislocation line along the η axis as the original and stable position. The dislocation motion is governed by the change ΔU in energy caused by deviations from the straight line. The slip plane is taken as the (ξ, η) plane and the dislocation line is defined by $\xi = f(\eta)$ (fig. 1). Then, by using eq (8) the following is obtained:

$$\Delta U = \int d\eta W_e [1 + f'^2]^{1/2} \{1 - m \cos^2(\Theta - \Theta')\} - (1 - m \cos^2 \Theta).$$

Here, $f' = \partial \xi / \partial \eta$, and $\Theta - \Theta' = \theta$ is the angle between the line segment and Burgers vector; Θ and Θ' are shown in figure 1. Introducing $\tan \Theta' = f'$ we obtain

$$\begin{aligned} \Delta U = \int d\eta W_e & \left\{ (1 + f'^2)^{1/2} \left[1 - \frac{m}{1 + f'^2} (\cos^2 \Theta \right. \right. \\ & \left. \left. + 2f' \sin \Theta \cos \Theta + f'^2 \sin^2 \Theta) \right] - (1 - m \cos^2 \Theta) \right\}. \end{aligned} \quad (10)$$

Assuming $f' < 1$ (i.e., moderate dislocation displacements), the integrand of (10) can be expanded in powers of f' . If one keeps terms up to the fourth power in f' , the result is given by

$$\begin{aligned} \Delta U = \int d\eta W_e & [-2mf' \sin \Theta \cos \Theta + \frac{1}{2}(1 + m \cos^2 \Theta \\ & - 2m \sin^2 \Theta)f'^2 + f'^3 \sin \Theta \cos \Theta - \frac{1}{8}(1 + 3m \cos^2 \Theta - 4m \sin^2 \Theta)f'^4]. \end{aligned} \quad (11)$$

If the dislocation is pinned at $\eta = 0$ and $\eta = L$, the deviations from the straight configuration should be the same for equal positive and negative stresses. In other words, ΔU should be symmetrical in terms of f' . Therefore, in eq (11) the terms containing f' and f'^3 should vanish.

The equilibrium condition for the line segment L can be obtained from a variational principle; i.e., the total energy $W = \Delta U - U_\tau$ should be an extremal, where U_τ is the work done by the external force and given by

$$U_\tau = \tau b \int_0^L f(\eta) d\eta,$$

and τ is the resolved shear stress in the glide plane and in the slip direction. The equilibrium condition becomes

$$\delta W = \delta(\Delta U - U_\tau) = 0$$

or, according to the Euler-Lagrange equation,

$$\frac{d}{d\eta} \left(\frac{\partial W}{\partial f'} - \frac{\partial W}{\partial f} \right) = 0.$$

The result is then

$$\begin{aligned} -f'W_e[1+m \cos^2 \Theta - 2m \sin^2 \Theta) \\ -\frac{3}{2}(1+3m \cos^2 \Theta - 4m \sin^2 \Theta)f'^2] = \tau b. \end{aligned} \quad (12)$$

If one assumes that the line energies of edge dislocations and of screw dislocations are equal, i.e., $m=0$, then eq (12) becomes

$$-W_e f' \left(1 - \frac{3}{2} f'^2 \right) = \tau b,$$

which is the case treated in references [1-3]. If one assumes further that the higher order term is negligible, the equation reduces to

$$-W_e f' = \tau b,$$

which is the case of the linear approximation treated by Granato and Lücke [7]. Even in an isotropic material, m is not equal to zero, and is given by

$$m = \nu = \frac{1}{3} (\nu, \text{Poisson's ratio}).$$

Thus, for an edge dislocation ($\Theta=\pi/2$), eq (12) reduces to

$$-\frac{1}{3} W_e f' \left(1 + \frac{3}{2} f'^2 \right) = \tau b$$

or, since $W_e/3 \approx \frac{1}{2} \mu b^2$,

$$-\frac{1}{2} \mu b^2 f' \left(1 + \frac{3}{2} f'^2 \right) = \tau b. \quad (13)$$

For a screw dislocation ($\Theta = 0$),

$$\begin{aligned} -(4/3)W_e f''(1 - (9/4)f'^2) &= \tau b, \\ -2\mu b^2 f''(1 - (9/4)f'^2) &= \tau b. \end{aligned} \quad (14)$$

Equations (13) and (14) reveal two important features: (a) The linear term of eq (13), $-\frac{1}{2}\mu b^2 f''$, is $\frac{1}{4}$ of the linear term of eq (14), $-2\mu b^2 f''$. This means that for a small applied stress, the displacement of an edge dislocation is approximately four times larger than that of a screw dislocation. Therefore, for a small oscillatory stress, it is expected that the contribution from edge dislocations is predominant for quantities such as attenuation and velocity change, provided that the density and loop lengths of the two types of the dislocations are similar [8, 11]. (b) The nonlinear term in eq (13), $-\frac{3}{2}f'^2$ is negative, while that of eq (14), $+(9/4)f'^2$ is positive. This means that, the stress-displacement relation for edge dislocations is "hardening" (as the applied stress increases, a larger stress increment is necessary to produce a given amount of displacement), while the stress-displacement relation for screw dislocations is "softening" (see fig. 2). Of course, the deviation from a linear stress-displacement relationship, whether it is softening or hardening, is the source of the harmonic generation.

The nonlinear relation between a static stress and the dislocation displacement of a pinned dislocation leads to the following equation of motion of a dislocation under the influence of combined static and oscillatory stresses (damping proportional to dislocation velocity is assumed):

$$A \frac{\partial^2 \xi}{\partial t^2} + B \frac{\partial \xi}{\partial t} - C \left[\left(\frac{\partial^2 \xi}{\partial \eta^2} \right) - C' \left(\frac{\partial \xi}{\partial \eta} \right)^2 \left(\frac{\partial^2 \xi}{\partial \eta^2} \right) \right] = bR\sigma,$$

where

σ is given by eq (3),

$A = \pi\rho b^2$ (effective mass of dislocation per unit length),

B is the damping coefficient,

$C = W_e(1 + m \cos^2 \Theta - 2m \sin^2 \Theta)$,

$C' = \frac{3}{2} \frac{(1 + 3m \cos^2 \Theta - 4m \sin^2 \Theta)}{(1 + m \cos^2 \Theta - 2m \sin^2 \Theta)}$,

m and Θ are the quantities defined in the previous section

\mathbf{b} is the Burgers vector,

R is the resolving shear factor converting the axial stress to the shear stress in the slip plane and in the slip direction.

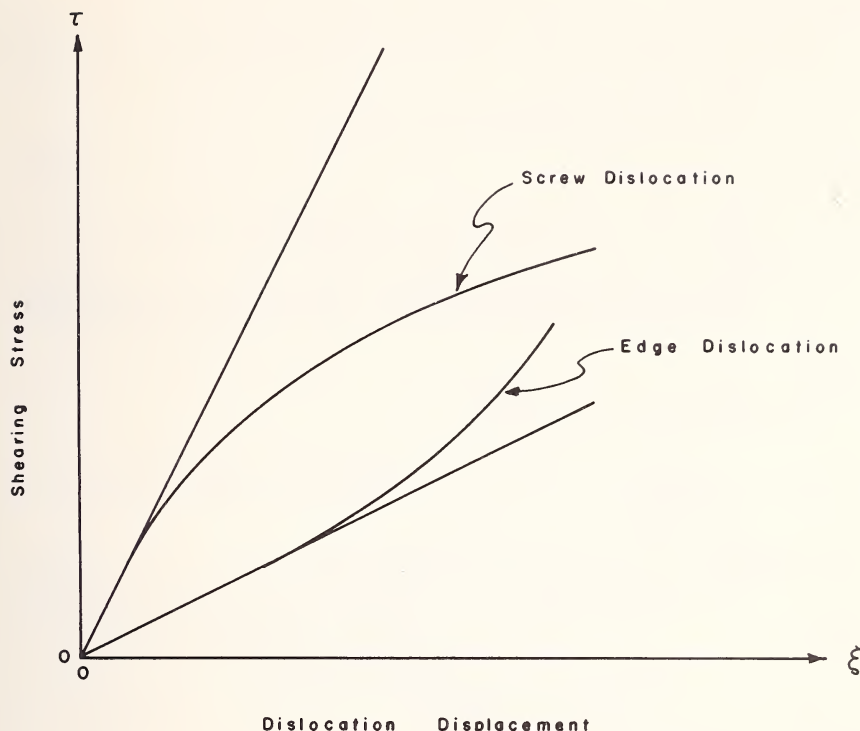


FIGURE 2. Stress-displacement relationship of screw and edge dislocations (schematic); straight lines give linear approximation.

The nonlinear differential eq (15) can be solved approximately by iteration. First, utilizing the Fourier expansion of $bR\sigma$, one obtains a solution ξ_1 for the linearized form of eq (15)

$$\xi_1 = \xi_{10} + \xi_{11} + \xi_{12} + \xi_{13}, \quad (16)$$

where

$$\xi_{10} = \frac{4bRA_0L_0^2}{\pi^3 C} \sum_0^\infty \frac{1}{(2n+1)} \sin \frac{(2n+1)\pi\eta}{L_0}$$

$$\xi_{11} = \frac{4bRA_1}{A\pi} \sum_0^\infty \frac{1}{(2n+1)} \frac{1}{S_n^{1/2}} \times \sin \frac{(2n+1)\pi\eta}{L_0} \cos (\omega\tau - kx - \delta_{1n}),$$

with

$$S_n = (\omega_n^2 - \omega^2)^2 + (\omega d)^2,$$

$$\omega_n = (2n+1) (\pi/L_0) (C/A)^{1/2},$$

$$\tan \delta_{1n} = \omega d / (\omega_n^2 - \omega^2),$$

$$d = B/A,$$

$$\xi_{12} = \frac{4bRA_2}{A\pi} \sum_0^\infty \frac{1}{(2n+1)} \frac{1}{M_n^{1/2}} \times \sin \frac{(2n+1)\pi\eta}{L_0} \cos 2(\omega t - kx - \delta_2 - \delta_{2n})$$

with

$$M_n = \{\omega_n^2 - (2\omega)^2\}^2 + (2\omega d)^2,$$

$$\tan 2\delta_{2n} = \frac{2\omega d}{\omega_n^2 - (2\omega)^2}$$

$$\xi_{13} = \frac{4bRA_3}{A\pi} \sum_0^\infty \frac{1}{(2n+1)} \frac{1}{T_n^{1/2}} \times \sin \frac{(2n+1)\pi\eta}{L_0} \cos 3(\omega t - kx - \delta_3 - \delta_{3n}),$$

with

$$T = \{\omega_n^2 - (3\omega)^2\}^2 + (3\omega d)^2,$$

$$\tan 3\delta_{3n} = \frac{3\omega d}{(\omega_n^2 - 3\omega^2)}.$$

In the following analysis, only the first terms ($n=0$) of each infinite series are taken into account.¹ Inserting $\xi = \xi_1 + \xi_2$ into eq (15), where ξ_2 is the iterated solution, and retaining those nonlinear terms containing only ξ_1 , one obtains the equation

$$\begin{aligned} A \frac{\partial^2 \xi_2}{\partial t^2} + B \frac{\partial \xi_2}{\partial t} - C \frac{\partial^2 \xi_2}{\partial \eta^2} &= -CC' \left(\frac{\partial \xi_1}{\partial \eta} \right)^2 \left(\frac{\partial^2 \xi_1}{\partial \eta^2} \right) \\ &= \frac{CC'}{4} \left(\frac{\pi}{L_0} \right)^4 \left(\sin \frac{3\pi\eta}{L_0} + \sin \frac{\pi\eta}{L_0} \right) \{A_0 P + A_1 Q \cos (\omega t - kx - \delta_{10}) \right. \\ &\quad \left. + A_2 K \cos 2(\omega t - kx - \delta_2 - \delta_{20}) + A_3 J \cos 3(\omega t - kx - \delta_3 - \delta_{30})\}^3, \end{aligned} \quad (17)$$

where

$$P = \frac{4bRL_0^2}{\pi^3 C}, \quad Q = \frac{4bR}{A\pi S_0^{1/2}}, \quad K = \frac{4bR}{A\pi M_0^{1/2}},$$

$$J = \frac{4bR}{A\pi T_0^{1/2}}.$$

¹ The displacement of the modes corresponding to $n > 0$ decreases very rapidly with increasing n and may be neglected for the purposes of this calculation.

Neglecting the term $\sin(3\pi\eta/L_0)$ and retaining the terms up to the third harmonic in the right-hand side of eq (17),² one obtains the solution ξ_2 ,

$$\xi_2 = \xi_{20} + \xi_{21} + \xi_{22} + \xi_{23}, \quad (18)$$

where

$$\xi_{20} = h \sin \frac{\pi\eta}{L_0} \frac{L^2}{\pi^2 C} \left[A_0^3 P^3 + \frac{3}{2} A_0 P A_1^2 Q^2 \right], \quad h = \frac{CC'}{4} \left(\frac{\pi}{L_0} \right)^4,$$

$$\begin{aligned} \xi_{21} = h \sin \frac{\pi\eta}{L_0} \frac{1}{AS_0^{1/2}} & \left[\left\{ \frac{3}{4} A_1^3 Q^3 + 3A_0^2 P^2 A_1 Q \right\} \cos(\omega t - kx - 2\delta_{10}) \right. \\ & \left. + 3A_0 P A_1 Q A_2 K \cos(\omega t - kx - 2\delta_2 - 2\delta_{20}) \right], \end{aligned}$$

$$\begin{aligned} \xi_{22} = h \sin \frac{\pi\eta}{L_0} \frac{1}{AM_0^{1/2}} & \left[\frac{3}{2} A_0 P A_1^2 Q^2 \cos 2(\omega t - kx - \delta_{10} - \delta_{20}) \right. \\ & \left. + 3A_0^2 P^2 A_2 K \cos 2(\omega t - kx - \delta_2 - \delta_{20}) \right], \end{aligned}$$

$$\begin{aligned} \xi_{23} = h \sin \frac{\pi\eta}{L_0} \frac{1}{AT_0^{1/2}} & \left[\frac{1}{4} A_1^3 Q^3 \cos 3(\omega t - kx - \delta_{10} - \delta_{30}) \right. \\ & \left. + 3A_0^2 P^2 A_3 J \cos 3(\omega t - kx - \delta_3 - 2\delta_{30}) \right. \\ & \left. + 3A_0 P A_1 Q A_2 K \cos 3 \left(\omega t - kx - \frac{1}{3} (\delta_{10} + 2\delta_2 + 2\delta_{20} + 3\delta_{30}) \right) \right]. \end{aligned}$$

Thus, after one iteration, one obtains for the solution of eq (15),

$$\xi = \xi_1 + \xi_2, \quad (19)$$

where ξ_1 and ξ_2 are given by expressions (16) and (18).

Once ξ is obtained in terms of η , $\partial u_d / \partial x$ can be calculated by the relation:

$$\frac{\partial u_d}{\partial x} = \frac{Nbq}{L_0} \int_0^{L_0} \xi d\eta, \quad (20)$$

where N is the effective dislocation density and q is a factor converting the shear strain to the longitudinal strain.

² When the term $\sin(3\pi\eta/L_0)$ is retained various parts of the solution are multiplied by numerical factors of order unity.

III. Amplitude of the Second and Third Harmonic

The amplitudes of the second and third harmonic are derived by solving the differential equations obtained from inserting expressions (3), (5) and (20) into eq (2) and equating separately the sine and cosine terms of each harmonic. After some simplifications the following results are obtained.

$$A_1 = A_{10} e^{-\alpha_1 x}, \quad (21)$$

$$\text{with } \alpha_1 = (\rho \omega^2 g / 2k) [Q \sin \delta_{10} + (3h/AS_0^{1/2}) A_0^2 P^2 Q \sin 2\delta_{10}], \quad (22)$$

$$k^2 - \alpha_1^2 = \rho \omega^2 \left\{ \frac{1}{E_1} - \frac{2a}{E_1^3} A_0 + g \left[Q \cos \delta_{10} + \frac{3h}{AS_0^{1/2}} A_0^2 P^2 Q \cos 2\delta_{10} \right] \right\}, \quad (23)$$

where A_{10} is the amplitude of the induced oscillatory stress at $x=0$, and $g=2Nbq/\pi$.

Expression (22) represents the attenuation of the fundamental wave. Since $k=\omega/v$ and $v=(E/\rho)^{1/2}$ (v is the velocity of sound in the material), the first term of the expression (22) can be written

$$\alpha_{10} = 4NE_1 b^2 q R \omega^2 d / v A \pi^2 S_0, \quad (24)$$

which agrees with Granato and Lücke's [7] results. The second term of the expression (22) represents the effect of bias stress on the attenuation. Although it increases with the square of the bias stress, its contribution to the attenuation turns out to be negligible in the stress range of interest here.

From eq (23), one can derive the velocity change $\Delta v/v$ of the fundamental wave,

$$(\Delta v/v) = (a/E_1^2) A_0 - \frac{1}{2} E_1 g \{Q \cos \delta_{10} + (3h/AS_0^{1/2}) A_0^2 P^2 Q \cos 2\delta_{10}\}. \quad (25)$$

The amplitude A_2 of the second harmonic is:

$$A_2 = \left[\frac{a}{2E_1^3} \sin 2\delta_2 - \frac{3}{2} \frac{hg}{AM_0^{1/2}} A_0 P Q^2 \sin 2(\delta_2 - \delta_{10} - \delta_{20}) \right] \frac{\rho \omega^2}{k} A_{10}^2 \frac{e^{-2\alpha_1 x} - e^{-\alpha_2 x}}{\alpha_2 - 2\alpha_1}, \quad (26)$$

with

$$\alpha_2 = (\rho \omega^2 g / k) \{K \sin 2\delta_{20} + (3h/AM_0^{1/2}) A_0^2 P^2 K \sin 4\delta_{20}\}, \quad (27)$$

where the following relation should also be satisfied:

$$\begin{aligned} d^2A_2/dx^2 = & [4k^2 - 4\rho\omega^2 \{(1/E_1) - (2a/E_1^3)A_0 + Kg \cos 2\delta_{20} \\ & + (3hg/AM_0^{1/2})A_0^2P^2K \cos 4\delta_{20}\}]A_2 + 4\rho\omega^2 \{(a/2E_1^2) \cos 2\delta_2 \\ & - \frac{3}{2}(hg/AM_0^{1/2})A_0PQ^2 \cos 2(\delta_2 - \delta_{10} - \delta_{20})\}A_1. \end{aligned} \quad (28)$$

If one compares the expression for α_2 [eq (27)] and that of the fundamental wave α_1 [eq (22)], it is easily seen that α_2 is equivalent to the attenuation of an independent wave propagating with a frequency 2ω . This means that since dispersion is assumed to be negligible, the following relation between k and α_2 should also hold.

$$\begin{aligned} 4k^2 - \alpha_2^2 = & 4\rho\omega^2 \{(1/E_1) - (2a/E_1^3)A_0 \\ & + g\{K \cos 2\delta_{20} + (3h/AM_0^{1/2})A_0^2P^2K \cos 4\delta_{20}\}\}. \end{aligned} \quad (29)$$

Substituting the expressions (26) and (29) into (28), one obtains the following relation for the phase angle δ_2 between the fundamental and the second harmonic wave:

$$\tan 2\delta_2 \cong \frac{a/2E_1 - (3h/AM_0^{1/2})A_0PQ^2 \cos 2(\delta_{10} + \delta_{20})}{(3h/AM_0^{1/2})A_0PQ^2 \sin 2(\delta_{10} + \delta_{20})} \quad (30)$$

If one neglects the dislocation contribution to the second harmonic, the phase angle becomes,

$$2\delta_2 = \pi/2.$$

On the other hand, if one neglects the lattice contribution, $2(\delta_2 - \delta_{10} - \delta_{20})$ is very close to $\pi/2$. Thus, one can express the amplitude of the second harmonic with reasonable accuracy as follows:

$$A_2 = \frac{\rho\omega^2}{k} [X^2 + Y^2 - 2XY \cos 2(\delta_{10} + \delta_{20})]^{1/2} A_{10}^2 \frac{e^{-2\alpha_1 x} - e^{-\alpha_2 x}}{\alpha_2 - 2\alpha_1}, \quad (31)$$

where

$$X = a/2E_1^2$$

$$Y = 48Nb^4R^3qC'A_0/\pi^2A^3S_0M_0^{1/2}L_0^2,$$

furthermore, in the case where $\omega_0 \gg 4\omega$, the factor

$$\cos 2(\delta_{10} + \delta_{20})$$

can be replaced by

$$(\omega_0/S_0 M_0^{1/2}) (\omega_0^4 - 5\omega_0^2 d^2).$$

The amplitude A_3 and the attenuation α_3 of the third harmonic are:

$$A_3 = \frac{3}{8} \frac{\rho \omega^2 g}{k} \frac{h Q^3 A_{10}^3 \sin 3(\delta_3 - \delta_{10} - \delta_{30})}{AT_0^{1/2}} \frac{e^{-3\alpha_1 x} - e^{-\alpha_3 x}}{\alpha_3 - 3\alpha_1} \quad (32)$$

$$\alpha_3 = \frac{3}{2} \frac{\rho \omega^2 g}{k} \left[J \sin 3\delta_{30} + \frac{3h}{AT_0^{1/2}} A_0^2 P^2 J \sin 6\delta_{30} \right], \quad (33)$$

As in the case of the second harmonic, expression (33) indicates that the third harmonic generated in the solid attenuates in the same manner as an independent wave of frequency 3ω introduced into the solid. This leads to the following condition determining the phase angle $3\delta_3$ between the fundamental and the third harmonic wave:

$$\tan 3(\delta_3 - \delta_{10} - \delta_{30}) = 6k/(\alpha_3 + 3\alpha_1).$$

Since the right-hand side of the above equation is a very large quantity, $3(\delta_3 - \delta_{10} - \delta_{30})$ is positive and very close to $\pi/2$. Thus, one can express the amplitude of the third harmonic with reasonable accuracy as follows,

$$A_3 = \frac{12\rho\omega^2 N b^4 q R^3 C C' A_{10}^3}{k A^4 S_0^{3/2} T_0^{1/2} L_0^4} \frac{e^{-3\alpha_1 x} - e^{-\alpha_3 x}}{\alpha_3 - 3\alpha_1} \quad (34)$$

It should be emphasized that expression (41) represents the contribution of dislocations only to the third harmonic and that the lattice contribution is neglected.

IV. Consequences of the Model

(a) Two contributions to the second harmonic have been treated. One of these arises from the lattice anharmonicity which is represented by the first term of expression (31), the other arises from the nonlinear dislocation motion which is represented by the second term of this expression. In addition, the existence of the phase angle $2(\delta_{10} + \delta_{20})$ between the two components leads to the cross term in expression (31). The factor Y is a function of dislocation density, of bias stress (internal or external), and of loop length (which in turn depends on bias stress), while

X is independent of the bias stresses in the range considered here and is a constant for a given solid and mode of wave propagation. In general, a separation of the two contributions is quite difficult because of the cross term in expression (31). Under certain circumstances, either X or Y is dominant and the cross term is unimportant. A separation of the two terms is also possible, of course, when $2(\delta_{10} + \delta_{20}) \approx (\pi/2)$ (δ_{10} and δ_{20} depend on loop length).

In the case of the third harmonic, the lattice contribution does not appear in the expression (34). This is simply because the terms in powers higher than the square of the displacement gradient are not included in expression (4). Although for the lattice part the magnitude of the cubic term relative to the linear and the square terms is not known at present, it is reasonable to assume that in most solids the lattice contribution to the third harmonic is negligible, compared to the dislocation contribution. Thus, the third harmonic observable near room temperature is considered to be due predominantly to the nonlinear motion of dislocations.

(b) The amplitudes of the second and third harmonic are proportional, respectively, to the square and cube of the amplitude of the fundamental wave as long as the dislocation loop lengths remain constant.

(c) At $x=0$, the amplitude of the harmonics is zero. As the fundamental wave propagates along the x axis, it starts generating the harmonics. However, both fundamental and harmonic waves suffer attenuation. The resulting initial buildup followed by a decay of the amplitude of the second and third harmonics as a function of propagation distance x are represented, respectively, by

$$(e^{-2\alpha_1 x} - e^{-\alpha_2 x}) / (\alpha_2 - 2\alpha_1) \quad (35)$$

and

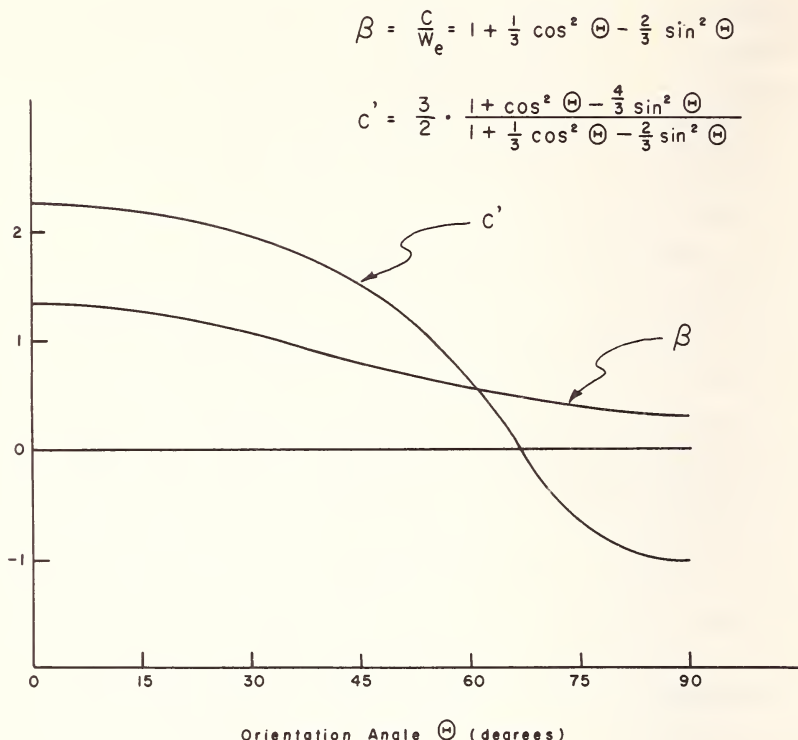
$$(e^{-3\alpha_1 x} - e^{-\alpha_3 x}) / (\alpha^3 - 3\alpha_1). \quad (36)$$

Each factor has a maximum at a distance $(x_2)_{\max}$ and $(x_3)_{\max}$ given by

$$(x_2)_{\max} = \frac{\ln(2\alpha_1/\alpha_2)}{2\alpha_1 - \alpha_2} \quad (37)$$

$$(x_3)_{\max} = \frac{\ln(3\alpha_1/\alpha_3)}{3\alpha_1 - \alpha_3}. \quad (38)$$

(d) Since C appears in the factors S_0 , M_0 , and T_0 , the magnitude and the sign of the harmonics depend on the values of C and C' , which are, of course, a function of the orientation angle Θ . In figure 3, the factors

FIGURE 3. Variation of the factors β and C' with orientation angle Θ .

$$\beta = C/W_e = 1 + m - 3m \sin^2 \Theta$$

and

$$C' = \frac{3}{2} \frac{(1 + 3m - 7m \sin^2 \Theta)}{(1 + m - 3m \sin^2 \Theta)}$$

are plotted as a function of Θ , taking $m = \nu = 1/3$ (ν is Poisson's ratio). As can be seen, C' changes its sign at approximately $\Theta = 67.5$ deg. This means that the harmonics generated by dislocations with Θ in the range $0 < \Theta < 67.5$ deg are opposite in sign to the harmonics generated by dislocations with Θ in the range $67.5^\circ < \Theta < 90^\circ$. In the case of the second harmonic, the applied static stress A_0 is, in fact, a parameter to indicate the degree of deviation of a bowed out dislocation from its straight-line configuration. Therefore, regardless of whether the static stress is tension or compression, the absolute value $|A_0|$ should be used in evaluating the expression (31). Thus, except for the factor C' , the quantities that appear in the dislocation contribution are all positive. The contribution of the dislocations may be of the same or opposite sign as the lattice term,

depending on the relative signs of X and Y , as well as on the sign of $(\omega_0^5 - 5\omega^2 d^2)$ — see eq (31). In the case of the third harmonic, the absolute value should be used in evaluating the expression (34).

The factor β (as well as C) also depends on the angle Θ . The larger the value of C , the smaller is the corresponding dislocation displacement for a given stress. Since the amplitude of the harmonics depends strongly on the dislocation displacement, it is expected that the dislocations with smaller C values will generate larger harmonics, other factors being the same.

As an example the Θ and loop-length-dependent part of the amplitude A_3 (disregarding the attenuation factor)

$$CC'/S_0^{3/2}T_0^{1/2}L_0^4 \quad (39)$$

is calculated numerically for edge, screw, and $\pi/3$ dislocations as a function of loop length L_0 , for a single loop and using the following values, $A = 7.6 \times 10^{-15}$ g cm $^{-1}$, $B = 5 \times 10^{-4}$ dyn s cm $^{-2}$, $\omega = 2\pi \times 10^7$ s $^{-1}$, $W_e = 1.2\mu b^2$, $\mu = 3 \times 10^{11}$ dyn cm $^{-2}$, $b = 3 \times 10^{-8}$ cm. The results are given in figure 4. As can be seen, the maximum amplitude of the third harmonic

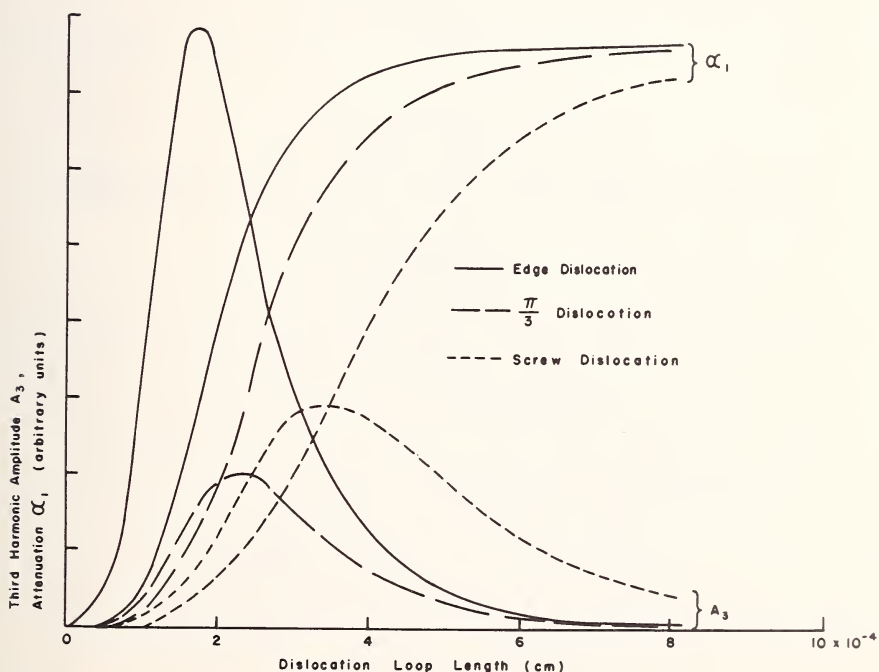


FIGURE 4. Amplitude of the third harmonic A_3 and attenuation of the fundamental wave α_1 for edge, screw, and $\pi/3$ dislocations as a function of loop length. (Arbitrary units for A_3 and α_1).

arising from edge dislocations is considerably larger than that arising from screw or $\pi/3$ dislocations. In this figure, the attenuation of the fundamental wave α_1 is also plotted for the three types of dislocations. In each case, the loop length for the maximum amplitude of the third harmonic coincides approximately with loop length corresponding to the inflection point in the attenuation curve. The maximum of the third harmonic, therefore, corresponds approximately to the transition between underdamped and overdamped behavior. The condition determining the loop length for the maximum amplitude A_3 is given by

$$\omega_0/\omega = 1.12(d/\omega)^{1/2}. \quad (40)$$

In plotting figure 4 the absolute values are taken for the third-harmonic amplitude A_3 . As mentioned earlier, the amplitude A_3 for dislocations whose orientation angles Θ are in the range $0 < \Theta < 67.5^\circ$ are opposite in sign to those whose orientation angles are in the range $67.5^\circ < \Theta < 90^\circ$.

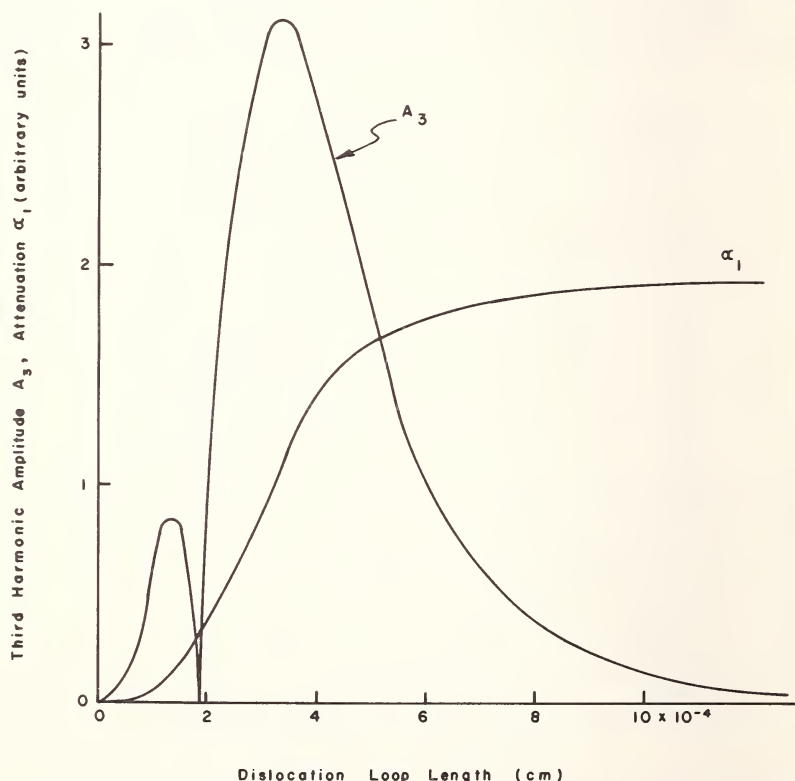


FIGURE 5. Amplitude of the third harmonic A_3 and attenuation of the fundamental wave α_1 averaged over the range $0 < \Theta < 90^\circ$.

Therefore, cancellations of amplitude A_3 will take place when the dislocations in the two ranges operate simultaneously. To see this effect, a simple average of the expression (40) over the range $0 \leq \Theta \leq 90^\circ$ was calculated as a function of loop length using the same numerical values as given above. The results are shown in figure 5. The cancellation occurs approximately at the loop length of 1.9×10^{-4} cm. Whether this effect becomes significant or not depends, of course, on the orientation distribution of dislocations.

V. Summary and Conclusions

The predictions of the model were found to be consistent with experimental results. This was demonstrated by studying the effect of small bias stresses on A_3 in single crystals with different initial dislocation loop lengths [12]. It is concluded, therefore, that the model provides a correct phenomenological description of harmonic generation due to dislocations.

In view of the difficulties in separating lattice and dislocation contributions in the case of the second harmonic, dynamic properties of dislocations are studied more easily through the generation of third harmonics. Attention is called to the fact that in order to study lattice anharmonicity by means of second-harmonic generation, it is necessary to eliminate the dislocation contribution.

VI. Acknowledgement

Research supported in part by the National Science Foundation.

VII. References

- [1] Hikata, A., Chick, B. B., Elbaum, C., Appl. Phys. Letters **3**, 196 (1963).
- [2] Hikata, A., Chick, B. B., and Elbaum, C., J. Appl. Phys. **36**, 229 (1965).
- [3] Suzuki, T., Hikata, A., and Elbaum, C., J. Appl. Phys. **35**, 2761 (1964).
- [4] Hikata, A., and Elbaum, C., Phys. Rev. **144**, 469 (1966).
- [5] Landau, L. D., and Lifshitz, E. M., Theory of Elasticity (Pergamon Press, Inc., New York, 1959) p. 115.
- [6] Koehler, J. S., Imperfections in Nearly Perfect Crystals (Wiley, New York, 1952).
- [7] Granato, A., and Lücke, K., J. Appl. Phys. **27**, 583 (1956).
- [8] Stern, R. M., and Granato, A., Acta Met. **10**, 92 (1962).
- [9] Foreman, A. J. E., Acta Met. **3**, 322 (1955).
- [10] de Wit, G., and Koehler, J. S., Phys. Rev. **116**, 1113 (1959).
- [11] Leibfried, G., Oak Ridge National Laboratory Progress Report No. ORNL 2829, 1959 (unpublished).
- [12] Hikata, A., Sewell, F. A., Jr., and Elbaum, C., Phys. Rev. **151**, 442 (1966).

A SOURCE OF DISSIPATION THAT PRODUCES AN INTERNAL FRICTION INDEPENDENT OF THE FREQUENCY

W. P. Mason

*Department of Engineering and Applied Science
Columbia University
New York, N.Y. 10027*

Many measurements of the internal friction of metals and other materials such as the earth's crust show that there is a component at low frequencies which produces a value independent of the frequency. It has been shown that this component is associated with dislocation motion.

Using a model for which dislocation motion results from the motion of kinks, it is shown that such a loss can be associated with the energy dissipated when kinks cross Peierls barriers. Theoretical calculations have shown that the energy dissipated in mechanical vibrations requires a dissipative force equal to from 0.01 to 0.1 of the Peierls stress to replace the energy lost. At the low stresses used in internal friction measurements, it requires a thermal activation to cause motions of the kinks. The lag of the motion behind the applied stress produces a drag coefficient B proportional to the temperature. The energy due to kink dissipation produces an internal friction to modulus change ratio β , equal to the ratio of the dynamic to the static kink stress. Measurements in copper and in the alloy Ti-6Al-4V indicate that this ratio is about 0.03, in agreement with calculations.

Key words: Internal friction; kink motion; Peierls stress.

I. Introduction

It has long been known that metals and a wide class of materials—such as the earth's crust [1]—have an internal friction Q^{-1} which is independent of the frequency. Early measurements by Wegel and Walther [2], shown by figure 3f-3, page 3-95, of the American Institute of Physics Handbook (1963), show that the internal friction for nonmagnetic materials is either constant or slightly decreasing with frequency. While no tests were made to ascertain the cause of the internal friction, it ap-

pears that the only defect which can move fast enough to cause the internal friction is the dislocation. More recently, measurements [3] have been made over wider frequency ranges—1 Hz to 40 KHz—with similar results. Tests have shown that this background internal friction is due to dislocations. It seems probable that the internal friction in the earth's crust is also due to dislocation motions, since the rocks are polycrystalline materials under enough pressure to generate a considerable number of dislocations.

As long as dislocations were assumed to lie across Peierl's energy barriers, as in the Granato Lücke model [4], the only cause of dislocation damping was due to the communication of energy to phonons and electrons, and this produces a drag coefficient proportional to the velocity. However, in the last few years, convincing evidence [5] has been produced that dislocations lie partly in Peierl's barriers with these parts connected by kinks lying across energy barriers, as shown by figure 1. When a stress is applied to the crystal, the dislocation moves by the kinks moving. As shown by Seeger and Schiller [5], such kinks have masses and damping constants and also kink energy barriers which have been calculated [6] to be

$$W = \frac{\sigma_k b^3}{5}; \quad \sigma_k = \frac{192}{\pi^2 \sqrt{3}} \left(\frac{1-\nu}{1+\nu} \right) \frac{b}{w} \left(\frac{\sigma_p}{\mu} \right)^2 \mu \quad (1)$$

where σ_k is the kink stress, W the kink energy barrier, ν is Poisson's ratio, b the Burger's distance, w the kink width, σ_p the Peierl's stress,

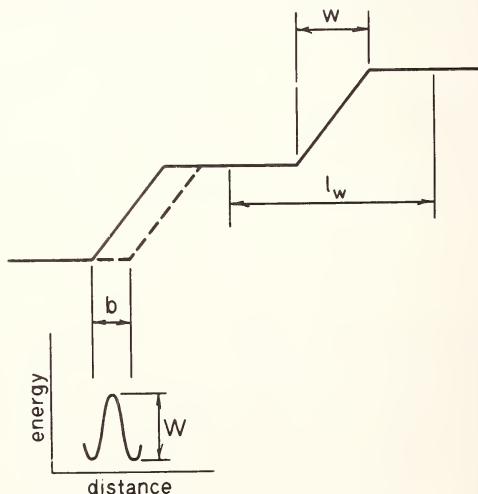


FIGURE 1. Dislocation kinks and kink energy barriers.

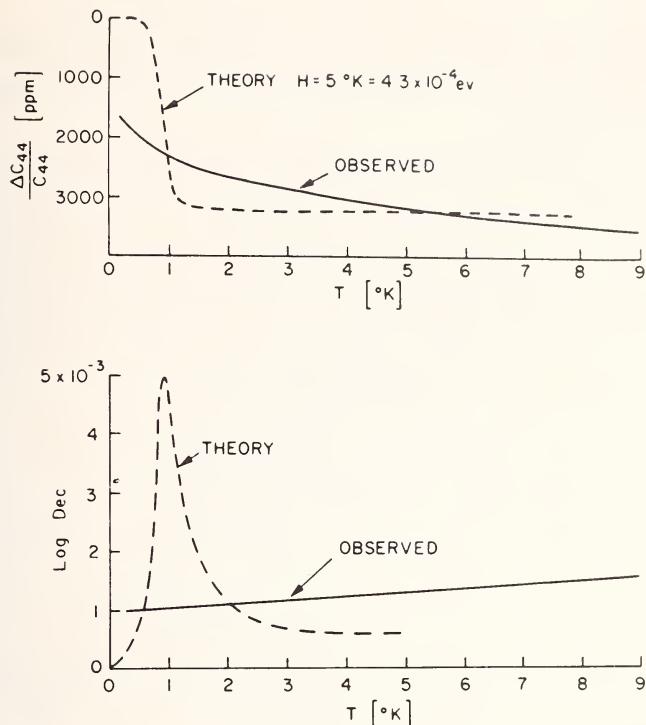


FIGURE 2. Modulus change and internal friction as a function of the temperature. Measurements made at 10 MHz. Dashed curves show calculated value of an activation energy process (after G. A. Alers and K. Salama).

and μ the shearing modulus. As shown by figure 2, the best evaluation of W comes from the work of Alers and Salama [7], which indicates that half the modulus defect has disappeared as the temperature is lowered to 0.1 K. This decrease in modulus defect requires a distribution of activation energies centered around $W = 1.25 \times 10^{-4}$ eV = 1.5×10^{-16} ergs, as can be seen from the calculation given in Section II. This corresponds to a kink stress of 4.5×10^7 dynes/cm², corresponding to a strain of 1.1×10^{-4} . This should also be the elastic limit at 0 K for very pure copper, which glides by kink motion [8]. Most measurements are from 10^{-5} to $10^{-4}\mu$ but at a temperature for which thermal activation can lower the limiting stress.

Since it requires strains in excess of 10^{-4} to cause kink motion over barriers, the strains of 10^{-8} to 10^{-7} usually used for internal friction measurements are not large enough to cause the kinks to cross their kink barriers. It requires thermal energy to accomplish this and this produces

a slight lag of the motion behind the applied stress, which results in a drag coefficient B of the same order as that calculated by Leibfried [9] for interactions with phonons. The thermal model and its consequences are discussed in section II.

In order to obtain an internal friction independent of the frequency, we have to have a source of energy loss proportional to the number of kink displacements rather than to their velocity. Such a source of loss has been calculated by Weiner [10] and by Atkinson and Cabrera [11]. Using a Frenkel-Kontorova model, they have shown that it takes a dynamic Peierl's stress of from 0.01 to 0.1 of the Peierl's stress to keep the dislocation moving after it first crosses the barrier. This stress is necessary to replace the energy lost to mechanical vibrations when the dislocation moves discontinuously across the barrier. Since on this thermal activation model, the displacement and hence the energy loss is proportional to the applied stress, this is equivalent to impressing a force $\tau^* = \tau(1 - j\beta)$ on the string model where β is the ratio of the dynamic to the static Peierl's stress. Section III shows the effect of applying such a stress to the string model. A low-frequency component results with a ratio of the internal friction Q^{-1} to the modulus change $\Delta E/E$ equal to β . At high frequencies, the drag coefficient B produces the highest internal friction. Using the results of Thompson and Holmes [12], the value of β appears to be from 0.04 to 0.09, which is within the calculated values. A recent measurement of one alloy Ti-6Al-4V gives a value of 0.03.

II. Thermal Activation Model for Kink Motion

The actual motion of the kinks for all stresses applied for internal friction measurements will be one Burger's distance or less. Hence the potential well model that we have to consider is the two-well model shown by figure 3, where the separation between wells is one Burger's distance b .

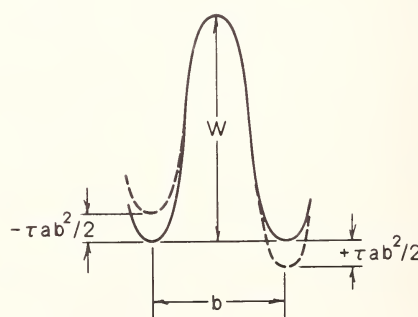


FIGURE 3. Dislocation potential well model.

The value W is the height of the potential barrier. The effect of a stress is to lower one barrier in the direction of motion and to raise the other in the direction away from the motion by amounts

$$W_1 = W - \frac{\tau ab^2}{2} \quad \text{and} \quad W_2 = W + \frac{\tau ab^2}{2} \quad (2)$$

where τ is the applied shearing stress and τab is the force exerted on the kink, where a is the kink height.

From reaction rate theory it is known that the average time to cross the barrier in the positive direction is

$$t = t_0 e^{(W - \frac{\tau ab^2}{2})/kT} \quad (3)$$

where t_0 is the time that kink will be attempting to cross the energy barrier. If ν_0 is the vibration frequency —usually taken to be about 10^{13} —then t_0 is usually taken to be

$$t_0 = \frac{1}{2\pi\nu_0} = \frac{1}{\omega_0} \doteq 1.6 \times 10^{-14} \text{ s.} \quad (4)$$

The number of jumps per second— α_{12} —in the forward direction is

$$\alpha_{12} = \omega_0 e^{-(W - \frac{\tau ab^2}{2})/kT}. \quad (5)$$

After the kink has crossed the barrier there is a certain probability that it will jump back against the applied stress. This results in the number of jumps per second α_{21} given by

$$\alpha_{21} = \omega_0 e^{-(W + \frac{\tau ab^2}{2})/kT}. \quad (6)$$

Hence the net rate of jumps per second is

$$\alpha_{12} - \alpha_{21} = \omega_0 e^{-W/kT} [e^{\tau ab^2/2kT} - e^{-\tau ab^2/2kT}]. \quad (7)$$

For shear stresses corresponding to strains of 10^{-7} often used in internal friction measurements, $\tau = 4 \times 10^4$ dynes/cm², a is in the order of 2×10^{-8} cm, and $b = 2.55 \times 10^{-8}$ cm for copper. Hence $\tau ab^2/2kT \ll 1$ even down to 0.1 K. Similarly the term $e^{-W/kT}$ is near unity for all values of T above 5 K. Hence the number of jumps per second should be

$$\alpha_{12} - \alpha_{21} = 2\pi \times 10^{13} \left[\frac{\tau ab^2}{kT} \right] e^{-W/kT}. \quad (8)$$

At room temperature for a strain of 10^{-7} —stress 4×10^4 dynes/cm²—the number of jumps per second should be about 8×10^8 . If we assume that it takes 2π jumps in the time of a cycle for a dislocation to follow the applied stress, this corresponds to a frequency of 125 MHz.

At low temperatures, on account of the exponential factor, there will be some frequency for which the dislocation will not follow the applied stress. According to figure 2, for measurements made at 10 MHz, half the dislocations are not able to follow the stress at 0.1 K. This allows one to estimate the value of W as

$$e^{-W/k(0.1)} = \frac{10^7}{10^{13} \left(\frac{4 \times 10^4 \times 2 \times 10^{-8} \times 6.5 \times 10^{-16}}{1.38 \times 10^{-16} \times 0.1} \right)} = \frac{1}{3.75 \times 10^4} \quad (9)$$

or $W \doteq 1.5 \times 10^{-16}$ ergs $= 1.25 \times 10^{-4}$ eV. It will be noted that this mechanism does not result in a peak in the attenuation as assumed in the dashed line of figure 2, since it results only in a gradual elimination of the number of dislocation loops that can move.

The lag in the dislocation motion behind the applied stress does result in a drag coefficient proportional to the velocity and the absolute temperature of the same order as that calculated by Leibfried [9]. To calculate this value we assume that there are no pinning points. The total displacement D of the dislocation kink per second will be

$$D = b(\alpha_{12} - \alpha_{21}) = \left[\frac{\omega_0 \tau ab^3}{kT} \right] e^{-W/kT}. \quad (10)$$

Hence this lag in displacement results in a drag coefficient B equal to

$$B = \frac{\tau b}{D} = \frac{kTe^{W/kT}}{\omega_0 ab^2} = (1.7) \times 10^{-7} T. \quad (11)$$

At room temperature B will have the value

$$B = 0.5 \times 10^{-4} \text{ dyne sec/cm}^2, \quad (12)$$

which is in the same order as the drag coefficient calculated by Leibfried [9] for interactions with phonons.

For slowly applied stresses, the number η of kinks crossing the barrier reaches an equilibrium value, since the kinks crossing the barrier have a stored energy of $\sigma_k ab^2/2$ gained from the negative slope of the barrier. The potentials on each side of the barrier reach an equilibrium value when

$$(\eta_0 - \eta)\tau ab^2/2 = (\sigma_k - \tau)ab^2/2 \quad \text{or } \eta = \eta_0\tau/\sigma_k,$$

where η_0 is the total number of kinks.

III. Internal Friction Independent of the Frequency

In order to obtain an internal friction independent of the frequency, we have to have a source of energy proportional to the number of kink displacements rather than to their velocity. Such a source of loss has been calculated by Weiner [10] and by Atkinson and Cabrera [11]. Using a Frenkel-Kontorova model they have shown that it takes a dynamic Peierls stress of from 0.01 to 0.1 of the Peierls stress to keep the dislocation moving after it first crosses the barrier. This stress is necessary to replace the energy lost to mechanical vibrations when the dislocation moves discontinuously across the barrier.

For the model shown by figure 1, an equivalent string model can be obtained by equating the area swept out by the kinks to the area determined by the displacement of the dislocations assumed initially to be straight lines. For the low frequency case considered here, we can neglect the damping due to the drag coefficient B . For $N(l)$ dislocations of length l , we can set

$$nab = N(l)\bar{x}l = N(l)Al^3/6 = \frac{\tau N(l)l^3}{6\mu b} \quad (13)$$

where n is the number of kink jumps, \bar{x} is the average displacement of the string, and A a constant given by eqs (21) and (23) with β and d set equal to zero. If n_0 is the number of kink jumps occurring when the kink stress σ_k is applied, then n_0 is

$$n_0 = \frac{N(l)\sigma_k bl^3}{6\mu ab^3}; \text{ also } n = \frac{N(l)\tau bl^3}{6\mu ab^3} \text{ or } n = \frac{n_0\tau}{\sigma_k} \quad (14)$$

When a kink crosses the barrier under the applied stress alone, it acquires an energy $\sigma_k ab^2/2$ from the negative slope of the potential well. This energy is applied to stretching the dislocation and hence the energy required to obtain the maximum extension of the dislocation is

$$\frac{1}{2}(n_0\sigma_k ab^2) = \frac{N(l)\sigma_k^2 l^3}{12\mu}. \quad (15)$$

The energy stored in the crystal is

$$\frac{\sigma_k^2}{2\mu'} = \frac{\sigma_k^2}{2\mu^E \left[1 - \frac{\Delta\mu}{\mu} \right]} = \frac{\sigma_k^2}{2\mu^E} \left[1 + \frac{\Delta\mu}{\mu} \right] \quad (16)$$

where μ' is the elastic constant including the effect of the dislocations and μ^E is the elastic constant without dislocations effects. Hence

$$\frac{\Delta\mu}{\mu} = \frac{N(l)l^3}{6}. \quad (17)$$

The energy dissipated when the kink goes over the barrier is equal to

$$\Delta W = (\frac{1}{2})n\tau_{dp}ab^2 = (\frac{1}{2})(n\beta\sigma_k ab^2) \quad (18)$$

where β is the ratio of the dynamic Peierls stress to the kink stress. Hence the ratio of the energy dissipated to the energy stored, which is by definition the internal friction of the system, is equal to the ratio β . However this is the internal friction of the dislocation system alone. To determine the internal friction of the complete crystal we have to multiply the denominator by the ratio $(\Delta\mu/\mu)$ and hence for the crystal

$$Q^{-1} = \beta(\Delta\mu/\mu). \quad (19)$$

For lower stresses and higher temperatures, the motion is accomplished by abstracting thermal energy from the bath of an amount required to take the kink across the barrier. The energy lost for this motion is again the value given by (18) and hence the same value of energy dissipated to energy stored is obtained.

For sinusoidal motions the same result is obtained by applying a stress $\tau^* = \tau(1 - j\beta)$ to the string model. At the same time the effect of the drag term B can be evaluated. Applying this stress to the string model we have for the stress applied in the shear plane, for simple harmonic motion

$$-\omega^2 Mx + j\omega Bx - T \frac{\partial^2 x}{\partial y^2} = \tau(1 - j\beta)b \quad (20)$$

where M is the mass of the dislocation per unit length, B the drag coefficient and T the tension of the dislocation which is often taken to be $\mu b^2/2$. For a slowly varying stress, a solution for the loop shape, assuming that the loop is pinned on both ends, is

$$x = (Aly - y^2); \frac{\partial^2 x}{\partial y^2} = -2A \quad (21)$$

where x is the displacement at any point y measured from one pinning point. Dislocations are overdamped, i.e., M can be neglected compared to B . Substituting (21) in (20) and integrating with respect to y from 0 to l , the loop length, the constant A takes the form for sinusoidal vibrations

$$\frac{j\omega BAL^3}{6} + \mu b^2 Al = \tau(1 - j\beta) bl \quad (22)$$

or

$$A = \frac{\tau(1 - j\beta)}{\mu b} \left[\frac{1}{1 + j\omega d} \right] \text{ where } d = \frac{Bl^2}{6\mu b^2}. \quad (23)$$

The average displacement \bar{x} is from (21)

$$\bar{x} = \frac{1}{l} \int_0^l x dx = \frac{Al^2}{6}. \quad (24)$$

The effect of $N(l)$ loops per cubic centimeter (of length l) on the shear strain S_s is obtained by adding to the elastic strain S_s^E a plastic strain S_s^P such that

$$S_s = S_s^E + S_s^P = S_s^E + N(l) sb \quad (25)$$

where s is the area of displacement of a single loop. Hence the shear modulus μ' is, since $\mu' = \tau/S_s$,

$$\frac{1}{\mu'} = \frac{1}{\mu} + \frac{N(l) sb}{\tau} = \frac{1}{\mu} + \frac{N(l) b \bar{x} l}{\tau} = \frac{1}{\mu} + \frac{N(l) l^3}{6\mu} \left[\frac{1 - j\beta}{1 + j\omega d} \right] \quad (26)$$

or since the last term is small compared to unity

$$\mu' \left[1 + \frac{j}{Q} \right] = \mu \left[1 - \frac{N(l) l^3}{6} \frac{[1 - j(\beta + \omega d)]}{1 + \omega^2 d^2} \right]. \quad (27)$$

Hence for a single loop length, we find

$$\frac{\mu - \mu'}{\mu} = \frac{\Delta\mu}{\mu} = \frac{N(l) l^3}{6 \left[1 + \left(\frac{\omega l^2 B}{6\mu b^2} \right)^2 \right]}, \quad \frac{1}{Q} = \frac{\Delta\mu}{\mu} \left[\beta + \frac{\omega l^2 B}{6\mu b^2} \right] \quad (28)$$

upon introducing the value of d from (23). We see for low frequencies, for which β exceeds $\omega Bl^2/6\mu b^2$, that

$$\frac{1}{Q} / \frac{\Delta\mu}{\mu} = \beta. \quad (29)$$

For any other type of stress, such as a longitudinal vibration, the same solution holds if we introduce an orientation factor R which relates the

average shear stress in the glide planes to the applied stress. This results in

$$\frac{\Delta E}{E} = \frac{N(l) R l^3}{6 \left[1 + \left(\frac{\omega l^2 B}{6 \mu b^2} \right)^2 \right]}, \quad \frac{1}{Q} = \frac{\Delta E}{E} \left[\beta + \frac{\omega l^2 B}{6 \mu b^2} \right]. \quad (30)$$

Actually the loops are not all of one length but probably follow an exponential law which has been assumed by Koehler [13] to take the form

$$N(l) dl = \frac{\bar{N}}{l_A^2} e^{-\eta l_A} dl \quad (31)$$

where \bar{N} is the total number of dislocations per square centimeter l_A is an averaged pinned loop length. Since the internal friction value Q^{-1} can be divided into two parts, one proportional to $\Delta E/E$ and the other to $(\Delta E/E)(\omega l^2 B / 6 \mu b^2)$, we can use a calculation due to Oen, Holmes, and Robinson [14] to evaluate the effect of the distribution of dislocations on the modulus and Q^{-1} factor. This calculation is shown schematically on figure 4, which shows the ratio of $\Delta E/E$ to $\bar{N} R l_A^2$ and Q^{-1} to $\bar{N} R l_A^2$. This part of Q^{-1} will be the part determined by the drag coefficient B . The other part due to the loss determined by kink barriers will be β times the value of $\Delta E/E$.

Some idea of the value of β can be obtained from the measurements of friction Q^{-1} that can be removed by neutron irradiation. For the low frequencies of 12,000 to 15,000 Hz the ratio of Q^{-1} to $\Delta E/E$ was found to be

$$\beta = Q^{-1}/(\Delta E/E) = 0.04 \text{ to } 0.09 \quad (32)$$

for the ten crystals given. These values are intermediate to the calculated values [10, 11]. More recent measurements [15] in the alloy Ti-6Al-4V give a value of 0.03.

If we assume a value of $\beta = 0.03$, we see from figure 4 that the low-frequency and high-frequency internal friction values will be equal when

$$\frac{\omega}{\omega_2} = 7.5 \times 10^{-3} \quad \text{or} \quad \omega = \frac{7.5 \times 10^{-3}}{B l_A^2}. \quad (33)$$

Granato and Stern [16] showed that for very pure copper, the internal friction at 15 KHz was in the order of the high frequency component. From eq (33) this would require the average loop length l_A to be equal to 1.8×10^{-4} cm or larger, a not unreasonable value.

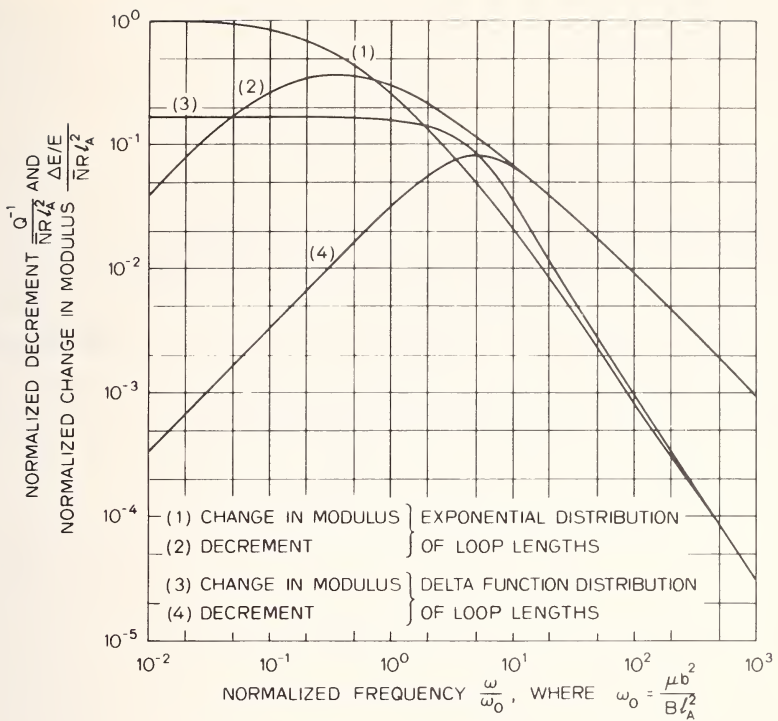


FIGURE 4. Internal friction and modulus change for an exponential dislocation distribution assuming a velocity drag coefficient damping (after Oen, Holmes, and Robinson).

Some other evidence for the loop length dependence of the internal friction is the rate that it disappears when the material is neutron irradiated. Using a torsional pendulum Routbort and Sack [3] find that the value caused by deformation disappears much more slowly than the high-frequency component. This is consistent with the square law loop dependence for the low-frequency component compared to the fourth power dependence of the high-frequency component. Granato and Stern [16] also found two components one of which disappears much faster than the other.

IV. References

- [1] Knopoff, L., in **Physical Acoustics, IIIB**, W. P. Mason, Ed. (Academic Press, 1965) Chap. 7.
 - [2] Wegel, R. L., and Walter, H., *Physics* **6**, 141 (1935).
 - [3] Routbort, J. L., and Sack, H. S., *J. Appl. Phys.* **37**, 4803 (1966).
 - [4] Granato, A. V., and Luke, K., in **Physical Acoustics, IVA**, W. P. Mason, Ed. (Academic Press, 1966) Chap. 6.

- [5] Seeger, A., and Schiller, P., in *Physical Acoustics, IIIA*, W. P. Mason, Ed. (Academic Press, 1966) Chap. 8.
- [6] Loc cit. p. 426.
- [7] Alers, G. A., and Salama, K., in *Dislocation Dynamics*, A. R. Rosenfeld, G. T. Hahn, A. L. Bement, Jr., and R. I. Jaffee, Eds. (McGraw-Hill, 1968) p. 211.
- [8] Friedel, J., *Dislocations* (Addison-Wesley, 1964) p. 58.
- [9] Leibfried, G., *Z. Physik* **127**, 344 (1950).
- [10] Weiner, J. H., *Phys. Rev.* **136**, A863 (1964).
- [11] Atkinson, W., and Cabrera, N., *Phys. Rev.* **138**, A763 (1965).
- [12] Thompson, D. O., and Holmes, D. K., *J. Appl. Phys.* **27**, 713 (1956).
- [13] Koehler, J. S., in *Imperfections in Nearly Perfect Crystals* (Wiley, New York, 1952) Chap. 7.
- [14] Oen, O. S., Holmes, D. K., and Robinson, M. T., U.S. Atomic Energy Comm. Rept. ORNL-3017, 3.
- [15] Mason, W. P., and Wehr, J., *J. Phys. and Chem. of Solids* (in press).
- [16] Granato, A. V., Stern, R. J., *J. Appl. Phys.* **33**, 2880 (1962).

Discussion on Papers by J. A. Garber and A. V. Granato, R. O. Schwenker and A. V. Granato, and W. P. Mason.

GILMAN: I would like to comment on Professor Granato's paper. In general, it seems to me this is a very nice technique, but there are some subtleties associated with the interpretation which make the given interpretation doubtful. One of the treacheries is that it's well known in deformed crystals, and especially alkali halides, that the density and the local modulus become changed. The simple proof is the fact that the region becomes birefringent. Therefore, the acoustic impedance is changed and one expects scattering from this, whether the dislocations move or not. Also, the given proof that radiation damage suppresses the reflection is not sufficient, because one knows that the damage is selective. That is, there is enhanced colorability in a deformed region. By Le Chatelier's principle it would tend to reduce the changed density and changed modulus selectively; and therefore, cause the acoustic impedance to come back to the normal value. Hence, the acoustic reflection would be suppressed by radiation. Let us now put the question of whether one is really getting a reflection as a result of motion of the dislocations aside, and assume you really get that effect. Then, it is known that in these crystals the relative concentration of monopoles compared with dipoles concentration is very small. So, most of the dislocations exist in dipoles, at moderate total dislocation densities. Therefore, they are strongly coupled one to another, and the spring constant associated with this coupling must be more important than the spring constant associated with the loop length. One can still use the formalism, probably, except that instead of the parameter L being the "loop length," it becomes the dipole moment. At very high dislocation densities one should probably properly consider the system to be essentially a dislocation plasma where everything is interacting with everything else.

Another thing one has to be careful about is the fact that the wall has a finite width. Therefore, if there is a change in the acoustic impedance in the slab, there will be an apparent attenuation associated with the phase shift between the front and the back of the wall, and this makes it difficult to get an absolute value of the attenuation.

GRANATO: Well, I appreciate the chance to discuss some of the experimental aspects that I felt I should leave out of the talk due to lack of time. The finite width of the wall is indeed a problem. In fact, we've never been able to get a wall that's completely satisfactory. [Here Professor Granato continued at the board.] For instance, the little echos

from the wall don't completely disappear upon radiation, some part is left and the part that's left varies. But we tried to account for it by assuming that the local modulus could change in those regions, for example, instead of by the assuming scattering from dislocations. But you just can't quantitatively get this size of effect that way. You have to assume that the elastic constants change by a factor of three, or something like that, which is out of the question. You simply can't get this magnitude effect from this kind of wall. Also the radiation level is extremely low, too low to produce any mechanical effects besides dislocation pinning.

About the business of monopoles and dipoles, all I can say is that the comparison of theory and experiment just supports the string model. There is a tremendous volume of data that fits the theory quantitatively; all the predictions are proved out. I've never seen a theory for dipoles that can predict enough data to be taken as seriously as the simple monopole string model.

ARSENAULT: I would just like to make one comment on Professor Granato's statement on measuring the Peierls stress. You would have to be extremely careful that you did not get any geometrical kinks in your crystal before you start doing any measurements, because, you would get unbelievably small values for the Peierls stress if you had any geometrical kinks in the dislocations.

ESHELBY: This isn't really a question. It is more a confession. I believe Professor Granato said he used my value for the radiation which I calculated in 1949. Unfortunately it is too low by a factor of two which I discovered in 1962. People have used it all that time—it just shows nobody checks anything.

GRANATO: The figures shown are drawn using the corrected value.

ESHELBY: Oh, good! Can I also put a plug in for the fact that for an edge dislocation the answer is almost exactly the same—it's about 10% bigger, and not 10 times as big as stated somewhere in the literature.

HIRTH: I would like to address my question to Professor Granato. Assuming that one did have a perfect tilt wall, and, particularly, if one had a fairly high angled tilt wall, then it seems to me that the dislocations would be strongly coupled together. Rather than behaving as a vibrating string in that case, they would perhaps behave as a vibrating membrane.

GRANATO: I would like to say, first of all, these were not tilt walls. We tried to make tilt walls and never found one that was mobile. Also you wouldn't have enough dislocations in a tilt wall, if it is just one line wide, to get an observable signal. About the interactions, we also thought that the interactions should be important, because the dislocations are fairly close, of the order of a micron spacing. But, if you use only the restric-

tions that would come from the tensions in a string model, you can calculate the displacement and it is within a factor of 2 of the observed displacements. I think that the main effects of any interactions would be to reduce the amount of displacement, and we take this fact, that there is such good agreement, to mean the interactions are less important than are the pinning interactions.

BACON: I have a question for Professor Mason. In your model the energy dissipation arises from a dynamical Peierls stress which you suggest is between .01 and .1 of the static Peierls stress. Do you think that is really significant in f.c.c. metals?

MASON: This is the calculation of Professor Weiner here; that's just a model, isn't it. These particular figures are for the Frenkel-Kontorova model.

BACON: A second aspect of this question, also to Professor Mason. How is this interpretation related to the microstrain results obtained by, for example, Roberts and Brown, Meakin and Lawley,¹ and many others, on h.c.p. and f.c.c. metals?

MASON: I am not sure how high a strain value they go to, if they go to a point where dislocation breakaway is a factor, then that could be the cause of the microstrain. You would certainly get an effect here, though, and it would not be very large. I don't know whether you could measure it at that low a strain value.

LOTHE: Perhaps I may ask one question, myself. I think it is very important what Professor Mason has pointed out about this frequency independent background. But I don't understand the model, quite. I don't understand how one can retain so to speak this low temperature velocity independent friction force in a range where thermal activation is very easy. I don't see, then, that the mechanism pointed out by Weiner, for example, applies. That is, I can see the model for low temperatures, but I don't see that you can retain this as something that you superpose at higher temperatures where thermal activation is easy.

MASON: The mechanism applies at all temperatures, since the kink stress to cross the barrier is greater than the applied stress. Hence, thermal activation is required. After the kink has crossed the barrier, the energy stored from the negative slope of the kink barrier causes the kink flow to be shut off. In a paper presented at the Internal Friction Conference at

¹ Roberts, J. M., and Brown, N., Trans. AIME, **218**, 454 (1960); Lawley, A., and Meakin, J. D., Acta Met., **14**, 236 (1966).

Brown University it is shown that the rate of kink flow is

$$\alpha_{12} - \alpha_{21} = \omega_0 [\exp(-w/kT)] [n_0\tau - n\sigma_k] ab^2/kT$$

where $(\alpha_{12} - \alpha_{21})$ is the number of kinks per second crossing the barrier, n_0 is the total number of kinks, τ is the applied stress, n is the number of kinks that have crossed the barrier, a is the height of the kink, ω_0 is the attempt angular frequency, and w is the height of the barrier. Hence the equilibrium number of kinks that have crossed the barrier is $n = n_0\tau/\sigma_k$.

IV APPLICATIONS OF THE GEOMETRY OF DISLOCATIONS

Chairman:

F. R. N. NABARRO

THE MEANING OF DISLOCATIONS IN CRYSTALLINE INTERFACES

W. Bollmann

*Battelle Institute
Advanced Studies Center
Geneva, Switzerland*

The extension of the dislocation concept to arbitrary crystalline interfaces is discussed. It is shown that invariance and continuity of the Burgers vector can be conserved and that in high angle boundaries the function of the standard or primary dislocation is the delimitation of ranges of coordination between the two crystals. In certain relative orientations where the superposition of the two crystals forms a highly periodic pattern (which is energetically favorable such that the crystal tends to conserve it) a slight deviation from that optimum pattern is corrected by a network of secondary dislocations. There is complete balance between the Burgers vectors of primary as well as secondary dislocations.

Key words: Dislocations; grain boundaries; interfaces; twinning.

I. Introduction

It is well known that the interface of two crystals of the same kind which slightly deviate from each other in orientation consists of a network of dislocations. The theory of these so-called subgrain boundaries was initiated by Frank [1], worked out and reviewed by Amelinckx and Dekeyser [2] and formulated in a dualistic manner by Bollmann [3]. The most recent reviews are given by Nabarro [4] and Hirth and Lothe [5].

The problems of high-angle boundaries were treated on the basis of the coincidence site lattice essentially introduced by Frank cited by Ranganathan and developed by Brandon et al. [6], Brandon [7] and Ranganathan [8].

A geometrical approach was given by Bollmann [9]. This approach allows an extension of dislocation networks to general crystalline interfaces. However the concept of "dislocation" will have to be reconsidered in this context.

We first develop the general geometrical theory of crystalline interfaces and then shall investigate what aspects of "dislocations" are conserved for arbitrary interfaces.

II. The 0-Lattice

The basic idea of the general theory can be introduced the following way:

Instead of two crystals joining at a boundary the two respective translation lattices (named lattice 1 and 2) are considered as interpenetrating. The interpenetrating lattices represent two possible sets of positions for every set of atoms, one in lattice 1, the other in lattice 2. We may choose for convenience a lattice point in lattice 1 as origin and translate lattice 2 so that one of its lattice points coincides with that origin. Now we may look for positions within the two interpenetrating lattices where the two lattices "match best." We may set the boundary through such positions, and then place the atoms at lattice points of lattice 1 on one side and of lattice 2 on the other. The boundary itself is then a remnant of the interpenetrating lattices.

The basic problem of this theory is to find an appropriate mathematical definition of what is meant by "best matching" of two periodic structures; and the next step is to localize those best matching spots within the interpenetrating lattices.

A first choice of positions of best fit may be the "coincidence sites" i.e., coincidences of lattice points of both lattices, which leads to the "coincidence site lattice." Mathematically expressed the two lattices are two translation groups i.e., two classes of points within the same space which may be related by a linear nondegenerate transformation \mathbf{A} that usually is homogeneous

$$\mathbf{x}^{(2L)} = \mathbf{Ax}^{(1L)}, \quad |\mathbf{A}| \neq 0. \quad (1)$$

(The index L means lattice point.) $|\mathbf{A}| \neq 0$ is the condition for a point to point relation of the two lattices. In this way all the lattice points of lattice 1 and of lattice 2 are "paired" by the relation (1) and hence the two classes of lattice points are related to each other. Coincidence sites in this terminology are *coincidences of elements of related classes*. They are not coincidences of related elements, as these are related by eq (1) and hence can coincide only at the origin.

This concept of the coincidence site lattice is not yet satisfactory because its configuration is strictly discontinuous with respect to any change in orientation of lattice 2 (while lattice 1 is considered as fixed). There may be orientations which furnish a high density coincidence site lattice, but a slight change in orientation destroys it completely while the change in the physical situation is expected to be continuous.

The coincidence site lattice may be generalized by considering not only the lattice points but the whole space i.e., not only a translation group

but also all its cosets. A coset is obtained by starting from a point *inside* a unit cell of the lattice and adding to it all the translation vectors of the translation group. Hence a coset which again is a class of points has a representative point within every unit cell of the lattice, and in a coordinate system where every lattice point has integer coordinates (and which we call the crystal coordinate system) all the points of a given coset have the same "internal coordinates"; thus the class of points may be named by them.

The coordinates of a specific point may be (12.318, 7.243, -4.421). Of these, the integers (12, 7, -5), which we may call the "external coordinates", characterize a specific element; and the internal coordinates (0.318, 0.243, 0.579) indicate the class of that element. The internal coordinates shall always be positive and < 1.

From a point of a given class we obtain any other point of the same class by adding a translation vector. Every coset in lattice 1 (as well as the translation group) has its image in lattice 2. A lattice is now not only represented by one class of points but by an infinity of them. A subdivision of the whole space into distinct equivalence classes is named a "partition." A related partition of lattice 2 is given by

$$\mathbf{x}^{(2)} = \mathbf{A}\mathbf{x}^{(1)} \quad (2)$$

where now $\mathbf{x}^{(1)}$ resp. $\mathbf{x}^{(2)}$ can be any point of the space. Hence instead of dealing with one pair of related classes we handle an infinity of them. Thus, every point in space belongs to two equivalence classes but for most points the two classes are not related by the transformation \mathbf{A} .

Now, in order to find a generalization of the coincidence site lattice we are looking for *coincidences of elements of related classes regardless of the values of the corresponding internal coordinates*. We call this kind of coincidence points 0-points and indicate them by $\mathbf{x}^{(0)}$; and consider them as the points of best matching of the two lattices. Lattice coincidence sites are coincidences of elements of the class [000], and as such they are special 0-points.

In order to find the 0-points we start with an arbitrary vector $\mathbf{x}^{(1)}$ of lattice 1 with arbitrary external and internal coordinates. It belongs to a class which we name $C^{(1)}$. Its related element (its image) in lattice 2 is $\mathbf{x}^{(2)} = \mathbf{A}\mathbf{x}^{(1)}$. This point belongs by definition to the related class named $C^{(2)}$. On the other hand we obtain a point belonging to the same class as $\mathbf{x}^{(1)}$ i.e., to $C^{(1)}$ in lattice 1 by adding a translation vector of lattice 1 which we name $\mathbf{b}^{(L)}$. Hence $\mathbf{x}^{(1)}$ and $\mathbf{x}^{(1)} + \mathbf{b}^{(L)}$ belong to the same class $C^{(1)}$ while $\mathbf{A}\mathbf{x}^{(1)}$ is an element of the related class $C^{(2)}$. If two such points coincide, we call the coincidence point $\mathbf{x}^{(0)}$, i.e.,

$$\mathbf{A}\mathbf{x}^{(1)} = \mathbf{x}^{(1)} + \mathbf{b}^{(L)} = \mathbf{x}^{(0)}.$$

From this we obtain the equation for $\mathbf{x}^{(0)}$:

$$\mathbf{x}^{(0)} = \mathbf{A}^{-1}\mathbf{x}^{(1)} + \mathbf{b}^{(L)}$$

$$(\mathbf{I} - \mathbf{A}^{-1})\mathbf{x}^{(0)} = \mathbf{b}^{(L)}$$

(3)

(\mathbf{I} = identity).

We obtain all $\mathbf{x}^{(0)}$ —positions by solving eq (3) for all possible translation vectors $\mathbf{b}^{(L)}$ of lattice 1. In contrast to the coincidence site lattice, the 0-lattice is in general a continuous function of the transformation \mathbf{A} i.e., of the relation between the two crystal lattices. While a slight rotation of lattice 2 with respect to the fixed lattice 1 the coincidence sites of lattice points disappear, the 0-points are just displaced continuously a small amount.

Instead of considering translation vectors, distributed over lattice 1, we form a separate lattice by translating them such that they start at a common origin in a separate space, the b -space. This lattice so formed is called the b -lattice; hence $\mathbf{b}^{(L)}$ is a lattice vector of the b -lattice. The b -lattice as a whole is identical with lattice 1.

We can now consider eq (3) as an *imaging relation* between the b -lattice and the 0-lattice with the latter located within the two interpenetrating crystal lattices.

There is a second interpenetration of the 0-lattice. Starting from a given origin we define lattice 2 from lattice 1 by the transformation A . We can show that we obtain the same lattice 2 in the same position from the lattice 1 by the same transformation A but starting from different origins. The pairing of related points is different for different origins. The 0-lattice is the lattice of all possible origins of this kind. With

$$\mathbf{x}^{(2L)} = \mathbf{A}\mathbf{x}^{(1L)}$$

$$(\mathbf{x}^{(2L)} - \mathbf{x}^{(0)}) = \mathbf{A}(\mathbf{x}^{(1L)} + \mathbf{b}^{(L)} - \mathbf{x}^{(0)})$$

leads to eq (3). For a new origin $\mathbf{x}^{(0)}$ another lattice point of lattice 1, namely $\mathbf{x}^{(1L)} + \mathbf{b}^{(L)}$, is related to $\mathbf{x}^{(2L)}$. The general theory of the 0-lattice is given in reference [9].

On applying the theory, first the transformation \mathbf{A} (i.e., the relation between the two lattices) has to be formulated, such that it relates the *nearest neighbors* in the two lattices. Then eq (3) is determined and solved by routine linear algebra techniques.

We call the solutions of eq (2) "0-elements." These may be 0-points, 0-lines, or 0-planes according to whether the rank of the matrix $(\mathbf{I}-\mathbf{A}^{-1})$ is 3, 2 or 1.

If the rank of $(\mathbf{I}-\mathbf{A}^{-1})$ is 2 then the three linear equations represented by (3) are linearly dependant. Hence, in order to furnish solutions certain restrictions have to be given for \mathbf{b} , which, in geometrical terms, confine their values to those lying in a plane through the origin in b -space. We call this plane a two-dimensional b -subspace. Hence only b -lattice points within that b -subspace are imaged as an 0-line. The orientation of the 0-line then is determined by the invariant eigenvector (eigenvalue $\lambda=1$) of the transformation \mathbf{A} . (In the case that rank $(\mathbf{I}-\mathbf{A}^{-1})=1$ the b -subspace is a line through the origin and the 0-elements are parallel planes.)

The complications arising when few or no b -lattice points lie within the b -subspace are discussed in reference [9]. b -lattice points lying next to the b -subspace can be perpendicularly projected onto the b -subspace and be imaged as 0-elements if within the transformation \mathbf{A} translation is allowed perpendicular to the b -subspace.

We now separate the different 0-elements by cell walls and so introduce a cell structure into the interpenetrating lattices. The most appropriate cell walls appear to be the images of Wigner-Seitz walls between b -lattice points. This leads, for a cell wall between the primary origin and a neighboring 0-element, to the equation:

$$\left[\tilde{\mathbf{b}}^{(L)} \mathbf{G} (\mathbf{I}-\mathbf{A}^{-1}) \right] \mathbf{x} - \frac{1}{2} (\tilde{\mathbf{b}}^{(L)} \mathbf{G} \mathbf{b}^{(L)}) = 0, \quad (4)$$

with $\tilde{\mathbf{b}}^{(L)}$ = transpose of $\mathbf{b}^{(L)}$ i.e., a line vector;
 \mathbf{G} = metric tensor of the chosen coordinate system.

This equation is derived in reference [10].

As mentioned above, every 0-point (within any 0-element) can be considered as an origin of the transformation \mathbf{A} between the *whole* of lattice 1 and the *whole* of lattice 2, but is considered only as an origin for the relation between the two lattices *within* the corresponding 0-lattice cell. Thus there are an infinity of origins throughout the two interpenetrating crystal lattices. At the cell wall the pairing, the coordination, changes by the vector \mathbf{b} which is the difference vector between the two b -lattice points, the images of which are the two 0-elements adjacent at the cell wall.

We summarize here briefly the procedure for calculating the 0-lattice:

(a) The transformation \mathbf{A} between the two lattices eq (2) has to be formulated. This point will be further discussed in the next chapter.

- (b) The 0-lattice is calculated by means of eq (3), and
- (c) the cell walls using eq (4).

III. The Transformation A

The formulation of the transformation A is discussed in references [9], [10], and [11]. We describe here briefly the basic problems.

There are many possibilities of imaging one lattice onto another. As an example we may think of a square lattice where \mathbf{A} may be a rotation by 10° . The same lattice 2 is obtained by a rotation of $90^\circ + 10^\circ$ etc. but also by a rotation of 10° and then a shear etc. Every transformation furnishes a different 0-lattice and the question arises which one is physically the most significant. Obviously it is the one for which \mathbf{A} relates the nearest neighbors in the two lattices. This is the one for which the determinant $|\mathbf{I} - \mathbf{A}^{-1}|$ has the smallest value and hence furnishes the largest unit cell for the 0-lattice. On varying the transformation continuously (e.g., increasing the angle of rotation) it may be needed to switch transformations in order to relate always the nearest neighbors. For example, for rotation over a range of 90° on the $\{112\}$ -plane in the bcc-structure, four different transformations are needed as shown by the author and A. J. Perry [10]. Hence, although the two crystals may be of the same nature, they often have to be treated as if they had different unit cells in order to relate the nearest neighbors. From the mathematical side there is very little difference whether we are dealing with grain- or with phase-boundaries.

IV. Problems Related to the Choice of the Crystal Boundary

When we choose a crystal boundary within the interpenetrating lattices we place it as far as possible through 0-elements. By doing this we have to cut cell walls. We call the line of intersection of a cell wall with the chosen crystalline interface a "mathematical dislocation" as it is the line where the coordination changes. Parallel to the choice of the crystal boundary we pick out all the b -lattice points corresponding to the intersected 0-elements. All these b -lattice points together form the b -net.

We now consider two limiting cases:

- (1) The 0-lattice unit is large compared to the crystal unit.
- (2) The 0-lattice unit is about the same size as the crystal unit.

In the case (1) the mathematical dislocation becomes a "physical dislocation" by relaxation of the atoms. The Burgers vector of this dislocation can be obtained from the b -lattice through the dualism between the dislocation network and its " b -net" (ref. [3]).

We summarize briefly the dualism between the dislocation network and the *b*-net.

<i>Dislocation network (L)</i>		<i>b</i> -net
(1) To every L-field (0-element) limited by dislocations	corresponds	a <i>b-node</i> (<i>b</i> -lattice point) in the <i>b</i> -net.
(2) To every L-node in the dislocation network	corresponds	a <i>closed b-polygon</i> in the <i>b</i> -net.
(3) A dislocation line separates two L-fields while	the corresponding	Burgers vector connects the two corresponding nodes of the <i>b</i> -net (<i>b</i> -lattice points).

The sign relation between line sense of the dislocation and the Burgers vector is given below by (4). It is a dualism between rotation (curl) and divergency. The line sense of the dislocation fixes a curl around the L-field and as such determines a curl vector perpendicular to the L-field (right hand screw). A Burgers vector can point out of a *b*-node or into it and thus defines a sign of a divergency (positive if the vector flows out). In this term the dualism 4 becomes:

- | | |
|---|--|
| (4) If the <i>curl vector</i> of the L-field of a given 0-element points into crystal 2 | the <i>divergency</i> of the corresponding <i>b-node</i> (<i>b</i> -lattice point) is <i>positive</i> . |
|---|--|

These dualisms hold for any mathematical dislocation network. The general meaning of these dislocations and Burgers vectors will be discussed in section V.

For example for the case of rotation by an angle θ of a fcc lattice around its $\langle 111 \rangle$ -axis, the 0-lattice is a hexagonal line-lattice with the 0-lines parallel to the axis of rotation, and the cell walls form a hexagonal honeycomb structure. The *b*-subspace is the $\{111\}$ -plane of the *b*-lattice. Choosing the boundary perpendicular to the axis of rotation furnishes a twist-boundary; and choosing a cut parallel to the axis a tilt-boundary which can be straight or stepped (reference [3]). For small angles θ of rotation eq (3) reduces to Frank's formula

$$\mathbf{b}^{(L)} = [\boldsymbol{\theta} \times \mathbf{x}^{(0)}]. \quad (5)$$

We may distinguish two kinds of problem related to the choice of the boundary:

(a) The two crystals with their relative orientations are given and hence the 0-lattice with its cell structure is determined. The question is as to what kinds of boundaries are possible and which ones are the most favorable. This type of problem was mentioned above in relation to subgrain boundaries.

(b) The two crystals are given but their relative orientation has to be determined such that a boundary (which is to be determined too) is stable in the sense that any change in the orientation of the boundary as well as of the crystals leads to an increase in energy.

For this type (b) of problem an energy criterion has to be defined. The calculation of the actual energy of a general phase boundary is very complicated. For a general grain or phase boundary formed by a "physical" dislocation network the actual energy function may be replaced by a geometrical function with the single property of behaving monotonically with the energy. With d the spacing of one type of dislocations in a dislocation network and b the absolute value of their Burgers vector, the following replacement function p was chosen:

$$p = \sum_i \left(\frac{b_i}{d_i} \right)^2 \quad (6)$$

where the sum is taken over the number of independent sets of dislocations (which may be 1 or 2).

This function is positive except when the dislocation spacing goes to infinity. Then p becomes zero but then there is no boundary left. p has a meaning only in the limiting case (1) (0-lattice unit large compared to crystal unit).

The procedure for calculating a boundary was tested on a monoclinic-triclinic two-phase system (exsolved alkali feldspar) where the calculated relative orientations of the crystals (see ref. [11] by the author and H.-U. Nissen) as well as the orientation of the optimal boundary agrees well with the previously measured values for this mineral.

The most striking aspect of that calculation is that the result is right although the only crystal data used are the two sets of six lattice constants. No knowledge was needed of how the unit cells are filled with atoms, nor of atomic forces, atomic positions and elastic constants. This shows that the best geometrical fit is (at least here) also energetically the most favorable one.

In the case No. 2 where the 0-lattice unit is comparable in size with the crystal unit, the "mathematical dislocations" may no longer contract to physical dislocations. But low energy boundaries will still be possible due to a highly periodic pattern of the lattice points (coincidence site lattice). We may divide the total *pattern* of the lattice points of the two crystal lattices into "pattern elements" i.e., the parts of the pattern within one 0-lattice cell. A periodic pattern will consist of a finite number of different pattern elements; a nonperiodic one of an infinity of them. For a given transformation \mathbf{A} a pattern element is given by the internal coordinates (i.e., the equivalence class) of its 0-point. Hence, in order

to find the number of different pattern elements one has to find the number of different related equivalence classes containing coinciding elements. A computer technique for this purpose was developed (ref. [10]).

If a minimum energy pattern exists and if the energy is such that the crystal tends to conserve the pattern on a slight change in orientation of lattice 2, then the crystal accomplishes this by means of a dislocation network of "secondary dislocations" or boundary dislocations. These secondary dislocations are calculated analogously to the primary ones except that the 02-lattice is now an O-lattice of two O-lattices instead of two crystal lattices (ref. [9], p. 395). More about secondary dislocations is given in the next section.

V. Dislocations in Crystalline Interfaces

As we shall extend the notion of dislocation to general crystalline interfaces, we shall have to point out a few known properties of single dislocations, and then we shall investigate what properties are conserved. We know the dislocation as a line with a strain field. Attributed to the dislocation is a pseudo-vector, the Burgers vector. The Burgers vector is invariant along the line and continuous on branching of the lines (Frank's node condition).

We should point out that dislocations with the invariance properties of the Burgers vector are only possible in a periodic or elastically distorted periodic substratum. In a continuum one could introduce a wedge-shaped Volterra cut, and there an invariant Burgers vector could not be defined. For the standard dislocations this substratum is given by the crystal itself. We shall see that for secondary dislocations the substrata are different.

First we have to review the definition of the Burgers vector. Frank's definition by a Burgers circuit imaged onto a reference lattice is a specific way to express that the Burgers vector is a *coordinate difference* independent of any elastic distortion of the coordinate system of the real crystal. Only as a coordinate difference is it conserved.

There is another way of defining the Burgers vector from the kinetic behavior of the dislocation through the so-called "movement rule." A dislocation line (line sense **I**, Burgers vector **b**) moving through a crystal in the direction **v** virtually divides the crystal into two parts. Then the part marked (i.e., labeled) by

$$\mathbf{m} = [\mathbf{l} \times \mathbf{v}] \quad (7)$$

is shifted by **b** when the dislocation passes by. The other part is considered as fixed.

Here only the state of the perfect crystal before and after the passage of the dislocation is considered. No strain field has to be taken into account. We ask, what does the (perfect) dislocation do to the crystal on moving through it? The answer is that it translates one part with respect to the other but such that the arrangement of lattice points, the pattern, is the same after the transition as before i.e., that structure as well as the position of the pattern is conserved. This definition is consistent with the others, i.e., with the pseudo-vector character of \mathbf{b} .

We shall now see how far these definitions and properties hold for dislocations in crystalline interfaces. We defined the "mathematical dislocation" as the line of intersection of the crystal boundary with the 0-lattice cell wall, and the Burgers vector by the dualism between 0- and b -lattice.

The question now arises how the above definitions by the Burgers circuit and the movement rule hold for the general "mathematical dislocations" e.g., in a twist boundary where the twist is 30° . Here surely the strain field of the "dislocation" will be completely different from the one of the single dislocation in the crystal.

A Burgers circuit may be started in crystal 1. Then we may pass in steps of translation vectors to a point $\mathbf{x}^{(1L)}$ in the field on the 0-element 0, go to $\mathbf{x}^{(2L)}$ which is related to $\mathbf{x}^{(1L)}$ by the eq (8)

$$\mathbf{x}^{(2L)} - \mathbf{x}^{(0)} = \mathbf{A}(\mathbf{x}^{(1L)} - \mathbf{x}^{(0)}). \quad (8)$$

From here we move within crystal 2 around the dislocation into the field of the 0-element 0' and from there back to crystal 1 (eq (9)).

$$\mathbf{x}^{(1L)'} - \mathbf{x}^{(0)'} = \mathbf{A}^{-1}(\mathbf{x}^{(2L)} - \mathbf{x}^{(0)}'). \quad (9)$$

We can introduce a reference lattice also here as a help for counting the coordinate steps. The related coordinate steps in lattice 1 and 2 are equivalent and points related by eq (8) resp. (9) are identical in this reference lattice.

Now, the Burgers circuit has to be such that its image in the reference lattice is closed. If the Burgers circuit forms a right-handed screw with the line sense l , b points from the *beginning* to the *end* of the circuit in the crystal lattice. It can be shown that all the steps cancel out except the two transitions from one lattice into the other.

By eliminating $\mathbf{x}^{(2L)}$ from eq (8) and (9) one obtains:

$$(\mathbf{I} - \mathbf{A}^{-1})(\mathbf{x}^{(0)'} - \mathbf{x}^{(0)}) = \mathbf{x}^{(1L)'} - \mathbf{x}^{(1L)}. \quad (10)$$

Hence the closure failure is a difference of two lattice vectors, and thus

a translation vector of lattice 1. On the other hand it follows from eq (3) that

$$(\mathbf{I} - \mathbf{A}^{-1})(\mathbf{x}^{(0)\prime} - \mathbf{x}^{(0)}) = \mathbf{b}^{(1)\prime} - \mathbf{b}^{(1)}, \quad (11)$$

which shows that the closure failure is identical with the difference of the two b -lattice vectors related to the two 0-points. If we begin and end in crystal 2 in the same sense of rotation we obtain a closure failure of $\mathbf{x}^{(2L)} - \mathbf{x}^{(2L)\prime}$, and this difference vector transformed to lattice 1 equals $\mathbf{b}^{(1\prime)} - \mathbf{b}^{(1)}$:

$$\mathbf{A}^{-1}(\mathbf{x}^{(2L)} - \mathbf{x}^{(2L)\prime}) = \mathbf{b}^{(1)\prime} - \mathbf{b}^{(1)}. \quad (12)$$

It thus corresponds to the Burgers vector defined by the dualism between the dislocation network and the b -net.

Actually the closure failures in the two crystals are two different vectors (in our example they are rotated by 30°) but if we consider them as *the* Burgers vector we have to understand them as *the identical coordinate difference* in the two different coordinate systems of the two crystals related by the transformation A.

The situation is exactly analogous to that of the single dislocation in the otherwise perfect crystal. The vector steps in the elastically distorted crystal which differ from place to place are taken as identical, just as we take the related coordinate differences in both crystals as identical.

The Burgers vector defined in this way is conserved not only within the crystals but also throughout the boundary. Even if a dislocation branches off from the boundary into the crystal there is complete balance of the system (ref. [12]).

The definition of the Burgers vector by the movement rule can be extended into the boundary as well. If a dislocation is moved by a definite amount v , so that a 0-point moves into the position of its neighbor, then that lattice which is marked by \mathbf{m} moves by one of its own translation vectors.

In these terms practically every crystalline interface is a "dislocation network" even if the dislocation spacing is of the order of the lattice constant. Exceptions, however, are undisturbed twin boundaries which fit over a whole 0-plane.

We call the dislocations discussed up to here in this section "primary dislocations." These include the standard dislocations in low angle boundaries but also the "mathematical dislocations" (intersection of boundary with 0-lattice cell walls) in arbitrary interfaces.

It was pointed out before that a dislocation with an invariant Burgers vector can only be defined on a periodic substratum. It may happen that

the pattern formed by the superposition of the two crystal lattices becomes highly periodic such that at the boundary the arrangement of a small group of atoms is periodically repeated. Such a pattern may form a minimum energy state, which the crystal tends to conserve on slight deviations from the optimum orientation. In the case of such an optimum pattern, the balance of the primary dislocation network can be closed and the whole pattern can be regarded as a new "perfect crystal" i.e., a periodic substratum for dislocations, the secondary dislocations. The Burgers vectors of secondary dislocations are, according to the movement rule, displacements which conserve the structure of the pattern but not necessarily its position. The periodic pattern is a kind of moiré pattern which can be displaced while one crystal is translated with respect to the other. The Burgers vectors of the secondary dislocations are rational fractions of those of the primary dislocations. Hence the Burgers vectors of the primary dislocations are included in the secondaries but a displacement by such a primary Burgers vector always conserves the position of the pattern as well. The analysis of patterns and the calculation of secondary dislocations are given in reference [10].

If we look at the problem of interfaces from the standpoint of primary dislocations, we can consider the two crystals as one crystal which contains a dislocation network. On the other hand if we investigate secondary dislocations we have to treat the two joining crystals as a sandwich of three crystals, crystal 1, the periodic interface and crystal 2, and we have to balance the Burgers vectors with respect to all three of them.

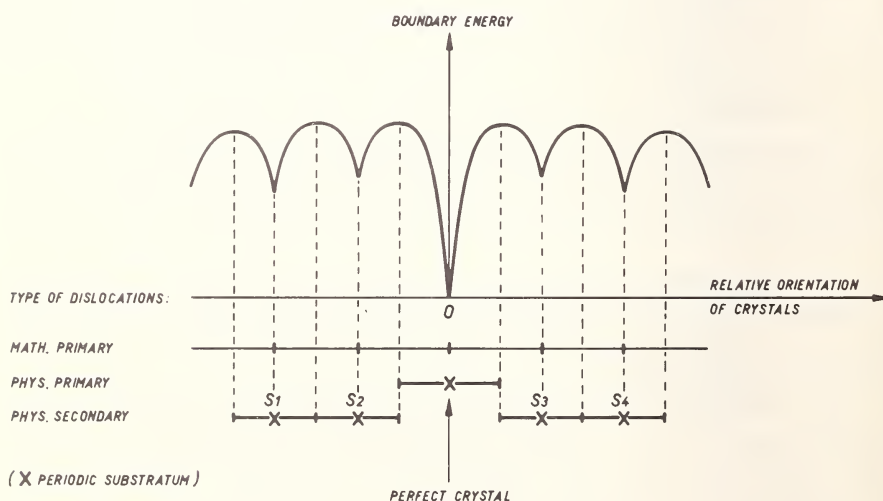


FIGURE 1. Schematic diagram of the ranges of different kinds of dislocations in boundaries.

In reference [12] figure 2 the situation of an edge dislocation passing through a twist boundary of $\theta = 36^\circ 52.2'$ on the {001} face in a cubic system is discussed. This twist furnishes a highly periodic pattern (ref. [10] table I). From the standpoint of primary dislocations, the edge dislocation in crystal 1 is identical to the one in crystal 2. The boundary network is balanced. But a secondary dislocation is left in the boundary. Hence from the standpoint of secondary dislocations, the edge dislocations in both crystals are different.

Figure 1 gives a schematic view of the ranges of different kinds of dislocations.

VI. Summary

It was shown that by means of the 0-lattice theory the dislocation concept can be extended to arbitrary crystalline interfaces. The extension of the standard dislocation is the primary dislocation. If a certain configuration forms a minimum energy pattern, then deviations from that pattern are secondary dislocations. On moving through the crystal primary dislocations conserve the structure as well as the position of the pattern, while in general secondary dislocations only conserve the structure but displace the pattern. The Burgers vectors of the secondary dislocations are rational fractions of those of the primary dislocations. While primary dislocations can exist throughout the crystals, secondaries are only possible within the boundary.

VII. Acknowledgements

The author would like to thank Dr. M. H. Boon for reading through the manuscript and the Battelle Institute for financial support.

VIII. References

- [1] Frank, F. C., in Conference on Plastic Deformation of Crystalline Solids (Mellon Institute, 1950) p. 150; in Conference on Defects in Crystalline Solids (Physical Society, London, 1955) p. 159.
- [2] Amelinckx, S., and Dekeyser, W.. Solid State Physics, **8**, F. Seitz and D. Turnbull, Eds. (Academic Press, London and New York, 1959) p. 325.
- [3] Bollmann, W., Phil. Mag. **7**, 1513 (1962); Discuss. Faraday Soc. **38**, 26 (1964).
- [4] Nabarro, F. R. N., Theory of Crystal Dislocations (The Clarendon Press, Oxford, 1967).
- [5] Hirth, J. P., and Lothe, J.. Theory of Dislocations (McGraw-Hill, New York, 1968).
- [6] Brandon, D. G., Ralph, B., Ranganathan, S., and Wald, M. S., Acta Met. **12**, 813 (1964).
- [7] Brandon, D. G., Acta Met. **14**, 1479 (1966).
- [8] Ranganathan, S., Acta Cryst. **21**, 197 (1966).
- [9] Bollmann, W., Phil. Mag. **16**, 363, 383 (1967).
- [10] Bollmann, W., and Perry, A. J., Phil. Mag. **20**, 33 (1969).
- [11] Bollmann, W., and Nissen, H.-U., Acta Cryst. **A24**, 546 (1968).
- [12] Bollmann, W., in Dislocation Dynamics, A. R. Rosenfield et al., Eds. (McGraw-Hill, New York, 1968) p. 275.

STRUCTURAL AND ELASTIC PROPERTIES OF ZONAL TWIN DISLOCATIONS IN ANISOTROPIC CRYSTALS

M. H. Yoo and B. T. M. Loh

Metals and Ceramics Division
Oak Ridge National Laboratory
Oak Ridge, Tennessee 37830

A descriptive definition of zonal twin dislocations for compound twin systems is given based on the well established rational crystallographic elements. Geometric characteristics of zonal twin dislocations in double lattice structures are thoroughly discussed. Equilibrium shapes of an incoherent twin boundary have been analyzed by using the anisotropic elastic properties of edge dislocations. Short-ranged structural properties of zonal twin dislocations are discussed based on a Peierls-Nabarro model. It is found that the "anisotropic parameter," $K_c S_{66}$, correctly predicts the active mode of crystallographically non-equivalent conjugate twin systems.

Key words: Dislocation geometry; twinning; zonal dislocations.

I. Introduction

Frank and van der Merwe [1] first pointed out that a state of strain similar to that around a perfect dislocation exists around a step in a coherent twin interface. Frank [2] defined this step as a *twin dislocation* and called the glissile-type a *twinning dislocation*,¹ of which Burgers vector, \mathbf{b}_t , is the closure failure of a Burgers circuit that would close in a perfectly coherent twin. The magnitude of the Burgers vector is determined as the height of the step multiplied by the twinning shear, g , such that for a single twin dislocation $b_t = g \cdot d$, where d is the interspacing of twin lattice planes. When such a twin dislocation moves along the twin interface, the result is to transform a layer of the lattice from matrix to twin, or the reverse, depending on the direction of movement.

¹ All the *twin dislocations* considered in this paper are Shockley type imperfect dislocations since their Burgers vectors lie in the twin plane, hence *twinning dislocations*. But for brevity, they will be called *twin dislocations* throughout the discussion.

In double lattice structures, the structures based on two interpenetrating lattices, a single step must necessarily be the one with the height of an integral multiple of d in order that the equivalence of the atomic configuration at the new interface to that at the original interface be maintained. This feature was first pointed out by Thompson and Millard [3], who suggested that for $\{10\bar{1}2\} \langle 10\bar{1}\bar{1} \rangle$ twinning in hexagonal-close-packed (h.c.p.) structure a "double" twin dislocation which signifies a step with the height $2d$ would be physically more meaningful than a single twin dislocation although the "double" twin dislocation would be energetically unstable due to the repulsion between its two components. Recognizing the fact that homogeneous shear occurs on every second $(10\bar{1}2)$ twin plane, Westlake [4] proposed that it would exist, not as two twin dislocations, but as one *zonal* twin dislocation, in analogy to the *zonal* slip dislocations in complex structures that were originally conceived by Kronberg [5]. The concept of zonal dislocations was extended by Rosenbaum [6] in his study of atom movements and formation of faults during $\{11\bar{2}2\} \langle 11\bar{2}3 \rangle$ slip and twinning in h.c.p. structure.

In view of the fact that deformation twinning is one of the two fundamental processes of plastic deformation in crystalline solids, slip being the other, it is deemed necessary to give a full account of geometric characteristics of zonal twin dislocations and to elucidate some basic properties inherent to these dislocations. In this paper a descriptive definition is given of zonal twin dislocations for compound twin systems in metallic structures, which is followed by a discussion on the geometric characteristics. For a total of fifty twin systems in various metals selected from cubic to orthorhombic crystal system, the long-range elastic properties of zonal twin dislocations are calculated by using anisotropic elasticity theory and applied in an analysis of stable configurations of an incoherent twin boundary. Some typical results are presented and discussed in this paper. Based on a Peierls-Nabarro type model an "anisotropic parameter" is introduced and tested as a factor of energetic criteria for operative twin modes.

II. ZONAL TWIN DISLOCATIONS

Consider a compound twin system with the well defined rational crystallographic elements, K_1 , K_2 , η_1 , and η_2 . The macroscopically homogeneous deformation of twinning can be completely described in terms of these crystallographic elements and the parameters that are given in figure 1. When a reference unit cell with the base vectors, η_1 , η_2 , and S , where S is the translation vector normal to the plane of shear S , is sheared homogeneously as described in figure 1, the result is a unit cell of the twinned lattice with the base vectors, η_1' , η_2' , and S . That

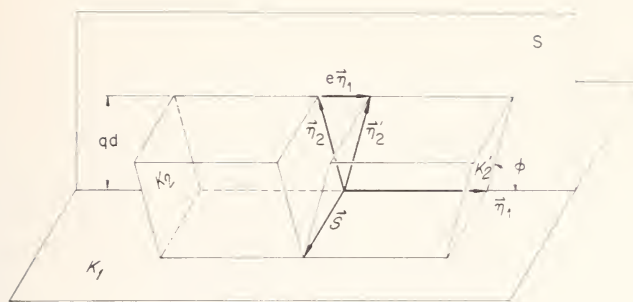


FIGURE 1. Crystallographic elements of twinning.

is, while K_1 , η_1 , and S remain fixed, K_2 and η_2 are rotated about S by $(\pi - 2\varphi)$ to become K'_2 and η'_2 , respectively, where φ is the acute angle between η_1 and η_2 (or η'_2). Hence, the twinning shear is $g = 2 \cot \varphi = e\eta_1/qd$, where q is the number of K_1 lattice planes intersected by the vector η_2 , and e is a numerical factor that depends on crystal structure [7]. From the following general relationship

$$\frac{e}{2} = \frac{1}{\eta_1} [\eta_2^2 - (qd)^2]^{1/2} \quad (1)$$

the expressions for e for the fifteen compound twin systems in structures ranging from cubic to orthorhombic crystal system are obtained and are given in tables 1 and 2 together with the crystallographic elements and other parameters. The numerical value of e is simply $2/3$ for both of the twin systems in cubic structures, whereas for the rest e is related to the axial ratio or angle of the unit cell of the Bravais lattice of the structure.

In double lattice structures inhomogeneous motion, shuffling, of some atoms in addition to a homogeneous shear deformation of the reference unit cell is generally required if the original crystal structure is to be restored after twinning. When q is even, however, as in all the compound twin systems under consideration, one can show that the atoms (or the double motif unit) at every n th twin plane are sheared to their correct positions, where $2n = q$, and that the shuffling is periodic with the period of nd . Therefore, a zonal twin dislocation can be regarded as a step in the interface with the step height of nd .

Based on the geometrical relationships described above, the Burgers vector of a zonal twin dislocation in compound twin systems can be expressed as $\mathbf{b}_z = n\mathbf{b}_t$, where \mathbf{b}_t is the Burgers vector of a *unit twin dislocation* as named by Yoo and Wei [7], and may be given as $\mathbf{b}_t = (e/q)\eta_1$.

TABLE 1. *Crystallographic elements and parameters of compound twin systems.* $\gamma = \frac{c}{a}$, $\beta = \frac{b}{a}$,
 $\alpha = \text{rhombohedral angle}$, and $A = (1 - \cos \alpha)(1 + 2 \cos \alpha)$

Crystal structure (type)	K_1	K_2	η_1	η_2	S	q	g	$\frac{e}{2}$	
								η_1	η_2
f.c.c. (A1)	{111}	{11̄1}	$\frac{1}{2}\langle 11\bar{2} \rangle$	$\frac{1}{2}\langle 112 \rangle$	$\frac{1}{2}\langle 1\bar{1}0 \rangle$	2	$\frac{1}{\sqrt{2}}$		$\frac{1}{3}$
b.c.c. (A2)	{112}	{11̄2}	$\frac{1}{2}\langle 1\bar{1}1 \rangle$	$\frac{1}{2}\langle 111 \rangle$	$\frac{1}{2}\langle 1\bar{1}0 \rangle$	2	$\frac{1}{\sqrt{2}}$		$\frac{1}{3}$
f.c.t. (A5) In	{101}	{10̄1}	$\frac{1}{2}\langle 10\bar{1} \rangle$	$\frac{1}{2}\langle 101 \rangle$	$\langle 0\bar{1}0 \rangle$	2	$\frac{\gamma^2 - 1}{\gamma}$		$\frac{\gamma^2 - 1}{\gamma^2 + 1}$
b.c.t. (A6) Sn	{301}	{10̄1}	$\langle \bar{1}03 \rangle$	$\langle 101 \rangle$	$\langle 010 \rangle$	4	$\frac{3\gamma^2 - 1}{2\gamma}$	$\frac{3\gamma^2 - 1}{9\gamma^2 + 1}$	$\frac{3\gamma^2 - 1}{\gamma^2 + 1}$
rhombohedral (A7, A10)	{110}	{001}	$\langle 00\bar{1} \rangle$	$\frac{1}{2}\langle 110 \rangle$	$\frac{1}{2}\langle 1\bar{1}0 \rangle$	2	$\frac{2\sqrt{2} \cos \alpha}{\sqrt{A}}$	$\cos \alpha$	$\frac{2 \cos \alpha}{1 + \cos \alpha}$
orthorhombic U (A20)	{130}	{11̄0}	$\frac{1}{2}\langle 3\bar{1}0 \rangle$	$\frac{1}{2}\langle 110 \rangle$	$[00\bar{1}]$	2	$\frac{\beta^2 - 3}{2\beta}$	$\frac{\beta^2 - 3}{\beta^2 + 9}$	$\frac{\beta^2 - 3}{\beta^2 + 1}$

TABLE 2. *Crystallographic elements and parameters of compound twin systems in h.c.p.
structure (A3).* $\gamma = \frac{c}{a}$

K_1	K_2	η_1	η_2	S	q	g	$\frac{e}{2}$	
							η_1	η_2
{10̄12}	{101̄2}	$\pm\langle 10\bar{1}1 \rangle$	$\pm\langle 10\bar{1}1 \rangle$	$\pm\frac{1}{3}\langle 1\bar{2}10 \rangle$	4	$\frac{\gamma^2 - 3^*}{\gamma\sqrt{3}}$		$\frac{\gamma^2 - 3^*}{\gamma^2 + 3}$
{10̄11}	{101̄3}	$\langle 10\bar{1}2 \rangle$	$\langle 30\bar{3}2 \rangle$	$\frac{1}{3}\langle 1\bar{2}10 \rangle$	8	$\frac{4\gamma^2 - 9}{4\gamma\sqrt{3}}$	$\frac{4\gamma^2 - 9}{4\gamma^2 + 3}$	$\frac{4\gamma^2 - 9}{4\gamma^2 + 27}$
{11̄22}	{112̄4}	$\frac{1}{3}\langle 11\bar{2}3 \rangle$	$\frac{1}{3}\langle 22\bar{4}3 \rangle$	$\langle 1\bar{1}00 \rangle$	6	$\frac{2(\gamma^2 - 2)}{3\gamma}$	$\frac{\gamma^2 - 2}{\gamma^2 + 1}$	$\frac{\gamma^2 - 2}{\gamma^2 + 4}$
{11̄21}	(0002)	$\frac{1}{3}\langle 1\bar{1}26 \rangle$	$\frac{1}{3}\langle 11\bar{2}0 \rangle$	$\langle \bar{1}100 \rangle$	2	$\frac{1}{\gamma}$	$\frac{1}{4\gamma^2 + 1}$	1

*Absolute value of the difference.

Hence, the Burgers vector of a zonal twin dislocation can be defined as

$$\mathbf{b}_z = \frac{e}{2} \boldsymbol{\eta}_1 \quad (2)$$

for the compound twin systems.² The present definition by eq (2) is consistent with the one given by Saxl [10], who used the notations introduced by Bilby and Crocker [11]. The Burgers vector of a zonal twin dislocation can be determined graphically also with a Burgers circuit by means of the start-to-finish right-handed rule given by Frank [2]. The Burgers circuit must be constructed following a lattice network generated by the two interpenetrating reference lattices with a translation vector [1/2, 1/2, 0] as shown in figure 2. The closure failure denoted by SF in figure 2b is equal to \mathbf{b}_z as defined by eq (2).

When $q=2$ ($n=1$), as for $\{111\} \langle 11\bar{2} \rangle$ in face-centered-cubic (f.c.c.), $\{112\} \langle 11\bar{1} \rangle$ in body-centered-cubic (b.c.c.), $\{11\bar{2}\bar{1}\} \langle \bar{1}\bar{1}26 \rangle$ twinning in h.c.p. structure, etc. (see table 1), it follows that the zonal twin dislocations are simply reduced to their unit twin dislocations. Furthermore, in the cubic structures the unit twin dislocation is identical with the imperfect slip dislocation. Such relationships between slip and twin dislocations can be generally correlated by using eq (2). Since $\boldsymbol{\eta}_1$ is a

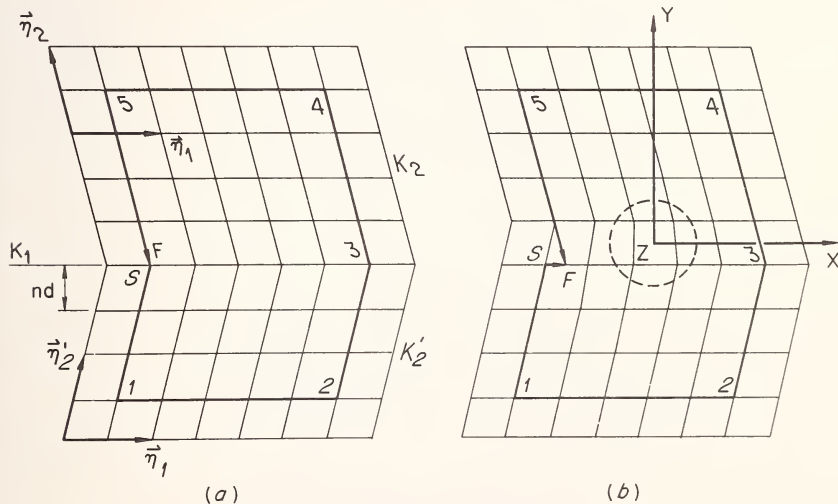


FIGURE 2. Start-to-finish right-handed Burgers Circuit in (a) a coherent twin boundary and (b) an incoherent twin boundary. The plane of drawing is the plane of shear and also $Z=0$.

² An alternative definition is given by Mendelson [8, 9].

lattice vector, $e/2$ must be equal to a ratio of two integers in order for any dislocation reaction involving perfect and imperfect dislocations to give rise to a zonal twin dislocation. Such a condition is satisfied only for f.c.c. and b.c.c. structures, that is, $e/2 = 1/3$. This may be a feature which constitutes the essential difficulty in envisaging a dislocation model of twin nucleation in non-cubic crystal structures. By whatever the nucleation mechanism, however, once a twin interface is created, production of zonal twin dislocations can be fully accounted for by various dislocation reactions possible at the interface as discussed by Bilby [12]. In an analysis of the incorporation processes of slip dislocations into twins, for instance the work on h.c.p. structure by Yoo [13], the concept of zonal twin dislocations ensures that no single imperfect slip dislocation trailing a fault behind it, will result in a twin when a slip dislocation is incorporated into the twin.

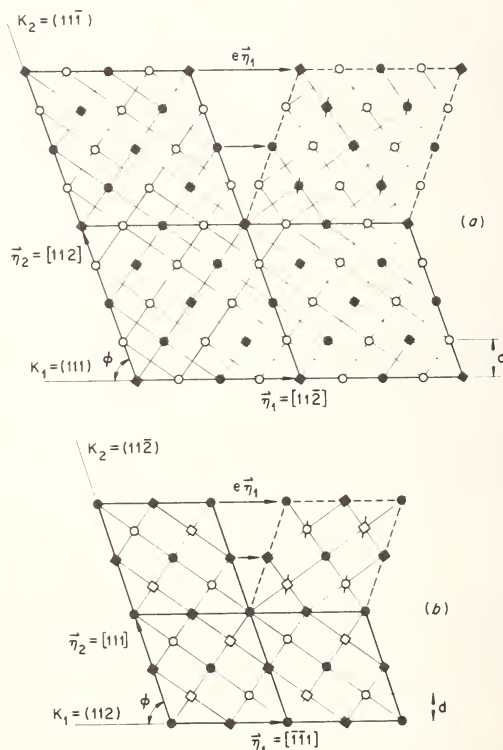


FIGURE 3. Twinning in ordered cubic alloys. $q = 4$, $\varphi = 70^\circ 32'$. (a) AB_3 alloy with $L1_2(\text{Cu}_3\text{Au})$ structure. (b) AB alloy with $B2(\beta\text{-brass})$ structure. Squares represent A atoms, and circles represent B atoms. Filled symbols represent atoms in the plane of projection, and open symbols represent those on the adjacent planes.

The present definition of zonal twin dislocations is a general one and applicable also to ordered structures. For fully ordered cubic structures ($L1_2$ and $B2$ types), as depicted in figure 3, η_1 , η_2 , S , and q should necessarily be twice as large as those for the corresponding $A1$ and $A2$ structures, their fully disordered structures.

III. Elastic Properties

The anisotropic elasticity theory of dislocations developed by Eshelby et al. [14] is applied to calculate the elastic properties of zonal twin dislocations. Since twin dislocations are situated in the twin interface, their long-range elastic properties will vary with the extent of the anisotropic media on both sides of the interface. Possible configurations of a twin in an infinite medium may be classified into the following three cases: (a) $N=n$, a monolayer twin, where Nd is the thickness of a twin; (b) $N > n$, a twin of a finite thickness; and (c) $N \gg n$, the thickness of a twin is much greater than the step height. The intermediate case (b) is a realistic representation of a twin of finite volume embedded in the parent matrix. For this case, one must solve a boundary value problem of anisotropic elasticity theory in order to obtain a solution of zonal twin dislocations. In this paper, the solutions of an edge zonal twin dislocation for the case (a) are calculated numerically using the procedures developed by Stroh [15], and, as a first approximation, they are used in the analysis of dislocation interactions.

With respect to the Cartesian coordinate system chosen such that x_3 -axis coincides with the dislocation line, and $x_2=0$ plane is K_1 plane, the stress fields of a straight dislocation in general can be given as

$$\sigma_{ij}(x_1, x_2) = \frac{Kb}{2\pi} \sum_{\alpha=1}^3 \frac{A_{ij\alpha}x_1 + B_{ij\alpha}x_2}{(x_1 + r_\alpha x_2)^2 + (q_\alpha x_2)^2}, \quad (3)$$

where b is the Burgers vector, and K is an energy factor. $A_{ij\alpha}$, $B_{ij\alpha}$, and K are real coefficients related to the elastic constants and also to r_α and q_α which are the real and imaginary parts of the complex roots for a sextic equation. Since a pure edge dislocation (x_3 -axis) lies perpendicular to the plane of shear S which is a symmetry plane, the secular equation governing the elastic solutions is a quartic equation, and $\alpha=1, 2$. For such a case in general, the numerical solutions of r_α and q_α and the explicit expressions of K , $A_{ij\alpha}$, and $B_{ij\alpha}$ have been obtained, which will be reported elsewhere [16]. As a typical result, σ_{11} , σ_{22} , $\bar{\sigma}_{12}$, and σ_{33} stress fields and Δ_e dilatation field are presented by contour plots in figure 4 for an edge twin dislocation of α -Fe with $\mathbf{b}_t=1/6 [11\bar{1}]$. As contrasted to the case discussed by Chou [17], where $x_2=0$ is also a symmetry

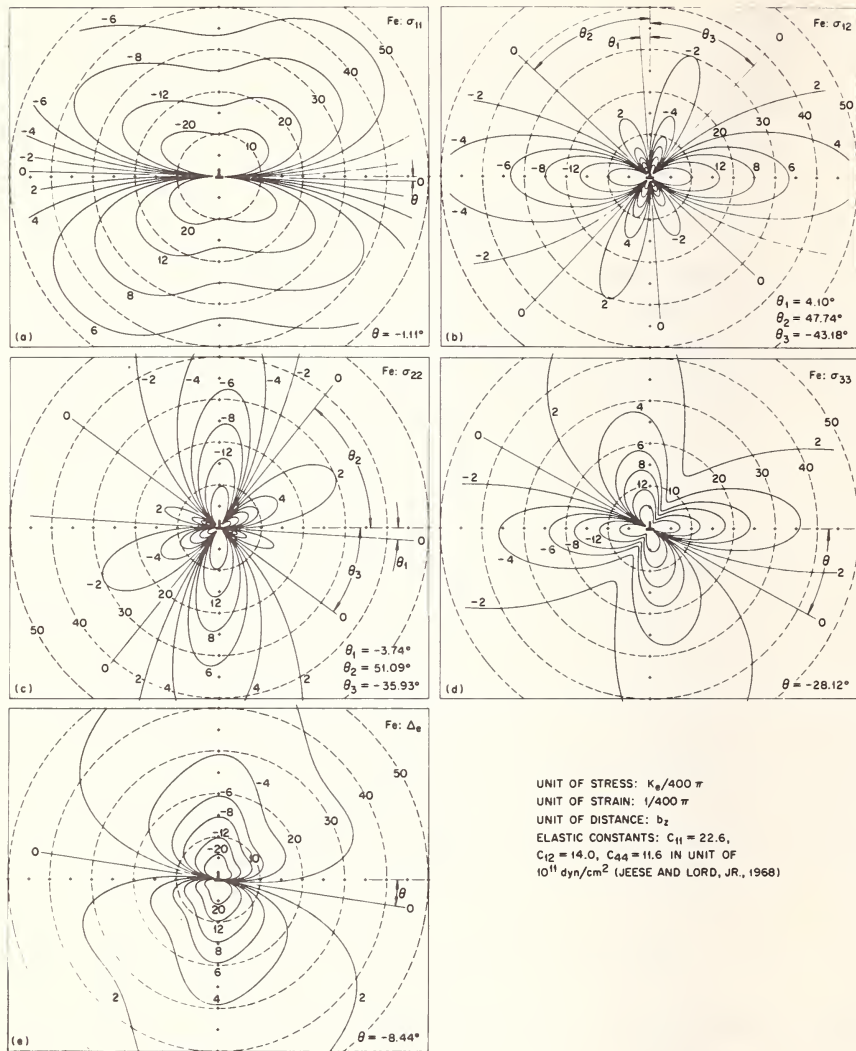


FIGURE 4. Stress fields and dilatation field of an edge twin dislocation. $\{112\} \langle 11\bar{1} \rangle$ twin of Fe.

plane, the symmetries of the stress and dilatation fields with respect to x_1 -axis and also to x_2 -axis are no longer present, that is, $\theta \neq 0$ and $\theta_1 \neq 0$ in figure 4. Also, the other zero-stress contours in σ_{12} and σ_{22} , that is, θ_2 and θ_3 in figures 4(b) and 4(c), deviate from the $\pm 45^\circ$ lines of the isotropic case.

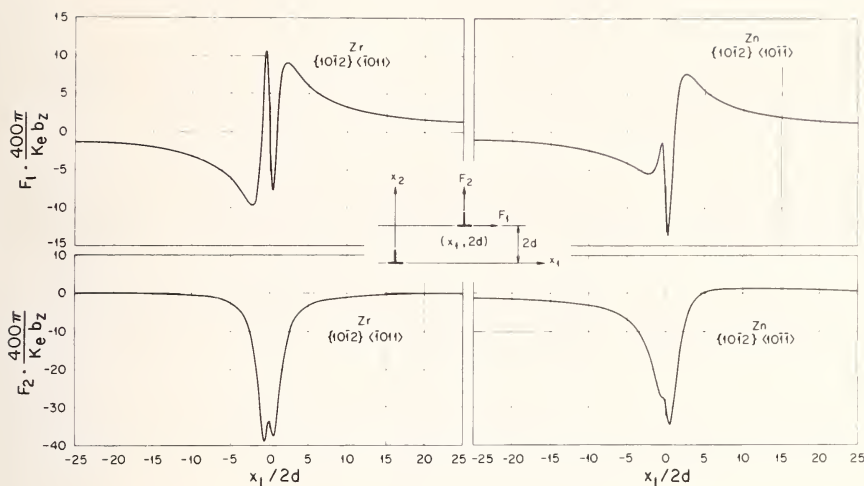


FIGURE 5. Interaction forces between two parallel edge zonal twin dislocations, {1012} type twin in Zr and Zn.

Interaction forces, F_1 and F_2 , between two parallel edge zonal twin dislocations have been computed, and the results for {1012} type twin in zirconium and zinc are given in figure 5. As may be expected from the feature of σ_{12} field discussed earlier, the centrosymmetry with respect to the origin is not present in the F_1 plot. This means, for instance, that in the case of zinc a dislocation situated at (x_1/nd) experiences greater repulsive force than it would experience at $-(x_1/nd)$. The reverse holds true in zirconium, as shown in figure 5.

In the analysis of equilibrium shapes of a twin, only the F_1 component is of importance and becomes a controlling factor since twin dislocations are subjected to glide in their twin plane. Consider an incoherent twin boundary, which consists of N straight edge zonal twin dislocations, in equilibrium under an applied stress τ_a . If it is assumed that an obstacle effectively blocks the leading dislocation, but not the other dislocations, then the equilibrium condition for an array of N dislocations is that the effective force on each dislocation be equal to zero; that is, for each dislocation the sum of the external force due to the applied shear stress and the interaction forces by all other dislocations must be zero. For {1012} $\langle 10\bar{1}\rangle$ twin in zinc, the equilibrium positions of the dislocations have been obtained numerically for various values of N and τ_a , and the results for $N=7$ are given in figure 6 for the three values of $\tau_a=0.9, 1.8$, and 2.7 kg/mm^2 . It is apparent from figure 6 that by doubling and tripling τ_a the equilibrium distance between a dislocation and the leading dislocation is reduced to approximately one-half and one-third.

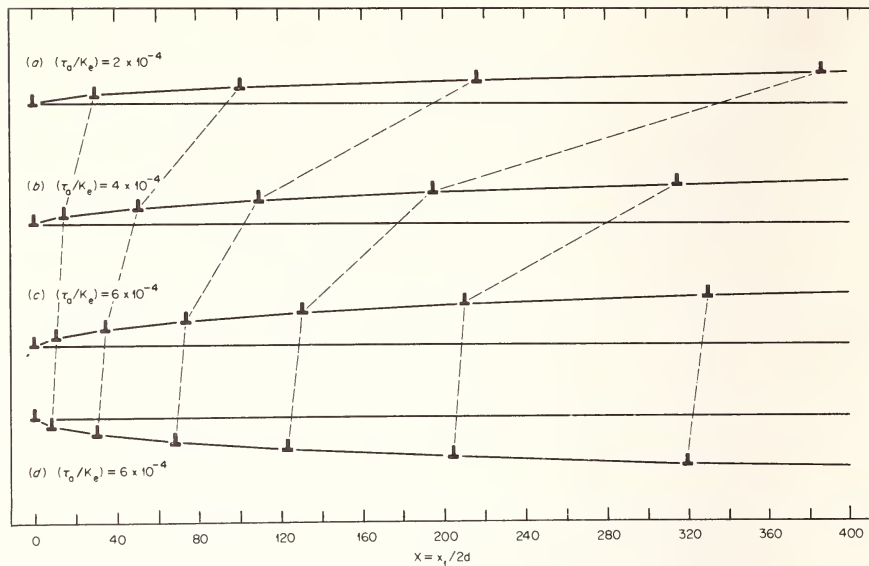


FIGURE 6. Effect of applied stress, τ_a , on equilibrium shape of an incoherent twin boundary consisting of N straight edge zonal twin dislocation. $N=7$. $\{10\bar{1}2\}$ $\{10\bar{1}1\}$ twin of Zn. Vertical scale is expanded four times.

respectively, of the original distance. This feature was pointed out by Marcinkowski and Sree Harsha [18], who made an analysis of equilibrium shapes of a blocked twin using isotropic elasticity theory. It was also noted that doubling τ_a while holding $(N-1)$ constant is in effect equivalent to doubling $(N-1)$ at a constant τ_a . Figures 6(c) and 6(d) together exhibit the asymmetry of an incoherent twin boundary which is a direct consequence of the F_1 interaction curve for zinc shown in figure 5.

IV. Structural Properties

In order to illustrate a point that the atomic model of dislocation developed by Peierls [19] and by Nabarro [20] can be directly applied to the present case of zonal twin dislocations, the cross section of an edge zonal twin dislocation is depicted in figure 7. A cut is made on a perfectly coherent twin along K_1 plane ($Y=0$) such that the medium above $A'-A$ surface be the parent matrix, and the medium below $B'-B$ surface be the twin. Before these two surfaces are welded back together, the relative displacements as indicated by the two arrows are applied across the interface, which may be considered to arise due to a continuous distribution of infinitesimal edge dislocations as suggested by Eshelby [21]. The net

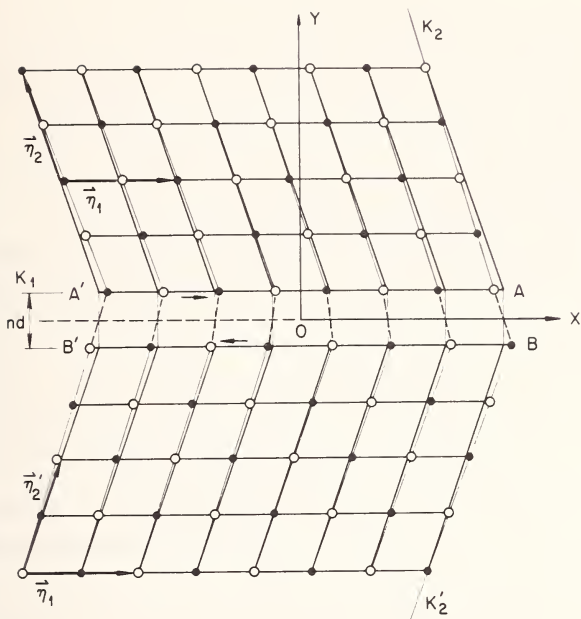


FIGURE 7. Schematic illustration of the cross section of an edge zonal twin dislocation. The atomic configuration is depicted for f.c.c. structure (A1).

result is a step in the twin interface as depicted in figure 7. Therefore, due to the close analogy, the original Peierls-Nabarro model or any model derived from it may be directly applicable to a zonal twin dislocation. One important point, however, is that a Peierls-Nabarro type model does not take into account the inhomogeneous motion of the atoms that must shuffle in a double lattice structure.

The Peierls-Nabarro stress, the stress necessary to move a zonal twin dislocation along the twin interface, depends sensitively on a factor $\exp(-\zeta/b_z)$. The exponent, which is a measure of ease of gliding, is given by Eshelby [21] as

$$\frac{\zeta}{b_z} = \frac{1}{2} (K_e S_{66}) \left(\frac{1}{g} \right), \quad (4)$$

where g is the twinning shear. It is expected that the larger the (ζ/b_z) parameter, the higher the probability is of a certain twin system to be active. As pointed out by Bilby and Crocker [11], that g must be small is the primary one of the geometric criteria for operative twin modes. K_e and S_{66} are both anisotropic coefficients varying with orientation. Hence, as a counterpart to g , the product $(K_e S_{66})$ may be defined as an "aniso-

tropic parameter" of energetic criteria such that in a crystal the higher the value of ($K_e S_{66}$), the higher is the mobility of dislocation.

In comparing the crystallographically non-equivalent conjugate (or reciprocal) pair of a compound twin system, the prevalence of one conjugate system over the other should be correctly predicted in terms of the ($K_e S_{66}$) anisotropic parameters since all the geometric factors (g , q , and shuffling) are essentially common to both systems. Other than {1121} $\langle\bar{1}\bar{1}26\rangle$ twinning in h.c.p. structure, of which conjugate system is (0002) $\langle\bar{1}\bar{1}\bar{2}0\rangle$ basal slip, the twinning shear of observed compound twin systems in non-cubic metals are small, and in most cases $g < 0.3$ and hence $81.5^\circ < \varphi < 90^\circ$. Therefore, one can be certain that crystal orientation with respect to the loading axis is not a critical factor, since at such a high value of φ the Schmid factors will be nearly the same for both conjugate systems. The validity of the present argument is tested by examining the five non-equivalent conjugate pairs for eight metals selected as listed in table 3. It is indeed found in each conjugate twin system that the higher value of ($K_e S_{66}$) is associated with the observed mode, according to the review by Christian [22].

In the case of rhenium it has not been clearly established as to whether or not the twin modes listed in table 3 are operative. Judging from the calculated values of anisotropic parameters, however, one should expect {1122} twin mode to be prevalent if and when the compound twin system is activated.

In comparing one compound twin system to another, it was found that the exponent (ζ/b_z) could serve only as a major factor but not as a com-

TABLE 3. Anisotropic parameters ($K_e S_{66}$) for non-equivalent conjugate twin systems. All values at room temperature, except 80 K for Hg

Metals	Twin systems	$K_e S_{66}$	Metals	Twin systems	$K_e S_{66}$
β -Sn	{301}$\langle\bar{1}03\rangle^*$	2.019	Mg	{101}$\langle10\bar{1}2\rangle^*$	1.362
	{101}$\langle101\rangle$	1.866		{10\bar{1}3}$\langle30\bar{2}2\rangle$	1.285
Bi	{110}$\langle00\bar{1}\rangle^*$	1.944	Re	{11\bar{2}2}$\langle11\bar{2}3\rangle$	1.302
	{001}$\langle110\rangle$	1.362		{11\bar{2}4}$\langle22\bar{4}3\rangle$	1.216
Hg	{110}$\langle001\rangle^*$	4.147	Zr	{11\bar{2}2}$\langle11\bar{2}3\rangle^*$	1.390
	{001}$\langle110\rangle$	3.157		{11\bar{2}4}$\langle22\bar{4}3\rangle$	1.294
α -U	{130}$\langle3\bar{1}0\rangle^*$	1.345	Ti	{11\bar{2}2}$\langle11\bar{2}3\rangle^*$	1.444
	{1\bar{1}0}$\langle110\rangle$	1.306		{11\bar{2}4}$\langle22\bar{4}3\rangle$	1.409

*The only, or more frequently, observed mode.

plete criterion for the relative mobilities of twin dislocations. The reason for this is of course the neglect of atomic shuffling. For instance, in h.c.p. structure, the main reason why $\{10\bar{1}1\}$ $\langle 10\bar{1}2 \rangle$ twinning seldom occurs in spite of its small g may be due to the complex atomic shuffling involved. On the other hand, more common occurrence of $\{11\bar{2}1\}$ $\langle \bar{1}126 \rangle$ twinning despite a large g is attributed to the relatively simple shuffling. Also, in each case of the ordered structures shown in figure 3 those A and B atoms with the stroked symbols must change places in order to reconstitute the stable ordered cubic lattice. Such atomic shuffling would not be energetically feasible at low temperatures since the atoms must move a large distance, $1/2 \langle 112 \rangle$ and $1/2 \langle 111 \rangle$ in $L1_2$ and $B2$ structures, respectively, and the lattice resistance resulting from the disruption of $A-B$ bonds will be extremely high. Hence the mobility of a zonal twin dislocation in the fully ordered alloys is expected to be very low.

Finally, the anisotropic parameters ($K_e S_{66}$) at high and low temperatures have been calculated for zirconium and titanium and plotted in figure 8. The results show that the differences in ($K_e S_{66}$)'s between $\{11\bar{2}2\}$ and $\{11\bar{2}4\}$ conjugate modes existing at room temperature and 4.2 K diminish at the high temperatures, 1133 K and 1156 K for zirconium and titanium. This suggests that $\{11\bar{2}4\}$ $\langle 22\bar{4}3 \rangle$ twinning may become equally probable mode as $\{11\bar{2}2\}$ $\langle 11\bar{2}3 \rangle$ twinning at the high temperatures. It is also interesting to note in figure 8 that the parameter for $\{11\bar{2}1\}$ twin is greater than those for other twins at low temperatures.

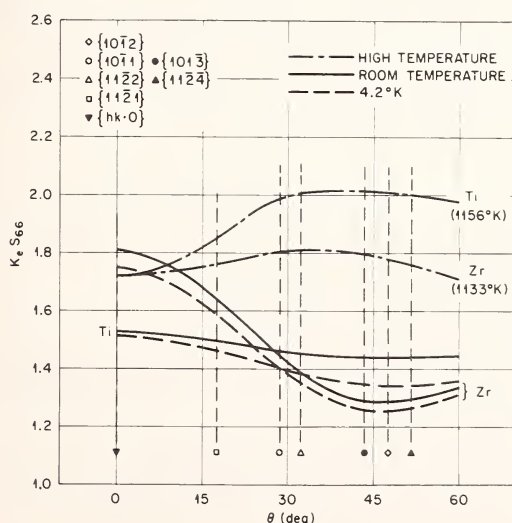


FIGURE 8. Anisotropic parameter ($K_e S_{66}$) versus θ , the angle between c axis and twinning direction, for Zr and Ti.

but becomes smaller at the high temperatures. Therefore, insofar as $(K_e S_{66})$ anisotropic parameters are involved, $\{11\bar{2}1\} \langle \bar{1}\bar{1}26 \rangle$ twinning in zirconium and titanium may occur much more readily at low temperatures.

V. Conclusions

1. A general definition of zonal twin dislocations is given as $\mathbf{b}_z = (e/2)\boldsymbol{\eta}_1$, and some geometric characteristics of the dislocations are discussed.
2. The σ_{ij} stress fields and the Δ_e dilatation field of edge zonal twin dislocations have been calculated numerically by using anisotropic elasticity theory.
3. The interaction forces, F_1 and F_2 , between a pair of edge zonal twin dislocations are obtained and used in the analysis of equilibrium shapes of an incoherent twin boundary.
4. Due to the close analogy to perfect dislocations, a Peierls-Nabarro type dislocation model can be directly applied to a zonal twin dislocation.
5. $(K_e S_{66})$ is introduced as an anisotropic parameter of energetic criteria for operative twin modes. The calculated parameters correctly predict the more active mode between a conjugate pair of crystallographically non-equivalent compound twin systems.

VI. Acknowledgements

The authors wish to express their appreciation to Dr. R. A. Vandermeer for helpful discussions. They are also grateful to Drs. R. O. Williams and C. J. McHargue for commenting on the manuscript.

Research sponsored by the U.S. Atomic Energy Commission under contract with the Union Carbide Corporation.

VII. References

- [1] Frank, F. C., and van der Merwe, J. H., Proc. Roy Soc. **A198**, 205 (1949).
- [2] Frank, F. C., Phil. Mag. **42**, 809 (1951).
- [3] Thompson, N., and Millard, D. J., Phil. Mag. **43**, 422 (1952).
- [4] Westlake, D. G., Acta Met. **9**, 327 (1961).
- [5] Kronberg, M. L., J. Nucl. Mater. **1**, 85 (1959).
- [6] Rosenbaum, H. S., in Deformation Twinning (Proc. TMS-AIME Conf., Gainsville, Florida, 1963), R. E. Reed-Hill, J. P. Hirth, and H. C. Rogers, Eds. (Gordon and Breach, New York, 1964) p. 43.
- [7] Yoo, M. H., and Wei, C. T., Phil. Mag. **14**, 573 (1966).
- [8] Mendelson, S., in Proc. Intern. Conf., on Strength of Metals and Alloys, Tokyo, Japan, 1967. Suppl. Trans. Japan Inst. Metals **9**, 812, 819 (1968).
- [9] Mendelson, S., in these Proceedings.
- [10] Saxl, I., Czech. J. Phys. **B18**, 39 (1968).
- [11] Bilby, B. A., and Crocker, A. G., Proc. Roy. Soc. **A288**, 240 (1965).

- [12] Bilby, B. A., *Phil. Mag.* **44**, 782 (1953).
- [13] Yoo, M. H., *Trans. TMS-AIME* **245**, 2051 (1969).
- [14] Eshelby, J. D., Read, W. T., and Shockley, W., *Acta Met.* **1**, 251 (1953).
- [15] Stroh, A. N., *Phil. Mag.* **3**, 625 (1958).
- [16] Yoo, M. H., and Loh, B. T. M., to be published in *J. Appl. Phys.*
- [17] Chou, Y. T., *J. Appl. Phys.* **34**, 429 (1963).
- [18] Marcinkowski, M. J., and Sree Harsha, K. S., *Trans. TMS-AIME* **242**, 1405 (1968).
- [19] Peierls, R. E., *Proc. Phys. Soc.* **52**, 34 (1940).
- [20] Nabarro, F. R. N., *Proc. Phys. Soc.* **59**, 256 (1947).
- [21] Eshelby, J. D., *Phil. Mag.* **40**, 903 (1949).
- [22] Christian, J. W., *The Theory of Transformations in Metals and Alloys* (Pergamon Press, Oxford, 1965) p. 765.

NON-PLANAR DISSOCIATIONS OF DISLOCATIONS

S. Mendelson*

2660 Somerset Blvd.
Troy, Michigan 48084

Non-planar dissociations of dislocations are studied in hcp, fcc, bcc, diamond lattice, tetragonal and orthorhombic crystal structures. The geometric and energetic conditions are shown to be favorable for various dissociations in each crystal structure. A general equation is formulated for dissociations into partials which are glissile on various twin planes of a common zone. The Burgers vector of the twinning dislocations are expressed in terms of orthogonal unit vectors which lie in the "plane of shear" of the twin mode. The twinning dislocations are generally of the "zonal" type, chosen to be consistent with minimum shear-strain and simple atomic shuffling criteria for twinning, and applied in derivations of the twinning elements and shear-strains for various twin modes. The sign of the shear-strain determines the "stress sense" characteristics for dislocation resistance and twinning and are shown to be consistent with behavior in various hcp and bcc metals. The maximum repulsive force on the twinning partials γ_m is computed using anisotropic elasticity, and compared with evaluations of twin lamella energies γ . In many cases it is found that $\gamma_m/\gamma > 1$, leading to an increase in dislocation resistance, locking, or twinning at lower temperatures. In the cases where $0 < \gamma_m/\gamma < 1$ the partialized dislocation model reduces to the "modified pseudo-Peierls-Nabarro model" for dislocation resistance.

Among various effects, the dissociations account for all twin modes in hcp metals and for the extreme difference in the flow behavior of Cd and Zn on one hand and Ti and Zr on the other. The stress dependent activation energies for motion of dissociated 60° dislocations in germanium are computed and compare favorably with the data of Kabler. A "lock" for kinks on 60° dislocations is described which can account for dragging points in the model of Celli et al.

Key words: Dislocation dissociation; lattice shuffling; partial dislocations; twinning; zonal dislocations.

I. Introduction

If a dislocation can dissociate into partials which are glissile on oblique planes, dislocation locks tend to form which have an orientation and

*Consultant Scientist.

Fundamental Aspects of Dislocation Theory, J. A. Simmons, R. de Wit, and R. Bullough, Eds. (Nat. Bur. Stand. (U.S.), Spec. Publ. 317, I 1970).

temperature dependent strength. The conditions necessary for non-planar dissociations are (i) that the dislocation line be parallel to the axis of stacking fault or twin planes, (ii) that the partial dislocations have Burgers vectors corresponding to the shear strain for stacking faults or twin lamellae on these planes, and (iii) that the resolved force on the glissile partials be repulsive. Earlier application of these conditions to various crystal structures suggested a partialized dislocation model for dislocation resistance [1-3]. In this study, anisotropic elasticity is applied to dislocation dissociations in h.c.p., f.c.c., b.c.c., diamond lattice, tetragonal, and orthorhombic crystal structures. This is preceded by formulations of the dissociation equation, zonal dislocation, twinning elements, and forces on the glissile partials. For conciseness the Burgers vectors are expressed in bi-pyramid or Thompson tetrahedron coordinates.

II. Formulation of Dissociation Equation and Twinning Parameters

When a dislocation line is parallel to the zone axis of several twin planes the possible non-planar dissociations can be represented by a general equation in which the Burgers vector, \mathbf{b}_0 , of the perfect dislocation on each twin plane κ_1 in the twinning direction $\boldsymbol{\eta}_1$ is taken as a linear sum of orthogonal unit vectors $\Psi\Omega_m$ and $T\xi_m$ which lie on the plane of shear S_m defined by the subscript m .

Various nomenclatures have been used for the twinning parameters and it is not possible to be consistent with any single set. The crystallography for twinning is illustrated in figure 1. The elements of the second undistorted (rotated) plane are κ_2 and $\boldsymbol{\eta}_2$. The normal to the plane of

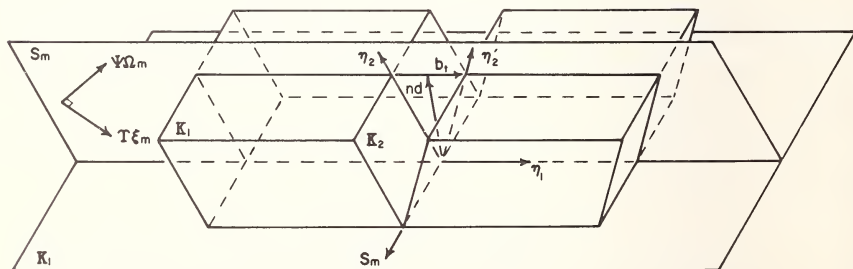


FIGURE 1. Twinning elements in crystals. κ_1 is the twin plane and $\boldsymbol{\eta}_1$ the shear direction. κ_2 and $\boldsymbol{\eta}_2$ are the elements for the second undistorted plans. S_m is the plane of shear containing $\Psi\Omega_m$ and $T\xi_m$ orthogonal unit vectors.

shear is given by $\mathbf{S}_m = \Psi\Omega_m \times \mathbf{Y}\xi_m$ and the Burgers vector of the perfect dislocation on its twin plane is¹

$$\mathbf{b}_0 = [\rho\Psi\Omega_m + \sigma\mathbf{Y}\xi_m] \quad (1)$$

where ρ and σ are positive integers.

The Burgers vector of the twinning dislocation is

$$\mathbf{b}_t = s\mathbf{b}_0 \quad (2)$$

where s is the fraction of \mathbf{b}_0 which produces the twinning shear. The shear-strain for twinning is given by

$$S = sb_0/nd \quad (3)$$

where d is the spacing of twin planes and n is the number of twin planes in the twin lamella. In multiple lattice structures such as hcp and diamond cubic (regarded as consisting of two interpenetrating lattices) each twin plane of spacing d may correspond to a rumpled plane or to two closely spaced planes.

The direction η_2 is given by

$$\eta_2 = [2n\mathbf{D} + s\mathbf{b}_0] \quad (4)$$

where \mathbf{D} is the twin normal of magnitude $|\mathbf{D}| = d$. κ_2 is established by the requirement that it contain the vectors $[\Psi\Omega_m \times \mathbf{Y}\xi_m]$ and η_2 , i.e., its normal is given by $\kappa_2 = [\Psi\Omega_m \times \mathbf{Y}\xi_m] \times \eta_2$.

The general equation for dissociation of dislocation \mathbf{QP} into multiple twinning partials on various twin planes of a common zone is given by

$$\mathbf{QP} \rightarrow \sum_{i=1}^{q-1} s_i [\rho_i \Psi\Omega_m + \sigma_i \mathbf{Y}\xi_m] + \left[\mathbf{QP} + \sum_{i=1}^{q-1} s_i \rho_i \Omega\Psi_m + \sum_{i=1}^{q-1} s_i \sigma_i \xi Y_m \right]. \quad (5)$$

The first summation on the right corresponds to the $q-1$ glissile twinning partials on their respective twin planes and the second bracketed vector is the stair-rod dislocation between them.

Since s has been measured for only a few twin modes in a few metals, it must be assumed. The choice is governed by minimum shear-strain [4, 5] and simple atomic shuffling [6] criteria. The first of these, originally proposed by Kiho [4] and later by Jaswon and Dove [5], suggests that the

¹ η_1 as given in various papers and books has unit indices and does not in general have the magnitude of \mathbf{b}_0 .

twin modes with smaller shear-strain will be favored. Bilby and Crocker [6] give a systematic description of the atomic shuffles which often occur and summarize the criteria as (i) the twinning shear should be small, (ii) the shuffle mechanism should be simple, (iii) the shuffle magnitudes should be small, and (iv) the shuffles should be parallel to the twinning direction rather than perpendicular to it. Conditions (iii) and (iv) are not mutually exclusive, since a smaller shuffle distance is often possible if it is permitted to have a component normal to the twinning direction [10]. The distortion energy of the twin boundary must also be considered as a criterion for twinning.

When a second twin mode has elements such that $\kappa'_1 = \kappa_2$, $\kappa'_2 = \kappa_1$, $\eta'_1 = \eta_2$ and $\eta'_2 = \eta_1$ it is said to be a conjugate or reciprocal twin mode. Both have the same shear-strain and similar, but not equal, atomic shuffling. Kiho [4] proposed that the more favorable conjugate twin mode will have the smaller b_t , while Bilby and Crocker [6] conclude that the mode with simplest atomic shuffling will be preferred, and that when no shuffles are necessary (homogeneous shear) both composition planes should be equally favorable. The twin boundary distortional energies must also be considered, since they can be very different for conjugate twin modes [10] and can play a significant role, at least when the first twinning partial passes through the virgin lattice.

If twinning occurs by homogeneous shear the smallest Burgers vector is often large and dissociation less likely. In many cases various dissociations become possible when the twinning dislocations are of the "zonal" type [7-11] since their Burgers vectors can be small. The concept of a zonal dislocation is inherent in the earlier studies [4-6] and corresponds to non-homogeneous shear in which a smaller s is paid for by atomic shuffling in a multi-layer twin lamella.

If n is the number of layers in the twin lamella which forms as the dislocation glides [11],

$$s = ns' - p \quad (6)$$

where s' is the shear for a single layer twin and p is an integer which gives the lowest absolute value of s . When $p=0$ ($n=1$), $s=s'$ and twinning is homogeneous, often with a large shear-strain. The zonal dislocation results for $n > 1$ and $p \geq 1$, and permits a reduction in shear-strain at the expense of atomic shuffling. Of the many possible values of s which satisfy eq (6) and for which dissociation is energetically favorable, the ones for which n is small give the best balance between the two effects; thicker lamellae require more atomic shuffling and are more difficult to nucleate and propagate. The sign of s determines the direction in which the partial must move, and consequently its stress-sense characteristics.

This can be illustrated by simple examples of twinning in cubic crystals. For bcc metals $\kappa_1 = \{112\}$, $\mathbf{b}_0 = 1/2[11\bar{1}]$ and $s' = 1/3$ giving, for homogeneous shear, $\mathbf{b}_t = 1/6[11\bar{1}]$ and $S = 1/\sqrt{2}$. For fcc metals $\kappa_1 = \{111\}$, $\mathbf{b}_0 = 1/2[11\bar{2}]$ and $s' = 1/3$ giving, for homogeneous shear, $\mathbf{b}_t = 1/6[11\bar{2}]$ and $S = 1/\sqrt{2}$. Substituting $n = (2+3N)$ or $(1+3N)$ where $N = 0, 1, 2, \dots$ gives $|s| = 1/3$ and no change in \mathbf{b}_t . If only the minimum shear-strain criterion applies, $S \rightarrow 0$ as $n \rightarrow \infty$, and thick lamellae would be favored.

The obvious anomaly is due to the neglected atomic shuffling which results when $n > 1$. For $n = 2$ ($N = 0$, extrinsic stacking fault)

$$s = 2(1/3) - 1 = -1/3$$

and the same Burgers vector must glide in the opposite direction, with atoms on the intermediate plane shuffling through $2\mathbf{b}_t$. In hcp metals twinning occurs on higher order planes for which the homogenous shear-strain is generally large. In these cases the atomic shuffling, resulting when $n > 1$, permits a significant decrease in \mathbf{b}_t and S , making these modes more favorable.

III. Forces on Twinning Dislocations

The resolved force on the twinning partial is computed by a force balance, where only the components which act in the twin plane are equilibrated. The morphologies of the partialized dislocations for symmetric and non-symmetric dissociations are illustrated schematically in figure 2. (a) shows a perfect dislocation while (b) and (c) correspond to symmetric and non-symmetric dissociations respectively. 1 and 2 are

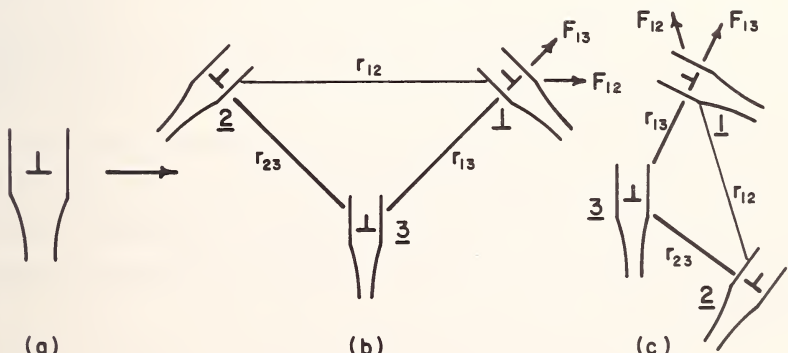


FIGURE 2. Schematic of twin lamellae morphologies for dissociation of dislocations. (a) perfect dislocation, (b) symmetric dissociation and (c) non-symmetric dissociation.

glissile twinning dislocations and 3 is a sessile stair-rod dislocation. s is positive at both partials for the symmetric case in (b). For the non-symmetric dissociation in (c) s is positive for 1 and negative for 2.

The initial dislocation energy E is equated to the energy of the resulting morphology and given by

$$E = E_1 + E_2 + E_3 + \mathbf{W}_{1,2} + \mathbf{W}_{1,3} + \mathbf{W}_{2,3} + \gamma_1 r_{1,3} + \gamma_2 r_{2,3} \quad (7)$$

where E_i are the self energies of the partials, \mathbf{W}_{ij} are the interaction energies for a separation between partials of r_{ij} and γ_i are the energies of the stacking faults or twin lamellae. The self and interaction energies are given by [12]

$$E_i = (\mathbf{K}_i \mathbf{b}_i^2 / 2\pi) \ln (r/r_0) \quad (8)$$

$$\mathbf{W}_{ij} = (\mathbf{K} \mathbf{b}_i \cdot \mathbf{b}_j / 2\pi) \ln (r_{ij}/r_0) + \mathbf{K}(\mathbf{b}_i \cdot \mathbf{r}_{ij})(\mathbf{b}_j \cdot \mathbf{r}_{ij})/\mathbf{r}_{ij}^2 \quad (9)$$

where \mathbf{b}_i is the Burgers vector of the i th dislocation and \mathbf{K} the elastic energy factor for the dislocation on its slip plane.

If the dislocations are constrained to translate by glide only, the force between two partials is given by

$$\mathbf{F}_{ij} = -\partial \mathbf{W}_{ij} / \partial \mathbf{r}_{ij} = (\mathbf{K}/2\pi) \mathbf{b}_i \cdot \mathbf{b}_j / \mathbf{r}_{ij}. \quad (10)$$

For the symmetric and non-symmetric dissociations the maximum stacking fault energy, γ_m , is equated to the force, F_i , on the twinning partial [13] resolved parallel to the twin plane when the partials are separated by $r_{i3} = a$ [14]. This is

$$\gamma_{mi} = F_i = (\mathbf{K}_i / 2\pi a) [\mathbf{b}_i \cdot \mathbf{b}_3 + 1/2 \mathbf{b}_1 \cdot \mathbf{b}_2] \quad (11)$$

where i is 1 or 2 for the glissile twinning partials and \mathbf{b}_3 is the Burgers vector of the stair-rod dislocation. If $r_{i3} = \epsilon a$ and $\epsilon > 1$ the values of γ_m would be divided by ϵ .

If each $\gamma_{mi}/\gamma_i > 1$ the dissociation can be spontaneous. For symmetric dissociations $\gamma_1 = \gamma_2 = \gamma$ and the equilibrium separation r_{i3} is given by an expression similar to eq (11) (i.e., substitute $a = r_{i3}$ and $\gamma_{mi} = \gamma$). If α is the angle between the twin lamellae the equilibrium separation for non-symmetric dissociations are obtained by the solution of two simultaneous equations given by

$$\gamma_i = (\mathbf{K}_i / 2\pi) [\mathbf{b}_i \cdot \mathbf{b}_3 / r_{i3} + (\mathbf{b}_1 \cdot \mathbf{b}_2 / r_{12}^2) (r_{i3} - r_{j3} \cos \alpha)] \quad (12)$$

with

$$r_{1,2}^2 = r_{1,3}^2 + r_{2,3}^2 - 2r_{1,3}r_{2,3} \cos \alpha$$

where i is 1 or 2 for the glissile twinning partials and \mathbf{b}_3 is the Burgers vector of the stair-rod dislocation. If $r_{i_3} = \epsilon a$ and $\epsilon > 1$ the values of γ_m would be divided by ϵ .

$$\gamma'_{mi} = (\tau_i b + \gamma_{mi}) > \gamma_i. \quad (13)$$

τ_i can develop when dislocations pileup. When the dislocation dissociates at an existing twin eq (13) does not apply, since no new twin boundary is created, and the dissociation can be spontaneous when $\gamma_m > 0$. Similarly after the initial dissociation the residual dislocation may spontaneously dissociate into successive twinning partials of the same twin mode.

Dislocations of large Burgers vector can generally dissociate into more than two glissile twinning partials on twin planes which are parallel to the dislocation axis. For $q-1$ glissile partials emanating from the stair-rod dislocation, with $r_{iq} = a$, γ_m is given by

$$\gamma_{mi} = (\mathbf{K}_i / 2\pi a) [\mathbf{b}_i \cdot \mathbf{b}_q + 1/2 \sum_{j \neq i}^{q-1} \mathbf{b}_i \cdot \mathbf{b}_j] \quad (14)$$

where $\mathbf{b}_1, \mathbf{b}_2, \dots, \mathbf{b}_{q-1}$ are the Burgers vectors of the glissile twinning partials and \mathbf{b}_q is that of the stair-rod dislocations between them.

A dissociation is considered to be favorable when all $\gamma_{mi} > 0$, and spontaneous if all $\gamma_{mi}/\gamma_i > 1$. If the γ_i are known, the equilibrium separations, r_{iq} , can be computed by solving $q-1$ simultaneous equations similar to eq (12). The more favorable dissociations correspond to those for which $R = (\gamma_{m(s)}\gamma_l/\gamma_{m(l)}\gamma_s)$ is largest, where $\gamma_{m(s)}$ and $\gamma_{m(l)}$ are the smallest and largest values of γ_m respectively; γ_s and γ_l are their respective twin lamellae energies. When internal stress fields exist many less favorable morphologies for which $\gamma_m > 0$ are possible.

The elastic energy factors for edge twinning dislocations in h.c.p. metals were computed numerically [15] with the equations developed by Eshelby [16]. For screw dislocations in h.c.p. metals they were approximated by $K(\theta) = (\bar{S}_{55}\bar{S}_{66})^{-1/2}$ where θ is the angle between the dislocation and the basal plane, the \bar{S}_{55} and \bar{S}_{66} are the transformed elastic compliances. This equation gives exact values when $\theta=0$ and 90° [17]. The errors are estimated to be less than several percent [15]. Similar approximations, having maximum errors estimated to be less than a few percent, are applied to dislocations on higher order fault planes in f.c.c. metals. The tabulated data of Head [18] are used to approximate the energy factors for screw dislocations on higher order planes in f.c.c. metals. For f.c.c., b.c.c., tetragonal, and orthorhombic metals, various energy factors are taken from published work [19-22] or computed with the analytic equations developed by Foreman [17].

IV. HCP Metals

In hcp metals the reported twin modes correspond to seven $\{\bar{2}11l\}$ and $\{\bar{1}01l\}$ planes, where $l=1, 2, 3$, and 4 for the $\{\bar{2}11l\}$ zone and $l=1, 2$, and 3 for the $\{\bar{1}01l\}$ zone. A $\{\bar{3}034\}$ habit is also found in Mg [23–25], but it is not known whether this is a new twin mode or a rotated $\{\bar{1}011\}$ twin; the latter has not been successfully rationalized [26–28]. The $\{\bar{3}034\}$ habit can be a real twin mode [10, 24] with elements $\kappa_1 = \{\bar{3}03\bar{4}\}$, $\eta_1 = \langle\bar{2}023\rangle$, $\kappa_2 = \{\bar{1}012\}$ and $\eta_2 = \langle\bar{1}01\bar{1}\rangle$, and a shear-strain of $S=-0.27$.

The dislocations which meet the criteria for partialization on the oblique planes of the two zones are **AB** edge, **AB** 60° and **A μ** Shockley partials on the basal plane, **AB** mixed and **$\phi\theta$** edge and mixed dislocations on the first-order prism plane, **$\phi\theta$** edge and mixed dislocations on the second-order prism plane, and **[AB + $\phi\theta$]** edge, screw and mixed dislocations on the second-order $\{\bar{2}112\}$ pyramidal slip plane. The vector representation corresponds to the bi-pyramid notation [29] as modified by Nabarro et al. [30]. The Burgers vector of perfect dislocations are listed in table 1 in bi-pyramid notation, Miller-Bravais, and Cartesian coordinates.

The Burgers vector of the perfect dislocations on the twin planes are

$$\mathbf{b}_0 = [\rho\mathbf{AB} + \sigma\mathbf{\mu\theta}] \quad \text{for planes of the } \{\bar{2}11l\} \text{ zone} \quad (15)$$

$$\mathbf{b}_0 = [\rho\mathbf{A\mu} + \sigma\mathbf{\mu\theta}] \quad \text{for planes of the } \{\bar{1}01l\} \text{ zone} \quad (16)$$

For the $\{\bar{2}11l\}$ zone $\sigma=2l$ and $\rho=(3/2)h$; for the $\{\bar{1}01l\}$ zone $\sigma=2l$ and $\rho=3h$. The h and l are indices in Miller-Bravais coordinates of the $[hkil]$ Burgers vector of the perfect dislocation on its twin plane. The values of ρ and σ are listed in table 1.

The single-layer and multi-layer twin shears for small n are given by

$$s' = 1/[\rho + (\sigma^2/4\rho)(c/a)^2] \quad \text{for } \{\bar{2}11l\} \text{ planes} \quad (17)$$

$$s = [n - \rho - (\sigma^2/4\rho)(c/a)^2]/[\rho + (\sigma^2/4\rho)(c/a)^2] \quad \text{for } \{\bar{2}11l\} \text{ planes} \quad (18)$$

$$s' = 1/[(1/3)\rho + (\sigma^2/4\rho)(c/a)^2] \quad \text{for } \{\bar{1}01l\} \text{ planes} \quad (19)$$

$$s = [n - (1/3)\rho - (\sigma^2/4\rho)(c/a)^2]/[(1/3)\rho + (\sigma^2/4\rho)(c/a)^2] \quad \text{for } \{\bar{1}01l\} \text{ planes} \quad (20)$$

Values of s for the seven reported twin planes, with small n , are listed in table 2. For the modes with $n > 1$ p is taken as unity in eq (6) giving eqs (18) and (20).

The shear-strain for twinning is given by eq (3) where

$$b_0 = a[\rho^2 + (1/4)\sigma^2(c/a)^2]^{1/2} \quad \text{for } \{\bar{2}11l\} \text{ planes} \quad (21)$$

$$d = a/2[1 + 4(\rho/\sigma)^2(a/c)^2]^{1/2} \quad (22)$$

TABLE I. *Types of dislocations in h.c.p. metals*

	Miller-Bravais coordinates				Bi-pyramid notation	Cartesian coordinates	Dislocation energy
Twin zone	Plane	Burgers vector b_0	ρ	σ	Burgers vector b_0	Burgers vector b_0	$E/K = b_0^2$
First-order pyramidal zone $\{\bar{1}01l\}$	(0001)	$1/3\langle\bar{1}010\rangle$	1	0	$A\mu$	$1/6 < 3\sqrt{3} 0 >$	$1/3$
	$\{\bar{1}01\bar{l}\}$	$\langle\bar{1}012\rangle$	3	4	$3A\mu + 2\phi\theta$	$1/2 < 3\sqrt{3} 4 >$	$3 + (c/a)^2$
	$\{\bar{3}03\bar{4}\}$	$\langle\bar{2}023\rangle$	6	6	$6A\mu + 3\phi\theta$	$< 3\sqrt{3} 3 >$	$12 + 9(c/a)^2$
	$\{\bar{1}01\bar{2}\}$	$\langle\bar{1}011\rangle$	3	2	$3A\mu + \phi\theta$	$1/2 < 3\sqrt{3} 2 >$	$3 + (c/a)^2$
	$\{\bar{1}01\bar{3}\}$	$\langle\bar{3}032\rangle$	9	4	$9A\mu + 2\phi\theta$	$1/2 < 9 3\sqrt{3} 4 >$	$27 + 4(c/a)^2$
	$\{\bar{1}010\}$ or $\{\bar{2}110\}$	[0001]	0	2	$\phi\theta$	[001]	$(c/a)^2$
Second-order pyramidal zone $\{\bar{2}11l\}$	[0001]	0	1		$\mu\theta$	$1/2[001]$	$(1/4)(c/a)^2$
	(0001)	$1/3\langle\bar{2}110\rangle$	1	0	AB	$\langle100\rangle$	1
	$\{\bar{2}11\bar{l}\}$	$1/3\langle\bar{2}116\rangle$	1	4	$AB + 2\phi\theta$	$\langle102\rangle$	$1 + 4(c/a)^2$
	$\{\bar{2}11\bar{2}\}$	$1/3\langle\bar{2}113\rangle$	1	2	$AB + \phi\theta$	$\langle101\rangle$	$1 + (c/a)^2$
	$\{\bar{2}11\bar{3}\}$	$1/3\langle\bar{2}112\rangle$	3	4	$3AB + 2\phi\theta$	$\langle302\rangle$	$9 + 4(c/a)^2$
	$\{\bar{2}11\bar{4}\}$	$1/3\langle\bar{4}223\rangle$	2	2	$2AB + \phi\theta$	$\langle201\rangle$	$4 + (c/a)^2$

and

$$b_0 = a[(1/3)\rho^2 + (1/4)\sigma^2(c/a)^2]^{1/2} \quad (23)$$

for $\{\bar{1}01l\}$ planes

$$d = a/2[(1/3) + 4(\rho/3\sigma)^2(a/c)^2]^{1/2} \quad (24)$$

Taking $|\phi\theta'| = 1/|\phi\theta| = a/c$, η_2 is given by eq (4) with

$$\mathbf{D} = [\sigma AB - 2\rho\phi\theta']/2[\sigma + 4(\rho^2/\sigma)(a/c)^2] \quad \text{for } \{\bar{2}11l\} \text{ planes} \quad (25)$$

$$\mathbf{D} = [3\sigma A\mu - 2\rho\phi\theta']/2[\sigma + (4/3)(\rho^2/\sigma)(a/c)^2] \quad \text{for } \{\bar{1}01l\} \text{ planes} \quad (26)$$

Table 2. s values for various twin modes in h.c.p. metals

Plane	n	Equation	Cd	Zn	Co	Mg	Re	Zr	Ti	Ru	Be
{\bar{2}111}	1	$\frac{1}{1+4(c/a)^2}$	0.0657	0.0676	0.0867	0.0875	0.0898	0.0903	0.0906	0.0923	
	1	$\frac{1}{1+(c/a)^2}$	0.2195	0.2248	0.2752	0.2775	0.2837	0.2843	0.285	0.2891	
{\bar{2}112}	3	$\frac{2-(c/a)^2}{1+(c/a)^2}$		-0.1744	-0.1744	-0.1675	-0.1489	-0.1471	-0.145	-0.1327	
	4	$\frac{3-(c/a)^2}{1+(c/a)^2}$	-0.122	* -0.1008							
{\bar{2}113}	1	$\frac{1}{3+(4/3)(c/a)^2}$	0.1292	0.1316	0.1533	0.1543	0.1571	0.1572	0.1579	0.1594	
	6	$\frac{3-(4/3)(c/a)^2}{3+(4/3)(c/a)^2}$		-0.0802	-0.0802	-0.0748	-0.0574	-0.0568	-0.0526	-0.0436	
{\bar{2}114}	3	$\frac{1-(1/2)(c/a)^2}{2+(1/2)(c/a)^2}$	-0.2059	-0.1945	-0.0955	-0.0955	-0.0925	-0.0805	-0.079	-0.0775	-0.0709
	4	$\frac{2-(1/2)(c/a)^2}{2+(1/2)(c/a)^2}$	0.0588	0.074	0.206	0.210	0.226	0.228	0.230	0.2388	

Table 2. *s* values for various twin modes in h.c.p. metals—Continued

IV. Dislocation dissociations

A. AB EDGE DISLOCATIONS ON THE BASAL PLANE

The general equation for dissociation of an **AB** edge dislocation on the basal plane into single twinning partials on $\{\bar{2}11l\}$ planes is given by

$$\mathbf{AB} \rightarrow [(1-\rho s)\mathbf{AB} + \sigma s \boldsymbol{\theta} \boldsymbol{\mu}] + s[\rho \mathbf{AB} + \sigma \boldsymbol{\mu} \boldsymbol{\theta}] \quad (27)$$

For symmetric twinning partials on $\{\bar{2}11l\}$ planes it is given by

$$\mathbf{AB} \rightarrow (1-2\rho s)\mathbf{AB} + s[\rho \mathbf{AB} + \sigma \boldsymbol{\mu} \boldsymbol{\theta}] + s[\rho \mathbf{AB} + \sigma \boldsymbol{\theta} \boldsymbol{\mu}] \quad (28)$$

and for non-symmetric partials on $\{\bar{2}11l\}$ planes by

$$\begin{aligned} \mathbf{AB} \rightarrow & [(1-s_1\rho_1 - s_2\rho_2)\mathbf{AB} + (s_2\sigma_2 - s_1\sigma_1)\boldsymbol{\mu} \boldsymbol{\theta}] \\ & + s_1[\rho_1 \mathbf{AB} + \sigma_1 \boldsymbol{\mu} \boldsymbol{\theta}] + s_2[\rho_2 \mathbf{AB} + \sigma_2 \boldsymbol{\theta} \boldsymbol{\mu}] \end{aligned} \quad (29)$$

B. AB 60° DISLOCATIONS ON THE BASAL PLANE

The general equation for dissociation of **AB** 60° dislocations on the basal plane into single twinning partials on $\{\bar{1}01l\}$ planes is given by

$$\mathbf{AB} \rightarrow [\mathbf{AB} + \rho s \boldsymbol{\mu} \mathbf{A} + \sigma s \boldsymbol{\theta} \boldsymbol{\mu}] + s[\rho \mathbf{A} \boldsymbol{\mu} + \sigma \boldsymbol{\mu} \boldsymbol{\theta}] \quad (30)$$

For symmetric twinning partials on $\{\bar{1}01l\}$ planes it is given by

$$\mathbf{AB} \rightarrow [\mathbf{AB} + 2\rho s \boldsymbol{\mu} \mathbf{A}] + s[\rho \mathbf{A} \boldsymbol{\mu} + \sigma \boldsymbol{\mu} \boldsymbol{\theta}] + s[\rho \mathbf{A} \boldsymbol{\mu} + \sigma \boldsymbol{\theta} \boldsymbol{\mu}] \quad (31)$$

and for non-symmetric partials by

$$\begin{aligned} \mathbf{AB} \rightarrow & [\mathbf{AB} + (\rho_1 s_1 + \rho_2 s_2) \boldsymbol{\mu} \mathbf{A} + (\sigma_2 s_2 - \sigma_1 s_1) \boldsymbol{\mu} \boldsymbol{\theta}] \\ & + s_1[\rho_1 \mathbf{A} \boldsymbol{\mu} + \sigma_1 \boldsymbol{\mu} \boldsymbol{\theta}] + s_2[\rho_2 \mathbf{A} \boldsymbol{\mu} + \sigma_2 \boldsymbol{\theta} \boldsymbol{\mu}] \end{aligned} \quad (32)$$

C. AB MIXED DISLOCATIONS ON THE $\{01\bar{1}0\}$ FIRST-ORDER PRISM PLANE

AB dislocations on the first-order prism plane (cross-slip plane) can dissociate into twinning partials on $\{\bar{2}11l\}$ and $\{\bar{1}01l\}$ planes when they assume specific orientations. For $\{\bar{2}11l\}$ planes these orientations are $\langle\bar{2}116\rangle$, $\langle\bar{2}113\rangle$, $\langle\bar{2}112\rangle$ and $\langle\bar{4}223\rangle$ for $l=1, 2, 3$, and 4 respectively, while for $\{\bar{1}01l\}$ planes the orientations are $\langle\bar{2}113\rangle$, $\langle\bar{4}223\rangle$ and $\langle\bar{2}111\rangle$ for $l=1, 2$, and 3 respectively. For single twinning partials on $\{\bar{2}11l\}$ planes eq (27) applies, and for single twinning partials on $\{\bar{1}01l\}$ planes eq (30) applies.

D. $A\mu$ EDGE DISLOCATIONS ON THE BASAL PLANE

The equation for dissociation of $A\mu$ edge dislocations into twinning partials on $\{\bar{1}01l\}$ planes are the same as eqs (30) to (32) when AB is replaced by $A\mu$. Their morphologies are the same as those for AB 60° dislocations with, in this case, the stair-rod dislocations being pure edge.

E. $[AB + \phi\theta]$ DISLOCATIONS ON THE $\{\bar{2}112\}$ SECOND-ORDER PYRAMIDAL SLIP PLANE

$\{\bar{2}112\}$ second-order pyramidal slip is common in Cd and Zn [31–37] when basal slip is unfavorable, but is found to be more difficult in other metals [38–45], and is not expected in terms of the usual criteria for the choice of slip system. The discrepancy is attributed to its stabilization by dissociation on the $\{\bar{2}112\}$ slip plane [10]. Various zonal dislocations are possible [9, 10, 46]. The partial dislocation could have a Burgers vector $s\mathbf{b}_0$ with $s=s'$, corresponding to single-layer twin fault, or $s=2s'$ for double-layer twin fault. Smaller Burgers vectors can result for thicker lamellae; this is the case in Cd and Zn for four-layer twin lamellae, and in metals for which $c/a < \sqrt{8/3}$ for three-layer twin lamellae.

Atomic shuffling is least when $s=s'$, and if γ is not too high the $[AB + \phi\theta]$ dislocation can dissociate into $q=4$ glissile partials in metals for which $c/a < \sqrt{8/3}$, with $s_1=s_2=s_3=s'$ and $s_4=1-3s'$ and $n=1, 2$, and 3 layers between successive partials. For Cd and Zn q could be 5 with $s_1=s_2=s_3=s_4=s'$ and $s_5=1-4s'$ and $n=1, 2, 3$, and 4 layers between successive partials. The large Burgers vector of $[AB + \phi\theta]$ allows for many non-planar dissociations given by eq (5), with

$$\mathbf{QP} = [AB + \phi\theta],$$

$\Psi\Omega_m = AB$ and $\mathbf{Y}\xi_m = \mu\theta$ for $\{\bar{2}11l\}$ planes, and $\Psi\Omega_m = A\mu$ for $\{\bar{1}01l\}$ planes. Edge dislocations dissociate into twinning partials on $\{\bar{2}11l\}$ planes; those on $\{\bar{1}01l\}$ planes result when the orientations are $\langle\bar{2}113\rangle$ (pure screw), $\langle\bar{2}243\rangle$ and $\langle\bar{2}753\rangle$ for $l=1, 2$, and 3 respectively.

The $s' [AB + \phi\theta]$ dislocation could also dissociate into single glissile twinning partials on $\{\bar{2}11l\}$ and $\{\bar{1}01l\}$ planes. γ_m is positive for twinning partials on $\{\bar{2}111\}$, $\{2114\}$, and $\{\bar{1}012\}$ planes in all metals and for $\{\bar{1}011\}$ and $\{\bar{1}013\}$ in metals for which $c/a < \sqrt{8/3}$. The γ_m are too small to initiate a twin lamella, but could enhance spontaneous dissociation at an existing twin and may contribute to nucleation of a twin at a dislocation pile up. Similar dissociations apply to $\phi\theta$ dislocations on first and second order prism planes [47].

F. DISCUSSION

Values of γ have been approximated [10] by applying anisotropic elasticity to changes in the closest atomic approach [48] at the twin boundaries, and when compared with γ_m permit an estimate of the tendency to dissociate for the various twin modes. These show several cases for which **AB** dislocations could lock. In these cases $\gamma_m/\gamma < 1$ for Cd and Zn and > 1 for Zr and Ti which show a strong temperature dependence for both basal and prism slip, but less so for prism slip [49]. This is consistent with the smaller γ_m for dissociation of **AB** on the prism plane.

Dissociations of **AB** and $[\mathbf{AB} + \phi\theta]$ dislocations can account for all the twin modes and various plastic flow behavior [47, 11]. For $\phi\theta$ dislocations it is found that $\gamma_m/\gamma > 1$ in many cases, indicating that the dislocations would lock soon after they form. The only evidence for $\phi\theta$ dislocations is in Zn [32] and Be [45] when $[\mathbf{AB} + \phi\theta]$ dislocations dissociate. This does not rule out a possible role in twinning if their formation preceded twinning, but it is unlikely that the origin of $[\mathbf{AB} + \phi\theta]$ dislocations is due to the interaction of **AB** and $\phi\theta$ dislocations [50].

The dissociation processes are affected by orientation and stress-sense effects. The $\{\bar{2}111\}$ and $\{\bar{2}113\}$ twin modes, with $n=1$ ($s=+$), are favored by tension along $\phi\theta$ and compression along **AB**, while the $\{\bar{2}112\}$ and $\{\bar{2}114\}$ twin modes, with $n=3$ ($s=-$), are favored by opposite stresses. The $\{\bar{1}011\}$ and $\{\bar{1}013\}$ twin modes with $n=4$ ($s=-$) in metals with $c/a < \sqrt{8/3}$, are favored by compression along $\phi\theta$ and tension parallel to $\mathbf{A}\mu$. This behavior is consistent with $\{\bar{1}011\}$ twinning in Mg [51, 52].

For the $\{\bar{1}012\}$ twin mode, twinning is favored for compression along $\phi\theta$ and tension parallel to $\mathbf{A}\mu$ in Cd and Zn ($s=-$), and for opposite stresses in metals for which $c/a < \sqrt{8/3}$ ($s=+$). The lack of $\{\bar{1}011\}$ and $\{\bar{1}013\}$ twins in Cd and Zn could be attributed to the large shear-strain (small γ_m when $n \leq 4$) and to the availability of the more favorable $\{\bar{1}012\}$ twin mode for the same stress conditions. In Mg, where $\{\bar{1}011\}$ and $\{\bar{1}013\}$ twins are found [25], the orientation and stress-sense effects are opposite to that of $\{\bar{1}012\}$ twins. In this case $\{\bar{1}011\}$ and $\{\bar{1}013\}$ twins are more favorable than $\{\bar{1}012\}$ twins for compression parallel to $\phi\theta$ or tension parallel to $\mathbf{A}\mu$. The $\{\bar{3}034\}$ twin mode has the same stress-sense characteristics as $\{\bar{1}011\}$. γ_m is greatest for the $\{\bar{1}013\}$ twin mode when **AB** dislocations dissociate, while it is greatest for the $\{1011\}$ twin mode when $[\mathbf{AB} + \phi\theta]$ dislocations dissociate.

Of the $\{\bar{2}111\}$ twin modes in Zr and Ti, $\{\bar{2}113\}$ is least frequently found [53–55]. This is consistent with the large shear-strain and smaller γ_m and γ_m/γ values when $n=1$ in most of the dissociations. In cobalt $\{\bar{2}111\}$ twins are reported by Davis and Teghtsoonian [56], while Seeger et al. [38] find $\{\bar{2}112\}$ and $\{\bar{2}114\}$ twins. The difference may be due to orienta-

tion and stress effects; these modes have opposite stress-sense characteristics. In Zr $\{\bar{2}11\}$ twin modes of lower l are more numerous at all temperatures [53, 54]. This is also the case in Ti at high temperatures [57, 58], but at -196°C the $\{\bar{2}114\}$ twin mode is found to be more numerous [55]. γ_m is largest for $\{\bar{2}114\}$ twins when **AB** dislocations dissociate, while it is largest for $\{\bar{2}111\}$ twins when $[\mathbf{AB} + \phi\theta]$ edge dislocations dissociate. Rosi et al. [55] find that the $\{\bar{2}114\}$ twins, which form in titanium at -196°C in tension, increase in frequency as the **AB** pole is approached. This is consistent with the stress-sense characteristics and with the view that locked **AB** dislocations in these crystals may not be able to thermally unlock at these low temperatures [49, 11].

The preference for $\{\bar{2}11\}$ twinning of lower l at higher temperatures suggests that these twin modes may be due to dissociation of $[\mathbf{AB} + \phi\theta]$ dislocations. This is consistent with studies in zinc. Burr and Thompson [59] find that $\{\bar{2}112\}$ slip precedes $\{\bar{1}012\}$ twinning at room temperature. These crystals were stressed parallel to the basal plane and show that twinning results in tension tests at 20 or 77 K at lower stresses than are required at room temperature, consistent with stress-sense effects and with the partialized dislocation model. Second order pyramidal slip is found in cadmium [31–34], zinc [35–37, 32], cobalt [38], zirconium [39, 40], hafnium [39] and beryllium [41–45].

V. FCC Metals

If $\mathbf{AB}(\mathbf{b} = 1/2[1\bar{1}0])$ dislocations are not dissociated into Shockley partials on their $\{111\}$ slip plane, they may dissociate into partials which are glissile on oblique planes [3]. The edge dislocation line is parallel to the $\langle 11\bar{2} \rangle$ zone axis of higher order fault planes. The general equation for symmetric dissociations of **AB** is given by

$$\mathbf{AB} \rightarrow (1 - 2\rho s)\mathbf{AB} + s[\rho\mathbf{AB} + \sigma\mathbf{D}\delta] + s[\rho\mathbf{AB} + \sigma\delta\mathbf{D}]. \quad (33)$$

$\mathbf{D}\delta = 1/3[111]$ and ρ and σ are integers given by $\sigma = 3l$ and $\rho = 2(h-l)$, where h and l are indices of the $[hkl]$ Burgers vector of the perfect dislocation on the fault plane. Various planes and Burgers vectors of this zone are listed in table 3 in Miller and Thompson tetrahedron [60] coordinates. s is given by eq (6) and

$$s' = 3\rho/[3\rho^2 + 2\sigma^2]. \quad (34)$$

$\{\bar{2}41\}$, $\{\bar{1}52\}$, and $\{174\}$ are imperfect boundaries with properties similar to $\{\bar{2}111\}$ and $\{\bar{2}113\}$ simple shear faults in h.c.p. metals [10], while $\{\bar{1}31\}$, $\{021\}$, and $\{132\}$ are perfect twin boundaries, similar to $\{\bar{2}112\}$ and $\{\bar{2}114\}$ twin boundaries in h.c.p. metals. The distortions are

TABLE 3. *Types of dislocations in f.c.c. metals.*

Plane	$\{\bar{1}10\}$	$\{\bar{2}41\}$	$\{\bar{1}31\}$	$\{\bar{1}52\}$	$\{021\}$	$\{174\}$	$\{132\}$	$\{111\}$
b_0	$\frac{1}{3}\langle 111 \rangle$	$\frac{1}{2}\langle 312 \rangle$	$\frac{1}{2}\langle 714 \rangle$	$\langle 201 \rangle$	$\frac{1}{2}\langle 5\bar{1}2 \rangle$	$\langle 3\bar{1}1 \rangle$	$\langle 4\bar{2}1 \rangle$	$\frac{1}{2}\langle 1\bar{1}0 \rangle$
ρ	0	1	3	2	3	4	6	1
σ	1	3	6	3	3	3	3	0
b_0	$D\delta$	$AB + 3D\delta$	$3AB + 6D\delta$	$2AB + 3D\delta$	$3AB + 3D\delta$	$4AB + 3D\delta$	$6AB + 3D\delta$	AB

more severe for the imperfect twins, limiting them to a possible role in Martensitic transformations. For the perfect twins the distortions are normal to the twin boundary and increase as ρ/σ increases; $\{\bar{1}31\}$ is the most favorable. The symmetric dissociation of AB into twinning partials on $\{\bar{1}31\}$ planes is given by

$$AB \rightarrow (1-6s)AB + s[3AB + 6D\delta]_{(\bar{1}31)} + s[3AB + 6D\delta]_{(3\bar{1}1)}. \quad (35)$$

The γ_m values for $s=s'$ are listed in table 4. γ_m is also positive for non-symmetric dissociations when the number of layers in the fault lamella for the second partial is $(1-s)/s$; these thicker lamellae are less likely to develop.

Non-edge dislocations on the $\{11\bar{1}\}$ plane with Burgers vector $AD=1/2[101]$ could also dissociate into glissile partials on these higher

TABLE 4. γ_m values for dissociation of dislocations in f.c.c. metals. The units are ergs/cm². The first column refers to the equations in the text.

Equation	α -brass	Al	Cu	Au	Pb	Ni	Ag	Th
35	130	83	144	104	38	232	104	115
36	305	206	355	235	88	609	251	294
38	152	90	167	109	52	282	117	144
39	136	84	148	105	39	241	107	120
41	164	133	189	143	50	320	140	144

order twin planes when **AD** assumes an orientation $\langle hkl \rangle$ which lies in the twin plane. For the $\{\bar{1}31\}$ twin mode $\langle hkl \rangle$ corresponds to the screw orientation of **AD** and the dissociation is given by

$$\mathbf{AD}_s \rightarrow 1/11[3\mathbf{AB} + 6\mathbf{D}\boldsymbol{\delta}]_{(\bar{1}31)} + 1/11[3\mathbf{BD} + 6\mathbf{A}\boldsymbol{\alpha}]_{(\bar{1}31)}. \quad (36)$$

The γ_m values are listed in table 4. Both partials are glissile on the $(\bar{1}31)$ cross slip plane. This dissociation becomes more favorable in higher $\{111\}$ stacking fault energy metals.

The distortion energy of the faults can be approximated from changes in the closest atomic approach by [48].

$$\gamma = (1/2) \alpha d \epsilon^2 E_\phi \quad (37)$$

where ϵ is the elastic strain, d the spacing of distorted planes, E_ϕ the tension modulus (Young's modulus) in the direction of the distortion, and α the number of distorted planes in the fault or relative density of distorted atoms in the fault. The resulting distortion energies for $1/11(714)\{\bar{1}31\}$ faults are listed in table 5. Comparing γ_m for eq (36) with the values in table 5 shows that $\gamma_m/\gamma \approx 1$ for dissociations of screws in α -brass, Pb, and Th, and 0.6 to 0.9 in the other metals. The tendency to dissociate by eq (36) may impose a drag on screws tending to lower their mobility at lower temperatures. For symmetric dissociations of edge dislocations on $\{\bar{1}31\}$ planes, $\gamma_m/\gamma \approx 1/3$. This is too small to affect isolated dislocations but might be effective at complex dislocation dipoles and braids, during work-hardening, where opposite sign partials may interact.

TABLE 5. γ values for $\{131\}$ faults in fcc metals. The units are ergs/cm².

Metal	α -brass	Al	Cu	Au	Pb	Ni	Ag	Th
γ	302	347	405	297	87	730	282	298

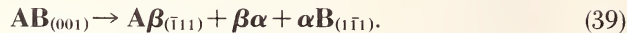
For dissociation into partials on the $\{021\}$ twin plane the orientation of **AD** is $\langle 3\bar{1}2 \rangle$ and the dissociation is given by

$$\mathbf{AD}_{(3\bar{1}2)} \rightarrow 1/5[\mathbf{BD} + 3\mathbf{AB} | \boldsymbol{\delta}\gamma] + 1/5[3\mathbf{AB} + 3\mathbf{D}\boldsymbol{\delta}]_{(021)}. \quad (38)$$

The γ_m values are listed in table 4. They are smaller than those for eq 36, and since γ is also larger on this plane, this dissociation is less favorable.

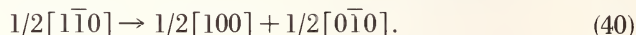
The **AB** screw dislocation could also slip on other planes ($\{001\}$ and $\{110\}$) of the zone which has its axis parallel to $\langle 1\bar{1}0 \rangle$. For slip on $\{001\}$, which is the next most widely spaced plane, the edge dislocation line is parallel to the $\langle 1\bar{1}0 \rangle$ zone axis of symmetric $\{\bar{1}11\}\langle 1\bar{1}2 \rangle$ and $\{\bar{1}\bar{1}1\}\langle 1\bar{1}2 \rangle$

twin systems and can dissociate according to

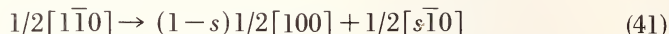


The γ_m values are listed in table 4. Comparing these with reported values of γ show that $\gamma_m/\gamma > 1$ in α -brass, Cu, Au and Ag; $\gamma_m/\gamma \approx 1$ in Pb, Ni and Th and $\gamma_m/\gamma < 1$ in Al. It suggests that $\{001\}$ slip is possible in aluminum but much less likely in the other metals. Equation (39) is the well-known Lomer-Cottrell lock proposed for interactions of $1/2\langle 110 \rangle$ dislocations on different $\{111\}$ planes. It can also form by cross-slip of AB screws from $\{111\}$ to $\{001\}$ [61]. Nabarro discussed Stroh's evaluations for the stability of this lock [62]. $\{001\}$ slip is reported in aluminum [63–65].

For $1/2\langle 1\bar{1}0 \rangle\{110\}$ slip, edge dislocations might dissociate according to



If one partial separates into the compressive region of the second, the closest atomic approach is reduced by $\sqrt{1/2}a - 1/2a$, severely distorting the lattice. If it separates into the tensile region it can reduce the Burgers vector of the second partial by this amount without affecting the closest atomic approach. This is given by



where $s = 1 - \sqrt{1/2} = 0.293$ and γ_m has the values listed in table 4. This dissociation could lock the edge dislocation if these values are greater than the energy due to the change in coordination from 12 to 9; $\{110\}$ slip has been proposed [66, 67], due to the smaller elastic energy factor for dislocations on this plane.

Equation (41) also applies to edge dislocations in the NaCl lattice. Many of these slip on the $1/2\langle 110 \rangle\{110\}$ system and show avalanche behavior in glide band formation [68, 69]. In this case the dissociation depends on the nature of the ionic forces and relative ionic radii. Various twin modes are found in this lattice. In PbS several $\{hh\ell\}$ twins are reported [70, 71]. These are of the same zone with a common $\{110\}$ plane of shear, and are readily explained by this model [72].

VI. Diamond Lattice

The **AB** dislocation in the diamond lattice can dissociate into Shockley partials on the $\{111\}$ plane [73]; $\gamma_m/\gamma > 1$ in both silicon and germanium. This is a double-lattice fcc structure, with the intrinsic stacking fault being a one-layer (double-plane) twin having two low-energy coherent twin boundaries. Motion of the Shockley partials (which can be considered

as zonal dislocations [3, 74]) creates and dissolves the twin lamella, and can be described in two equivalent ways: (i) by shear between closely spaced {111} planes as contrasted with shear between widely spaced planes for the perfect dislocation. This requires breaking three times as many atomic bonds and should be more difficult [75], (ii) by shear between widely spaced planes accompanied by a rotation of atom pairs through 120° as the first Shockley partial passes and a similar rotation as the second one passes [76] [see fig. 3a]. In the latter it is necessary that atoms along the dislocation line pass through a 12 percent reduction in the closest atomic approach, consistent with the high Peierls-Nabarro lattice resistance, and thermally activated flow behavior.

Due to the open nature of the lattice, various stacking faults are possible for which both the closest atomic approach and coordination number are maintained. A Type II fault [77] of this type corresponds to a $\frac{1}{6}[11\bar{1}]$ displacement which, for dissociation of an **AB** type dislocation, results by

$$\frac{1}{2}[10\bar{1}] \rightarrow \frac{1}{6}[11\bar{1}] + \frac{1}{6}[2\bar{1}\bar{2}], \quad (42)$$

where $\gamma_m = Ka/24\pi$, the same as for the Shockley dissociation. This is illustrated in figure 3(b). The Burgers vector is along $[11\bar{1}]$ but the separation is along $[11\bar{2}]$ on (111). The Shockley dissociation is likely in annealed crystals whereas eq (42) may be favored during plastic flow if rotation of atom pairs to form the intrinsic twin fault is difficult. Since the $\frac{1}{6}[11\bar{1}]$ par-

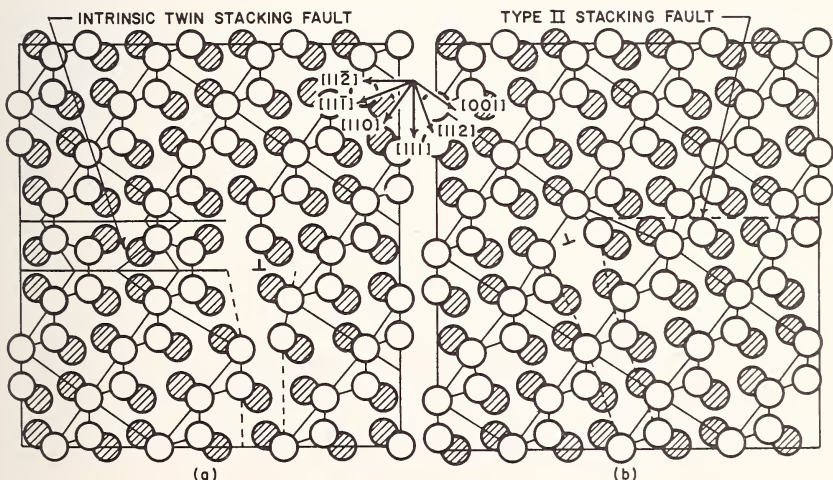


FIGURE 3. (a) Atomic model of a Shockley edge dislocation at an intrinsic stacking fault in the diamond lattice. (b) Type II stacking fault with $b = 1/6 [11\bar{1}]$. The projection plane is $(1\bar{1}0)$ and the hatched circles lie at $a\sqrt{1/8}$ behind the plane of the paper.

tial has a component normal to the $\{111\}$ slip plane its formation would tend to stabilize edge dislocation dipoles.

Dislocations in this lattice could also dissociate into partials which are glissile on $\{132\}$ planes [3]; this is a report twin plane [78] in various semiconductors. For symmetric partials on $\{132\}$ planes the dissociation is



For $s = s' = 1/7$, given by eq (34), the distortions at the twin boundary are very severe.² A non-symmetric fault which maintains the closest atomic approach results when $s = -1/14$. In this case $\gamma_m = 431$ and 516 ergs/cm² for Ge and Si respectively. The elements of the second undistorted plane are $\kappa_2 = \langle 1\bar{1}0 \rangle$ and $\boldsymbol{\eta}_2 = \langle 111 \rangle$, and the shear-strain for faulting is $S = 0.524$.

Non-edge \mathbf{AD} dislocations on the $\{11\bar{1}\}$ plane could dissociate into partials which are glissile on the $\{132\}$ plane when they assume the $\langle 5\bar{3}2 \rangle$ orientation. In this case



$\gamma_m = 334$ and 424 ergs/cm² for Ge and Si respectively. The sessile partial, of the form $1/14[326]$, can further dissociate into a $\gamma\mathbf{D}$ Shockley partial giving



γ_m on the Shockley partial is 368 and 453 ergs/cm² for Ge and Si respectively, and on the $1/14[6\mathbf{AB} + 3\mathbf{D}\boldsymbol{\delta}]$ partial it is 211 and 248 ergs/cm² in Ge and Si respectively. If AD is dissociated into widely spaced Shockley partials on the $\{11\bar{1}\}$ slip plane, the $\mathbf{A}\gamma$ partial can dissociate according to



$\gamma_m = 121$ and 141 ergs/cm² for Ge and Si respectively.

VI.1. Dislocation mobilities in germanium

Both the planar and non-planar dissociations predict a high dislocation resistance in this lattice [79, 80]. Studies of glide band formation in silicon [81], deformed at low strain-rates, show characteristics quite similar to that found in alkali-halide single crystals [68, 69]. The narrow glide bands taper to a single plane at opposite ends and the dislocation morphology

² This is so great that it is questionable whether the reported defects are mechanical twins. Christian [28] suggests that later work makes it doubtful the $\{123\}$ twins do in fact exist in diamond lattice.

in the bands, as revealed by their phase retardation birefringence characteristics, are in the form of large concentric loops on neighboring planes with staggered sources in the central region of the band.

Dislocation motion in this lattice is strongly temperature dependent and can be expressed by

$$\nu = \nu_0 \exp [-E(\tau)/kT] \quad (47)$$

where $E(\tau)$ is the activation energy for motion of the dislocation. Kabler [82] made careful studies of the motion of *isolated* dislocations in germanium and found that the activation energy for 60° dislocations decreases from 2.25 eV at stresses of $\tau < 0.8 \text{ kg/mm}^2$ to 1.49 eV at $\tau > 8 \text{ kg/mm}^2$. The activation energy for screw dislocations is found to be independent of stress and equal to 1.47 eV.

If the pre-exponential term, ν_0 , is constant or an increasing function of stress, a plot of $\ln \nu$ versus $\ln \tau$ would be concave upwards. In Kablers studies the curve is concave downward, and can only result if ν_0 is a decreasing function of stress for the intermediate stresses. To account for this behavior, Celli et al. [83] proposed that the dislocation lines contain randomly distributed dragging points which limit the movement of kinks along the dislocation line. The orthogonal kink on the 60° dislocation makes an angle of 30° with the Burgers vector, $6\frac{1}{2}^\circ$ off the $\langle 5\bar{3}2 \rangle$ orientation. If the kinks are at $83\frac{1}{2}^\circ$ instead of 90° they can lock and serve as dragging points. Since only large kinks can lock, dragging points are not expected at low stresses, while at much higher stresses the dragging points can be overcome. Locking is possible for kinks on screws only when they make an angle of $36\frac{1}{2}^\circ$ with the dislocation line.

The decreasing activation energy with stress for 60° dislocation can be accounted for if the high activation energy for $\tau < 0.8 \text{ kg/mm}$ corresponds to motion of dissociated dislocations and the lower value for $\tau > 8 \text{ kg/mm}$ to motion of almost perfect ones. The decreasing intermediate values could then be related to the energy required to constrict and recombine the Shockley partials. The activation energy is given by [84]

$$E[\tau] = E_c + Rx^* \quad (48)$$

where E_c is the constriction energy, R the recombination energy, and x^* the length of the recombined segment, equal to the critical kink separation l . When $l > x^*$ the dislocation can dissociate ahead of the line to effectively displace the segment by a distance h . The sequence of configurations during a thermal vibration of the activated process is similar to that proposed by Friedel [84].

The recombination energy for a pair of Shockley partials at a 60° dislocation is given by [85]

$$R = (Ka^2/24\pi) \ln (d/eb) \quad (49)$$

where a is the lattice parameter, b the Burgers vector of the perfect dislocation, and d the spacing of the partials. The constriction energy is given by [86].

$$E_c = 0.032Gb^2d[\ln (d/eb)]^{1/2} \quad (50)$$

where $G = K(1 - \nu)$ and the core radius is taken as $r_0 = eb$, as for recombination.

The separation of partials depends on both the applied stress and the effective stacking fault energy, and is given by [85]

$$d = Ka^2/24\pi(\gamma + \tau b_1) \quad (51)$$

where b_1 is the Burgers vector of the Shockley partial.

The interaction energy for kinks on a dissociated dislocation can be approximated from that for a perfect dislocation [87, 88] by

$$E_k = [(Gb_1^2h_1^2\beta)/8\pi l][1 + s(d_0 - d)/(d_0 - eb)] \quad (52)$$

where h_1 is the height of the Shockley kinks, d_0 the separation of Shockley partials at $\tau = 0$, and $\beta = (1 - 2\nu)/(1 - \nu)$ for kinks in approximately screw orientation. The first term on the right corresponds to the interaction energy of kinks on a Shockley edge dislocation while the second term includes the interaction from the kinks on the neighboring Shockley partial. s is a normalizing factor ($= 5.75$) chosen to give the interaction energy of kinks on a perfect dislocation when $d = eb$.

The critical separation of the kinks, $l = x^*$, occurs when $E_k = W$ where $W = \tau bhl$ is the work done by the applied stress to displace the segment. This gives

$$x^* = \{(Gb^2\beta/36\sqrt{3}\pi\tau)[1 + s(d_0 - d)/(d_0 - eb)]\}^{1/2}. \quad (53)$$

Substituting eqs (49), (50), (51), and (52) into eq (48) for a value of $\gamma = 192$ ergs/cm², the $E(\tau)$ values are plotted in figure 4. The theoretical curve is compared with the activation energies computed from the data of Kabler [82]. For $0.8 > \tau > 8$ kg/mm², $E(\tau)$ is taken as the constant upper and lower values corresponding to dissociated and almost perfect dislocations respectively. The value of $E = 1.47$ eV for screws is consistent with undissociated dislocations, since the repulsive force is smaller and dangling bonds must be created by dissociation [73].

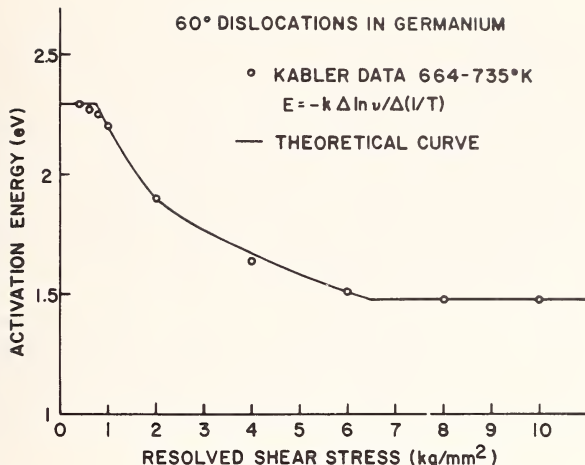


FIGURE 4. Activation energy for dislocation motion by double-kink formation at dissociated dislocations in germanium when $\gamma = 192 \text{ ergs/cm}^2$. These are compared with the activation energies computed from the data of Kabler [82].

The pre-exponential term has the form $v_0 = B\tau^m$ in each of the three stress ranges. For $\tau < 0.8 \text{ kg/mm}^2$, $m_1 = 3.32$ and $B_1 = 1.55 \times 10^{10}$; for $1 < \tau < 6 \text{ kg/mm}^2$, $m_2 = -4.64$ and $B_2 = 7.87 \times 10^9$, while for $\tau > 8 \text{ kg/mm}^2$, $m_3 = 2.1$ and $B_3 = 4.33 \times 10^4$. The negative value of m_2 for intermediate stresses is attributed to dragging points at deeper kinks which develop by coalescence of unit kinks as the stress increases. Unit kinks which form at lower stresses cannot lock, while at higher stresses the dragging points can be overcome. The value of $\gamma = 192 \text{ ergs/cm}^2$ is twice the reported stacking fault energy [89]; this may be related to effects which prevent equilibrium separation under dynamic conditions for the intrinsic twin stacking fault, or it may correspond to the Type II stacking fault. Hirth and Lothe [74] place the two partials on different planes displaced by $1/2\mathbf{D}\delta$ and propose that the second partial glides by shuffling a row of interstitials (or vacancies). This description is equivalent to shear between widely spaced planes accompanied by a rotation of atom pairs, but the assumption of different slip planes is not necessary since the equivalent model of shear between closely spaced planes creates the perfect twin fault lamella with shear on a single plane. Ice crystals show similar flow behavior [90]. The basal plane of this lattice is a double layer structure with a similar intrinsic stacking fault, consistent with the above model for the flow behavior.

VII. BCC Metals

In bcc metals both screw and edge dislocations meet the criteria for partialization. The low index Burgers vectors in this crystal lie on a

bi-pyramid of $\{110\}$ surfaces. The (001) square base, $ABCD$, has μ at its center and $\langle 100 \rangle$ edges; the oblique edges of the pyramids are $1/2\langle 111 \rangle$ with θ at the top of the pyramid, and ϕ at the bottom of the inverted pyramid. In this notation, $\mathbf{AB} = [100]$, $\mathbf{AD} = [010]$ and $\mathbf{\phi\theta} = [001]$; $\mathbf{A\theta} = 1/2[111]$, $\mathbf{B\theta} = 1/2[\bar{1}11]$, $\mathbf{C\theta} = 1/2[\bar{1}\bar{1}1]$ and $\mathbf{D\theta} = 1/2[\bar{1}\bar{1}\bar{1}]$; $\mathbf{A\mu} = 1/2[110]$, $\mathbf{AC} = [110]$, $\mathbf{B\mu} = 1/2[\bar{1}10]$ and $\mathbf{BD} = [\bar{1}10]$. The other $\langle 110 \rangle$ vectors are given by sums such as $[101] = [\mathbf{AB} + \mathbf{\phi\theta}]$ etc. Similarly all other vectors are represented by sums of unit vectors which lie on the plane of shear for the fault mode.

$\mathbf{A\theta}$ screw dislocations are parallel to the zone axis of three $\{112\}$ and three $\{110\}$ planes and can dissociate into three $s\mathbf{A\theta}$ partials which are glissile on these planes, or three $s\mathbf{AC}$ type partials which are glissile on $\{110\}$ planes [91–96]. $s = 1/3$ for $\mathbf{A\theta}$ partials and $1/8$ for \mathbf{AC} type partials. The dissociations are given by

$$\mathbf{A\theta}_s \rightarrow 1/3\mathbf{A\theta} + 1/3\mathbf{A\theta} + 1/3\mathbf{A\theta} \quad (54)$$

$$\mathbf{A\theta}_s \rightarrow 1/2\mathbf{A\theta} + 1/8\mathbf{AC} + 1/8[\mathbf{AB} + \mathbf{\phi\theta}] + 1/8[\mathbf{AD} + \mathbf{\phi\theta}]. \quad (55)$$

The faults which result for separation of $1/3\mathbf{A\theta}$ partials on $\{112\}$ and $\{110\}$ planes have a 5.73 percent reduction in the closest atomic approach normal to the boundary. If the partials lie on the slip plane the dislocation is glissile but an additional resistance results as the stacking fault *wedges* its way through the lattice. Taking $\epsilon = 0.0573$, $d = 2d_{\langle 112 \rangle}$ ($d_{\langle 112 \rangle}$ is the spacing of $\{112\}$ planes) and $\alpha = 2$, the energy of the $\{112\}$ fault can be approximated with eq (37). If the distortions are permitted to relax ϵ can reduce to $\epsilon_R = 0.01523$ with $\alpha = 6$. ϵ_R is computed by permitting the two sides of the stacking fault to separate to an equilibrium distance for which the remaining reduced spacing is equal to the increased spacing with neighboring atoms. The resulting unrelaxed and relaxed stacking fault distortion energies are listed in table 6. γ_R may apply to twin lamelae or widely extended faults, while γ would apply to stacking faults at partialized dislocations. The values of γ are four times those given by Wasilewski [48].

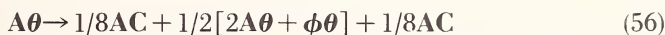
For $1/8[110](\bar{1}\bar{0})$ faults the crystal structure changes to b.c. monoclinic, which is almost orthorhombic. The parameters are $\alpha' = \beta' = 90^\circ$, $\gamma' = 88.1^\circ$, $c' = a$, $a'/c' = 0.885$ and $b'/c' = 1.132$. The elements of the second undistorted plane are $\kappa_2 = \{430\}$ and $\eta_2 = \langle \bar{3}40 \rangle$ and the shear-strain is $S = 0.25$. In this structure two nearest neighbors increase their spacing by 2.19 percent, while a next-nearest neighbor becomes a nearest neighbor with the same spacing. The distortion energy can be approximated by equating it to that of the three distorted bonds. The resulting values are approximately $1/4$ of those for $\{112\}$ faults listed in table 6.

TABLE 6. γ values for {112} and {103} faults in bcc metals. The units are ergs/cm².

Fault plane	Fault energy	α -Fe	Ta	W	V	Cr	Mo	Nb
{112}	γ	168	171	345	100	204	271	82
{112}	γ_m	36	37	74	21	44	58	17
{103}	γ	1018	1218	2960	959	2525	2020	935

This does not include the effect of an increase in coordination number from 8 to 9 for a single-layer fault and to 10 for a multiple layer lamella. As noted by Crussard [97] the larger interstitial sites enhance fault formation when interstitials are mobile.

Single-layer fault forms on {110} when the dislocation dissociates into 1/8[110] partials by [97, 98].



and double layer fault when it dissociates into 1/4[110] partials by



γ_m is 60 percent greater for the double layer faults but the distortion energy is estimated to be about twice as large, while still only about 1/2 that of 1/6 [111] faults. The γ_m values for eq (57) are listed in table 7.

TABLE 7. γ_m values for dissociation of dislocations in bcc metals. The units are ergs/cm². The first column refers to the equation in the text.

Equation	Dislocation	α -Fe	Ta	W	V	Cr	Mo	Nb
57	Edge	600	656	1390	455	867	1137	431
	Screw	419	434	1010	291	696	796	263
59	Edge	288	289	570	181	388	445	165
60	Edge	960	1050	2224	728	1388	1818	691
61	Screw	314	326	707	219	522	597	199
62	Edge	446	448	904	287	535	704	262
63	Edge	1360	1360	2510	816	1403	2015	739
66	Edge	1920	2100	4448	1456	2776	3636	1383

γ_m/γ is greater than unity for both eqs (56) and (57), which may play a role in Martensitic transformations.

Non-planar dissociations of screw dislocations have been studied by various authors [91–96] and can account for orientation and stress-sense effects [99–103] and thermally activated flow behavior [104–107]. A tensile stress parallel to $\langle 110 \rangle$ or compressive stress parallel to $\langle 001 \rangle$ tends to retard the sessile-glissile transformation for screw dislocations which are partialized on symmetric $\{112\}$ planes, while the reverse stresses enhance this transformation. This is consistent with stress-sense studies [99–103]; no asymmetry exists for screw dislocations when they are partialized on symmetric $\{110\}$ planes.

$\text{A}\theta$ edge dislocations can also dissociate into partials which are glissile on oblique planes. The Cottrell-Bilby dissociation for edge dislocations on a $\{11\bar{2}\}$ plane is given by [108]

$$\text{A}\theta_{(11\bar{2})} \rightarrow 1/3\theta\text{C}_{(112)} + 2/3[\text{A}\theta + \mu\theta]. \quad (58)$$

This is not favorable at isolated dislocations since the fault energy is high and, to a first approximation, the force between partials is zero. Motion of the $1/3\theta\text{C}$ partial to form intrinsic stacking fault requires an energy of γ , whereas motion in the opposite direction forms a double-layer stacking fault in the tensile region of the sessile dislocation, which can relax the distortions to lower the stacking fault energy and reduce the Burgers vector of the sessile partial to

$$(1-s)1/3[112]; s = 2(0.0573 - 0.01523) = 0.08414$$

is the relaxation of the two sides of the fault. The dissociation is

$$1/2[111] \rightarrow (1-s)1/3[112] + (1+2s)1/6[11w] \quad (59)$$

where

$$w = (4s-1)/(1+2s)$$

The γ_m are listed in table 7. In each metal $\gamma_m/\gamma_R \gg 1$ and $\gamma_m/\gamma > 1$, suggesting that edge dislocations on $\{112\}$ planes should tend to lock at low temperatures.

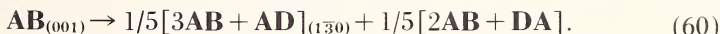
Vitek [109] recently applied a central force interaction between atoms at stacking faults in bcc metals, and finds an energy increase (with no minima or plateau) for $s\langle 111 \rangle\langle 112 \rangle$ faults as s increases. Several different potentials were used giving different numerical values, but the same γ surface contour. In the present study the strain at the bond which is normal to the fault increases to 5.73 percent as s increases from zero to

the 1/3 value. If s is taken as 1/6 the distortion at this bond is smaller but other atomic bonds increase in length and the distortion is found to be approximately twice that for $s = 1/3$.

In the Vitek approximation it would be less, suggesting the possibility for dissociations into glissile partials of smaller Burgers vector. In this case $\mathbf{A}\theta$ might dissociate into six $1/6\mathbf{A}\theta$ partials which separate on symmetric {112} and {110} planes. The smaller γ values for these faults permit partialization with γ_m approximately 1/2 as large as it is for $1/3\mathbf{A}\theta$ partials. It might further dissociate into nine $1/9\mathbf{A}\theta$ partials or twelve $1/12\mathbf{A}\theta$ partials (if extrinsic stacking faults are allowed) which separate on symmetric {112} and {110} planes. This *dilated core structure* would be more mobile than the three-partial morphologies. Nonscrew $\mathbf{A}\theta$ dislocations on $\{1\bar{1}0\}$ can dissociate into $1/3\mathbf{A}\theta$ type partials on oblique {111} planes [110]. In this case $\gamma_m/\gamma \approx 1/2$ is too small to be effective at isolated dislocations, but may play a role at tangles.

Perfect dislocations having other Burgers vectors can form by interactions of slip dislocations on different planes [111]. Favorable reaction products are $\langle 100 \rangle \{001\}$ and $\langle 100 \rangle \{011\}$ dislocations; this Burgers vector is found in α -Fe [112, 101]. $\langle 100 \rangle \{001\}$ edge dislocations can dissociate into $s\langle 310 \rangle$ twinning partials on $\{\bar{1}\bar{3}0\}$ planes. In this case $s' = 2/5$ with $s = -1/5$ when $n = 2$, and $s = 1/5$ when $n = 3$. In the former the elements of the second undistorted plane are $\kappa_2 = \{110\}$ and $\eta_2 = \langle 1\bar{1}0 \rangle$ and in the latter they are $\kappa_2 = \{100\}$ and $\eta_2 = \langle 010 \rangle$. The shear-strain for twinning is $S = 1$ when $n = 2$ and $S = -2/3$ when $n = 3$. The mode corresponding to $n = 2$ is listed for iron alloy martensites by Bevis et al. [116]. The $\langle 310 \rangle$ Burgers vector in bi-pyramid notation has the form $[3\mathbf{AB} + \mathbf{AD}]$ or $[2\mathbf{AD} + \mathbf{AC}]$. The former is used in dissociation of \mathbf{AB} and the latter in dissociations of \mathbf{AC} .

For single $(\bar{1}\bar{3}0)$ twin lamellae the dissociation of \mathbf{AB} is given by



The γ_m values are listed in table 7. The {103} twin lamella energies, evaluated from changes in the closest atomic approach with eq (37), are listed in table 6. Comparing these with γ_m for eq (60) show that γ_m/γ goes from 0.94 in α -Fe to 0.74 in the other metals, except Cr which has a value of 0.55. {103} stacking faults with the $\langle \bar{3}01 \rangle$ shear direction are found in niobium crystals [113], and {103} twins form in iron alloys [114]. The shear direction for the twins was not established, but suggested to be $\langle 5\bar{3}1 \rangle$. Hartley [115] has shown that {103} twinning could be produced by $1/10\langle 5\bar{3}1 \rangle$ partial dislocations which form when $\langle 100 \rangle$ screw dislocations dissociate. In this case the twinning shear-strain is $S = 1.9$. If the minimum shear-strain criterion applies, the $s\langle 310 \rangle$ shear mode would be more favorable.

If the **AB** edge dislocation dissociates into twinning partials on symmetric $\{103\}$ planes γ_m is 20 percent of those for eq (60). The **AB** 45° dislocation can dissociate into $1/8[110]$ screw dislocations on $\{1\bar{1}0\}$. For single twin lamellae the dissociation of **AB** is



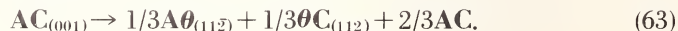
The γ_m values are listed in table 7. For dissociation into two $1/8\mathbf{AC}$ screw dislocations γ_m is 80 percent of those for eq (61). In each case $\gamma_m/\gamma > 1$.

$\langle 001 \rangle \{1\bar{1}0\}$ dislocations can develop by cross-slip of $\langle 001 \rangle \{100\}$ screws or by interactions of slip dislocations. If the edge component of $\phi\theta$ dissociates into single $1/3\mathbf{A}\theta$ twinning partials the reaction is



The γ_m values are listed in table 7. $\phi\theta$ screws have a pole-strength equivalent to double-layer fault on $\{112\}$ and permit continuous twin multiplication by the pole mechanism for tension parallel to $\langle 110 \rangle$ or compression parallel to $\langle 001 \rangle$. If $\phi\theta$ dissociates into symmetric $1/3\mathbf{A}\theta$ type partials γ_m are 20 percent greater than those for eq (62).

$\langle 110 \rangle$ Burgers vectors have been found in α -Fe [116, 117]; they cannot form by spontaneous interactions of $1/2\langle 111 \rangle$ dislocations, but might develop at intersecting pile ups. $\langle 110 \rangle \{001\}$ edge dislocations can dissociate into $1/6\langle 111 \rangle$ twinning partials on $\{112\}$ planes. For symmetric partials the dissociation is



The γ_m values are listed in table 7. For single twinning partials



γ_m is 106 percent and 141 percent of that for eq (62) for the $1/3\mathbf{A}\theta$ and $2/3\mathbf{A}\theta$ partials respectively. \mathbf{AC} screws have a pole-strength equivalent to double-layer fault. In this case continuous twin multiplication occurs with eq (64) for tension parallel to $\langle 110 \rangle$ and compression parallel to $\langle 001 \rangle$, and with eq (65) for opposite stresses. If the pole mechanism does not operate, twin growth could occur by successive dissociations of dislocations which meet the twin. For dissociation of \mathbf{AC} into $1/3\mathbf{A}\theta$ twinning partials $\gamma_m > 0$ for $N=3$ successive dissociations. A fourth dissociation has $\gamma_m = 0$.

AC dislocations on the $\{1\bar{1}0\}$ plane could dissociate into various glissile and sessile morphologies [118]. It could dissociate into as many as eight $1/8\text{AC}$ glissile partials for a role in Martensitic transformations. The edge dislocation line is parallel to the zone axis of $\{130\}$ and $\{110\}$ fault planes and can dissociate into glissile partials on these planes. For three-twinning partials on $\{130\}$ planes

$$\begin{aligned}\mathbf{AC}_{(1\bar{1}0)} \rightarrow & 1/5[\mathbf{AC} + 2\mathbf{AD}]_{(3\bar{1}0)} + 1/5[\mathbf{DB} + 2\mathbf{AB}]_{(130)} \\ & + 1/5[\mathbf{AC} + 2\mathbf{AD}]_{(3\bar{1}0)}.\end{aligned}\quad (66)$$

The most favorable morphology corresponds to the third partial at the stair-rod position, with the γ_m values listed in table 7. For dissociation into single $1/5[130]$ twinning partials the γ_m values are twice as large as those for eq (66). The **AC** screw has a pole strength equivalent to two $\{310\}$ planes, permitting continuous twin multiplication with a shear-strain of $S=1$.

VIII. Tetragonal Structure

In β -tin slip occurs on $[001](100)$ and $1/2[111](1\bar{1}0)$ systems while twinning occurs on $[103](301)$ and 101 systems [119–121]; the former twin mode is most frequently found. When crystal plates have the *c*-axis perpendicular to the tensil axis the slip system is $1/2[111](1\bar{1}0)$ and no twinning is found [120], consistent with the view that twinning is related to $[001](100)$ slip [3]. The edge dislocation line for this system is parallel to the $[010]$ zone axis of $\{301\}$ and $\{101\}$ twin planes and can dissociate into $s\langle 103 \rangle$ and $s\langle 101 \rangle$ twinning partials on these planes. The bi-pyramid notation of the preceding section is also applicable to tetragonal and orthorhombic crystal structures.

For $\{301\}$ twins the thinnest favorable twin mode corresponds to $n=2$ with

$$s' = 6(c/a)^2/[1 + 9(c/a)^2] \quad (67)$$

giving [3]

$$s = [3(c/a)^2 - 1]/[1 + 9(c/a)^2] \quad (68)$$

For single $\{301\}$ twin lamellae the dissociation is given by

$$\phi\theta_{(100)} \rightarrow [s\mathbf{BA} + (1 - 3s)\phi\theta] + s[\mathbf{AB} + 3\phi\theta]_{(\overline{3}01)}. \quad (69)$$

Substituting $s=0.02935$ and $K=3.207 \times 10^{11}$ dynes/cm², $\gamma_m=68.3$ ergs/cm². For symmetric $\{301\}$ twin lamellae the equation is given by

$$\phi\theta_{(100)} \rightarrow (1-6s)\phi\theta + s[\mathbf{AB} + 3\phi\theta]_{(301)} + s[\mathbf{BA} + 3\phi\theta]_{(301)} \quad (70)$$

with $\gamma_m = 79$ ergs/cm². The separation of {301} twin planes is $d = ca/b_0$ and the twinning shear-strain for $n=2$ is

$$S = (3/2)(c/a) - (1/2)(a/c). \quad (71)$$

This is the same equation reported by Ishii and Kiho [122], giving $S=0.1$. The elements of the second undistorted plane are $\kappa_2=(10\bar{1})$ and $\eta_2=[101]$.

For {101} twins the thinnest favorable twin mode corresponds to $n=2$ with

$$s' = 2(c/a)^2/[1+(c/a)^2] \quad (72)$$

giving [3]

$$s = [3(c/a)^2 - 1]/[1+(c/a)^2] \quad (73)$$

For single {101} twin lamellae the dissociation is given by

$$\phi\theta_{(100)} \rightarrow [s\mathbf{BA} + (1-s)\phi\theta] + s[\mathbf{AB} + \phi\theta]_{(10\bar{1})}. \quad (74)$$

Substituting $s=0.083$ and $K=3.25 \times 10^{11}$ dynes/cm², $\gamma_m=48$ ergs/cm². In this case $\kappa_2=(301)$ and $\eta_2=[10\bar{3}]$, and {101} and {301} twin modes are reciprocal [28].

IX. Orthorhombic Structure

In $\alpha-U$ the principal slip and twin systems are [100](010) and [310](130) respectively [123]. The edge dislocation line is parallel to the [001] zone axis of {130} twin planes and can dissociate into single $s<310>$ twinning partials.

$$\mathbf{AB}_{(010)} \rightarrow [(1-3s)\mathbf{AB} + s\mathbf{DA}] + s[3\mathbf{AB} + \mathbf{AD}]_{(1\bar{3}0)} \quad (75)$$

where [3]

$$s' = [1-3(a/b)^2]/2[1+9(a/b)^2]. \quad (76)$$

The favorable twin mode corresponds to $n=1$. Substituting $s=s'=0.0471$ and $K=9.655 \times 10^{11}$ dynes/cm², $\gamma_m=491$ ergs/cm². The shear-strain for twinning is [3]

$$S = (1/2)(b/a) - (3/2)(a/b). \quad (77)$$

$S=0.3$, $\kappa_2=(1\bar{1}0)$ and $\eta_2=[110]$, as found by Cahn [123]. For symmetric {130} twin lamellae the dissociation is given by

$$\mathbf{AB}_{(010)} \rightarrow (1-6s)\mathbf{AB} + s[3\mathbf{AB} + \mathbf{AD}]_{(1\bar{3}0)} + s[3\mathbf{AB} + \mathbf{DA}]_{(130)}. \quad (78)$$

$\gamma_m = 719$ ergs/cm. Other twin modes are accounted for by dissociations of various dislocations on primary and secondary systems.

X. Discussion

When $\gamma_m/\gamma > 1$ for all glissile partials the dissociation is defined and will tend to lock at low temperatures. When $\gamma_m/\gamma < 1$ the partialized dislocation model reduces to the modified pseudo Peierles-Nabarro model [124] for dislocation resistance. In this model the edge dislocation can be represented as an *oblated core* and the screw as a *dilated core* in which multiple partials tend to separate under hydrostatic forces onto planes of least distortion. The degree of separation, the stress-sense characteristics, the tendency to twin, and consequently the dislocation resistance would depend on the number and relative strength of the fault planes. The possibilities are (i) few planes with relatively low distortion energy, (ii) many planes with low distortion energy and (iii) one or zero planes with low distortion energy. Greatest resistance is expected for (i) and least resistance for (iii), with (ii) having intermediate effects.

When (i) applies, dislocation resistance will be strongly orientation and stress-sense dependent and controlled by thermally activated processes. For (ii) orientation and stress-sense effects will be less, while for (iii) they will have no effect. Screw dislocations in bcc metals may be described by (i) or (ii).

Among the various properties which can be affected by, or attributed to, partialized dislocations are (i) the lattice frictional resistance along the slip plane, (ii) the locking of an otherwise favorable slip system, (iii) orientation and stress-sense effects, (iv) internal friction and thermally activated flow behavior, (v) stabilization of dislocation dipoles and braids during workhardening, (vi) delay times and avalanche behavior in glide band formation, (vii) twinning at low temperatures or high strain-rates, (viii) embrittlement (or strengthening) of a crystal, and (ix) it can serve as a vehicle for Martensitic transformations.

Avalanche behavior in glide band formation is found in many crystal structures and is characteristic of low strain-rates when a single slip system operates. First reported by Joffe [125] in NaCl and zinc crystals, it has since been established for insulators [125-127, 68, 69], metals [128-136], and semiconductors [81], by independent and combinations of studies of (i) slip lines [128-133], (ii) jerky stress-strain behavior [133], (iii) electrical resistivity changes [134, 135], (iv) refined acoustic measurements [136], and (v) birefringence effects in transparent crystals [125-127, 68, 69]. In the latter, a refined birefringence technique [137], supplemented by etch pit studies, was used in the most direct confirmation of avalanche behavior in alkali halide crystals [68, 69]. In these studies at low strain-rates on soft crystals, glide bands form in pro-

gressive avalanches, which last about 1/10 s, and increase in rate until the entire gage length is consumed. The behavior is consistent with the double cross-slip model of Koehler [138], originally proposed to account for the dependence of strain-rate on the number of lamellae in glide bands of aluminum [130]. The above behavior cannot, in general, be attributed to impurity locking effects.

XI. References

- [1] Mendelson, S., in Work Hardening (AIME Symp., Chicago 1966) J. P. Hirth and J. J. Weertman Eds. (Gordon and Breach Sci. Publ. 1968) p. 363.
- [2] Mendelson, S., Bull. Am. Phys. Soc. **12**, 412 (1967); Bull. Met. Soc. AIME **2**, No. 2 62 (1967).
- [3] Mendelson, S. (Intern. Conf. on Strength of Metals and Alloys, Tokyo, Japan 1967), Suppl. J. Japan Inst. Metals **9**, 819 (1968).
- [4] Kiho, H., J. Phys. Soc. Japan **9**, 739 (1954); **13**, 269 (1958).
- [5] Jaswon, M. A., and Dove, D. B., Acta. Cryst. **9**, 621 (1956); **10**, 14 (1957); **13**, 232 (1960).
- [6] Bilby, B. A., and Crocker, A. G., Proc. Roy. Soc. **A288**, 240 (1965).
- [7] Kronberg, M. L., J. Nucl. Mater. **1**, 85 (1959).
- [8] Westlake, D. G., Acta Met. **9**, 327 (1961); Deformation Twinning. R. E. Reed-Hill, J. P. Hirth, and H. C. Rogers Eds. (Gordon and Breach Sci. Publ. 1964) p. 29.
- [9] Rosenbaum, H. S., in Deformation Twinning, R. E. Reed-Hill, J. P. Hirth, and H. C. Rogers Eds. (Gordon and Breach Sci. Publ. 1964) p. 43.
- [10] Mendelson, S., Mater. Sci. Eng. **4**, 231 (1969).
- [11] Mendelson, S., in Intern. Conf. Strength of Metals and Alloys, Tokyo 1967, Suppl. J. Japan Inst. Metals **9**, 812 (1968).
- [12] Nabarro, F. R. N., Adv. Phys. **1**, 269 (1952).
- [13] Hirth, J. P., J. Appl. Phys. **32**, 700 (1961).
- [14] Teutonico, L. J., Acta Met. **13**, 605 (1965).
- [15] Mendelson, S., J. Appl. Phys. **40**, 1988 (1969); J. Met. **20**, No. 8 12A (1968).
- [16] Eshelby, J. D., Phil. Mag. **40**, 903 (1949).
- [17] Foreman, A. J., Acta Met. **3**, 322 (1955).
- [18] Head, A. K., Phys. stat. sol. **5**, 51 (1964).
- [19] Duncan, T. R., and Kuhlmann-Wilsdorf, D., J. Appl. Phys. **38**, 313 (1967).
- [20] Wasilewski, R. J., Acta Met. **11**, 63 (1963).
- [21] Reid, C. N., Acta Met. **14**, 13 (1966).
- [22] Yoo, M. H., Abstract Bull. Met. Div. AIME **2**, No. 2 17(1967).
- [23] Couling, S. A., and Roberts, C. S., Acta Met. **9**, 972 (1956).
- [24] Reed-Hill, R. E., and Robertson, W. D., Acta Met. **5**, 717 (1957); Trans. AIME **212**, 256 (1958).
- [25] Reed-Hill, R. E., Trans. AIME **218**, 554 (1960).
- [26] Crocker, A. G., Phil. Mag. **8**, 1077 (1963).
- [27] Hartt, W. H., and Reed-Hill, R. E., Trans. AIME **239**, 1511 (1967).
- [28] Christian, J. W., The Theory of Transformations in Metals and Alloys (Pergamon Press, Oxford, 1965).
- [29] Berghezan, A., Fourdeux, A., and Amelinckx, S., Acta Met. **9**, 464 (1961); Damiano, W., Trans. AIME **227**, 288 (1963).

- [30] Nabarro, F. R. N., Basinski, Z. S., and Holt, D. B., *Adv. Phys.* **13**, 193 (1964).
- [31] Price, P. B., *J. App. Phys.* **32**, 1750 (1961).
- [32] Price, P. B., in *Electron Microscopy and Strength of Crystals*, G. Thomas and J. Washburn Eds. (Interscience Publ. Co., New York 1963) p. 41.
- [33] Stoloff, N. S., and Gensamer, M., *Trans. AIME* **224**, 732 (1962).
- [34] Risebrough, N. R., and Teghtsoonian, E., *Can. J. Phys.* **45**, 591 (1967).
- [35] Bell, R. L., and Cahn, R. W., *Proc. Roy. Soc. A* **239**, 494 (1957).
- [36] Price, P. B., *Phil Mag.* **5**, 873 (1960).
- [37] Rosenbaum, H. S., *Acta Met.* **9**, 742 (1961).
- [38] Seeger, A., Kronmuller, H., Boder, O., and Rapp, M., *Phys. Stat. Sol.* **3**, 1107 (1963).
- [39] Baldwin, D. H., and Reed-Hill, R. E., *Trans. AIME* **233**, 248 (1965).
- [40] Dickson, J. I., Dedo, A., and Craig, C. B., *J. Met.* **20**, No. 8 85A (1968).
- [41] Pointu, P., Azou, P., and Bastien, P., *C. R. Acad. Paris* **252**, 1984 (1961).
- [42] Walters, C. P., van den Walt, C. M., and Makin, M. J., *J. Nucl. Mat.* **11**, 335 (1964).
- [43] Taylor, W., and More, A., *J. Nucl. Mater.* **13**, 23 (1964).
- [44] Scott, V. D., and Lindsay, M., *J. Nucl. Mater.* **18**, 176 (1966).
- [45] Damiano, V. V., London, G. J. and Conrad, H., *Trans. AIME* **242**, 987 (1968).
- [46] Frank, F. C., and Nicholas, J. F., *Phil. Mag.* **44**, 1213 (1953).
- [47] Mendelson, S., *J. Appl. Phys.* **41** (April 1970).
- [48] Wasilewski, *Scripta Met.* **1**, 45 (1967).
- [49] Levine, E. D., *Trans. AIME* **236**, 1558 (1966).
- [50] Shvidkovsky, E. G., Tjapunina, N. A., Predvoditelev, A. A., and Martinuk, G. K., (Proc. Intern. Conf. Crystal Lattice Defects), *Suppl. J. Phys. Soc. Japan* **18**, 89 (1963); Yoo, M. H., *Scripta Met.* **2**, 537 (1968).
- [51] Wosiewics, B. C., and Backofen, W. A., *Trans. AIME* **239**, 1422 (1967).
- [52] Kelly, E. W., and Hosford, W. F., *Trans. AIME* **242**, 5 (1968).
- [53] Rapperport, E. J., and Hartley, C. S., *Trans. AIME* **218**, 869 (1960).
- [54] Reed-Hill, R. E., in *Deformation Twinning*, R. E. Reed-Hill, J. P. Hirth, and H. C. Rogers Eds. (Gordon and Breach Sci. Publ., New York 1964) p. 295.
- [55] Rosi, F. D., Perkins, F. C., and Seigle, S. S., *Trans. AIME* **206**, 115 (1956).
- [56] Davis, K. G., and Teghtsoonian, E., *Acta Met.* **10**, 1189 (1962).
- [57] Rosi, F. D., Dube, C. S., and Alexander, B. H., *Trans. AIME* **197**, 257 (1953).
- [58] Liu, T. S., and Steinberg, M. A., *Trans. AIME* **194**, 1043 (1952).
- [59] Burr, D. J., and Thompson, N., *Phil. Mag.* **11**, 229 (1965).
- [60] Thompson, N., *Proc. Phys. Soc. London* **B66**, 481 (1953).
- [61] Hosford, W. F., and Fleicher, R. L., *Acta Met.* **7**, 817 (1959).
- [62] Nabarro, F. R. N., *Theory of Crystal Dislocations* (Oxford Univ. Press, London 1967) p. 220.
- [63] Schmid, E., and Boas, W., *Plasticity of Crystals* (F. A. Hughes and Co. Ltd. London 1950) p. 85.
- [64] Servi, I. S., Norton, J. T., and Grant, N. J., *Trans. AIME* **194**, 965 (1952).
- [65] Johnson, R. D., Young, A. P., and Schweppe, A. D., in *Creep and Fracture of Metals at High Temperatures* (Her Majesty's Stationery Office, London 1956) p. 25.
- [66] Foreman, A. J., and Lomer, W. M., *Phil. Mag.* **46**, 73 (1955).
- [67] Duncan, T. R., Kuhlmann-Wilsdorf, D., *Appl. Phys. Letters* **10**, 105 (1967).
- [68] Mendelson, S., *J. Appl. Phys.* **33**, 2175 (1962).
- [69] Mendelson, S., *Phil. Mag.* **8**, 1633 (1963).
- [70] Seifert, H., Neus. Jb. Mineral., Beil. Bd. **57**, 690 (1928).
- [71] Elleman, A. J., and Wilman, H., *Proc. Phys. Soc. London* **61**, 164 (1948).
- [72] Mendelson, S., unpublished.
- [73] Hornstra, J. *Phys. Chem. Solids* **5**, 129 (1958).

- [74] Hirth, J. P., and Lothe, J., Theory of Dislocations (McGraw-Hill, New York, 1968) p. 353.
- [75] Shockley, W., Phys. Rev. **91**, 228 (1953); Reed, W. T., Phil. Mag. **45**, 775 (1954); Haasen, P., and Seeger, A., Halbleiterproblem **4**, 68 (1958); Friedel, Dislocations (Addison Wesley 1964) p. 155.
- [76] Mendelson, S., J. Appl. Phys. **38**, 1573 (1967).
- [77] Mendelson, S., J. Appl. Phys., to be published.
- [78] Bullough, R., Proc. Roy. Soc. **A241**, 568 (1957); Churchman, A. T., Geach, G. A., and Winton, J., Proc. Roy. Soc. **A238**, 194 (1956).
- [79] Mendelson, S., Bull. Am. Phys. Soc. **13**, 360 (1968).
- [80] Mendelson, S., Bull. Am. Phys. Soc. **13**, 74 (1968).
- [81] Mendelson, S., Bull. Met. Soc. AIME **2**, No. 2 61 (1967).
- [82] Kabler, M. N., Phys. Rev. **131**, 54 (1963).
- [83] Celli, V., Kabler, M. N., Ninomiya, T., and Thompson, R., Phys. Rev. **13**, 58 (1963).
- [84] Friedel, J., Internal Stresses and Fatigue in Metals, G. M. Rossweiler and W. L. Grube Eds. (Elsevier Press, Amsterdam 1959) p. 220.
- [85] Dorn, J. E., Energetics in Metallurgical Phenomena, I, W. M. Mueller Ed. (Gordon and Breach Sci. Publ. 1965), p. 241.
- [86] Stroh, A. N., Proc. Phys. Soc. London, **B67**, 427 (1954).
- [87] Kroupa, F., and Brown, L. M., Phil. Mag. **6**, 1267 (1961).
- [88] Seeger, A., and Schiller, P., Acta Met. **10**, 348 (1962).
- [89] Art, A., Aerts, E., Delavignette, P., and Amelinckx, S., Appl. Phys. Letters, **2**, 40 (1963).
- [90] Higashi, A., Mae, S., and Fukuda, A. (Intern. Conf. Strength of Metals and Alloys), Suppl. J. Japan Inst. Metals **9**, 784 (1968).
- [91] Hirsch, P. B., Fifth Intern. Crystallographic Congress, Cambridge (1960).
- [92] Sleeswyk, A. W., Phil. Mag. **8**, 1967 (1963).
- [93] Mitchell, T. E., Foxall, R. A., and Hirsch, P. B., Phil. Mag. **8**, 1895 (1963).
- [94] Kroupa, F., Phys. stat. sol. **3**, 391 (1963).
- [95] Kroupa, F., and Vitek, V., Czech. J. Phys. **B14**, 337 (1964).
- [96] Wasilewski, R. J., Acta Met. **13**, 40 (1965).
- [97] Crussard, C., C. R. Acad. Sci. (France) **252**, 273 (1961).
- [98] Cohen, J. B., Hinton, R., Lay, K., and Sass, S., Acta Met. **10**, 894 (1962).
- [99] Taoka, T., Takeuchi, S., and Furubayashi, E., J. Phys. Soc. Japan **19**, 701 (1964).
- [100] Sestak, B., and Zorubova, N., Phys. stat. sol. **10**, 239 (1965).
- [101] Reid, C. N., Gilbert, A., and Hahn, G. T., Acta Met. **14**, 975 (1966).
- [102] Sestak, B., Zorubova, N., and Sladek, B., Can. J. Phys. **45**, 1031 (1967).
- [103] Argon, A. S., and Maloof, S. R., Acta Met. **14**, 1449 (1966).
- [104] Vitek, V., Kroupa, F., Phys. stat. sol. **18**, 703 (1966); Can. J. Phys. **45**, 945 (1967); Czech. J. Phys. **B18**, 464 (1968).
- [105] Escaig, B., J. de Physique **27**, C3-205 (1966); 464 (1968).
- [106] Foxall, R. A., Duesbery, M. S., and Hirsch, P. B., Can. J. Phys. **45**, 607 (1967).
- [107] Duesbery, M. S., and Hirsch, P. B., in Dislocation Dynamics, A. R. Rosenfield, G. T. Hahn, A. L. Bement, Jr., and R. I. Jaffee Eds. (McGraw-Hill, New York, 1968), p. 57.
- [108] Cottrell, A. H., and Bilby, B. A., Phil. Mag. **42**, 573 (1951).
- [109] Vitek, V., Phil. Mag. **18**, 773 (1968).
- [110] Mitchell, T. E., Scripta Met. **2**, 591 (1968).
- [111] Hartley, C. S., Phil. Mag. **14**, 7 (1966); Trans. AIME **242**, 1101 (1968).
- [112] Hirsch, P. B., J. Inst. Met. **87**, 406 (1959; Carrington, W., Hale, K. F., and McLean, D., Proc. Roy. Soc. **A259**, 203 (1960); Berghezan, A., and Fourdeux, A., Coll. Met. Centre Etudes Nucl. Saclay, 1960 (Presse Univ. de France, Paris, 1961), p. 127;

- Banerjee, B. R., Capenos, J. M., Hauser, J. J., and Hirth, J. P., *J. Appl. Phys.* **32**, 556 (1961); Keh, A. S., and Weissman, S., in *Electron Microscopy and Strength of Crystals*, G. Thomas and J. Washburn Eds. (Interscience Publ., New York, 1963) p. 231; Hull, D., ibd. p. 291; Ohr, S. M. and Beshers, D. N., *Phil. Mag.* **8**, 1343 (1963).
- [113] Segall, R. L., *Acta Met.* **9**, 975 (1961).
- [114] Richman, R. H., in *Deformation Twinning*, R. E. Reed-Hill, J. P. Hirth and H. C. Rogers Eds. (Gordon and Breach Sci. Publ. 1964) p. 237.
- [115] Hartley, C. S., *Phil. Mag.* **14**, 1207 (1966).
- [116] Bevis, M., Rowlands, P. C., and Action, A. F., *Trans. AIME* **242**, 1555 (1968).
- [117] Dingley, D. J., and Hale, K. F., *Proc. Roy. Soc. A* **295**, 55 (1966); Smith, D. A., Morgan, R., and Rolf, B., *Phil. Mag.* **18**, 869 (1968).
- [118] Mendelson, S., to be published.
- [119] Friedel, J., *Dislocations* (Addison-Weseley Publ. Co., 1964) p. 458.
- [120] Hirokawa, T., Yomogita, K., and Honda, K. (*Proc. Intern. Conf. Strength of Metals and Alloys*) Suppl. *J. Japan Inst. Metals* **9**, 837 (1968).
- [121] Maruyama, S., and Kiho, H., *J. Phys. Soc. Japan* **11**, 516 (1956).
- [122] Ishii, K., and Kiho, H. *J. Phys. Soc. Japan* **18**, 1122 (1963).
- [123] Cahn, R. W., *Acta Met.* **1**, 49 (1953).
- [124] Nabarro, F. R. N., and Conrad, H. Agenda Discussion, in *Dislocation Dynamics*, A. R. Rosenfield, G. T. Hahn, A. L. Bement, Jr., and R. I. Jaffee, Eds. (McGraw-Hill Book Co., 1968) p. 475.
- [125] Joffee, A. F., *The Physics of Crystals* (McGraw-Hill Book Co. 1928).
- [126] Schmid, E., and Boas, W., *Plasticity of Crystals* (F. A. Huges and Co. Ltd., London, 1950).
- [127] Pratt, P. L., *Acta Met.* **1**, 103 (1953).
- [128] Heidenreich, R. D., and Shockley, W., *Strength of Solids* (Phys. Soc. London, 1947) p. 57.
- [129] Maddin, R., Mathewson, C. H., and Hibbard, W. R., *Trans. AIME* **175**, 86 (1948).
- [130] Brown, A. F., *J. Inst. Met.* **80**, 115 (1951).
- [131] Brown, A. F., *Adv. in Phys.* **1**, 427 (1952).
- [132] Leibfried, G., *Z. Phys.* **127**, 580 (1950); Haasen, P., and Leibfried, G., *Z. Metallk.* **43**, 317 (1952).
- [133] Ardley, C. W., and Cottrell, A. H., *Proc. Roy. Soc. London* **219**, 328 (1953).
- [134] Rozhanskii, V. N., Goriunov, Iv. V., and Shchukin, E. D., *Dodladay Akas. Nauk. USSR* **105**, 80 (1955).
- [135] Shchukin, E. D., Goriunov, Iv. V., Perlsov, N. V., and Rozhanskii, Soviet Phys.-Doklady **3**, 96 (1958).
- [136] Fisher, R. M., and Lally, J. S., *Can. J. Phys.* **45**, 1147 (1967).
- [137] Mendelson, S., *J. Appl. Phys.* **32**, 1999 (1961); Mendelson, S., and Kear, B. H., *J. Opt. Soc. Am.* **53**, 250 (1963).
- [138] Koehler, *Acta Met.* **1**, 377 (1953); *Phys. Rev.* **86**, 52 (1952).

PROPAGATION OF GLIDE THROUGH INTERNAL BOUNDARIES

M. J. Marcinkowski

*Engineering Materials Group and
Department of Mechanical Engineering
University of Maryland
College Park, Maryland 20742*

It has been shown that when an internal boundary such as a grain boundary is cut by a crystal glide dislocation, a disturbance is left at the boundary. This disturbance closely resembles that about a crystal dislocation with the exception that (a) there is no extra half plane associated with the dislocation and (b) the Burgers vector associated with this disturbance is a variable which depends on the nature of the internal boundary. These boundary dislocations have been termed virtual dislocations.

The nature of the virtual boundary dislocations has been treated in detail for the symmetrical tilt boundary. Both homogeneous and heterogeneous type glide across these boundaries have in turn been applied to grain boundary crack formation and propagation, grain boundary rotation, preferred orientation, etc.

Key words: Boundary dislocations; glide propagation; grain boundaries; virtual dislocations.

I. Introduction

Perhaps no deformation mechanism remains so obscure as that which occurs in polycrystals. At the heart of this dilemma is the lack of knowledge concerning what happens to the grain boundary itself, i.e., its structure, during the deformation process. In the following paragraphs consideration will be given to the simplest of all boundaries, the symmetrical tilt boundary, as a first step in trying to understand the deformation behavior of grain boundaries in general.

Fundamental Aspects of Dislocation Theory, J. A. Simmons, R. de Wit, and R. Bullough, Eds., (Nat. Bur. Stand. (U.S.), Spec. Publ. 317, I 1970).

II. Simple Type of Internal Boundary

One of the simplest of internal boundaries is that formed when two substances of the same crystal structure but differing lattice constant, i.e., A and a in figure 1a, are joined together. For simplicity A was taken equal to $2a$. One method of joining the two crystals together would be as shown in figure 1b, where the strain is taken up equally in both crystals, in turn altering the lattice constant to the common value of $B = (a + A)/2$. However, long-range stresses of high constant value are introduced throughout the entire volume of both crystals. By allowing the crystals to relax to their characteristic lattice constant as the distance from the boundary increases, as shown in figure 1c, the strains can be reduced considerably. Furthermore, the stress field associated with the boundary (shown dashed) in figure 1c can be imagined as equivalent to an array of edge dislocation of Burgers vector $b = A - a$ inserted between each plane of the original crystal. These dislocations are shown dotted in figure 1c.

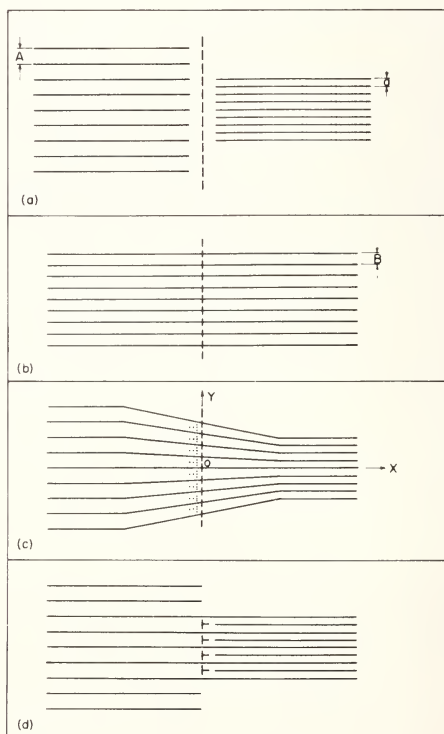


FIGURE 1. Sequence of steps (hypothetical) in the formation of an incoherent boundary: a) before joining, b) after joining rigidly, c) after introduction of virtual dislocations (shown dotted), d) after introduction of crystal dislocations (shown solid).

Since they are not real dislocations, in the sense of having associated with them an extra half plane, they will be referred to as virtual dislocations.

Although the virtual dislocations in figure 1c are shown as discrete dislocations with Burger vector $b = A - a$, they may be more correctly visualized as a continuous distribution of edge dislocations of strength dy such that the following relation as shown by Weertman [1] is satisfied

$$\int_{-L}^{+L} D(y) dy = nb \quad (1)$$

where $+L$ and $-L$ refer to the upper and lower surfaces of the crystal, $D(y)$ is a distribution function and n the total number of dislocations in the boundary. From inspection of figure 1c, it is apparent that $D(y)$ was taken to be $8(A-a)/2L$. It also follows that by increasing n from 8 to ∞ and decreasing b correspondingly from $(A-a)$, the boundary would be more accurately thought of as a continuous distribution of dislocations infinite in number and of infinitesimally small Burgers vector. Thus it will also be convenient to refer to the virtual dislocations as continuum dislocations.

Finally, the long-range stresses associated with the virtual dislocations in figure 1c can be entirely eliminated by the introduction into the boundary of the real crystal dislocations or interface dislocations such as shown in figure 1d. The crystal dislocations have Burgers vectors equal to a when referred to the smaller crystal structure and $A/2$ when referred to the larger. In general the number of interface dislocations required to completely cancel the long-range stress field of the virtual dislocations is given by nb/A or 4 in the specific case of figure 1d.

As shown by Friedel [2], the discrete stress fields of the crystal dislocations in figure 1d will only cancel the continuous stress field of the virtual dislocations at a distance on the order of the separation of the crystal dislocations. If the shear stress field σ_{xy} from the virtual dislocations in figure 1c is high enough, i.e., on the order of $\mu/10$, Marcinkowski and Leamy [3] have shown that glide dislocations will be nucleated spontaneously parallel to the boundary. A portion of the loop will remain stuck in the crystal as the interface dislocation, while the remaining portion of opposite sign will glide out of the crystal so as to produce the offset such as shown in figure 1d. If on the other hand, as Marcinkowski and Fisher [4] have demonstrated, the temperature is sufficiently high, prismatic dislocation loops can be nucleated normal to the boundary under the influence of the compressive component of stress σ_{yy} of the vertical dislocation array shown in figure 1d. Specifically, there will be a stress induced diffusion of atoms from the large crystal to the small crystal in figure 1c. Diffusion-induced interface dislocation generation gives

rise to no offset at the crystal surface. Li [5] has given explicit expressions for the stress fields about various linear dislocation arrays and finds that only for the case where b is normal to the infinite linear array do the long-range stresses vanish.

III. Glide Across a Symmetrical Tilt Boundary (Disordered Alloy)

A second important type of internal boundary within a crystal is the symmetrical tilt boundary such as is shown in figure 2. In the case where θ is small, i.e., less than 10° , Cottrell [6] shows that the boundary can be visualized in terms of well-defined edge dislocations such as in figure 2a. On the other hand, when θ is large, as in figure 2b, the dislocations comprising the boundary are so close together that their cores overlap. At this point, it becomes less meaningful to describe the boundary in terms of individual dislocations, and to emphasize this point it is shown dashed in figure 2b.

For convenience, the grain to the left of the boundary in figure 2 will

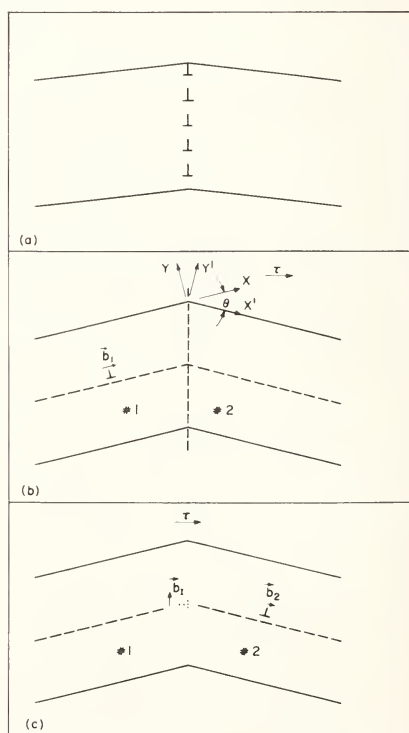


FIGURE 2. a) Low angle symmetrical tilt boundary, b) high angle symmetrical tilt boundary before passage of dislocation through it, c) same as b) but after passage of dislocation through grain boundary.

be referred to as grain #1 while that given to the right of the boundary will be designated as grain #2. Now consider the passage of a single glide dislocation through the symmetrical tilt boundary as shown in figures 2b and 2c. In order that a glide dislocation \mathbf{b}_1 in grain #1 shown in figure 2b pass through the boundary and into grain #2 to become the glide dislocation \mathbf{b}_2 shown in figure 2c, it is necessary that a dislocation \mathbf{b}_1' be introduced into the boundary. According to Friedel[2]

$$\mathbf{b}_1 = \mathbf{b}_2 + \mathbf{b}_1'. \quad (2)$$

In the above $|\mathbf{b}_1| = |\mathbf{b}_2| = |\mathbf{b}|$. The dislocation \mathbf{b}_1' is a virtual dislocation since there is no extra half plane associated with it.

A very simple pictorial representation showing the meaning of \mathbf{b}_1' in eq 3 can be seen by referring to figure 3. Specifically \mathbf{b}_1' is nothing more than the change in interplanar spacing between the slip planes in grain #2 from their equilibrium values prior to slip from grain #1 to grain #2 in order that continuity across the slip planes be preserved. A deeper insight into these virtual grain boundary dislocations (VGBD) will be given shortly.

The coordinates of \mathbf{b}_2 in eq 2 must be referred to the same axes as that of \mathbf{b}_1 and will be designated as \mathbf{b}_2 . In particular using the coordinate system referred to grain #1,

$$\bar{\mathbf{b}}_2 = \mathbf{R}\mathbf{b}_2 = \mathbf{R}\mathbf{b}_1 \quad (3)$$

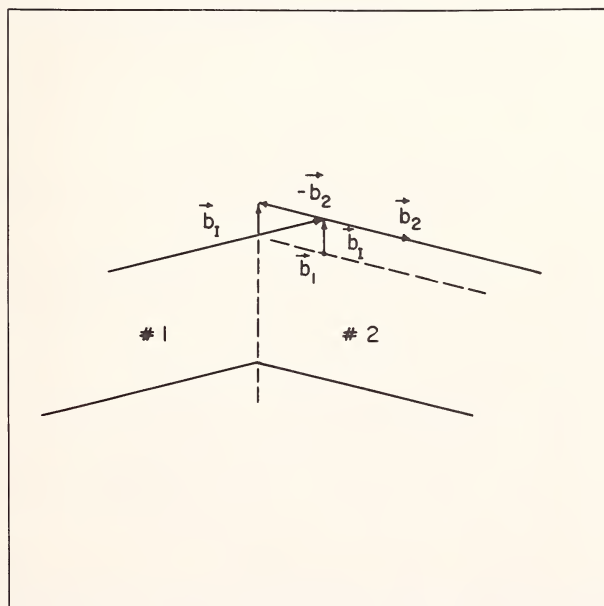


FIGURE 3. Displacement \mathbf{b}_1' occasioned by slip from grain #1 to grain #2.

where \mathbf{R} is the rotation matrix given by

$$\mathbf{R} = \begin{bmatrix} \cos \theta & -\sin \theta & 0 \\ \sin \theta & \cos \theta & 0 \\ 0 & 0 & 1 \end{bmatrix} \quad (4)$$

Combining eqs 4, 3, and 2 we obtain

$$\mathbf{b}_1 = \begin{bmatrix} b_{1,x} \\ b_{1,y} \\ b_{1,z} \end{bmatrix} = \begin{bmatrix} b_{1,x} \\ 0 \\ 0 \end{bmatrix} - \begin{bmatrix} \cos \theta & -\sin \theta & 0 \\ \sin \theta & \cos \theta & 0 \\ 0 & 0 & 1 \end{bmatrix} \begin{bmatrix} b_{1,x} \\ 0 \\ 0 \end{bmatrix} \quad (5)$$

where the matrix to the left of the minus sign above refers to \mathbf{b}_1 while the product to the right of the minus sign refers to \mathbf{b}_2 .

Expanding eq 5 and realizing that θ is negative in figure 2 gives

$$\begin{bmatrix} b_{1,x} \\ b_{1,y} \\ b_{1,z} \end{bmatrix} = b_{1,x} \begin{bmatrix} 1 - \cos \theta \\ \sin \theta \\ 0 \end{bmatrix}. \quad (6)$$

Next define a unit vector \mathbf{n} which lies in the $x-y$ plane and normal to the grain boundary. If \mathbf{n} points away from grain #1 then

$$\mathbf{n} \equiv \begin{bmatrix} n_x \\ n_y \\ n_z \end{bmatrix} \equiv \begin{bmatrix} \sin(\pi/2 - \theta/2) \\ -\cos(\pi/2 - \theta/2) \\ 0 \end{bmatrix} = \begin{bmatrix} \cos(\theta/2) \\ \sin(\theta/2) \\ 0 \end{bmatrix}. \quad (7)$$

Also, since

$$\mathbf{b}_1 \cdot \mathbf{n} = b_{1,x} [\cos(\theta/2) - \cos(\theta/2)\cos(\theta) - \sin(\theta)\sin(\theta/2)] = 0, \quad (8)$$

it follows that \mathbf{b}_1 must lie in the plane $x-y$ and be parallel to it, i.e., lie in the grain boundary. As will become apparent shortly, for a non-symmetrical grain boundary, \mathbf{b}_1 is perhaps better described as lying in the mean direction defined by y and y' .

Two rather interesting limiting cases exist for \mathbf{b}_1 . In particular, when $\theta \rightarrow 0$ eq 6 shows that the VGBD has a Burgers vector $\theta b_{1,x}$. On the other hand, for $\theta \rightarrow \pi/2$ the same equation gives $b_{1,x}$ for the Burgers vector of the VGBD. It is therefore apparent that the magnitude of the VGBD is a strong function of grain misorientation.

Two very interesting VGBD configurations arise as a result of two distinct types of plastic deformation in the bicrystals shown in figure 2. These two particular types of plastic deformation will be referred to as homogeneous and heterogeneous shear. The case of homogeneous shear

is shown in figure 4 where figure 4a is the bicrystal before deformation. Now if grain #1 is given a simple shear on the plane whose normal is y and in the x direction, while grain #2 is given the same shear but in the plane whose normal is y' and whose direction is x' , figure 4b obtains. The shear can be thought of as being accomplished by the motion of a glide dislocation on each successive plane. In order to maintain continuity across the slip planes in both grains #1 and #2, as well as to accommodate the strain equally between both grains, the interplanar spacings in grains #2 and #1 must be increased and decreased respectively with respect to their equilibrium values shown in figure 4a. If, on the other hand, the

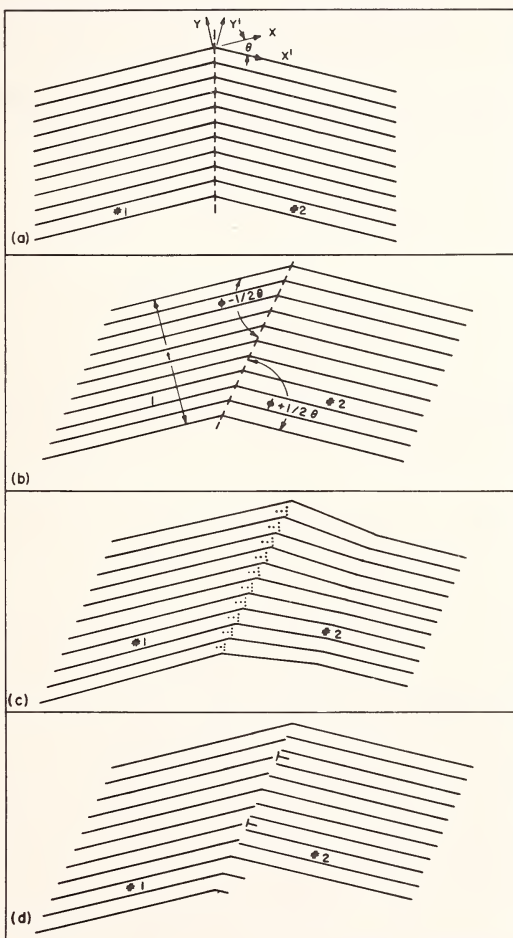


FIGURE 4. Sequence of steps (hypothetical) in the homogeneous shear of a symmetrical tilt boundary: a) before shear, b) after rigid shear, c) after introduction of virtual dislocations (shown dotted), d) after introduction of crystal dislocations (shown solid).

crystal is allowed to relax to its equilibrium configuration at large distances from the boundary, the condition in figure 4c obtains, i.e., the boundary can be thought of as being composed of an array of virtual dislocations each with a Burgers vector given by eq 6. On the other hand, figure 4d shows that the long-range stresses at the boundary in figure 4c can be eliminated in large part by the introduction of crystal or misfit dislocations at the boundary. The correspondence between the sequences in figures 1 and 4 are in principle identical although at first glance they appear quite different.

Note that the crystal dislocations in figure 4d are shown to be generated in grain #2 only, presumably by the generation of dislocation loops near the boundary due to the high stress fields of the VGBD of figure 4c. This is shown again more schematically in figure 5a. Alternately the crystal dislocations could have all been generated in grain #1 as shown in figure 5b. However in both these cases, although the component $b \cos(\theta/2)$ of

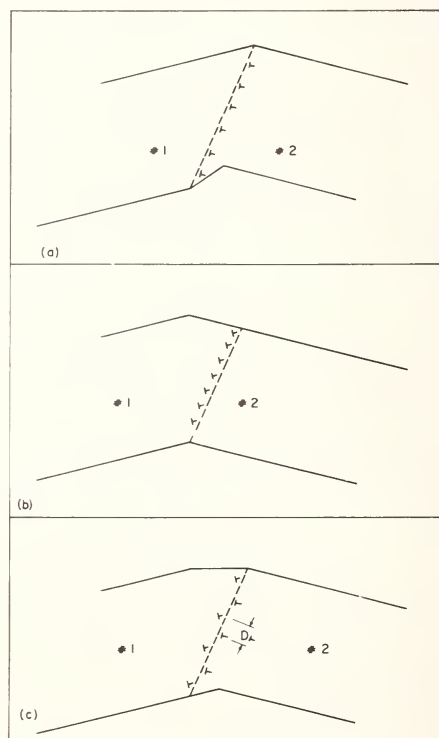


FIGURE 5. Relief of long range stresses at grain boundary due to virtual grain boundary dislocations by the generation of crystal dislocations in: a) grain #2 only, b) grain #1 only, c) both grains #1 and #2.

the glide dislocation can essentially eliminate the long-range stress fields due to the \mathbf{b}_1 type virtual dislocations, they introduce a component of magnitude $\pm b \sin (\theta/2)$ which generates a new long-range stress field. Also, because this component of the crystal dislocation lies either parallel or antiparallel to those that comprise the original undistorted symmetric tilt boundary, the degree of tilt may be either further increased as in figure 5b or decreased as in figure 5a. These particular two cases are special types of preferred orientation generated by the deformation of a polycrystal and may in fact provide the basis for a general theory of preferred orientation. When the crystal dislocations are generated at the grain boundaries in equal numbers in both grains #1 and #2, figure 5c obtains and the long-range stresses can be entirely cancelled so that no preferred orientation is induced in the grains.

It is instructive at this point to obtain a relationship between the density of misfit dislocations at the grain boundary and the degree of asymmetry imparted to it by glide. The interface dislocation is a glide dislocation with Burgers vector of magnitude $|\mathbf{b}|$. It will accommodate the misfit \mathbf{b}_1 at the grain boundary occasioned by glide across it when the following relation is met

$$N_{G\perp} = |\mathbf{b}| / |\mathbf{b}_1| \cos (\theta/2) \quad (9)$$

where $N_{G\perp}$ refers to the number of glide dislocations passing through the grain boundary. Using eq 6, $N_{G\perp}$ is readily found to be given as

$$N_{G\perp} = 1/(2 - 2 \cos \theta)^{1/2} \cos (\theta/2) = 1/2 \sin (\theta/2) \cos (\theta/2). \quad (10)$$

$N_{G\perp}$ of course must be the nearest integer value. None of the previous arguments depend on the magnitude of θ .

Figure 4 approximates the case where large numbers of dislocations, which are more or less distributed randomly throughout the crystal, pass through a grain boundary under an applied stress τ , i.e., homogenous glide. In the first place, it will be noted that the grain boundary is rotated so as to lie more nearly parallel to the direction of glide. This feature of the present analysis is in agreement with the parallel alignment of grain boundaries along the rolling direction in plastically worked materials illustrated by Williams and Homerberg [7].

Now assume that the density of \mathbf{b}_1 type glide dislocations in grain #1 is ρ . If grain #1 is one unit wide and t units thick, and all of the glide dislocations contained therein cross the grain boundary; the angle $(\phi - \theta/2)$ between the grain boundary and the x axis of grain #1 will be given by the

following relationship:

$$\tan(\phi - \theta/2) = t / [\rho tb + t \tan(\theta/2)]. \quad (11)$$

Note that ϕ is the angle that the grain boundary makes with the mean x direction. With the aid of eqs 9 and 10, the number of interface dislocations generated at the boundary will be given by

$$\rho t / N_{G\perp} = [t/b \tan(\phi - \theta/2) - t \tan(\theta/2)/b] 2 \sin(\theta/2) \cos(\theta/2). \quad (12)$$

Since the length of the grain boundary l after deformation is readily found from figure 4b to be given by

$$\sin(\phi - \theta/2) = t/l, \quad (13)$$

the spacing D_{\perp} of interface dislocations along the boundary can be found from eqs 12 and 13 to be

$$\begin{aligned} D_{\perp} &= l N_{G\perp} / \rho \\ &= b/2 \sin(\theta/2) \cos(\theta/2) \sin(\phi - \theta/2) [1/\tan(\phi - \theta/2) - \tan(\theta/2)] \end{aligned} \quad (14)$$

and which upon simplifying leads to

$$D_{\perp} = b/2 \cos \phi \sin(\theta/2). \quad (15)$$

Equation 15 is precisely the same relationship derived by Read [8] for an asymmetrical tilt boundary where no deformation of any type was invoked and where no restriction was placed on the magnitudes of ϕ or θ . Thus the asymmetrical tilt boundaries generated either by deformation or by annealing, etc., are identical with respect to dislocation content and configuration. It is also important to note that eq 15 only applies strictly to a boundary such as is shown in figure 5c where the stresses are fully compensated. Also, in the case of figure 5c, if the value of θ is sufficiently small so that the dislocations in the original symmetrical tilt boundary can be resolved as individual dislocations, their spacing measured along the boundary after deformation is readily found to be given by

$$D_{\perp} = b/2 \sin(\theta/2) \sin \phi, \quad (16)$$

which again is identical to that given by Read [8].

The second important type of glide through a grain boundary occurs when the dislocations all move on a single slip plane. This is the heterogeneous type of deformation mentioned earlier. An example of this is

shown in figure 6a where slip has occurred between the planes shown divided by the dashed line.

In figure 6a the misfit strain has been distributed equally and rigidly in both grains, while in figure 6b the strain at large distances from the boundary has been relaxed, in turn allowing the crystal to revert to its strain-free dimensions. Figures 6a and 6b have their analogs in figures 4b and 4c respectively for the case of homogeneous shear. Thus the displaced grain boundaries in figure 6b can be visualized as being connected by a series of VGBD's shown dotted. Their magnitude as usual is given by eq 6 while their horizontal spacing is $\cos(\theta/2)$. In the strictest sense however the VGBD's in figure 6b should, as in the case of figure 1c, be treated as a continuous distribution of dislocations of infinitesimal strength, which, along the lines used to obtain eq 1, gives the following relation:

$$\int_0^{b \cos(\theta/2)} D(x) dx = 2b \sin(\theta/2). \quad (17)$$

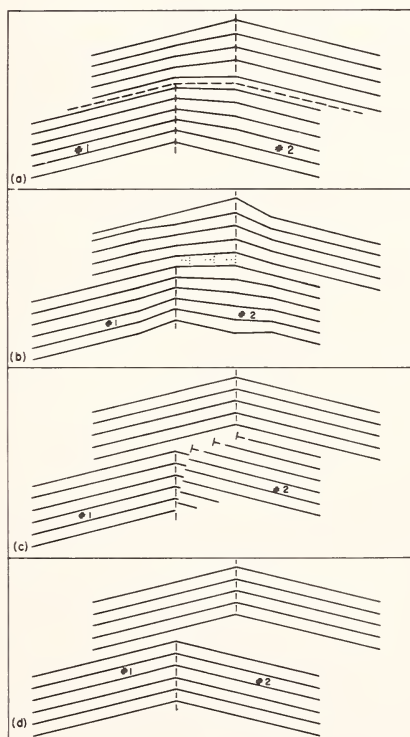


FIGURE 6. Sequence of steps (hypothetical) in the heterogeneous shear of a symmetrical tilt boundary: a) after rigid shear, b) after introduction of virtual dislocations (shown dotted), c) after introduction of crystal dislocations (shown solid), d) after fracture.

The strain due to the VGBD can be almost fully relaxed by the introduction of crystal misfit dislocations such as shown in figure 6c. Again the misfit dislocations are presumed to be nucleated as loops in the vicinity of the grain boundary due to the stress field of the VGBD's. Note that in the particular case of figure 6c the introduction of three misfit dislocations overcompensates for the distortion associated with the VGBD's. This in turn causes some matching difficulties along the lower portion of the grain boundary, which in effect is the same as saying that some long-range stress fields still remain.

As in the case of homogeneous glide in figure 5, the various ways in which the stress can be relieved along the grain boundary by heterogeneous glide are shown in figure 7. Again, it is only for the case shown in figure 7c that the long-range stresses due to the VGBD's can be completely relieved, i.e., the case where the misfit dislocations are generated in equal numbers in both grains #1 and #2. It is a simple matter to calculate the spacing of the misfit dislocations required to compensate

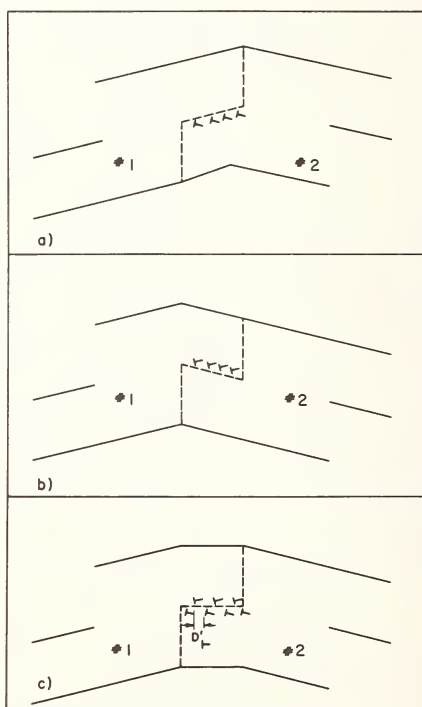


FIGURE 7. Relief of long range stresses at grain boundary due to virtual grain boundary dislocations by the generation of crystal dislocations in: a) grain #2 only, b) grain #1 only, c) both grains #1 and #2.

fully for the VGBD strain. In particular it is given by

$$D_{\perp}^1 = N_{G\perp} 2 b \sin (\theta/2) = b/\cos (\theta/2), \quad (18)$$

where $N_{G\perp}$ is the number of glide dislocations giving a misfit that can be compensated for by one crystal dislocation, while the second term is the spacing between the VGBD's.

A second way in which the VGBD strain can be relieved is by complete rupture or fracture across the glide plane and this is shown in figure 6d. This will occur when the energy of the new surfaces created is less than the strain energy associated with the VGBD array in figure 6b.

It is important to realize that the VGBD's behave exactly as crystal dislocations with respect to their interaction with one another. In particular, the horizontal array in figure 6b is stable. On the other hand, a pair of VGBD's of like sign would repel if the angle between their Burgers vector and radius vector were greater than 45° and would attract if this angle were less than 45° . Note also that the VGBD can glide along the grain boundary but only in the mean y direction of both grains.

The VGBD's have actually been observed by Gleiter, Hornbogen, and Bäro [9] using transmission electron microscopy techniques and do in fact confirm many of the postulates discussed up to now.

IV. Glide Across A Symmetrical Tilt Boundary (Ordered Case)

Figure 8a shows the dislocation configuration in a low angle symmetrical tilt boundary in an ordered alloy, i.e., say of the $B2$ type. Specifically,

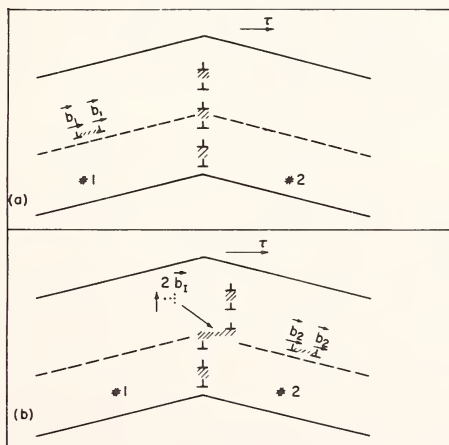


FIGURE 8. Symmetrical tilt boundary in an ordered alloy, a) before glide through the boundary, b) after glide through the boundary.

Marcinkowski [10] has shown that the dislocations are vertically aligned coupled pairs, each pair being connected by an antiphase boundary (APB). As the angle of tilt θ increases, the length of each APB strip becomes more nearly equal to the length of the ordered strip between adjacent coupled dislocation pairs. This situation presumably also prevails at large values of θ , i.e., large angle boundaries.

Figure 8b shows what happens when the superlattice glide dislocation, originally in grain #1 of figure 8a, passes through the boundary. In particular it is shown to pass through the APB of a vertically aligned pair. It is apparent that this process requires an expenditure of a great deal of energy. In the first place, a VGBD of magnitude $2b_1$ must be created in the boundary, i.e., twice that for the disordered alloy. Secondly, an APB energy ledge of energy $2b_2$ must also be created, requiring an additional expenditure of energy $2b_2 \gamma$ where γ is the APB energy per unit area.

On the average, an APB ledge will be created in only about half the cases for homogeneous glide in an ordered alloy, since in the remaining cases the superlattice dislocations will pass in between adjacent vertically coupled dislocation pairs. Thus, grain boundary resistance to shear is very high in the case of ordered alloys, leading to blocking of large numbers of superlattice dislocations. Relief of stresses by dislocation loop nucleation in the vicinity of the grain boundaries is made difficult by ordering. Marcinkowski and Leamy [3] and Marcinkowski and Fisher [11] have shown that the reason for this is that an antiphase boundary must first be created during the formation of the first loop. Thus, it is conceivable that the normal components of stresses resulting from these blocked dislocations, coupled with the disorder of the APB, are responsible for the intergranular brittleness which Marcinkowski and Miller [12], Marcinkowski and Chessin [13], and Marcinkowski and Campbell [14] have shown is so common to ordered alloys in general. Finally it is important to note that VGBD's are not coupled by APB's.

V. Summary and Conclusions

It is found that when dislocation glide occurs across an internal boundary a disturbance is produced in the boundary. The stress fields associated with this disturbance resemble an actual crystal dislocation in many ways. On the other hand, there is no extra half plane associated with these non-crystal dislocations and furthermore they may have a Burgers vector of variable magnitude, depending on the nature of the boundary. These boundary dislocations have been termed virtual dislocations. The stress fields associated with a virtual dislocation may be largely compensated by the stress-induced nucleation of a crystal dislocation loop in the vicinity of the virtual dislocation.

Two specific cases of glide across a grain boundary have been treated.

The first involves homogeneous glide across a symmetrical tilt boundary. This particular case leads to grain boundary rotation and possibly preferred orientation of the grains. In the second case, where glide occurs on only a single slip plane across the boundary (heterogeneous deformation), a jog is produced in the boundary, which in turn may lead to crack nucleation.

The above analysis has been extended to ordered alloys, where it is found that glide across grain boundaries in such alloys is extremely difficult. This difficulty arises because (1) an antiphase boundary ledge may have to be produced in the grain boundary, and (2) the magnitude of the virtual dislocation left in the grain boundary after it is intersected by a superlattice dislocation has twice the magnitude of its counterpart in the disordered alloy. The above process is believed to result in the intergranular fracture which is so characteristic of ordered alloys.

VI. Acknowledgements

The author would like to express his sincere appreciation to Drs. R. W. Armstrong and R. J. Arsenault of the Engineering Materials Group of the University of Maryland for a series of very stimulating discussions as well as for their criticisms and comments. He is also indebted to the Department of Mechanical Engineering and the Center of Materials Research of The University of Maryland for their financial support during this investigation.

VII. References

- [1] Weertman, J., and Weertman, J. R., *Elementary Dislocation Theory* (MacMillan Co., New York, 1964).
- [2] Friedel, J., *Dislocations* (Addison-Wesley Publ. Co., Reading, Mass., 1964).
- [3] Marcinkowski, M. J., and Leamy, H. J., *Phys. Stat. Sol.* **24**, 149 (1967).
- [4] Marcinkowski, M. J., and Fisher, R. M., in *Int. Conf. on Electron Microscopy*, I (Maruzen Co., Ltd., Tokyo, 1966) p. 299.
- [5] Li, J. C. M., in *Electron Microscopy and Strength of Crystals*, G. Thoman and J. Washburn, Eds. (Interscience Publ., New York, 1963).
- [6] Cottrell, A. H., *Dislocations and Plastic Flow in Crystals* (The Clarendon Press, London, 1953).
- [7] Williams, R. S., and Homerberg, V. O., *Principles of Metallography* (McGraw-Hill Book Co., Inc., New York, 1948).
- [8] Read, W. T., Jr., *Dislocations in Crystals* (McGraw-Hill Book Co. Inc., New York, 1953).
- [9] Gleiter, H., Hornbogen, E., and Bärö, G., *Acta Met.* **16**, 1053 (1968).
- [10] Marcinkowski, M. J., *Phil. Mag.* **17**, 159 (1968).
- [11] Marcinkowski, M. J., and Fisher, R. M., *Trans. AIME* **233**, 293 (1965).
- [12] Marcinkowski, M. J., and Miller, D. S., *Phil. Mag.* **6**, 871 (1961).
- [13] Marcinkowski, M. J., and Chessin, H., *Phil. Mag.* **10**, 837 (1964).
- [14] Marcinkowski, M. J., and Campbell, D. E., *AIME Symposium on Intermetallic Compounds* (September 1969).

Discussion on Papers by W. Bollmann, M. H. Yoo and B. T. M. Loh, and S. Mendelson, Including a Written Contribution by J. P. Hirth.

HIRTH: [This written contribution: "A Dislocation Mechanism for Phase Transformation" replaces Professor Hirth's oral presentation.]

The present idea on transformation dislocations was stimulated by some hot-stage transmission electron microscope observations of the f.c.c.-h.c.p. transformation in cobalt and its dilute alloys.¹ Occasionally, the transformation was incubated when moving dislocations, activated by thermal stresses induced by the electron beam, intersected either other dislocations or stacking fault ribbons.

The case of dislocation intersection in principle could be explained by a variant of the dislocation pole-mechanisms proposed as superjog sources for dislocation twinning in f.c.c. metals.^{2,3} Let us briefly consider these two mechanisms at the outset. In the first,³ a dislocation **BA**(d), in Thompson's notation,⁴ dissociates into a sessile partial **BC/A α** and a glissile partial **α C**, bounding an intrinsic stacking fault (see fig. 23-9a in footnote 5). Under an appropriate resolved stress, the partial **α C** could glide around the **BA** "pole" dislocation and produce a transformation to h.c.p. by the mechanism proposed by Seeger.⁶ The difficulty in this mechanism, however, is that for each sweep around the pole, the partial must intersect one other (or a group of other) forest dislocation with a net Burgers vector component normal to the glide plane and equal in magnitude to one interplanar distance; otherwise an f.c.c. twin or a faulted f.c.c. region would be formed instead of an h.c.p. region. On a statistical basis, the above requirement is unlikely to be fulfilled. Also, the **BC/A α** partial is a high-energy one, so the initial dissociation is energetically unfavorable.

In the second case,² a dislocation **AC**(d) dissociates into a sessile partial **α A** and a glissile partial **C α** bounding an intrinsic stacking fault (see fig. 23-9c in footnote 5). Under an appropriate resolved stress the partial **C α** could glide around the pole dislocation **AC** and would then recombine with **α A** on the same glide plane. The recombined dislocation **AC** then

¹ Kennedy, E. M., Ph.D. Thesis (Ohio State University, Columbus, Ohio, 1968).

² Venables, J. A., Phil. Mag., **6**, 379 (1961).

³ Hirth, J. P., in Deformation Twinning, R. E. Reed-Hill, J. P. Hirth, and H. C. Rogers, Eds., (Gordon and Breach, New York, 1964) p. 112.

⁴ Thompson, N., Proc. Phys. Soc. (London), **66B**, 481 (1953).

⁵ Hirth, J. P., and Lothe, J., Theory of Dislocations (McGraw-Hill Book Co., New York, 1968).

⁶ Seeger, A., Z. Metallk. **44**, 247 (1956).

cross-slips on (d) by an amount equivalent to two interplanar spacings normal to (a), then redissociates into $\alpha\mathbf{A}$ and $\mathbf{C}\alpha$, and the process repeats. The h.c.p. phase is thus propagated in a "ratchet-pole" variant of Venable's twinning mechanism.²

The difficulties in this mechanism are that the partial $\mathbf{C}\alpha$ must complete an entire revolution and recombine over an appreciable length before cross-slip can occur, so that the transformation velocity is limited, and there must be an appropriate resolved shear stress on the cross-slip plane. Also, it is conceivable that some constriction of a sessile configuration would be required before cross-slip could occur.

Hence, there is some question about the applicability of the pole mechanisms to the transformation for the dislocation-intersection case and neither would apply to the stacking fault-intersection case. An alternative model which could rationalize both cases and which avoids some of the difficulties discussed above is presented in figure 1. Linear, continuum-elastic calculations indicate that the model is energetically favorable. However, such calculations are highly unrealistic for the critical-sized nucleus, whose dimensions are of the order of the dislocation core radius for such a configuration. Hence, rather than give such calculations quantitatively, we present the model qualitatively; hopefully, atomic calculations will demonstrate its feasibility.

Intersection of a stacking fault, whether a wide ribbon or the portion at the center of an extended dislocation, by a moving dislocation $\mathbf{D}\mathbf{A}(c)$ creates the configuration in figure 1a. Along the line of intersection, a dislocation dipole $\mathbf{A}\delta\text{-}\delta\mathbf{A}$ is formed.⁷ This could further react to form the stair-rod dipole $\gamma\delta\text{-}\delta\gamma$, or equivalently, to form a jog line;⁸ the consequences of all three possibilities would be the same.

Consider now the nucleation of a partial loop $\mathbf{A}\delta$ as indicated in figure 1b. Elastic interaction with the adjacent $\delta\mathbf{A}$ partial reduces the elastic energy of formation of the loop.^{9,10} More importantly, the "stacking fault" energy of the incipient loop is *negative*, since growth of the loop propagates the thermodynamically stable h.c.p. phase. Together, these factors make the nucleation process favorable in the elastic approximation.

Continued loop nucleation, as in figure 1c, continues the transformation. The line of $\mathbf{A}\delta\text{-}\delta\mathbf{A}$ dipoles, or $\gamma\delta\text{-}\delta\gamma$ dipoles, or jog lines, left in the h.c.p.

⁷ Jouffrey, B., Daniel, A., and Escaig, B., J. de Phys., Suppl. C-3, **27**, 114 (1966).

⁸ Thompson, N., in *Defects in Crystalline Solids* (Physical Society, London, 1955), p. 153.

⁹ Frank, F. C., in *Symposium on Plastic Deformation of Crystalline Solids* (Office of Naval Research, Washington, D. C., 1950), p. 89.

¹⁰ Hirth, J. P., in *Relation Between Structure and Strength in Metals and Alloys* (H. M. Stationery Office, London, 1963), p. 218.

phase is exactly equivalent to the $\{11\bar{2}2\}$ stacking fault in hcp crystals associated with the motion of a $\langle 11\bar{2}3 \rangle$ type zonal dislocation on a $\{11\bar{2}2\}$ glide plane.¹¹ Thus, the net free energy change as the f.c.c.-h.c.p. interface advances is the chemical driving-force term minus the energy of the above stacking fault. This net change is large and negative for supercoolings greater than $\sim 2^\circ\text{C}$.

Another factor which could favor the proposed process is the local adiabatic temperature rise in the wake of the dislocation **DA** associated with the energy absorbed from the moving dislocation by phonons via their damping constraint to the motion. This would be particularly effective if shear modes were excited in plane (d).

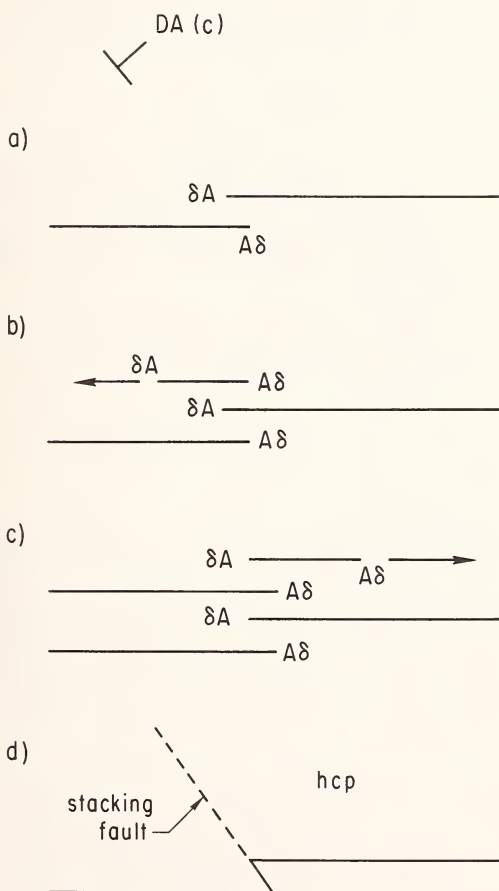


FIGURE 1.

¹¹ Rosenbaum, H. S., in Deformation Twinning, R. E. Reed-Hill, J. P. Hirth, and H. C. Rogers, Eds., (Gordon and Breach, New York, 1964) p. 43.

Generically, the mechanism in figure 1 somewhat resembles one proposed some time ago by Bollmann.¹² He considered a mechanism wherein a partial dislocation gliding in the fcc phase encountered a stacking fault and reflected back two interplanar distances removed. The internal stress concentration at the point of intersection provided the driving force for dislocation nucleation analogous to the present example. However, his model differs in the detailed description of the configuration at the site of intersection and would have obvious differences with regard to both the habit plane of the transformation and the final microstructure.¹³

MENDELSON: [Written comment on Professor Hirth's contribution.] Zonal dislocations having a Burgers vector $b_s = sb_o$ can also apply to phase transformations when the definition of s is rewritten as

$$s = (n/n')s' - p$$

where s' is the shear for a unit-lamella of martensite formed by n' atomic layers and n is the number of layers which are converted to martensite by the zonal dislocation. (n/n') is an integer equal to the number of unit-lamellae of martensite and p is again an integer chosen to give the smallest absolute value of s .

The f.c.c. \rightarrow h.c.p. phase transformation discussed by Professor Hirth is a simple one because both structures are close-packed, having the same atomic density. Stacking faults which form when perfect **AB** dislocations dissociate into Shockley partials on the close-packed plane transform each structure into the other.¹⁴ In this case $s' = 1/3$ for $n' = 2$ with $\mathbf{b}_o = 1/2[112]$, giving $\mathbf{b}_s = 1/6[112]$ and $S = sb_o/nd = 1/\sqrt{8}$. The elements of the transformation are $\kappa_1 = (1\bar{1}\bar{1})$, $\eta_1 = [112]$, $\kappa_2 = (5\bar{5}7)$ and $\eta_2 = [7,7,\overline{10}]$. An atomic model illustrates this in figure 2. The plane of soft shear is $S_m = (1\bar{1}0)$ and the hatched circles lie at a level $a_f/\sqrt{8} = a_h/2$ below the plane of the paper. For the reverse transformation, $S_m = (\bar{1}2\bar{1}0)$ and $\mathbf{b}_s = 1/3[\bar{1}010]$ with $\kappa_1 = (0001)$, $\eta_1 = [\bar{1}010]$, $\kappa_2 = (\bar{3}0\bar{3}\bar{1})$ and $\eta_2 = [\bar{1}016]$. This transformation can also occur for $n = 4$ with $s = 2(1/3) - 1 = -1/3$, $\eta_2 = [5\bar{5}6]$ and $\kappa_2 = (335)$; the shear-strain is reduced by $1/2$, but the greater atomic shuffling makes it less likely.

The more general phase transformation involves a change in density, requiring lattice deformation as well as rotation. Zonal dislocations can also apply to these cases if the volume change direction is in the plane of shear. If it is also normal to κ_1 the transformation can be represented by

¹² Bollman, W., Acta Met. **9**, p. 972 (1961).

¹³ This research was supported by the U. S. Office of Naval Research.

¹⁴ Christian, J. W., The Theory of Transformations in Metals and Alloys (Pergamon Press, New York, 1965).

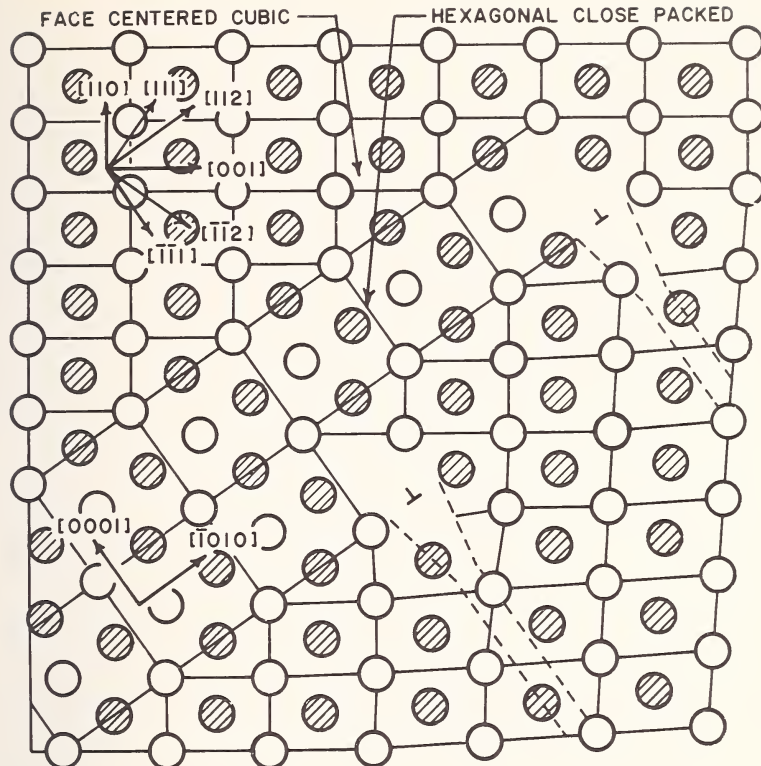


FIGURE 2.

a shear parallel to η_1 together with a collapse (or expansion) normal to κ_1 . The former is accomplished by the zonal dislocation \mathbf{b}_s and the latter by the displacement vector $\mathbf{b}_n = \zeta \mathbf{b}_{on}$ where \mathbf{b}_{on} is the lattice translation normal to κ_1 and ζ is the fraction of \mathbf{b}_{on} which produces the volume change. For a particular orientation relationship the volume change direction is normal to the plane in which two mutually perpendicular vectors are lattice translation vectors in both phases.

The transformations can have relatively simple habits when the closest atomic approach of close packed planes in the two phases are parallel. This corresponds to the Burgers¹⁵ orientation relationship in the b.c.c. \rightarrow h.c.p. transformation and to the Kurdjumow-Sachs¹⁶ orientation relationship in the f.c.c. \rightarrow b.c.c. transformation. When the volume change is

¹⁵ Burgers, W. G., *Physica* **1**, 561 (1934).

¹⁶ Kurdjumow, G., and Sachs, G., *Z. Physik* **64**, 325 (1930); *Naturwiss* **18**, 534 (1930).

normal to κ_1 the b.c.c. \rightarrow h.c.p. transformation can result for $\kappa_1 = (112)_b$, $\eta_1 = [1\bar{1}\bar{1}]_b$, $\mathbf{b}_o = 1/2[1\bar{1}\bar{1}]_b$ and $\mathbf{b}_{on} = [\bar{1}\bar{1}\bar{2}]_b$, with $s' = 1/6$ and $\zeta = (1/3 - a_b/(a_b \sqrt{8}))$ for $n' = 2$. The transformation can be assumed to occur by shear of $1/12[1\bar{1}\bar{1}]_b$ on $(112)_b$ followed by collapse of $(1/3 - a_b/(a_b \sqrt{8}))[\bar{1}\bar{1}\bar{2}]_b$, with the resulting habit being $(112)_b$. This habit is found in certain alloys. If \mathbf{b}_n combines with \mathbf{b}_s , the total dislocation \mathbf{b}_t would glide on an oblique plane of the same zone. Substituting values for the lattice parameters in titanium alloys $\mathbf{b}_t = \mathbf{b}_s + \mathbf{b}_n = 0.0355 [2, 2, \bar{3}, 1]_b$; this is close to the $[2\bar{2}\bar{3}]_b$ direction in the $(334)_b$ habit plane reported^{17,18} in titanium and some of its alloys. A pole mechanism can apply with $\mathbf{A}\theta = 1/2[111]_b$ type screw poles.

Similarly for the f.c.c. \rightarrow b.c.c. transformation the volume change direction is normal to $\kappa_1 = (112)_f$ with $\eta_1 = [1\bar{1}0]_f$, $S_m = (111)_f$, $\mathbf{b}_o = 1/2[1\bar{1}0]_f$, $s' = 1/6$, $\mathbf{b}_{on} = 1/2[1\bar{1}\bar{2}]_f$ and $\zeta = [(2/3)a_b/a_f - 1/2]_f$ for $n' = 3$. The $\{1\bar{1}\bar{2}\}_f$ habit is found for martensite in Fe-Ni alloys.¹⁹ A pole mechanism can apply with $\mathbf{BC} = 1/2[10\bar{1}]_f$ type screw poles. Zonal dislocations can also apply²⁰ to various higher order habits found with the Nishiyama²¹ and Greninger and Troiano,²² etc., orientation relationships.

BESHERS: [To Professor Hirth] Do you have any idea of the time the process you suggest would take?

HIRTH: I envision that it would happen more or less instantaneously in the wake of the moving dislocation.

BULLOUGH: I wonder if Dr. Bollmann would speculate whether his sophisticated geometrical methods could possibly predict martensitic habit planes or twin planes in complex crystalline systems.

BOLLMANN: I am sorry, but I am no prophet.

BULLOUGH: There is nothing in principle to tell you that it would not work?

BOLLMANN: No.

MENDELSON: Concerning twinning, one notes that in order to predict the active twin mode of various possible twin systems in terms of an anisotropic parameter, the differences in the parameter should be significantly greater than any other differences. By examining reciprocal or conjugate twin modes, as in the study of Drs. Yoo and Loh, one

¹⁷ Gaunt, P., and Christian, J. W., *Acta Met.* **7**, 534 (1959).

¹⁸ Hammond, C., and Kelly, P. M., *Acta Met.* **17**, 969 (1969).

¹⁹ Patterson, R. L., and Wayman, C. M., *Acta Met.* **14**, 347 (1966).

²⁰ Mendelson, S., to be published.

²¹ Nishiyama, Z., *Sci. Rep. Tohoku Imp. Univ.* **23**, 637 (1934).

²² Greninger, A. B., and Troiano, A. R., *Trans. AIME* **140**, 307 (1940).

can eliminate most of the differences in atomic shuffling, generally present for non-conjugate twin modes: there is still a difference, but not a great one, due to the fact that the spacing between twin planes d and their Burgers vectors sb_o are different. The assumption of equal atomic shuffling is approximately valid because n and sb_o/d are the same for the conjugate twin modes, giving the same shear-strain. However there is still another factor which is probably more important than these when comparing the properties of twinning dislocations on different twin planes, that is the difference in twin boundary energy. As an example, the distortional energy for the $\{\bar{2}114\}$ twin boundary is five times greater than that for the conjugate $\{\bar{2}112\}$ twin. Thus if one is concerned with differences in atomic mobility for twinning dislocations on the two conjugate twin planes, these distortions would certainly play a very significant role, at least in the case when the first twinning partial passes. They will play a lesser role for twin growth, but I wouldn't rule them out even for twin growth since the difference between the dislocation width parameters found by Drs. Yoo and Loh is only less than 10%, whereas the distortions for this case differ by 500%.

If I can make one other comment on the definition of the twinning dislocation . . . [At this point Dr. Mendelson went to the blackboard.] As in my definition of the twinning dislocation, the Burgers vector is given as $s\mathbf{b}_o$ whereas Drs. Yoo and Loh give $(e/2)\boldsymbol{\eta}_1$: these are essentially equivalent. \mathbf{b}_o is a unit lattice vector, defined as a perfect Burgers vector on the twin plane in the $\boldsymbol{\eta}_1$ direction and s (or $e/2$) is the fraction of \mathbf{b}_o that produces the twinning shear. The substitution of $\boldsymbol{\eta}_1$ for \mathbf{b}_o confuses the definition, since a fudging factor is required for the cases where $|\boldsymbol{\eta}_1| \neq |\mathbf{b}_o|$. $s\mathbf{b}_o$ defines a twinning dislocation; whether it is a zonal dislocation depends on how one chooses s . We cannot really define this quantity, as Dr. Yoo has, with the relation $(1/\eta_1)\{\eta_2^2 - (qd)^2\}^{1/2}$ (this is the reverse of my eq 4) primarily because we do not know $\boldsymbol{\eta}_2$. What Dr. Yoo has done was to go into the literature and take the values of $\boldsymbol{\eta}_2$ that people have listed and used them to define $(e/2)$. The $\boldsymbol{\eta}_2$ values themselves were originally computed from s which was either measured experimentally or assumed by applying minimum shear-strain and simple atomic shuffling criteria, as in my definition. What of the cases where more than one value of $\boldsymbol{\eta}_2$ is proposed, and how does the definition by Drs. Yoo and Loh apply if the $\boldsymbol{\eta}_2$ value is wrong?

There are only a small number of cases in the many metals where the shear-strain has actually been measured. Twinning by homogeneous shear requires a large Burgers vector and is not consistent with experimental studies in non-cubic metals. Rather, it has been suggested that minimum shear-strain should be a principal criterion for twinning, and this has been developed by several authors. It is discussed in some detail

by Bilby and Crocker.²³ Another criterion is that the reduction in shear-strain be accomplished without introducing enormous amounts of atomic shuffling. In the definition I give, $s = ns' - p$, this is accomplished providing that n is not too large. If $n = 1$, $p = 0$ and $s = s'$ corresponding to homogeneous shear and a large shear-strain. In selecting a likely twin mode corresponding to a particular κ_1 and η_1 we choose n to give a small Burgers vector with reasonable atomic shuffling. This is essentially what others have done in evaluating η_2 , the element that Drs. Yoo and Loh now use in reverse to define the zonal twinning dislocation. A quantity which is defined in terms of another assumed quantity (equivalent to the defined quantity itself) is not a definition. The correct way to define the zonal twinning dislocation is from first principles and in terms of minimum shear-strain and small atomic shuffling criteria: one cannot eliminate p from my definition, as Drs. Yoo and Loh apparently have, and cannot define the twinning dislocation in terms of η_2 . Similarly, the zonal twinning dislocation cannot be defined by $n\mathbf{b}_t$. \mathbf{b}_t defined as a "unit twinning dislocation," has no physical significance: it is not a twinning dislocation, nor is it glissile—it is only related to the particular zonal dislocation from which it was evaluated.

YOO: I admit that there are oftentimes some ambiguities in the literature as to how closely the experimental data points for twinning elements on stereographic projection converge onto rational crystallographic indices. Those who are familiar with the crystallography of martensitic transformation will be well aware of this problem, namely the determination of habit planes, etc. It is not our problem here, however, to verify the twinning elements reported in the literature.

We are concerned with the properties of zonal twin dislocations in compound twin systems with the *well defined rational* crystallographic twinning elements, K_1 , K_2 , η_1 , and η_2 . Therefore, once the four elements are known, the Burgers vector of a zonal twin dislocation is defined explicitly by our eq (2). The atomic shuffling takes place in the core region of a twin dislocation as it glides along the twin interface. The reason for introducing the concept of *zonal* dislocations is to satisfy the necessary condition that the new twin interface created by the movement of a twin dislocation must be both crystallographically and atomistically equivalent to the original twin interface. Hence, it is this requirement together with the four crystallographic elements that completely determines the Burgers vector of a zonal twin dislocation.

We have taken fifteen compound twin systems in structures ranging from cubic to orthorhombic crystal systems that are reported in the

²³ Bilby, B. A., and Crocker, A. G., Proc. Roy. Soc. (London) **A288**, 240 (1965).

recently published books and review papers. The simple expressions for the numerical factors, e 's, for these twin systems are given in the first two tables in the text. So, once the twinning elements are taken, the Burgers vector is determined as a direct consequence of the lattice geometry involved, not the energetic feasibilities of dislocation dissociations discussed by Dr. Mendelson. You do not have any room to choose what the parameter, p , should be.

MENDELSON: Yes, that's true. If you take η_2 , as a basic quantity then you don't have any choice. But my point here is that η_2 is a variable; it is not known, in general. For a κ_1 and η_1 there is no unique η_2 and κ_2 . There are, at least in h.c.p. metals, an infinite number of possibilities, but most of these are not reasonable and can be eliminated when minimum shear-strain and small atomic shuffling criteria are applied. When n is large the atomic shuffling is large and dislocation motion becomes prohibitive. In defining the zonal twinning dislocation one chooses the most reasonable s value (from which η_2 and κ_2 are calculated) consistent with minimum shear-strain and small atomic shuffling criteria. Drs. Yoo and Loh arrive at the correct answers because they are using η_2 values which were determined by various authors from s values which were either measured experimentally or evaluated by applying minimum shear-strain and small atomic shuffling criteria. To repeat the point a definition should be based on first principles. Yours is not a definition because you are defining the zonal twinning dislocation in terms of another quantity which was originally evaluated from the quantity you wish to define.

NABARRO: Dr. Yoo, you have 60 seconds.

YOO: Since sixty seconds are hardly enough for what I have in mind, let me ask a simple question instead. In body-centered-cubic structures, K_1 and K_2 planes are $\{11\bar{2}\}$ variant, and η_1 and η_2 directions are $\langle 111 \rangle$ variant. Along the $[111]$ direction, the translation vector is $1/2[111]$. Now, do you accept that $\eta_2 = 1/2[111]$?

MENDELSON: Well, in this case η_2 corresponds to homogeneous shear and the twinning dislocation is not a zonal dislocation. It turns out that twinning on this plane in b.c.c. is favored by homogeneous shear ($n=1$), but in hexagonal metals homogeneous shear is not the best mode for most twin planes. For the common twin planes in cubic metals you cannot do much better than twin by homogeneous shear. For example, for $n=1$, $s=s'=1/3$ and the Burgers vector on $(11\bar{2})$ in bcc is $\mathbf{b}_t=1/6[111]$. If $n=2$ (corresponding to an extrinsic stacking fault), $s=2(1/3)-1=-1/3$ and the Burgers vector has the same absolute magnitude. The shear-strain is reduced from $S=\sqrt{2}/2$ to $\sqrt{2}/4$, but atomic shuffling is

required. This mode is still possible, having opposite stress-sense characteristics and different η_2 and κ_2 . The two modes are illustrated in figure 3. [This figure was added at a later date.] The projection plane is $S_m = (\bar{1}\bar{1}0)$ and the hatched circles are $a/\sqrt{2}$ below those in the plane of the paper. (a) is for $n=1$ and (b) for $n=2$. $\mathbf{b}_t = 1/6[111]$, with $\eta_2 = [\bar{1}\bar{1}\bar{1}]$ and $\kappa_2 = (112)$ for $n=1$, and $\eta_2 = [113]$ and $\kappa_2 = (331)$ for $n=2$. These modes are listed by Crocker²⁴ for twinning in b.c.c. martensite. The same effects

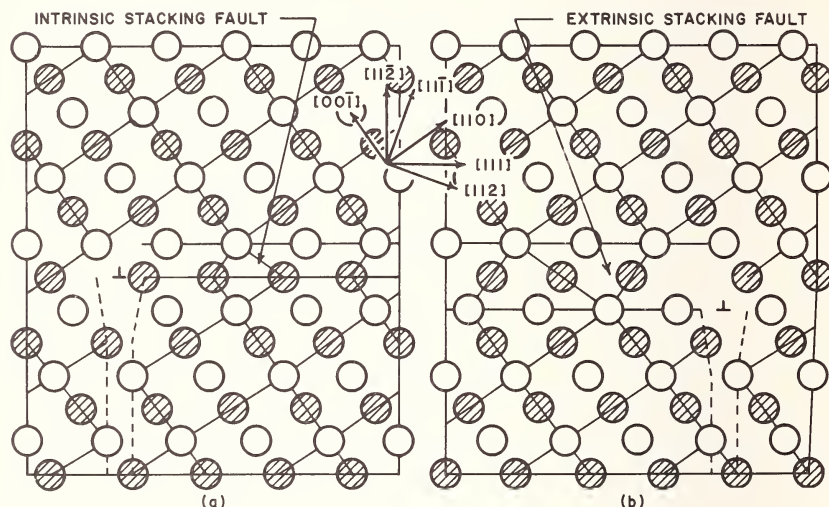


FIGURE 3.

apply to intrinsic and extrinsic stacking faults in fcc metals. Similar atomic models illustrate this for twin modes in hcp metals,²⁵ where the choice is wider and atomic shuffling for larger n is often accompanied by a decrease in \mathbf{b}_t as well as S . In these cases there are various values of η_2 and κ_2 for any particular κ_1 and η_1 , and reasonable assumptions are necessary to choose the most likely one, unless you have experimentally determined the shear-strain. There are only a small number of twin modes for which the shear-strain was experimentally determined. Examples of this are $\{\bar{1}012\}$ ($n=2$) twinning in cadmium and zinc and $\{\bar{2}112\}$ ($n=3$) twinning by Rapperport and Hartley in zirconium,²⁶ others have been reported for certain metals and some are in dispute. What is pertinent and repeated here is that it is meaningless to define the zonal

²⁴ Crocker, A. G., in Deformation Twinning, R. E. Reed-Hill, J. P. Hirth, and H. C. Rogers, Eds., (Gordon and Breach, New York, 1964), p. 272.

²⁵ Mendelson, S., Mat. Sci. Eng. **4**, 231 (1969).

²⁶ Rapperport, E. J., and Hartley, C. S., Trans. AIME **218**, 869 (1960).

twinning dislocation in terms of a quantity which is not unique or basic and which itself was evaluated from the quantity to be defined. The definitions you give are incorrect imitations of correct ones which were published²⁷ and reported earlier. [This is discussed further elsewhere.²⁸]

DUNCAN: I don't know how many people noticed the anisotropy of the shear stress of {211} <111> dislocations in Dr. Yoo's paper. I have calculated the same thing and I got the same anisotropy. I had high hopes that the anisotropy in the shear stress would correlate with the anisotropy in the flow stress of b.c.c. crystals, but unfortunately it does not. As far as I can see you cannot explain or even relate the anisotropy of the flow stress in b.c.c. metals in compression and tension with the anisotropy of the shear stress of the glide dislocations in the {211}<111> system.

BOLLMANN: May I comment on Professor Marcinkowski's paper. [The following is a written contribution.] It shall be shown how by means of the 0-lattice method that the equilibrium dislocation arrangement of the symmetrical tilt boundary and the unsymmetrical tilt boundary can be derived. In addition the concept of Marcinkowski's virtual dislocation can be understood on the basis of the 0-lattice theory. In the standard procedure of the 0-lattice method, first the relation between the two crystal lattices is given. We assume cubic lattices where lattice No. 2 is rotated by the angle θ around the z-axis with respect to lattice No. 1. We formulate the problem two-dimensionally

$$\mathbf{x}^{(2)} = \mathbf{A}\mathbf{x}^{(1)}$$

with

$$\mathbf{A} = \mathbf{R} = \begin{pmatrix} \cos \theta & -\sin \theta \\ \sin \theta & \cos \theta \end{pmatrix} \quad (2)$$

From the basic equation of the 0-lattice follows

$$\mathbf{x}^{(0)} = (\mathbf{I} - \mathbf{A}^{-1})^{-1} \mathbf{b}^{(1)}$$

i.e.
$$\begin{pmatrix} \mathbf{x}^{1(0)} \\ \mathbf{x}^{2(0)} \end{pmatrix} = \begin{pmatrix} \frac{1}{2} & \left(\frac{1}{2}\right) \cotan(\theta/2) \\ -\left(\frac{1}{2}\right) \cotan(\theta/2) & \frac{1}{2} \end{pmatrix} \begin{pmatrix} \mathbf{b}^{1(1)} \\ \mathbf{b}^{2(1)} \end{pmatrix}.$$

The $\mathbf{b}^{(1)}$ -vectors are the lattice vectors of the b-lattice and as such are identical with the translation vectors of the lattice. The two basal vectors of the b-lattice in the chosen coordinate system are of the form <1,0>.

²⁷ Mendelson, S., Proc. Int. Conf. on Strength of Metals and Alloys, Tokyo, Japan, 1967. Suppl. J. Japan Inst. Met. **9**, 812 and 819 (1968).

²⁸ Mendelson, S., Scripta Met. **4**, 5, (1970); Yoo, M. H., Scripta Met. **4**, 9 (1970).

Hence, the basal vectors of the 0-lattice are

$$\mathbf{x}_1^{(0)} = [\frac{1}{2}, (\frac{1}{2}) \cotan(\theta/2)],$$

$$\mathbf{x}_2^{(0)} = [(\frac{1}{2}) \cotan(\theta/2), \frac{1}{2}].$$

In the z -direction the 0-elements are lines parallel to the axis of rotation. Figure 4 shows the situation for $\theta = -10^\circ$. The chosen boundary A is a symmetrical tilt boundary, B is unsymmetrical.

The virtual grain boundary dislocation (VGBD) can be treated as a non-linear problem by superposing two lattices rotated with respect to one another, where each contains an edge dislocation of the same type. A calculation of this kind was published elsewhere.²⁹ The difference of the two Burgers vectors (translation vectors) in the two crystals is the Burgers vector of the VGBD and as such is not a translation vector in either lattice.

I should like to propose to define the Burgers vector of the VGBD for the low angle boundary by $\mathbf{b}_1 = \mathbf{b}_2 - \mathbf{b}_1$ instead of the inverse sign of Mankowski's definition (his eq 3) in order to keep crystal 1 as the invariable basis and to do all the operations on crystal 2.

It should be mentioned that Sleeswyk³⁰ worked on similar problems.

KRÖNER: I have one question for Dr. Bollmann. You developed your whole theory considering two equivalent lattices which were rotated with respect to each other. It is very easy to see that this works well, but it does not seem so obvious to me that it would also work well if they are different lattices, like monoclinic and triclinic. Are there extra difficulties?

BOLLMANN: Not at all. The problem is how to formulate the linear transformation which "generates" lattice 2 out of lattice 1

$$\mathbf{x}^{(2)} = \mathbf{A}\mathbf{x}^{(1)}.$$

We may start from an orthogonal lattice with unit length 1 Å and produce lattice No. 1 out of it

$$\mathbf{x}^{(1)} = \mathbf{S}^{(1)}\mathbf{x}^{(orth)}.$$

Lattice 2 may be produced in the same manner and by an additional rotation \mathbf{R} the orientation of lattice 2 may be varied

$$\mathbf{x}^{(2)} = \mathbf{R}\mathbf{S}^{(2)}\mathbf{x}^{(orth)}.$$

²⁹ Bollmann, W., in Dislocation Dynamics, A. R. Rosenfield, G. T. Hahn, A. L. Bement, Jr., and R. I. Jaffee, Eds., (McGraw-Hill Book Co., New York, 1968) p. 275.

³⁰ Sleeswyk, A. W., Physique des Dislocations (Presses Universitaires de France, Paris, 1967) pp. 63-78.

On eliminating $\mathbf{x}^{(orth)}$ we obtain:

$$\mathbf{x}^{(2)} = (\mathbf{R}\mathbf{S}^{(2)}\mathbf{S}^{(1)-1})\mathbf{x}^{(1)} := \mathbf{A}\mathbf{x}^{(1)}.$$

In order to relate the closest neighbors, sometimes additional unimodular transformations are needed (c.f. ref. [10] of my paper). In this way any arbitrary transformation \mathbf{A} can be constructed.

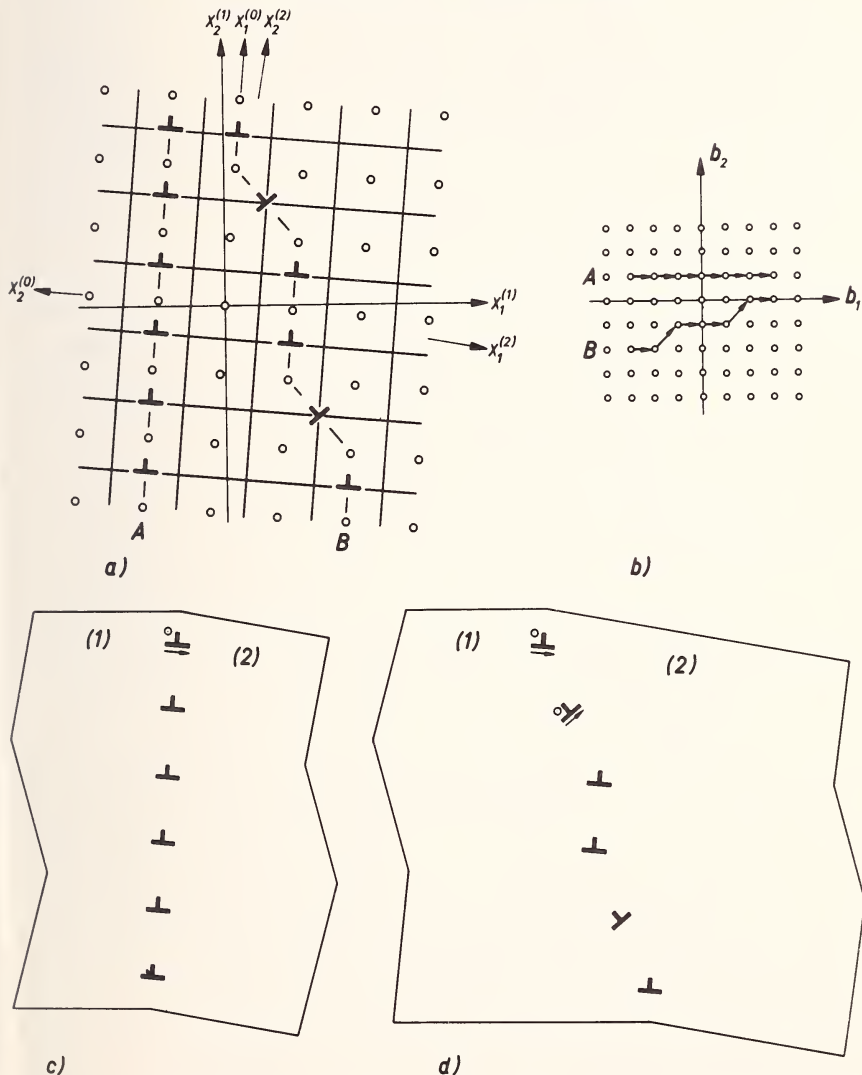


FIGURE 4. (a) 0-lattice for $\theta = -10^\circ$. (b) b-lattice enlarged 2X (i.e. the crystal units are half the size of the drawn b-lattice). (c) Symmetrical tilt boundary (boundary A in fig. 4(a)). (d) Unsymmetrical tilt boundary (boundary B in fig. 4(a)).

SIMMONS: You did not mention that your formulation was invariant under the point group in that you can put in any other unimodular point group matrix connecting a base for the lattice with another base. But your formulation is invariant under such unimodular transformations?

BOLLMANN: No! Two given lattices can be related by many different transformations \mathbf{A} ($\mathbf{x}^{(2)} = \mathbf{Ax}^{(1)}$). For example a square lattice may be rotated by 10° or by $90^\circ + 10^\circ$, etc. The point configuration of the two lattices is always the same and hence is invariant under these unimodular transformations. However, the 0-lattice as solution of the equation $(\mathbf{I} - \mathbf{A}^{-1})\mathbf{x}^{(0)} = \mathbf{b}^{(L)}$ is different in every case. The physically significant 0-lattice is the one which is produced by that \mathbf{A} which relates the closest neighbors, i.e. in our case the rotation by 10° . At the same time it is that 0-lattice with the largest unit cell, i.e. that for which the determinant $|\mathbf{I} - \mathbf{A}^{-1}|$ has the smallest value.

Figure 5 shows an example in a $\{110\}$ -plane in the b.c.c.-structure. Both point configurations formed by the two lattices are the same, but the correlations between the points and hence the 0-lattices are different. In the three-dimensional arrangement the 0-elements in figure 5a are vertical lines, in figure 5b vertical planes.

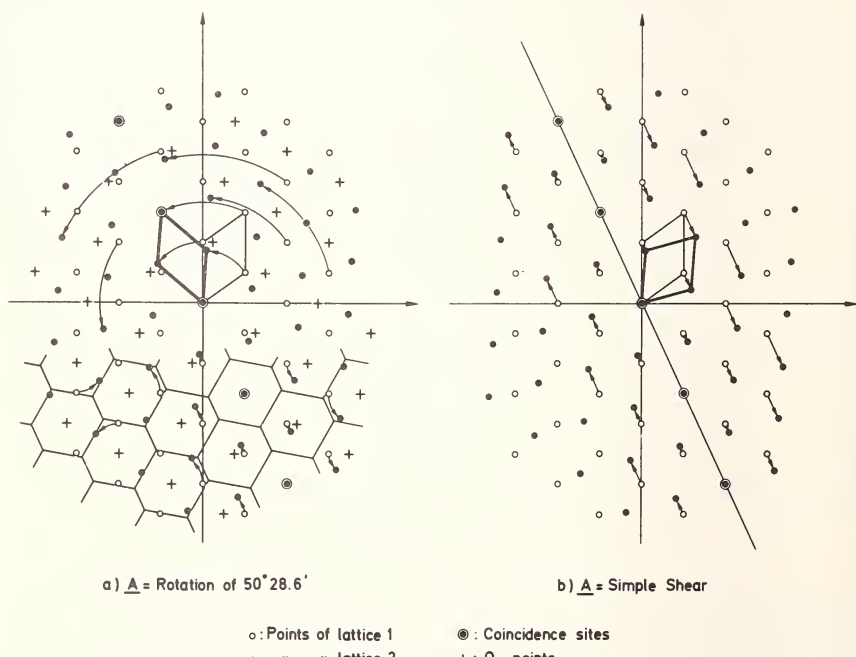


FIGURE 5

BULLOUGH: I just wanted to make one quick remark back to you. The whole problem in martensitic transformation theory is the choice of correspondence from which you start the game. Now in your case, you choose this correspondence in the knowledge that you know where the interface is, because you are able to locate the relative positions in the interface and make a decision on those grounds. If you do not know where the interface is, just how do you get going?

BOLLMANN: In the moonstone case (c.f. ref. [11] of my paper) I knew about where the boundary was, but the calculation made no use at all of this knowledge. Only at the end the calculated results were compared with the measured ones.

BULLOUGH: That is why I asked the question. It seems so incredible and I have not got it quite clear. Maybe everyone else has.

BOLLMANN: The point is that I could not show all the pictures, because it would have taken too much time. In order to determine the relative orientation of the crystals and the orientation of the boundary for which the boundary energy is a minimum, we do not need to know the energy itself. The energy function can be replaced by some function which we know behaves monotonically with the energy. For a phase boundary of the type of a low angle boundary, a geometrical parameter which corresponds to the square of the dislocation strain was chosen. Then the relative orientation of the crystals for which the smallest of these parameters showed a minimum was determined. The details are given in ref. [11] of my paper.

CHANG: Have you tried to superimpose a four-fold pattern onto a three-fold pattern of a cubic lattice? What kind of Moiré pattern would you get?

BOLLMANN: I haven't tried, but one could do it.

VOICES FROM AUDIENCE TO BOLLMAN: Do you mean it's trivial?

BOLLMANN: Yes, in principle.

AUDIENCE: Laughter.

NABARRO: In principle this discussion is concluded.

KINKS, VACANCIES, AND SCREW DISLOCATIONS

Robb M. Thomson

*Department of Materials Science
State University of New York at Stony Brook
Stony Brook, New York 11790*

A vacancy on a nonsplit pure screw dislocation can dissociate into a set of kinks. This dissociation is demonstrated geometrically for the NaCl lattice, showing that no geometrical constraints are violated by the dissociation. The kinks thus generated also splinter and spread the charge of the vacancy along the line. The effective vacancy association energy on the line is thus much higher than has been supposed hitherto, and is partly due to the delocalization of the charge singularity of the point defect and partly due to the delocalization of elastic singularity. When the Peierls energy is low, the vacancy will always dissociate, while if it is high, the dissociation will occur only when the total kink energy is less than the vacancy energy. Vacancy contributions to both climb and pipe diffusion are discussed in terms of the kink dissociation process. Results are that interstitial pipe diffusion is entirely symmetric to vacancy pipe diffusion, no motion energy is needed, and the formation energy for diffusion is related to the Peierls energy.

Key words: Dislocation geometry; dislocations; kinks; pipe diffusion; vacancies in dislocations.

I. Introduction

From the very beginning of dislocation theory, the problem of point defect interactions with dislocations has been one of the central problems. It is our purpose in the present paper to discuss the qualitative aspects of the core of a screw dislocation containing vacancies or interstitials. We shall take up a suggestion originally made by F. C. Frank [1] that it is possible to dissociate the vacancy in the core, and shall show that in the case of the NaCl lattice, such a dissociation is probable. Since it may be difficult to persuade oneself that no stacking-fault-like defects are generated in the process, the kinks thus generated will be considered in detail.

Fundamental Aspects of Dislocation Theory, J. A. Simmons, R. de Wit, and R. Bullough, Eds. (Nat. Bur. Stand. (U.S.), Spec. Publ. 317, I, 1970).

Our discussion is restricted to the case of whole, or non-dissociated dislocations. Since the dislocations in metals are so commonly dissociated, our discussion would appear to have its most interesting application to ionic crystals.

II. Effective Charge of Kinks

In ionic crystals, it is important to consider the charge on a screw dislocation kink. Hirth and Lothe [2] have shown that the charge is $q \equiv \pm e/4$, and in the appendix we demonstrate the same theorem by a different route.

III. Point Defect Dissociation

When a negative ion vacancy is added to a screw dislocation, the vacancy is equivalent to the four kinks shown in figure 1. Each of these kinks corresponds to a charge $+e/4$, and the sum is of course the same as the whole effective charge of the negative ion vacancy. The self energy of a vacancy in the lattice is composed partially of polarization energy, partly of Madelung energy, and partly of repulsive energy. The first two of these

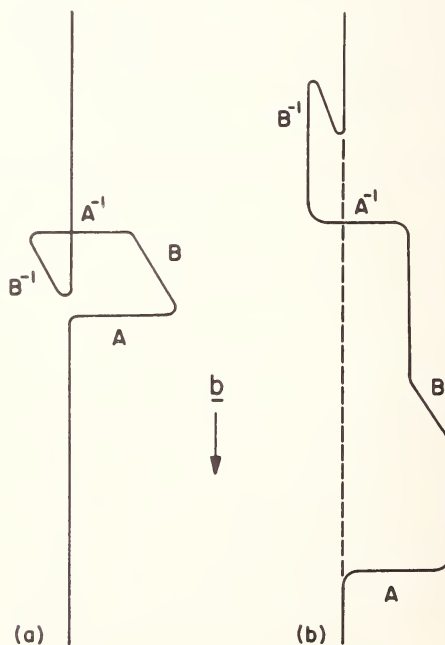


FIGURE 1. Dissociation of point defect on screw dislocation. (a) Initial prismatic configuration in cubic crystal. (b) Dissociated vacancy as series of kinks.

are decreased by breaking up the vacancy into a system of kinks. From the point of view of dislocation theory, the vacancy is a highly localized kink system, but if the Peierls energy is low, this kink system by de-localizing itself over many atomic distances along the line, will lower the energy of the vacancy. Likewise, once separated, the kinks will repel one another with a Coulomb repulsion.

An interstitial on the dislocation is just the reverse of the vacancy case. In figure 1, if the Burgers vector is reversed, or the sense of the rotation around the rectangle in (1a) is reversed, then the dislocation platelet represents an extra atom. The sign of the charges must also be changed, of course, for the extra atom case.

Visualization of the atomic placement in the vicinity of a kink is difficult. It is helpful, however, to consider the following sequence of operations: (1) Create a screw dislocation in a perfect crystal. (2) Slice the crystal on a plane normal to the screw and separate. Since the "plane" is in reality a spiral ramp, one must first cut the ramp on a line terminating at the dislocation and extending out to the external surface. When the two half crystals are separated, the ramp on each half crystal terminates at the familiar ledge along the cut line, the ledge emanating out from the dislocations. (3) Rigidly translate the two half crystals parallel to their surfaces of separation in direction of the desired kink, and by the amount of the desired kink length; and (4) weld the surfaces back together. The surfaces weld uniformly except along the cut ledges. The result is depicted in figure 2, where there is a thin wedge of missing material

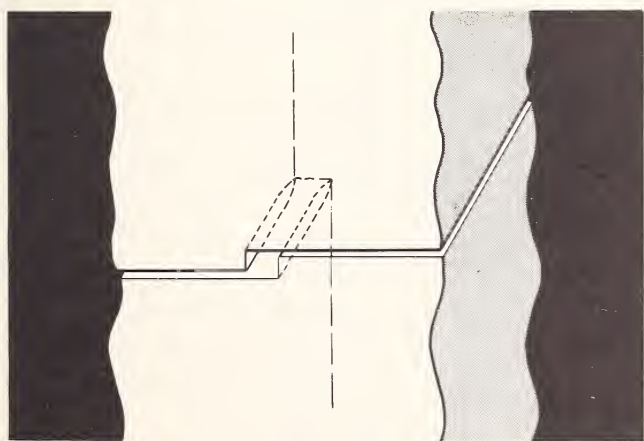


FIGURE 2. The figure shows how a kink is created by cutting a screw dislocated crystal perpendicular to the line of the screw, and displacing the two halves of the crystal in the plane of the cut. The extra "half plane" of atoms for the kink which results is manifested as the empty slot into which new material must be inserted.

where the ledges have moved apart by the amount of the translation of step 3. (The dislocation is represented by the vertical dashed lines joined in the center by the kink shown as the short horizontal dashed line.) The wedge of course simply represents the "extra half plane" of the edge dislocation corresponding to the kink and must be filled with added material. For a kink of minimum length, the wedge is a single line of atoms terminating at the kink. (For a displacement with opposite direction in step 3, of course, material would have to be subtracted in a manner analogous to all dislocation constructions.)

Figures 3 and 4 show detailed drawings of the atom placement in the core region of [110] and [100] kinks, respectively. The dislocation is represented in the figures by the heavy vertical lines. The circled ions at the kink sites are the ends of the extra line of ions described in the above paragraph. The light dashed and solid lines show the rows of ions in their deformed positions on the dislocation ramp. Only one plane of ions is shown, that just above the dislocation line. The heavy dashed lines represent the cross section of the surface first opened and then welded together in the construction of the previous paragraph.

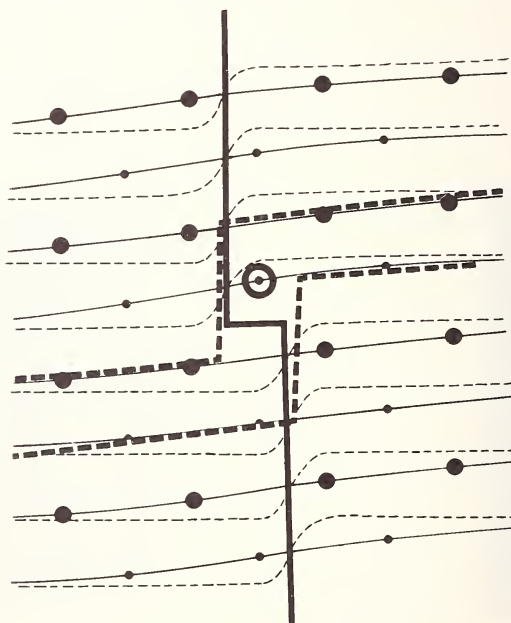


FIGURE 3. Kinked dislocation with kink in the [110] direction. All circles shown are on a single [100] plane. Large circles, for example, are negative ions, small circles positive ions.

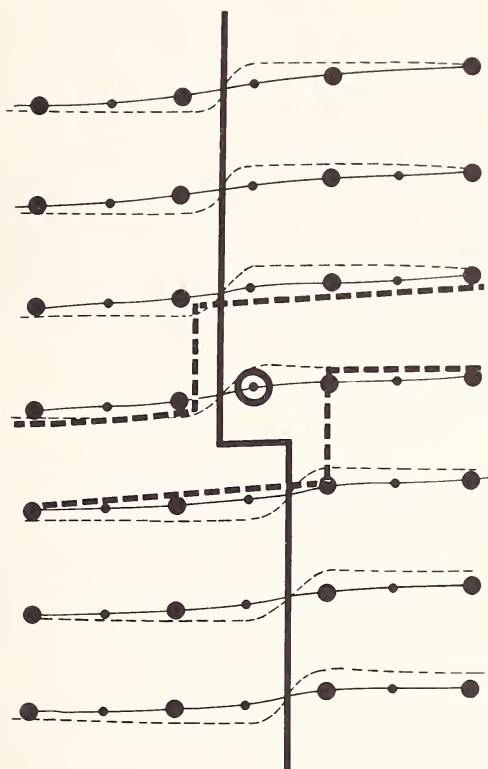


FIGURE 4. Kinked dislocation with kink running in [100] direction. (Ibid. fig. 3.)

III.1. Association energy of point defects

It has long been assumed that the large affinities which vacancies appear to have for dislocations is due to the stress relaxation in the core of the dislocation caused by the vacancy. However, uniquely for the case of the screw dislocation, the breakup of the vacancy into a kink system, when the kinks are relaxed, very nearly amounts to the total disappearance of the vacancy, and the association energy of the vacancy to the dislocation approaches the vacancy formation energy, itself. The criterion for breakup of the vacancy is obviously

$$4E_k < E_v, \quad (1)$$

where E_k is the kink energy, and E_v is the vacancy energy. The Schottky energy of NaCl is 2.02 eV per vacancy pair so that, provided the kink energy is less than about 0.25 eV per kink, the vacancy will dissociate.

(We neglect the difference in formation energies of positive and negative vacancies for simplicity.) Although various speculations have been made regarding the Peierls energy in the ionic crystals, the author is of the opinion that no evidence exists that it is strong enough to prevent the kink break up, even for the [100] kink.

One interesting possibility remains, namely that the vacancy has an activation energy barrier for breakup, with a local minimum for the localized vacancy. In such a case, measurements analogous to those of D. Thompson, et al. [3] would probably show an anomalous effect. The question then becomes what is the lifetime of a localized whole vacancy on the dislocation before dissociation occurs?

IV. Kink Kinetics

In the earlier paper by Thomson and Balluffi [1] it was suggested that a convenient notation in a four-fold lattice would be “*a*” to represent a positive kink, say in the [110] direction, and “*a*⁻¹” to represent a negative one. Then $aa^{-1}=1$ corresponds to annihilation. A “*b*” kink would be a [100] kink, etc. *a* and *b* kinks cannot pass easily through one another, since climb would result. (We term this process commutation in the following.) Thus $ab \neq ba$.

There is a serious problem associated with vacancy production by a screw dislocation line once the vacancies become completely dissociated. Production of a vacancy on the line requires bringing the appropriate four kinks together against their Coulomb repulsion, and then making the diffuse kink system “materialize” a localized vacancy once more. This process not only requires energy, but involves a very complicated reaction path. It is a very unlikely process involving a four-body collision, and equilibrium between vacancies in the lattice and the dislocation line will require a very highly kinked line.

Another mechanism for vacancy production on the line will undoubtedly predominate. If a kink pair breaks the forbidden commutation rule, climb occurs. The pair *ab* represents in our notation a “half” vacancy because it is half of the clockwise turn $aba^{-1}b^{-1}$. *ba*, on the other hand, represents a “half” interstitial because it is half of the sequence $bab^{-1}a^{-1}$. Thus a vacancy is produced in the lattice by the commutation $ab \rightarrow ba$. Furthermore, this is a simple bi-molecular collision process, and no collective localization is necessary. We note also that in a kink sequence $aba^{-1}b^{-1}$, once the commutation occurs, then $aba^{-1}b^{-1} \rightarrow baa^{-1}b^{-1} \rightarrow 1$, and the original dissociated vacancy, $aba^{-1}b^{-1}$, completely disappears. Thus vacancy production on a screw dislocation should be a very efficient

process, but it will be physically completely different from what occurs on an edge.

One final point must be made regarding the commutation process in an ionic lattice. Clearly, if $aba^{-1}b^{-1}$ represents a positive ion vacancy, and $bab^{-1}a^{-1}$ represents an extra positive ion, then $ab \rightarrow ba$ changes the signs of the two kinks. The annihilation bb^{-1} mentioned in the previous paragraph is thus facilitated by the opposite signs of the b and b^{-1} kinks. For kinks in ionic lattices, one probably should devise a notation which immediately distinguishes the charge. Hence, if "a" is a positive kink, "a*" will denote a negative kink, etc. Hence commutation must be written

$$ab \rightarrow b^*a^* + [\text{vac}]^- \quad (2)$$

The conditions for equilibrium between kinks and vacancies on the dislocation can now be written. The flux onto the dislocation will be written ϕ . The vacancy production rate by commutation of the kinks ab will be given by $\nu_{ab} \exp(-E_{ab}/kT)$, where ν_{ab} is a relatively complicated frequency factor for the collision rates. In equilibrium, then

$$\phi = \nu_{ab} e^{-E_{ab}/kT}. \quad (3)$$

The frequency factor, ν_{ab} , which must be calculated from the excitation spectrum of the kink system is of course a very complicated object. However, we note that any two adjacent kinks, a and b , of different kind must have the same sign of the charge, and thus repel one another. This theorem follows from the geometrical constraints placed upon how the ordering of the various types of kinks must proceed. Although the long-range character of the Coulomb repulsion between kinks will be important in generating plasma-like excitations, one can to a degree approximate the force law as a truncated two-body Coulomb potential, where the cutoff distance is the length, r_k , of the kink itself.

$$E_{kk} = \frac{e^2}{16\kappa r} \quad (4)$$

$r > r_k.$

The factor 16 is due to the effective charge of the kinks. Within r_k , the energy is a constant. r_k is several lattice spacings in length for a smooth kink in a crystal with low Peierls energy. κ is the dielectric constant. If a particular a -kink is caught between two b -kinks, and the b -kinks are held stationary, then the a -kink will oscillate in the Coulomb well with a

frequency characteristic of this nonlinear oscillator. The frequency, valid for small oscillations will be

$$\nu_{ab} = \frac{1}{2\pi} \left\{ \left[\frac{\frac{\partial^2 E_{kk}}{\partial r^2}}{m} \right] R_k \right\}^{1/2}. \quad (5)$$

In this equation, m is the inertial mass of the kink, and of course should be some type of reduced mass, since normally the b -kinks will not be pinned, as in this exercise. R_k is the average kink separation distance on the line. Substitution of (4) into (5) yields

$$\nu_{ab} = \frac{e}{8\pi R_k^{3/2}} \sqrt{\frac{2}{\kappa m}}. \quad (6)$$

For kinks separated about 20 lattice spacings apart and kink energy $\approx 10^{-1}$ eV, this frequency becomes approximately 10^{-11} sec $^{-1}$. Our estimate, (6), is of course very crude, but does show that ν_{ab} will depend upon the kink density to the 3/2 power. If the kinks were freely colliding particles (high-temperature approximation), then ν_{ab} would depend upon the first power of the kink density.

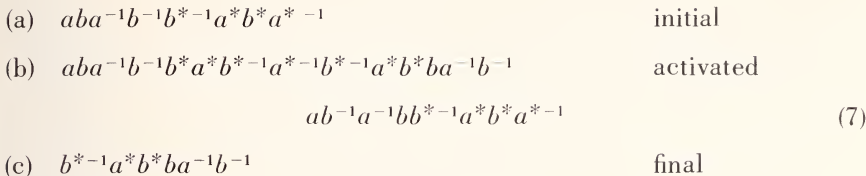
IV. 1. Dekinking

The problem remains of how a dislocation starting from a tight corkscrew unwinds itself into an open spiral. For example, if $aba^{-1}b^{-1}$ represents the vacancy of figure 1, $aba^{-1}b^{-1}aba^{-1}b^{-1}$ will be two vacancies of the same sign stacked on top of one another along the dislocation. $aba^{-1}b^{-1}b^{*-1}a^{*}b^{*}a^{*-1}$ represents a neutral pair. $b^{*-1}a^{*}b^{*}ba^{-1}b^{-1}$, however, also represents a neutral pair with two of its original kinks annihilated. Thus there are two nonequivalent ways of putting a neutral vacancy pair on the line. One sequence begins to form a larger spiral while the other simply coils up the line.

The crucial step in uncoiling the spiral is the one in which a divacancy kink system of the first type in the previous paragraph becomes one of the second type. The first kink system represents a small spiral of two turns, the second type only one.

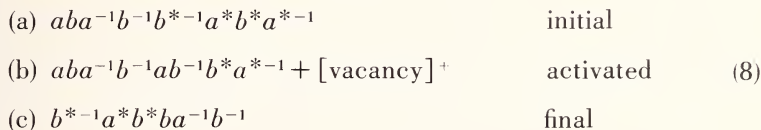
There are several ways to nucleate the process. One is to nucleate the equivalent of two positive and two negative complete turns in the middle

of the kink system, and let the activated state die by kink collisions:



A total of 8 new kink pairs (of the classic glide type usually discussed in kink theory) must be formed in this process.

Another process is the following:



The vacancy formed in the activated state moves up the dislocation line and forms a new kink system to the left of (8a) by diffusion of a localized vacancy. If the localized vacancy has a significant lifetime on the dislocation, the diffusion will be by pipe diffusion, otherwise the vacancy must leave the dislocation, diffuse through the lattice and return to it. The rate of dekinking by this process will be much facilitated by the presence of a metastable localized vacancy on the dislocation because of the relatively much faster pipe diffusion.

The two processes, (7) and (8), show that in general the dekinking process can take place by two types of process. One occurs by winding up the dislocation in the midst of the kink system, and then allowing kink annihilation to effect the final configuration. In the second, the dislocation produces a localized vacancy (or extra atom) which must move to a different point on the line, and then break apart again. Obviously which of these processes predominates will depend upon the activation energies involved and the length of reaction paths to be covered. However, when the kink is a low energy configuration, the line fluctuations will be easy and fast, and the first method will predominate. As kink energy becomes significant, then the vacancy production in the intermediate state will have to be considered.

V. Diffusion

Another interesting phenomenon relates to the pipe diffusion possibilities for dissociated kinks on a screw. The first point to be made is that on an edge dislocation, a vacancy or extra atom retains its individuality as it diffuses down the line. On the screw dislocation, the same is true only if the

defect is localized. If the defect dissociates into a kink system, the motion of the kink is slip-like rather than diffusion-like. To be concrete, if an extra atom enters onto an edge dislocation pipe on one surface, it can itself be transported to the opposite surface by diffusion. If an extra atom enters a screw dislocation on one surface, and a kink system moves to the opposite surface, then the original atom is incorporated into the lattice just under the first surface, and an atom originally belonging to the lattice just under the second surface is punched out on that surface. The passage of the kink system is analogous to the interstitialcy mechanism, while the passage of a localized extra atom is analogous to interstitial diffusion. Hence, one cannot obtain fast transport of marked atoms along a screw by kinks.

These remarks do not mean, however, that matter transport cannot take place quickly along screw dislocation. In fact, in the limit of zero Peierls energy, it will occur with activation energy for motion approaching zero, as we shall demonstrate. To be specific, we take the case where matter is being removed from the point where the dislocation breaks the surface, as in an etching experiment. Matter transport can occur by pair production:

- (a) aa^{*-1}
- (b) $abb^{*-1}a^{*-1}$
- (c) $aba^{-1}ab^{**-1}a^{*-1}$
- (d) $aba^{-1}b^{-1}b^*a^*b^{*-1}a^{*-1}$ (9)

The first step is just the standard kink pair nucleation familiar in classic glide theory. The final step, however, is a vacancy-extra atom pair. If extra atoms are being removed from the surface region, the extra atom kink system diffuses toward the surface, leaving the vacancy kinks in the interior. Since the kinks are free particles on the line, the only activation energy appearing in the process is that associated with the various steps, (9). Entropy is not negligible, however, and will contribute a temperature dependence of its own. Also, depending upon exactly how matter is extracted at the surface, localization energy for the extra atoms may be necessary there.

There is some evidence the [100] glide kinks in the NaCl type lattice may have a significant Peierls energy, in which case the glide activation energy in that glide plane would be equal to the pipe diffusion energy along the screws. In more conventional terms, the pipe diffusion has all its activation energy contained in formation energy, and this formation energy is just the formation energy of a double kink pair on the [100] glide plane. We would like to emphasize here, as we did in reference [1], that

extra atom diffusion on both screws and edges is a very likely process in contrast to the case of interstitial diffusion in a close packed perfect lattice. On a screw, there is complete symmetry between the two, provided dissociation takes place. On the edge, symmetry is not complete.

VI. Conclusions

- A. In low Peierls energy crystals, we can expect vacancies and extra atoms to dissociate on the dislocation into a low energy kink system.
- B. The charge of the kinks on [110] dislocations in the NaCl lattice is $e/4$.
- C. Vacancy production from a screw dislocation is by commuting kinks past one another.
- D. Dekinking of a dislocation can occur either by commuting kinks and diffusing the vacancy, or by multiple pair production in the middle of the kink system. If the Peierls energy is very low, the second will be preferred, and will not be an activated process.
- E. Pipe diffusion is extremely fast with no motion energy. The formation energy in the diffusion process is the same as the kink pair formation energy. Pipe diffusion is completely symmetric to vacancy or extra atom diffusion.

VII. Appendix

The importance of the charge on the screw is obvious from the preceding. Hirth and Lothe have already given a rule for obtaining the charge associated with various configurations of screws in the NaCl lattice, and we present here a technique capable of generalizing the procedure. If we start from a neutral configuration (perfect crystal) and add various arrays of semi-infinite ions, the long range potential from which the effective charge (or more complicated higher pole) may be inferred is obtained by the sum

$$V(x, y, z) = \sum_n \frac{e_n}{\{(x - x_n)^2 + (y \pm y_n)^2 + (z - z_n)^2\}^{1/2}} \quad (\text{A-1})$$

For example, this sum is often a simple sum over a line of ions. If the line is along the x axis, the potential as a function of the distance, y , from the axis is

$$V(y) = e \sum_{n=0}^N \frac{(-1)^n}{(x_n^2 + y^2)^{1/2}}. \quad (\text{A-2})$$

The sum may be represented as the integration over a series of δ -functions; however, more generally a continuous charge distribution would be represented by a Fourier series. If we use only the first term in the Fourier series (higher terms do not contribute to first order), the result is

$$V(y) \approx \frac{\pi e}{2} \int_0^N \frac{\sin \pi x}{(x^2 + y^2)^{1/2}} dx. \quad (\text{A-3})$$

Integration by parts yields

$$V(y) = 1/2 \left[\frac{e_0}{(x_0^2 + y^2)^{1/2}} + \frac{e_N}{(x_N^2 + y^2)^{1/2}} \right] + O(1/R^3). \quad (\text{A-4})$$

The potential is simply that of half charges at the two ends of the line. This result was obtained by Seitz [4] in calculating the charge at a jog on an edge.

The same reasoning can be applied to a calculation of the corner charge of a ledge on the surface of an ionic crystal. A square array of alternating charge gives the result

$$\begin{aligned} V(x_p, y_p) &= \frac{e\pi^2}{4} \left\{ \int_0^N \sin \pi y dy \right\} \\ &\quad \left\{ \int_0^N (\sin \pi x) [(x - x_p)^2 + (y - y_p)^2]^{-1/2} dx \right. \\ &\quad \left. \cong \frac{e}{4} \left\{ \frac{1}{x_p^2} + \frac{1}{y_p^2} \right\}^{-1/2} \right. . \end{aligned} \quad (\text{A-5})$$

If the array is not square, of course, the integration yields a more complex result.

One further case is important, namely the warped array. For example, a line of ions along the [110] direction in NaCl is a corrugated series of alternating charges. The potential is then

$$\begin{aligned} V(y) &= e \sum_n \frac{(-1)^n}{\{x_n^2 + (y + (-1)^n y_0)^2\}^{1/2}} \\ &= \frac{e\pi}{2} \int_0^N \frac{\sin \pi x}{[x^2 + (y - y_0 \sin \pi x)^2]^{1/2}} dx \\ &= 1/2 \left[\frac{e_0}{(x_0^2 + y^2)^{1/2}} + \frac{e_N}{(x_N^2 + y^2)^{1/2}} \right] + O(1/R)^3 \end{aligned} \quad (\text{A-6})$$

and corrugation is seen not to have an effect to first order.

One could use the previous method to calculate the charge on the kink directly but the integrations are difficult, and an approximate result is obtained in the following way by first calculating the charge on the surface where the screw emerges. Figure 5 shows the [110] plane in NaCl, and the screw emergent point is labelled *S*. If the ledge on the surface caused by the screw lies in the [001] direction, then by adding a quarter plane of ions (the corner lying at *S*), the ledge is turned to the [110] ledge.

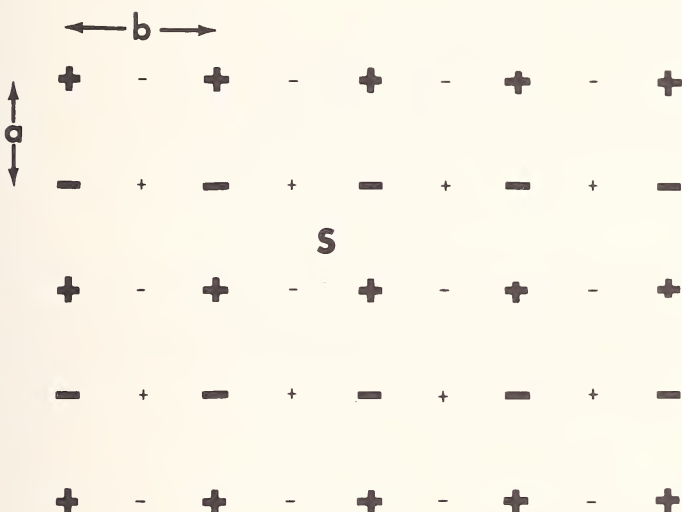


FIGURE 5. Schematic drawing of the ion positions on the [110] plane of NaCl with lattice parameters *a* and *b*. The screw emerges at *S*. The ledge caused by the screw can run in either the [001] direction (vertical) or in the [110] direction (horizontal). The heavy ions are the surface ions; the light ones are those lying a distance *b*/2 below the surface. When a quarter plane is added to turn a vertical ledge into a horizontal one, $\pm e/4$ is added to the screw emergent point.

Since a quarter plane of ions by (A-5) has an effective charge of $\pm e/4$, and if the charge on the screw as quarter planes are added (thus winding up the spiral ramp of the screw dislocation) is symmetric about zero, then the charge on the screw at the surface is $\pm e/8$. The plus sign corresponds to the ledge at the screw ending at a positive ion, and vice versa for the negative charge. The complexity of the integrals appearing in (A-1) for a spiral ramp suggests that the screw is *not* exactly symmetric about zero, as we suggest, but $e/4$ is seen as an upper limit for the charge, and $e/8$ appears as a fair approximation.

The charge on the kink is then obtained by taking two half crystals with screws emerging from their surfaces, placing them into contact again

with the screws one atom distance out of registry, as shown again by figure 2. The charge on the kink is then obtained by adding (1) the charge on the screws at their surface emergent points and (2) the charge at the end of the extra line of atoms which must be added to fill in the vacant wedge showing in figure 2. If the kink is in the [110] direction, the screws will each have (say) a charge of $-e/8$; the extra line of ions has a charge at its end of $+e/2$; and the final sum of the charges at the kink is then $+e/4$. Similar arguments show that the shortest kink in the [100] direction has charge also $\pm e/4$.

VIII. Acknowledgements

The author would like to thank C. Bauer, D. Thompson, and J. Hirth for comments and discussion relating to this paper.

IX. References

- [1] Frank, F. C., Nuovo Cim. Suppl. **7**, 386 (1958). See also R. Thomson and R. W. Balluffi, J. Appl. Phys. **33**, 803 (1962).
- [2] Hirth, J. P., and Lothe, J., Theory of Dislocations (McGraw-Hill, New York, 1968).
- [3] Thompson, D., Buck, O., Huntington, H. B., and Barnes, R. S., to appear J. Appl. Phys.
- [4] Seitz, F., Rev. Mod. Phys. **26**, 7 (1954).

Discussion on Paper by R. M. Thomson

BULLOUGH: From the symmetry you emphasized between the vacancy and the interstitial here, I have the impression that you are implying their formation energies will be equal.

THOMSON: That's right. That is, the formation energies on the line—not in the lattice, but on the line.

BULLOUGH: But they don't exist in halides?

THOMSON: That's right. The difference between the formation energy of vacancies and interstitials in the lattice will show up as a difference in association energy to the dislocation. Symmetry, however, requires equivalence for the dissociated kink configuration.

BESHERS: Isn't that equivalent to the generation of a spiral prismatic dislocation?

THOMSON: It certainly is an atomic version of the spiral prismatic dislocation. The question was how does one get an open spiral prismatic one from a highly kinked line? I am suggesting that you can get it by either of two mechanisms. If the Peierls energy is really high, then you have to deal with old fashioned vacancy motion. When the Peierls energy is low, you can simply curl the line up by a series of pair formations, and the kink system collapses into an open spiral.

ELBAUM: I would like to point out that several years ago some experiments were done on the charge of edge and screw dislocations in alkali-halides. At that time it was shown fairly convincingly that no charge was associated with the screw dislocation, which would make one think that screw dislocations are not actually very effective sources or sinks for vacancies.

THOMSON: That's an interesting point. However, it certainly also has been demonstrated with various pictures which I can remember but cannot quote that one does get spirals in ionic crystals and ionic lattices. I wonder if it has to do with the complete symmetry of the positive and negative ion vacancy on the screw. I'm not sure what that boundary condition does to you.

ELBAUM: I don't know either except that as far as charge conservation is concerned it would seem that two kinks would cancel, so that would still leave a spiral without showing a charge.

THOMSON: A second point is that a spiral prismatic dislocation does not move under stress, and the effective charge would not show as a

polarization under stress. If I know what you are talking about in the experiments you allude to, you move the screw back and forth and watch for induced polarization.

MITCHELL: There is one question that bothers me a little about this, and that is: It appears to me that in the beginning of the mechanism, if one is going to transform a screw into a helical or spiral dislocation, there is one essential ingredient that definitely one needs with one defect, namely supersaturation. It requires supersaturation or undersaturation, before you can go from the straight screw to a helical dislocation.

THOMSON: A supersaturation, or undersaturation, certainly will kink up the line. However, in addition, there will be an equilibrium kink (or vacancy) density on the line which, though normally small, is nevertheless present. The effects I discuss relate first to the configuration of the point defects on the line from whatever cause, and second to the possible kinetic transformations the kinked line can undergo.

TOPOLOGICAL RESTRICTION ON THE DISTRIBUTION OF DEFECTS IN SURFACE CRYSTALS AND POSSIBLE BIOPHYSICAL APPLICATION

W. F. Harris

Department of Chemical Engineering
Institute of Technology
University of Minnesota
Minneapolis, Minnesota 55455

Many thin biological structures such as some plasma membranes and virus capsids appear to be made up of units packed in two-dimensional lattices. Such structures are termed *surface crystals*. Dislocations and disclinations are observable in some of these crystals. The perfect surface crystal is described by a *pair* of basis vectors and the conventional crystal by a *triplet* of basis vectors; both are regarded as embedded in three-dimensional space. This difference allows the existence of defects which have no counterpart in conventional crystals. The various defects are classified as local or global, intrinsic or extrinsic. Surface crystals that form closed surfaces are considered and it is shown that the sum of the rotations of intrinsic (screw) disclinations in them must equal $2\pi\chi$ where χ is the Euler-Poincaré characteristic of the surface. The biophysical consequences are discussed briefly.

Key words: Dislocations in biophysics; protein structure; surface crystals; surface dislocations.

I. Introduction

In the biological literature, particularly of recent years, there are many examples of thin structures that exhibit periodicity in two dimensions. Such structures include bacterial cell walls [24], bacterial flagella [17], cell membranes [4, 22, 23] and protein coats of viruses [3, 5, 8, 9]. After disruption many of them are able to reassemble or crystallize spontaneously under suitable conditions [2, 12, 17, 21]. It is possible to identify dislocations in one of Watson and Remsen's [24] micrographs of a cell wall and disclinations in models (Caspar and Klug [7]; Hull, Hills, and Markham [14]; Kellenberger [15, 16]), if not in actual micrographs, of some viruses.

Fundamental Aspects of Dislocation Theory, J. A. Simmons, R. de Wit, and R. Bullough, Eds. (Nat. Bur. Stand. (U.S.), Spec. Publ. 317, I, 1970).

In the simpler viruses the protein coat is usually either a spherical or cylindrical shell around a nucleic acid or nucleoprotein core but toroidal shells have been observed (Dmochowski et al. [10]). Membranes of cytoplasmic organelles can be highly convoluted and many appear to be shells of high connectivity.

Caspar et al. [6] refer to viral protein coats as *surface crystals*. It is useful to generalize this term to include all structures exhibiting periodicity in two dimensions. Harris and Scriven [13] have discussed the passage of dislocations through cylindrical surface crystals and have suggested that dislocations may be involved in the contraction of certain viruses and in other biophysical processes. In this paper the importance of *disclinations* in biology is brought out.

II. The Perfect Surface Crystal

A *perfect surface lattice* is an infinite set of points invariant under translation by all vectors of the form

$$\mathbf{T} = n_\alpha \mathbf{a}_\alpha \quad (1)$$

and only those vectors; any two points can be connected by a vector of the same form. Summation is understood over repeated indices, the *basis vectors* of the lattice. \mathbf{T} is a *lattice translation vector* or translational symmetry operation. A *perfect surface crystal* is obtained by adding a *unit cell* to each lattice point in such a way that \mathbf{T} is still a symmetry operation.

In this paper only perfect dislocations and disclinations are considered. Dislocations, therefore, must have Burgers vectors \mathbf{b} of the form given by eq (1) and disclinations must have rotation vectors $\boldsymbol{\omega}$ which are rotational symmetry operations of the perfect surface crystal (Nabarro [19, p. 123]).

The perfect surface lattice is contained, of course, in a planar surface. This surface is regarded as being embedded in the surface crystal and as deforming with the latter, when defects are introduced. It can be termed conveniently *the surface* of the surface crystal. It is the geometry of this surface that is referred to when the surface crystal is said to have some particular shape.

The surface crystal is defined with reference to a *pair* of basis vectors whereas the conventional crystal is referred to a *triplet* of basis vectors. Both are regarded as being embedded in three-dimensional space (3-space). *This difference between the two types of crystal allows defects in surface crystals which have no counterpart in conventional crystals.*

The symmetry operations \mathbf{T} and $\boldsymbol{\omega}$, where $\boldsymbol{\omega}$ is normal to the surface of the perfect surface crystal, imply displacements in the plane of the

surface. Such displacements would be readily understood by the inhabitants of Abbott's Flatland [1]; they result in *intrinsic defects*. All other displacements carry material out of the 2-space (the surface); they lead to *extrinsic* defects. Since no displacement carries material out of 3-space all defects in conventional crystals must be intrinsic defects. Extrinsic defects in 3-space paralleling those in surface crystals may arise from general relativity (Marder [18]; Nabarro [19, p. 590]).

Below the term defect is restricted to the class of defects of the Weingarten-Volterra type, i.e., defects resulting from rigid-body-type relative displacement of cut faces (Nabarro [19, p. 16]).

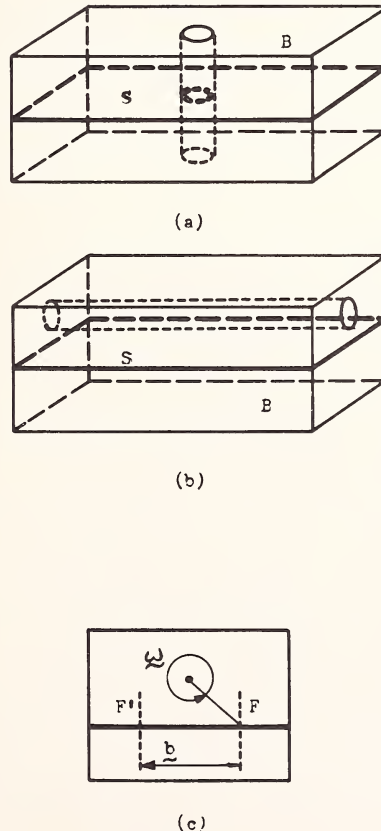


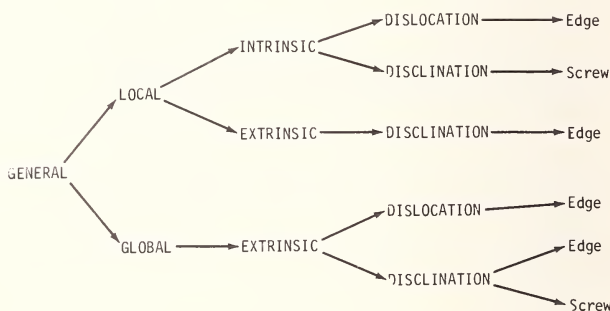
FIGURE 1. The surface crystal S embedded in a doubly-connected body B. In (a) the hole penetrates S, in (b) it does not. The right-hand end view of (b) is shown in (c) to illustrate the introduction of a global defect by rotation through 2π and translation through b: the defect results in a cylindrical surface crystal.

III. The Imperfect Surface Crystal

The various types of defects in surface crystals can be enumerated by considering a surface crystal embedded in an imaginary doubly-connected body B. The embedding (see fig. 1) can be such that the hole (a) intersects the surface crystal S or (b) does not intersect S. A defect can be introduced by the usual method of making a cut to render B simply connected and displacing one surface relative to the other by a rigid-body-type displacement. The cut must intersect S and the relative displacement must be a symmetry operation of S.

The defect line threads the hole. Where the latter penetrates S is a point or *local* defect in the surface crystal. If the latter does not penetrate S then the surface crystal contains a global defect. Local defects may be intrinsic or extrinsic. Intrinsic displacements in figure 1b are certainly possible but they leave the surface crystal unstrained. Insisting that strains in a defective surface crystal must not be zero everywhere one concludes that global defects are always extrinsic. The hierarchy of defects is shown in table 1.

TABLE 1. *Classification of defects in surface crystals.*



IV. Global Defects

The only symmetry properties that imply rigid-body-type displacements out of the plane of S are axes of rotation not normal to S. Perfect surface crystals may have 2-fold axes in their midplanes and all, of course, have an infinity of 1-fold axes everywhere. Rotation by π about 2-fold axes leads to folded or twisted sheets which spring flat when applied stresses are released; i.e., no defect results. Rotation by 2π about any 1-fold axis similarly results in no defect. Therefore none of these operations alone leads to a defect.

If the rotation by 2π is made about the axis of the hole in figure 1b and it is accompanied by translation in accordance with the translational

symmetry eq (1) (see fig. 1c) then a cylindrical surface crystal results. If S is inextensible then the circumference of the cylinder, measured in S , is the magnitude of the translation. The global defect thus produced may be thought of as having two components, disclination with $\omega = 2\pi$ and dislocation with \mathbf{b} equal to the circumference of the cylinder formed by S if S is inextensible. The disclination has screw character and the dislocation edge character. This global defect can also be regarded as a pair of screw disclinations whose combined angle of rotation is 2π and whose axes of rotation are parallel but not coincident. However, since the Burgers vector of the dislocation is related directly to the circumference of the cylinder the first description would appear preferable. A cylindrical crystal is shown in figure 2.

Harris and Scriven [13] discuss cylindrical crystals in detail. The Burgers vector of the dislocation component corresponds to the characteristic vector \mathbf{C} in their paper and the rotation vector of the disclination component is parallel to their vector \mathbf{z} .

A cylindrical crystal can, of course, be obtained simply by identifying opposite sides x of a rectangular portion of a perfect surface crystal where



FIGURE 2. A cylindrical surface crystal; global defect with (screw) disclination and (edge) dislocation components.

the other two sides can be represented by \mathbf{b} (fig. 3a). (A rectangle is chosen only for convenience.) If, in addition, the sides y are identified as in figure 3b then the result is a toroidal crystal. This corresponds to the introduction of a second global defect, of screw-disclination and edge-dislocation character, at right angles to the first. In figure 3c the one side is rotated through an angle π about a 2-fold axis at right angles to the imaginary defect line and then rotated through 2π and translated by \mathbf{b} as before. This is in fact the introduction of an edge-disclination component ω_e into the global defect. S assumes the shape of a Möbius strip and is nonorientable or one-sided (in 3-space). An example is shown in figure 4. If interpenetration is allowed then the addition of a second global defect, with screw-disclination (ω_{2s}) and edge-dislocation (\mathbf{b}_2) components, to the Möbius crystal results in a crystal of the shape of a Klein bottle (fig. 3d).

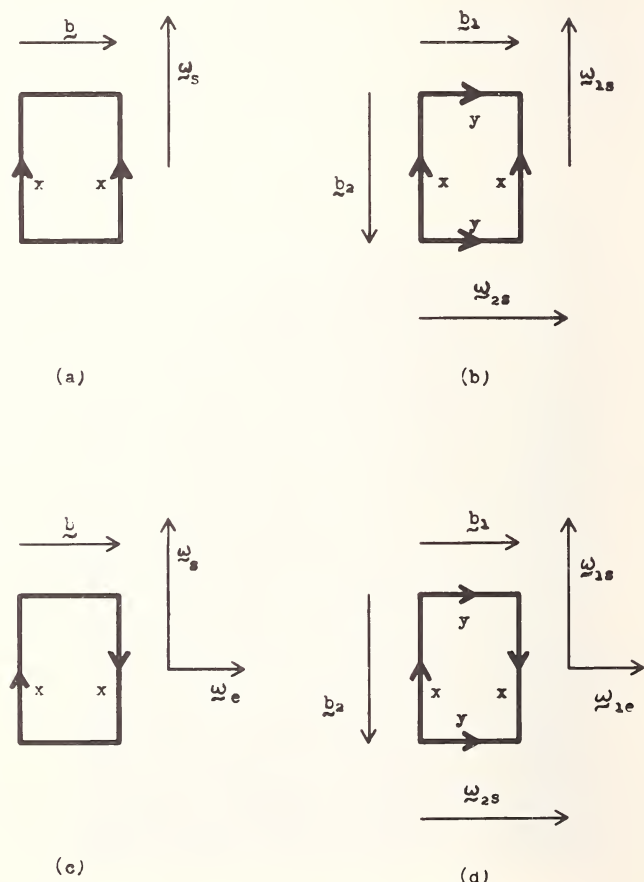


FIGURE 3. Identification of sides as shown leads to global defects with Burgers and rotation vectors as shown: (a) cylinder, (b) torus, (c) Möbius strip, (d) Klein bottle.

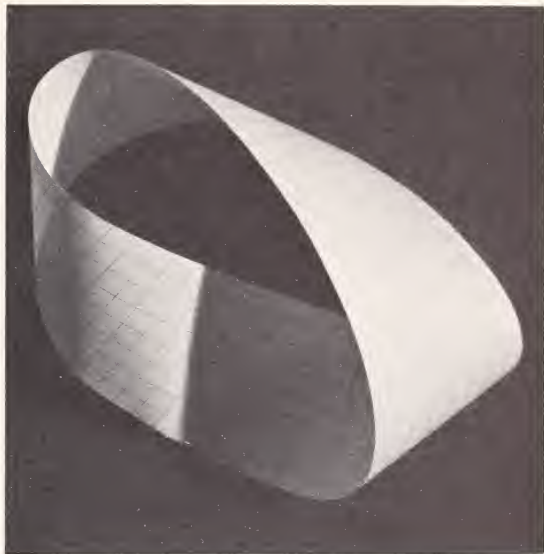


FIGURE 4. Global defect (Möbius strip) with components edge disclination ($\omega = \pi$), screw disclination ($\omega = 2\pi$) and edge dislocation.

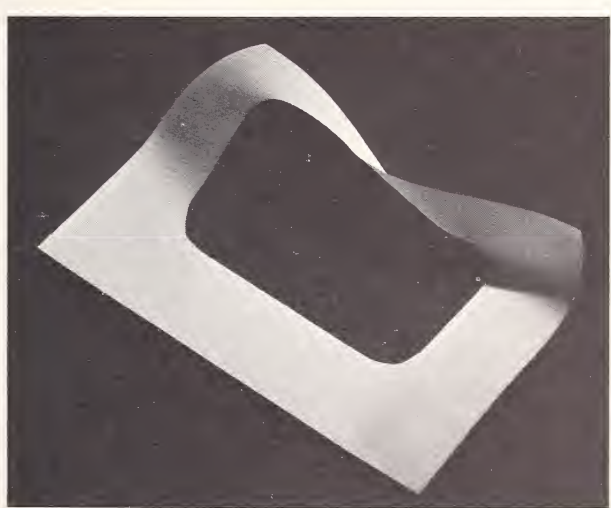


FIGURE 5. Extrinsic local defect (Möbius strip). It is purely edge disclination with $\omega = \pi$.

V. Local Defects

Local defects result from Weingarten-Volterra dislocations introduced into figure 1a. Rotation about axes normal to S leads to intrinsic defects and rotation about other axes (1-fold and possibly 2-fold in the midplane of the perfect surface crystal) to extrinsic defects. Dislocations are intrinsic defects and are clearly edge in character.

Figure 5 shows an extrinsic local defect made by rotation through π about a 2-fold axis in the midplane of the perfect crystal: the surface is a Möbius strip. The difference between figures 4 and 5 should be noted. Rotation by 2π about the same axis leads to a Möbius strip of two half-twists. This last axis could, of course, be a one-fold axis. Rotation by 2π about other one-fold axes leads to Möbius strips of two half-twists or interpenetrating surfaces if they are allowed. Extrinsic local defects may be regarded as edge in character.

Intrinsic defects are of two basic types: (edge) dislocation and (screw) disclination. Two of the latter are shown in figures 6 and 7. The axes of rotation for intrinsic disclinations are normal to S and may be s -fold where $s=1, 2, 3, 4$, or 6. The rotation angle is of the form (Nabarro [19, p. 124])

$$\omega = 2\pi n/s \quad (2)$$

where n is any integer.

The vector \mathbf{b} and the angle ω describing any defect depend only on the translational and rotational symmetry of the perfect surface crystal. A network of regular hexagons has the same appropriate symmetry properties as any perfect hexagonal surface crystal and therefore can be used to represent the latter. Similarly a network of squares can represent a surface crystal with 4-fold rotation axes. By introducing defects into such networks and using the simple yet powerful Euler's formula it is shown below that the number and strength of intrinsic disclinations possible in surface crystals depends on the Euler-Poincaré characteristic χ of the surface. Results for crystals of lower symmetry can be obtained by simple argument as special cases of the above. No similar restrictions are found for intrinsic dislocations.

The nomenclature used in the graph theory below is that of Ore [20]. The number of end points of edges coinciding at a vertex is the *valence* ρ of that vertex. The number of boundary edges of a face in the graph is the *dual valence* ρ^* of that face: an edge which is on the boundary of one face, only, is counted twice. A graph is *regular* if every vertex has the same valence. It is *dually regular* if every face has the same dual valence. It is completely regular if it is both regular and dually regular.

The hexagonal lattice of figure 8a has 6-fold rotation axes at face centers (A) and 3-fold axes at vertices (B). A disclination with $\omega = \pi/3$ produces a

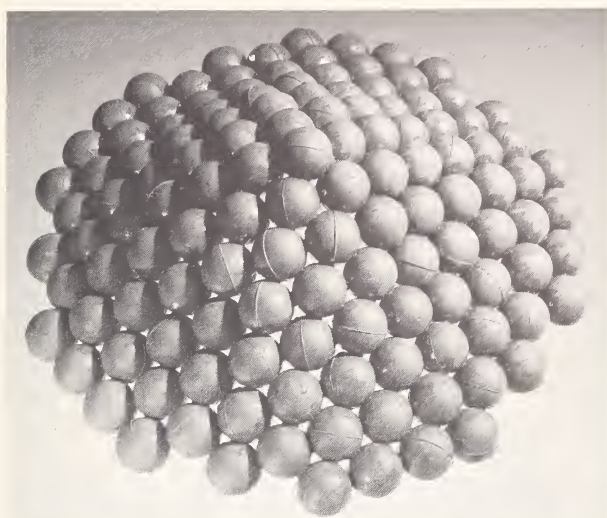


FIGURE 6. Local positive screw disclination with $\omega = \pi/3$.

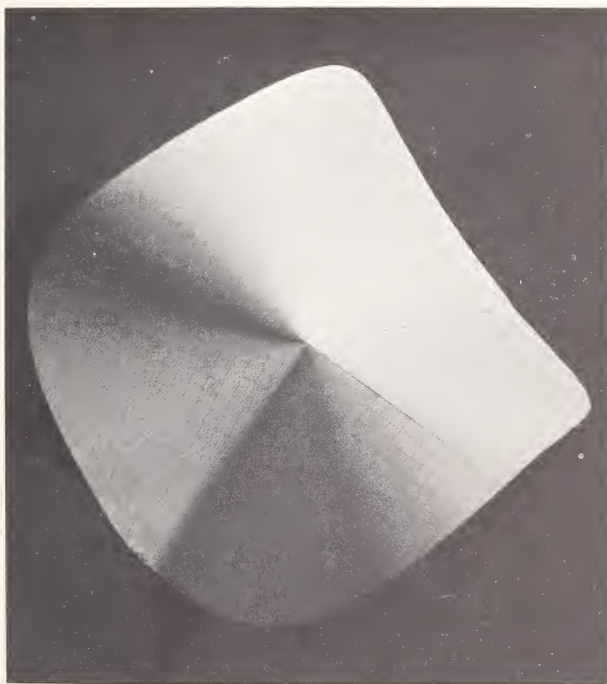


FIGURE 7. Local negative screw disclination with $\omega = -\pi/2$.

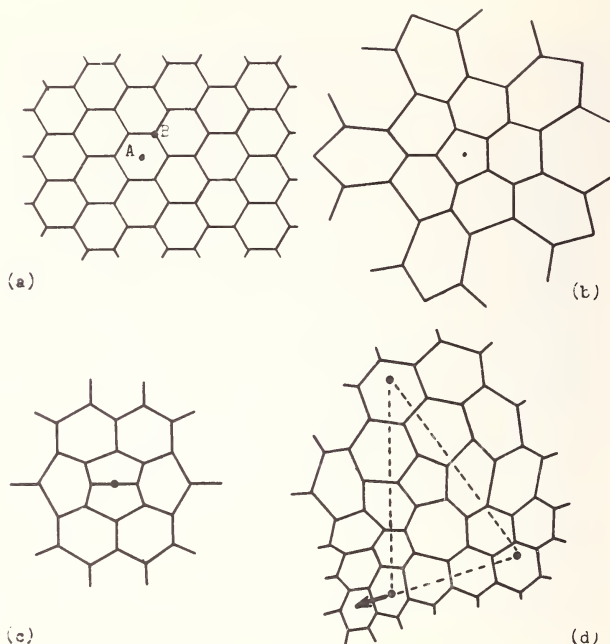


FIGURE 8. (a) Perfect hexagonal lattice. (b) Screw disclination ($\omega = \pi/3$) at a face center. (c) Screw disclination ($\omega = 2\pi/3$) at a vertex. (d) Edge dislocation appearing as a pair of disclinations of opposite sign.

pentagon surrounded by hexagons (fig. 8b). The graph is regular with $\rho = 3$. In general a disclination with $\omega = 2\pi n/6$ results in a regular graph ($\rho = 3$) with a $(6-n)$ -gon surrounded by 6-gons. The integer n is restricted to values less than 6. A disclination with rotation $\omega = 2\pi/3$ about B results in a dually regular graph ($\rho^* = 6$) with one vertex valence 2 and the rest valence 3 (fig. 8c). In general a disclination at B with $\omega = 2\pi n^*/3$ leads to a dually regular graph ($\rho^* = 6$) with one vertex valence $(3 - n^*)$ and the rest valence 3; n^* is restricted to less than 3.

In a similar manner disclinations can be introduced into a square lattice (fig. 9). The two lattices can be dealt with together. A disclination with angle $\omega_n = 2\pi n/s$ ($n < s$) about a point in a face of an s -gonal lattice ($s = 4, 6$) appears as a regular graph ($\rho = 4$ for $s = 4$; $\rho = 3$ for $s = 6$) with an $(s - n)$ -gon surrounded by s -gons. A disclination of angle $\omega_{n^*} = 2\pi n^*/\rho$ ($n^* < \rho$) at a vertex appears as a dually regular graph ($\rho^* = s$) with one vertex valence ($\rho = n^*$) and the rest valence ρ .

Consider a graph containing v_n disclinations of angle ω_n and v_{n^*} of angle ω_{n^*} on a closed surface of Euler-Poincaré characteristic χ . For such a graph (Eves [11])

$$v - e + f = \chi \quad (3)$$

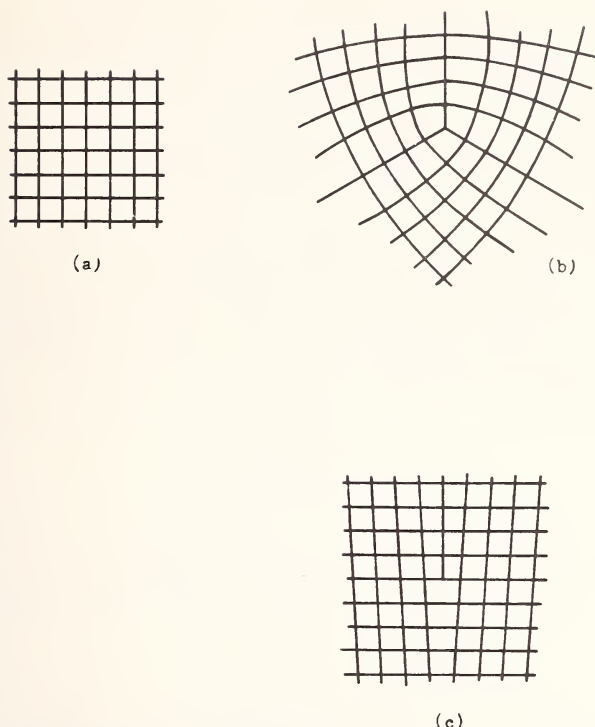


FIGURE 9. (a) Perfect square lattice. (b) Screw dislocation ($\omega = \pi/2$) at a vertex. (c) Edge dislocation.

where v , e , and f are the number of discrete vertices, edges and faces respectively. Then

$$f = \sum_n v_n \quad (4)$$

where summation is from $(-\infty)$ to $(s-1)$ and v_0 is the number of s -gons. (The s -gons are, of course, disclinations of zero rotation.) Also

$$e = \frac{1}{2} \sum_n (s-n)v_n. \quad (5)$$

If $v_{n*} = 0$ for all n^* then each vertex is shared by ρ faces and the number of vertices is

$$v_0 = \frac{1}{\rho} \sum_n (s-n)v_n. \quad (6)$$

If $\nu_{n*} = 1$ for $n^* = n_1^*$ and $\nu_{n*} = 0$ for $n^* \neq n_1^*$ then one vertex has valence $(\rho - n_1^*)$ and $(\rho - n_1^*)$ polygons share that vertex. Equation (6) must be corrected by adding $\{1 - (\rho - n_1^*)/\rho\}$ or n_1^*/ρ . Generally

$$v = \frac{1}{\rho} \sum_n (s - n) \nu_n + \frac{1}{\rho} \sum_{n*} n^* \nu_{n*}. \quad (7)$$

Substitution of eqs (4), (5), and (7) in (3) gives

$$\left(\frac{1}{2}\rho - 1\right) \sum_n n \nu_n + \sum_{n*} n^* \nu_{n*} + \left\{ s \left(1 - \frac{1}{2}\rho\right) + \rho \right\} \sum_n \nu_n = \rho \chi.$$

For both $s = 4$ and 6

$$s \left(1 - \frac{1}{2}\rho\right) + \rho = 0. \quad (8)$$

$$\therefore \left(\frac{1}{2}\rho - 1\right) \sum_n n \nu_n + \sum_{n*} n^* \nu_{n*} = \rho \chi$$

and

$$s \left(\frac{1}{2}\rho - 1\right) \sum_n \nu_n \omega_n + \rho \sum_{n*} \nu_{n*} \omega_{n*} = 2\pi \rho \chi.$$

From eq (8)

$$\sum_n \nu_n \omega_n + \sum_{n*} \nu_{n*} \omega_{n*} = 2\pi \chi.$$

This can be written simply

$$\sum_i \omega_i = 2\pi \chi. \quad (9)$$

where ω_i is the rotation of disclination i .

The dislocations of figures 8d and 9c can be regarded as pairs of disclinations the sum of whose rotations is zero. Similarly dislocations with larger Burgers vectors may be regarded as groups of disclinations of zero total rotation. Clearly, therefore, the above argument leads to no restriction on the number or Burgers vectors of dislocations in surface crystals.

By restricting rotations in a hexagonal lattice to $2\pi n/3$ one sees that a crystal with 3-fold axes is a special case of the hexagonal lattice and eq (9) must hold for the crystal. Similarly crystals with 2 and 1-fold axes normal to the surface are special cases of the square lattice. Equation (9), therefore, holds for all surface crystals on closed surfaces at least for intrinsic disclinations of rotation less than 2π .

VI. Conclusion

The smallest possible intrinsic disclination has rotation $\pi/3$: it can occur only in a surface crystal with 6-fold symmetry. For a sphere $\chi=2$. Therefore, from eq (9), 12 such disclinations are necessary in a sphere. A spherical surface crystal containing 12 disclinations is shown in figure 10: it is in fact a model of a small spherical virus (Caspar and Klug [7]; Kellenberger [15, 16]).

The only closed surfaces that need not contain intrinsic disclinations are those with $\chi=0$: i.e., the torus and the Klein bottle (Eves [11]). These surfaces, of course, contain global defects with disclination components as discussed in section IV. Any closed, noninterpenetrating surface is topologically equivalent to a sphere with p handles. The Euler-Poincaré characteristic for such a surface is (Eves [11])

$$\chi = 2 - 2p. \quad (10)$$

From eqs (9) and (10) one sees that, except for spherical and toroidal surface crystals (0 and 1-handled spheres), any closed, noninterpenetrating surface crystal must contain at least one negative intrinsic disclination.

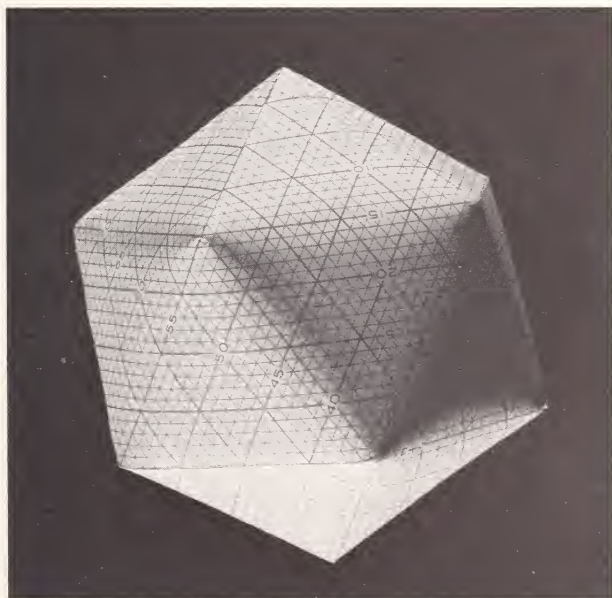


FIGURE 10. Spherical surface crystal containing 12 intrinsic disclinations of rotation $\pi/3$. It is model of a spherical virus.

Without change in the topology of its surface the shape of a surface crystal may be altered by rearranging its local defects or, perhaps, even by changing their number. Change in the topology of the surface generally involves change in both local and global defects. The writer is at present studying the details of these processes. The ability to undergo these types of changes is nothing less than a very characteristic of living systems.

VII. Acknowledgements

The writer wishes to express his gratitude to L. E. Scriven for his continuing advice and encouragement. This work was supported by the Air Force Office of Scientific Research, under AFOSR Grant No. 219-67, L. E. Scriven, Principal Investigator.

VIII. References

- [1] Abbott, E. A., *Flatland* (Dover, New York, 1952).
- [2] Bancroft, J. B., Hills, G. J., and Markham, R., *Virology* **31**, 354 (1967).
- [3] Bradley, D. E., and Robertson, D., *J. Gen. Virol.* **3**, 247 (1968).
- [4] Brightman, M. W., and Reese, T. S., *J. Cell Biol.* **40**, 648 (1969).
- [5] Caspar, D. L. D., *Adv. Protein Chem.* **18**, 37 (1963).
- [6] Caspar, D. L. D., Dulbecco, R., Klug, A., Lwoff, A., Stoker, M. P. G., Tournier, P., and Wildy, P., *Cold Spring Harbor Symp. Quant. Biol.* **27**, 49 (1962).
- [7] Caspar, D. L. D., and Klug, A., *Cold Spring Harbor Symp. Quant. Biol.* **27**, 1 (1962).
- [8] Coetzee, H. L., de Klerk, H. C., Coetzee, J. N., and Smit, J. A., *J. Gen. Virol.* **2**, 29 (1968).
- [9] Crawford, L., in *Molecular Basis of Virology* (ACS Monograph 164), H. Fraenkel-Conrat, Ed. (Reinhold, New York, 1968) p. 435.
- [10] Dmochowski, L., Grey, C. E., Padgett, F., and Sykes, J. A., in *Viruses, Nucleic Acids and Cancer* (Univ. of Texas, M. D. Anderson Hospital and Tumor Inst.), (Williams and Wilkins, Baltimore, 1963) p. 85.
- [11] Eves, H., *A Survey of Geometry*, **2** (Allyn and Bacon, Boston, 1965) pp. 346 ff.
- [12] Green, D. E., and MacLennan, D. H., *BioScience* **19**, 213 (1969).
- [13] Harris, W. F., and Scriven, L. E., *J. Theoret. Biol.* **26**, (1970), in press.
- [14] Hull, R., Hills, G. J., and Markham, R., *Virology* **37**, 416 (1969).
- [15] Kellenberger, E., in *Principles of Biomolecular Organization* (Ciba Foundation Symp.), G. E. W. Wolstenholme and M. O'Connor, Eds. (Churchill, London, 1966) p. 192.
- [16] Kellenberger, E., *Scientific American* **215** (6), 32 (1966).
- [17] Lowy, J., Hanson, J., Elliott, J. F., Millman, B. M., and McDonough, M. W., in *Principles of Biomolecular Organization* (Ciba Foundation Symp.), G. E. W. Wolstenholme and M. O'Connor, Eds. (Churchill, London, 1966) p. 7.
- [18] Marder, L., *Proc. Roy. Soc. A* **252**, 45 (1959).
- [19] Nabarro, F. R. N., *Theory of Crystal Dislocations* (Clarendon Press, Oxford, 1967).
- [20] Ore, O., *The Four-Color Problem* (Academic Press, New York, 1967).
- [21] Poglazov, B. F., *Structure and Function of Contractile Proteins* (Academic Press, New York, 1966) p. 125.
- [22] Robertson, J. D., in *Principles of Biomolecular Organization* (Ciba Foundation Symp.), G. E. W. Wolstenholme and M. O'Connor, Eds. (Churchill, London, 1966) p. 357.
- [23] Staehelin, L. A., *Proc. Roy. Soc. B* **171**, 249 (1968).
- [24] Watson, S. W., and Remsen, C. C., *Science* **163**, 685 (1969).

DISCLINATIONS IN SURFACES

F. R. N. Nabarro

*Department of Physics
University of the Witwatersrand
Johannesburg, South Africa*

The screw disclination is essentially a 2-dimensional object. Screw disclinations provide a convenient classification of star polygons. By considering the disclinations in vector fields lying on surfaces, it is possible to relate Euler's theorem for polyhedra inscribed on a sphere (faces – edges + corners = 2) to the fixed-point theorem for continuously-varying small displacements of points on a sphere. The changes in the Euler characteristic produced by the addition of holes, handles and cross caps are related to the disclinations which these singularities introduce into vector fields lying on the surface. These disclinations may be localized into the neighbourhood of their corresponding singularities.

Key words: Crystal surface imperfections; disclinations; screw disclinations.

I. Introduction

The idea of a disclination has been developed in three dimensions (cf. Nabarro [1], sec. 3.1). The special case of a screw disclination is essentially two-dimensional. We consider a surface which has at every point a pattern which defines a direction or a set of equivalent directions lying in the surface. We take a closed circuit Γ in the surface, and record the total change in the orientation of the pattern when the circuit is traversed once. If this change is not zero, we say that the circuit encloses a disclination. The strength of the disclination is the number of complete rotations of the pattern in the sense in which the circuit is described. If the pattern is a continuous vector field \mathbf{V} defining a unique direction at almost all points of the surface, the strength S of the disclination may be defined as

$$S = \frac{1}{2\pi} \oint_{\Gamma} d\theta,$$

where θ is the angle between some constant direction \mathbf{V}_0 and the vector field \mathbf{V} (fig. 1). An alternative definition is based on the angle ϕ between

Fundamental Aspects of Dislocation Theory, J. A. Simmons, R. de Wit, and R. Bullough, Eds. (Nat. Bur. Stand. (U.S.), Spec. Publ. 317, I, 1970).

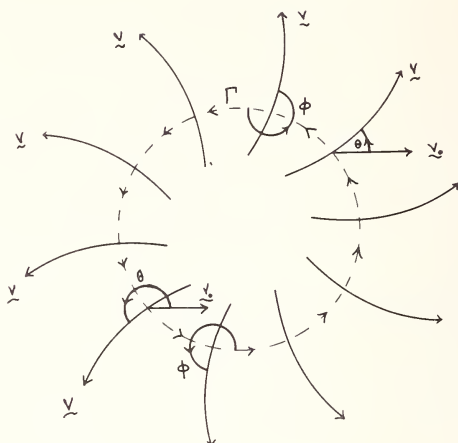


FIGURE 1. The strength of a disclination in a surface is defined by the integral round a circuit Γ of the change in the angle θ or the angle ϕ .

an element of the circuit Γ and the local vector field (fig. 1). The strength is then given by

$$S = \frac{1}{2\pi} \oint_I d\theta + 1.$$

The definitions are equivalent if the surface (but not necessarily the pattern on the surface) is regular on and within Γ . If the surface is singular on or within Γ , there may be difficulty in defining the parallel transport of the vector V_0 , and the second definition must be used.

In such a continuous vector field, isolated disclinations must have integral strengths. Figures 2 (a), (b), and (c) illustrate disclinations of strength + 1, figure 3 a disclination of strength + 2, and figure 4 a disclination of strength - 1. If the elements of the pattern have n -fold rotational symmetry, disclinations of strength p/n , with p any integer, are possible. For example, the pattern of figure 5(a), which has three-fold symmetry, admits the disclination + 1/3 of figure 5(b). Figure 6 illustrates by the special case $(+2) + (-1) = +1$ the important result that the disclination associated with a circuit is the sum of the elementary disclinations enclosed by the circuit. Disclinations of fractional strength are joined by lines of constant misorientation (fig. 7 (a) and (b)), and the relations $1/2 + 1/2 = 1$ and $1/3 + 1/3 + 1/3 = 1$ are illustrated. It is necessary to adopt the convention that sudden changes in direction on crossing a line of constant misorientation are neglected.

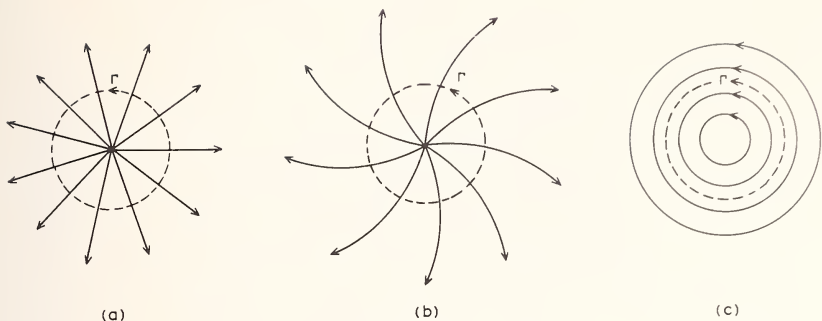


FIGURE 2(a), (b), (c) Three configurations of the disclination + 1.

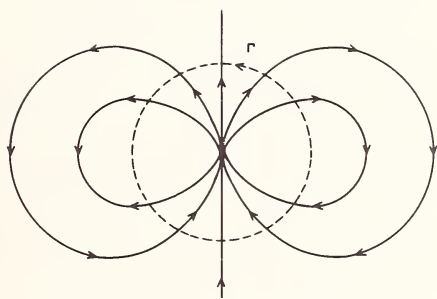


FIGURE 3. The disclination + 2.

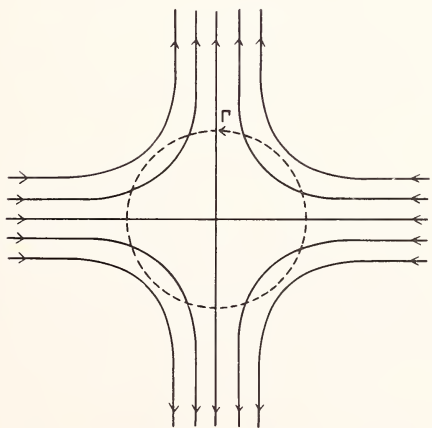


FIGURE 4. The disclination - 1.

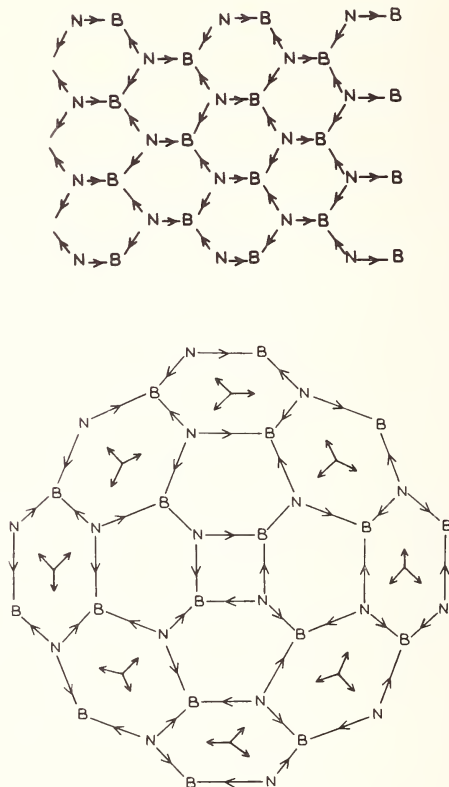


FIGURE 5(a). A pattern with three-fold symmetry. (b) A disclination + 1/3 in this pattern.

To justify this neglect, we map the figure on a surface carrying a pattern of higher symmetry for which the constant misorientation represents a symmetry element of the pattern. In the latter map the line of constant misorientation is no longer a singularity in the pattern. For example, the pattern in the neighbourhood of Γ_1 in figure 7(a) may be mapped on to a surface carrying a pattern with two-fold symmetry, as in figure 3.5 of Nabarro [1]. The disclination of strength + 1/2 remains, but the line singularity has disappeared. Similarly, the neighbourhood of either end of the singular line in figure 7(b) may be mapped on a surface carrying a pattern with three-fold symmetry. The resulting map is figure 5(b).

II. Regular and Star Polygons in the Plane

If a tangent rolls once around any polygon in a plane, it turns through 2π radians. In a regular n -gon, the angle at each corner is $2\pi/n$, and the

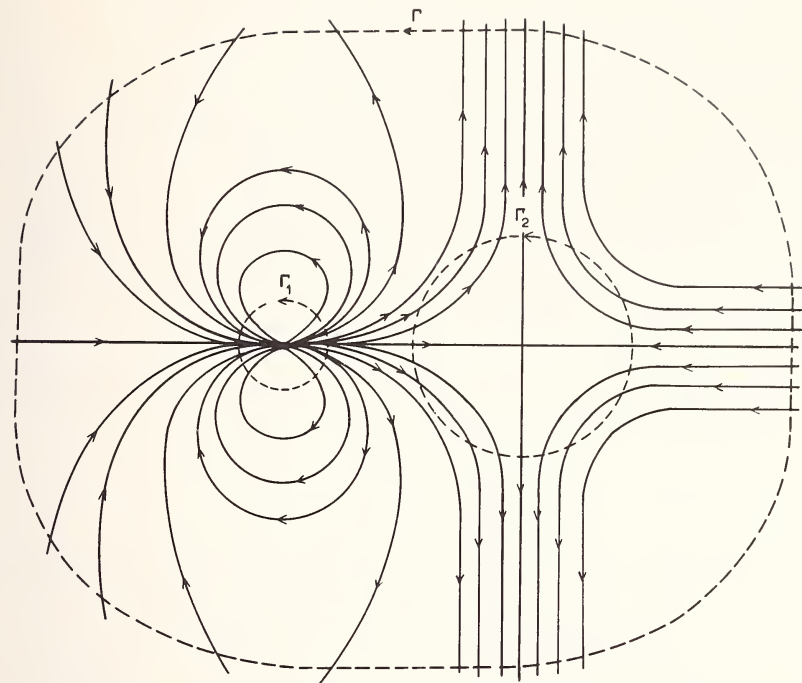
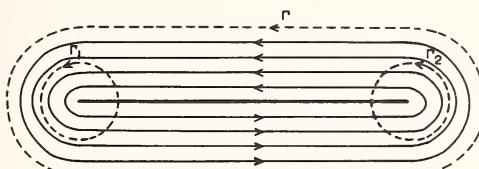
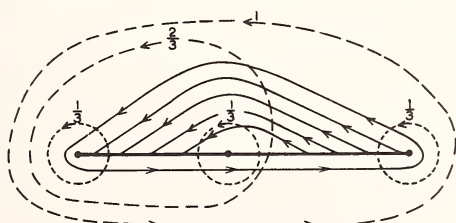


FIGURE 6. The circuit Γ_1 encloses a disclination $+2$, the circuit Γ_2 a disclination -1 , and the outer circuit Γ a disclination $+1$.



(a)



(b)

FIGURE 7(a). The addition theorem $+1/2 + 1/2 = +1$. (b) The addition theorem $+1/3 + 1/3 + 1/3 = +1$. In both figures it is necessary to neglect the discontinuity across the heavy line, which is a line of constant misorientation.

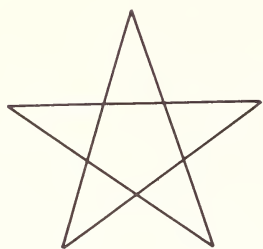


FIGURE 8. A star pentagon.

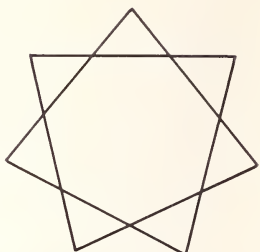


FIGURE 9. A star heptagon.

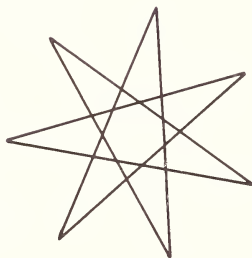


FIGURE 10. A double star heptagon.

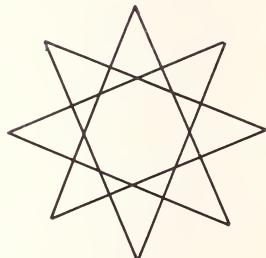


FIGURE 11. A double star octagon.

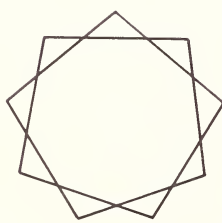


FIGURE 12. A star nonagon.

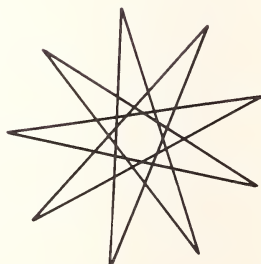
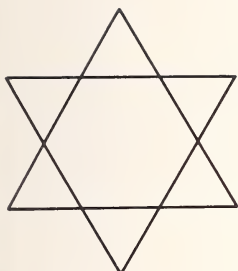
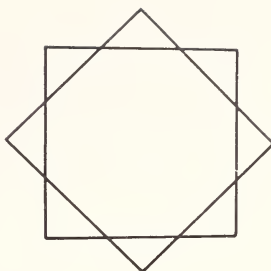


FIGURE 13. A triple star nonagon.



(a)



(b)

FIGURE 14(a). A representation of a triangle described twice. (b) A representation of a square described twice.

TABLE I

n	p	figure
3	0	triangle
4	0	square
5	0	pentagon
5	1	star pentagon (fig. 8)
6	0	hexagon
6	1	triangle described twice
7	0	heptagon
7	1	star heptagon (fig. 9)
7	2	double star heptagon (fig. 10)
8	0	octagon
8	1	square described twice
8	2	double star octagon (fig. 11)
9	0	nonagon
9	1	star nonagon (fig. 12)
9	2	triangle described thrice
9	3	triple star nonagon (fig. 13)
...
10	3	star pentagon described twice.

interior angle is therefore $2\pi[1/2 - 1/n]$. Now suppose that the n -gon is a circuit surrounding a disclination of strength p . Then the tangent turns through an additional angle $2p\pi$. If the resulting figure is still a closed n -gon, p must be an integer. The interior angle at each corner is now $2\pi[1/2 - (p+1)/n]$. A new figure is produced for each value of p for which this expression remains positive. (See figures 8-14b.) The possible values of p for small n are indicated in table 1.

When $p+1$ and n have a common factor q , the figure degenerates into a simpler figure described q times. While (6, 1) and (8, 1) may be symbolically represented as in figure 14 (a) and (b), these representations (contrary to the statement of Lyusternik [2]) are not regular polygons in our sense.

III. Polyhedra on the Topological Sphere

The idea of disclinations, together with the addition theorem for the strength of disclinations, gives added precision to the fixed-point theorem for vector fields on the surface of a sphere, and relates this theorem to Euler's theorem that if a polyhedron on a topological sphere has f faces, e edges, and c corners, then the Euler characteristic $C \equiv f - e + c = 2$. The method can be extended to surfaces with other Euler characteristics.

We can show that if a sphere is covered by a vector field which is continuous everywhere except for a finite number of isolated points, then the sum of the strengths of the disclinations at these points is +2. We describe a small circuit Γ in a regular part of the pattern. The sum of the disclinations within this circuit is $(1/2\pi)\int d\theta + 1 = -1 + 1 = 0$. We now regard the same curve as a circuit enclosing the remainder of the surface of the sphere. The positive sense of describing the circuit is now reversed, and we now find $(1/2\pi)\int d\theta = +1$. The sum of all the disclinations on the sphere is thus $+1 + 1 = 2$.

Now consider a polygon lying on the sphere. Introduce a vector field in the following way. On each face, and just inside the boundary, draw a field line which describes the boundary anticlockwise as viewed from outside the sphere. Continue this pattern inside the face as shown in figure 15. Then in the middle of each face there is a disclination of strength +1, giving a total strength of $+f$.

There are also disclinations at the corners. We remember the convention that sudden changes of direction on crossing a boundary are neglected. At a corner where s edges meet, the strength of the disclination is $1 - (1/2)s$. The sum of all disclinations at corners is $\sum_c [1 - (1/2)s] = c - 1/2 \sum_c s$. Now each edge joins 2 corners, so that $1/2 \sum_c s = e$. There are no other

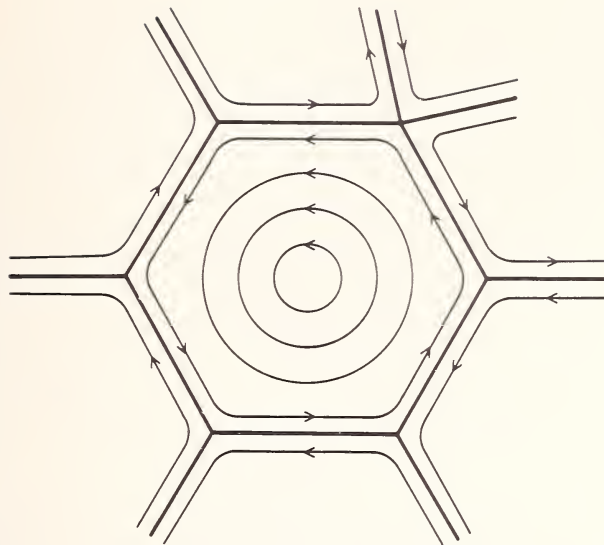


FIGURE 15. The vector field associated with a polyhedron.

disclinations, so the sum of the strengths of all disclinations is $D=f+c-e$. Since the polyhedron lies on a sphere, this sum is $D=2$, and so $C=:f-e+c=2$.

IV. Holes, Loops, and Channels

By a hole in a surface we mean a region of the surface which has been removed, leaving a boundary which is not connected to any other part of the surface. We may take the shaded region in figure 16 to be such a hole, and we see that the introduction of a hole requires the introduction of a disclination of strength -1 . Thus, for a polyhedron having h holes in its faces, the total strength of all disclinations is $D=f-e+c-h$.

Similarly, figure 17 shows the vector field in the neighbourhood of two boundaries. These boundaries may be connected by a loop outside the surface or by a channel inside the surface, and the vector lies on the surface of the loop or channel without discontinuities. The disclination associated with a loop or channel is of strength -2 . Thus, if in addition to h holes there are l loops or channels, the total number of disclinations is $D=f-e+c-h+2l=2+h-2l$. For example, a torus has $h=0$ and $l=1$, so that $D=0$, in agreement with the fact that one can cover a torus with a vector field which is free from singularities.

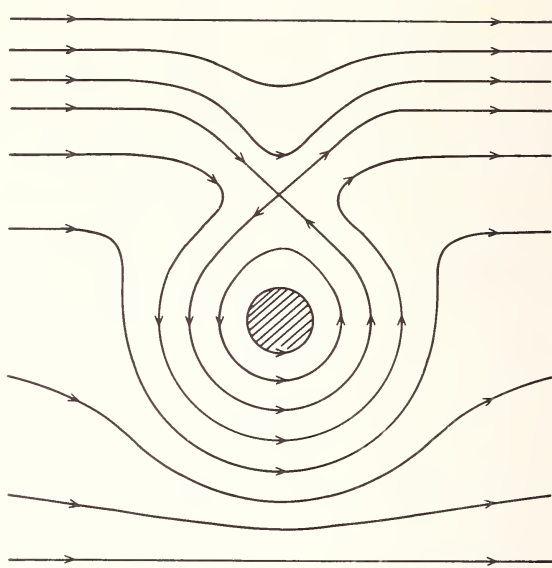


FIGURE 16. A disclination dipole $(+1) + (-1)$ does not disturb the vector field at distant points. The shaded area may be removed to leave a hole in the surface.

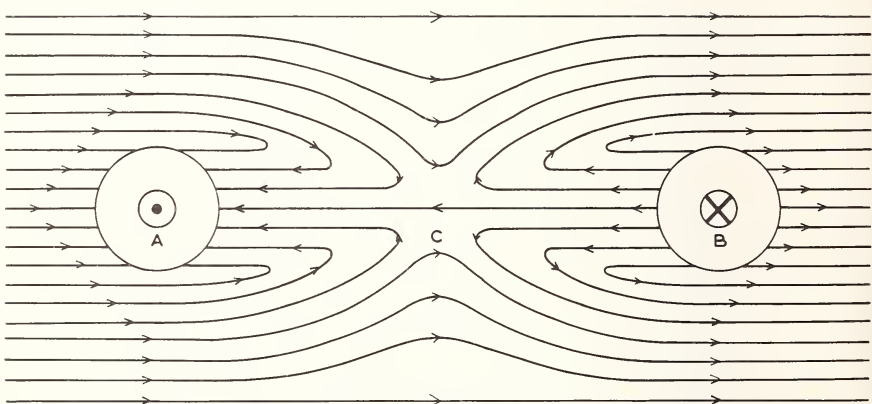


FIGURE 17. The vector field near a smoothly fitting handle on a surface has a disclination -2 .

V. One-Sided Surfaces¹

As a typical one-sided surface we consider the model of the projective plane which is made by placing a cross cap on a hemisphere (fig. 18). Its characteristic $C = f - e + c$ is well known (e.g., Lietzmann [3]) to be $C = 1$.

¹ Note added in proof: The arrangement of Section V is faulty. The contribution of a cross cap both to the Euler characteristic and to the total disclination strength is -2 .

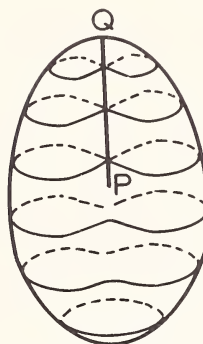


FIGURE 18. The projective plane represented by a sphere fitted with a cross cap.

We now prove and generalize this result by the use of disclinations.

The model of a cross cap in figure 18 involves an unpleasant singularity at P . A more easily analyzed model is formed by half of a heptahedron (fig. 19 (a) and (b)). On a regular portion $ABCD$ of the outer surface of a two-sided figure are placed two faces R_1QR_2 and R_3QR_4 of a pyramid, the vertex Q of the pyramid lying outside the surface. If P is the centre of the square $R_1R_2R_3R_4$, the triangles R_1PR_2 and R_3PR_4 are removed from the surface, thus exposing its inside. The intersecting triangles R_1QR_3 and R_2QR_4 complete the cap.

Suppose the vector field in the neighbourhood of $ABCD$ was regular. There is no loss of generality in assuming that on the outside of the original surface it ran parallel to R_1R_2 and to R_4R_3 . Then it is clear from figure 19 that the vector field is continuous everywhere (except perhaps at the singular points R_i , P , and Q), if the pattern on the "outer" surface, viewed along QP , is unchanged when the cross cap is added, while the pattern on the "inner" surface runs everywhere in the opposite direction to that on the "outer" surface. On the side of the triangle R_1QR_3 nearer to R_1 the vectors are parallel to PQ , and on the side nearer to R_2 the vectors are parallel to QP . The vector field is continuous where the triangle R_1QR_3 is intersected by the triangle R_2QR_4 .

Although the vector field is continuous, it is not free from disclinations, because the surface on which it lies is singular. It is easily seen that circuits round the points R_i or their "images" R'_i do not contain disclinations. It may also be seen that the circuit round Q sketched in figure 19, which runs "outside" the tetrahedron R_1R_2PQ and "inside" the tetrahedron R_3R_4PQ , does not contain a disclination. Its "image" circuit "inside" R_1R_2PQ and "outside" R_3R_4PQ is also of strength zero. However, the circuit around P which is illustrated, and which runs "out-

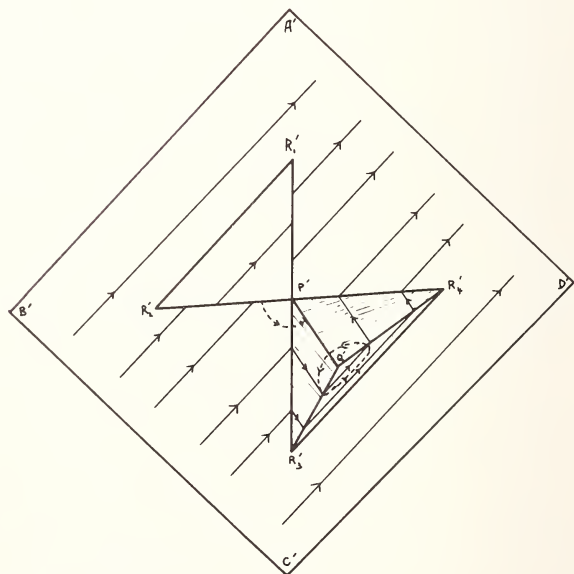
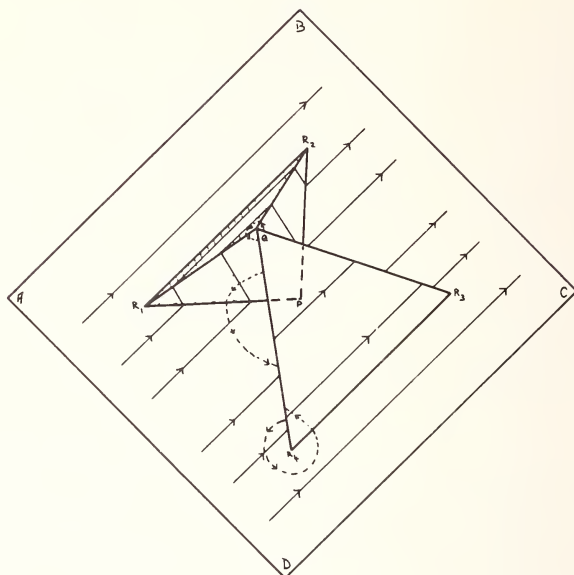


FIGURE 19(a). A cross cap in the form of half of a heptahedron is fitted to a plane surface. A uniform vector field runs across the surface. (b) The same configuration viewed from inside the original surface.

side" the triangle R_1PQ , "outside" the original surface from R_1P to R_4P , "outside" the triangle R_4PQ , "inside" the triangle $R'_2P'Q'$, "inside" the original surface from R'_2P' to R'_3P' , "inside" the triangle $R'_3P'Q'$, and so back to the "outside" of the triangle R_1PQ , contains a disclination of strength -1 . Its "image" circuit also contains a disclination of strength -1 .

The cross cap, treated as an isolated entity, thus contributes -2 to the disclination strength, or to the Euler characteristic. But the cross cap is itself a polyhedron, and Euler's formula and its generalizations do not apply to surfaces containing isolated polyhedra. The isolated polyhedron must be linked to the main polyhedron by an edge joining one of its corners to a corner of the main polyhedron. This edge, which joins two existing corners and delimits no new faces, contributes -1 to the Euler characteristic.² The contribution of a cross cap to the Euler characteristic is thus $-2 - 1 = -3$.

Now suppose we have a two-sided surface with characteristic $2 + h - 2l$, and we attach to it x cross caps. The first cross cap exposes the inside of the surface, and so doubles the characteristic. If $H(z)$ is defined to be zero when z is negative and unity when z is positive, the contribution to the characteristic of all regions remote from the cross caps is $[1 + H(x - 1/2)](2 + h - 2l)$. In addition, the neighbourhood of each cross cap contributes -3 , so that the final formula for the characteristic is

$$C = [1 + H(x - 1/2)](2 + h - 2l) - 3x.$$

For example, the projective plane is a sphere with $h = l = 0$, fitted with one cross cap. It has $C = [1 + H(1/2)] \cdot 2 - 3 = 4 - 3 = 1$. For a sphere with two cross caps, $C = [1 + H(3/2)] \cdot 2 - 6 = -2$. For a torus with a cross cap, $C = [1 + H(1/2)] \cdot 0 - 3 = -3$.

² Consider, for example, a polyhedron on a sphere, for which $C \equiv f - e + c = 2$. Inscribe an isolated triangle on a face of the polyhedron. This triangle contributes $\delta f = +1$, $\delta e = +3$, and $\delta c = +3$. Thus $\delta C = +1$, and the Euler rule is not valid. If we join a corner of the triangle to a corner of the original polyhedron, we add $\delta'f = 0$, $\delta'e = +1$ and $\delta'c = 0$, giving $\delta'C = -1$, and restoring the validity of the Euler rule. A smoothly fitting handle is not a polyhedron, for it has $f = e = c = 0$. It is not necessary to join its neighbourhood to the main polyhedron. If we choose to join a point on it to a corner of the main polyhedron, we have $\delta f = 0$, $\delta e = +1$, $\delta c = +1$, and $\delta C = 0$, so that Euler's rule remains valid. Alternatively, if the handle is a polyhedral arch placed on a face of the original polyhedron, it has $C = 0$. It is then necessary to link one corner of each foot of the arch to a corner of the original polyhedron, contributing $\delta C = -\delta e = -2$.

VI. Acknowledgements

I am grateful to Professor H. Rund for a helpful discussion, to Mrs. O. L. Prior, Mrs. K. Peach and Mr. S. Angellini for model building and drawings, and to the South African Council for Scientific and Industrial Research for financial support.

VII. References

- [1] Nabarro, F. R. N., Theory of Crystal Dislocations (Clarendon Press, Oxford, 1967).
- [2] Lyusternik, L. A., Convex Figures and Polyhedra (Dover, New York, 1963).
- [3] Lietzmann, W., Visual Topology (Chatto and Windus, London, 1965).

APPLICATION OF DISLOCATION THEORY TO LIQUID CRYSTALS

J. Friedel and M. Kléman

Laboratoire de Physique des Solides

Faculté des Sciences

91 Orsay, France

After an introduction which recalls some of the properties of liquid crystals, a general theory of dislocations in a mesomorphic medium is outlined. On the basis of their symmetry properties, and of viscosity relaxation, it is first shown that perfect disclinations in nematic crystals may take any shape, are restricted to straight lines in smectic crystals, and that both types exist in cholesteric crystals, where there are two possible axes of rotation. The second part is specialized to the case of cholesteric crystals for which a mechanism of pairing of dislocations is proposed which allows a multiple disclination to take any shape, at the expense of a small increase of energy in the faulted ribbon.

Key words: Cholesteric crystals; faulted ribbon; liquid crystals; nematic crystals; smectic crystals.

I. Introduction

The so-called "liquid crystals" form an independent thermodynamic state of matter, discovered at the end of the 19th century by Reinitzer, an Austrian botanist, who at that time synthesized cholesteryl benzoate. This substance melts at 145 °C to a liquid of turbid appearance, which turns to an ordinary transparent liquid after further heating, at 179 °C. Lehmann [1] determined that the turbid phase is strongly optically anisotropic. Later, Lehmann discovered other liquid substances, such as p. azoxyanisole, p. azoxyphenetole, etc . . . , which were shown to display, like cholesteryl benzoate, very strong optical anisotropies. For a detailed review of chemical and physical properties of liquid crystals, the reader is referred to G. W. Gray's book [2], and Chistyakov's and Chatelain's papers [3, 4]. We shall here first briefly recall some of these properties and then proceed to our main topic, i.e., the description of the topological singularities, observed by the optical microscope, in natural or polarized light, which constitute, for the present-day physicist, a very fascinating example of application of the notions of translation and rotation dislocations.

Fundamental Aspects of Dislocation Theory, J. A. Simmons, R. de Wit, and R. Bullough, Eds. (Nat. Bur. Stand. (U.S.), Spec. Publ. 317, I 1970).

II. General Properties of Liquid Crystals

II.1. Physical and crystallographic properties

Chemically, liquid crystals are made of rod-like organic molecules, which display long-range order. A typical length of the molecule is 20 Å for p. azoxyanisole. Aqueous solutions of some soaps, of some viruses, of synthetic polypeptides, with much longer molecules, give formations resembling ordinary liquid crystals and can be included in the description of their topological properties.

G. Friedel [5], on the basis of a study of their optical properties and of their structure singularities, gave a classification of the liquid crystals, which he called "mesomorphic states", as follows (fig. 1):

(i) — The nematic state. The molecules are oriented in the same direction, their centers of gravity being at random. It is assumed, as for the other mesomorphic states, that the molecule oriented \mathbf{n} is equivalent to the molecule $-\mathbf{n}$.

The crystal symmetry elements are

- any translation
- any rotation about the direction of the molecules
- a rotation of π about any axis perpendicular to the molecules.

(ii) — The cholesteric state. The molecules spiral with a pitch $p = \frac{2\pi}{q_0}$

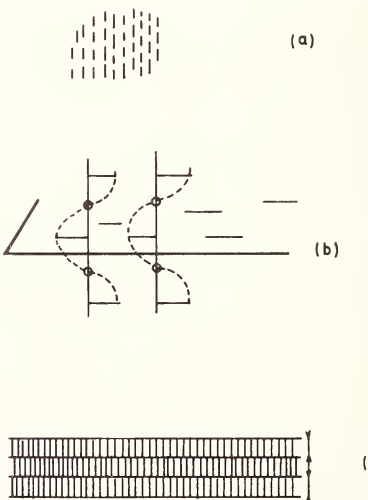


FIGURE 1. Mesomorphic phases—schematic arrangement of the molecules: (a) nematic, (b) cholesteric, (c) smectic.

about a constant direction, the so-called cholesteric axis. In any plane perpendicular to this axis (the cholesteric plane), the molecules are parallel, as in the nematic state. A cholesteric medium is either left-handed or right-handed.

The crystal symmetry elements are

- any translation in the cholesteric plane
- any rotation-translation along the cholesteric axis (a rotation $2\pi\alpha$ and a translation $-2\pi\alpha/q_0$ for a left-hand cholesteric, defined by $\theta = -q_0 z$).
- a rotation $\Omega = \pi$ perpendicular to the cholesteric axis, about a molecule or perpendicular to a molecule.
- a rotation $\Omega = \pi$ about the cholesteric axis.
- a translation π/q_0 along the cholesteric axis.

(iii) — The smectic state. The molecules are assembled in plane layers of equal thicknesses d , perpendicularly to the layers. The crystal symmetry elements are:

- any translation in the plane of the layers
- any rotation about an axis perpendicular to the layers
- a translation of magnitude d along the molecules
- a rotation π about any axis perpendicular to the molecules and located in the plane between two layers or midway between two planes.

A glass plate, rubbed along a preferred direction, and in contact with a liquid crystal, aligns the molecules along this direction (Chatelain [6]). This is the ordinary way of crystallising a nematic droplet, between two glass plates rubbed along parallel directions. Cholesteric crystals are prepared in the same way. Use is also made of rubbed wedges or a fresh clivage wedges of mica. On the other hand, carefully cleaned glass plates give the so-called homeotropic phases, where the molecules have the least possible contact with the plate, and stand perpendicular to it.

The cholesteric and the nematic states are, according to G. Friedel [5], the same thermodynamic state. A liquid crystal may undergo a transition from the smectic to the nematic or the cholesteric state, but never undergoes a nematic \rightleftharpoons cholesteric transition under a change of temperature. The smectic state always appear at a lower temperature than the nematic state. This result agrees with the fact there is more "solid-type" crystallinity in the smectic phase, which is generally more viscous than the other phases.

Liquid crystals are anisotropic in their magnetic properties. The nematic phase p. azoxyanisole is diamagnetic and the molecules orient themselves parallel to the field. This is a way of crystallising the phase. A diamagnetic cholesteric crystal turns to a nematic crystal under a field applied perpendicularly to the cholesteric axis. This transition has

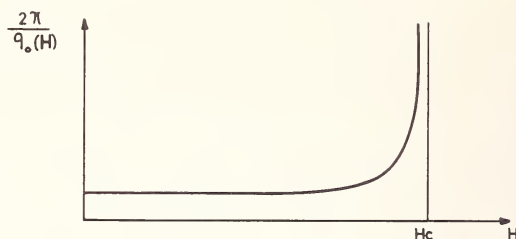


FIGURE 2. Variation of the pitch with a magnetic field perpendicular to the spiral axis.

been predicted by de Gennes [7] (fig. 2) and experimentally verified by G. Durand and co-workers [8].

Nematic and smectic crystals are uniaxial positive, the axis being along the molecule. The birefringence is generally high and varies with temperature. They show also very marked dichroism. These optical properties have been thoroughly studied by Mauguin [9], who related the observations to the structural defects in the nematic crystals. Moreover, nematic crystals scatter and depolarize light very strongly. This phenomenon, first attributed to the existence of "swarms" of molecules all identically oriented, taking part in the brownian movement of the liquid, with a size of typically 10^{-5} cm [10], has recently been explained by de Gennes [11] on the basis of long wavelength elastic fluctuations of the orientation.

Cholesteric crystals are apparently uniaxial negative, the axis being along the cholesteric axis, but are uniaxial positive along the spiraling molecules. They show a strong rotatory power, which may reach values as high as $60,000^\circ/\text{mm}$ in some substances. The rotatory power changes sign for a certain wavelength λ_0 depending on temperature [12], for which there is an intense scattering of the right-hand circularly polarized component of the incident light for a right-hand cholesteric, the left-hand component being transmitted without attenuation. For $\lambda < \lambda_0$, the rotatory power is to the left. The converse results are true for a left-hand cholesteric.

II.2. The Oseen-Zocher-Frank elasticity equations

Most of the preceding results, like the action of a magnetic field or the scattering of light, and also the molecules distributions around singularities and their energies, may be described quantitatively in the frame of the macroscopic elasticity equations derived first by Oseen [13] and Zocher [14], and later established on a firmer basis by Frank [15].

Let \mathbf{n} be a unit vector representing the direction of the molecule at the point \mathbf{r} . \mathbf{n} and $-\mathbf{n}$ are equivalent. The most general distortion of the molecular assembly is represented locally by the six local components of

curvature. Consider a local axis z along the molecule and the small variation of \mathbf{n} with respect to that direction in the neighborhood of \mathbf{r} . We distinguish three basic modes of distortion, as follows

$$\text{splay} \quad s_1 = \frac{\partial n_x}{\partial x} \quad s_2 = \frac{\partial n_y}{\partial y}$$

$$\text{twist} \quad t_1 = -\frac{\partial n_y}{\partial x} \quad t_2 = \frac{\partial n_x}{\partial y}$$

$$\text{bend} \quad b_1 = \frac{\partial n_x}{\partial z} \quad b_2 = \frac{\partial n_y}{\partial z}$$

On figure 3 we have represented such distortions assuming s_1 , t_1 , and $b_1 \neq 0$.

By expanding the free energy to second-order terms in curvature, and

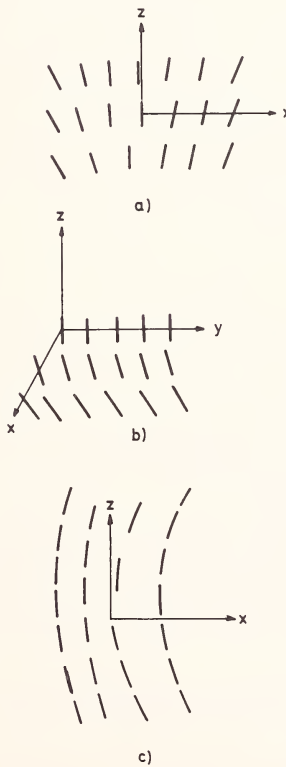


FIGURE 3. The three types of distortion in the neighborhood of a molecule \mathbf{n} : (a) splay, (b) twist, (c) bend.

using straightforward symmetry considerations, the free energy density appears to be of the form

$$F_0 = 1/2 \{ K_{11} (\operatorname{div} \mathbf{n})^2 + K_{22} (\mathbf{n} \cdot \operatorname{rot} \mathbf{n} - q_0)^2 + K_{33} (\mathbf{n} \wedge \operatorname{rot} \mathbf{n})^2 \} \quad (1)$$

where K_{11} , K_{22} , and K_{33} correspond respectively to splay, bend, and twist. q_0 , the inverse of the pitch ($p = 2\pi/q_0$), is zero for nematic and smectic crystals. Frank adds to (1) a term in K_{24} which was shown by de Gennes [11] to introduce a volume term of the same form as K_{11} .

If we take into account the influence of a magnetic field \mathbf{H} , we must add a term

$$F_{\text{mag}} = -1/2 \chi_a (\mathbf{n} \cdot \mathbf{H})^2 \quad (2)$$

where χ_a is the difference $\chi_{||} - \chi_{\perp}$ between the susceptibilities for \mathbf{H} parallel to \mathbf{n} and normal to \mathbf{n} .

The reader is referred to de Gennes' papers [7, 11, 16] for the applications of these equations to the influence of a magnetic field and the scattering and depolarization of light.

Frank has pointed the relationship between splay and polarization: a polar medium should be splayed in its ground state but liquid crystals are not polar. More recently Meyer [17] has shown that there is a coupling between the induced polarization and the splay through the shape of the molecules, which should explain some of the properties of liquid crystals under applied electric fields.

III. Topological Properties of Perfect Dislocations

III. 1. General dislocation

A general dislocation in a liquid crystal is defined, as in a solid crystal, by the position of the line \mathbf{L} and the total displacement imposed to the cut surface \mathbf{S} bounded by the line \mathbf{L} .

Let \mathbf{r} be the position of a point on \mathbf{S} with respect to the axis of rotation ν , the relative displacement \mathbf{d} of the lip \mathbf{S}_1 on the cut surface with respect to the lip \mathbf{S}_2 contains two terms, one of pure translation (that of the ordinary translation dislocation), the other of pure rotation, and may be written

$$\mathbf{d} = \mathbf{b} + 2 \sin \frac{\Omega}{2} \cdot (\boldsymbol{\nu} \wedge \mathbf{r}). \quad (3)$$

\mathbf{b} is a translation symmetry element of the lattice, and $(\Omega, \boldsymbol{\nu})$ a rotation symmetry element. The displaced part \mathbf{d} is either removed or filled in with extra matter of perfect crystal, and the medium allowed to relax.

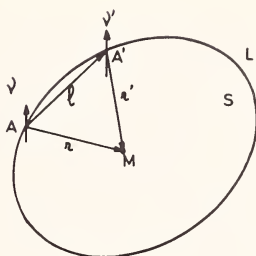


FIGURE 4. Variation of the position of the axis of rotation along a disclination line.

We shall restrict the use of the word disclination to the case where the displacement \mathbf{d} contains a rotation.

In a liquid crystal, for some kinds of the allowed dislocations, the relaxation of the preceding process of cut and removal (or introduction) of matter is not only elastic, but can be *viscous*. This process of relaxation leads to a uniform density of molecules and tends to suppress any dislocation with displacement \mathbf{d} which can be varied continuously to zero, without breaking the symmetry properties of the medium. This viscous relaxation may be considered as the dispersion of an initial dislocation (\mathbf{b}, Ω) in a continuous distribution of dislocations $(d\mathbf{b}, d\Omega)$. So that non-quantized symmetry elements do not lead to stable dislocations in a medium at rest. For example: translation dislocations in a nematic phase.

This property can lead to an indeterminacy in the position of a disclination line with respect to the axis of rotation. In a *solid* crystal, it is quite clear that the axis of rotation \mathbf{v} and the line \mathbf{L} must be confounded, otherwise the core of the disclination would suffer a large displacement, i.e., would have a large energy: disclinations in consequence must be straight. Consider on the other hand a disclination line \mathbf{L} in a *liquid* crystal, two points \mathbf{A} and \mathbf{A}' (fig. 4) on that line, and assume that the displacement of the cut surface may be described with the axis of rotation either in \mathbf{A} or in \mathbf{A}' . These two descriptions of the disclination are equivalent if the difference δ between the displacements \mathbf{d} and \mathbf{d}' can be relaxed by a viscous process, i.e., if

$$\delta = 2 \sin \frac{\Omega}{2} (\mathbf{v} \wedge \mathbf{AA}')$$

is a non-quantized translation of the medium. Applications of this property will be found in the following paragraphs.

III. 2. Perfect disclinations in a nematic crystal

The only quantized symmetry element in a nematic crystal is the two-fold symmetry axes perpendicular to the molecules.

(1) *Screw disclinations.* Following the nomenclature adopted by Nabarro [18], screw disclinations have their axis (Ω , ν) along the line. Owing to the energy considerations stated above, this should be the common case for most of the disclinations in different media, although it is not the only possible case for a nematic phase.

For a medium with an n -fold axis, the possible screw disclinations correspond to rotations of the form $\Omega = 2\pi s/n$ (s and n integers). $S = s/n$ will be referred as the strength of the screw disclination. In a nematic phase $n=2$. Figure 5 shows the cases $S = \pm 1/2, \pm 1, 3/2, 2$, following Frank [15]. It is to be noted that the minus signs correspond to a Volterra process in which matter is added, and conversely, the plus signs correspond to the removal of matter. The same sign convention agrees with Harris theorem [19], stating that for screw disclinations perpendicular to a given surface, the algebraic sum of the strengths is equal to the Euler's characteristic of the surface.

The nematic state is named from the apparent threads seen within the fluid under the microscope. Typical screw disclinations were first reported by Lehmann [1], then by G. Friedel and Grandjean [20], and later by Mauguin [9], who explained their nature from their observation in polarized light. Plate I is from G. Friedel's report [5]: disclinations in azoxyphenetol are seen end on, between crossed polars; disclinations of strength unity have four branches, and disclinations of strength $1/2$ have two branches.

The actual configurations around screw disclinations were first calcu-

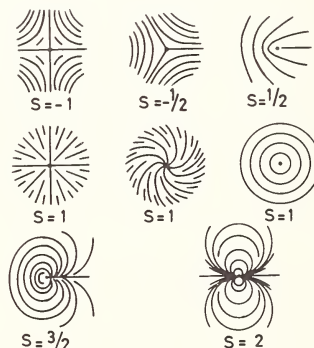


FIGURE 5. Simple screw disclinations in a nematic crystal (after Frank).

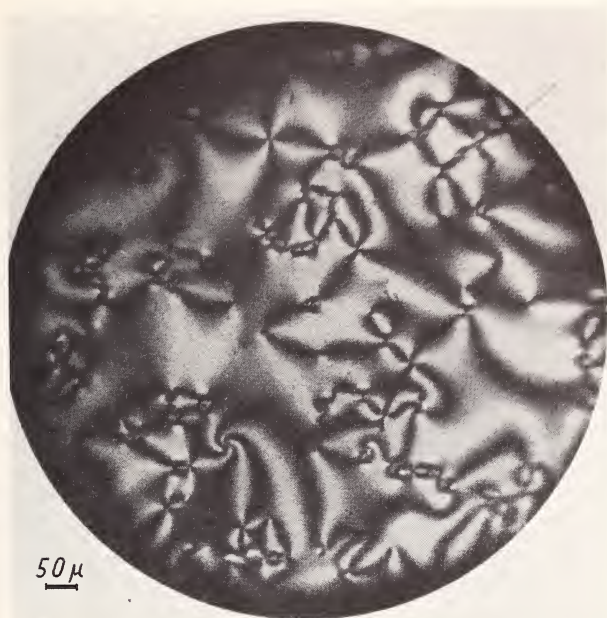


PLATE I. Nematic phase of azoxyphenetol; disclinations of strength 1 (four branches) and 1/2 (two branches) are seen end on, between crossed polars. (After G. Friedel.)

lated by Oseen [13], assuming $K_{11} = K_{22} = K_{33}$. The Oseen-Zocher-Frank equations thus reduce to

$$\nabla^2 \phi = 0, \quad (4)$$

ϕ being the azimuthal angle of \mathbf{r} in a plane perpendicular to the line, and \mathbf{n} being restricted to that plane. The most general solution of (4) is

$$\phi = S\psi + \phi_0. \quad (5)$$

ψ being the azimuthal angle of \mathbf{r} . It is worth noticing (cf. fig. 5) that the constant ϕ_0 is not a meaningless parameter: it may be defined as the azimuthal angle of the cut surface. If the cut surface rotates along the line, ϕ_0 may depend on the coordinate z on the line. For a disclination of strength $S = \pm 1/2$, the configuration of the molecules rotates as a whole with the cut surface, but for, say, $S = 1$ (cf. fig. 5), the configuration depends on ϕ_0 , and changes therefore along the line if the cut surface rotates.

(2). *Edge disclination.* In a nematic phase, owing to the viscous relaxation of translation dislocations, any line shape is allowed, and the axis of rotation subsequently may be located anywhere. In particular the

Volterra process may consist in rotating *each molecule* about a rotation axis passing through its center of gravity.

Consider a line perpendicular to the axis of rotation (a straight-edge disclination, or a "prismatic" loop), and **S** the cut surface. The introduction of the disclination consists in the creation of a spiral structure in a cylinder parallel to the axis of rotation and bounded by the line **L** (fig. 6). For $\Omega = \pm\pi$, this spiral goes through half a pitch between the ends of the cylinder, which are at infinity or on the boundaries of the medium. The sign plus or minus corresponds to a left or a right hand spiral. It is noticeable that the distorted cylinder depends on the position of the cut surface (compare the situations in which the cut surface is inside or outside **L**), and that the distortion extends to a long distance. In actual cases, where inhomogeneities in the rubbing conditions exist, this type of disclination may be formed in order to compensate for a twist on the molecules at the surface of the glass plates.

(3). *General disclinations.* General disclinations are a combination of the two former types. Their existence was first appreciated by Friedel and de Gennes [21], who showed that, assuming an isotropic nematic crystal ($K_{11} = K_{22} = K_{33} = K$), and **n** parallel to a constant plane, the actual configuration is given by

$$\phi(\mathbf{r}) = \frac{\Omega_s(\bar{r})}{4} + \dots \quad (6)$$

where Ω_s is the solid angle under which the line is seen from **r**.

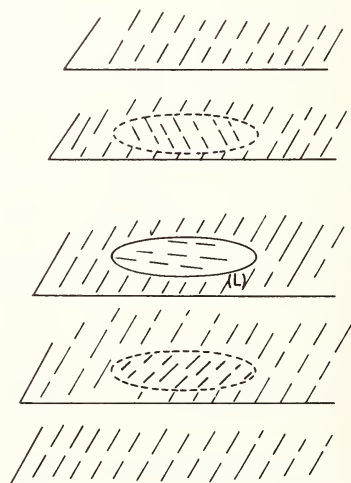


FIGURE 6. Edge disclination in a nematic crystal.

III.3. Perfect Disclinations in a Smectic Crystal

The quantized symmetry elements lead to the possible dislocations, as follows:

- translation dislocations with \mathbf{b} Burger's vector equal to the lattice parameter and parallel to the molecules.
- disclinations $\Omega = n\pi$ (n integer) about twofold axes ν perpendicular to the molecules and passing either through the extremities of the molecules or through the middle.

The translation dislocation does not need a long commentary here: as any translation dislocation in a crystal, it involves only one (or possibly two) \mathbf{b} vectors, and may take any shape. The disclinations $\Omega = n\pi$ are necessarily rectilinear; because of the viscosity of the smectic phase, which relaxes any translation in the smectic plane, the disclination has to be located in the plane of the molecular axis and the rotation axis; but in that plane the disclination must be passing through the extremely of the middle of a molecule, i.e., must be straight.

Figure 7 describes the creation of such a disclination $\Omega_a = \pi$, following the general definition of a dislocation and assuming ν between two molecu-

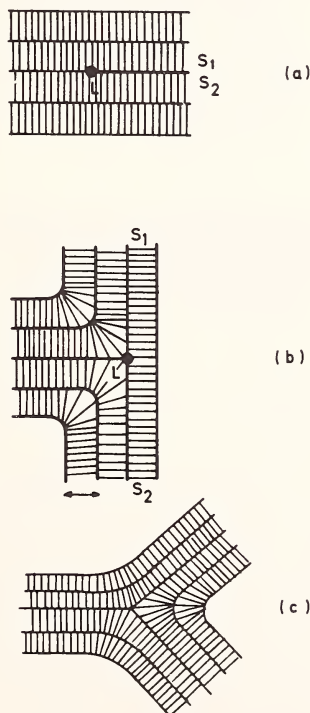
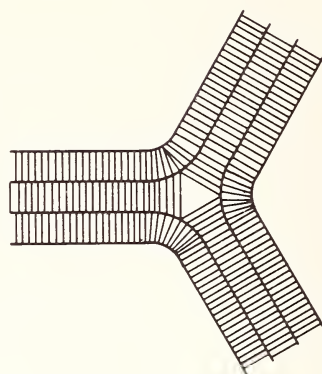
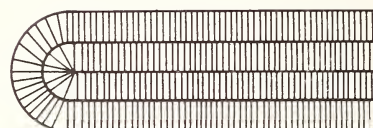


FIGURE 7. Creation of a $\Omega_a = \pi$ in a smectic crystal.

FIGURE 8. $\Omega_b = \pi$ in a smectic crystal.

(a)



(b)

FIGURE 9. $\Omega_a = -\pi$ and $\Omega_b = -\pi$ (smectic crystal).

lar layers. The line is perpendicular to the plane of the figure. Figure 8 shows the analogous situation for the second type $\Omega_b = \pi$, and figure 9 the corresponding $\Omega_{a,b} = -\pi$ disclinations. The disclinations $\Omega_a(+\pi)$ and $\Omega_b(+\pi)$ are not equivalent. The cores energies are certainly different. But the long-range configurations are also different. This may be seen in the following way. Draw a circuit $A B C D E F G A$ which encloses the core of Ω_a (fig. 10). Due to the importance of the actual cut surface in the final result, an origin A on the circuit has to be chosen. Consider an equivalent circuit around the core of Ω_b , starting from a point equivalent to A . The circuit around Ω_b does not close, the closure failure being

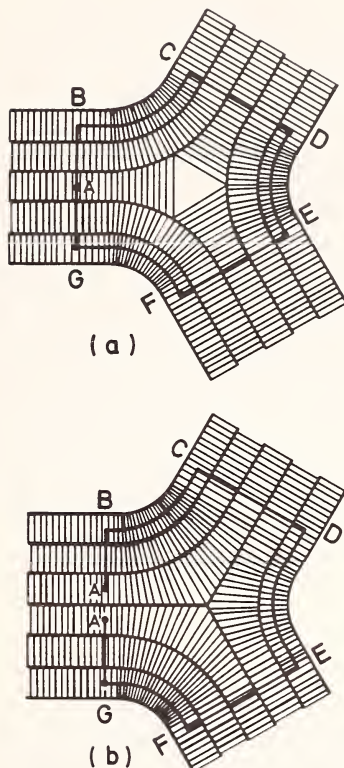


FIGURE 10. Equivalent Burger's circuits for an $\Omega_b(\pi)$ compared to an $\Omega_a(\pi)$ in a smectic crystal.

equal to a unit translation along the molecules. A similar situation exists for the cholesteric phase and will be discussed in more details.

It has been pointed by Frank [22] that the Burger's circuit used above is not of the usual type. It is a way of comparing the topologies of different disclinations at infinity, which could be done also by enumerating the layers and trying to fit the different enumerations.

It is likely that the elastic energy of the disclinations in smectic crystals is very large, and they do not seem to have been observed. The singularities in smectic crystals are cofocal domains, which we shall now briefly describe.

III.4. Cofocal domains

The geometry of cofocal domains has been studied in great detail by G. Friedel [5]. A cofocal domain (fig. 11) consists of two cofocal conics,

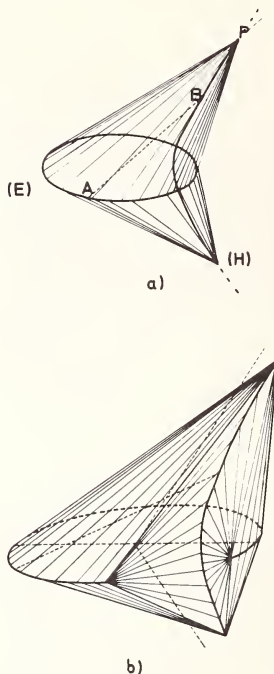


FIGURE 11. Scheme of a cofocal domain in smectic crystals (after G. Friedel).

an ellipse and a branch of hyperbola. The molecules are along the lines drawn between a point A on the ellipse (E) and a point B on the hyperbola (H). All the lines starting from A and describing (H) form a cone of revolution and similarly for the lines starting from any point on (H) and describing (E). The smectic layers are perpendicular to these lines and form a family of Dupin cyclides. The cofocal domains are limited by the cones tapering to the limiting points on (E) and (H) (fig. 11.b) and are tangent to the adjacent cofocal domains along these cones. A correlated interesting point is that the layers surfaces are then limited to hyperbolic parts of the Dupin cyclides. This configuration leads to beautiful arrangements, described by Friedel [5] as feathers, fan-tailed fields, etc. . . . Plate II shows a typically terraced smectic droplet, in which the layers are plane, and bounded by families of tiny cofocal domains. Plate III shows a droplet in which large cofocal domains are present.

The occurrence of cofocal domains may be easily understood on the basis of a layered structure, if not easily described in terms of singularity lines. The layers can easily glide upon each other, but less easily deform along the smectic axis. This has to be understood as a competition between viscous relaxation along the layers and elastic relaxation throughout the layers. Any distorted structure should then preserve layers of equal thick-



PLATE II. Terraced smectic droplet (after G. Friedel) of ethyl azoxybenzoate.



PLATE III. Cofocal domains in ethyl azoxybenzoate. Most of the ellipses are in the plane of the glass plate. Crossed polars.

ness, which means that the layers surfaces have common normals and the same centers of curvature along the same normal. These centers of curvature describe the so-called focal surfaces, which are singularities of the structure on which the smectic phase must stop (cf. a similar discussion in Nye [23]). But, the smectic phase being a liquid with no empty space, the surface singularities must be reduced to line singularities. This means that the radii of curvature of the smectic layers are constant along curvature lines, i.e. that curvature lines are circles. Therefore the smectic layers are Dupin cyclides, and the line singularities cofocal conics.

Sackmann and Demus [24] claim to have observed other types of structural defects in smectic crystals, which they relate to different smectic modifications of the same crystal, but no more is known at the present time on these structural defects.

III.5. Perfect disclinations in a cholesteric crystal

Perfect dislocations in a cholesteric crystal correspond to the two kinds of quantized rotations, along the cholesteric axis and in the cholesteric plane, and to the translation π/q_0 along the cholesteric axis. It will be shown that the translation dislocation and the disclination with ν along the cholesteric axis are equivalent descriptions of the same singularity.

(1) *Axis of Rotation Perpendicular to the Spiral Axis.* Such disclinations, for reasons similar to those stated for the smectic crystal, are necessarily straight. We shall denote $\tau^{n+}(z)$, $\tau^{n-}(z)$ the disclinations transverse to the molecules, z is the coordinate of the line measured along the spiral axis, and varies discontinuously, by quantities equal to the half-pitch. The signs plus and minus are chosen with the same convention as for the similar nematic screw disclinations. n is the number of π rotations involved in the Volterra process. Similarly, we introduce the symbols $\lambda^{n+}(z)$, $\lambda^{n-}(z)$ for the disclinations running lengthwise the molecules. Figures 12 and 13 show perpendicular sections of these four types for $n=1$. The points represent the molecules viewed end-on, the continuous line or the dashed-line the molecules in the plane of the figure; an intermediary position is represented by a nail with its pointed spike directed towards the observer. The figures are drawn for left-hand spirals.

It is to be noted that a λ and a τ are not equivalent. It is likely that the core energy of a λ is smaller than the core energy of a τ . Moreover, as stated for the smectic screw disclinations, the topological properties at infinity are not the same : one transforms a λ into a τ , and vice-versa, by emission or absorption of a χ dislocation, which will now be described.

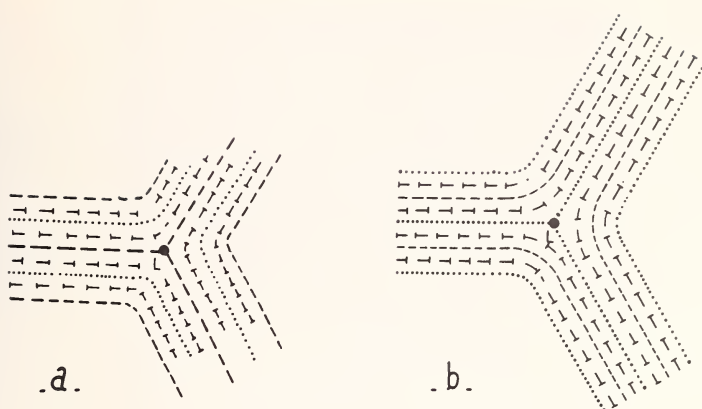


FIGURE 12. λ^- and τ^- in a cholesteric crystal; section perpendicular to the axis of rotation.

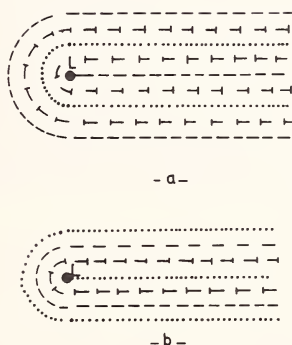


FIGURE 13. λ^+ and τ^+ in a cholesteric crystal; section perpendicular to the axis of rotation.

(2) *Axis of Rotation Parallel to the Spiral Axis.* Such disclinations, which we shall denominate χ disclinations, because of the location of the rotation axis along the axis of chirality, may take any shape, owing to the viscosity in the cholesteric plane. There is on the other hand a viscosity of rotation-translation along the spiral axis : any rotation $\Omega = \alpha$, followed by a translation $T = -\alpha/q_0$ (minus sign for a left hand cholesteric¹) is relaxed. We can write symbolically

$$(\Omega, T) \equiv (\alpha, -\alpha/q_0) \equiv 0. \quad (7)$$

¹ By definition, a right-hand spiral is analytically represented by the expression $\theta = +q_0 z$ in a right-hand system of reference.

Conversely, we have

$$(\alpha, \alpha/q_0) \equiv (2\alpha, 0) \equiv (0, -2\alpha/q_0). \quad (8)$$

This equation states the equivalence, for $\alpha = \pi/2$, between the rotation $\Omega = \pi$, the translation $T = -\pi/q_0$ (the half-pitch), and the right-handed translation-rotation $(\pi/2, \pi/2q_0)$ for the left-hand helix.

χ disclinations are very similar to disclinations in nematic crystals. Screw χ disclinations have the same cross-section configurations than the nematic disclinations. Let ϕ be the azimuthal angle of $\mathbf{n}(r)$; in the perfect state, we have, for a left-handed spiral

$$\phi = -q_0 z. \quad (9)$$

Introduce a χ , i.e., a screw dislocation $b = \pm \frac{\pi}{q_0}$. Equation (9) becomes,

$$\text{with } z \rightarrow z \pm \frac{1}{q_0} \frac{\psi}{2},$$

$$\phi = -q_0 z \pm 1/2\psi + \text{relaxation terms} \quad (10)$$

where ψ is the azimuthal angle of \mathbf{r} . Therefore the configuration of the molecules is the same as for a nematic screw with a cut surface rotating like the cholesteric spiral.

χ edge disclinations have been first proposed by de Gennes [25] in order to explain the occurrence of the so-called Grandjean-Cano "walls" [26, 27], which appear in a wedge single crystal of a cholesteric phase (fig. 14), when the boundary conditions impose to the molecules to keep parallel to the surfaces. If in A (see fig. 14) the thickness of the wedge is equal to say, one pitch, and in B to three half-pitches, the domain in between must display a singularity where the number of half spirals change abruptly

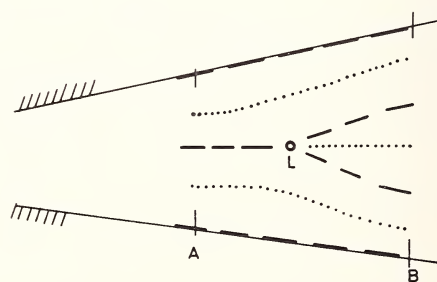


FIGURE 14. Grandjean-Cano walls in a small-angle wedged single cholesteric crystal.



PLATE IV. High pitch cholesteric phase (dilute solution of a cholesterol ester in p. azoxyanisol): observation of Grandjean-Cano walls. (Courtesy Orsay Liquid Crystal Group.)

from 2 to 3. The photograph of plate IV obtained by the Orsay Liquid Crystal Group [28], from a high pitch cholesteric phase ($\left(\frac{2\pi}{q_0}\right) \sim 100\mu$) shows parallel Grandjean-Cano walls with a regular spacing. They have shown that the spacing of the first lines (at the bottom of the picture) agrees with a χ of Burgers vector equal to half-pitch, but that the following should be double χ 's.² In fact another model has been proposed for these "double" lines [29], which explains also their behaviour in a magnetic field. This model, which assumes the pairing of disclinations of opposite sign, will be explained further.

The energy and the configuration of a χ edge disclination have been calculated by de Gennes for the isotropic case [25]. A perturbation calculation of the influence of the anisotropy on the energy has also been performed and shows that the energy varies with the position of the edge disclination along the spiral axis [30].

² The simple lines look faintly contrasted on the plates, and the double lines strongly contrasted.



PLATE V. Same situation after application of a magnetic field perpendicular to the spiral axis (Courtesy Orsay Liquid Crystal Group).

(3) *Other Kinds of Singularities in Cholesteric Crystals.* For some singularities which have been observed, the thickness of the cholesteric layers (the pitch) is kept constant. Such is the case for the cofocal domains observed by G. Friedel [5] (plate VI) and the spherulites observed by C. Robinson [31]. It seems, following G. Friedel, that a cholesteric phase displays, either the typical Grandjean-Cano "walls," or the cofocal domains, which constitute a metastable distortion. More work is certainly needed to compare and explain these fundamentally different kinds of singularities.

IV. Pairing of Disclinations in Cholesteric Crystals

IV.1. Impossibility of a curved λ or τ

Let us suppose that a λ or a τ is curved. This would mean that, in each point A_1 of the line L_1 , the distortion may be defined by a *local* axis of rotation ν_1 parallel (or perpendicular) to the molecule in A_1 . Consider two position $A_1, A'_1 = A_1 + ds$, on the line, ν_1 and ν'_1 the corresponding axes of

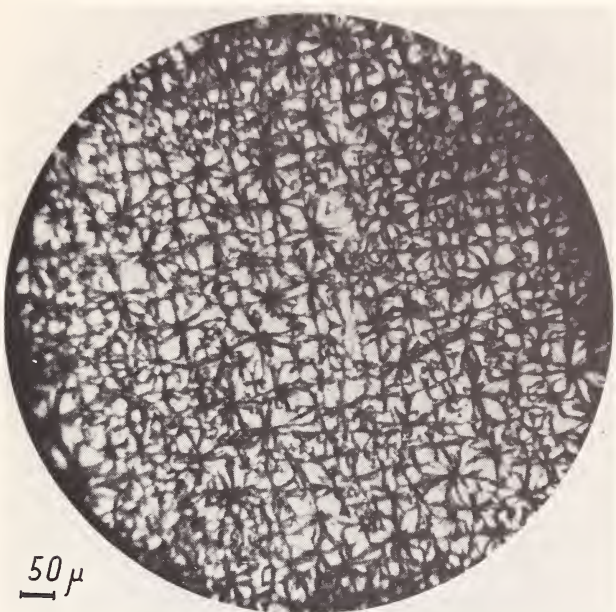


PLATE VI. Cholesterol butyrate. Cofocal domains seen between crossed polars (after G. Friedel).

rotation, \mathbf{r}_1 and \mathbf{r}'_1 the distance of \mathbf{A}_1 and \mathbf{A}'_1 to a point M on the cut surface S . The difference $\delta = \mathbf{d}_1 - \mathbf{d}'_1$ of the displacements of \mathbf{M} is given by (fig. 16)

$$\delta = 2 \sin \frac{\Omega_1}{2} \{ d\boldsymbol{\nu}_1 \wedge \mathbf{r}_1 - \boldsymbol{\nu}_1 \wedge d\mathbf{s}_1 \}, \quad (11)$$

where $d\boldsymbol{\nu}_1 = \boldsymbol{\nu}'_1 - \boldsymbol{\nu}_1$.

δ corresponds to a continuous distribution of infinitesimal dislocations of two types

— a density of disinclinations $d\boldsymbol{\nu}_1$

— a density of translation dislocations $-\boldsymbol{\nu}_1 \wedge d\mathbf{s}_1$.

These infinitesimal dislocations cannot be viscously relaxed, and are therefore impossible if we assume a relative displacement of the cut surface lips of the form stated eq (3).

IV.2. Pairing of straight λ or τ

It is possible to reduce to zero at long distance these continuous distributions by pairing two disinclinations of opposite sign at short distance one from the other.

The simplest case consists in pairing two straight disinclinations. For

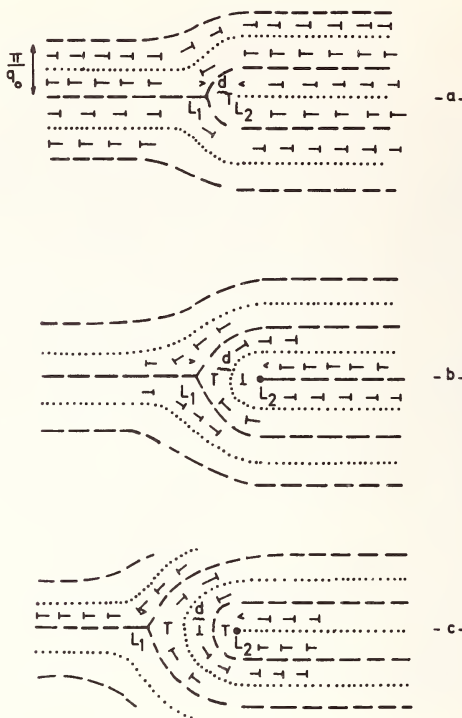


FIGURE 15. Pairing of two λ or τ disclinations of opposite signs.

in this situation there are no continuous dislocations in the ribbon separating them. Figure 15 illustrates this possibility. Let \mathbf{d} be the distance between the two disclinations. The total effect of the pair on the cut surface is given by

$$2 \sin \frac{\Omega_1}{2} (\boldsymbol{\nu}_1 \wedge \mathbf{r}_1 + \boldsymbol{\nu}_2 \wedge \mathbf{r}_2) = 2 \sin \frac{\Omega_1}{2} (\boldsymbol{\nu}_1 \wedge \mathbf{d}) = 2(\boldsymbol{\nu}_1 \wedge \mathbf{d}). \quad (12)$$

This is equivalent to a translation dislocation, possible if $2d$ is equal to a lattice parameter. This condition leads to the relation

$$d = \frac{n\pi}{2q_0} \quad (13)$$

the cases $n = 1, 2, 3$ are represented figure 15 and correspond to pairs of increasing energy.

The possibility of such a pairing of disclinations has already been assumed in solids by Friedel [32].

The preceding discussion shows that such pairs are equivalent at long distances to χ disclinations. But the core is very different, and involves a $\pi/2$ rotation of the cholesteric axes. This point has been very important

in the understanding of the zigzag instability of "double" lines [29] under a magnetic field. Plate V corresponds to plate IV after application of a magnetic field. The lines have moved towards the top, in the region where the wedge is thicker, in order to accommodate the increase of the pitch $\frac{2\pi}{q_0(H)}$. At the same time, for a field $H_z \sim H_c/2$, the "double" lines become zigzagging, and the "simple" lines stay stable. Bearing in mind that the cholesteric phase is diamagnetic, so that the molecules tend to align parallel to the applied field, i.e., the cholesteric axis perpendicular to \mathbf{H} , a pair tends to rotate by an angle of $\pi/2$ about the cholesteric axis. This effect is larger when the core is larger, and a crude calculation [29] leads to the conclusion that the instability field H_z is of the order of H_c/n , where n is the number of half-pitches of the pair. Therefore a "simple" line could as well be a pair or a χ , as it would not display any instability before the critical field H_c .

IV.3. Lines of pairs

Consider a line L_1 , and be ν_1 , on each point \mathbf{A}_1 of the line, a rotation axis either parallel or perpendicular to the local molecule. It is possible, by a generalization of the preceding paragraph, to pair this line with a line L_2 (fig. 16) such that:

- the rotation axis ν_2 at the point \mathbf{A}_2 , coupled with \mathbf{A}_1 , is opposite to ν_1 .
- $\mathbf{A}_1\mathbf{A}_2 = \mathbf{d}$ is in the cholesteric plane.
- $d = \frac{n\pi}{2q_0}$ is a constant.

Such a pair is equivalent at long distances to a translation dislocation of Burgers vector $\frac{n\pi}{q_0}$. The faulted ribbon between L_1 and L_2 is covered by

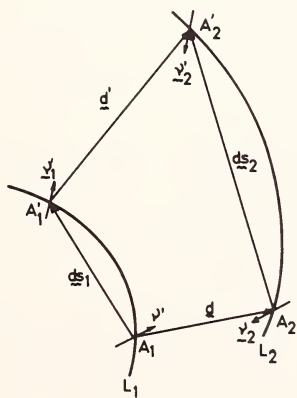


FIGURE 16. Line of pairs : general case.

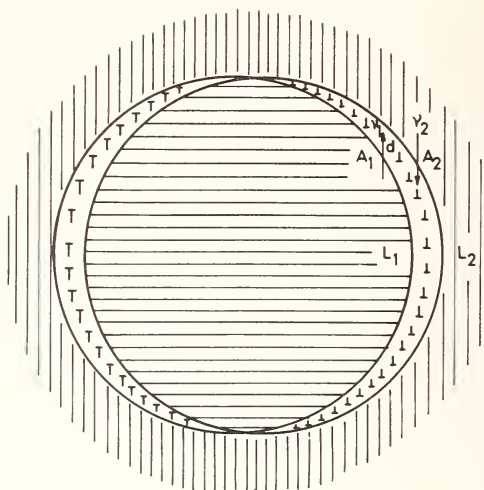


FIGURE 17. Translated plane loops parted in order to give a translation dislocation line.

a continuous distribution of infinitesimal dislocations, directed along $\mathbf{A}_1\mathbf{A}_2$, and of density $d\nu_1$ in rotation and $\nu_1 \wedge d\mathbf{s}_1$ in translation.

Among the possible configurations which achieve the preceding result, there are two simple cases:

(i) — *Translated plane loops.* L_1 and L_2 are two loops in the same cholesteric plane $\cdot \nu = \nu_1 - \nu_2$ is a constant vector. The faulted ribbon is composed uniquely of translation dislocations (fig. 17).

(ii) — *Helicoïdal concentric loops.* Such loops have the same pitch as the cholesteric crystal. The faulted ribbon is composed uniquely of rotation dislocations radially spread, with a density equal to the curvature of the projection of the helix on the cholesteric plane.

F. C. Frank [22] has pointed out that the inner region of the cylinder has not the same pitch as the outer region. We consider three possible cases:

- The effect of the helicoïdal pair is to introduce n half-pitches *inside* the cylinder for each pitch of the pair. The inner pitch is given by $\frac{2\pi}{q_0} = \frac{2\pi}{q_0} \left(\frac{2}{2+n} \right)$, figure 18a represents a median section of the configuration for $n=1$.
- The effect of the pair is to introduce one half-pitch *outside* the cylinder. The inner pitch is therefore twice the outer pitch (fig. 18b).
- The effect of the pair is to introduce two half-pitches *outside* the cylinder for each pitch of the pair. The inner part is then nematic (fig. 18c).

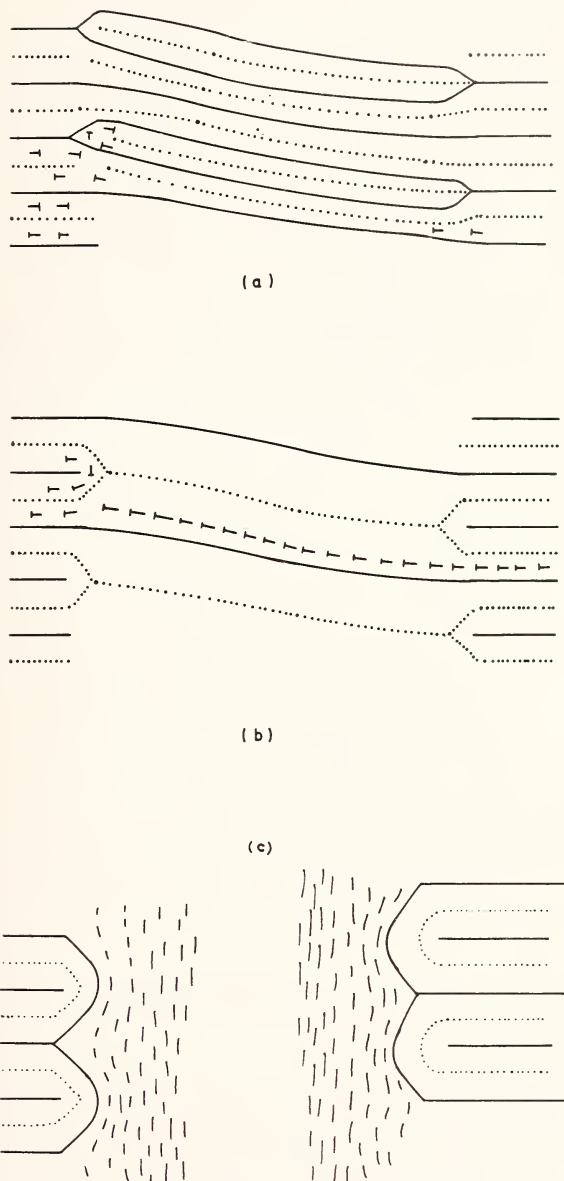


FIGURE 18. Helicooidal pair : the pitch inside the cylinder is different from the pitch of the matrix crystal (see text).

V. Glide of Disclinations in a Cholesteric Crystal

V.1. Screw disclinations

Let us consider the possibility for a screw disclination τ^- , for example, to glide parallel to itself (fig. 19) along the cholesteric axis by a distance x , and let us assume $x < \frac{\pi}{4q_0}$. In the intermediary state of figure 19b, the molecules at the boundary on the upper part of the cut surface are not parallel to the molecules at the boundary on the lower part. It is therefore necessary to deform the left part of the crystal by a rotation $2xq_0$ of the molecules of the half-plane, or by opposite rotations $\pm 2xq_0$ of the molecules of the two half-planes, in order that the deformed crystal matches the perfect crystal introduced on the right. The result is described figure 19c; the axis S is an axis of symmetry. It is clear that this process leads to an excited state of τ^- , because a simple redistribution of the molecules in the core gives τ^- back.

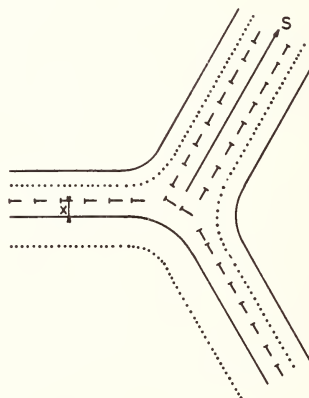
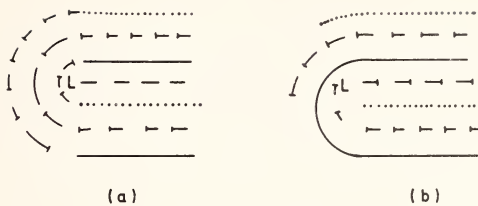


FIGURE 19. Creation of an imperfect τ^- .

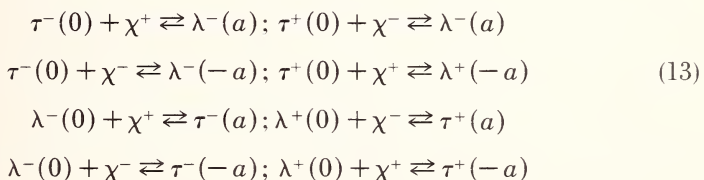
It should have been as well possible to rotate the molecules of the half-plane on the left part by an amount $-\pi + 2xq_0$, which is equivalent to adding a χ to τ^- . The result is then an excited state of λ^- .

A similar analysis can be made for λ^+ and τ^+ . A displacement of the disclination by a distance x upwards is equivalent to a rotation xq_0 of each molecule about the local spiral axis, which leads finally to a higher energy distribution in the core. Figure 20a shows this rotation, and figure 20b shows the isoclinal lines of the same disclination.

FIGURE 20. Configuration of an imperfect τ^+ .

V.2. Absorption and emission of χ 's by a λ or a τ (Frank)

The preceding analysis shows clearly that a λ (or a τ) is transformed in a τ (or a λ) by the absorption or emission of a χ parallel to the screw disclination line, and that the process is attended by the glide of the λ (or the τ) along the cholesteric axis. More precisely, we can write the following reactions (cg. F. C. Frank, Montpellier Juin 69, Colloque sur les cristaux liquides).



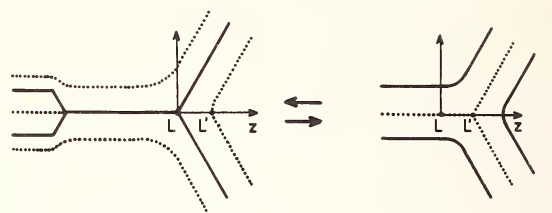
The two first reactions are illustrated in figure 21. It is interesting to note the similarity between these reactions introduced here through the concept of glide and the Burger's circuit description, used above in the case of disclinations in a smectic crystal, and which apply evidently to the present cases.

Frank has also made the following remark:

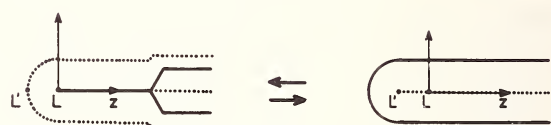
Let us now imagine a χ^+ (fig. 22) rotating counterclockwise about a $\tau^-(0)$ by an angle of 2π . The χ^+ is transformed in a χ^- in this process, which can be as well described as the absorption of the χ^+ by the τ^- on one axis of symmetry and the emission of the χ^- on an other axis of symmetry. By the preceding results the τ^- has moved during this process by a distance $-2a$. So that it is possible to move a τ or λ by letting a χ rotate about it.

V.3. Glide of pairs

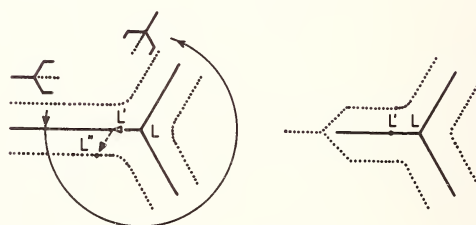
The glide of a pair, say, from a $\lambda^+\tau^-$ configuration to a $\lambda^-\tau^+$ configuration is, owing to the preceding analysis, describable as the exchange of a χ



a

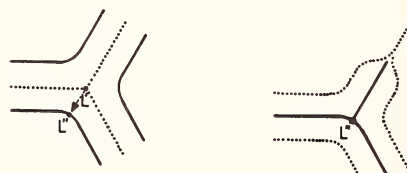


b



a

b



c

d

FIGURE 22. Rotation of a χ about a τ and displacement of the τ from L to L' : (a) rotation of a χ ; (b)(c)(d) steps of an equivalent circuit.

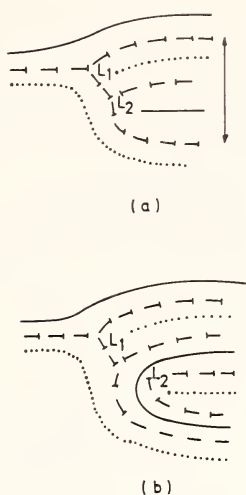


FIGURE 23. Glide of a pair (excited state).

between the two cores. The intermediate situation, at the beginning of the glide is shown in figure 23.

VI. Conclusion

The liquid crystals offer a very remarkable medium for the application of the notion of disclination. Although the analysis here presented is far from being complete and from explaining all the experimental facts, we have the feeling that it gives a very secure basis for further progress. An important step would be also to solve the elasticity equations in order to compute the real configurations in these media where the anisotropy effects are certainly important.

VII. Acknowledgements

The authors are particularly indebted to F. C. Frank, with whom they had a complete and fruitful discussion on most of the topics hereabove discussed. They took also advantage of many comments by the members of the Orsay Liquid Crystal Group and P. G. de Gennes.

VIII. References

- [1] Lehmann, O. Z. Phys. Chem. **4**, 468 (1889).
- [2] Gray, G. W., Molecular Structure and Properties of Liquid Crystals (Academic Press, New York, 1962).
- [3] Christyakov, I. G., Sov. Phys. Uspekhi **9**, 551 (1967).

- [4] Chatelain, P., Bull. Soc. Franç. Miner. Crist. **77**, 323 (1954).
- [5] Friedel, G., Ann. Physique **18**, 273 (1922).
- [6] Chatelain, P., C. R. Acad. Sci. Paris **213**, 875 (1941).
- [7] de Gennes, P. G., Sol. State Comm. **6**, 163 (1968).
- [8] Durand, G., Léger, L., Rondelez, F., and Veysié, M., Phys. Rev. Letters **22**, 227 (1969).
- [9] Mauguin, C., Bull. Soc. Franç. Miner. Crist. (1911); in *Traité de Chimie Organique*, **1**, V. Grignard Ed. (Masson, Paris, 1947) p. 82.
- [10] Chatelain, P., Acta Cryst. **1**, 315 (1948); **4**, 453 (1951).
- [11] de Gennes, P. G., Proc. of the 2nd Intern. Liquid Crystal Conf. (Kent University, 1968), to be published.
- [12] de Vries, H., Acta Cryst. **4**, 219 (1958).
- [13] Oseen, C. W., Trans. Faraday Soc. **29**, 883 (1933).
- [14] Zocher, H., Trans. Faraday Soc. **29**, 945 (1933).
- [15] Frank, F. C., Disc. Faraday Soc. **25**, 19 (1958).
- [16] de Gennes, P. G., C. R. Acad. Sci. Paris **266**, 15 (1968).
- [17] Meyer, R. B., Phys. Rev. Letters **22**, 918 (1969).
- [18] Nabarro, F. R. N., *Theory of Crystal Dislocations* (Clarendon Press, Oxford, 1957) Chap. III.
- [19] Harris, W. F., These proceedings.
- [20] Friedel, G., Grandjean, F., Bull. Soc. Franç. Mine. Crist. (1911).
- [21] Friedel, J., and de Gennes, P. G., C. R. Acad. Sci. Paris **268**, 257 (1969).
- [22] F. C. Frank, private communication.
- [23] Nye, J. F., Acta Met. **1**, 153 (1953).
- [24] Sackmann, H., and Demus, D., in *Liquid Crystals* (Gordon and Breach, London, 1966) p. 341.
- [25] de Gennes, P. G., C. R. Acad. Sci. Paris, **266**, 571 (1968).
- [26] Grandjean, F., C. R. Acad. Sci. Paris **172**, 71 (1921).
- [27] Cano, R., Thesis (Montpellier, 1966).
- [28] Orsay Liquid Crystal Group, Phys. Letters **28A**, 687 (1969).
- [29] Kléman, M., and Friedel, J., J. de Physique **30**, C-43 (1969).
- [30] Caroli, C., and Dubois-Violette, E., Sol. State Comm. **7**, 799 (1969).
- [31] Robinson, C., in *Liquid Crystals* (Gordon and Breach, London, 1966) p. 147.
- [32] Friedel, J., *Dislocations* (Pergamon Press, 1964) p. 10.

NONMETRIC CONNEXIONS, QUASIDISLOCATIONS AND QUASIDISCLINATIONS. A CONTRIBUTION TO THE THEORY OF NONMECHANICAL STRESSES IN CRYSTALS

K. H. Anthony

*Institut für Theoretische und Angewandte Physik der Universität
Stuttgart Germany*

Nonmechanical stresses produced, for instance, by a temperature gradient or by an internal magnetic field are related to an affine lattice connexion, which is nonmetric with respect to the elastic metric. The covariant derivative of the elastic metric with respect to the lattice connexion is regarded as source-function for this kind of internal stresses. It may easily be determined from experimental data. The calculation of mechanical stresses is based on this quantity.

Instead of describing nonmechanical stresses by a nonmetric lattice connexion we alternatively may use an elastic connexion which is metric with respect to the elastic metric. In the elastic connexion are involved the tensors of quasiplastic torsion and of quasidisclination-density, which are regarded as source functions of nonmechanical stresses. Both tensors are intimately connected. They are a natural generalization of the quasidislocation tensor of the linear theory of nonmechanical stresses.

From the theory of quasidisclinations we obtain the following statement: In general, nonmechanical stresses cannot be eliminated solely by a dislocation movement. An additional distribution of crystal disclinations is necessary.

Key words: Affine connexions; continuum mechanics; curvature tensor; disclination; internal stresses; quasidisclination.

I. States and Quantities

In order to describe nonmechanical stresses in a crystal which, for instance, is endowed with a temperature gradient or with an internal

Fundamental Aspects of Dislocation Theory, J. A. Simmons, R. de Wit, and R. Bullough,
Eds. (Nat. Bur. Stand. (U.S.), Spec. Publ. 317, I, 1970).

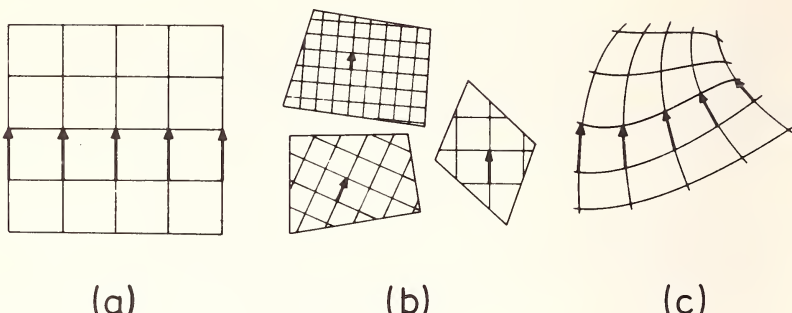


FIGURE 1. (a) Ideal state, (b) natural state, (c) final state.

magnetic field one considers three states of the crystal (see fig. 1) [1].

In the stress-free *ideal state* (f) one observes the regular undisturbed crystal lattice. If we confine ourselves to the case where real crystal dislocations and crystal disclinations are absent, we go by a compatible deformation from the ideal state to the *final state* (k), which presents elastic internal stresses. This deformation may, e.g., be due to the building-up of a temperature gradient. Both states are realized as a compact body in Euclidean space. The final state is referred to coordinates x^k with basis vectors \mathbf{f}_k , $k = 1, 2, 3$.

The *natural state* (κ) may be produced from the final state by a tearing process which relaxes all elastic strains. In this state the volume elements of the crystal in general cannot be fitted together as a compact body. The crystal structure in the elements is not the regular one. In the case of thermal stresses the lattice shows different dilatations on different volume elements according to their local temperature. In addition the lattice will be sheared inhomogeneously in the case of magnetostrictive internal stresses.

Nonlinear theory starts by defining in the final state the following quantities [1–5]:

- (1) The *elastic metric tensor* $\mathbf{a} = (a_{ij})$ defines distances of material points x^k and $x^k + dx^k$ which they assume in the natural state:¹

$$d\sigma^2 = a_{ij} dx^i dx^j. \quad (1)$$

- (2) The *lattice-metric tensor* $\mathbf{b} = (b_{ij})$ measures distances of material points which they assume in the ideal state:

$$d\varsigma^2 = b_{ij} dx^i dx^j. \quad (2)$$

¹ Summation convention implied.

(3) The affine *lattice-connexion* $\Gamma = (\Gamma_{ij}^k)$ describes the crystal lattice in the final state. The lattice defines the Γ -parallelism corresponding to Γ , i.e., if $\mathbf{v}(x)$ is any field of equivalent lattice vectors in the final state, this vectorfield varies according to

$$dv^k = -\Gamma_{ij}^k v^j dx^i. \quad (3)$$

By using the Euclidean metric tensor $\mathbf{g} = (g_{ij})$ and the connexion $\{\Gamma_{ij}^k\}$ of Euclidean parallelism we derive in the final state from the quantities $\mathbf{a}, \mathbf{b}, \Gamma$ the following tensors:

(1) The *elastic strain tensor* $\mathbf{e} = (e_{ij})$ measures the elastic change of distances, when deforming the crystal from the natural to the final state:

$$ds^2 - d\sigma^2 = 2e_{ij} dx^i dx^j, \quad (4)$$

$$e_{ij} = 1/2 (g_{ij} - a_{ij}). \quad (5)$$

The Euclidean distance of material points in the final state is given by

$$ds^2 = g_{ij} dx^i dx^j. \quad (6)$$

(2) When we deform the crystal from the ideal state into the final state distances between material points change according to

$$ds^2 - d\varsigma^2 = 2t_{ij} dx^i dx^j, \quad (7)$$

where $\mathbf{t} = (t_{ij})$ is the *total strain tensor*:

$$t_{ij} = 1/2 (g_{ij} - b_{ij}). \quad (8)$$

(3) The *quasiplastic strain tensor* $\mathbf{q} = (q_{ij})$ and the elastic strain tensor add to the total strain tensor:

$$t_{ij} = q_{ij} + e_{ij}, \quad (9)$$

i.e.,

$$q_{ij} = 1/2 (a_{ij} - b_{ij}). \quad (10)$$

The tensor \mathbf{q} belongs to the quasiplastic deformation which produces the natural state from the ideal state:

$$d\sigma^2 - d\varsigma^2 = 2q_{ij} dx^i dx^j. \quad (11)$$

To illustrate the meaning of \mathbf{q} we cut the ideal state in small pieces and impose on each volume element, e.g., its final local temperature.

(4) The deviation of the final state crystal lattice from an undisturbed lattice structure is measured by the *hyperdeformation tensor* $\mathbf{H} = (H_{ij}^k)$:

$$H_{ij}^k = \left\{ \begin{matrix} k \\ ij \end{matrix} \right\} - \Gamma_{ij}^k. \quad (12)$$

The tensor \mathbf{H} compares the Γ -parallelism with the Euclidean parallelism [2]. It contains the *hyperstrain tensor* $\mathbf{E} = (E_{imn})$,

$$E_{imn} = H_{im}^k a_{kn}/(mn), \quad (13)$$

and the *structure curvature tensor* $\mathbf{K} = (K_{imn})$,

$$K_{imn} = H_{im}^k a_{kn}/[mn]. \quad (14)$$

(5) The covariant derivative of the elastic metric with respect to the lattice connexion

$$Q_{kij} = -\overset{\Gamma}{\nabla}_k a_{ij} \quad (15)$$

$$= -(\partial_k a_{ij} - \Gamma_{ki}^p a_{pj} - \Gamma_{kj}^p a_{ip}) \quad (16)$$

is the fundamental quantity in this paper.

II. Naturalization

Each of the three quantities \mathbf{a} , \mathbf{b} , Γ defined in the final state belong to a certain tearing process: Distances with respect to the elastic metric \mathbf{a} become Euclidean if we drag along this metric with the deformation which carries the final state into the natural state. An analogous consideration may be associated with the lattice metric \mathbf{b} if we take the deformation from the final to the ideal state. The same deformation transforms the Γ -parallelism of the final state into a Euclidean parallelism in the ideal state, if we drag along the Γ -parallelism with this deformation.

By means of the following statements these physical features are involved into a differential geometrical description, based on the quantities \mathbf{a} , \mathbf{b} , Γ [3].

The elastic metric tensor $\mathbf{a} = (a_{ij})$ defined in the final state is said to be *naturalizable*, if there exists a new basis system in the same state.

$$\mathbf{n} = A_{\kappa}^k \mathbf{f}_k, \quad \kappa = 1, 2, 3, \quad (17)$$

relative to which the metric has the components

$$a_{\kappa\lambda} = \delta_{\kappa\lambda}, \quad (18)$$

where

$$a_{\kappa\lambda} = A_{\kappa}^k A_{\lambda}^l a_{kl}. \quad (19)$$

Similarly the lattice connexion $\Gamma = (\Gamma_{ij}^k)$ is said to be *naturalizable* if we can find in the final state a new basis system

$$\overset{\text{I}}{i} = B_i^k \overset{\text{f}}{k}, \quad f = 1, 2, 3, \quad (20)$$

in which the connexion has the components

$$\Gamma_{ij}^p = 0. \quad (21)$$

We obtain these components by means of the transformation formula²

$$\Gamma_{ij}^p = B_i^l B_j^m B_k^p \Gamma_{lm}^k - B_i^l B_j^m \partial_l B_k^p \quad (22)$$

In view of (17) to (22) the naturalizations of the metric **a** or the connexion Γ mean therefore the construction of certain basis systems relative to which the metric or the connexion show Euclidean features. These processes take place in the *compact* final state and have a priori nothing to do with the tearing of the body. The variations of the naturalizing basis systems $\overset{\text{n}}{\kappa}$ and $\overset{\text{i}}{f}$ in the final body manifold visualize incompatibilities involved in the final state.

Especially a basis system $\overset{\text{i}}{f}$, $f = 1, 2, 3$ naturalizes the connexion Γ if and only if it is displaced parallel with respect to Γ , i.e., the lattice connexion always naturalizes, for example, in a basis system which is defined from the lattice vectors in the final state.

On the other hand, the naturalizing basis system $\overset{\text{n}}{\kappa}$, $\kappa = 1, 2, 3$, of the metric **a** is only determined up to an arbitrary "orthonormal basis transformation,

$$\overset{\text{n}}{\kappa'} = D_{\kappa}^{\kappa'} \overset{\text{n}}{\kappa}, \quad \kappa' = 1, 2, 3, \quad (23)$$

$$D_{\kappa}^{\kappa'} D_{\lambda}^{\lambda'} \delta_{\kappa\lambda} = \delta_{\kappa'\lambda'}. \quad (24)$$

² $\partial_i = \frac{\partial}{\partial x_i}$, B_i^f inverse of B_i^l .

i.e., \mathbf{n}_κ is determined up to an arbitrary rotation relative to the metric \mathbf{a} .

A positive definite metric and a connexion with vanishing Riemannian curvature can always be naturalized in certain basis systems which at least are anholonomic relative to the coordinate system x^k [3]. In the case of nonvanishing Riemannian curvature we generalize the definition of the naturalization in such a way that it is valid on arbitrary lines in the final state [3].

Of fundamental importance in this paper is the *simultaneous naturalization* of a *metric and a connexion*. If both quantities are assumed to be naturalizable, in general they do not naturalize simultaneously, i.e., there is no common basis system, in which both quantities naturalize. The following lemma is not hard to prove [3]:

The connexion Γ and the metric \mathbf{a} naturalize simultaneously (naturalizability of each quantity presumed) if and only if Γ is a metric connexion with respect to \mathbf{a} , i.e.,

$$Q_{kij} = 0. \quad (25)$$

(See (15, 16)).

In the case where Γ has nonvanishing torsion (dislocation density) and Riemannian curvature (disclination density) this lemma is valid too.

Naturalization of a quantity is intimately connected with a certain tearing process. To illustrate this we assume, e.g., the coordinates x^k of the final state to be orthonormal Cartesian coordinates in Euclidean space. Then we consider for instance the inverse of eq (17) not as a basis transformation that leaves the body undeformed in the final state but as a material mapping of the body into the Euclidean space such that in each material point the material vectors \mathbf{n}_κ are mapped into the vectors \mathbf{f}_k . This means a deformation of the final state such that distances according to the metric \mathbf{a} appear as Euclidean distances.

Therefore this mapping leads to the natural state (κ) mentioned above. The naturalization process of the elastic metric \mathbf{a} is a mathematical image in the final state for the physical tearing process which leads from the final state to the natural state.

Arbitrary rotations of the volume elements in the natural state have no physical meaning. This corresponds to the uncertainty (23) of the naturalizing basis.

An analogous consideration is valid for the naturalization of the lattice connexion Γ . After the material mapping, which by eq (20) carries the material basis vectors \mathbf{i}_k into the vectors \mathbf{f}_k , the Γ -parallelism of the final state becomes Euclidean. The mapping leads to the ideal state.

One should keep in mind that this mapping is only a geometrical process, which leaves, e.g., a temperature gradient invariant. By the mapping which corresponds to eq (20) we get the structure of the ideal state though the lattice is not free of elastic strains.

Tearing processes are in a one-to-one correspondence to naturalization processes. Therefore as a consequence of the difference of the natural and the ideal state the lattice-connexions Γ and the elastic metric a do not naturalize simultaneously in the case of nonmechanical stresses. From this follows [3, 5]:

The lattice-connexion is non-metric relative to the elastic metric³, i.e.,

$$Q_{kij} \neq 0. \quad (26)$$

The tensor \mathbf{Q} may be regarded as *source-function for nonmechanical internal stresses*. It is invariant with respect to physically unessential rotations of the natural state.

Because of the fact that the lattice metric \mathbf{b} and the lattice-connexion Γ are both referred to the ideal state, they naturalize simultaneously, which means that Γ is metric with respect to \mathbf{b} :

$$\nabla_k^{\Gamma} b_{ij} = 0. \quad (27)$$

From (10), (15), (27) we obtain

$$Q_{kij} = -2 \nabla_k^{\Gamma} q_{ij}. \quad (28)$$

The tensor \mathbf{Q} may be determined from experimental data.

III. Examples

(a) In the case of thermal stresses we have a quasiplastic, isotropic change of length

$$d\tilde{s} \rightarrow d\sigma = (1 + f(T)) d\tilde{s}, \quad (29)$$

where $f(T)$ is the isotropic thermal dilatation coefficient (T =temperature). From (29) we obtain

$$d\sigma^2 - d\tilde{s}^2 = ((1 + f)^2 - 1) d\tilde{s}^2. \quad (30)$$

³ Bilby et al. came to the same result by other considerations [6].

and together with (11), (2). (28) we finally get

$$Q_{kij} = -2 \frac{df/dT}{1+f} (\nabla_k T) \cdot a_{ij} \quad (31)$$

(∇_k = Euclidean derivative in the final state). This result is exact. It should be remarked that the elastic strain \mathbf{e} is included in the elastic metric \mathbf{a} .

(b) We consider a spontaneously magnetized cubic crystal. Magnetostrictive strains are assumed to be very small so that to a good approximation the crystal remains cubic in the final state. If the coordinate system x^k of the final state is Cartesian, the lattice-connexion Γ differs not very much from zero. If in addition the coordinate system coincides with the cubic axis we obtain in good approximation for the quasi-plastic strain tensor [7]

$$\mathbf{q} = \begin{pmatrix} \lambda_0(\alpha_1^2 - 1/3) & & & \text{symm.} \\ \lambda_1\alpha_1\alpha_2 & \lambda_0(\alpha_2^2 - 1/3) & & \\ \lambda_1\alpha_1\alpha_3 & \lambda_1\alpha_2\alpha_3 & \lambda_0(\alpha_3^2 - 1/3) & \end{pmatrix}. \quad (32)$$

λ_0, λ_1 are material constants and α_i the direction cosines of the magnetization vector relative to the cubic axes.

In linear approximation we get

$$Q_{kij} = -2((\lambda_0 - \lambda_1)\delta_{ij} + \lambda_1)\partial_k(\alpha_i\alpha_j). \quad (33)$$

— no summation —

From (31) and (33) we see that thermal or magnetostrictive stresses vanish if we have a constant temperature or a homogeneous magnetization in the crystal.

(c) Stresses caused by extramatter are another example for the theory of nonmetric lattice-connexions [1, 5, 6]. Especially, point defects constitute extramatter.

IV. Elasticity Theory of Nonmechanical Stresses in Crystals Using Nonmetric Lattice-Connexions

If we confine ourselves to pure nonmechanical stresses the crystal lattice in the final state is topologically undisturbed. Therefore the lattice-connexion Γ is free of torsion,

$$S_{ij}{}^k \equiv \Gamma_{[ij]}{}^k = 0, \quad (34)$$

and free of Riemann-Christoffel curvature:

$$\Gamma_{ijk}{}^l \equiv 2(\partial_i\Gamma_{jk}{}^l + \Gamma_{im}\Gamma_{jk}{}^{ml})_{[ij]} = 0. \quad (35)$$

Equations (34) and (35) are the compatibility conditions of the problem. Equation (35) may be brought into the form

$$\Gamma_{ijkl} \equiv \Gamma_{ijk}{}^m a_{ml} = 0. \quad (36)$$

By means of the identities for the Riemann-Christoffel curvature tensor⁴ only six equations are left. Using the formula⁵

$$\Gamma_{ij}{}^k = 1/2 a^{im} (\partial_i a_{jm} + \partial_j a_{im} - \partial_m a_{ij}) + 1/2 a^{km} (Q_{ijm} + Q_{jim} - Q_{mij}) \quad (37)$$

and eq (5) we get these equations in terms of the elastic strain tensor:⁶

$$(-\epsilon^{inm} \epsilon^{jlk} \nabla_n \nabla_i e_{mk} + 1/2 \epsilon^{inm} \epsilon^{jlk} \nabla_n Q_{lkm})_{(ij)} \\ = 1/2 \epsilon^{inm} \epsilon^{jlk} q_{nmkl}/_{(ij)}. \quad (38)$$

Of these equations only three equations are independent because of the Bianchi-identity for the Riemann-Christoffel curvature tensor.⁴

The left-hand side of (38) consists only of linear terms. The vanishing of this expression generalizes deSaint Venant's compatibility conditions to the present problem.

The term q_{nmkl} in (38) includes all nonlinear effects:

$$q_{nmkl} = H_{nkp} (H_{mlq} + Q_{mlq}) a^{pq}, \quad (39)$$

where H_{ijk} is the total covariant hyperdeformation tensor:

$$H_{ijk} = H_{ij}{}^m a_{mk} \quad (40)$$

(see eq (12)).

Equations (37) and (14) lead to the following expression for the structure curvature:

$$K_{imn} = 2 \nabla_{[m} e_{n]i} - Q_{[mn]i}. \quad (41)$$

The general decomposition of a connexion Γ with regard to a metric \mathbf{a} ⁵

$$\Gamma_{ij}{}^k = \frac{1}{2} a^{km} (\partial_i a_{jm} + \partial_j a_{im} - \partial_m a_{ij}) - a^{km} (S_{imj} - S_{mji} + S_{jim}) \\ + \frac{1}{2} a^{km} (Q_{ijm} + Q_{jim} - Q_{mij}), \quad (42)$$

⁴ [8] p. 144 ff.

⁵ [8] p. 132.

⁶ ∇ = Euclidean derivative, ϵ^{ijk} permutation symbol.

$$S_{ijk} = S_{ij}{}^m a_{mk}, \quad (43)$$

allows one to show that eqs (41) are equivalent to the torsion part (34) of the compatibility conditions. Therefore we use (41) as the nine compatibility conditions concerning torsion.

Equations (38) and (41) together with the equations of equilibrium and the material constitutive equations constitute the basic equations for the elastic problem.

If we include couple stresses into the consideration the energy-density-function depends on the elastic strain $\mathbf{e} = (e_{ij})$ and on the structure curvature $\mathbf{K} = (K_{imn})$.

From (38) and (41) we obtain $\mathbf{Q} \neq 0$ as a necessary condition for the existence of nonmechanical internal stresses. For $\mathbf{Q} = 0$ eqs (38) and (41) become compatibility conditions of a compatible deformed medium.

V. Quasidislocation and Quasidisclination Theory

Nonmechanical internal stresses may be included in a *linear* dislocation theory if one defines from the quasi-plastic distortion $\overset{Q}{\beta}$ the tensor of quasidislocation density⁷

$$\overset{Q}{\alpha} = \text{rot } \overset{Q}{\beta}. \quad (44)$$

$\overset{Q}{\beta}$ contains the quasi-plastic strain tensor $\overset{Q}{\epsilon}$ as well as a quasi-plastic rotation $\overset{Q}{\omega}$. However, the tensor $\overset{Q}{\omega}$ is physically underdetermined. In general one avoids this difficulty by omitting the quasi-plastic rotation and defining the quasi-dislocation density by

$$\overset{Q}{\alpha} = \text{rot } \overset{Q}{\epsilon}. \quad (45)$$

In this paper we generalize the idea of quasidislocations. To this aim we take the nonlinear theory of crystal dislocations as a guide [5].

For real dislocations the lattice connexion naturalizes simultaneously with the elastic metric [1, 3]. In comparison with the elastic metric the

⁷ [9] eq I.48.

lattice-connexion contains only the structure curvature \mathbf{K} as defined in (14) as an additional information.⁸ The hyperstrain \mathbf{E} , defined on (13), brings no additional information compared with \mathbf{a} .

In order to join the theory of nonmechanical stresses to the dislocation theory we define in the final state for the case of nonmechanical stresses an affine *elastic connexion*: $\gamma = (\gamma_{ij}^k)$ such that

- (1) γ naturalizes simultaneously with the elastic metric \mathbf{a} ,
- (2) gives via its connected hyperdeformation tensor

$$h_{ij}^k = \left\{ \begin{matrix} k \\ ij \end{matrix} \right\} - \gamma_{ij}^k \quad (46)$$

a curvature tensor

$$k_{imn} = h_{im}^k a_{kn} / [mn] \quad (47)$$

which equals the structure curvature \mathbf{K} of the lattice-connexion:

$$k_{imn} = K_{imn}. \quad (48)$$

The connexion γ exists uniquely. Because of condition 1 it is a metric connexion with respect to \mathbf{a} , i.e.,

$$\gamma_{ij}^k = \frac{1}{2} a^{km} (\partial_i a_{jm} + \partial_j a_{im} - \partial_m a_{ij}) - a^{km} (s_{imj} - s_{mji} + s_{jmi}) \quad (49)$$

(see (42)). We call its torsion tensor

$$s_{ijk} = \gamma_{[ij]}^{\quad p} a_{pk} \quad (50)$$

the *quasiplastic torsion tensor* $\overset{Q}{\alpha} = (\overset{Q}{\alpha}_{ijk})$. From (48), (49) and (37) we obtain

$$\boxed{\overset{Q}{\alpha}_{ijk} = -\frac{1}{2} Q_{[ij]k}} \quad (51)$$

Equation (28) leads to

$$\boxed{\overset{Q}{\alpha}_{ijk} = \nabla_{[i} q_{j]k}} \quad (52)$$

which is the nonlinear generalization of (45).

⁸ Lowering of the index with the elastic metric is important.

In general, the Riemann-Christoffel curvature tensor of the elastic connexion does not vanish. Together with (36) and

$$\gamma_{ijk} = \gamma_{ij}^m a_{mk}, \quad (53)$$

we obtain

$$\gamma_{ijk}^m a_{ml} \equiv \gamma_{ijkl} \equiv 2(\partial_i \gamma_{jkl} - \gamma_{ilp} \gamma_{jkq} a^{pq})_{[ij]} = -\overset{Q}{\theta}_{ijkl} \quad (54)$$

where

$$\boxed{\overset{Q}{\theta}_{ijkl} = \frac{1}{2} Q_{ilp} Q_{jkq} a^{pq} / [ij]} \quad (55)$$

is the tensor of the *quasi-disclination density*.

Equations (54) are completely equivalent to the compatibility conditions (36), whereas the compatibility conditions (41) read in terms of the quasi-plastic torsion

$$K_{imn} = k_{imn} = 2 \nabla_{[m} e_{n]}_i - (\overset{Q}{\alpha}_{imn} - \overset{Q}{\alpha}_{mni} + \overset{Q}{\alpha}_{nim}) \quad (56)$$

Both the tensors of quasi-disclination density and of quasi-plastic torsion are invariant with respect to physically unessential rotations of the natural state. Because of the identities for the Riemann-Christoffel curvature tensor they are intimately connected. Therefore the pair of tensors $\overset{Q}{\alpha}, \overset{Q}{\theta}$ as a whole is the nonlinear generalization of the quasi-dislocation density in linear theory.

The tensors $\overset{Q}{\alpha}$ and $\overset{Q}{\theta}$ are in close analogy to crystal dislocations and crystal disclinations [10, 11, 4]. Especially $\overset{Q}{\alpha}$ is analogous to the total torsion of dislocation-disclination-theory, where total torsion may be decomposed into dislocation-torsion and disclination-torsion. $\overset{Q}{\theta}$ corresponds to real disclination density.

For this reason we reserve the terminology *quasi-dislocation density* for the tensor $\overset{Q}{\alpha}$ to those special cases, where $\overset{Q}{\theta}$ vanishes.

The quasi-disclination density describes exclusively nonlinear effects. It disappears in the special case of thermal stresses as can easily be shown from (55) and (31). For magnetostrictive stresses it does not vanish. In linear approximation only the quasi-dislocation density is left over.

Generalizing the theory by adding real dislocations and disclinations we easily obtain the following statements: In general nonmechanical internal

stresses cannot be eliminated solely by a dislocation movement. An additional distribution of crystal disclinations is necessary [5].

In linear approximation dislocation movements suffice to eliminate nonmechanical stresses. The same is true within the nonlinear theory in the special case of thermal stresses.

These facts concerning the relation between real dislocation-disclination arrangements and nonmechanical stresses arise from the additive superposition of real and quasi-disclination density and of real total and quasiplastic torsion. The elastic connexion γ is constructed quite in the same way as in the case where real dislocations and disclinations are absent.

VI. Acknowledgement

I am very grateful to the Deutsche Forschungsgemeinschaft, which enabled me by a generous financial support to participate in the conference on Fundamental Aspects of Dislocation Theory.

VII. References

- [1] Kröner, E., Arch. Rat. Mech. Anal. **4**, 273 (1960).
- [2] Teodosiu, C., Rev. roum. sci. techn., sér. méc. appl. **12**, 961 and 1061 (1967).
- [3] Anthony, K. H., to appear in Arch. Rat. Mech. Anal. (1970).
- [4] Anthony, K. H., Die Theorie der Disklinationen. To be published.
- [5] Anthony, K. H., Theorie der nichtmetrischen Spannungen in Kristallen. To be published.
- [6] Bilby, B. A., Gardner, L. R. T., Grindbert, A. and Zorawski, M. Proc. Roy. Soc. **A292**, 105 (1966).
- [7] Becker, R. and Döring, W., Ferromagnetismus (Springer-Verlag, Berlin, 1939).
- [8] Schouten, J. A., Ricci-Calculus (Springer-Verlag, Berlin, 1954).
- [9] Kröner, E., Kontinuumstheorie der Versetzungen und Eigenspannungen Ergebn. Angew. Mathem. **5** (Springer-Verlag, Berlin, 1958).
- [10] Nabarro, F. R. N., Theory of Crystal Dislocations (Clarendon Press, Oxford, 1967).
- [11] Anthony, K. H., Essmann, U., Seeger, A., and Träuble, H., in Mechanics of Generalized Continua (IUTAM-Symposium Freudenstadt-Stuttgart, 1967) E. Kröner, Ed. (Springer-Verlag, Berlin, 1968) p. 355.

LINEAR THEORY OF STATIC DISCLINATIONS

R. deWit

*Metallurgy Division
National Bureau of Standards
Washington, D.C. 20234*

A brief review of compatible and incompatible elasticity theory is given. It is shown how dislocation theory was developed from classical compatible elasticity. Then disclination theory is developed from dislocation theory in an analogous way. The disclination and dislocation density tensors are defined from the plastic deformation. The total deformation satisfies the classical condition of compatibility. By combining these two concepts the geometric basic laws or field equations are found, which relate the elastic deformation to the defect content. The contortion or Nye curvature tensor is found to be a useful equivalent for the dislocation density. Weingarten's theorem motivates the generalization of the Burgers vector and the definition of the analogous rotation vector of disclinations. Finally the dualism between the geometry of disclination theory and the statics of couple-stress theory, as well as the relation of disclination theory to "motor calculus" are pointed out.

Key words: Burgers vector; compatibility; continuum; contortion; Cosserat; couple-stress; defect; deformation; disclination; dislocation; dualism; elasticity; incompatibility; motor calculus; plasticity.

I. Introduction

This work was motivated by recent interest in disclinations—for example, Nabarro [1] who has discussed some of their crystallographic aspects and Anthony et al. [2] who have observed such defects. Usually this type of defect has been ignored in the literature and no theory was available for it until Schaefer's recent papers [3]. However, Schaefer presents his results in the framework of the exterior calculus, into which he has incorporated his motor analysis [4]. Furthermore, he applies this to the Cosserat continuum and disclinations are then discussed as a special example of this general theory. This approach has not been helpful for the dislocation theorists as Schaefer [5] himself recognizes: "On the question of whether or when [the disclination density] vanishes

no clarity seems to exist in dislocation theory." This paper treats the theory from a more elementary and direct point of view.

Disclination theory is developed from dislocation theory in a way quite analogous to the way dislocation theory is developed from compatible classical elasticity theory by Kröner [6]. Actually it is a combined disclination and dislocation theory. In the same sense Kröner's theory is a combined compatible and incompatible theory, i.e., it is integrable in the rotation but not integrable in the displacement. The transition to disclination theory consists simply in the extension to non-integrable rotations. In this transition we find that many equations from dislocation theory generalize into pairs of equations in disclination theory.

The general approach is the same as that of Kröner. The *plastic deformation* is arbitrary and defines the defect content of the body. The *total deformation* satisfies the classical compatibility conditions for a body that undergoes an elasto-plastic deformation without breaking. By combining these two concepts we find the geometric basic laws or field equations that relate the *elastic deformation* to the defect content.

Section II reviews the classical compatibility conditions and section III Weingarten's theorem for multiply-connected bodies. Section IV reviews incompatible theory without specifying the nature of the defects. Section V reviews classical dislocation theory. Section VI develops disclination theory and section VII shows how Weingarten's theorem motivates the definition of the Burgers vector and the analogous rotation vector for disclinations. Section VIII shows the dualism between geometry and statics in defect theory, and in particular between disclination and couple-stress theory. Section IX shows the relation to Schaefer's new motor analysis.

II. Review of Compatible Theory

If a continuous simply-connected body undergoes an elastic deformation, then this deformation satisfies the classical conditions of compatibility. These conditions are a consequence of the fact that a *displacement* vector function \mathbf{u} can be defined for every point of the continuous body; hence, they are integrability conditions. In this section we find the compatibility conditions for the important field variables, namely the distortion β , the strain ϵ , the rotation ω , and the bend-twist κ .¹ We also discuss what these compatibility conditions, in turn, imply about the displacement.

(1) *The distortion* is defined:

$$\beta = \text{grad } \mathbf{u} \equiv \nabla \mathbf{u} \quad (2.1)$$

¹ The dyadic or symbolic notation is used for the sake of compactness. See, for example, Nadeau [7], Chapter One. The whole paper could equally well have been written in the index notation.

Assuming the existence of \mathbf{u} , then this definition implies that $\boldsymbol{\beta}$ satisfies the necessary condition:

$$\operatorname{curl} \boldsymbol{\beta} \equiv \nabla \times \boldsymbol{\beta} = 0, \quad (2.2)$$

which is the compatibility condition for $\boldsymbol{\beta}$. Conversely, by potential theory (Nadeau [7], p. 20), condition (2.2) is sufficient to assure the existence of a single-valued continuous solution of (2.1) for \mathbf{u} , up to a constant translation \mathbf{u}_0 .

(b) The strain is defined as the symmetric part of $\boldsymbol{\beta}$:

$$\boldsymbol{\epsilon} = \operatorname{def} \mathbf{u} \equiv 1/2 (\nabla \mathbf{u} + \mathbf{u} \nabla), \quad (2.3)$$

and the *rotation tensor* as the antisymmetric part of $\boldsymbol{\beta}$:

$$\boldsymbol{\omega} = 1/2 (\nabla \mathbf{u} - \mathbf{u} \nabla), \quad (2.4)$$

so that

$$\boldsymbol{\beta} = \boldsymbol{\epsilon} + \boldsymbol{\omega}. \quad (2.5)$$

For the antisymmetric tensor $\boldsymbol{\omega}$, we can equivalently use the *rotation vector* defined by (see appendix):

$$\vec{\boldsymbol{\omega}} \equiv 1/2 \langle \boldsymbol{\omega} \rangle. \quad (2.6)$$

Then the definition equivalent to (2.4) is

$$\vec{\boldsymbol{\omega}} = 1/2 \nabla \times \mathbf{u}, \quad (2.7)$$

which can be verified by substituting (2.4) into (2.6). Now, the definitions (2.3) and (2.7) imply that $\boldsymbol{\epsilon}$ and $\boldsymbol{\omega}$ satisfy the necessary conditions:

$$\operatorname{inc} \boldsymbol{\epsilon} \equiv \nabla \times \boldsymbol{\epsilon} \times \nabla = 0, \quad (2.8)$$

$$\nabla \cdot \vec{\boldsymbol{\omega}} = 0, \quad (2.9)$$

which are compatibility conditions for $\boldsymbol{\epsilon}$ and $\boldsymbol{\omega}$.

These conditions are also implied by (2.2). To show this, write (2.2)

$$\nabla \times \boldsymbol{\epsilon} + \boldsymbol{\delta} \nabla \cdot \vec{\boldsymbol{\omega}} - \vec{\boldsymbol{\omega}} \nabla = 0 \quad (2.10)$$

by (2.5), (2.6), and (A.6), where δ is the idemfactor or unit dyadic. The trace of this expression gives (2.9). Substituting (2.9) into (2.10) we have:

$$\nabla \times \boldsymbol{\epsilon} - \vec{\boldsymbol{\omega}} \nabla = 0. \quad (2.11a)$$

For convenience, we also note that the transpose of this equation is

$$-\boldsymbol{\epsilon} \times \nabla - \nabla \vec{\boldsymbol{\omega}} = 0. \quad (2.11b)$$

Conditions (2.8) and (2.9) now follow directly from these equations by taking the curl and the trace. From the above derivation we also see that (2.11) is completely equivalent with (2.10) and hence with (2.2).

We now want to consider the converse problem and ask what is implied by the compatibility conditions (2.8) and (2.9). We have seen that they are necessary for the existence of the displacement, but are they also sufficient? It will be shown that the answer to this is *no* (even though we are only considering a simply-connected body here).

Consider first condition (2.8). By potential theory (Fung [8], p. 99), this condition is sufficient to assure the existence of a single-valued continuous solution of (2.3) for \mathbf{u} , up to a rigid motion ($\mathbf{u}_0 + \vec{\boldsymbol{\omega}}_0 \times \mathbf{r}$). However, since we are not assuming that (2.2) is satisfied, this solution \mathbf{u} of (2.3) may not represent the displacement (whether or not (2.9) holds). Its existence only implies that

$$\boldsymbol{\beta} = 1/2(\nabla \mathbf{u} + \mathbf{u} \nabla) + \boldsymbol{\omega} \quad (2.12)$$

by (2.5), which is not equivalent to (2.1), unless (2.4) or (2.7) is also satisfied by the same solution \mathbf{u} . So (2.8) is a less restrictive condition than (2.2), for it puts no limitations on $\boldsymbol{\omega}$. But if now the condition (2.2) in the form (2.11a) is also imposed, we have

$$\left(1/2\nabla \times \mathbf{u} - \vec{\boldsymbol{\omega}}\right) \nabla = 0 \quad (2.13)$$

from (2.3). This condition implies that for this \mathbf{u} (2.7) is also satisfied by $\vec{\boldsymbol{\omega}}$, up to a constant rotation $\vec{\boldsymbol{\omega}}_0$, which can be determined from \mathbf{u} and $\vec{\boldsymbol{\omega}}$. Hence, \mathbf{u} now does represent the displacement, up to the rigid motion, and for this \mathbf{u} (2.1) is satisfied by $\boldsymbol{\beta}$, up to the constant rotation $\boldsymbol{\omega}_0$. So by redefining the total displacement to be ($\mathbf{u} + \mathbf{u}_0 + \vec{\boldsymbol{\omega}}_0 \times \mathbf{r}$) we obtain (2.1) and thus an alternate method of solution to that of subsection (a) above.

On the other hand, by potential theory (Phillips [9], p. 104), condition (2.9) is sufficient to assure the existence of a single-valued continuous

solution of (2.7) for \mathbf{u} , up to a potential deformation, which is defined by a displacement $\nabla\phi$. Again, this solution may not be the displacement (this time whether or not (2.8) holds). We can only write

$$\boldsymbol{\beta} = \boldsymbol{\epsilon} + 1/2(\nabla\mathbf{u} - \mathbf{u}\nabla), \quad (2.14)$$

which is not equivalent to (2.1), unless (2.3) is also satisfied. But once more, if condition (2.11a) is also imposed, we have

$$\nabla \times (\boldsymbol{\epsilon} - 1/2\mathbf{u}\nabla) = 0 \quad (2.15)$$

from (2.7). This condition implies that for this \mathbf{u} (2.3) is satisfied by $\boldsymbol{\epsilon}$, up to a potential deformation $\nabla\nabla\phi$, which can be determined from \mathbf{u} and $\boldsymbol{\epsilon}$. Hence, \mathbf{u} now does represent the displacement, up to the potential deformation, and for this \mathbf{u} (2.1) is satisfied by $\boldsymbol{\beta}$, except for the potential deformation $\nabla\nabla\phi$. By now redefining the displacement $(\mathbf{u} + \nabla\phi)$ we again arrive at the solution of subsection (a).

We may therefore remark that conditions (2.8) and (2.9) by themselves are not sufficient to assure the existence of a displacement function \mathbf{u} .² This point is usually not made by classical elasticity texts in the discussion of the compatibility conditions, because of the assumption that a displacement function exists.

(c) *The bend-twist*³ is defined:

$$\boldsymbol{\kappa} = \overrightarrow{\nabla\omega}. \quad (2.16)$$

This definition leads to the first compatibility condition for $\boldsymbol{\kappa}$:

$$\nabla \times \boldsymbol{\kappa} = 0. \quad (2.17)$$

The second compatibility condition for $\boldsymbol{\kappa}$ is found from (2.16) and (2.11b):

$$\boldsymbol{\kappa} = -\boldsymbol{\epsilon} \times \nabla. \quad (2.18)$$

² This is illustrated by an example from incompatible theory: For a constant distribution of edge dislocations, the displacement \mathbf{u} does not exist, since (2.2) is violated (c.f. 5.6), but (2.8) and (2.9) are satisfied by the strain $\boldsymbol{\epsilon}(=0)$ and the rotation $\vec{\omega}(=\mathbf{r} \cdot \mathbf{K})$, with $\mathbf{K} = \text{const.}$ and $K = 0$.

³ The term “bend-twist” is newly coined in this paper. The diagonal components described a twisting and the off-diagonal ones a bending. Mindlin and Tiersten [10] call it the curvature-twist and Koiter [11] the torsion-flexure. The elastic bend-twist is also frequently called the lattice curvature. The new term avoids possible confusion with the Riemann-Christoffel curvature and the Cartan torsion, which occur in the non-Riemannian formulation of the theory.

Note that (2.18) with (2.17) implies (2.8). Again, condition (2.17) is sufficient to assure the existence of a single-valued continuous solution of (2.16) for the rotation $\vec{\omega}$, up to a constant $\vec{\omega}_0$. If in addition condition (2.18) is also imposed, then (2.11b) follows. This implies that for this $\vec{\omega}$ there exists a single-valued continuous solution of (2.3) and (2.7) for \mathbf{u} , up to a constant translation \mathbf{u}_0 . For this \mathbf{u} (2.1) is satisfied by $\boldsymbol{\beta}$, up to the constant rotation $\vec{\omega}_0$. By redefining the rotation $(\vec{\omega} + \vec{\omega}_0)$ and the displacement $(\mathbf{u} + \mathbf{u}_0 + \vec{\omega}_0 \times \mathbf{r})$ we arrive at the solution of subsection (a) once more.

The third compatibility condition for κ is the vanishing of its trace

$$\kappa \equiv \text{Tr } \kappa = 0. \quad (2.19)$$

which follows from (2.18). Note that (2.19) with (2.17) implies (2.9).

So far we have only shown the *existence* of $\vec{\omega}$ and \mathbf{u} for compatible deformation of a simply-connected body. Actually, it is possible to give explicit expressions for these quantities. Suppose the fields κ and ϵ are known and satisfy the conditions (2.17), (2.18), and (2.19). Then it is only necessary to know $\vec{\omega}$ and \mathbf{u} at some particular point \mathbf{r}_0 to find their spatial dependence. The expressions can be derived as follows:

$$\vec{\omega}(\mathbf{r}) = \vec{\omega}(\mathbf{r}_0) + \int_{\mathbf{r}_0}^{\mathbf{r}} d\vec{\omega},$$

or

$$\vec{\omega}(\mathbf{r}) = \vec{\omega}_0 + \int_{\mathbf{r}_0}^{\mathbf{r}} d\mathbf{r}' \cdot \boldsymbol{\beta}(\mathbf{r}'), \quad (2.20)$$

$$\begin{aligned} \mathbf{u}(\mathbf{r}) &= \mathbf{u}_0 + \int_{\mathbf{r}_0}^{\mathbf{r}} d\mathbf{r}' \cdot \boldsymbol{\beta}(\mathbf{r}') \\ &= \mathbf{u}_0 + \int_{\mathbf{r}_0}^{\mathbf{r}} d\mathbf{r}' \cdot [\boldsymbol{\epsilon}' + \vec{\omega}'] \\ &= \mathbf{u}_0 + \int_{\mathbf{r}_0}^{\mathbf{r}} [d\mathbf{r}' \cdot \boldsymbol{\epsilon}' - d\{\vec{\omega}' \times (\mathbf{r} - \mathbf{r}')\} + d\vec{\omega}' \times (\mathbf{r} - \mathbf{r}')] \end{aligned}$$

or

$$\mathbf{u}(\mathbf{r}) = \mathbf{u}_0 + \vec{\omega}_0 \times (\mathbf{r} - \mathbf{r}_0) + \int_{\mathbf{r}_0}^{\mathbf{r}} d\mathbf{r}' \cdot [\boldsymbol{\epsilon}' + \boldsymbol{\kappa}' \times (\mathbf{r} - \mathbf{r}')]. \quad (2.21)$$

These results are single-valued if the line integrals are independent of path, or if they vanish for every closed C curve in the body. That this is so follows from Stokes' theorem with (2.17), (2.18), and (2.19):

$$\oint_C d\mathbf{r}' \cdot \boldsymbol{\kappa}' = \int_S d\mathbf{S}' \cdot \nabla' \times \boldsymbol{\kappa}' \\ = 0 \quad (2.22)$$

$$\oint_C d\mathbf{r}' \cdot [\boldsymbol{\epsilon}' + \boldsymbol{\kappa}' \times (\mathbf{r} - \mathbf{r}')] = \int_S d\mathbf{S}' \cdot \nabla' \times [\boldsymbol{\epsilon}' + \boldsymbol{\kappa}' \times (\mathbf{r} - \mathbf{r}')] \\ = \int_S d\mathbf{S}' \cdot [\nabla' \times \boldsymbol{\epsilon}' - (\nabla' \times \boldsymbol{\kappa}') \times (\mathbf{r} - \mathbf{r}') + \delta \boldsymbol{\kappa}' - \ddot{\boldsymbol{\kappa}}'] \\ = 0. \quad (2.23)$$

It is now easily verified that (2.20) and (2.21) satisfy (2.1), (2.3), (2.4) or (2.7), (2.9), (2.11), and (2.16).

In classical or compatible elasticity the elastic deformation of a simply-connected body satisfies all the equations of this section. The next section shows how these results may be modified for a multiply-connected body. The subsequent sections will then show that for defect or incompatible elasticity the elastic compatibility conditions are usually violated. However, for a simply-connected body that undergoes an elasto-plastic deformation without breaking, the *total* deformation will still be compatible and satisfy all the results of this section.

III. Multiply-Connected Bodies and Weingarten's Theorem

Consider a multiply-connected body for the purposes of this section only. We shall then define it as a compatible body if the compatibility conditions are satisfied.

What do these conditions now imply about the rotation and displacement functions, such as given by (2.20) and (2.21)? It is no longer possible to prove that they are single-valued by using Stokes' theorem as in (2.22) and (2.23) if C is irreducible (that is, it cannot be deformed continuously into a point without leaving the body). We shall now investigate the meaning of $\vec{\omega}$ and \mathbf{u} under these conditions. Let C_0 be a closed curve inside the body, which starts and ends at the point \mathbf{r}_0 , see figure 1. Then, if C_0 is irreducible, $\vec{\omega}$ and \mathbf{u} may not return to their original values on following this circuit around. The changes are given by setting $\mathbf{r} = \mathbf{r}_0$ in (2.20) and (2.21):

$$[\vec{\omega}] = \oint_{C_0} d\mathbf{r}' \cdot \boldsymbol{\kappa}', \quad (3.1)$$

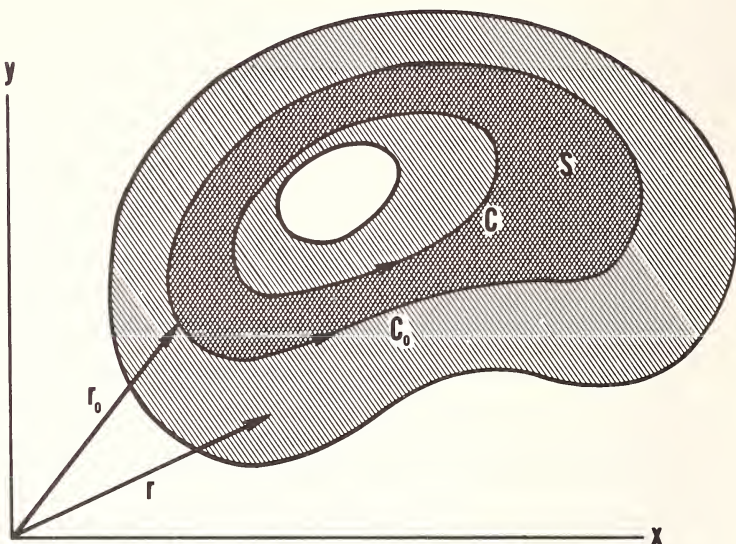


FIGURE 1

$$[\mathbf{u}] = \oint_{C_0} d\mathbf{r}' \cdot [\boldsymbol{\epsilon}' + \boldsymbol{\kappa}' \times (\mathbf{r}_0 - \mathbf{r}')]. \quad (3.2)$$

These expressions can be rewritten as follows

$$[\vec{\omega}] = \vec{\Omega}, \quad (3.3)$$

$$[\mathbf{u}] = \mathbf{b} + \vec{\Omega} \times \mathbf{r}_0, \quad (3.4)$$

where we have defined the constants

$$\vec{\Omega} \equiv \oint_C d\mathbf{r}' \cdot \boldsymbol{\kappa}', \quad (3.5)$$

$$\mathbf{b} \equiv \oint_C d\mathbf{r}' \cdot [\boldsymbol{\epsilon}' - \boldsymbol{\kappa}' \times \mathbf{r}'], \quad (3.6)$$

and where C is any curve reconcilable to C_0 (that is, it can be deformed continuously into C_0 without leaving the body). *Proof:* For $C = C_0$ the result is obvious. Otherwise there exists a surface S inside the body bounded by both C and C_0 (fig. 1), to which we can apply Stokes' theorem. Then by (2.17), (2.18), and (2.19) it easily follows that

$$\vec{\Omega}(C) = \vec{\Omega}(C_0) \text{ and } \mathbf{b}(C) = \mathbf{b}(C_0).$$

For a simply-connected body every circuit is reducible, so that C can be deformed into a point and $\vec{\Omega} = \mathbf{b} = 0$ or $[\vec{\omega}] = [\mathbf{u}] = 0$, as shown in section II for well-defined single-valued functions $\vec{\omega}$ and \mathbf{u} . For a multiply-connected body where C encircles a hole it is irreducible so that $\vec{\Omega}$ and \mathbf{b} do not necessarily vanish, but are constant for all reconcilable curves. In this case we can still regard $\vec{\omega}$ and \mathbf{u} as functions, but they could possibly be multiple-valued.

The relations (3.3) and (3.4) embody *Weingarten's Theorem*: On following around an irreducible circuit in a multiply-connected body satisfying the classical compatibility conditions, the rotation and displacement change by an amount that would be possible for a rigid body.

Further discussions of Weingarten's theorem are given by Nabarro [1] and Kessel [12]. It may be taken as the point of departure for a theory of discrete defects, where the defect region, which does not satisfy the compatibility conditions, is cut out of the body and we are left with a multiply-connected but compatible body. This approach is not pursued further in this paper. The next sections treat an alternate approach, where the defects are distributed continuously in a simply-connected but incompatible body.

IV. Review of Incompatible Theory

If a simply connected body undergoes an arbitrary plastic deformation, then this deformation does not necessarily satisfy the compatibility conditions. If the *plastic strain* $\boldsymbol{\epsilon}^P$ is prescribed, then this allows us to define the *incompatibility tensor*:

$$\boldsymbol{\eta} \equiv -\nabla \times \boldsymbol{\epsilon}^P \times \nabla. \quad (4.1)$$

For a compatible plastic deformation $\boldsymbol{\eta} = 0$, so that $\boldsymbol{\eta}$ measures the deviation from compatibility. The *fundamental meaning* of this equation is that an arbitrary plastic strain leads to incompatibility, which is just another word for defects. The *continuity condition*

$$\nabla \cdot \boldsymbol{\eta} = 0 \quad (4.2)$$

follows directly from (4.1).

Equation (4.1) is not useful for solving problems because $\boldsymbol{\epsilon}^P$ is not a state quantity, i.e., it cannot be determined from the state of the body. But the *elastic strain*⁴

$$\boldsymbol{\epsilon} = \boldsymbol{\epsilon}^T - \boldsymbol{\epsilon}^P \quad (4.3)$$

⁴The superscript E is dropped from the *elastic* quantities, such as strain $\boldsymbol{\epsilon}^E$, distortion β^E , rotations $\boldsymbol{\omega}^E$ and $\vec{\omega}^E$, and bend-twist $\boldsymbol{\kappa}^E$.

is a state quantity. Here $\boldsymbol{\epsilon}^T$ is the *total* strain. We now obtain the *geometric basic law* or field equation for $\boldsymbol{\eta}$:

$$\nabla \times \boldsymbol{\epsilon} \times \nabla = \boldsymbol{\eta} \quad (4.4)$$

from (4.3), (2.8) applied to $\boldsymbol{\epsilon}^T$, and (4.1). The *geometric meaning* of this equation is that if defects are present with a distribution given by $\boldsymbol{\eta}$, then elastic strain $\boldsymbol{\epsilon}$ is produced according to this law in order to insure the continuity of matter. Consequently this equation is the mathematical formulation of the statement that incompatibility is the source of elastic strain.

The basic problem of the linear static continuum theory of defects is defined by eq (4.4), together with the equilibrium equation for the stress, and the constitutive law between stress and strain. This problem has been treated by Kröner [6]. However, that treatment does not indicate the nature of the defects that contribute to $\boldsymbol{\eta}$.

V. Review of Dislocation Theory

If, in addition to the plastic strain $\boldsymbol{\epsilon}^P$, the plastic rotation $\boldsymbol{\omega}^P$ is also prescribed, then the defects may be identified as dislocations. In this case we can say, alternatively, that the plastic distortion

$$\boldsymbol{\beta}^P = \boldsymbol{\epsilon}^P + \boldsymbol{\omega}^P \quad (5.1)$$

is prescribed arbitrarily, where $\boldsymbol{\epsilon}^P$ and $\boldsymbol{\omega}^P$ are the symmetric and anti-symmetric parts of $\boldsymbol{\beta}^P$.

There are two ways of formulating dislocation theory, namely in terms of the dislocation density tensor, $\boldsymbol{\alpha}$, or the contortion tensor, \mathbf{K} .

(a) *The dislocation density* is defined:

$$\boldsymbol{\alpha} \equiv -\nabla \times \boldsymbol{\beta}^P. \quad (5.2)$$

This definition is motivated by (2.1) and (2.2). For a compatible plastic deformation $\boldsymbol{\alpha}=0$, so that $\boldsymbol{\alpha}$ gives a measure of the plastic incompatibility, i.e., $\boldsymbol{\alpha}$ contributes to $\boldsymbol{\eta}$. In fact, we see that

$$\boldsymbol{\eta} = (\boldsymbol{\alpha} \times \nabla)^S \quad (5.3)$$

from (4.1) and (5.2), where the superscript *S* stands for the symmetric part of the quantity in parentheses. The fundamental meaning of (5.2) is that an arbitrary plastic distortion leads to dislocations. The continuity condition

$$\nabla \cdot \boldsymbol{\alpha} = 0 \quad (5.4)$$

follows directly from (5.2). It implies that dislocations do not end inside the body. Now the elastic distortion is given by

$$\boldsymbol{\beta} = \boldsymbol{\beta}^T - \boldsymbol{\beta}' \quad (5.5)$$

and the geometric basic law or field equation for $\boldsymbol{\alpha}$:

$$\nabla \times \boldsymbol{\beta} = \boldsymbol{\alpha} \quad (5.6)$$

is obtained from (5.5), (2.2) applied to $\boldsymbol{\beta}^T$, and (5.2). The geometric meaning of this equation is that for a dislocation distribution, $\boldsymbol{\alpha}$, the elastic distortion, $\boldsymbol{\beta}$, is produced according to this law in order to insure the continuity of matter. Consequently this equation shows that dislocations are the source of elastic distortion.

(b) *The contortion*⁵ is defined:

$$\mathbf{K} \equiv -\boldsymbol{\epsilon}^P \times \nabla - \nabla \vec{\omega}^P. \quad (5.7)$$

This definition is motivated by (2.11b). For a compatible plastic deformation $\mathbf{K} = 0$, so that \mathbf{K} gives a measure of incompatibility. In fact

$$\boldsymbol{\eta} = \nabla \times \mathbf{K} \quad (5.8)$$

from (4.1) and (5.7). The fundamental meaning of (5.7) is that an arbitrary plastic strain and rotation leads to contortion. But the strain and rotation define the distortion, eq (5.1). Therefore \mathbf{K} must be related to $\boldsymbol{\alpha}$. To show this, first note that the transpose and trace of \mathbf{K} are

$$\hat{\mathbf{K}} = \nabla \times \boldsymbol{\epsilon}^P - \vec{\omega}^P \nabla, \quad (5.9a)$$

$$\mathbf{K} = -\nabla \cdot \vec{\omega}^P \quad (5.9b)$$

from (5.7). Now (5.2) can be written

$$\boldsymbol{\alpha} = -\nabla \times \boldsymbol{\epsilon}^P - \boldsymbol{\delta} \nabla \cdot \vec{\omega}^P + \vec{\omega}^P \nabla \quad (5.10a)$$

by (5.1) and (A.6). The trace is

$$\alpha = -2 \nabla \cdot \vec{\omega}^P. \quad (5.10b)$$

⁵ The use of the term “contortion” has been recommended by Kröner [13]. It is usually known as the Nye curvature. Note that the contortion, which is a source quantity, must be distinguished from the bend-twist, which is a field quantity.

Comparing (5.9) and (5.10) we see that

$$\alpha = \delta K - \overset{*}{\mathbf{K}}, \quad (5.11a)$$

$$\mathbf{K} = 1/2 \delta \alpha - \overset{*}{\alpha}. \quad (5.11b)$$

Now the elastic rotation is given by

$$\vec{\omega} = \vec{\omega}^T - \vec{\omega}^P \quad (5.12)$$

and the geometric basic law or field equation for \mathbf{K}

$$\epsilon \times \nabla + \nabla \vec{\omega} = \mathbf{K} \quad (5.13)$$

is obtained from (4.3), (5.12), (2.11b) applied to the total deformation, and (5.7). The geometric meaning and interpretation of this equation is similar to that for (5.6). Of course, (5.13) is equivalent to (5.6). This can be shown by noting first that

$$\beta = \epsilon + \omega \quad (5.14)$$

by (5.5), (2.5) applied to β^T , (5.1), (4.3), and (5.12). Then (5.6) can also be written

$$\nabla \times \epsilon + \delta \nabla \cdot \vec{\omega} - \vec{\omega} \nabla = \alpha \quad (5.15)$$

by (A.6). We see that this is equivalent to (5.13) by (5.11).

In this section we can also define the plastic bend-twist

$$\kappa^P = \nabla \vec{\omega}^P. \quad (5.16)$$

Defining the elastic bend-twist by

$$\kappa = \kappa^T - \kappa^P \quad (5.17)$$

we also have

$$\kappa = \nabla \vec{\omega} \quad (5.18)$$

from (2.16) applied to $\vec{\omega}^T$, (5.16), and (5.12). Then (5.7), (5.9), (5.10), (5.13), and (5.15) could equally well have been written in terms of these bend-twists. Note that (5.6) implies that the elastic displacement is undefined in this section, i.e., $d\mathbf{r} \cdot \beta$ need not be integrable, though $\vec{\omega}$ is well-defined.

VI. Disclination Theory

Since the elastic rotation of section V is a rigid body motion, it is not a true state quantity, but rather its variation is related to the state of the body. This suggests that the elastic bend-twist κ is the proper state quantity, together with the elastic strain ϵ . Then the elastic rotation is left undefined, a situation analogous to that for the elastic displacement in section V.

Similarly, to describe the defect content of the body, we leave the plastic rotation undefined, but prescribe arbitrarily the plastic bend-twist κ^P , together with the plastic strain ϵ^P . Then the results of section II for the total deformation and section IV remain valid, but those of section V are modified as we shall see below.

In the transition from classical elasticity to dislocation theory, (2.2) motivated the definition (5.2). Similarly, in the transition from dislocation to disclination theory, (2.17) motivates the following definition of the *disclination density*:

$$\theta \equiv -\nabla \times \kappa^P. \quad (6.1)$$

When only dislocations are present, then $\theta=0$ from (5.16), so that θ measures the deviation of the defects from pure dislocations. The *fundamental meaning* of this equation is that an arbitrary plastic bend-twist leads to disclinations. The continuity condition for θ :

$$\nabla \cdot \theta = 0 \quad (6.2)$$

follows directly from (6.1). It implies that disclinations do not end inside the body.

Now with arbitrarily prescribed ϵ^P and κ^P there may also be dislocations present. As in section V they can be described either by the dislocation density tensor α or the contortion tensor K . However, the definitions of these quantities in section V are no longer applicable. But the substitution of (5.16) into (5.10a) and (5.7) suggests the following definitions:

$$\alpha \equiv -\nabla \times \epsilon^P - \delta \kappa^P + \overset{*}{\kappa^P}, \quad (6.3)$$

$$K \equiv -\epsilon^P \times \nabla - \kappa^P. \quad (6.4)$$

These definitions imply that, when the disclination density vanishes, the results of this section will reduce to those of section V; for when $\theta=0$ (6.1) is essentially equivalent to (5.16) as we saw in section IIc. We see that α and K are still related by (5.11):

$$\alpha = \delta K - \overset{*}{K}, \quad (6.5a)$$

$$\mathbf{K} = 1/2 \delta \boldsymbol{\alpha} - \overset{*}{\boldsymbol{\alpha}}. \quad (6.5b)$$

For a compatible plastic deformation we know that $\boldsymbol{\alpha} = \mathbf{K} = 0$, so that $\boldsymbol{\alpha}$ and \mathbf{K} still give a measure of incompatibility. In fact we can now see how the dislocations and disclinations each contribute to the incompatibility:

$$\boldsymbol{\eta} = (\boldsymbol{\alpha} \times \nabla - \boldsymbol{\theta})^s \quad (6.6)$$

$$= \nabla \times \mathbf{K} - \boldsymbol{\theta} \quad (6.7)$$

from (6.3), (6.4), (6.1), and (4.1). The *fundamental meaning* of (6.3) and (6.4) now is that an arbitrary plastic strain and bend-twist leads to dislocations or contortion. The continuity condition for $\boldsymbol{\alpha}$:

$$\nabla \cdot \boldsymbol{\alpha} + 2\vec{\boldsymbol{\theta}} = 0 \quad (6.8)$$

follows from (6.3), (6.1), and (A.7). We suggest that this equation implies that dislocations can only end on disclinations, in which case the disclination density $\boldsymbol{\theta}$ is asymmetric. However, K. H. Anthony has a different interpretation for (6.8). (See the Discussion at the end of this Conference Session and Panel on Intrinsic Properties of Dislocations.) In terms of \mathbf{K} the continuity condition reads

$$\nabla \mathbf{K} - \mathbf{K} \cdot \nabla + 2\vec{\boldsymbol{\theta}} = 0 \quad (6.9)$$

by (6.5a). We now investigate the consistency of (6.6) and (6.7) with the requirements on $\boldsymbol{\eta}$ of symmetry, (4.1), and continuity, (4.2). The symmetry of (6.6) is obvious and the continuity follows from (6.2), (A.8), and (6.8):

$$\begin{aligned} 2\nabla \cdot \boldsymbol{\eta} &= \nabla \cdot \boldsymbol{\alpha} \times \nabla - \nabla \cdot \boldsymbol{\theta} - \boldsymbol{\theta} \cdot \nabla \\ &= \nabla \cdot \boldsymbol{\alpha} \times \nabla - 2\nabla \times \vec{\boldsymbol{\theta}} \\ &= (\nabla \cdot \boldsymbol{\alpha} + 2\vec{\boldsymbol{\theta}}) \times \nabla \\ &= 0. \end{aligned}$$

The continuity of (6.7) follows immediately from (6.2) and the symmetry from (A.7) and (6.9):

$$\begin{aligned} 2\vec{\boldsymbol{\eta}} &= (\nabla \times \mathbf{K}) - 2\vec{\boldsymbol{\theta}} \\ &= \mathbf{K} \cdot \nabla - \nabla \mathbf{K} - 2\vec{\boldsymbol{\theta}} \\ &= 0. \end{aligned}$$

The *geometric basic law* or field equation for θ :

$$\nabla \times \kappa = \theta \quad (6.10)$$

is found from (5.17), (6.1), and (2.17) applied to κ^T , and those for α and \mathbf{K} :

$$\nabla \times \epsilon + \delta\kappa - \overset{*}{\kappa} = \alpha, \quad (6.11)$$

$$\epsilon \times \nabla + \kappa = \mathbf{K} \quad (6.12)$$

from (4.3), (5.17), (2.18) and (2.19) applied to the total deformation, (6.3), and (6.4). When (5.18) holds we see that (6.10) vanishes, (6.11) reduces to (5.15), and (6.12) reduces to (5.13). The *geometric meaning* of (6.10), (6.11), and (6.12) is that for disclination and dislocation distributions given by θ and α or \mathbf{K} elastic strain and bend-twist are produced according to these laws to insure the continuity of matter. Consequently these equations show that disclinations and dislocations are the sources of elastic strain and bend-twist. Note that when disclinations are present the dislocations are no longer the source of elastic distortion, which does not then exist.

VII. Rotation and Burgers Vectors

Weingarten's theorem, discussed in section III, is used to motivate the definitions of the following quantities in an incompatible simply-connected body:

$$\vec{\Omega} = \oint_C d\mathbf{r} \cdot \kappa, \quad (7.1)$$

$$\mathbf{b} = \oint_C d\mathbf{r} \cdot [\epsilon - \kappa \times \mathbf{r}], \quad (7.2)$$

where C is a closed curve called the *Burgers circuit*. These quantities can be related to θ and α by applying Stokes' theorem to any surface S inside the body bounded by C :

$$\begin{aligned} \vec{\Omega} &= \int_S d\mathbf{S} \cdot \nabla \times \kappa \\ &= \int_S d\mathbf{S} \cdot \theta, \end{aligned} \quad (7.3)$$

$$\begin{aligned} \mathbf{b} &= \int_S d\mathbf{S} \cdot [\nabla \times \epsilon - (\nabla \times \kappa) \times \mathbf{r} + \delta\kappa - \overset{*}{\kappa}] \\ &= \int_S d\mathbf{S} \cdot [\alpha - \theta \times \mathbf{r}] \end{aligned} \quad (7.4)$$

by (6.10) and (6.11). We therefore have the following interpretation: $\vec{\Omega}$ is the *rotation vector* of the disclinations crossing S and \mathbf{b} is the *general*

Burgers vector of the dislocations and disclinations crossing S . We know that the diagonal and off-diagonal components of α correspond to the screw and edge components of the dislocations. Equation (7.3) shows that the diagonal components of θ correspond to the wedge components of the disclinations. It was suggested at this Conference to call the off-diagonal components of θ the twist components of the disclinations.⁶ (See Panel on Intrinsic Properties of Dislocations.)

Now let S be a closed surface bounding the volume V . Then, applying the divergence theorem:

$$\begin{aligned}\vec{\Omega} &= \int_V dV \nabla \cdot \theta \\ &= 0, \\ \mathbf{b} &= \int_V dV \nabla \cdot (\alpha - \theta \times \mathbf{r}) \\ &= \int_V dV [\nabla \cdot \alpha - (\nabla \cdot \theta) \times \mathbf{r} + \vec{\theta}] \\ &= 0\end{aligned}$$

by (6.2) and (6.8). So the continuity equations for θ and α correspond to conservation theorems for $\vec{\Omega}$ and \mathbf{b} .

VIII. Relation to Couple-Stress Theory

The *dualism* between the geometry and statics of defect theory has been pointed out by Kondo [14]. The equilibrium equation for the stress tensor σ is

$$\nabla \cdot \sigma = 0, \quad (8.1)$$

when no body forces are present. By potential theory we can therefore find a tensor ϕ such that

$$\sigma = \nabla \times \phi \times \nabla, \quad (8.2)$$

for a symmetric stress, where ϕ is called the *Beltrami stress function tensor*. It is seen that (8.1) and (8.2) are dual to (4.2) and (4.4). The connection between geometry and statics is provided by Hooke's law

$$\sigma = c : \epsilon \quad (8.3)$$

in classical elasticity. These results are summarized in table 1.

⁶ Nabarro [1] calls them screw and edge disclinations, respectively.

TABLE 1. *Dualism between geometry and statics of defect theory*

Geometry	Statics
η	σ
ϵ	ϕ
$\nabla \cdot \eta = 0$	$\nabla \cdot \sigma = 0$
$\nabla \times \epsilon \times \nabla = \eta$	$\sigma = \nabla \times \phi \times \nabla$
<i>Relation between geometry and statics</i>	
$\sigma = c : \epsilon$	

An alternative and more detailed dualism exists between the geometry of disclination theory and the statics of couple-stress theory.⁷ In addition to (8.1) there is then an equilibrium equation for the couple-stress tensor μ

$$\nabla \cdot \mu + 2\vec{\sigma} = 0, \quad (8.4)$$

when no body-couples are present. Now σ is no longer necessarily symmetric. By potential theory the pair (8.1) and (8.4) again assures the existence of two tensors \mathbf{F} and \mathbf{G} , such that

$$\sigma = \nabla \times \mathbf{F}, \quad (8.5)$$

$$\mu = \nabla \times \mathbf{G} + \delta \mathbf{F} - \mathbf{F}^*, \quad (8.6)$$

where \mathbf{F} and \mathbf{G} are called the *Günther stress functions tensors* [15]. Equations (8.1), (8.4), (8.5), and (8.6) are now dual to (6.2), (6.8), (6.10), and (6.11). This dualism suggests the following connection between the geometry of disclination theory and the statics of couple-stress theory:

$$\sigma = d : \kappa + c : \epsilon, \quad (8.7)$$

$$\mu = a : \kappa + b : \epsilon. \quad (8.8)$$

These results are summarized in table 2.

⁷A simple derivation of couple-stress theory is given by Mindlin and Tiersten [10].

TABLE 2. *Dualism between geometry of disclination theory and statics of couple-stress theory.*

Geometry	Statics
θ	σ
α	μ
κ	F
ϵ	G
$\nabla \cdot \theta = 0$	$\nabla \cdot \sigma = 0$
$\nabla \cdot \alpha + 2\theta = 0$	$\nabla \cdot \mu + 2\sigma = 0$
$\nabla \times \kappa = \theta$	$\sigma = \nabla \times F$
$\nabla \times \epsilon + \delta \kappa - \kappa = \alpha$	$\mu = \nabla \times G + \delta F - F$

Relation between geometry and statics

$$\begin{aligned}\sigma &= d : \kappa + c : \epsilon \\ \mu &= a : \kappa + b : \epsilon\end{aligned}$$

The constitutive equations (8.7) and (8.8) are more general than those for *compatible* couple-stress theory as given by Mindlin and Tiersten [10]. This is because *incompatible* couple-stress theory no longer has the restriction that κ vanishes, as can be seen from (6.11) or (6.12). However, they are a special case of those for the *Cosserat-continuum* as given by Kessel [16], because ϵ is symmetric. Disclination theory is an *incompatible constrained Cosserat theory* in Kessel's terminology, or a *theory of the incompatible pseudo-Cosserat-continuum* in Schaefer's words [5], or an *incompatible "indeterminate" couple stress theory* according to Eringen [17]. This suggests that the present theory could easily be extended into an incompatible Cosserat theory by generalizing κ and ϵ into the Cosserat deformation tensors.

Kröner [18] has considered the dualism from a somewhat different point of view. Instead of the Günther stress function tensors he uses the stress functions

$$\psi = 1/2\delta\mu - \overset{*}{\mu}, \quad (8.9)$$

$$\chi = G^S, \quad (8.10)$$

dual to K and ϵ . Then by eliminating F (8.5) and (8.6) can also be written

$$\sigma = -\nabla \times \chi \times \nabla + \nabla \times \psi \quad (8.11)$$

$$\mu = \delta\psi - \overset{*}{\psi}, \quad (8.12)$$

which are dual to (6.7) with (4.4) and (6.5a). However this dualism suggests different constitutive equations:

$$\sigma = d : \mathbf{K} + c : \epsilon, \quad (8.13)$$

$$\mu = a : \mathbf{K} + b : \epsilon, \quad (8.14)$$

which Kröner prefers. These results are summarized in table 3.

TABLE 3. *Dualism between geometry of disclination theory and statics of couple-stress theory, according to Kröner*

Geometry	Statics
θ	σ
α	μ
\mathbf{K}	ψ
ϵ	χ
$\theta = -\nabla \times \epsilon \times \nabla + \nabla \times \kappa$	$\sigma = -\nabla \times \chi \times \nabla + \nabla \times \psi$
$\alpha = \delta K - \bar{K}$	$\mu = \delta \psi - \bar{\psi}$
<i>Relation between geometry and statics</i>	
$\sigma = d : \mathbf{K} + c : \epsilon$	
$\mu = a : \mathbf{K} + b : \epsilon$	

These dualisms show how an understanding of the geometry of defects may provide an insight into the statics of continuum mechanics. For example, Kondo [14] has reduced the study of many physical phenomena, such as yielding, to a study of geometry in Schaefer-space. The dualisms also explain the new terminology, such as dual dislocations for couple-stresses.

IX. Relation to Motor Calculus

Note that \mathbf{b} is not invariant under a coordinate translation. If a new origin of coordinates, $0'$, is chosen whose position is, \mathbf{r}_c , with respect to the old system, 0 , then the new radius vector, \mathbf{r}' , is related to the old, \mathbf{r} , by

$$\mathbf{r}' = \mathbf{r} - \mathbf{r}_c. \quad (9.1)$$

We now find

$$\vec{\Omega}' = \vec{\Omega} \quad (9.2)$$

$$\mathbf{b}' = \mathbf{b} + \vec{\Omega} \times \mathbf{r}_c \quad (9.3)$$

either from (7.1) and (7.2) or from (7.3) and (7.4). A pair of finite vectors that behaves this way is called a *motor*, and the motor algebra was developed by von Mises [19] more than forty years ago to describe the motion of rigid bodies.

Schaefer [4,3] recently made this into a motor analysis by extending the meaning of the ∇ -operator when it acts on an infinitesimal motor (\mathbf{V}, \mathbf{W}) as follows

$$\nabla \begin{pmatrix} \mathbf{V} \\ \mathbf{W} \end{pmatrix} \equiv \begin{pmatrix} \nabla \mathbf{V} \\ \nabla \mathbf{W} + \mathbf{V} \times \boldsymbol{\delta} \end{pmatrix}, \quad (9.4)$$

which is suggested by (9.2) and (9.3). This relation gives the gradient of a motor. By inserting a dot or a cross it also defines the divergence and curl,

$$\nabla \cdot \begin{pmatrix} \mathbf{V} \\ \mathbf{W} \end{pmatrix} \equiv \begin{pmatrix} \nabla \cdot \mathbf{V} \\ \nabla \cdot \mathbf{W} + \mathbf{V} \cdot \boldsymbol{\delta} \end{pmatrix}, \quad (9.5a)$$

$$\nabla \times \begin{pmatrix} \mathbf{V} \\ \mathbf{W} \end{pmatrix} \equiv \begin{pmatrix} \nabla \times \mathbf{V} \\ \nabla \times \mathbf{W} + \mathbf{V} \times \boldsymbol{\delta} \end{pmatrix}. \quad (9.5a)$$

These relations were also assumed to hold for a higher rank tensor motor. Kessel [20] has used this approach to obtain special results for the Cosserat continuum. In the present paper we see that this formulation simplifies many pairs of equations as follows

$$\begin{pmatrix} \boldsymbol{\theta} \\ \boldsymbol{\alpha} \end{pmatrix} \equiv -\nabla \times \begin{pmatrix} \boldsymbol{\kappa}^P \\ \boldsymbol{\epsilon}^P \end{pmatrix}, \quad (6.1,3)$$

$$\nabla \cdot \begin{pmatrix} \boldsymbol{\theta} \\ \boldsymbol{\alpha} \end{pmatrix} = 0, \quad (6.2,8)$$

$$\nabla \times \begin{pmatrix} \boldsymbol{\kappa} \\ \boldsymbol{\epsilon} \end{pmatrix} = \begin{pmatrix} \boldsymbol{\theta} \\ \boldsymbol{\alpha} \end{pmatrix} \quad (6.10,11)$$

$$\nabla \cdot \begin{pmatrix} \boldsymbol{\sigma} \\ \boldsymbol{\mu} \end{pmatrix} = 0, \quad (8.1,4)$$

$$\begin{pmatrix} \boldsymbol{\sigma} \\ \boldsymbol{\mu} \end{pmatrix} = \nabla \times \begin{pmatrix} \mathbf{F} \\ \mathbf{G} \end{pmatrix}, \quad (8.5,6)$$

$$\begin{pmatrix} \boldsymbol{\sigma} \\ \boldsymbol{\mu} \end{pmatrix} = \begin{pmatrix} d & c \\ a & b \end{pmatrix} : \begin{pmatrix} \boldsymbol{\kappa} \\ \boldsymbol{\epsilon} \end{pmatrix}. \quad (8.7.8)$$

It is next interesting to note that these equations, except for (8.5,6), are identical in form to those for Kröner's [6] classical dislocation theory, i.e., (5.2), (5.4), (5.6), (8.1), and (8.3). Schaefer has noted this result in the non-Riemannian formulation of the theory. In this formulation of classical dislocation theory $\boldsymbol{\alpha}$ becomes equivalent to the Cartan torsion in a three-dimensional space with distant parallelism. Schaefer [3] generalizes this concept to disclination theory by making $(\boldsymbol{\theta}, \boldsymbol{\alpha})$ equivalent to the Cartan torsion motor in a six-dimensional motor space with distant parallelism.⁸

X. Summary and Discussion

We've given a short review of compatible, incompatible, and dislocation theory. Then we showed that disclination theory is a logical step in the extension of the continuum theory of defects. In this transition we found that many equations from dislocation theory generalize into pairs of equations in disclination theory. We found that the contortion \mathbf{K} can be used as an alternative description for the dislocation density $\boldsymbol{\alpha}$ when disclinations are present. Weingarten's theorem motivates the generalization of the Burgers vector \mathbf{b} and the definition of the analogous rotation vector $\vec{\Omega}$ for disclinations. We have pointed out the dualism between the geometry of disclinations and the statics of couple-stress theory, which could be a useful guideline for further research. We have also pointed out the relation to motor calculus, which may be another direction for future research.

A further step in the extension of the theory of defects might be the introduction of the continuum analog of point defects. These could be represented either by Eshelby's [21] "stress-free strain" \mathbf{e}^T or Kroupa's [22] dislocation loop density $\boldsymbol{\gamma}$. It would be interesting to see how this would generalize the results of dislocation theory. For example, it is expected at first sight that (6.6) and (6.7) would become

$$\begin{aligned} \boldsymbol{\eta} &= (\nabla \times \boldsymbol{\gamma} \times \nabla + \boldsymbol{\alpha} \times \nabla - \boldsymbol{\theta})^S \\ &= -\nabla \times \mathbf{e}^T \times \nabla + \nabla \times \boldsymbol{\kappa} - \boldsymbol{\theta} \end{aligned}$$

in the linear formulation of the theory.

⁸ Another non-Riemannian formulation of disclination theory is to make $\boldsymbol{\alpha}$ and $\boldsymbol{\theta}$ equivalent to the Cartan torsion and Riemann-Christoffel curvature in a three-dimensional space. For non-vanishing $\boldsymbol{\theta}$ there is, then, no distant parallelism.

XI. Appendix

We derive the three identities for dyadics that are used in this paper by specializing to Cartesian components. See Nadeau [7] for details. The rotation and curl of a tensor τ are defined by:

$$\langle \tau \rangle = e_{ijk} \tau_{ij} \mathbf{a}_k, \quad (\text{A.1})$$

$$\nabla \times \tau = \mathbf{a}_i e_{ijk} \partial_j \tau_{kl} \mathbf{a}_l, \quad (\text{A.2})$$

where e_{ijk} is the permutation symbol, \mathbf{a}_i the Cartesian base vector, and the Einstein summation convention is used. Furthermore, the associated rotation vector is defined:

$$\vec{\tau} = 1/2 \langle \tau \rangle, \quad (\text{A.3})$$

or in index notation:

$$\tau_k = 1/2 e_{ijk} \tau_{ij}. \quad (\text{A.4})$$

It follows that the antisymmetric part of τ_{ij} is

$$\tau_{ij}^A = e_{ijk} \tau_k. \quad (\text{A.5})$$

We now derive the first identity:

$$\begin{aligned} \nabla \times \tau^A &= \mathbf{a}_i e_{ijk} \partial_j e_{klm} \tau_m \mathbf{a}_l \\ &= (\delta_{il} \delta_{jm} - \delta_{im} \delta_{jl}) \mathbf{a}_i \partial_j \tau_m \mathbf{a}_l \\ &= \mathbf{a}_i \partial_j \tau_j \mathbf{a}_i - \mathbf{a}_i \partial_j \tau_i \mathbf{a}_j \\ &= \boldsymbol{\delta} \nabla \cdot \vec{\tau} - \vec{\tau} \nabla, \end{aligned} \quad (\text{A.6})$$

where

$$\boldsymbol{\delta} = \mathbf{a}_i \mathbf{a}_i$$

is the idemfactor or unit dyadic.

The second identity is:

$$\begin{aligned} \langle \nabla \times \tau \rangle &= e_{ilm} e_{ijk} \partial_j \tau_{kl} \mathbf{a}_m \\ &= (\delta_{lj} \delta_{mk} - \delta_{lk} \delta_{mj}) \partial_j \tau_{kl} \mathbf{a}_m \\ &= \partial_j \tau_{kj} \mathbf{a}_k - \partial_j \tau_{kk} \mathbf{a}_j \\ &= \tau \cdot \nabla - \nabla \tau. \end{aligned} \quad (\text{A.7})$$

The third identity is:

$$\begin{aligned}
 2\nabla \times \vec{\tau} &= 2\mathbf{a}_i e_{ijk} \partial_j \tau_k \\
 &= \mathbf{a}_i e_{ijk} \partial_j e_{klm} \tau_{lm} \\
 &= (\delta_{il} \delta_{jm} - \delta_{im} \delta_{jl}) \mathbf{a}_i \partial_j \tau_{lm} \\
 &= \mathbf{a}_i \partial_j \tau_{ij} - \mathbf{a}_i \partial_j \tau_{ji} \\
 &= \boldsymbol{\tau} \cdot \nabla - \nabla \cdot \boldsymbol{\tau}.
 \end{aligned} \tag{A.8}$$

XII. References

- [1] Nabarro, F. R. N., Theory of Crystal Dislocations (Clarendon Press, Oxford, 1967).
- [2] Anthony, K., Essmann, U., Seeger, A., and Trauble, H., in Mechanics of Generalized Continua (Proc. IUTAM Symposium, Freudenstadt-Stuttgart, 1967), E. Kröner, Ed. (Springer-Verlag, Berlin, 1968) p. 355.
- [3] Schaefer, H., ZAMM **47**, 319 (1967) and in Mechanics of Generalized Continua (Proc. IUTAM Symposium, Freudenstadt-Stuttgart, 1967), E. Kröner, Ed. (Springer-Verlag, Berlin, 1968) p. 57.
- [4] Schaefer, H., Bull. Acad. Pol. Sci. **15**, 63, 69 (1967).
- [5] Schaefer, H., ZAMM **47**, 485 (1967).
- [6] Kröner, E., Erg. Angew. Math. **5**, 1 (1958).
- [7] Nadeau, G., Introduction to Elasticity (Holt, Rinehart and Winston, New York, 1964).
- [8] Fung, Y. C., Foundations of Solid Mechanics (Prentice-Hall, Englewood Cliffs, N.J., 1965).
- [9] Phillips, H. B., Vector Analysis (Wiley, New York, 1963).
- [10] Mindlin, R. D., and Tiersten, H. F., Arch. Rat. Mech. Anal. **11**, 415 (1962).
- [11] Koiter, W. T., Proc. Kon. Ned. Akad. Wetensch. **B67**, 17 (1964).
- [12] Kessel, S., Abh. d. Brschw. Wiss. Ges. **17**, 51 (1965).
- [13] Kröner, E., in Mechanics of Generalized Continua (Proc. IUTAM Symposium, Freudenstadt-Stuttgart, 1967), E. Kröner, Ed. (Springer-Verlag, Berlin, 1968) p. 330.
- [14] Kondo, K., in Mechanics of Generalized Continua (Proc. IUTAM Symposium, Freudenstadt-Stuttgart, 1967), E. Kröner, Ed. (Springer-Verlag, Berlin, 1968) p. 200.
- [15] Günther, W., Abh. d. Brschw. Wiss. Ges. **10**, 195 (1958).
- [16] Kessel, S., Abh. d. Brschw. Wiss. Ges. **16**, 1 (1964).
- [17] Eringen, A. C., in Mechanics of Generalized Continua (Proc. IUTAM Symposium, Freudenstadt-Stuttgart, 1967), E. Kröner, Ed. (Springer-Verlag, Berlin, 1968) p. 18.
- [18] Kröner, E., Appl. Mech. Rev. **15**, 599 (1962). Int. J. Engng. Sci. **1**, 261 (1963). Mat. Sci. Res. **1**, 281 (1963).
- [19] von Mises, R., ZAMM **4**, 155, 193 (1924).
- [20] Kessel, S., ZAMM **47**, 329 (1967), and in Mechanics of Generalized continua (Proc. IUTAM Symposium, Freudenstadt-Stuttgart, 1967), E. Kröner, Ed. (Springer-Verlag, Berlin, 1968) p. 114.
- [21] Eshelby, J. D., Progr. Sol. Mech. **2**, 89 (1961).
- [22] Kroupa, F., Czech. J. Phys. **B12**, 191 (1962).

Discussion on Papers by F. R. N. Nabarro, K. H. Anthony, and R. de Wit.

MURA: Professor Nabarro, in your definition of disclinations you have to introduce a vector field, otherwise you cannot define the disclinations. The original definition of Volterra's rotational dislocation is given without introducing the vector field. It appears to me that there are several ways to define disclinations, and yours might be one of them, and there could be others. This is a matter of definition of rotation. Do you agree?

NABARRO: I agree entirely, and you have hit upon the weakness of what I have done. It seems to me that I would have done better not to deal with the vector field but to deal with the field of undirected lines, because I have to use in this discussion the convention that I can cross a line of constant misorientation and take no notice of it. The difficulty with the Volterra definition is that it deals with the elastic distortion of a body. It refers to an initial state of the body. Here we have not got an initial state, we have got a body as it is. I would add one further complication. One needs to distinguish, in the case of a surface carrying a pattern, between the disclination of the pattern and the disclination of the surface. In the case of the cross cap there is no disclination in the pattern but there is in the surface underlying it.

MURA: I have another question for Dr. de Wit. In your theory can you express your total distortion at the sum of plastic distortion and elastic distortion?

DE WIT: The distortion does not exist when there are disclinations.

MURA: Consider a twisted circular surface, as Professor Bollmann discussed, which then has an edge type disclination around its boundary. Now I can define the plastic distortion¹ $\beta_{z\theta}^* = \omega r \delta(z)H(R=r)$ and define nicely the disclination line. So I don't understand why you can not define the plastic distortion.

DE WIT: For a discrete disclination you can define the distortion away from the disclination, but it would be multiple-valued in the same way that for a discrete dislocation the displacement is multiple-valued.

¹ ω = constant rotation angle.

r = radius from the center of rotation

δ = Dirac delta function

H = Heavyside function

R = radius of the disclination loop

MURA: I see. Thank you.

DE WIT: I have a question for Professor Nabarro. The reason I have a whorl, here, on the top of my head is due to the furry ball theorem, but I don't have two of them because my whole face is not covered with hair; is that right?

NABARRO: May I quote from that great man, Dirac: "That is not a question; it is a statement."

ANTHONY: Dr. de Wit, you mention in your paper that in certain cases there is a possibility that disclinations become sources of dislocation lines. This would be a very important physical feature. Can you give any idea for visualizing this fact in terms of crystal lattice structures.

DE WIT: I have not worked this out. So I don't know yet what the significance of this equation is. One should work out an example.

ANTHONY: May I give a short discussion of this effect: As I have pointed out at the IUTAM-Symposium in 1967,² I also believed in a possibility that certain arrangements of disclination lines become sources of dislocations. This opinion was based on the mathematical structure of continuum theory. But now I am convinced that this standpoint is wrong because of the following facts: A disclination is characterized by a non-absolute lattice parallelism, whereas dislocations always belong to an absolute lattice parallelism. Now, if a certain disclination arrangement defines the source distribution of a certain dislocation arrangement, the disclination arrangement may be produced by adding the dislocations successively, i.e. a non-absolute lattice parallelism is produced by a superposition of absolute parallelisms. Obviously this is impossible. Therefore disclinations can never be sources of dislocation lines.

BEN-ABRAHAM: I would like to cut into this discussion between Dr. de Wit and Dr. Anthony. Dr. de Wit states a theorem that disclinations do not end inside the crystal. The general formulation of this theorem is the well-known Bianchi identity³ and the disclinations are the curvature in mathematical language. Now on the right-hand side of this equation we have a term which is essentially the product of curvature and torsion (i.e. dislocations), so that this theorem just holds under a certain assumption. On the other hand, I would like to answer Dr. Anthony: I believe that as long as we have a crystal and the crystal is defined in terms of continuum theory by vanishing curvature, it is right that there can be no disclina-

² Anthony, K., et al., in Mechanics of Generalized Continua, (Proc. IUTAM Symposium, Freudenstadt-Stuttgart, 1967), E. Kröner, Ed. (Springer-Verlag, Berlin, 1968) p. 355.

³ See eq (III.5.19) in Schouten, J. A., Ricci-Calculus (Springer-Verlag, Berlin, 1954).

tions because the curvature has to be zero and that defines distant parallelism. But the things we have to think about are liquids, or—as we already heard today—liquid crystals or glass-like structures. Well, then, neither the theorem that dislocations don't end in the body, nor the theorem that disclinations don't end in the body is valid, but rather both kinds of defects are present. That is where disclinations are really relevant, or, as we have seen, in two dimensions.

ANTHONY: From the point of view of continuum theory I agree with your arguments concerning sources of dislocations and disclinations. For instance in non-linear continuum theory the Bianchi identity in general seems to establish sources of disclination lines. But in my opinion this fact is only due to the continuum theory and it has no correspondence to the properties of real discrete disclinations in crystals, i.e. I think continuum theory fails to be a good tool with respect to the source properties of dislocation and disclination lines. To improve this weak point we have to develop a theory which deals with arbitrary distributions of discrete line defects. The fact that linear continuum theory describes source properties in the right way seems to be only a lucky chance without an essential background. Furthermore continuum theory, even in its non-linear form, gives always only a very rough approximation to describe disclinations. In the case of crystal disclinations, continuum theory is in contradiction to the discrete structure of the crystal point group. In contrast, continuum theory is the right way to describe dislocations, for the translation group of the crystal is continuous from the macroscopic point of view.

SIMMONS: Your quasi-disclinations, on the other hand, would be properly described in a continuum theory, however?

ANTHONY: Yes, that's right.

BEN-ABRAHAM: I just want to say that the Bianchi identity has some equivalent in the theory of discrete disclinations, exactly like the divergence theorem on torsion has an equivalent in the theory of discrete dislocations.

DE WIT: [Written contribution] In answer to Dr. Anthony's earlier question, I shall give an example of a dislocation line ending on a disclination line in a crystal.

Consider a positive wedge disclination of strength $\pi/3$ in a hexagonal crystal. (The crystal type is not important, similar arguments hold for other structures.) It is normal to the basal plane shown in figure 1 and localized at atom A. It is easily seen that the disclination can be moved to a new location by removing the plane of atoms AB. For the indicated

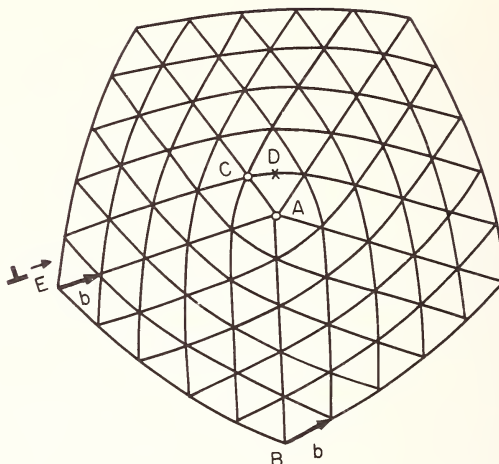


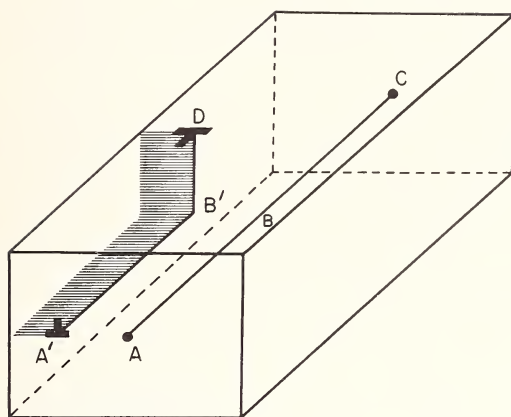
FIGURE 1. Positive wedge disclination of strength $\pi/3$ localized at atom A. The removal of plane AB or the glide of an edge dislocation along plane EA will cause atom C to move to location D and become the new location of the disclination.

Burgers vector \mathbf{b} , atom C will move to position D and become the new location of the disclination. The same result will be obtained if an edge dislocation glides into the disclination along the slip plane EA. The disclination moves one interatomic distance.

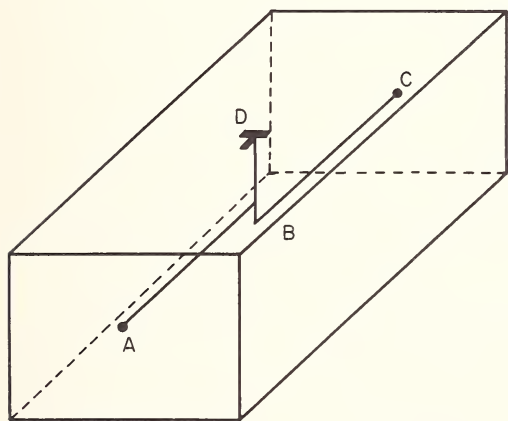
Next, consider figure 2(a), where such a wedge disclination ABC runs from the front face of a crystal to the back face. An L-shaped edge dislocation A'B'D glides into the crystal from the left face. The disclination lies in the glide plane of the leg A'B', and the other leg B'D emerges through the top face. When the dislocation reaches the disclination, the leg A'B' will cause part AB to move up by one interatomic distance. This will leave the disclination with a jog at B, from which a dislocation emerges, figure 2(b).

Though the relation of this example to eq (6.8) of my paper may seem somewhat remote, both results are consistent. For example, eq (6.8) implies that dislocations can end on twist disclinations for which θ may be asymmetric, but not on wedge disclinations for which θ is symmetric. The example shows the dislocation emerging from the jog, which is just a small segment of twist disclination.

I would also like to comment on Dr. Ben-Abraham's remarks about the Bianchi identity, eq (III.5.19) in Schouten, which is the non-linear continuity equation for disclinations. It is true that the right hand side in this equation is non-zero, but this represents the non-linear effect and arises



(a)



(b)

FIGURE 2. (a) Wedge disclination ABC and L-shaped edge dislocation A'B'D. (b) Wedge disclination ABC, with a kink at B, from which emerges an edge dislocation BD.

because of the “local” formulation of this equation. If the equation is put in its “true” formulation the right hand side vanishes, eq (III.5.42) in Schouten, and it is then a straightforward generalization of my eq (6.2). Hence the theorem that disclinations do not end inside the crystal is also rigorous non-linearly.

A similar argument holds for what is sometimes called the first Bianchi identity, eq (III.5.2) in Schouten, which is the non-linear continuity equation for dislocations. Again due to the “local” formulation this equation contains on the righthand side a dislocation square term. Again this term is missing in the “true” formulation, eq (III.5.41) in Schouten, which is now a straightforward generalization of my eq (6.8). So even non-linearly we have the theorem that dislocations can end on disclinations.

For disclination-free dislocation theory the difference between the “local” and “true” formulation of the non-linear continuity equation for dislocations has already been pointed out by Kröner and Seeger.⁴

⁴ Kröner, E., and Seeger, A., Arch. Rat. Mech. Anal., **3**, 97 (1957), eqs (29) and (36).

V PANEL: INTRINSIC PROPERTIES OF DISLOCATIONS

Chairman: **J. P. HIRTH**

Panel Members: **R. BULLOUGH**
 R. DEWIT
 C. ELBAUM
 J. D. ESHELBY
 P. HAASEN
 P. B. HIRSCH

INTRODUCTION TO THE PANEL DISCUSSION “INTRINSIC PROPERTIES OF DISLOCATIONS”

J. P. Hirth

*Department of Metallurgical Engineering
The Ohio State University
Columbus, Ohio 432100*

Since the future directions of dislocation theory were to be discussed in another panel, the purpose of the panel discussion reproduced in the following section was to assess the current status of the theory of dislocations, with emphasis on the intrinsic properties of the dislocations as opposed to those of other physical entities influenced by dislocations. (For example: the theory of crystal growth by a spiral ledge mechanism involving a screw dislocation.) In order to set the stage for the discussion to follow, some comment on the historical development of the theory is in order.

As is now well known, dislocation theory originated with the work in the early part of the century by elasticians, notably Volterra, Somigliana and Weingarten, on macroscopic dislocations in isotropic continua.¹ Modern dislocation theory began, however, with the invention of microscopic, crystalline dislocations; the edge by Orowan, Taylor and Polanyi in 1934 and the screw by Burgers in 1939.² Following this discovery, there have been several bursts of theoretical developments.

The first of these involved essentially the mathematical treatment of straight dislocations in infinite media using isotropic, continuum elasticity. These developments were nominally complete by the early 1950's, as exemplified in the books of Read [3] and of Cottrell [4]. Also, in this period, a number of quasi-phenomenological, model theories—based on the straight dislocation results—were generated to explain such macroscopic deformation phenomena as work hardening, creep, fatigue and fracture. Again, a number of these are treated in Cottrell's book.

The second period, continuing to the present time, encompassed a number of embellishments of the theory, including treatments of elastic anisotropy, simple free surface effects, curved dislocations, non-linear elasticity, and atomic calculations of core configurations. On the basis of these extensions, more elaborate theories were generated for many dislocation processes and for many dislocation configurations. The impetus for the new theoretical work was largely the most important development of

¹ For a review of these developments see pp. 8-21 of ref. [1].

² An interesting historical account of these is given by two papers in ref. [2]; those by G. Taylor, p. 355, and by E. Orowan, p. 359.

the technique of direct observation of dislocations by electron transmission microscopy by Hirsch, Horne, Whelan, and Bollmann [5] in 1956. Also, of course, the progress in computer technology during this period enabled both the atomic calculations and the more complicated elasticity calculations to be performed. The transmission results showed that, rather than the simple configurations envisioned earlier, most complicated arrays were present: For example the dislocation tangles observed in work-hardened metals. Many of the results from this period of burgeoning of dislocation theory are considered in the recent books of Nabarro [1] and of Hirth and Lothe [6]. What, then, is the status of dislocation theory today? A number of problems, usually involving fairly simple configurations, have been solved satisfactorily. One example is the theory of small angle grain boundaries which is in excellent agreement with experimental observations [7]. Another is the theory of pileups, where excellent agreement with experiment is also obtained. In the latter case, the theories include treatments of elastic anisotropy [8] and of interphase interface image effects [9]. Also, the treatment of a pileup as a continuous distribution of infinitesimal dislocations [10] provides a bridge between the discrete dislocation approach (related to atom displacements) of materials science and physics and the elastic-plastic continuum approach of mechanics.

At the other extreme, there are topics which remain highly controversial. These include most macroscopic mechanical properties. An example is the theory of work hardening, in which there are a number of rather different viewpoints³ all of which plausibly rationalize most experimental results in a self-consistent way, but which are not consistent with one another. Many of these problems involve the treatment of about 10^{18} dislocation segments, arbitrarily shaped, and each of which is in a differing state of effective stress. There is some progress in developing statistical treatments of such problems. Also, there is a beginning effort to develop a continuum-statistical theory, the three-dimensional extension of the two-dimensional case exemplified by the pileup calculations discussed above, to bridge the gap between continuum mechanics and discrete dislocation theories. The latter developments have been extensively discussed in the conference transcribed in the present volume and in one whose proceedings have been edited by Mura [14].

Between these extremes are problems whose solutions are agreed upon qualitatively, but upon which there remains quantitative disagreement. This category was selected as the basis for the following panel discussion with the hope that some guidelines could be generated toward a more complete answer. The agenda was comprised of five topics: (1) Core structures in metals: e.g. Peierls energy barriers, atomic calculations, non-linear

³ For example see the differing viewpoints in refs. [11,12,13].

elasticity, adsorption, b.c.c. faults and anisotropic elasticity; (2) Dislocation drag mechanisms: e.g. damping, inertial effects, electron interactions, thermoelastic effects and magnetic effects; (3) Core structure in covalent and polar materials: e.g. jogs, kinks, diffusion, interaction with conduction electrons and holes, and interaction with ionic defects; (4) Equilibrium configurations: e.g. disclinations, dipoles, junctions, superjogs, grain boundaries, nodes, and fault tetrahedra; and (5) Critical configurations: e.g. cross-slip, intersection, bow-out, and Peierls and quasi-Peierls barriers in b.c.c. crystals.

The first four topics are discussed fairly fully. However, the discussion on disclinations earlier in the conference was limited, so it was given additional time in the panel with the consequence that the last topic was not discussed, a circumstance that perhaps can be remedied at the next conference.

The panel members were R. Bullough, R. deWit, C. Elbaum, J. D. Eshelby, P. Haasen, P. B. Hirsch, and J. P. Hirth (Chairman). The proceedings follow.

References

- [1] Nabarro, F. R. N., *Theory of Crystal Dislocations* (Oxford University Press, 1968).
- [2] The Sorby Centennial Symposium on the History of Metallurgy (Gordon and Breach, N.Y., 1965).
- [3] Read, W. T., Jr., *Dislocations in Crystals* (McGraw-Hill, N.Y., 1953).
- [4] Cottrell, A. H., *Dislocations and Plastic Flow in Crystals* (Oxford University Press, 1953).
- [5] Hirsch, P. B., Horne, R. W., and Whelan, M. J., *Phil. Mag.* **1**, 677 (1956); Bollman, W., *Phys. Rev.* **103**, 1588 (1956).
- [6] Hirth, J. P., and Lothe, J., *Theory of Dislocations* (McGraw-Hill, N. Y., 1968).
- [7] Amelinckx, S., and Dekeyser, W., *Solid State Phys.* **8**, 325 (1959).
- [8] Armstrong, R. W., and Head, A. K., *Acta Met.* **13**, 759 (1965).
- [9] Dundurs, J., In *Mathematical Theory of Dislocations*. Mura, T., Ed. (Am. Soc. Mech. Eng. N.Y., 1969) p. 70.
- [10] Chou, Y. T., and Li, J. C. M., *ibid.*, p. 116.
- [11] Nabarro, F. R. N., Basinski, d Z. S., and Holt, D. B., *Adv. in Phys.* **13**, 192 (1964).
- [12] Hirsch, P. B., and Mitchell, T. E., in *Work Hardening*. Hirth, J. P., and Weertman, J., Eds. (Gordon and Branch, N.Y., 1968) p. 65.
- [13] Seeger, A., *ibid.*, p. 27.
- [14] Mura, T., Ed. *Mathematical Theory of Dislocations* (Am. Soc. Mech. Eng., N.Y., 1969).

Proceedings of the Panel on Intrinsic Properties of Dislocations¹

HIRTH: The title of the panel is "Intrinsic Properties" as a counterbalance to the final panel on "Future Directions," and we can also think of this as "Where do we stand today in dislocation theory?"

Although this is a theoretical meeting, I discovered on talking to several members of the panel that they and myself, *a priori*, do not know what a panel discussion really is, so we will be conducting somewhat of an experiment here this morning.

We will begin with the consideration of core structures in metals. We have the questions of the Peierls energy, of dislocation extension, of atomic calculations of core structure and of atomic force laws. I wonder if, to begin, Dr. Bullough might give us his thoughts on these matters.

BULLOUGH: Thank you. I would like to make the following points regarding these kinds of calculations. One is the purely practical point that if we are going to try to determine the configuration and energy of the core of a dislocation, then at the moment we are forced to use a two-body approach, with, of course, the appropriate volume dependent terms. In my opinion, the important justification for such calculations, again at the moment, is that they must be shown to be superior to a harmonic calculation. We heard yesterday from Professor Ashcroft on the practical impossibility of getting the band structure energy term. This band structure term, of course, depends on the ion configuration, which is the very thing we are trying to get. That immediately provides a fundamental difficulty.

So, I would say that we must insure that whatever model for cohesion we take, it should at least be consistent with the phonon dispersion properties of the crystal, since we wish to discuss movements of ions. This difficulty of getting agreement with the phonon dispersion data is a prime problem facing the quantum mechanists. You heard from Professor Ashcroft about the difficulty of selecting the appropriate dielectric function. Thus, I think we have to compromise immediately if we wish to attempt this kind of calculation.

There is another very important point about dislocations; namely, that the core structure is incredibly sensitive to the stacking fault energy. In view of this it is quite pointless to attempt a core calculation, in my opinion, if we do not insure that the potential we adopt gives stacking

¹ - edited by J. P. Hirth.

fault energies consistent with those observed by the experimentalists or at least values with the right sign. Again, it is frightfully difficult to construct a potential from basic principles that is consistent with stacking fault energies. Maybe we will have some comments from the audience on this point.

There is a particular problem in the b.c.c. materials, because in those materials we have many possible stacking faults. Again, it is essential, if we are going to study dislocations in such materials, that the potential be such that all the stacking fault energies are positive. It is quite ludicrous to use a potential that gives a negative fault energy and then pretend that the results have some physical meaning when applied to a configuration where such a fault can appear geometrically. Also, of course, the calculated fault energies must be pretty large to agree with experiment; on the order of 700 or so ergs per square centimeter.

I would sum up my attitude to the b.c.c. case as follows: We must satisfy the phonon dispersion data as accurately as possible. We must insure that all the stacking fault energies that can appear in the lattice associated with the core are positive and reasonably large. The potential, in addition, should be consistent with the surface energy of the material. This is particularly important if we are expecting any kind of loss of cohesion in the core region. This last feature is, to my knowledge, almost completely ignored.

We have recently been concentrating our attention on constructing what we think is a decent potential covering all these aspects. When I refer to "phonon dispersion," I also mean, of course, that particular care be taken to fit the long wavelength limit. This is a potential constructed by Roy Perrin.² [See here fig. 1.] It is a set of quintic polynomials. The point here is that we have dropped the spline procedure in this case, because we want to have the flexibility to fit this potential to the anharmonic properties. We have not done such fitting yet, but we have enough degrees of freedom to do it.

This potential has the great advantage that the lattice is stable. This remark is not so funny as it appears at first sight, because there are many potentials around in which the lattice is unstable against inhomogenous deformation. Whilst the eigenvalues of the dynamic matrix may all be positive, and may give a decent phonon dispersion, it is perfectly possible for the lattice to be unstable against an inhomogeneous deformation, which is precisely what a fault-shift is. Well, our potential does not give

² Bullough, R., and Perrin, R. C., in *Radiation Damage in Reactor Materials* (I.A.E.A., Vienna, 1968).

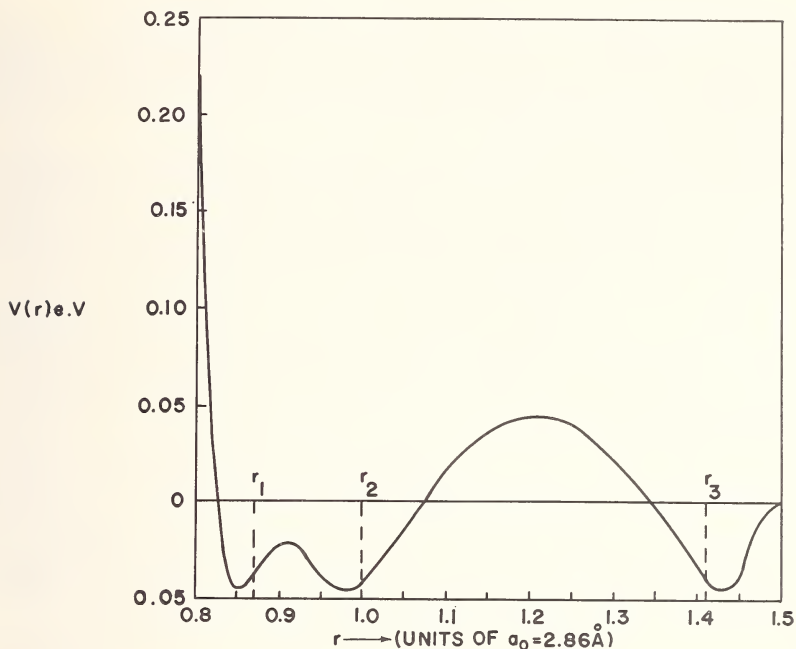


FIGURE 1. The third neighbour pair potential for body centered cubic iron. $r_1 = 2.48 \text{ \AA}$, $r_2 = 2.86 \text{ \AA}$ and $r_3 = 4.04 \text{ \AA}$ are the first, second and third neighbour separations respectively. The absolute value of the potential is set equal to -0.04 eV at each equilibrium separation to ensure an effective surface energy of 10^3 ergs/cm^2 and the physically reasonable stacking fault energies: 730 ergs/cm^2 for $a/6 \langle 111 \rangle$ on (110) ; 737 ergs/cm^2 for $a/8 \langle 110 \rangle$ on (110) and 844 ergs/cm^2 for $a/6 \langle 111 \rangle$ on (112) . Courtesy of R. Bullough.

an unstable lattice. It has positive stacking faults, and they are all healthily large as required for correlation with all the systems with experimentally known fault energies.

In the face-centered cubic case, we are, in my opinion, in some ways in a lot healthier position—but in some ways a lot more difficult one. It is well known that the geometrical fault energy depends on deviations from the third neighbor positions in the face-centered lattice. This means that it depends on the long-range part of the potential. For real-space relaxation calculations long-range potentials are a nuisance. They may not be a nuisance in a Fourier transformation procedure for the dislocation configuration, and on this topic I would like to hear the views of Professor Hardy.

On the other hand there is the distinct advantage that we know what the long-range potential is in the case of some of the face-centered cubic materials. We have some confidence, I think, in the Friedel oscillations, and we are interested in the asymptotic regime, where the form is, of

course, $\cos(2\mathbf{k}_F \cdot \mathbf{r})/r^3$: I think Professor Saada would probably concur with that.³ We know we can be fairly confident about fitting the stacking fault energy with the asymptotic form. However, there are the practical difficulties mentioned before.

HIRTH: Would anybody on the panel care to comment on Dr. Bullough's remarks? I might just say that another experimental test that would seem to be desirable for a potential would be whether it would reproduce a Peierls energy of something like 10^{-4} to 10^{-2} times the modulus.

BULLOUGH: Yes, I agree. The real problem is calculating the Peierls energy. As a matter of fact, I have to plead ignorance here; I was not aware of that beautiful method Professor Suzuki mentioned, Kurosawa's method,⁴ involving a homogeneous shear procedure.

We have tried many times to calculate the Peierls energy; the real difficulty is, of course, that you can get to the inflection point on the energy-distance curve at absolute zero but you cannot go past it because the dislocation then moves. I have great difficulty in understanding how people creep past the inflection point, in any, shall I say, mechanical experiment. How can they hold the configuration in an unstable state?

HIRTH: That is without going to finite temperatures where thermal activation can help.

BULLOUGH: Yes; well, we have to wait about a hundred years for a computer to do that, I think.

HIRTH: Professor Hirsch, you've recently looked at faults and core configurations in b.c.c. materials. Do you want to comment on that topic?

HIRSCH: Yes, I will say a few words about this matter. The first question I think one might ask oneself is: Why, apparently, is the Peierls energy high in body-centered cubic metals, and not in f.c.c. ones? Now, that is a very simple question; some people might even dispute it. I think it is true. Further, I think the answer to it, and a very obvious one, I suppose, is that it arises from the difference in the crystallography of the lattices.

AUDIENCE: General laughter.

HIRSCH: Now, let me make this perfectly obvious statement slightly more specific. Two models have been postulated for giving us a picture of why the Peierls stress in b.c.c. metals, in particular for screw dislocations, is high. One of these is Professor Suzuki's very beautiful model, which he

³ \mathbf{k}_F is the Fermi wave number, 2π over the energy of the highest filled states, and r is the radial distance from a given ion core.

⁴ Kurosawa, T., J. Phys. Soc. Japan **19**, 2096 (1964).

discussed yesterday;⁵ let me just remind you of it. If we look down a $\langle 111 \rangle$ direction we realize that the structure consists of rods of atoms which are at positions 1, $1/3$ and $2/3$. These appear in the projection as two types of triangles. Depending on the sign of the dislocation, either it will have low energy in triangle A or it will have low energy in triangle B; the other position in either case being the one of high energy. Well, that is a very simple idea, which shows that there is a good reason why the Peierls energy might be high in this lattice for screw dislocations because of the geometry.

The other reason that has been put forward is that because the screw dislocation has threefold symmetry, it is possible for the dislocation to dissociate on more than one plane. This dissociation again is a characteristic of this particular lattice. When the dislocation is dissociated in this way, then it is difficult for it to move.

Now, I would like to remark further about this possibility. The models which have been used in the past are, of course, very hypothetical models, with the dislocation dissociated into stacking faults which are postulated to be on particular planes. Of course, the dislocations turn out to be very narrow in these calculations and then, of course, the meaning of the stacking fault energy effectively disappears.

But the point about this sort of model is that it does not really matter whether these are stacking faults in the true sense; in the b.c.c. structure, the dislocation is a sort of animal which is split, that is where the misfit is distributed not on one plane, as it is in the f.c.c. structure, but in fact is spread out on several planes. The consequence of this splitting is that the dislocation is difficult to move.

It seems to me that both of these ideas are based on the configuration of the atoms in the b.c.c. lattice, and that one must do core calculations now to find out the exact details of the core structure. One must make quite sure, as Dr. Bullough said, that the potentials are at least such that the lattice is stable—that is a rather important criterion.

Well, if I may just summarize the way I see the results so far, a number of people have in fact calculated core structure using inter-atomic potentials of various types, including Suzuki; Bullough and Perrin; Gehlen, Hahn and Rosenfield; Chang; and Vitek.⁶ While all give configurations which appear to be split, most of these authors appear to obtain slightly different splittings. Thus, at the present time the situation is not very satisfactory because these results appear not to agree. Presumably this

⁵ See the paper by H. Suzuki in these Proceedings.

⁶ Suzuki, H., in *Dislocation Dynamics*, A. R. Rosenfield, G. T. Hahn, A. L. Bement, and R. I. Jaffee, Eds., (McGraw-Hill, N.Y., 1968) p. 679; Bullough, R., and Perrin, R. C., *ibid.*, p. 175; Gehlen, P. C., Hahn, G. T., and Rosenfield, A. R., *J. Appl. Phys.* **39**, 5246 (1968); Chang, R., *Phil. Mag.*, **16**, 1021 (1967); Vitek, V., *Phil. Mag.* **18**, 773 (1968).

requires looking into the questions of the way the calculations are done, the potentials, the boundary conditions that are used, and so on.

Another very trivial point, which perhaps might be overlooked, is that it is not so easy, actually, to characterize a core-structure once one sees it. I am not yet entirely convinced that all these structures which are being observed by these various people are actually all that different. I think that they may turn out to be alternative ways of describing the same structure.

Another thing, which I think the theoreticians ought to bear in mind, is that there are certain experimental results which have to be explained. For examples, the asymmetry effect, in which the slip on $\{112\}$ planes is easier in one direction than in the other, and, also, the fact that for certain b.c.c. metals, slip occurs on $\{110\}$ planes for certain crystal orientations and $\{112\}$ planes for other orientations. Thus, whatever potentials are used for core calculations, I think that the above experimental results have to be borne in mind; they have to be explained.

Finally, in my opinion, the effect of stress on the core configuration must be looked at. Calculations ought to be carried out in which, in effect, a stress is put on the crystal and the change in the structure is observed.

BULLOUGH: I would like to make one remark on what Professor Hirsch has said; namely, that I do recommend that people use that potential I put up on the board [fig. 1].

HIRTH: At this time we open the floor for general questions.

SAADA: Regarding these lattice calculations, I would like to make a very simple remark, namely, that underlying this calculation is the very important postulate that you can, in fact, describe a metal by a pairwise atomic interaction. However, even in the simplest metals, the only thing which has been shown from first principles by treating the whole problem is that this is true only to the second order of perturbation. For very simple metals like lithium, sodium and some close-packed metals like magnesium or aluminum, one can indeed express the total energy with a formula using some pairwise interaction, but the result is valid only to the second perturbation order.

Therefore, the main postulate on which all these calculations rely is not very certain. For example, one knows that in some pathological metals—like copper, which is pathological for other reasons—the fact that the surface does not cut the Brillouin zone but just pushes it, makes the convergence process at least very poor, or, probably, inapplicable. Thus, my feeling is that whatever experimental potential is taken for such lattice calculations, it will be a phenomenological potential, most of the time.

GILMAN: Well, it seems to me that Dr. Saada's points are well-taken, but that one can also criticize the attention paid solely to the crystallography. If one takes the simple case of the sodium-chloride structure, there is a vast variety of behavior. For an ordinary salt such as rock salt the Peierls force is very small for the highly pure crystal. On the other hand, a semiconductor like lead telluride is still fairly soft but the behavior is completely different because the glide plane switches from {110} to {100}. Finally, another type of compound with the rock salt structure is a carbide, such as titanium carbide, which has a very high Peierls force. Clearly, then, simple crystallography is a relatively minor part of the picture, and I do not see how one can avoid worrying about the electronic structure. For example, I have done experimental work on the intermetallic compound gold aluminide. In the presence of a large concentration of dislocations, the color of this compound changes from bright purple to grayish purple, which shows that its electronic structure has been significantly changed. One also knows from studies of the pressure dependences of the band structures of semiconductors that when the specific volume is changed the electronic properties change significantly. In some metals, where there is a large dilatation at the dislocation core, local bound states might form.

MENDELSON: [Written contribution] Dr. Gilman's suggestion that electronic effects are more important than crystal structure can be contrasted with studies of dislocation dissociations which suggest the opposite. In pure metals the electronic characteristics determine the stability of the existing phase and its elastic properties, but the differences of metals with the same structure are generally of magnitude rather than character. The flow behavior of b.c.c., f.c.c. and h.c.p. crystal structures differ because they have different slip systems and possible dislocation dissociations. The strong covalent forces in Si and Ge are responsible for tetrahedral bonding and the resulting diamond lattice, but the properties of these crystals can also be explained in terms of the crystal structure and the manner in which dislocations dissociate.

In compound crystals the electronic effects can be more varied and Dr. Gilman's suggestion becomes more tenable, but I find it more realistic to consider that the electronic effects alter the role played by crystallography rather than that they play the primary role themselves. The example of the differences in the behavior of ionic NaCl and covalent PbS, both of which have the same rock-salt crystal structure, illustrates the point. PbS shows different slip systems and twins on various planes which are unlikely in NaCl. The lack of strong ionic forces in PbS allows for various possible dissociation modes for dislocations to lock or twin on, and hence alters the role played by the crystal structure. Similarly

the Burgers vector and the dislocation dissociations possible in b.c.c. metals are not favorable in ionic CsCl-type compound crystals (the same Bravais lattice) and here again the electronic effects can be considered as altering the role played by the crystal structure.

CHANG: I would like to comment on Dr. Bullough's talk. I think that his points are well taken. In addition, I believe that anybody who works in this field would like to construct a potential following first principles as much as possible. Say, that for a given potential the computation shows that the stacking fault energy is negative; then the researcher would be upset—I would not like it myself.

Also, I think that fitting the phonon dispersion is not too difficult. However, according to some of the theorists in our lab such fitting is not sufficient to yield a valid potential. I would like to appeal to anybody working in this field to proceed to construct a potential in such a way as to cover first principles as much as possible, if he can.

A second comment—to Professor Hirsch's discussion of the five parties working on the screw dislocation:⁶ At least three of us agree on the core configuration. It is gratifying to know that there is some agreement. Also, those in agreement used different potentials.

THOMSON: This is a question to Dr. Bullough—it is really along the same line as Dr. Chang's: What is your feeling about using the theoretically suggested force laws for aluminum, where there is a stronger effect from the oscillations than, for example, in the case of copper that you showed earlier? Along this line, are those wiggles in the iron curve supposed to be screening oscillations, or are they purely phenomenological in origin? I guess the thrust of my question is: What is your feeling about using a light touch with what one can get from theoretical suggestions about the force law? Of course, I agree with your comments that one does have to insist that these lattices be stable, and so forth; but this, I suspect, is something that could be done after one takes his first cue from the theoretical suggestions.

A second point is that I am puzzled by your comment about not being able to calculate the Peierls energy. Why can you not simply do as Professor Hirsch suggested? That is, put a stress on the crystal with your potential, and then look for the energy—or the situation—where the thing goes to pot; or, in other words, where the dislocation goes over the top of the Peierls barrier? This really would be, I think, the thing that you are looking for.

BULLOUGH: Well, let me answer first what is in my mind, the question of Peierls energy. It is just that the critical force is achieved when you reach the inflection point in the energy curve, that is all.

HIRTH: One really determines the Peierls stress, but not the energy.

BULLOUGH: That is right. And I did not mean anything else.

HIRSCH: That is worth doing.

BULLOUGH: Yes. We do try.

AUDIENCE: General laughter.

BULLOUGH: As a matter of fact, we do take a cue from the theorists—the quantum theorists, I mean. The cue is that one can divide the cohesion into a pair-wise interaction potential and a volume term. Then, taking in Dr. Saada's point at the same time, we do not enforce equilibrium under a pair potential alone; this is very important. Equilibrium is achieved with this potential plus a volume term. If we did force equilibrium based on the pair potential alone, I would be the first to condemn it. It would be wrong harmonically, for one thing, since the Cauchy relations would be forced.

With regard to the aluminum question, I could not agree more. We have the greatest intentions now in this direction. In particular, because of Parsons' beautiful work at Chalk River,⁷ we really have something to compare with. I am sure you all know Parsons' work; he is actually getting resolution now of two Ångstroms in the electron microscope—seeing the atoms around the dislocation. I have the slides of this if anyone wishes to see them. There you can actually observe the lattice configuration for the first time, I think, around the dislocation. So, if the theoretical configuration does not agree there, you have had it, so to speak.

In answer to Dr. Chang: It is all very well saying you should work from basic principles, but one gets absolutely nowhere. I am the first to try this; I have tried very hard. In general, one cannot even get a positive stacking fault energy. So, one has to decide whether this kind of calculation is worth doing. That is the question, I think; not that you should waste your time with the present state of the theory . . . Well, that was a bit of an overstatement: One can get a positive stacking fault energy sometimes, but only in the case of aluminum has there also been a really successful correlation with the phonons. This is a very important point. Another interesting point concerns the kind of calculation that Professor Hardy and I did on a harmonic lattice. In a sense everyone finds this terribly respectable, because we used Fourier transformation procedures, worked from a dynamical matrix, and did not dirty our hands with computing. Yet there is no more physics going into that calculation than into the one I discussed earlier and it is very important, I think, to remember that.

⁷ Parsons, J. R., and Hoelke, C. W., *J. Appl. Phys.* **40**, 866 (1969).

Also, using our potential we got an interaction between vacancies in copper and aluminum which is very close to the observed binding energies of the di-vacancies. Further, the calculation was based purely on a relaxation interaction. Now, March does his electron, rigid-ion calculations and gets almost the same results.⁸ Is this purely coincidence or is there an underlying explanation?

HEAD: Could I ask Dr. Bullough: In his opinion, at the moment, for how many metals is a decent atomic potential calculation plus everything possible? That is, in which we have a good potential expression and so on; not just counting the ones you know, but in your opinion, how many metals are handleable with present knowledge?

BULLOUGH: However I answer that, it will be misunderstood! It depends upon which coat I put on. If I speak as a rigorous solid-state theorist, who really wants to believe in his description of the cohesion, then I have to stay with aluminum.⁹ I think that is fair. But, if I am satisfied with a potential which is better—far better—than a harmonic approximation, then I would say that the calculations for copper using the potential that Dr. Englert constructed are not far from the truth as far as small deviations from the equilibrium positions are concerned.¹⁰ At least the restoring forces are correct from a harmonic point of view. Of course, we are staying with metals . . . or ionic crystals?

HEAD: I meant metals, only.

BULLOUGH: In the case of iron, I would say either the potential that I put on the board [fig. 1] or Dr. Chang's—there is very little to choose between them. Dr. Chang's has the advantage that he has fitted it deliberately to the anharmonic properties, but I believe the consistency with fault energies is much safer with our potential.

HIRTH: I think we can move on now to the second topic, "Dislocation Drag Mechanisms." Dr. Eshelby?

ESHELBY: What I am thinking of, when I speak of drag, is the frictional force acting on a moving dislocation. I am not thinking of drag caused by jogs, or what one might call geometrical things like that. Also, for a sort of simple-minded theorist who has done mostly elasticity and that kind of thing, the force is exciting and awesome, because it depends on the interaction of dislocations with practically every other property of the material.

⁸ Alfred, L. C. R., and March, N. H., Phil. Mag. **2**, 985 (1957); Corless, G. K., and March, N. H., Phil. Mag. **6**, 1285 (1961).

⁹ The original transcription replaced "with aluminium" by "without a menu," which, while incorrect, perhaps aptly describes the situation.

¹⁰ See the paper by A. Englert, H. Tompa, and R. Bullough in these Proceedings.

There was a very nice paper by Professor Lothe some years ago¹¹ where he discusses a number of these mechanisms—it seems to me about a dozen. He comes out—perhaps I exaggerate a little—with the conclusion that each of them gives about $(0.1)b^2$ times the thermal energy density, ϵ , which is the old Leibfried value. Now, one wonders if some of them are not the same mechanism under assumed names. One then wonders whether of these dozen, perhaps several are not as big as you thought, and therefore the answer of only one of them, perhaps, is right, and therefore, it has the value $(0.1)b^2\epsilon$; or whether you ought to multiply by 10, and so forth.

The kind of thing I have in mind is, for example, the interaction with electrons. There is Professor Mason's electron viscosity. Then there is a thing in Professor Nabarro's book,¹² which incidentally contains a nice summary of all these matters, in which you say: Well, if we have already calculated the electrical resistance of a dislocation, then, instead of considering the dislocation to be moving through the crystal, we can stop it, let the electrons drift past, and find the mechanical resistance by comparing the electrical and mechanical dissipations. Also, I think there is some work done by Dr. Louat and his colleagues on the interaction of electrons with dislocations.¹³ I am not quite clear about the connection or lack of connection between these calculations. In addition, one has to consider possibly whether in doing these calculations one can treat the dislocation as a straight thing moving forward or whether it is advancing by kinks sliding along it. In certain cases, if it is going by kinks sliding along, some of the properties will be nearly identical with what they would be if it were moving rigidly.

Another question involves the effects of dispersion, or, if you like, that the velocity of phonons gets less near the top of the first Brillouin zone. This, I think, is a very small effect, but I was shocked to see some pictures got by the neutron diffraction people of body-centered things where the frequency versus wave number curve hangs down in a horrible sag at quite low wave numbers. What effect does that have?

I do not know that one can say anything general here except that there is an interaction of the dislocation with a large number of, what one might call, non-dislocation properties of the material; and that only experts in each of these, having got hold of an expert in dislocation theory, might do something definitive about the interaction by working together.

I see on the topic outline it says "thermo-elastic." Well, I think one can skip that; I do not think it is important. Furthermore, various physicists having done this some time ago, applied mathematicians have suddenly

¹¹ Lothe. J., J. Appl. Phys. **33**, 2116 (1962).

¹² Nabarro, F. R. N., Theory of Crystal Dislocations (Clarendon Press, Oxford, 1968).

¹³ See the paper by G. Huffman and N. Louat in these Proceedings.

woken up to thermoelasticity and are madly doing it. When they finish doing waves, perhaps we can persuade them to get around to doing elaborate problems for dislocations; but I think that for honest physicists the topic has become part of applied mathematics.

HIRTH: Dr. Elbaum, would you like to comment on this topic?

ELBAUM: Yes. There is one specific aspect to which, I believe, there is something to be added: I will also talk about this matter Friday afternoon,¹⁴ and that is the question of the drag of dislocations caused by conduction electrons in metals. There are, I believe, right now, two major tendencies that are rather in conflict for reasons that I shall try to explain.

Dr. Eshelby just mentioned the work of Professor Mason,¹⁵ who has predicted a drag that we call B for convenience, proportional to the inverse of the electrical resistivity of a metal. The point of departure for this treatment was the assumption that one could consider the dislocation (or its strain field) to be moving within a viscous gas (the electron gas) and that one could, therefore, use a semi-classical approach, and solve the problem essentially, though not explicitly, in the spirit of $ql < 1$; that is where q represents some appropriate wave number of a component of the moving strain field and l the mean free path of electrons in the metal.

Work of a similar character, but using different algebraic techniques, was carried out by Huffman and Louat.¹⁶ To be specific; these gentlemen used the Boltzmann transport equation, applied it to the situation which is really $ql > 1$ in the case of a crystal—for reasons that, again, I shall come back to in a moment—and came up, as you might expect, once more with a drag coefficient proportional to the reciprocal of the electrical resistivity. Now, there is a very basic problem here. In the drag on a dislocation caused by conduction electrons, we are faced really with two aspects: One is the magnitude of the drag and the second one its possible temperature dependence, if any. As for the magnitude of the drag, this is perhaps a particularly tall order in terms of calculations from first principles. However, the problem of the temperature dependence can be handled in a somewhat simpler, more straightforward and more physical way. Since, in the approximations used first by Professor Mason and subsequently by Drs. Huffman and Louat, a proportionality of the drag to the reciprocal resistivity was found, there is also a temperature dependence in the drag coefficient following the temperature

¹⁴ See the paper by C. Elbaum in these Proceedings.

¹⁵ Mason, W. P., J. Acoust. Soc. Am. **32**, 458 (1960).

¹⁶ See their paper in these Proceedings.

dependence of the resistivity. The ingredients that go into this approach are, however, somewhat questionable in my opinion. As you will see, I line up rather squarely behind the temperature independent drag for reasons that I shall try to explain.

First of all, consider a physical argument: If one considers that the displacement field of a dislocation is decomposed thus:

$$u = \sum_q u_q \exp(i\mathbf{q} \cdot \mathbf{r}),$$

an approach that was first pointed out by Holstein,¹⁷ then each one of the components of this Fourier series can be thought of as a wave in its own right—a wave with wave vector q and amplitude u_q . The important components of this Fourier decomposition are the ones corresponding to short wavelengths or large q . This is so because the strain field of a dislocation falls off with the negative square power of the distance r from the dislocation, so that most of the strain field is concentrated near the core; and this is where the most important contribution is going to arise.

Since we are talking about components with large q of the order of 10^6 to 10^7 cm^{-1} —but probably not any smaller—it would take a remarkably small mean-free path for the electrons to give $ql < 1$. In fact, an unrealistically small mean-free path of the order of 10^{-7} cm or less would be required to achieve the condition $ql < 1$ for which the smeared-out approach—the viscosity approach—or the Boltzmann transport equation can be used in good faith. However, if one takes a realistic mean-free path, which is commonly of the order of hundreds or thousands of interatomic distances, especially at low temperatures, it is the condition $ql > 1$ that is achieved.

The question also arises as to the appropriate method to use in calculating the interaction. Now, in the $ql > 1$ case, if we agree for a moment that this is indeed the proper view to adopt, simple first-order perturbation theory, such as is normally used for calculating electrical resistivity, yields a drag coefficient B that is temperature independent.

Furthermore, one can rationalize this result on very simple-minded physical grounds as follows. If, indeed, this kind of a representation is acceptable, the strain field of a dislocation is a frozen-in configuration which is temperature-independent save for such small high-order corrections as can arise from thermal expansion. The conduction electrons, being Fermions, have a temperature dependence which is certainly not of any importance in first order calculations. Therefore, if one combines these two properties, one would expect a temperature-independent behavior. Where, then, does the temperature independence come from

¹⁷ See the paper by C. Elbaum and A. Hikata in these Proceedings. Also, Holstein, T., summarized by Tittmann, B. R., and Bommel, H. E., Phys. Rev. **151**, 178 (1966).

in the case of electrical resistivity caused by scattering by phonons? Obviously, it comes from the temperature dependence of the phonon distribution; i.e. the fact that phonons obey Bose-Einstein statistics.

But here we do not have Bose-Einstein statistics; we are considering a frozen-in configuration of pseudo-phonons, i.e. the Fourier components mentioned earlier. I suggest, therefore, that the drag coefficient, or specifically the electronic contribution to it, is temperature-independent. It so happens that at least one kind of experiment shows this to be, indeed, the case. On the contrary, Dr. Huffman and Dr. Louat have interpreted the temperature-dependence of yield stress in b.c.c. metals as arising from their calculated value of the temperature-dependence of the electronic drag coefficient. Well, since these gentlemen are here, I suppose that they will have an opportunity to remark on this matter.

BULLOUGH: There are two points that I would like to mention. The first point is in regard to the distinction between f.c.c. and b.c.c. crystals. It should be interesting to see if Professor Hirsch agrees, but I get the impression that the difference in flow stress is often rationalized by asserting that the dislocations are much narrower in b.c.c. materials—I think this is Dr. Louat's thesis—whereas the spreading in the f.c.c. destroys the temperature dependence of the flow stress. It seems to me that this postulate is a little dangerous. Just because the Peierls energy is high does not mean that the degree of dissociation is small.¹⁸ High elastic moduli can offset the other factors and still give large dissociations. This is particularly likely in the b.c.c. materials where the elastic moduli tend to be rather large. For instance, the edge dislocation on a {110} plane, the one which splits up into three ⟨111⟩ partials, is spread out over about six Burgers vectors; which is hardly narrow.¹⁹

The second point is really a theoretical point which I do not understand, but which I think Professor Elbaum covered. It seems to me that in Dr. Louat's calculation the electron relaxation time is extremely small. So why do the electrons not just flow instantaneously around the moving defect? Why is it not like incompressible flow, and so where does the drag come from? Quite a dilemma!

LOTHE: I just want to state that I agree with Professor Elbaum, and that an alternative method of calculating the drag would be to use the imaginary part of the self-consistent dielectric constant which does give a dissipation of exactly the nature that Professor Elbaum indicates.

¹⁸ Or the stacking fault energy.

¹⁹ Presumably this refers to the atomic calculations for iron by Bullough, R., and Perrin, R. C., in Dislocation Dynamics, op., cit, p. 175.

Secondly, I think that the problem that is being discussed here is also similar to the problem with Professor Mason's phonon viscosity and is related to the appropriate inner cut-off at a dislocation core. I always have had the feeling that one could not apply Professor Mason's concept to a region closer to the core than the phonon mean-free path. I stated this in 1962.²⁰ The problem raised by Professor Elbaum is similar. For, outside the dislocation core at long distances away from the dislocation, one can probably do a calculation—such as Dr. Huffman and Dr. Louat have done in spirit—but the excluded inner region will then be so big that the damping contribution will be fairly small. I think it is important to discuss this, because in both of the cases mentioned above better agreement with experiment is claimed when these difficulties are ignored.

LOUAT: I think at this stage it would only be profitable merely to comment on Dr. Bullough's point with reference to dislocation width. One is referring to dislocation width in the Peierls' sense, not in the dissociation sense.

For the other points, I think perhaps they would be better treated on Friday.²¹

HUFFMAN: I would like to make one comment. It is that the impression has been given that our calculation is equivalent to Professor Mason's calculation; whereas this, in fact, is not the case. Objections have been raised to Professor Mason's calculation because he uses the viscosity concept and uses a short-wave-length cut-off; basically, because he takes a cut-off at $r = b$, or something like that.

Our calculation is done in the spirit of ql large compared to unity. We will be talking about this on Friday, so I do not want to go into it too much. But, basically, the situation is the following: We realize that one is on a little bit dangerous ground using concepts of quantum mechanical screening in a semi-classical approach like that of the Boltzmann equation. But the physical picture that we get is appealing. When one is dealing with very short wavelengths, the screening becomes imperfect. This means that in the acoustic attenuation theory one is going from what is essentially a constant current system to what is a constant voltage system, and this is what produces the conductivity-type dependence. I would like to remark, also, that the calculation does reduce to exactly the same results as Holstein's calculation²²—with the temperature independent result—when one neglects the effect of this imperfect screening. As

²⁰ Lothe, J., op. cit.

²¹ See the paper by G. Huffman and N. Louat in these Proceedings.

²² Holstein, T., op. cit.

Dr. Louat indicated, we feel that the temperature independent case occurs for f.c.c. metals. There the width of the dislocation—i.e. of the core distortion—is much more spread out, and one would expect the electrons to be able to screen the positive charge shift associated with the dislocation much better.

HIRTH: Our next topic is: "Core Structure in Covalent and Polar Materials." Professor Haasen, would you lead off on this one?

HAASEN: I would like to limit myself to some covalent crystals like silicon and germanium. As you all know, these crystals are intrinsically brittle at normal temperatures, without thermal activation. So there is no doubt in my mind that they are typical of crystals with high Peierls forces and rather limited widths of the dislocations.

The experimental situation is quite clear.²³ We know how dislocations move in these materials, their velocity, activation energy and so on. Theoretically, several calculations of the Peierls force have been done using various potentials: Some fitted to elastic constants and the phonon spectrum, some using a pseudo-potential approach, and maybe some tight-binding calculations. The results are surprisingly similar, but I do not think that we really have a good solution for the Peierls force yet. In particular, we have no calculation for the 60° dislocation as yet; all these calculations are for the screw dislocation only.

Concerning electronic effects on the Peierls force, I will talk about this a bit on Friday.²⁴ It looks like the dislocation carries a charge in these materials. While the effect of this charge on the Peierls potential is not known theoretically, experimentally we know something about it. So in order to find the dislocation structure in such a case, we must know what the charge state is at its core and then consider its influence on the Peierls potential.

Now, let us turn to the stacking fault extending between partial dislocations. I think that there is a clear indication that dislocations in the diamond structure are not extended; mobile dislocations at least are not extended and dislocations climb rapidly. However, the stacking fault energy certainly is rather low. A careful look at the diamond structure shows that the shear causing plastic slip by complete dislocations occurs between *one* set of planes, while the shear to create a stacking fault occurs on *another*.²⁵ So those two phenomena are really independent of each other.

²³ See Alexander, H., and Haasen, P., Solid State Physics **22**, 28 (1948).

²⁴ See the paper by P. Haasen and W. Schröter in these Proceedings.

²⁵ The slip process referred to involves shear between {111} planes locally separated by a distance $1/4\langle 111 \rangle$. The fault process occurs between {111} planes locally separated by $1/12\langle 111 \rangle$. The discussion returns to this point below.

Another interesting question which is unsolved, so far, involves the movement of kinks. We know we have *to create* kinks in order to move a dislocation over the Peierls potential barrier. On the other hand, we do not know what energy it takes *to move* kinks. It would be very valuable to have some information about kink mobilities from internal friction studies. The kink potential is a bit out of reach of the calculations so far. We still use the elastic "arc tangent" type of displacement, and certainly this is not sufficient for such an atomic scale configuration.

HIRTH: I would like to pose one question. Just looking at a strong covalent bonding picture, one would anticipate an extremely low stacking fault energy in the diamond cubic structure. Yet one seems to find experimentally that it is not all that low. Why?

HAASEN: I must admit that I was surprised about this too. I wonder whether we really have a valid experimental indication of the stacking fault energy. Theoretically, only the third nearest neighbors are disturbed across a stacking fault, so its energy should be extremely low. Let me ask you what experiment you are referring to, in particular.

HIRTH: I was thinking of the node measurements.

HAASEN: The old node results, I think are out. L. M. Brown,²⁶ at Cambridge, England, showed that previous node measurements were not done properly from the point of view of electron microscopy. If one did them properly, then one saw no extended dislocations.

HIRTH: Perhaps Professor Siems would rather answer that. But, I can state that Amelinckx disagrees with that view and still thinks that his microscopy was correct in indicating a small extension. In any case the puzzlement about the fault energy not being much smaller remains.

BULLOUGH: I have two short points, both concerned with ionic solids. The first is that it is frequently said that these are the crystals that we should do calculations on, because we know the potential. But, as a matter of fact, we do not know the repulsive part of the potential. Do we take a Born-Mayer potential, or what? Most people know how sensitive the simple point-defect-center formation energies are to the assumed form of the repulsive potential, so that things are not plain sailing in the sense of a well defined potential.

The second point is that, of course, these potentials have at least the feature that they are long-range, as is the polarization. I would like to address a remark on this, I think, to Professor Hardy. They gave the impression in their talk that the Kanzaki approach was ideal for such situations.²⁷

²⁶ Booker, G. R., and Brown, L. M., Phil. Mag. **11**, 1315 (1965).

²⁷ Kanzaki, H., J. Phys. Chem. Solids **2**, 24 (1959).

Clearly, given a long-range potential, its reciprocal space form will be short-ranged. However, one has the problem that the pertinent real space super-cells will have to be enormous, and therefore the density of points in the corresponding reciprocal space reduced zone will have to be equally enormous. So one has, as far as I can see, transferred the problem of the real space extent of the potential, which is a numerical problem, into another numerical problem involved in the final quadrature of unfolding the Fourier transform.

HAASEN: One point on ionic crystals: I think one should consider stacking faults in these materials on various planes. We have gotten used to the idea that dislocations are not extended in ionic crystals. However, Fontaine has recently done some calculations which show that extended dislocations actually exist on various planes,²⁸ especially on the {110} and on the {111} planes. I think effects of this sort could be seen experimentally, and calculations of the dislocation core structure in the sodium-chloride lattice should include the consideration of stacking faults.

ELBAUM: I would like to comment very briefly on one of the items mentioned in the agenda, namely the interaction of dislocations with conduction electrons and holes. I would like to point out that the calculation of the interaction with conduction electrons and holes, particularly the calculation of electronic energy states associated with a dislocation, is quite different depending on whether we deal with a covalent-ionic or a purely covalent crystal. The essential point physically is that in a covalent crystal such as germanium or silicon an extra half-plane associated with a dislocation—where electrons can, shall we say, become attached—is a plane where all the ions have the same charge. Therefore, the total Coulomb term in the energy, associated with the change of the charge-carrier population by unity, is substantial.

On the other hand if one deals with a crystal that is partly covalent and partly ionic, one can select dislocations which are known experimentally to be mobile and in which the extra half-plane is an alternation of ions of opposite sign. Thus, the inherent Coulomb term associated with such a half-plane is large to begin with, and the change of the Coulomb term when a charge carrier is added or taken away from this extra half-plane becomes, I believe, in most cases negligible. This renders calculation of the electronic energy states rather feasible.

HIRTH: An afterthought on the nodes.²⁹ Professor Haasen mentioned that in these materials there are charges carried by the dislocations. Perhaps

²⁸ Fontaine, G., J. Phys. Chem. Solids **29**, 209 (1968).

²⁹ See the previous exchange between P. Haasen and J. P. Hirth.

the charges profoundly affect the node configuration and influence stacking fault energy.

HAASEN: I think you are right. If the node extension is really small then the core structure would become quite important and this would depend on the charge.

BULLOUGH: Could I raise one further point? It occurs to me that it would be interesting to hear from Professor Maradudin about how he thinks the dislocation could be dealt with by lattice statics. A calculation he did many years ago at Bristol, I think, is the only one which has been performed.³⁰ He treated a screw dislocation and defined the dislocation by forcing the displacement field to be multi-valued. This is a kind of displacement dipole approximation in the Simmons-Bullough jargon.³¹ Considering how one would do an edge dislocation, one could conceivably do this by a semi-infinite sheet of forces defining the extra plane. This procedure is the analog of what Professor Hardy and I did for the vacancy, and this is a kind of force dipole situation.³² It just intrigues me to know whether you could do a force dipole for a screw; that is really what I am getting at. Is there some kind of "force" way of thinking of a screw dislocation?

MARADUDIN: The reason that I did the screw dislocation the way that I did it was simply because I found it very difficult to do a force model. It was much easier to slice the crystal along the dislocation line and simply hook the atoms on one side of the cut back again—not to the neighbors that they had before the cut was made, but to the neighbors below, for example. Then at the expense of adding a few Kronecker deltas here and there, the solution went through very nicely.

I think one can, in fact, do the edge dislocation by the half-sheet of forces in a manner mathematically similar to the way that Max Wagner³³ suggested a few years ago for treating an analogous lattice dynamical problem. The problem was that of calculating the dynamical properties associated with impurities which have internal degrees of freedom.

I do not want to go into the formal aspects of how one does this extension-matrix-partitioning technique. I think the upshot is that you do represent the edge dislocation by a set of additional forces acting on the atoms of the undislocated crystal. The problem then reduces to expressing the displacement field as a double-Fourier integral and solving the corresponding difference equations that way. It has not been done, but I think it can be.

³⁰ Maradudin, A., J. Phys. Chem. Solids **9**, 1 (1959).

³¹ See their paper in these Proceedings.

³² Simmons, J., and Bullough, R., op. cit.

³³ Wagner, M., Phys. Rev. **131**, 2520 (1963); **133**, A750 (1964).

HARDY: I just wanted to make one or two comments on Dr. Bullough's question in regard to the use of long-range forces in lattice statics. In fact we have applied this technique to charged point defects in ionic crystals, and we find that everything goes through very nicely. One gets the formation energies, the displacements in the vicinity of the defect, and so on without any particular problem. The only problem is that when one calculates the relaxation energy, one has a summation over reciprocal space. As Dr. Bullough suggested, one requires a fairly dense sample of wave vectors in reciprocal space to get that sum to settle down; but it is possible to do this. In fact, in our papers in the proceedings of this meeting, we describe the results we have obtained in this way.

But, as regards the actual displacements themselves, there is no particular problem. In the case of the dislocation I think the problem is more apparent than real. In fact, Professor Maradudin and I were discussing over coffee the point that the long-range part of the Coulomb field does not directly affect the dislocation configuration. The long-range part of the Coulomb field is something that remains actually uniform as you displace, say the ion rows of the dislocation. It is the periodic part that varies, and the periodic part is relatively short-range.

THOMSON: I just want to pick up the comment that Professor Haasen made having to do with the mobility of the kinks on dislocations in the diamond lattice. There have, of course, been two approaches to this; one, the abrupt kink originally suggested by Dr. Brailsford³⁴ and taken seriously more lately by Dr. Gilman, and the other view that the kinks on dislocations in these lattices are freely moving.

Now what is the experimental situation here? I believe there were some attempts, or at least some good intentions, of measuring the kink mobility. I wonder if people in the room have anything to say about this?

HAASEN: Are you referring to Russian work³⁵ on some internal friction maximum at low temperatures — about 110°K in germanium and silicon?

THOMSON: I believe there were several people who attempted to do this.

HAASEN: I'm afraid the work did not suffice to identify the process. The authors of the most recent work³⁶ found a peak; and related it to kink movement; but there really is no proof that this is the true explanation of the peak.

THOMSON: I dimly remember some work by people at Shockley's place some years back about the motion of [small angle dislocation] boundaries

³⁴ Brailsford, A. D., Phys. Rev. **122**, 778 (1961).

³⁵ Kromer, P. F., and Khiznichenko, L. P., Phys. Stat. Solidi **21**, 81 (1967).

³⁶ Ibid.

in these crystals, which apparently was relatively easy, but I do not remember the details.

GILMAN: First, I shall answer Professor Thomson, and then I shall ask my question. It seems to me that the most direct evidence about kink mobilities is given simply in Dr. Dash's pictures³⁷ of dislocation loops in silicon, where the loops have discrete hexagonal shapes for certain rates of deformation and temperatures. It is very hard to account for the shape unless the kinks have difficulty in moving. If they are freely moving, one would expect ellipsoidal loops. The situation is similar to that encountered in etch pit formation where the ratio of the kink formation rate to the movement rate determines the shape of a mono-surface step. Polygonal shapes are found only if the ratio is near unity. If it deviates from unity in either direction, circular or ellipsoidal shapes result.

THOMSON: It is not that there is a Peierls energy. I think everyone agrees to that. It is a question of whether the kinks, themselves, can move freely.

GILMAN: But if they could move freely along the line, then the loop could not possibly have a hexagonal shape.

HAASEN: You know, those pictures of hexagonal shaped loops are very nice. However, if one looks at dislocations in silicon under the electron microscope in transmission, then they are not hexagonal or kinked. They are like dislocations in any other material. Hence, I wonder whether the situation has not changed a bit since those pictures were taken?

GILMAN: I would like to ask my question now. This is directed to Professor Haasen, primarily. As we all know, there is much evidence that the stacking fault energies are in fact relatively low in some of these crystals: this is indicated by the poly-typism of silicon-carbide and zinc sulfide; and the fact that it is hard to grow silicon crystals epitaxially without getting stacking faults, and so forth.

This raises the question of whether or not the issue is associated with a nucleation barrier to the extension of a dislocation. Such a barrier might be expected because there is a high Peierls force. Then one would not get spontaneous extension. My question is: Have people worried about this, and if so what do they conclude about the height of the activation barrier for decomposition?

HAASEN: I think basically that my view, too, is that a nucleation barrier is involved. In diamond cubic structure a view parallel to a {111} plane is like this [fig. 2]. Here the atoms are bound tetravalently. The slip by

³⁷ Dash, W. C., J. Appl. Phys. **27**, 1193 (1956).

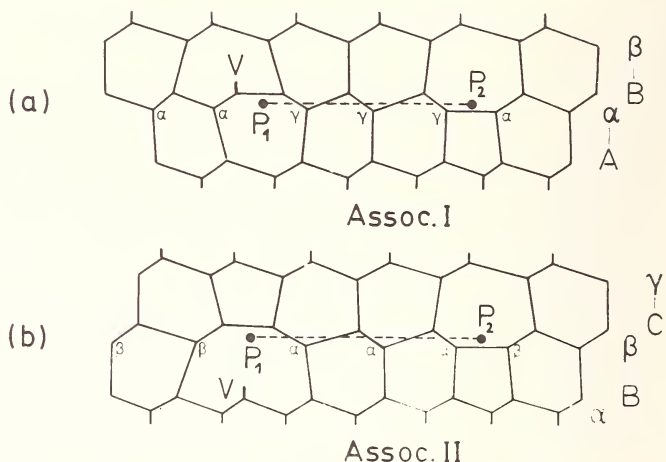


FIGURE 2. Possible associations of a complete (perfect) dislocation V and two partials of opposite sign, $P_1 - P_2$, extending a stacking fault in the diamond structure. The stacking order of the perfect lattice is $A \alpha B \beta C \gamma \dots$ in this picture. The lattice is projected normal to (110) . Courtesy of P. Haasen.

$1/2 \langle 110 \rangle$ dislocations shears the widely spaced plane, [between β and B , for example, in fig. 2] while in order to make a stacking fault, one must shear in between here [between α and B in fig. 2] or rotate the tetrahedron, which is equally difficult.

If one has a dislocation between the widely spaced planes [between β and B] one might associate this dislocation with two partial dislocations of opposite signs between the narrow planes [α and B]. If the stacking fault energy is low, the configuration will extend quite a bit and elastically act like a split dislocation. The array is, however, on two planes one interatomic distance apart, so only from the elasticity point of view does one have a single extended dislocation. As Dr. Gilman was remarking, there is the problem of nucleating at the core of the dislocation two partials of opposite sign which move apart to extend a stacking fault. One might, then, have a situation where upon applying a stress the complete dislocation runs away and the stacking fault shrinks to nothing, the two equal and opposite partials annihilating.

HIRTH: The next topic includes "Disclinations and Equilibrium Configurations."

DE WIT: Well, I shall confine myself to disclinations for obvious reasons. Yesterday, we saw many different ways we can look at disclinations, and

I shall assume you all know what they are by now. There are several small problems, though, that may still have to be settled, such as the one that Dr. Anthony brought up about a statement I made that dislocations can only end on disclinations. He has the same formula in his paper, incidentally, on which I based the statement.³⁸ Also of interest, is that I have a letter from Professor Schaefer, who has the same formulas in his paper. He also asked the question: "How can you visualize geometrically what this means?" That is an interesting question to follow-up to see what the answer is.

What I want to try to do here is assess the position of disclinations with respect to the theme of the conference:

First, I think that disclination theory is a logical extension of dislocation theory as it was developed by Professor Kröner. Hence, it motivates a search for a more complete theory of defects, from just a continuum point of view, for instance. One can confine oneself to linear theory, as I have done, or one could go to non-linear theory. In the non-linear theory we use non-Riemannian geometry where the Riemann-Christoffel curvature tensor would describe disclinations and where the torsion tensor would describe dislocations. What disclinations then do is to spoil distant parallelism and to introduce difficulties on that account—which one would have to look into.

A second point that I can mention is that there is a dualism—pointed out, I think, by Kondo first³⁹—which shows how the geometry of disclinations and defects in general meshes into couple-stress theories. Hence, it motivates generalizations in that connection: for instance, to Cosserat and more generalized continua.

A third point is that the theory fits into Schaefer's theory,⁴⁰ called "motor analysis." "Motors" as algebraic objects were introduced by Clifford, who is also responsible for Clifford Algebra, and were used by Von Mises in an application to mechanics. For this purpose Von Mises employed the term "motor algebra." Clifford described motors by using double numbers. An alternative description is via dual numbers, introduced by Study—the word "dual" is used here in a different sense from that in my second point. Von Mises suppressed dual numbers, feeling that the usage was confusing in mechanics, but Schaefer has reintroduced

³⁸ The equation in Anthony's reply below.

³⁹ Kondo, K., RAAG Memoirs of the Unifying Study of Basic Problems in Engineering and Physical Sciences by Means of Geometry, I—III (Gakujutsu Bunko Fukyu-Kai, Tokyo. 1955. 1958, 1962); see also Kondo, K., in Mechanics of Generalized Continua (Prop. IUTAM Symposium, Freudenstadt-Stuttgart, 1967) E. Kröner, Ed. (Springer-Verlag, Berlin, 196) p. 200.

⁴⁰ Schaefer, H., in IUTAM Symposium, op. cit., p. 57, and ZAMM 47, 319 (1967).

them.⁴¹ Schaefer's theory very nicely generalizes the idea of a Burgers vector. The combination of the Burgers vector and the rotation vector of a disclination forms a motor from his point of view.

I thought that these three points showed a relation between the general theme of the conference — defects — and how disclination theory might provide a path by which other theories can be brought in or new theories can be evolved. These ideas I had before. I now realize from the discussion yesterday that there are even practical applications for disclinations.

One other historical point may be of interest. I notice on the agenda the word "disclinations" as well as the word "disinclinations." The original term, "disinclinations," is due to F. C. Frank,⁴² who used it in 1958 at a Faraday Society meeting. The word in Professor Nabarro's book is "disclinations."⁴³ I think it would be best if I leave it to Professor Nabarro to explain this later, if he does not mind, because I think it would be interesting to know how this word developed.

BULLOUGH: I do not want to spoil the subject of disinclinations, but there are other items also in this topic. I was going to ask if anyone thinks it is worthwhile to use anisotropic elasticity to calculate the equilibrium energies of tetrahedra and collapsing tetrahedra? Is this really the best way to get stacking fault energy from the giant-jog spectra? Maybe it is being done. I would be very interested to know.

HIRTH: In turning to the general discussion, first we will revert to the question of disinclinations or disclinations. Professor Nabarro?

NABARRO: Well, I think this is just a typical piece of bogus history. As I remember, Frank's account of it is that he used the word "disinclination." He then wondered if this was the wisest word and consulted the Professor of English at the University of Bristol, whose name is forgotten, and he said he was disinclined to use that word.

AUDIENCE: General laughter.

NABARRO: May I take the opportunity of being on my feet to show two slides? Now, this [fig. 3] is clearly a screw disclination. It is made, as I understand it, of a flexible magnetic material and one can see that it does all the things that it ought to do. Incidentally, there was a very recent

⁴¹ These and further historical remarks were given by H. Schaefer in a lecture "Die Motorfelder des dreidimensionalen Cosserat-Kontinuums in Kalkül der Differentialformen" at Padua (March 28-29, 1968), which will appear in Italian translation in Università di Trieste—Instituto di Meccanica, Lezioni Conferenze.

⁴² Frank, F. C., Disc. Faraday Soc. **25**, 19 (1958).

⁴³ Op. cit.



FIGURE 3. A screw (wedge) disclination of strength - 1. Courtesy of F. R. N. Nabarro.



FIGURE 4. Three screw (wedge) disclinations of strength - 1. Courtesy of F. R. N. Nabarro.

paper of, I think, deGennes and Pincus⁴⁴ on the singularities of an isotropic magnetic fluid in which they show a screw disclination of strength +1. This [fig. 3] is a screw disclination of strength -1 and I am sure it is a lot older. One of the questions I want to ask is whether there is anybody who can tell me where I got these pictures? Because, I think they have now because of historical interest. The next slide [fig. 4] I have been analyzing during the course of this morning. It seems to me that what this represents is the intersection of three orthogonal screw disclinations, each of strength -1. That is to say, you draw the cubic axes through these, and that is all there is to it. But, I do think it is a figure of great beauty. I think it probably comes from one of the books of Lehmann some fifty or sixty years ago, but I should be very grateful to be reminded where it does come from.

KRÖNER: With respect to disclinations, I would like to say that certainly they are not important in normal, three-dimensional crystals; maybe they are important in surface crystals. They have been observed in the lattice of flux lines in superconductors and I think that is a reason why we should be interested in them, but not in using them to construct a theory of internal stress or dislocations or plasticity and so on. I cannot really see how we can construct even something like a continuous distribution of these disclinations. The reason, of course, is that a disclination would be a configuration that has so much energy that the crystal just cannot bear it. Just because of this the disclination does not appear in ordinary crystal lattices.

Now, we can think of quasi-disclinations. But this word does not seem to be appropriate, because we are thinking of special point configurations when we speak of disclinations. Instead of using the word "quasi-disclinations" we could also use the word "incompatibility," because this is just the same thing.

KLÉMAN: Since Professor Kröner advocated the possibility of application of the notion of disclinations to flux-lines in magnetic materials, I would like to comment on the application of this notion to heli-magnetics. In heli-magnetics, nobody has ever guessed what are the modes by which the flux is conducted, and nobody has ever seen something which is routine, like walls or flux-lines. [Dr. Kléman proceeded to give a nice presentation of a logical mechanism for conducting flux inside a heli-magnet by means of a combination of a +5 disclination and a -5 disclination. The explanation was heavily based on blackboard drawings which were not retained, and hence it is not repeated in detail here.]

⁴⁴ Orsay Liquid Crystal Group, Phys. Lett. **28A**, 687 (1969).

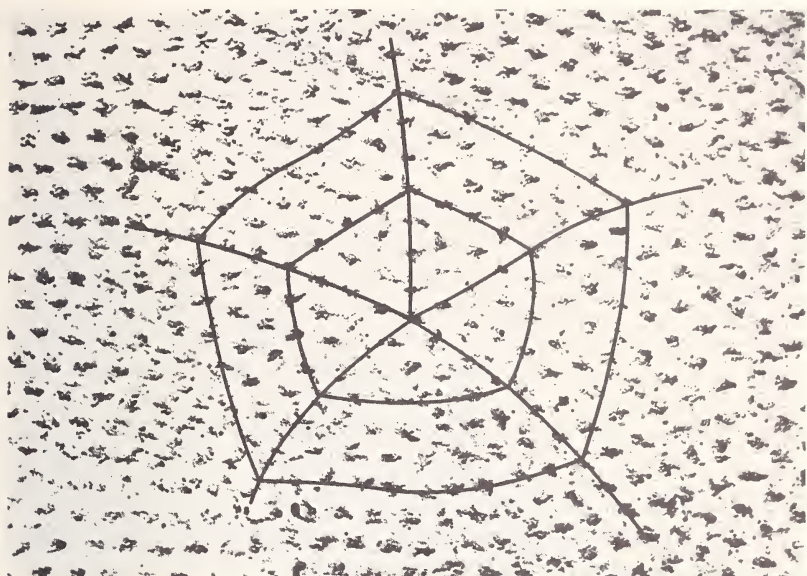


FIGURE 5. A wedge-disclination in the two-dimensional lattice formed by magnetic flux lines in the mixed state of type II superconductors. From Anthony, K. H., Essmann, U., Seeger, A., and Träuble, H., in Mechanics of Generalized Continua, (IUTAM-Symposium, Freudenstadt/Stuttgart, 1967) E. Kröner, Ed. (Springer-Verlag, Berlin/Heidelberg/New York, 1968). Courtesy of K. H. Anthony.

ANTHONY: May I have the slide, [fig. 5] please? Here, you see a disclination which is observed in the lattice formed by magnetic flux lines in the mixed state of type II superconductors. In this state the magnetic flux enters into the body from the boundary of the superconducting probe. The physical background is as follows: If a magnetic field acts on a superconducting specimen and if the magnitude of the field and the temperature are below certain critical values, the superconductor is in the so-called Meissner-state in which there is no flux inside the specimen. By increasing the magnetic field we go to the mixed state where the flux enters through the boundary. This magnetic flux is quantized in form of the flux lines which arrange themselves in the so-called Abrikosov lattice. In this lattice one can find, for instance, such defects as the disclination in the slide, which is called a screw disclination by Professor Nabarro. I agree with Professor Kröner that such a defect is quite insignificant in a solid crystal. The lattice curvature is very large, too large to exist in a solid crystal. But if one has a very soft crystal, for

instance this two-dimensional lattice formed by magnetic flux lines, one can find such defects.

The equation

$$\partial_i \alpha_{ij} + \epsilon_{jmn} I_{mn} = 0,$$

which is basic in the linear theory of disclinations, seems to establish a geometrical correlation between dislocations and disclinations. I is the tensor of the disclination density, α the contracted torsion tensor of the lattice parallelism, and ϵ_{jmn} is the Einstein permutation operator. I am convinced that α cannot be interpreted as a dislocation density, i.e. there is no connection between dislocations and disclinations because of the following facts:

We have two sorts of disclinations: The one sort, the screw- or wedge-disclination, is characterized by a rotation failure for a closed circuit round the disclination line, the vector of which is parallel to the disclination line. For this reason we have a Burgers vector which decreases to zero if the radius of the Burgers-circuit round the disclination line decreases to zero. In order to explain this behaviour, it is sufficient to assume a non-vanishing disclination density I . The other case is a disclination which shows a rotation failure perpendicular to the disclination line. Such a disclination cannot be produced in a singly connected crystal; the lattice would be destroyed. But it is possible if one has a crystal which is doubly connected, i.e. which contains a cylindrical hole. Now in this case, the Burgers vector doesn't decrease to zero if we contract the circuit to the disclination line. For this reason, the disclination density I is not sufficient to characterize such a disclination. We need a non-vanishing torsion tensor α , too, which is called disclination-torsion and which in the linear approximation is related to the disclination density by equation (1). The tensor α is an intrinsic property of the disclination and cannot be interpreted as a dislocation density as can easily be shown by means of the lattice parallelisms which belong to disclinations and dislocations, respectively.

DE WIT: Maybe, as you say, α is part of the disclination density; that is something that I would like to look at. At the moment it seems to me perhaps an opinion. But I think your equation (1) is the one that needs interpretation, and I will look at it when I have some time.

Another comment I would like to make is about energy. Professor Kröner says that there is a lot of energy associated with a disclination, but the disclination picture that Dr. Anthony showed [fig. 5] also has a lot of dislocations in its neighborhood. This is one way that the stresses are relieved. Maybe this is a way that would enable disclinations to occur more easily. Here, we would have a cloud of dislocations around the dis-

clination analogous to the situation of a Cottrell atmosphere of point defects around the ordinary dislocation.

The next point is that I do not like very much the words "screw" and "edge" disclinations which Professor Nabarro uses. The Stuttgart school prefers "wedge" instead of "screw" disclination. This is much more descriptive, I think, and less likely to lead to error. There does not seem to be a screw associated with such a disclination, but there is a wedge associated with it. You only call it a screw disclination by analogy, because the rotation vector points in the same direction as the disclination line. But it is not even the same kind of a vector as the Burgers vector. It is an axial vector, whereas the Burgers vector is a polar vector.

NABARRO: What is the fourth word, then, screw, edge, wedge and . . .?

DE WIT: That is what I want a word for.

NABARRO: Well, that is up to you.

DE WIT: But there is no obvious reason to call disclinations screw and edge. Perhaps someone has some ideas on this. [At this juncture, Dr. Eshelby suggested the word "wrench" to replace "edge" disclination. Then, during some of the succeeding discussion, Eshelby, Hirth and deWit caucused, sotto voce, and endorsed "twist" disclination as a physically descriptive replacement for "edge." Hirth announced this at a later point in the proceedings, but it seemed appropriate to insert it after the above colloquy.]

ESHELBY: I wanted to note that if anybody wants to hunt for a disclination, another thing to look at is a collection of screw dislocations going through a thin film. I know of one nice picture which has got an edge super-dislocation in an array of screw dislocations going through a thin film. I tried to interest Professor Hirsch in it—it was taken by his school—but all they were keen on was verifying that elasticity theory was O.K. and that diffraction theory was O.K. I could not enthuse them about the fact that these things formed a nice lattice with an edge dislocation in it. But I think if one examined some of these pictures, he might well find the odd disclination. The point is that they interact with a very short range repulsion. Anything that pushes them together forms them into a lattice. It is a fairly sloppy one, so I think one might well find a disclination—or even make one, somehow.

BULLOUGH: I would like to take up the point that, of course, there are regions in crystals where we could legitimately say the Riemann-Christoffel curvature tensor does not vanish. Right in the grain boundaries where the lattice correspondence is lost, for example. What about the suggestion that when dislocations slip into grain boundaries we call them infinitesimal disclinations? In other words, they go back into curvature.

Then when they are generated from grain boundaries, they come out of curvature, pop back into torsion, and become dislocations.

DE WIT: May I just make a short comment? Dr. Eshelby⁴⁵ showed some time ago that one gets the elastic results for edge dislocations by differentiating that for a wedge disclination, so they seem very closely related.

GILMAN: I have a partial question and a partial comment. Is it not true that there is a whole class of applications of disclinations when they come in pairs; that is, dipoles? For example, do I not have one in my watch, which consists of the spring wound up and held by the ratchet, which, in time, gradually releases the disclination dipole as the watch operates? Or, another case is the little paddle at the back end of a type of child's boat. You know; you wind it up against the torque extended by attached rubber bands, fix it in place, and put the boat into the water. When you release it the disclination dipole gradually disappears and the boat goes forward through the water.

AUDIENCE: General laughter; applause.

HIRTH: We might put that into the category of a Dirac comment in light of Professor Nabarro's remark of yesterday.⁴⁶

BESHERS: Is it known that there is a conservation theorem for this so that one disclinates the water?

AUDIENCE: General levity, light remarks and laughter.

ERINGEN: I would like to remind the audience that dislocation theory came from the theory of incompatible elasticity. Now it seems that there is a general tendency here against accepting disclinations. They can be very easily understood if we extend the boundaries of classical elasticity into the so-called deformable Cosserat continua. Now, without taking some of the points from our paper tomorrow, I would like to indicate that disclinations and, in fact, continuous distributions of disclinations, can be brought into the framework of mechanics through the incompatibility of the stretchable directors. In this sense, then, we must sort of abandon the non-Riemannian geometry of three-dimensional space. It turns out, however, that if one works with six-dimensional space and looks at the curvature tensor in it, then it will be quite natural that disclinations as well as dislocations come in. I think if one examined this, the disagreement between Dr. Anthony and Dr. de Wit would be resolved.

⁴⁵ Eshelby, J. D., Brit. J. Appl. Phys. **17**, 1131 (1966).

⁴⁶ See p. 676.

BEN-ABRAHAM: I would like to comment on the last remark. I do not believe that disclinations can be found in good crystals, except as Dr. Bullough pointed out, in grain boundaries, especially large angle grain boundaries. However, in hunting for disclinations the place where we always find them is in liquids. In the continuum theory, we define solids by saying that the lattice directions are everywhere well defined, which mathematically means that we have a distant parallelism. Now, this is destroyed in a liquid. While, in physical terms, short-range order persists, long-range order does not. In mathematical terms we have defined connection, but we do not have distant parallelism.

Physically, that means one starts out at an atom, looks at the configuration of its nearest neighbors, and finds something very similar to a crystal. However, if one wanders around the crystal with some vector on a path and comes back to the origin, one winds up with curvature instead of with the original vector, and curvature in our terminology means disclination. So that in the case of the liquid, we have just a body which is continuously disclinated in a "macroscopic" sense—notice here the implicit question: what is macroscopic?

Thus, a liquid, as opposed to a solid, would be characterized by a non-zero Riemannian curvature. Why? We shall be looking into this a little bit more carefully; it turns out that there are still very severe restrictions.

For one thing, on a macroscopic scale a liquid has to be isotropic. This restricts one to a scale of curvature different from zero and also reasonably small as compared to unity. Otherwise, the liquid will not be derivable from the crystal.

KRÖNER: I think in the sense that you use fluids here, you could say the same for polycrystalline aggregates. I do not see how the change in energy comes in, however.

Also, I do not share the view of Dr. Bullough that grain boundaries have anything to do with disclinations. Instead, in my opinion one should describe the entire assembly of atomic points by a general affine connection, which also has a metric part. To the metric part belong both the dislocations and the disclinations, because they preserve the lattice. In fact, in dislocated and disclinated lattices one can compare distances by counting atomic steps. However, if one goes through a grain boundary, one does not know how to go from one point to the next because there is quite a choice of going in different directions. So, I would say that the grain boundaries are regions of the crystal which are non-metric. One cannot compare lengths by counting lattice points on a path which goes through a grain boundary.

In summary I think grain boundaries and lattices would fit quite well into the general scheme of differential geometry. But, as I said before, I think

the disclination is completely different from the grain boundary; the former leaves the lattice intact.

BULLOUGH: You object to infinitesimal disclinations, do you?

KRÖNER: You could say quasi-disclinations, but there is nothing infinitesimal in the lattice.

HIRTH: Well, I think we might give some time to the other topics that were on the agenda at this point. Dealing with the question of whether one might calculate tetrahedra energies using anisotropic elasticity, I think Dr. Head has something to say.

HEAD: Yes. Well, you are not referring to complete tetrahedra, because the Stuttgart school years ago produced energies for them.

BULLOUGH: No; the unwrapping tetrahedra.

HEAD: Oh! The trouble here is that for a given configuration of dislocation one can think of ways of getting its energy in anisotropic theory, but in the cases one is interested in here there are mobile elements whose position is not known in advance. These have to take up their equilibrium position.

Just thinking of the dissociation of a triangular Frank loop, for instance, where are the Shockley partials running up the planes that are going to be the faces of the tetrahedron? They will be curved dislocations whose position will be determined by equilibrium conditions, but how to handle this sort of mobile dislocation problem *in anisotropy* I have no idea at all. We would like to know how to do it, but it is a very difficult problem—even computerwise. I mean, one could write something and put it in a computer, but it might take months of computing time. It is impossible to get that much time.

BULLOUGH: I was really thinking, with your experience at anisotropy and so on, whether you think it is worthwhile. Whether it would improve the accuracy of stacking fault estimates. You mentioned absurd errors in stacking fault energies in your talk, and I wondered whether this would be one way to logically reduce the error?

HEAD: Well, you are going to a more complicated configuration than the usual nodes, and it is rather hard to handle in anisotropic theory.

BULLOUGH: Is not the super-jog the best way to do it?

HEAD: Well, it is not clear to me that it is in fact do-able—in practice, anyway. As a practical computational method, I do not know of any computer that could handle it.

HIRTH: Could I say something here? What about Gallagher's configuration of three parallel partials?⁴⁷ That should be amenable directly to anisotropic elastic calculations.

HEAD: Sure; I mean, you have got a two-dimensional situation there. That should be straightforward. Ordinary elasticity is bad enough in three dimensions, but anisotropic cases are more difficult.

HIRSCH: I am not quite clear whether it would be possible to do the sessile jog. Perhaps this is what Dr. Bullough was getting at. It would be very nice to test whether all these proposed configurations for dissociated jogs really exist using anisotropy.

BULLOUGH: I was really referring to the super-jog mechanism for getting the maximum-size tetrahedron.

HIRSCH: Right! But at least in that case you are not worried about bowed-out dislocations, are you?

BULLOUGH: Well, what is wrong with Jøssang and Hirth's piecewise continuous dislocation model?⁴⁸ Do you have to put a bow-out on? It seems an incredible complication unless it's really necessary.

HIRSCH: Well, I think it would be a very interesting thing to do, if it can be done. It also has relevance to another topic on the agenda: that is dissociated dipoles. Are they in fact formed from dissociated jogs?

LOTHE: I have one comment. In the planar cases, I think the anisotropy problem is manageable. An example is the extended node which can be handled using energy factors for straight dislocations, such as are becoming more and more available, combined with Brown's formula,⁴⁹ say, or with piecewise straight dislocation formulas.⁵⁰ The planar curved dislocations can be handled in the anisotropic case using Brown's formula in the same way he did for the isotropic case, requiring only infinite straight dislocation parameters.

DE WIT: In most of the treatments of equilibrium configurations, except for the straight dislocation, there occurs in the formulas a logarithmic term with a core cut-off parameter. It sometimes makes as much as an 8% difference to the experimentalist, depending on what one chooses for this core cut-off parameter⁵¹ — for instance, when using the formula of Brown for dislocation nodes.⁵² So, my question is: Do those people that have

⁴⁷ Gallagher, P. C. J., *J. Appl. Phys.* **37**, 1710 (1966).

⁴⁸ Jøssang, T., and Hirth, J. P., *Phil. Mag.* **13**, 657 (1966).

⁴⁹ Brown, L. M., *Can. J. Phys.* **45**, 893 (1967).

⁵⁰ See paper by J. Lothe in these Proceedings.

⁵¹ Ruff, A. W., Jr., *Metall. Trans.* **1**, 2391 (1970).

⁵² Brown, L. M., *Phil. Mag.* **10**, 441 (1964).

worked on the core-structure statics have a way of using their results to come up with a better cut-off parameter for use in such continuum theory? The experimentalists, I think, would very much like to know this.

BULLOUGH: Perhaps I could comment? It is a terribly difficult question!

But my own opinion is that in these calculations involving elastic energies of stable configurations, I at least find it esthetically pleasant to completely separate the two: the unknown hole (the dislocation core) down the middle and the harmonic energy around it. So I make a little plea for putting in the correct core-surface traction term. This traction term is the quantity you have to add on to the surface-integral expression for the energies so that it actually equals the volume integral of the strain energy density. I know that will start something!

KRÖNER: Just a short comment. In my old book on continuum theory of dislocations and internal stress,⁵³ I have done something on this core problem. One can calculate the total dislocation energy, for instance, by using Peierls' method, fit this to the ordinary elasticity solution, and choose the cut-off radius so that the Peierls solution is matched. I think that what the Peierls solution gives in excess of the elasticity solution is just the core energy. This is a way to do it, I think.

BULLOUGH: My difficulty with your continuous distribution approach in the core is the following. I have always been puzzled by the fact that you are describing an atomic region by a continuous distribution of dislocations and getting the energy from that via the interaction between the infinitesimal elements. In a way this is just the region where one does not want infinitesimal elements. You criticized my previous remark on the grain boundaries because you said there are atoms. [General laughter.] But that is not how the Peierls energy is found. As I understand the Peierls model in your general theory, you have an arbitrary distribution of infinitesimal dislocations which goes into the general energy expression. The Peierls energy, however, is a fully atomistic energy that is handled separately.

TEUTONICO: I want to get back to Professor Hirth's comment about Gallagher's three-fold ribbon. One cannot calculate its energy analytically, in general anisotropic theory, for the {111} plane. One can get it for a ⟨112⟩ direction or a ⟨110⟩ direction. Thus, there is an analytic solution every thirty degrees, in the {111} plane, but that is all; it cannot be done in general for that plane. However, I have performed the calculation numerically.

⁵³ Kröner, E., Ergeb. angew. Math. 5, (1958).

HIRTH: But, if Dr. Head gets his solution to the general sextic equation, an analytic solution would be available.

HEAD: Yes. Hyperelliptic functions are analytic functions, so one can do the problem analytically.⁵⁴

HARTLEY: I would like to make a comment on the calculation of the criterion for dissociation of dislocations, apropos of what Dr. Bullough said. We have done a bit of an extension in pushing linear elasticity to calculate the energetics of the dissociation of perfect dislocations in f.c.c. crystals into two Shockley partials. The aim was to see just what additional corrections to the more-or-less classical, linear result one gets by including the correct core-surface traction terms; by including the fact that the continuum elastic core radii will probably change in the ratio of the moduli of the Burgers vectors; and by including the geometrical fact that the only region that has a constant—or anything like a constant—stacking fault energy is the region between the boundaries of the cores.

With these three corrections, and not taking into account any consideration of the anisotropy of the core energy itself it turns out that the energy change accompanying dissociation of a perfect screw dislocation does not become less than zero until separations are reached of about ten times the core radius. This value replaces that of 2.7 (more exactly the number e) times the core radius which is obtained without considering the core tractions and without considering these other geometrical things.⁵⁵

Also, for the edge, instead of 2.7 the factor is 4.1 times the core radius. Thus, the point is that including these corrections makes it even less likely that a dislocation will dissociate with a given fault energy.

HIRTH: Yes. I might make a brief comment on that. I think what Dr. Bullough had in mind was that there are, as far as I can count back, three schemes for taking the core into account in the elastic solution:⁵⁶ One is the core traction method that Bullough mentioned; one that of Professor Kröner of more-or-less averaging a core screw-edge energy and including

⁵⁴ See, for example, for the general quintic: Klein, F., *Lectures on the Icosahedron and the Solution of Equations of the Fifth Degree* (Dover Publications, N.Y., 1956); for the analogy between the general quintic and the general sextic: Klein, F., *Math. Ann.* **61**, 50 (1905); and for the general sextic: Gordon, P., *Math. Ann.* **61**, 453 (1905), **68**, 1 (1910), Coble, A. B., *Math. Ann.* **70**, 337 (1911).

⁵⁵ Hartley, C. S., *Phil. Mag.* **14**, 7 (1966) or Friedel, J., *Dislocations* (Pergamon Press, 1964), p. 159.

⁵⁶ Bullough, R., and Foreman, A. J. E., *Phil. Mag.* **9**, 316 (1964); Kröner, E., *Erg. angew. Math.* **5**, (1958); Jossang, T., Lothe, J., and Skylstad, K., *Acta Met.* **13**, 271 (1965); Jossang, T., *Phys. Stat. Solidi* **27**, 579 (1968).

it; and one that Jøssang suggested of just using the interaction energy between two screw dislocations to establish a core parameter. All of these are self-consistent and as long as one restricts interactions to a given glide plane, they lead to no problems. But, all lead to some problem in determining the interaction energy if there are displacements of the dislocations in other than radial directions. So it is a question of self-consistency and of realizing that there are these problems with what one might call the torque terms.

HEAD: Could I just dispute the fact that there are three methods you have just named taking the core into account? You can only take the core into account when you know it — on the atomic scale.

HIRTH: I mean artificially taking it into account.

HEAD: Artificially, yes. As one example, consider the sort of variation you can get if you consider the question: Does a triangular Frank loop have a higher or lower energy than the corresponding stacking fault tetrahedra when the sizes are of the order of 50 Å?

The whole business essentially hinges on the core. It is the core energy that determines the difference here. All of these conventions can give you *any* answer; you just have to know the real core energy. Perhaps such comparisons with experiment provide a way of determining core energies, or of determining which convention is better for a particular case. But it does not mean that when you change the Burgers vector or something else that the convention stays good.

HIRTH: My point was that none of the conventions is, *a priori*, better than the others, but that one can choose one and then use it *self consistently* as an artificial way of describing the core in the absence of actual knowledge of it.

HEAD: If you had some way of calibrating it absolutely to start with, yes.

BULLOUGH: Your comment is rather negative because we do not know the core energy. I would dispute strongly that we took into account something that we did not know. Ours was an elastic calculation and all we tried to do was make sure we got the unique elastic energy; and if this satisfactorily explained the results — which it did — this was our definition of contentment.

HEAD: Sure. Well, what you did was very good in that it separated clearly what you knew about the linear elastic energy into which — if you ever knew the core value — you could plug that result. It gave you a clear description of the linear elastic energy, but not of the total energy.

BULLOUGH: I never said it did.

HEAD: No, but people are using it as being a better description of the total energy than some of the other cut-off parameters.

BULLOUGH: Well, they should not be.

HEAD: O.K. But they are! I mean, it is represented as being a better description of the total energy. Not by you, but by other people. I say that none of these cut-offs is anything more than a conventional description of the total energy.

BULLOUGH: I must say we get misquoted many times regarding this paper, the one with Foreman on the energies of rhombus-shaped loops.⁵⁷ We actually did a Peierls calculation in that paper. We discussed clearly what we were missing out, and we put it in, to the Peierls approximation. So I mean, I do not understand why people misquote us.

HEAD: Well, this is always a problem. I think we all have this cross to bear some way or other. We all have a paper that everyone misquotes, and we can never understand why.

DE WIT: This brings me back to the original question.

AUDIENCE: Applause.

DE WIT: Do the people who do lattice statics have anything to contribute that would be helpful? Because they presumably are calculating the core structure.

HIRTH: This might be a question that we could continue in the "Future Directions" panel; it seems to be a future question.

BULLOUGH: It is very much in the future.

HIRTH: As a final remark, somebody passed up a paper and suggested a name replacing the edge disclination as a "lock-washer" disclination.

On that note, I suggest we adjourn. [Whereupon the session was adjourned.]⁵⁸

⁵⁷ Op. cit.

⁵⁸ Although the panel did not have time to discuss topic (5), "Critical Configurations," in a conversation after the panel P. B. Hirsch said that there was one point relative to this topic that he felt should be noted. To wit: that someone should theoretically treat Fleischer's mechanism for cross slip of an extended dislocation at a particle. See Fleischer, R. L., *Acta Met.* **7**, 134 (1959).

CONTRIBUTOR INDEX

- ANTHONY, K. H., **637**, 676, 677, 713
ARSENAULT, R. J., 311, 460, 997, 1107, 1164, 1166
ASHCROFT, N. W., **179**, 201, 202, 203, 247, 1175, 1255, 1258
BACON, D. J., **35**, 461
BARNETT, D. J., **125**, 832, 836
BEN-ABRAHAM, S. I., 250, 309, 310, 676, 677, 717, 835, **943**, **999**, 967, 1021, 1255
BENNETT, L. H., 1175
BERG, H. M., **71**
BESHERS, D. N., 84, 395, 552, 577, 716, 1164, 1166, 1227
BLOOM, J. E., **71**
BOLLMANN, W., **465**, 552, 557, 558, 560, 561
BRAILSFORD, A. D., 417, 1165, 1166
BULLOUGH, R., 84, **89**, 173, 202, 203, 247, 249, 250, 251, 252, **273**, 311, 396, 552, 561, 577, 687, 690, 692, 694, 695, 696, 700, 703, 705, 710, 715, 718, 719, 720, 722, 723, 835, 836, 966, 998, 1135, 1167, 1175
CHANG, R., 201, **299**, 561, 694
CLAUS, W. D., JR., **1023**, 1054, 1055
COTTERILL, R. M. J., **285**
DATTA, B. K., **737**
DE ROSSET, W., **1099**
DEWIT, R., **651**, 675, 676, 677, 708, 714, 715, 716, 719, 723, 832, 997
DOYAMA, M., **285**
DUESBERY, M. S., **1115**, 1135
DUNCAN, T. R., **47**, 557
EISENBERG, M. A., **925**
ELBAUM, C., 247, 312, 359, **427**, 577, 698, 704, **1291**, **1293**
ENGELKE, H., **397**, 415, 417, **1137**, 1164, 1165
ENGLERT, A., **273**
ERINGEN, A. C., 716, 831, 832, 834, **1023**, 1055, 1057
ESHELBY, J. D., 3, 175, 250, 251, 252, 415, 417, 460, 696, 715, 998
FLOCKEN, J. W., **219**
FOREMAN, A. J. E., **1083**
FOX, N., 965, **1041**, 1056, 1059, 1061
FRANK, W., **1065**, 1107, 1110, 1113
FRIEDEL, J., **607**
GARBER, J. A., **419**
GEHLEN, P. C., 201, 202, **305**, 311
GILMAN, J. J., 459, 693, 707, 716
GRANATO, A., 83, 359, 361, 395, **419**, **423**, 459, 460, **1099**, 1112, **1223**, 1227, 1228
GROVES, P. P., **35**
GRUNER, P., 360, **363**, 395, 396, 965
HAASEN, P., 702, 703, 704, 705, 706, 707, 1111, **1231**, 1255, 1256, 1258
HAHN, G. T., **305**
HARDY, J. R., **219**, 247, 249, 252, 706
HARRIS, W. F., **579**
HARTLEY, C. S., 721, **925**, 966
HEAD, A. K., 5, 84, 85, 86, 696, 718, 719, 721, 722, 723
HIKATA, A., **427**, **1291**
HIRSCH, P. B., 309, 690, 695, 719, **1083**, **1115**
HIRTH, J. P., 84, 310, 460, 547, 552, **683**, 687, 690, 692, 695, 696, 698, 702, 703, 704, 708, 710, 716, 718, 719, 721, 722, 723, 1111, 1113
HOBART, R., **1157**
HOLDER, J., **1223**
HOLMES, R. R., **1293**
HÖLZLER, A., **291**
HUFFMAN, G. P., 701, **1303**
HUMPHREYS, F. J., **1083**
ISHII, H., **71**
KLÉMAN, M., **607**, 712
KLEMENS, P. G., **391**, 395, 396
KOCKS, U. F., **1077**, 1108, 1110, **1179**
KOehler, J. S., 83, 84, 173

- KONDO, K., **761**
 KRÖNER, E., 173, 248, 249, 416, 558, 712, 717, 718, 720, **729**, **737**, 831, 832, 833, 834, 835, 836, 965, 1058, 1059, 1061, 1062
 KUHLMANN-WILSDORF, D., **47**, 84, 310
 KUNIN, I. A., **747**
 LI, J. C. M., **147**
 LOH, B. T. M., **479**
 LOTHE, J., **11**, 85, 86, 417, 461, 700, 719, 1111, 1112
 LOUAT, N., **135**, 701, **1303**
 MALÉN, K., **23**, 83, 84, 85, 86
 MARADUDIN, A. A., **205**, 247, 248, 249, 250, 251, 252, 705, 834, 1176
 MARCINKOWSKI, M. J., **531**
 MARION, R. H., **71**
 MASON, W. P., **447**, 461
 MENDELSON, S., **495**, 550, 555, 693, 1255, 1256
 MITCHELL, J. W., 578, 1110
 MISICU, M., **783**
 MURA, T., 675, 676, 965, **977**, 997, 998
 NABARRO, F. R. N., 395, 416, 555, 561, **593**, 675, 676, 710, 715
 NINOMIYA, T., **315**, 359, 360, 361
 NOURTIER, C., **1259**
 PEASE, D. E., **71**
 RIVLIN, R. S., 1056
 ROSENFIELD, A. R., **305**
 SAADA, G., 84, 202, 692, **1259**, 1289, 1290
 SCHOECK, G., 249, 311, 1107, 1110, 1113
 SCHRÖTER, W., **1231**
 SHWENKER, R. O., **423**
 SCATTERGOOD, R. O., **1179**
 SEGER, A., **397**, **877**, 1107, 1108, 1109, 1110, 1111, 1112, 1163, 1164, 1165, 1166, 1176, 1227, 1289, 1290, **1329**
 SENDECKYJ, G. P., **57**
 SIEMS, R., **291**, 309, 312
 SIMMONS, J. A., **89**, 174, 247, 560, 677, 963, 997, 1021, 1055, 1059, 1061, 1062
 SMITH, E., **151**
 SPRENG, D. T., **71**
 STOJANOVIC, R., **817**
 STONEHAM, A. M., **1169**, 1175, 1176, 1227
 SUZUKI, H., **253**, 311, 312, 359, 396
 TEODOSIU, C., 249, **837**, **877**, 965, 966, 1053
 TEUTONICO, L. J., 83, 87, 720
 THOMSON, R. M., 415, 416, 417, **563**, 577, 578, 694, 706, 707, 1163, 1164, 1258, **1279**, 1323
 TOMPA, H., **273**
 TUCKER, M. O., **163**
 VANDER SANDE, J. B., **71**
 VON TURKOVICH, B., 998
 WAISMAN, A. M., **747**
 WANG, C.-C., **907**
 WEERTMAN, J., **71**
 WEINER, J. H., 360, **403**, 415, 416, 967
 WILKENS, M., **1191**, **1195**
 YOO, M. H., **479**, 554, 555

